PARTICULATE FLUXES IN THE SUBTROPICAL CONVERGENCE REGION AND OTHER MARINE ENVIRONMENTS OF NEW ZEALAND

A thesis submitted

in fulfilment of the requirements

for the Degree of

Doctor of Philosophy

in

Earth Sciences

at the

University of Waikato

by

Scott Davidson Nodder

University of Waikato

1997

ABSTRACT

The thesis was designed to address two themes: (1) sediment trap methods and technique development; and (2) oceanic sediment fluxes within the Chatham Rise-Subtropical Convergence ecosystem, east of New Zealand. Accordingly, the principal objectives of Theme 1 were to design, construct and deploy a sediment trap system for sampling sinking marine particles and to evaluate hydrodynamic biases in sediment traps from field studies. Theme 2 focuses on biological and physical processes affecting modern particulate sedimentation in the vicinity of the Subtropical Convergence Zone, and the magnitude and composition of particulate fluxes within the Chatham Rise-Subtropical Convergence region.

An overall conservative strategy was adopted for the sediment trap design criteria since critical aspects of the bio-physical environment of Chatham Rise-Subtropical Convergence were poorly known. A multiple arrangement of 8 to 12 baffled cylindrical traps deployed at set water depths on free-floating sediment trap arrays was the preferred design. Basal high density brines with formalin as a poison/preservative were employed for deployments scheduled to last 2-3 days in the winter and spring of 1993. Pilot studies in autumn 1992 and 1993 allowed practicalities of sediment trap deployments to be evaluated. Field experiments in Evans Bay, Wellington Harbour, showed that there were minimal hydrodynamic interactions between traps on the same array. Furthermore, baffles did not significantly affect trapping efficiency, whereas brine volume had a profound effect. In the latter case, traps filled completely with a high-density salt brine collected 2-3 times less material than traps with basal brine thicknesses equal in height to 1- and 2.5-cylinder diameters.

The resultant free-floating sediment trap arrays were deployed as part of the multi-disciplinary New Zealand Joint Global Ocean Flux Study (JGOFS) in winter and spring 1993. This study was designed to determine the trophic pathways and transferal rates of carbon within pelagic food webs in contrasting water masses (subantarctic and subtropical) on either side of the Subtropical Convergence. The sediment trap work was undertaken to evaluate the efficiency of the "biological pump" in removing particulate material from the surface layers of the ocean, as

part of Theme 2 of the thesis. Despite substantial temporal and spatial differences in physical and biological parameters measured in subantarctic, convergence and subtropical waters, total mass and particulate phosphorus fluxes were not significantly different across the three water types in winter or spring. High levels of variability between trap samples are attributed to errors associated with subsampling procedures; a problem that appears to be widespread in other, more exhaustive sediment trap experiments in oligotrophic environments. In order to improve the statistical power of the experiments, more than two free-floating sediment trap moorings are required in similar studies to discriminate between water type differences. Particulate fluxes appeared to be decoupled from upper ocean primary production, and in the case of deployments within the Subtropical Convergence, affected markedly by resuspension of bottom sediments from the crest of Chatham Rise caused probably by strong tidal currents that are known to operate across the Rise.

The presence of photosynthetic pigments in trap samples from 100 to 550 m depths suggests that sinking material must be transported rapidly out of well lit surface waters, probably as intact marine aggregates or mesozooplankton faecal pellets. The low concentrations of phaeopigments, normally attributed to zooplankton grazing or algal senescence, suggest that organic material has not been degraded in the upper ocean prior to sinking. This observation is perhaps attributable to the aforementioned rapid sedimentation, or the occurrence of unbleached pigments preserved in faecal pellets due to low conversion rates of chlorophyll *a* to phaeopigments in zooplankton guts. Furthermore, low rates of pigment export as a function of phytoplankton biomass and primary production (<5%) suggest that other processes were operating in the upper water column to prevent pronounced sedimentation of organic material out of surface layers. Microzooplankton grazing of organic material is likely to be important in preferentially increasing particle residence times in the upper ocean. This mechanism may be concomitant with other processes including bacterial decomposition, mesozooplankton foraging activities and shallow surface stratification, especially in spring.

The Southwest Pacific Ocean is recognised as an important regional, probably biologically mediated sink for atmospheric carbon dioxide. Sediment trap results from Chatham Rise-Subtropical Convergence are statistically ambivalent in terms of assessing the efficiency of the "biological pump" in removing carbon in organic material from the upper ocean by sinking processes. However, the persistence of undegraded pigmented material at 550 m depth, the

continental margin affinities suggested by relatively high mean mass fluxes, and the observation that particulate carbon can comprise up to 40% of mass flux, all suggest that "biological pump" efficiency is also enhanced in this region.

More work is required, however, to determine the temporal and spatial variability of particulate fluxes in the Southwest Pacific Ocean in order to develop an understanding of how the "biological pump" functions in this region. Future studies will have to overcome the statistical design criteria suggested by the present study (i.e., three or more free-floating arrays to be deployed at any one time), and should investigate the collection of longer time-series measurements made possible by the use of deep ocean, bottom-moored, time-incremental sediment traps. In order to fully understand sediment trap interpretations, contemporaneous measurements of food web structure and processes must also be made in an oceanic region largely devoid of extensive biological oceanographic data-sets.

In conclusion, despite the shortcomings of the sediment trap method (i.e., hydrodynamic biases, zooplankton contamination, lack of independent calibration), traps remain the only technique available to the oceanographic community that provides a quantifiable measurement of export fluxes from the upper to deep ocean. Until modern technology develops a truly neutrally buoyant sediment trap system with zooplankton exclusion devices, relatively simple sediment trap arrays, as utilised by the present study, will continue to provide the best initial estimates of oceanic particulate fluxes from previously uncharacterised regions of the global ocean.

ACKNOWLEDGEMENTS

My thanks are extended to the many people who have supported me over the course of this research project. Janet Grieve and Rob Murdoch (NZOI, NIWA) made initial approaches to me with respect to undertaking the sediment trap sampling programme within the New Zealand JGOFS framework, and have provided continued encouragement and scientific advice. My supervisors Professor Cam Nelson (University of Waikato) and Lionel Carter (NZOI, NIWA) made enormous sacrifices to ensure that the thesis was finally completed under a self-imposed strict deadline. Both Cam and Lionel have been sources of inspiration in terms of science and general outlooks on life.

Many thanks are given to the professional scientists, technicians and laboratory staff within NIWA who have provided logistic support and expertise, in particular, my colleague and friend Bridget Alexander, Mark Gall, Mike Page, George Payne, Stu Pickmere, Megan Oliver, Malcolm Downes, Helen Neil, John Hunt, Hoe Chang, Julie Hall, Mark James, Kim Currie, Bill Main and Dick Singleton. Bridget was a conscientious lab assistant, even when the thought of filtering yet another volume of water was sometimes too much. Alistair MacDiarmid (NZOI, NIWA) helped me through the rigours of statistical analysis, and Rose-Marie Thompson (NZOI, NIWA) sorted out obscure references. Overseas colleagues, namely Liz Sikes (Antarctic CRC, Hobart, Australia), Mike Sturm (EAWAG, Zürich, Switzerland) and Jonathan Sharples (University of Southampton, U.K.), were also highly supportive. Special thanks to Rob, Jonathan, James and especially Helen who got me through the madness of the final night of thesis compilation. Resources to ensure the successful completion of this project were provided generously first by DSIR and more recently by NIWA. Acknowledgement is also given to the officers and crews of the research vessels that were used in the course of this project, namely G.R.V. *Rapuhia* and R.V. *Akademik M.A. Lavrentyev*.

Finally, all my love to my partner Lynne Silcock, who kept the big stick ready when I threatened to wander off the thesis path, and to my parents and sisters, who have supported me emotionally through the years. Lynne also made light work of my reprint collection in generating a definitive reference list. Lastly, it is with both sadness and pride that I dedicate this thesis to the memory of my aunt Lorna Tingay and to the small bundle of joy that replaced her, my daughter, Louise Blake Nodder.

p. 121, para. 1, line 8: "tintiniid" should be "tintinnid"
p. 130, para. 3, line 13: replace "paper" with "study"
p. 135, 1st line: replace "*Gryodinium*" with "*Gyrodinium*"
p. 137, para. 2, line 9: replace "it's" with "its"
p. 139, line 4: Note that peak 9 has a retention time of >10 min in Fig. 6.1, but over all the chromatograms that were used, the *average* retention time for this peak was 9.44 min
Table 6.3: upper figure for dinoflagellates, winter, STC, should be 153.55, not 53.55
p. 147, para. 2, 3rd line from bottom: "west" should be "east"
p. 152, line 13: replace "reinjestion" with "reingestion"
p. 163: add ", V. L." between "Asper" and "(1987a)"
p. 175: replace "Hansen" with "Hansell"
p. 178: "Jannasch et al. (1980)" should come after "James & Hall (1997)"
p. 181: "Khripounoff & Crassous (1994)" should come after " Keeling & Shertz (1992)"
Appendix 7B, Filter 369: replace "*Struthialaria*" with "*Struthiolaria*"
Appendix 7B, Filter 303: "Scuptured" should be "Sculptured"
Appendix 7B, Filter 217: replace "aggreagates" with "aggregates"

Chapter 4 - DYNAMICS OF CHATHAM RISE-SUBTROPICAL CONVERGENCE ECOSYSTEMS IN WINTER AND SPRING 1993

Chapter 5 - PARTICULATE FLUXES IN CHATHAM RISE-SUBTROPICAL CONVERGENCE REGION

LIST OF FIGURES

LIST OF TABLES

Chapter 1

INTRODUCTION

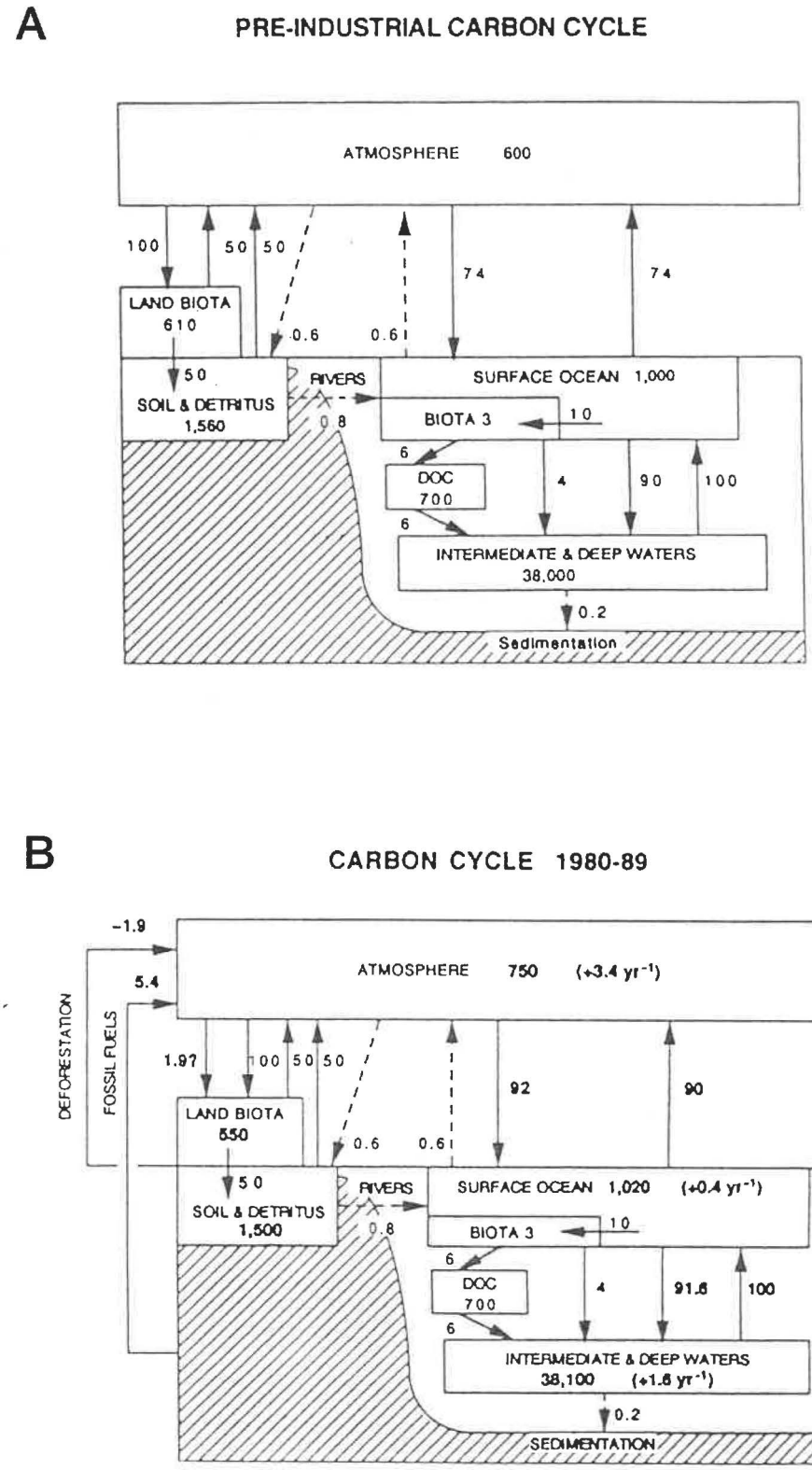

Fig. 1.1 Global carbon reservoirs (boxes) and fluxes (arrows) in gigatonnes (1 Gt = 10^{15}g) of carbon and gigatonnes of carbon per year, respectively (from Siegenthaler & Sarmiento, 1992). Pre- (A) and Post-Industrial (B) carbon cycles are depicted.

Chapter 1

INTRODUCTION

1.1. The oceanic carbon cycle and the biological pump

1.1.1. The global carbon cycle and relationships to oceanic processes

The oceanic reservoir of dissolved and particulate carbon is the most significant of the global carbon reservoirs, comprising an estimated 40 000 Gt (where 1 Gt = 10^{15}g) or 93.4% of the total global carbon pool (Siegenthaler & Sarmiento, 1993) (Fig. 1.1). These values are compared with 600 Gt of CO_2 in the pre-industrial (<1750 A.D.) atmosphere and 2170 Gt of carbon stored in terrestrial ecosystems. The effect of deforestation and fossil fuel burning by humans since industrialisation has been to increase the concentration of CO_2 in the atmosphere by 3.2 to 3.4 Gt C y^{-1} (Siegenthaler & Sarmiento, 1993; Sarmiento, 1995; Wallace, 1995). The oceans are thought to have responded to this anthropogenic perturbation by absorbing approximately 2.0 Gt more carbon on an annual basis (Siegenthaler & Sarmiento, 1993), which is about a third of all global carbon emissions (Tans et al., 1990; Wallace, 1995). By taking into account all of the important sinks and sources for CO_2, there is an apparent deficit in the global carbon cycle of about 1.8 Gt C y^{-1}, which has been a topic of continued controversy as to its actual size and location. Many carbon cycle modelers favour a large terrestrial sink (e.g., Tans et al., 1990; Hesshaimer et al., 1994; Ciais et al., 1995; Denning et al., 1995; Francey et al., 1995) whereas others have presented evidence for an oceanic sink (e.g., Keeling & Heimann, 1986; Keeling et al., 1989; Broecker & Peng, 1992; Keeling & Shertz, 1992; Sarmiento & Sundquist, 1992; Siegenthaler & Sarmiento, 1993). Notwithstanding these uncertainities, the magnitude of the oceanic carbon pool suggests that fluxes of various reduced and oxidised variants of carbon will affect profoundly global biogeochemical cycles.

Up to 90% of oceanic carbon takes the form of the dissolved bicarbonate ion with most of the balance made up in carbonate ions according to the following equilibrium reactions (e.g., Baes et al., 1985; Millero, 1995):

$$CO_2\,(g) = CO_2\,(aq) \qquad \text{[eqn. 1]}$$

$$CO_2\,(aq) + H_2O = H_2CO_3\,(aq) \qquad \text{[eqn. 2]}$$

$$H_2CO_3\,(aq) = H^+ + HCO_3^- \qquad \text{[eqn. 3]}$$

$$HCO_3^- = H^+ + CO_3^{2-} \qquad \text{[eqn. 4]}$$

The exchange rate of gaseous CO_2 in the atmosphere with the surface waters of the ocean is rapid, with full equilibration of the global surface ocean occurring in approximately one year (Broecker & Peng, 1982). The air-sea transfer of CO_2 is driven by partial pressure differences between atmospheric and oceanic concentrations of CO_2 (pCO_2^{air} and pCO_2^{sea}, respectively). The solubility of CO_2 in sea-water is affected primarily by pressure, salinity and temperature (Baes et al., 1982; Millero, 1995), such that at lower temperatures the capacity of sea-water to absorb higher concentrations of atmospheric CO_2 is increased by 3-4% per °C of cooling (Sarmiento & Sundquist, 1992). The physical transfer of atmospheric CO_2 into the upper ocean is facilitated by other factors, such as turbulence (and, hence, is dependent on wind speed; Tans et al., 1990) and bubble formation by breaking waves (Woolf, 1993), and by biological processes such as photosynthesis.

1.1.2. The biological pump and uptake of atmospheric CO_2 by the ocean

During biological fixation, CO_2 is converted from its dissolved states as inorganic (DIC = $[H_2CO_3]$ + $[HCO_3^-]$ + $[CO_3^{2-}]$) and organic (DOC) carbon to reduced particulate forms in the euphotic zone by biological uptake by marine plants (phytoplankton) during photosynthesis. Particulate and dissolved carbon are then transformed by processes of respiration and oxidation during the consumption of carbon in the upper ocean by other components of the food web, namely microbial and zooplankton elements. Volk & Hoffert (1985) conceptualised the processes involved in the so-called "biological pump" as either "soft-tissue" or "carbonate" components, with the

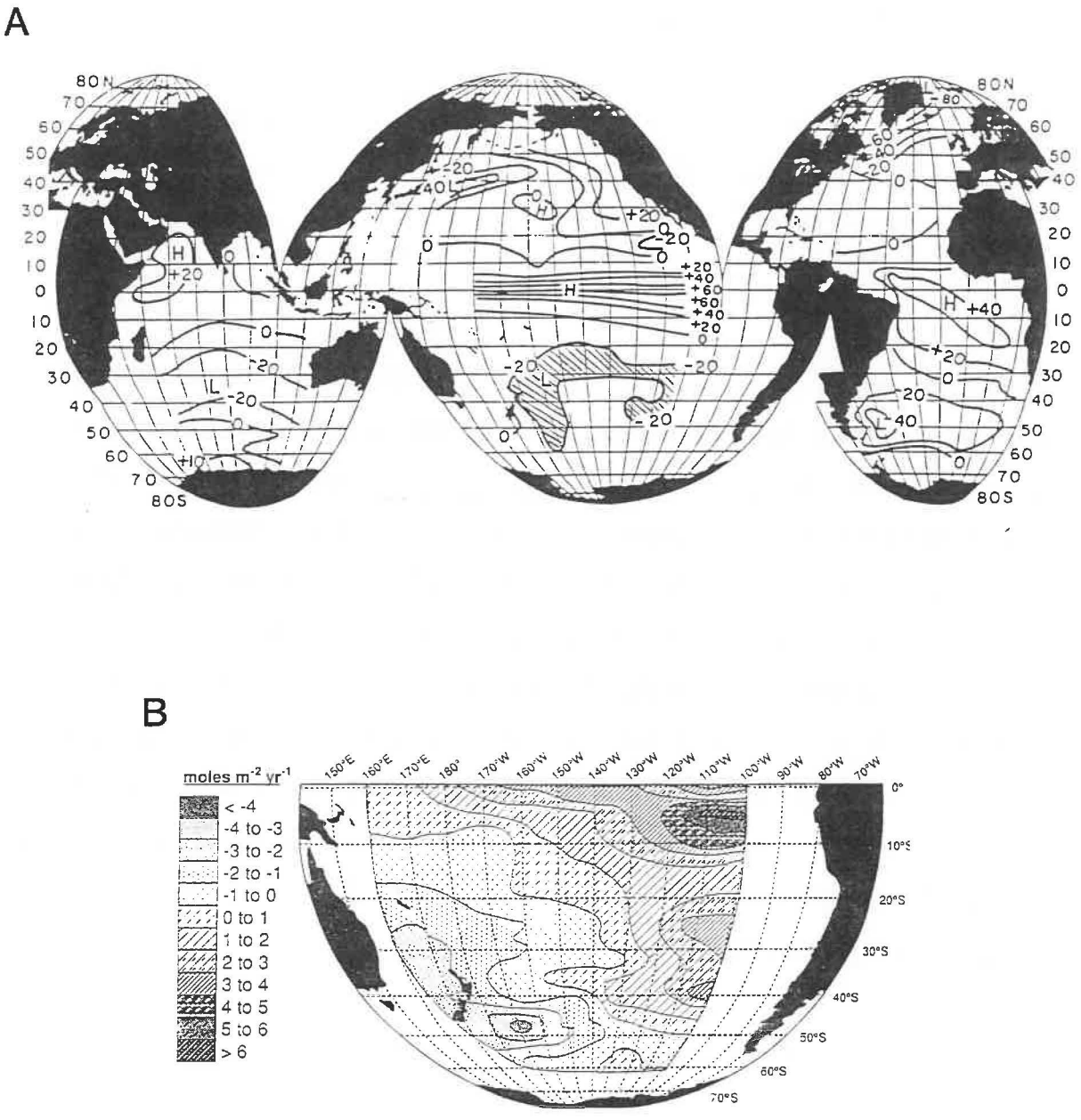

Fig. 1.2 (A) Global distribution of ΔpCO_2 in µatm observed in summer during the GEOSECS Program with area of significant oceanic uptake in Southwest Pacific Ocean highlighted (from Takahashi & Azevedo, 1982). (B) Regional annual molar flux of atmospheric CO_2 in South Pacific Ocean during February to May, between 1984-89 (from Murphy et al., 1991).

former associated with photosynthetic mechanisms and the latter with shell carbonate formation by marine protozoa. Photosynthesis and carbonate formation can be represented stoichiometrically by the following respective equations:

$$106CO_2 + 16NO_3^- + H_2PO_4^- + 17H^+ + 122H_2O \rightarrow (CH_2O)_{106}(NH_3)_{16}(H_3PO_4) + 138O_2\,(g) \quad \text{[eqn. 5]}$$

$$Ca^{2+} + 2HCO_3^- = CaCO_3\,(s) + CO_2 + H_2O \quad \text{[eqn. 6]}$$

These processes affect pCO_2^{sea} in opposite senses, with photosynthesis driving the oceanic uptake of atmospheric CO_2 and carbonate precipitation having an ambiguous effect on pCO_2^{sea}, but generally leading to an increase in pCO_2 (e.g., Robertson & Watson, 1993; Gattuso et al., 1995, and references therein) and a reduction in the total alkalinity (TA) of surface waters (where TA = $[HCO_3^-] + 2[CO_3^{2-}]$; Baes et al., 1985).

Ultimately, it is the complex balance between physical and biological processes in the world's oceans that determines the relative uptake of atmospheric CO_2. Thus, regions of the earth's surface can be regarded as representing on average either CO_2 sources, such as the equatorial zones, or CO_2 sinks, such as at mid- to high latitudinal areas (e.g., Takahashi & Azevedo, 1982; Baes et al., 1985) (Fig. 1.2A). Despite considerable controversy regarding the magnitude of the oceans as a global sink for CO_2 (e.g., Keeling et al., 1989; Tans et al., 1990; Broecker & Peng, 1992; Sarmieto & Sundquist, 1992; Siegenthaler & Sarmiento, 1993; Hesshaimer et al., 1994; Ciais et al., 1995), a "best-guess" estimate of 2.0±0.6 Gt y^{-1} of carbon is transferred as CO_2 across the air-sea interface on a global basis (Siegenthaler & Sarmiento, 1993). This figure has been recently revised by Sarmiento (1995) to 1.5±0.5 Gt y^{-1}. Surface waters of the Southern Ocean (>40°S) are a potential natural sink of atmospheric CO_2 on the basis of their relatively cold temperatures, compared with waters in equatorial regions, and their highly productive nature as suggested by a few primary production measurements (e.g., Bradford, 1980a, b; Knox, 1994) and by ocean colour satellite interpretations (e.g., Comiso et al., 1993; Sullivan et al., 1993). Studies by Takahashi & Azevedo (1982) and Murphy et al. (1991) have highlighted the importance of the Southwest Pacific

Ocean as a regional sink for CO_2 with ΔpCO_2 deficits of less than -20 μatm (where $\Delta pCO_2 = pCO_2^{air} - pCO_2^{sea}$) (Fig. 1.2). Similarly, Currie & Hunter (1997) show that waters to the east of New Zealand are a weak to moderately strong sink (-10 to -110 μatm) in spring, especially in the vicinity of the Subtropical Convergence (STC) at about 43°S. Whether the observed ΔpCO_2 deficit in the Southwest Pacific Ocean is due to physical solubility or biological effects has not been fully evaluated. Murphy et al. (1991) concluded that the -10 to -40 μatm deficit observed in autumn during their study was more likely to have a biological origin as reflected by elevated surface ocean pigment concentrations (from satellite imagery, e.g., Comiso et al., 1994) and enhanced production within the STC (e.g., Bradford, 1980a, b, 1983). Strong seasonal and interannual variability in the magnitude and sign of ΔpCO_2 are expected, however, from similar studies conducted in the southwestern Indian sector of the Southern Ocean (e.g., Poisson et al., 1994).

1.1.3. The role of the Southern Ocean in air-sea fluxes of carbon

Despite favouring a northern hemisphere terrestrial, rather than oceanic, sink for CO_2, Tans et al. (1990) clearly show that the oceanic areas at southern latitudes (15°-50°S) have the potential to absorb an estimated 1.1-2.3 Gt C y^{-1} compared with other oceanic sinks such as the North Atlantic and Pacific oceans (both less than 1.4 Gt C y^{-1}; table 3, p. 1435). Inversion studies using 2-dimensional atmospheric transport models also predict a similar effect of elevated CO_2 uptake at southern latitudes which follows expected seasonality trends related to the seasonal growth and decline of marine phytoplankton (e.g., Enting & Mansbridge, 1989). Broecker & Peng (1992) proposed that the pre-industrial south to north hemispherical transportation of atmospheric CO_2 (e.g., Keeling & Heimann, 1986) would have been balanced by a counter flow of carbon within the deep ocean circulation of the Atlantic Ocean. They estimated that about 0.6 Gt C y^{-1} was exported into the Southern Hemisphere, which Sarmiento & Sundquist (1992) surmised would be effluxed into the atmosphere from the sea at high southern latitudes. Sophisticated modelling using a zonally averaged global circulation model led Stocker et al (1994) to conclude that 30% of excess anthropogenic carbon in CO_2 was absorbed by the surface waters of the Southern Ocean (>45°S), compared with

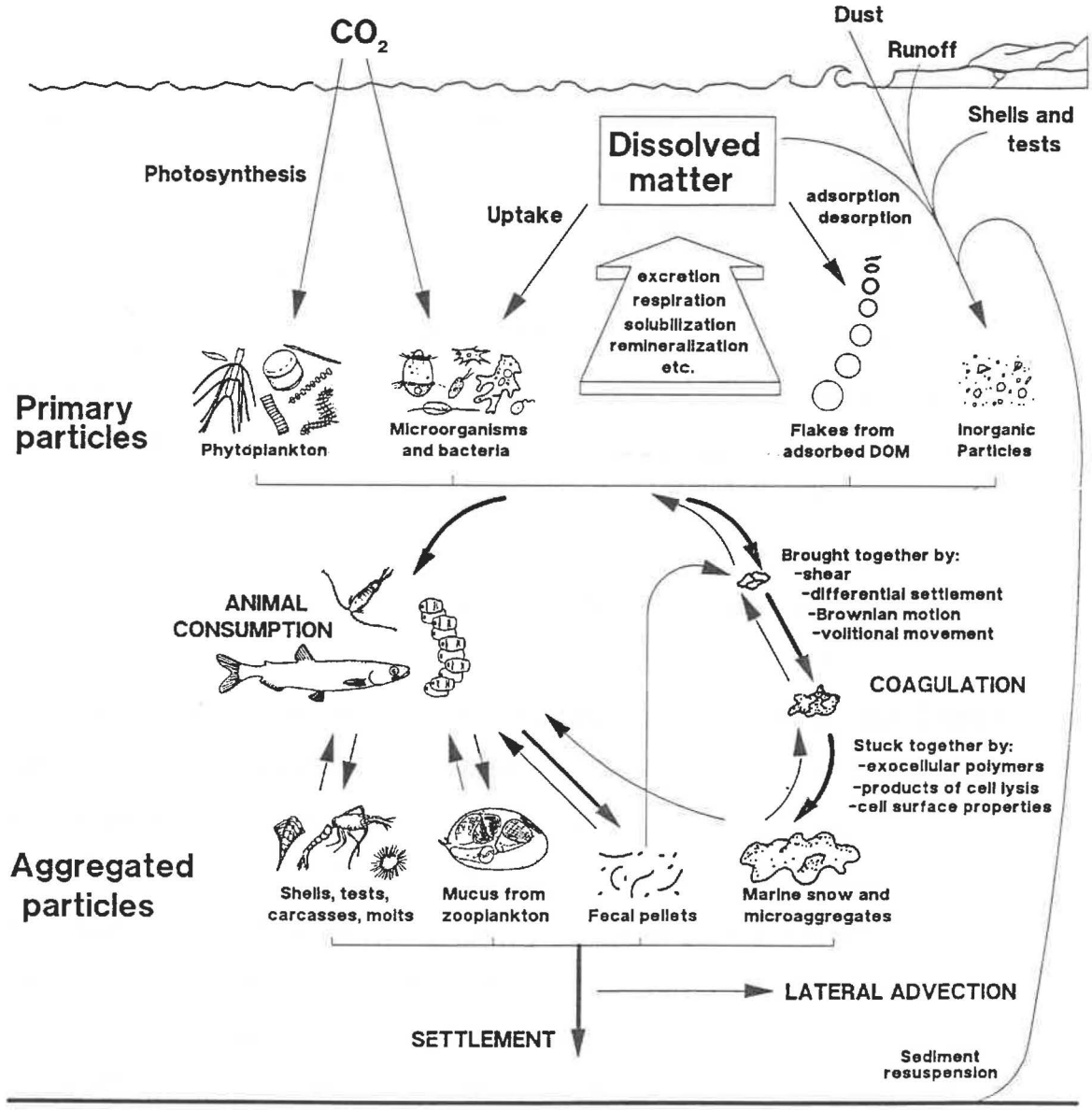

Fig. 1.3 Major sources and transformations of particles in sea-water, and contribution of aggregated and primary particles to sedimentation in the marine environment (from Karl et al., 1991a). The rates at which inorganic carbon is sequestered by phytoplankton and sinks from the surface layers of the world's oceans are critical rate-determining steps within the global carbon cycle.

only 10% in the North Atlantic; both observations were ascribed to the effect of deep convection in these regions. On a global scale, however, the zonal partitioning of atmospheric CO_2 using $\delta^{13}C$ measurements suggests that, although the oceans between 30 and 90°S can be a prominent sink, accounting for 1.0-1.1 Gt C y^{-1}, the most significant sink was at northern hemisphere latitudes (30-90°N) in 1991-92 when fluxes were in the order of 3-4 Gt C y^{-1} (Ciais et al., 1995). Since oceanic influences are limited over this northern latitudinal range, the sink in 1991-92 was therefore probably related to a temperate latitude terrestrial sink (e.g., Tans et al., 1990).

1.1.4. Role of particulate fluxes in global carbon cycle

The near-equilibrium situation that exists between the surface ocean and the atmosphere (e.g., Baes et al., 1985) suggests that one of the important mechanisms in the functioning of the oceanic carbon cycle is the rate at which dissolved and particulate carbon is removed from surface waters and transported to the deep ocean. Intermediate and deep ocean water masses form the most significant reservoir of carbon in the ocean (approximately 38 000 Gt C, or 97% of the total pre-industrial carbon ocean pool, Siegenthaler & Sarmiento, 1993) (Fig. 1.1), and the removal of carbon from surface waters represents effectively a "loss" from the pool of carbon that may be exchanged freely between the ocean and the atmosphere. Energy and metabolic requirements of organisms below the euphotic zone (defined as the depth of the 1% level of light in the ocean) and at the sea-floor are determined by the supply of dissolved and particulate phases of carbon from the upper to the deep ocean. While surface waters equilibrate rapidly with the atmosphere, the rate determining step in the dynamics of oceanic CO_2 uptake is the rate at which dissolved CO_2 and its various reduced and oxidised forms are transported vertically downwards into the deep ocean by diffusion, advection (Toggweiler, 1989) and particulate matter transfer (Peterson, 1981) . The mechanisms of diffusion and advection have equilibration time-scales with the atmosphere of about 1000 years (Siegenthaler & Sarmiento, 1993), whereas the transport of particles to the deep ocean operates on scales of days to months. Mechanisms of particle formation in sea-water are conceptualised in Fig. 1.3. Sinking of primary particles (e.g., phytoplankton, microzooplankton, inorganic material) may contribute directly to

particulate fluxes. It is generally perceived, however, that aggregation of these particles, via physical coagulation mechanisms and consumption by other organisms, enhances sinking rates of organic material from the upper ocean (e.g., McCave 1975, 1984b; Honjo, 1978, 1980; Knauer et al., 1979; Fowler & Knauer, 1986; Martin et al., 1987; Karl et al., 1991a). Particle aggregation by consumption is characterised by the formation of tests, carcasses, moults and faecal material by zooplankton. The multiple sources and dynamic pathways by which particles may be transformed and modified (Fig. 1.3) suggest that particulate transfer from the upper ocean to the deep sea is not a simple process, but is the result of a combination of numerous, complex, interrelated steps that characterise food web functioning and structure in the ocean.

As outlined by Longhurst's (1991) summary of the "biological pump", particulate transfer processes in the world's oceans include active vertical migration of zooplankton (Angel, 1989) and phytoplankton (Villareal et al., 1993), and gravitational settling of organic and inorganic matter (McCave, 1975, 1984b). The global significance of diel zooplankton migration was evaluated by Longhurst (1991) who proposed that this process may be capable of transporting up to 30% of sinking flux across the thermocline, in addition to contributions made at mid-water depths by excretion, respiration and over-wintering trends. In a subsequent paper, however, Longhurst & Williams (1992) concluded that on a global scale this effect was probably as small as 0.01-0.02 Gt C y^{-1}, or about 0.1% of the total sedimentary flux of carbon. In addition, it is apparent that considerable variability occurs at different oligotrophic sites with Dam et al. (1995), for example, estimating that between 18-70% of exported carbon could be accounted for by this mechanism in the Sargasso Sea.

Ultimately, therefore, it is the rapid downward vertical transport of particulate material at daily sinking rates of higher than 100 m (Fowler & Knauer, 1986) that has the most significant impact on the efficiency of the biological pump at removing particulate carbon from the surface waters of the ocean. Peterson (1981) suggested an annual "baseline" or "pre-anthropogenic" rate of only 2-3 Gt C, which he used to question the importance of particulate transport in the global carbon cycle. More recent work, however, has indicated that the magnitude of total particulate carbon export is poorly known with fluxes ranging

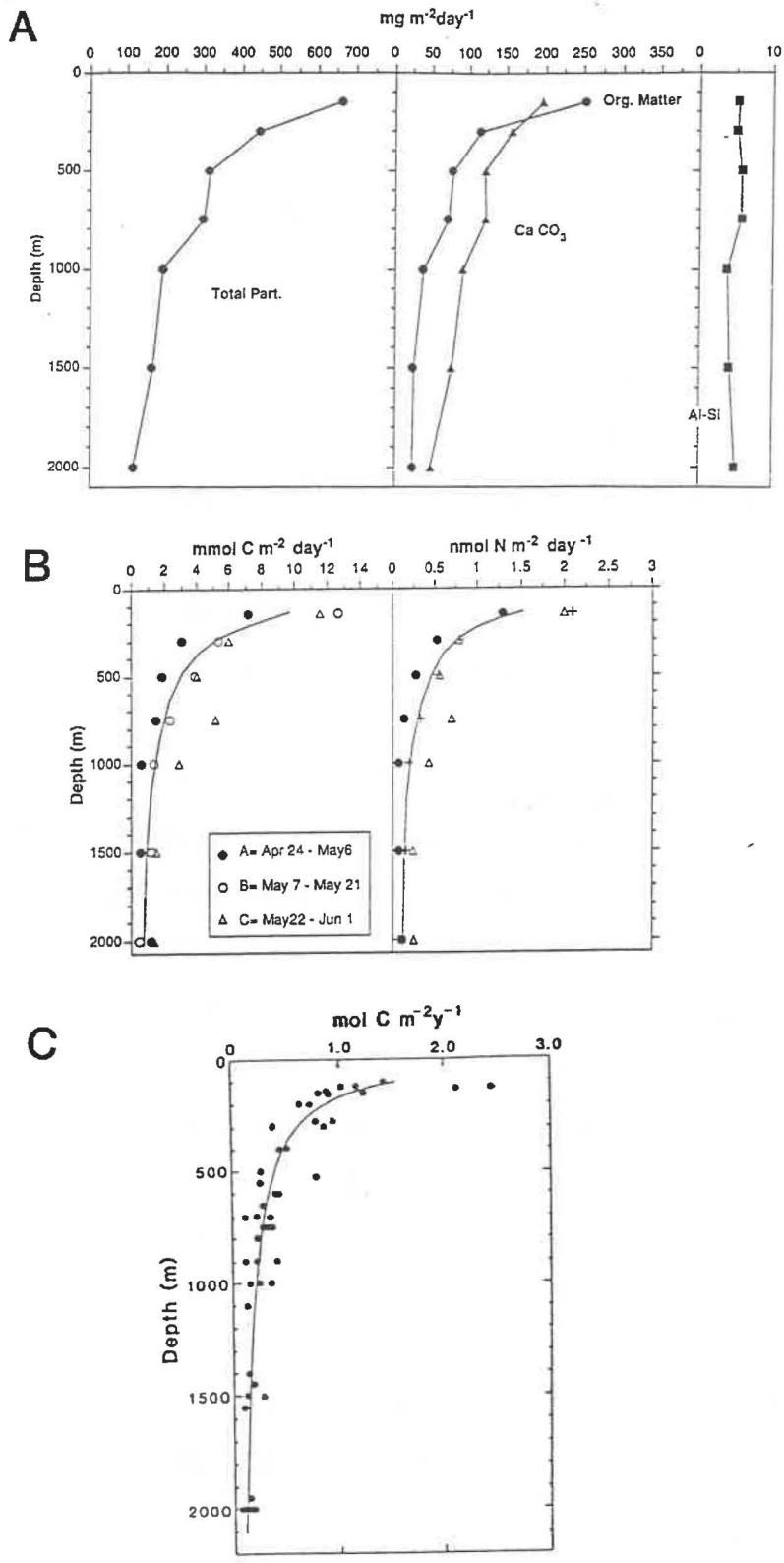

Fig. 1.4 (A) Average total particulate mass, organic matter, calcium carbonate and alumino-silicate fluxes with varying depth in northeast Pacific Ocean. (B) Particulate organic carbon and nitrogen fluxes with depth (z) and fitted power curves in northeast Pacific Ocean where:

$$\text{C flux} = 14.35(z/100)^{-0.946} \text{ and N flux} = 2.34(z/100)^{-1.02}.$$

(C) Open ocean composite fluxes (F) for organic carbon using the means of replicates from a variety of depths and environments in western Pacific Ocean where:

$$F = 1.53(z/100)^{-0.858},\ r^2 = 0.81,\ n = 48.$$

All measurements made during VERTEX programme (from Martin et al., 1987).

from 2 to 20 Gt C y^{-1} (Suess, 1980; Betzer et al.,1984; Martin et al., 1987; Siegenthaler & Sarmiento, 1993; Iverson & Esaias, 1995; Karl et al., 1996). Steady-state scenarios (on the order of months to years) have been used previously to relate sedimentary flux to the amount of new production occurring in the world's oceans (e.g., Eppley & Peterson, 1979; Knauer et al., 1979; Martin et al., 1987). New production is defined as the proportion of primary autotrophic production available for export which is balanced by the introduction of all sources of nitrogen (e.g., Dugdale & Goering, 1967; Eppley & Peterson, 1979). Since nitrogen in marine particulate material is related stoichiometrically to carbon in the form of the average Redfield ratio C:N:P = 106:16:1 (Fleming, 1940; Redfield et al., 1963; see eqn. 5), estimates of new production have been made using sediment traps deployed below the euphotic zone or mixed-layer (references above). In addition, the ratio of nitrate-based new production to total primary production (termed the *f*-ratio, Eppley & Peterson, 1979) also provides insights into the balance between the source of nutrients available for autotrophic production and the downward flux of particulate material. The highest rates of degradation and dissolution of particulate material occur in the uppermost 200 m of the water column (e.g., Knauer et al., 1979; Martin et al., 1987) (Fig. 1.4) and are believed to be related empirically to water depth (z) and primary productivity (PP) via various non-linear power functions that have been devised over the last 15 years, including:

(1) C flux (z)= $PP/0.0238z + 0.212$ (r^2=0.79, Suess, 1980)

(2) C flux (z) =$a.PP^{1.41}/z^{-0.63}$ where log a = -0.388±0.585 (Betzer et al., 1984)

(3) C flux (z) = $3.523z^{-0.734}PP^{1.000}$ (r^2=0.69; Pace et al., 1987)

(4) N flux (z) = $0.432z^{-0.843}PP^{1.123}$ (r^2=0.76; Pace et al., 1987)

In oligotrophic waters, however, the *f*-ratio typically exhibits considerable variability, with ranges of 0.03 to 0.84 reported by Platt & Harrison (1985). A recent study by Knauer et al. (1990) indicated that while no obvious relationship existed between new production and primary production, low *f*-ratios generally corresponded with times of high total primary production and low export flux. In addition, existing paradigms concerning the empirical relationship between the sedimentary flux of particulate organic carbon out of the upper ocean and near-surface autotrophic primary production (e.g.,

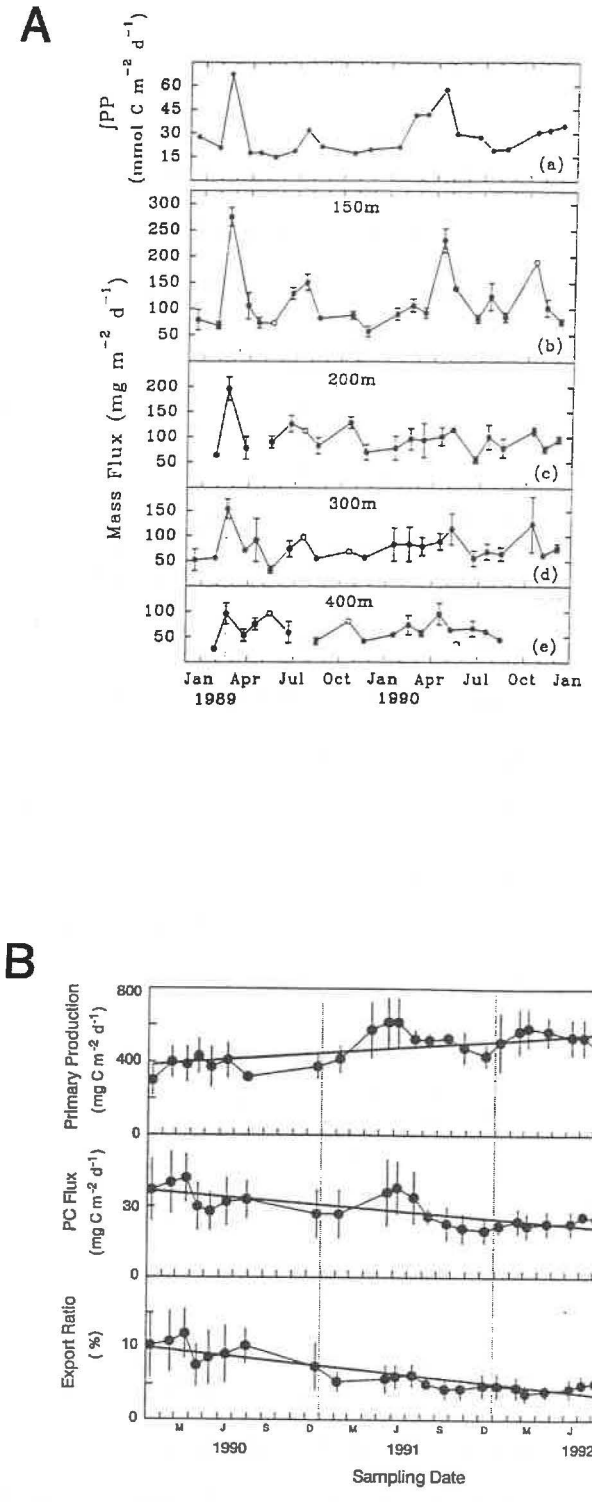

Fig. 1.5 Relationships between primary production (PP) and particulate fluxes at (A) Bermuda Atlantic Time-series Study (BATS) site (from Lohrenz et al., 1992), and (B) Hawaii Ocean Time-series (HOT) station ALOHA (from Karl et al., 1996). These results show that a current paradigm of biological oceanography, concerning the direct relationship between primary production and export flux (e.g., Eppley and Peterson, 1979; Suess, 1980), is being seriously challenged by recently collected time-series data.

Eppley & Peterson, 1979; Suess, 1980; Hargrave, 1985; Pace et al., 1987) has been challenged seriously by the recent presentation of time-series data collected at oligotrophic sites near Hawaii and Bermuda since 1989 (e.g., Lohrenz et al., 1992; Karl et al., 1996; Michaels & Knap, 1996). At these sites over 5-6 years of monthly monitoring, there was only a weak correlation between export and primary production of carbon (Fig. 1.5), despite close pelagic-benthic coupling observed at Bermuda in the first 2 years of the sampling programme (Asper et al., 1992).

1.1.5. Fate of sinking particulate material

Between 1-3% of primary production and less than 10% of particulate organic carbon exported from the upper surface waters of the ocean reaches the sea-floor where a significant proportion of this material (approximately 66%) is consumed and oxidised rapidly by benthic organisms (e.g., Berger et al., 1989; Siegenthaler & Sarmiento, 1993). Thus, the distribution of benthic community biomass and structure (i.e., feeding behaviour) is determined ultimately by the supply of organic material to the sea-floor (e.g., Hinga et al., 1979; Rowe, 1983; Jumars & Wheatcroft, 1989) with the organic supply exhibiting considerable heterogeneity on many temporal and spatial scales. Once at the sea-floor, particulate material, generally in the form of biogenic opal, carbonate and organic carbon (>80%; Dymond & Collier, 1988), is degraded or transformed by biologically mediated processes, such as bacterial and protozoan metabolism (e.g., Gooday, 1988), benthic consumption (e.g., Pfannkuche & Lochte, 1993; Smith et al., 1994) and bioturbation (e.g., Smith et al., 1994) or physical mechanisms, such as resuspension (e.g., Lampitt, 1985) and geochemical transformations in early diagenesis (e.g., Reimers, 1989). A recent summary of organic carbon distribution in bottom sediments of the world's oceans indicates that approximately 60-70% of particulate organic carbon flux to the deep ocean occurs within 30° latitude of the equator and that flux rates in the Atlantic and Pacific ocean basins are similar while highest rates occur in the Indian Ocean (Jahnke, 1996).

The highest proportions of sedimentary organic carbon (generally <2.5% by weight) and burial rates (up to 55 mmol C m^{-2} y^{-1} or 660 mg C m^{-2} y^{-1}) are found along continental

margins (Jahnke, 1996), where it is estimated that up to 50% of organic carbon that is exported to the adjacent open ocean may have an anthropogenic source (i.e., 0.4-0.5 x 10^9 tons C y^{-1} of an estimated total of 10^9 tons C y^{-1}; Walsh, 1989). Organic carbon input to the global ocean from continental erosion is estimated to be about 0.4 Gt C y^{-1} with 45% of this amount in particulate form (Ludwig et al., 1996). The distribution of sedimentary inorganic carbon in the form of calcium carbonate is also highest along the margins of ocean basins, although the relatively low percentages in deep ocean sediments by weight (<1%; Jahnke, 1996) are a reflection of the pressure-related dissolution of calcite below water depths of about 4500 m for the Atlantic, Pacific and Indian oceans (Broecker & Peng, 1982). This simple relationship, however, is modified further by the effect of deep ocean respiration, which is stronger in the Pacific compared with the Atlantic Ocean, resulting in better preservation of deep-sea carbonates in the less acidified waters of the Atlantic (Archer, 1996).

1.1.6. Summary of the potential role of the Southern Ocean and regional particulate fluxes to the global carbon cycle

In summary, the waters of the Southern Ocean are believed to act as a significant natural sink for atmospheric CO_2, accounting for 1-2 Gt of carbon transported across the air-sea interface on an annual basis. In addition, modelling work suggests that 30% of excess anthropogenic atmospheric CO_2 could potentially be absorbed by the Southern Ocean. Spatially and temporally, it is expected, however, that certain regions of this vast oceanic province will act as both sources and sinks for atmospheric CO_2. One of the critical rate-determining steps in the global carbon cycle is the rate at which carbon is removed from surface layers and transported to the deep ocean. An important process in this step is the sinking and transformation of particles in the form of inorganic and organic carbon (i.e., as carbonate and/or organic material). Since the waters to the east of New Zealand exhibit pronounced deficits in ΔpCO_2 (i.e., the oceans act as a sink for atmospheric CO_2) at certain times of the year (e.g., Takahashi & Azevedo, 1982; Murphy et al., 1991; Currie & Hunter, 1997), it is necessary to investigate particulate fluxes in this region to determine whether the efficiency of the "biological pump" in sequestering atmospheric CO_2 is similarly enhanced.

Consideration of particulate fluxes in water masses either side of a globally important ocean frontal zone, the Subtropical Convergence, may enable broad comparisons to be drawn with other similar regions of the Southern Ocean.

1.2. Objectives of thesis and thesis format

Biological oceanographic studies within the New Zealand region in the past were concerned primarily with descriptions of phytoplankton and zooplankton assemblages and their spatial distributions as related to regional physical features (e.g., Heath & Bradford, 1980; Bradford, 1983). Little information on the rate of organic matter production and the subsequent fate of this material has been conducted, except in waters off the west coast of South Island where primary production, nutrient regeneration and uptake rates and microbial processes have been described (e.g., Bradford & Chang, 1987; Hall et al., 1993; Chang et al., 1995).

In 1992, a scientific programme was developed at New Zealand Oceanographic Institute (NZOI, now National Institute of Water & Atmospheric Research Limited (NIWA)) to investigate the fluxes of carbon between the main components of pelagic oligotrophic ecosystems in New Zealand waters, under the auspices of the New Zealand Joint Global Ocean Flux Study (JGOFS). The principal objective of JGOFS is to evaluate the effect of biological processes on carbon sequestration by the world's oceans. Major field work initiatives by JGOFS-affiliated scientists have been undertaken in the North Atlantic (e.g., Lochte et al., 1993), Arabian Sea (e.g., Nair et al., 1989), equatorial Pacific (e.g., Murray et al., 1995; Karl et al., 1996) and Sargasso Sea (e.g., Michaels and Knap, 1996). Prior to 1992, no JGOFS work had been undertaken in the Southern Ocean, with scientists affiliated to the United States of America JGOFS programme not scheduled to conduct field work until 1996 to 2000. The absence of any integrated information on pelagic food web dynamics and carbon cycling in the Southwest Pacific Ocean sector of the Southern Ocean in 1992 provided the main focus of the planned New Zealand JGOFS research voyages in 1993. Of particular relevance to this thesis was a lack of data on the rates at which organic material is exported from surface waters in the Southwest Pacific region, which

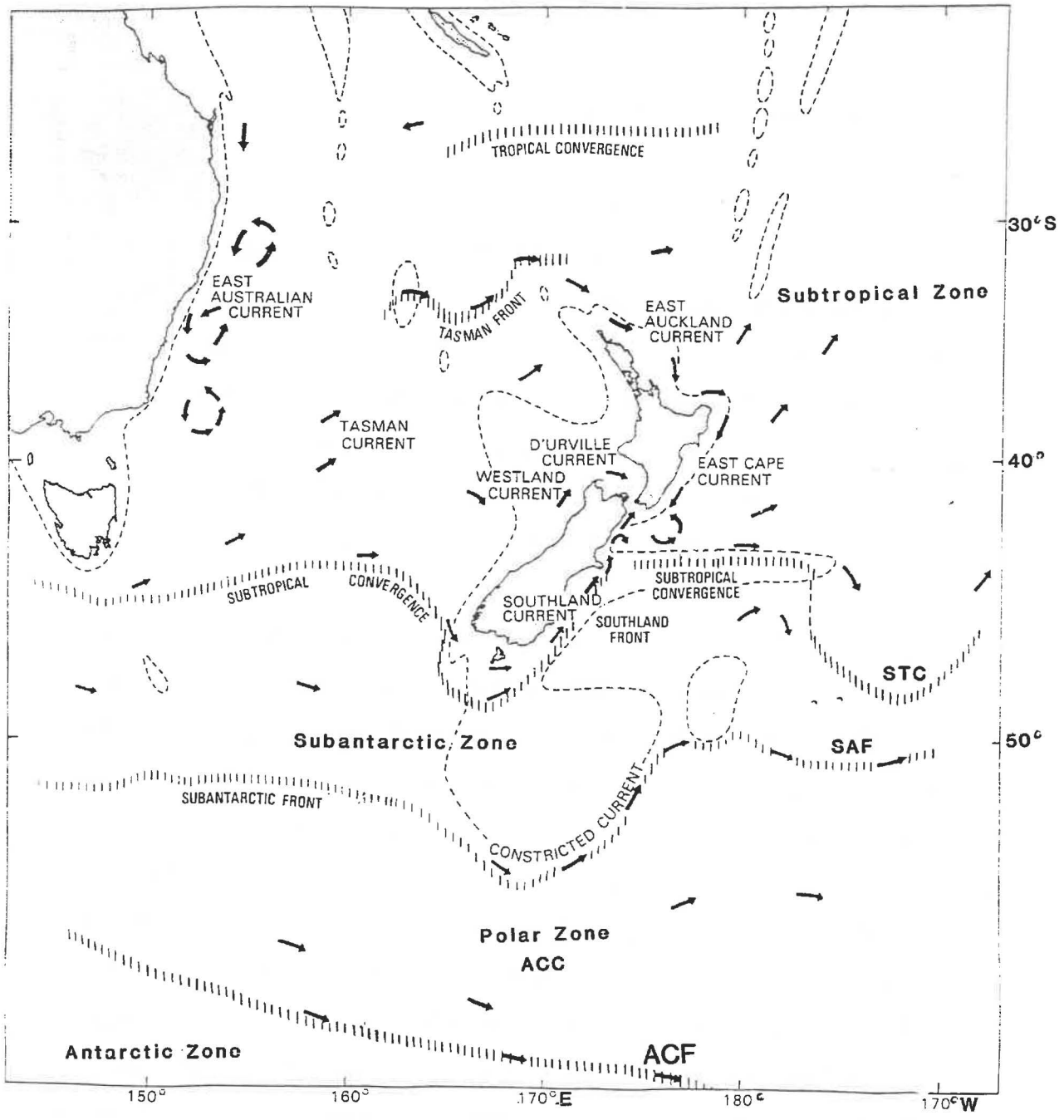

Fig. 1.6 Summary of generalised oceanic circulation patterns and positions of oceanic fronts in the Southwest Pacific Ocean (after Heath, 1985). STC = Subtropical Convergence, SAF = Subantarctic Front, ACC = Antarctic Circumpolar Current, ACF = Antarctic Circumpolar Front. The dashed line is a schematic 1000 m isobath.

necessitated the instigation of a sediment trap sampling programme upon which the present study is based.

As a consequence, the organisation of the thesis is based around two primary themes: (1) sediment trap methods and technique development (remainder of Chapter 1 and Chapter 2); and (2) oceanic sediment fluxes east of New Zealand and relationships to the Chatham Rise-Subtropical Convergence ecosystem (Chapters 3, 4, 5 and 6). Accordingly, the main objectives of the thesis are:

(a) To design, construct, test and deploy a sediment trap system for sampling sinking marine particles (Theme 1);

(b) to evaluate hydrodynamic biases in sediment traps from field studies (Theme 1);

(c) to assess biological and physical processes affecting modern particulate sedimentation in the vicinity of the Subtropical Convergence, east of New Zealand (Theme 2); and

(d) to characterise the nature and composition of particulate fluxes within the Subtropical Convergence zone in the Southwest Pacific region (Theme 2).

The main study area is located in oceanic waters to the east of New Zealand in the vicinity of the Subtropical Convergence (STC), a globally significant oceanic front that is confined geographically in this region along the crest of the submarine ridge forming the Chatham Rise (Fig. 1.6 & 1.7). The STC represents the mixing zone between warm, saline, nutrient-depleted **subtropical** waters to the north and cold, nutrient-replete **subantarctic** waters to the south. As part of thesis field work, pilot sediment trap studies were conducted in April 1992 and May 1993 (austral autumn) in subtropical waters, and were followed by two extensive research voyages in June-July (early winter) and October (spring) 1993 that analysed trophic interactions and carbon fluxes within three open ocean water types (subantarctic, STC and subtropical) east of New Zealand. Laboratory work and a series of *a posteriori* experiments investigating sediment trapping efficiency were

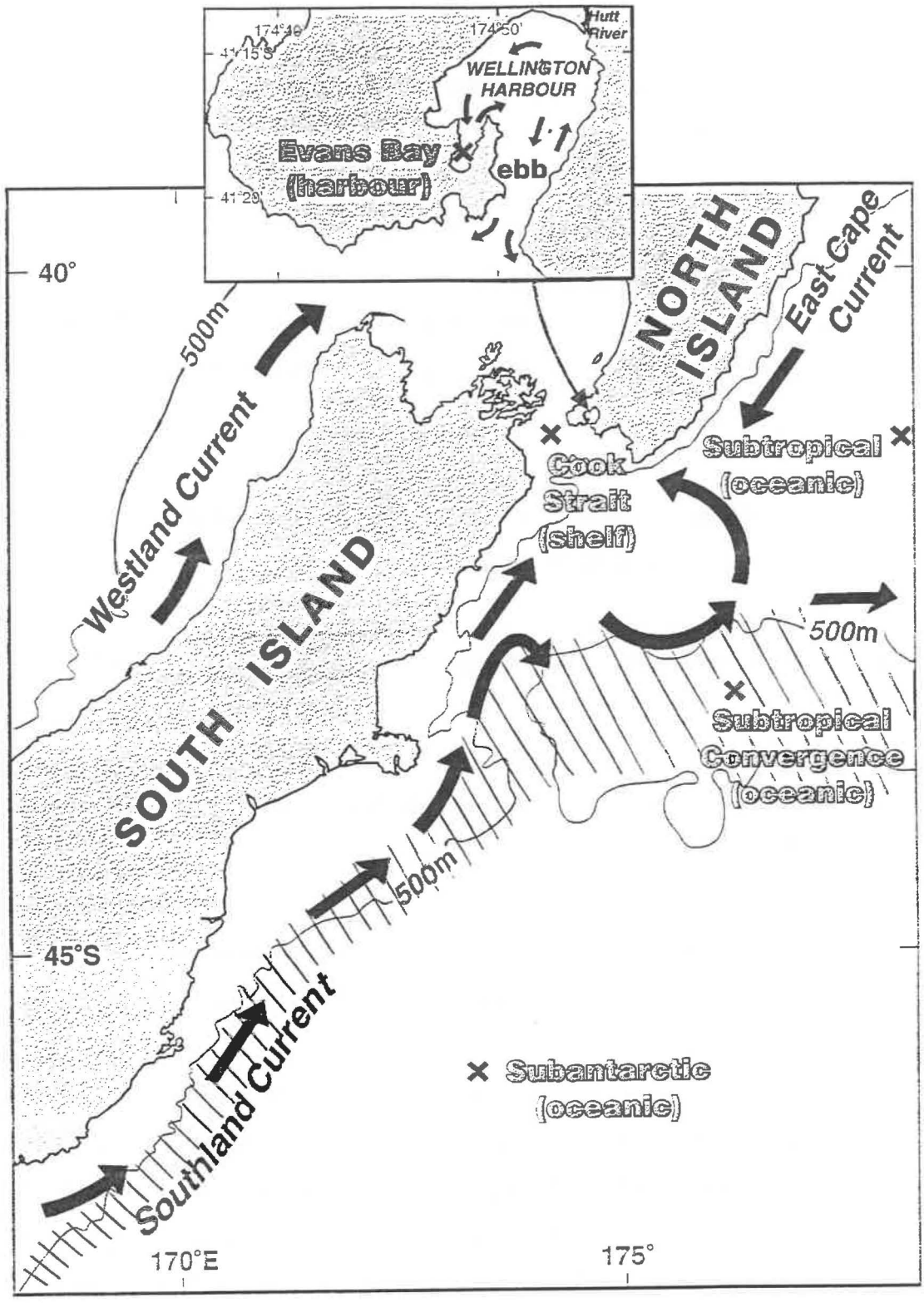

Fig. 1.7 Locations of sediment trap experiments conducted in New Zealand marine environments between 1993 and 1995. Studies in Cook Strait and Evans Bay are discussed in Chapter 2; the work at open ocean sites to the east of New Zealand in subtropical, Subtropical Convergence (approximate location shown by diagonal lines) and subantarctic waters are presented variously in Chapters 4, 5 and 6. Bathymetric contours are in metres below sea-level.

completed in 1994-95. The experiments in Evans Bay, Wellington Harbour, were conducted after the main phase of field work due to observations of variable flux results that were apparent from the 1993 JGOFS deployments. These variations could not be explained adequately by contemporaneous biological and physical measurements (Chapter 5).

The chronological sequence of field work and experimentation outlined above is not followed by the organisation of this thesis, which first presents a brief overview of sediment trap methods (remainder of Chapter 1). This chapter is followed by a section outlining the design rationale used for the traps constructed at NZOI in 1992, in association with results from two sediment trap pilot studies conducted in 1992 and 1993, and from the *a posteriori* experiments undertaken in 1994-1995 (Chapter 2). A literature review of the bio-physical environment of the STC region is then presented (Chapter 3) which is followed by a chapter describing the methods and interpreted results from biological and physical measurements made during the 1993 JGOFS field work in the STC region (Chapter 4). Results from Chapter 3 and 4 provide background information to subsequent chapters concerning aspects of sediment trap studies conducted in the STC region. Specifically, the main aim of Chapter 5 is to determine whether observed temporal and spatial variations in the physical environment and plankton community (Chapter 4) affected the magnitude of particulate fluxes in water masses either side of and within the STC. Potential sources in variability in sediment trap data are emphasised further in Chapter 5. In order to investigate the influence of changes in planktonic community structure and functioning on the composition of sinking particles, the fluxes of photosynthetic pigments are used as process tracers and phytoplankton biomarkers in Chapter 6.

1.3. Brief history of sediment trapping

Particle-collecting traps have been used in many physical environments as a technique for evaluating the fate of falling or sinking material. For example, pollen collectors and rain gauges are traps that are used to determine the amount of material falling out of the atmosphere to the surface of the earth. The first recorded use of a sediment trap began

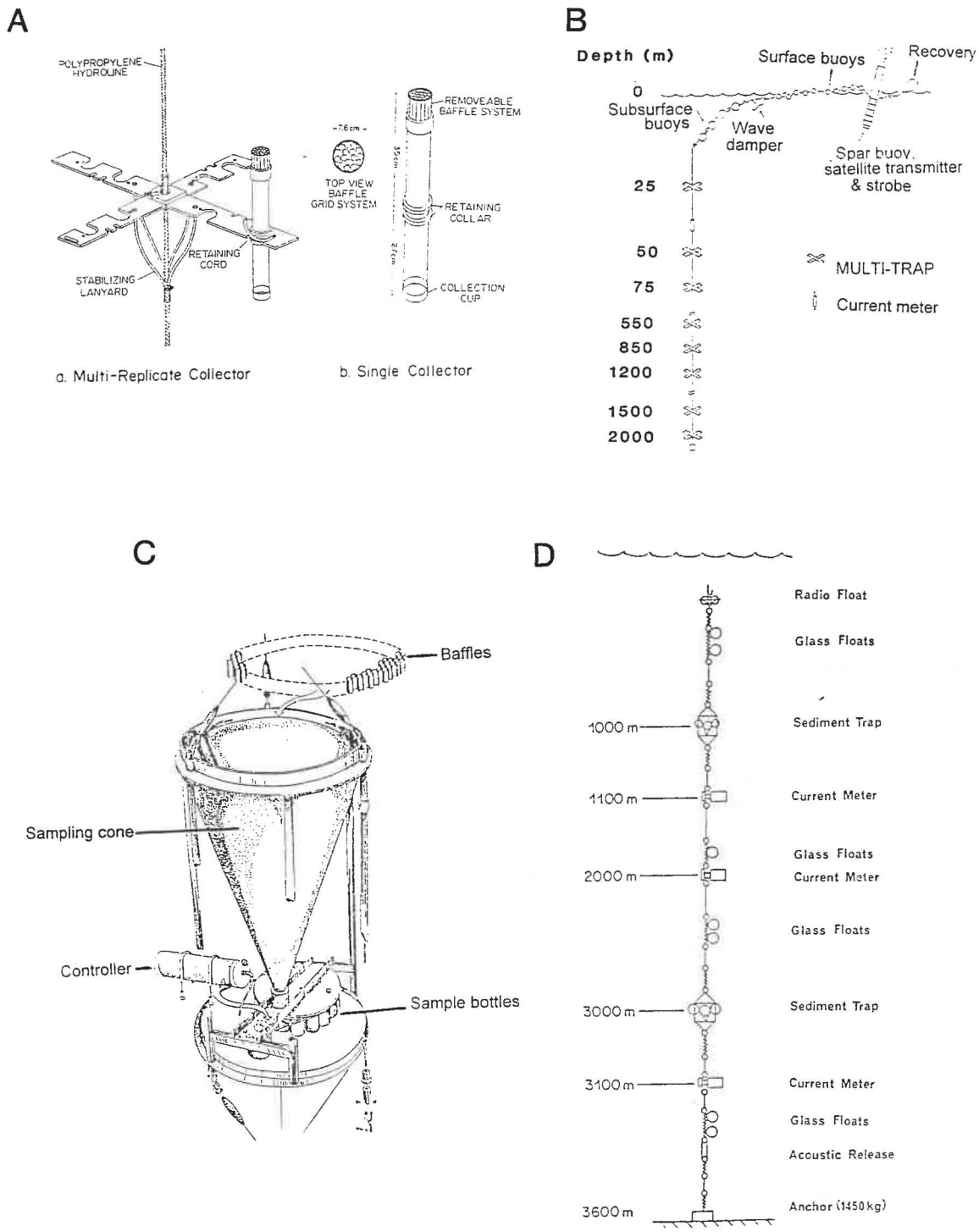

Fig. 1.8 Various sediment trap designs (A and C) and mooring configurations (B and D). (A) MULTI-trap (or Particle Interceptor Trap) used in VERTEX, BATS and HOT programmes (from Knauer et al., 1979). (B) Typical free-floating sediment trap array (from Knauer et al., 1979). (C) Time-incremental sediment trap designed and used by Honjo & Doherty (1988) showing conical sampling funnel, baffled opening and sampling bottles, controller housing and step motor used to advance the rotating plate over pre-determined time intervals. (D) Typical deep-ocean, bottom-anchored sediment trap mooring (from Asper, 1987b). An acoustic release is placed above the anchor and once released allows the entire mooring to float towards the sea surface to be recovered by a vessel. Note that the amount of buoyancy depicted in this diagram is schematic only; typically between 500-700 kg of buoyancy is required for a deep-ocean mooring that has 1-2 sediment traps deployed in 1500 m of water.

with the pioneering work of Albert Heim at the turn of the century (1900, *in* Bloesch & Burns, 1980). Since this time, sediment traps have been used in rivers to determine bedload transport rates and in lakes to assess the impact of sinking phytoplankton and zooplankton-derived particulate material on pelagic and benthic ecosystems. Similar applications have been made in the marine environment where traps of varying designs and modes of construction have been employed in a variety of settings, ranging from the surf zone on beaches (e.g., Krause, 1987), to the deep ocean where research on particle transport and transformations has provided insights into biological processes in the upper ocean and at bathyal depths (e.g., Wiebe et al., 1976; Knauer et al., 1979; Honjo et al., 1982a, b; 1995; Martin et al., 1987; 1993; Lohrenz et al., 1992; Karl et al., 1995, 1996; and many others). The history of sediment trapping has been reviewed by Bloesch & Burns (1980) and Blomqvist & Håkanson (1981). These two references cover many of the applications of sediment traps in lacustrine and oceanic regimes prior to the 1980's, as does an annotated bibliography by Reynolds et al. (1981).

Sediment trap applications in oceanic settings have increased dramatically since the 1970s due to technological advances in methods and materials (e.g., Asper, 1987b; U.S. GOFS Report 10, 1989). Traps have been used extensively in two modes: (1) free-floating, surface-tethered arrays deployed for periods of hours to weeks; and (2) bottom-anchored moorings that are recovered after periods ranging from weeks to years (Fig. 1.8). Pioneering work by Staresinic et al. (1978), Knauer et al. (1979) and Lorenzen et al. (1981) using drifting sediment trap arrays were precursory studies that attempted to minimise the effects of ambient turbulence on trapping efficiency by using traps as Lagrangian drifters. These early studies led to an upsurge of similar Lagrangian applications in the 1980s until the present-day (e.g., Betzer et al., 1984; Martin et al., 1987; 1993; Karl et al., 1991a, b; 1996; etc) (Fig. 1.8A, B). Similarly, classic deep ocean studies by Wiebe et al. (1976) and Hinga et al. (1979), among others (e.g., Honjo, 1978; 1980; Rowe & Gardner, 1979; Honjo et al., 1980; Dunbar & Berger, 1981; Dymond et al., 1981), using rudimentary traps that were anchored to the sea-floor, were followed by investigations using more technologically advanced, time-incremental sampling instruments (e.g., Zeitzschel et al., 1978; Jannasch et al., 1980; Deuser et al., 1981; Baker & Milburn, 1983; Honjo & Doherty, 1988) (Fig. 1.8C, D).

The modern-day analogues of these time-incremental traps have been employed in particle transport studies throughout the ocean basins of the world (e.g., Honjo et al., 1982a, b, 1995; Wefer et al., 1982, 1988; Deuser, 1986; Nair et al., 1989; Heussner et al., 1990; Tsunogai & Noriki, 1991; Honjo & Manganini, 1993; Hargrave et al., 1994; Honjo et al., 1995; etc.).

Despite acknowledged reservations regarding sediment trap methods and interpretations (e.g., Asper, 1987b; U.S. GOFS Report 10, 1989), traps remain the best method for determining the *in situ* flux of particulate material in marine environments, given present-day technological constraints. Other sampling techniques that have also provided useful information on the fate of sinking marine particles include large volume filtration systems (e.g., Bishop et al., 1986) and ocean cameras (e.g., Honjo et al., 1984; Asper, 1987a; Ratmeyer & Wefer, 1996; Diercks & Asper, 1997).

Data from sediment trap samples have been critical in improving our understanding of many open ocean biogeochemical processes, including:

(1) the rapid rate of particle transport from the upper ocean to the deep ocean sea-floor (e.g., Knauer et al., 1979; Martin et al., 1987) with implications for the transfer of radio-nuclides, trace metals and other chemical compounds (e.g., Spencer et al., 1978; Jickells et al., 1984; Kremling & Streu, 1993);

(2) the importance of bottom resuspension and mid-water flux maxima in continental margin environments (e.g., Rowe & Gardner, 1979; Honjo et al., 1982a; Walsh & Gardner, 1992; Gardner & Richardson, 1992)

(3) the significance of terrestrial particles to open ocean processes from material deposited from the atmosphere (e.g., Jickells et al., 1991);

(4) coupling between upper ocean productivity cycles and organic material fluxes in the deep ocean (e.g., Deuser et al., 1981; Asper et al., 1992), leading to development of empirical relationships between primary production and export flux (e.g., Eppley & Peterson, 1979; Suess, 1980; Hargrave, 1985; Martin et al., 1987; Pace et al., 1987);

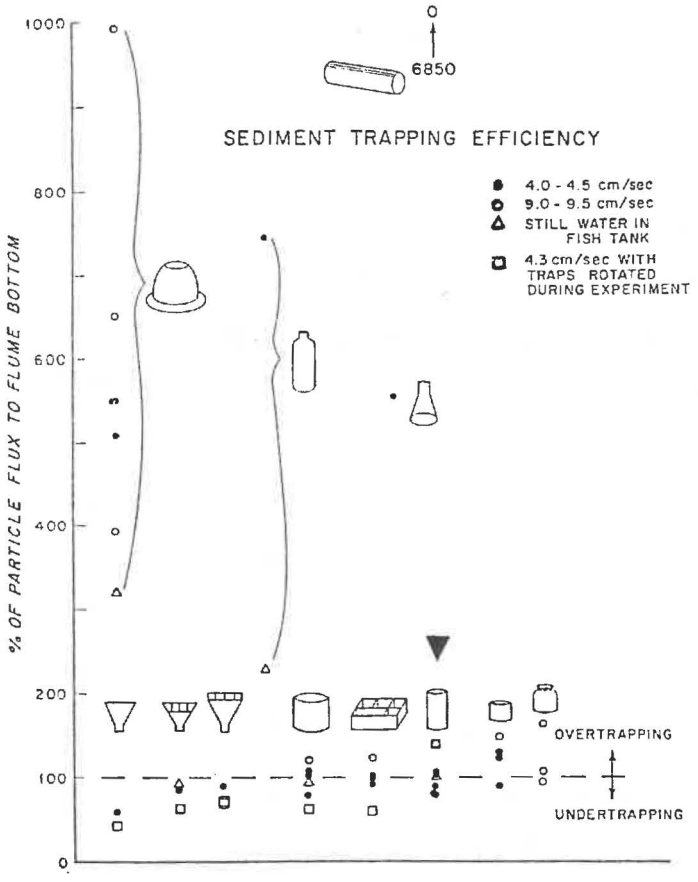

Fig. 1.9 Trapping efficiency of different shaped traps placed under a variety of environmental and experimental conditions in a flume, showing that on average cylindrical sediment traps are the most efficient trap (as arrowed) (modified from Gardner, 1980a). In the flume experiments, trapping efficiency was measured as percentage of released particles that sedimented to the bottom of the flume. If traps collected an identical amount of material as was deposited on the base of flume, then the traps were deemed to be "100% efficient". Hence, funnels generally undercollected material in the presence of currents (• 4-4.5 cm s^{-1} and o 9-9.5 cm^{-1}) and under stagnant water conditions (Δ), whereas bottles and flasks typically overcollected and boxes were variably efficient traps.

(5) dissolution and degradation rates of organic material within the water column (e.g., Honjo et al., 1982b; Gardner et al., 1983) and preferential decomposition of organic compounds (e.g., Wakeham et al., 1984; Wakeham & Lee, 1989, 1993) with inferences regarding nutritional quality of sinking material to pelagic and benthic organisms (e.g., Hinga et al., 1979; Billet et al., 1983; Lampitt, 1985);

(6) evidence of microbial transformations of sinking particles at meso- and bathy-pelagic water depths (e.g., Karl & Knauer, 1984a, b; Turley & Mackie, 1994);

(7) imbalances in oceanic carbon cycle models on basis of input from measured particulate carbon fluxes, leading to suggestions that significant amounts of organic carbon could be transported in dissolved states (e.g., Toggweiler, 1989; Michaels et al., 1994);

(8) seasonal and interannual variations in particulate fluxes related to fluctuations during El Niño periods (e.g., Honjo & Manganini, 1993; Karl et al., 1995, 1996) and other physical forcing mechanisms, such as storm event frequency (e.g., Deuser et al., 1995); and

(9) inferences regarding how changes in plankton community structure (e.g., Legendre, 1990; Passow & Peinert, 1993) and physical mechanisms, such as mixed-later dynamics, can influence particle residence times in the upper ocean (e.g., Eppley et al., 1983).

1.4. Principles of sediment trap dynamics

The hydrodynamics of sediment trapping have been addressed by earlier workers (e.g., Hargrave & Burns, 1979; Bloesch & Burns, 1980; Blomqvist & Håkanson, 1981). Many of the field and laboratory studies in 1970-1980s were concerned primarily with determining the most efficient sediment trap design, and recognised that differences between trap shape and size could affect significantly the trapping efficiency (e.g., Lau, 1979; Gardner, 1980a, b) (Fig. 1.9). Subsequently, Butman (1986) and Butman et al. (1986) identified three dimensionless parameters that were critical to sediment trapping efficiency:

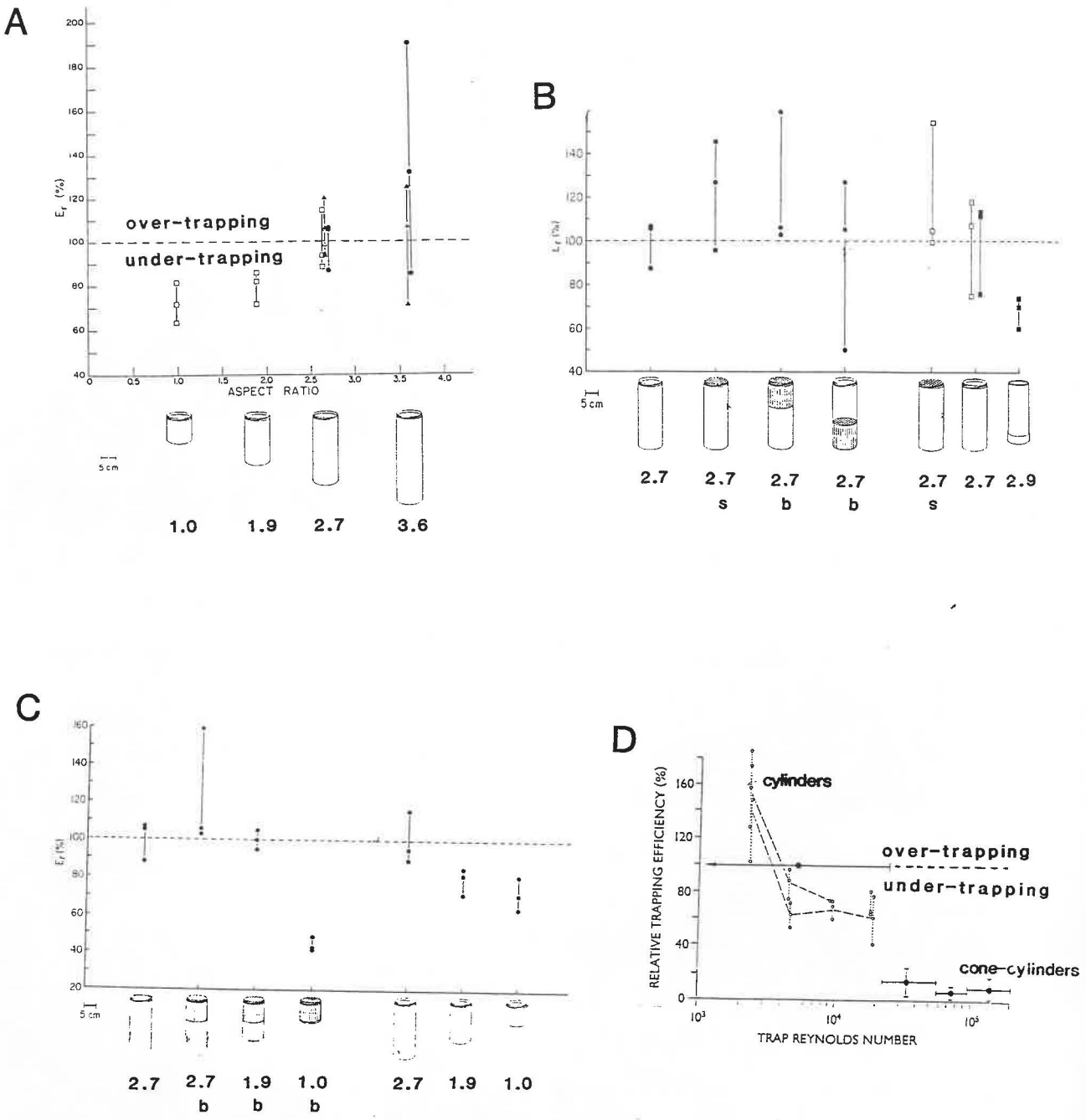

Fig. 1.10 Relative particle collection efficiency (E_r %) as a function of (A) trap aspect ratio (shown below cylindrical traps on x-axis), (B) flow obstructions (screens (s) and baffles (b)) in traps with an aspect ratio of about 3.0, (C) baffled (b) and unbaffled traps over a variety of aspect ratios, and (D) trap Reynolds number for straight-sided cylinders (upper left) and conical-cylinder collectors (lower right). (A) suggests that traps with an aspect ratio of about 3.0 are more efficient than traps with higher or lower aspect ratios. (B) and (C) show the variable effect of baffles and screens on trapping efficiency. (D) indicates that collection efficiency is reduced at high Reynolds numbers (>3000). All figures, except (D) which is from Baker et al. (1988), are modified from Butman (1986).

(1) Trap Reynold's Number (R_t) where:

$R_t = uD_o/\upsilon$ u = flow at height of trap mouth

D_o = outside diameter of trap mouth

υ = kinematic viscosity of the fluid medium [eqn. 7]

(2) Trap Aspect Ratio (AR) where:

$AR = H/D_i$ H = trap height

D_i = inside diameter of trap mouth [eqn. 8]

(3) Ratio of flow speed to particle fall velocity (R_v) where:

$R_v = u/W$ W = gravitational sinking speed of particles [eqn. 9]

With respect to these parameters, Butman (1986) and Butman et al. (1986) showed that trapping efficiency of unbaffled, straight-sided cylinders decreased over a range of increasing R_t and W (Fig. 1.10), as was later validated in field tests by Baker et al. (1988) (Fig. 1.11). In addition, trapping efficiency increased with increased AR over a specific range. The work of Butman and co-workers confirmed previous observations that cylinders were on average the most efficient sediment trap over a range of current speeds up to about 10 cm s^{-1} (e.g., Lau, 1979; Hargrave & Burns, 1979; Bloesch & Burns, 1980; Gardner, 1980a, b; Blomqvist & Håkanson, 1981; Blomqvist & Kofoed, 1981). Funneled traps tend to undercollect sinking material and bottle-like traps perform as overcollectors (e.g., Gardner, 1980a) (Fig. 1.9). Staresinic et al. (1982) observed higher fluxes and lower carbon-to-nitrogen ratios for cylindrical (AR=3) traps, compared with conical traps (Zeitzschel et al., 1978), although this result was attributed to differences in sample processing. Notwithstanding these observations, field tests of various trap designs, ranging from cylinders and cones to boxes, indicate no significant differences in moored trapping efficiency over periods of months (Dymond et al., 1981; Honjo et al., 1992), highlighting the "smoothing" effect that sampling times can have on trapping efficiency.

Limited work has been conducted to accurately test the effect of Reynold's Number (R_t) on trapping efficiency. The most comprehensive studies were those of Hawley (1988) and Baker et al. (1988). In Hawley's (1988) flume study, progressive destruction of the bottom tranquil layer by deepening eddy formation within traps

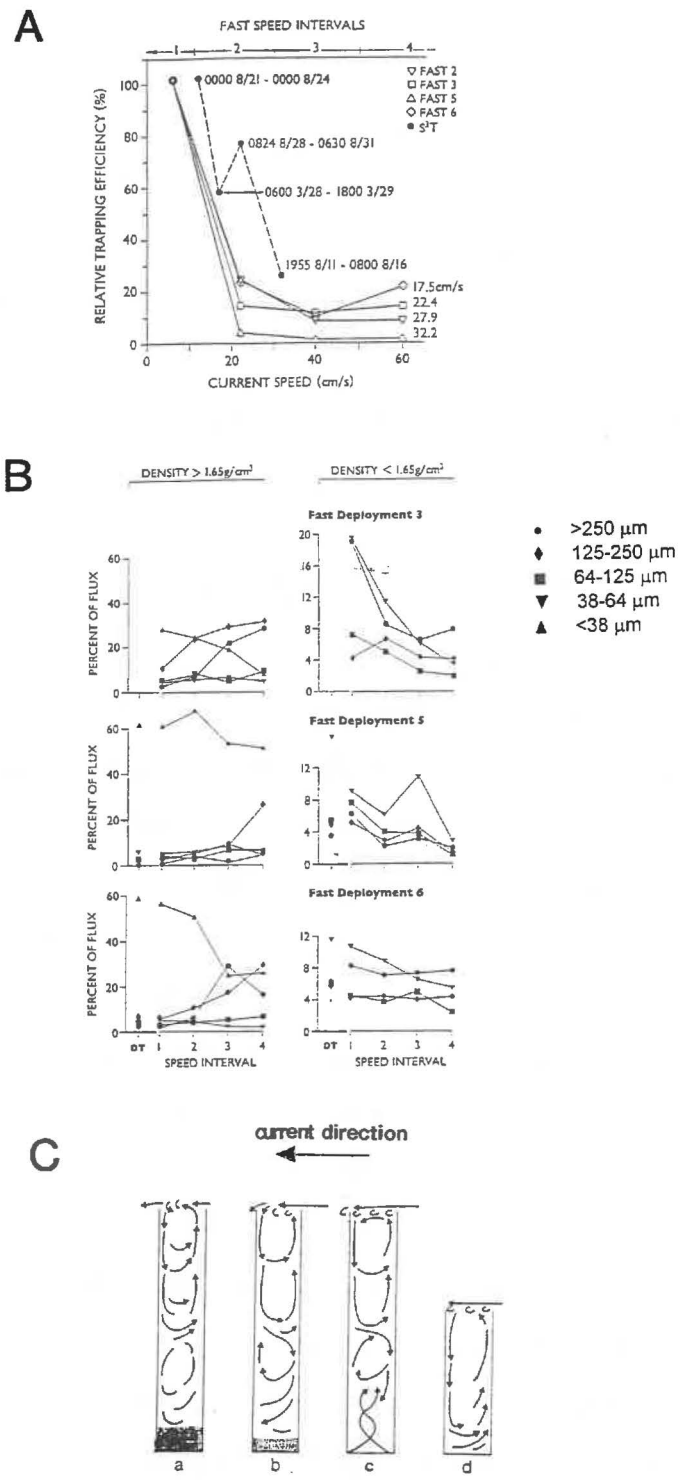

Fig. 1.11 (A) Relative trapping efficiency as a function of current speed showing that particle collection rates decrease markedly once currents are >12 cm s^{-1} (from Baker et al., 1988). (B) Size and density fractionation of mass flux collected under different current speeds (intervals 1-4) and during a drifting sediment trap deployment (DT). As current speed increases, larger particles comprise a proportionally greater component of the total flux in two density fractions (from Baker et al., 1988). (C) Flow patterns in traps generated by steady flow at various Reynolds numbers where for *a-c*, aspect ratio = 5 and for *d*, aspect ratio = 3 (from Hawley, 1988). In *a*, Reynolds number = 4300, *b* 8000, *c* 10 000 and for *d* 6000. This analysis shows that a tranquil bottom layer is preserved in traps at moderate Reynolds numbers (<10 000) and that as aspect ratio decreases this tranquil layer is destroyed at progressively lower Reynolds numbers.

occurred as R_t increased, resulting in a reduction in net deposition within cylindrical traps (AR ranging from 1 to 8) (Fig. 1.11C). For traps with AR=3, complete removal of a bottom boundary layer occurred at $R_t > 6000$ whereas for AR=5, decay of the basal tranquil layer (described as a logarithmic process by Lau, 1979) was observed as R_t exceeded 8500, and was not recorded even at R_t=20 000 for traps with AR=8. Baker et al. (1988) extended these observations to the field and showed that moored cylindrical traps (D_i=20 cm) with a steep internal funnel experienced a decrease in trapping efficiency of 20-25% in the velocity range of 12-30 cm s^{-1} (R_t=24 000-60 000), compared to the same trap design that was deployed as a drifting array in the same environment at the same time (Fig. 1.11A, B). In addition to the absolute effects of R_t on overall trapping efficiency are the impact of changing R_t on the composition and size ranges of particulate material collected by traps. Baker et al. (1988) showed that the mean size and density of trapped particles increased at current speeds greater than 12 cm s^{-1} (Fig. 1.11B) and Gardner (1980b) has demonstrated that "over-efficient" traps tend to collect preferentially fine (<63 μm) particles.

As shown above, aspect ratio (AR) is an important consideration in trap design and early workers, such as Bloesch & Burns (1980), recommended that ARs of greater than 5 should be used in small lakes and ARs greater than 10 in more turbulent environments, such as the open ocean (Hargrave & Burns, 1979). Subsequent researchers have advocated that ratios of greater than 3 should be sufficient for most oceanic sediment trap studies (e.g., Gardner, 1980a, b; U.S. GOFS Report 10, 1989), particularly in environments where R_t is less than 6000 (Hawley, 1988). As R_t increases then so should the AR of the trap to ensure effective collection of sinking particles (Hawley, 1988). Gardner (1979; 1980b) also observed that cylinders with ratios higher than 2-3 tended to overtrap material, resulting in overestimated flux measurements.

The ratio of flow speed relative to particle fall velocity is perhaps more difficult to account for in *a priori* trap experiments (e.g., Butman et al., 1986). In most instances, however, where consideration is given to R_v, assumptions have to be made concerning the settling behaviour of sinking particles based upon theoretical approximations using

Stoke's Law. In this relationship W, the gravitational sinking speed of particles, is proportional to particle diameter and the density differential between the particles and the fluid medium through which the material is sinking. Basic assumptions for Stoke's Law include that all the particles are spherical and have the same density, both of which are unlikely to be satisfied by actual sinking particle populations in the marine environment which are typically heterogenous (e.g., McCave, 1975, 1984b). Difficulties in obtaining accurate estimates of sinking speeds and the wide size range of marine particles in the field suggest that the effect of R_v on trapping efficiency remains at best poorly known. There is a suggestion from work by Peck (1972, *in* Butman et al., 1986) on pollen grains that trapping efficiency decreases with decreasing grain size, suggesting that since particle flux is dominated by rare, large (>32 μm) particles that sink relatively rapidly (McCave, 1975), trapping efficiency will not be compromised significantly due to the preferential collection of such material by sediment traps.

1.5. Other physical mechanisms in trap designs and methods

Other considerations in trap design include trap separation on multi-trap arrays and the use of brines, baffles, screens, closure mechanisms, flow separation guides, gimbals and vanes (e.g., U.S. GOFS Report 10, 1989). Butman (1984, *in* U.S. GOFS Report 10, 1989) indicated that multiple traps deployed at the same water depth should have effective separation of $3D_0$ in an across-flow direction and $10D_0$ in a down-stream direction (where D_0 = outside trap diameter). In many sediment trap studies involving multi-trap arrays (e.g., Knauer et al., 1979; Martin et al., 1987, 1993; Karl et al., 1995, 1996), often the criteria of trap separation is ignored and each trap is regarded as a "replicate sample" which is incorrect given that they are best described as "pseudo-replicates".

High-density salt brine solutions are used in traps to minimise sample and additive wash-out from the tranquil layer present at the bottom of cylindrical traps (e.g., Gardner, 1980a, b). Despite observations that the presence of a basal brine changes the AR of a trap by acting as an effective bottom (Gardner, 1979), and recommendations that traps only require a brine volume equivalent to the depth of $1D_0$ (U.S. GOFS

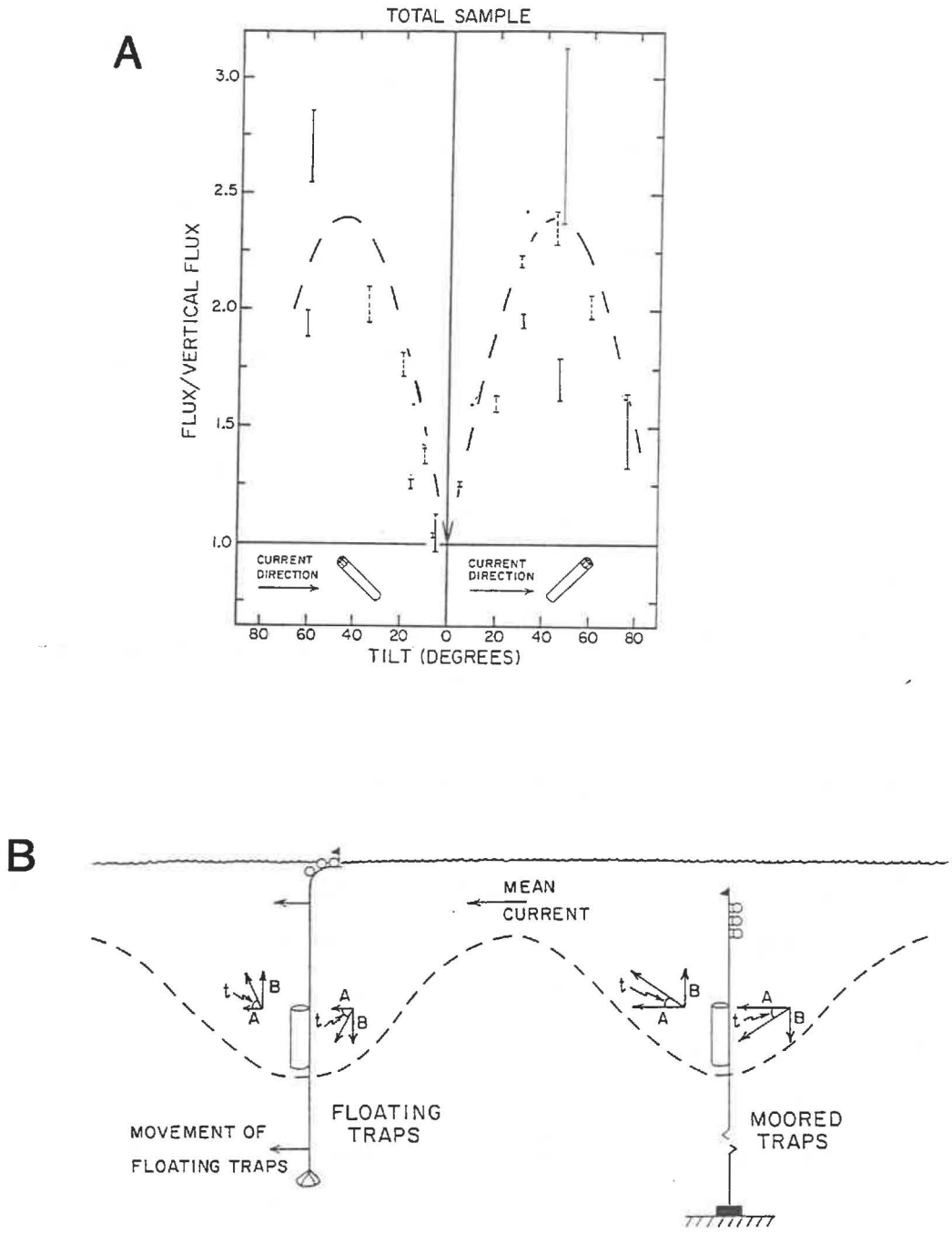

Fig. 1.12 Effect of (A) trap tilt and (B) effective tilt due to the passage of internal waves on trapping efficiency in floating and moored traps (from Gardner, 1985). In (A), traps had an aspect ratio of 5.2 and bars indicate the range of flux ratios from two replicate traps at each tilt angle (x-axis). Dashed bars refer to current velocities of 0-15 cm s^{-1} and solid bars to 15-62 cm s^{-1}. The flux ratio indicates that fluxes measured by inclined traps are higher by 2-3 times, relative to a trap collecting the "true" vertical flux of particles. The effect of tilt angle on fluxes seems to be maximal at angles of 40-50° and diminishes at angles below and above this threshold regardless of current speed.

Report 10, 1989), many experiments continue to utilise traps that are filled completely with brine (e.g., Martin et al., 1987, 1993; Lohrenz et al., 1992; Karl et al., 1996).

Mechanisms designed to modify or mitigate the flow and turbulence regimes around traps, such as baffles, screens, lids, lips, gimbals and vanes, have not been rigorously investigated to determine the exact effects of using such design strategies (U.S. GOFS Report 10, 1989). Baffles appear to improve the under-trapping efficiency of conical traps (Gardner, 1980a), but have an apparent ambiguous effect on trapping characteristics of cylinders. For example, Gardner (1980b) implied that increases in the AR of baffles and the proportion of the trap that the baffles occupy results in increases in flux measurements, whereas Martin et al. (unpublished data, *in* U.S. GOFS Report 10, 1989) showed that baffles reduced trapping efficiency over a range of cylinder heights. Similarly, no consensus has been reached about the use of many other trap modifications, in general because of insufficient laboratory and field testing. Closure mechanisms were a common feature of early traps (e.g., Rowe & Gardner, 1979; Lorenzen et al., 1981, 1983a, b), but more recently it has been recognised that "open traps recovered vertically can retain their samples intact, especially if brines are used" (U.S. GOFS Report 10, 1989, p.25). Examples of this successful open cylinder technique include the VERTEX (Vertical Transport & Exchange), HOT (Hawaii Ocean Time-series) and BATS (Bermuda Atlantic Time-series Study) programmes (e.g., Martin et al., 1987; Lohrenz et al., 1992; Karl et al., 1995, 1996).

In addition to concerns regarding actual trap designs, consideration has also been given to the effects of mooring configurations on trapping efficiency. In general, in terms of hydrodynamic effects, it is considered essential that flow is minimised relative to the traps and that traps are maintained in a vertical orientation during the deployment period (U.S. GOFS Report 10, 1989). Earlier work by Gardner (1985) also highlighted the potential impact that simple mooring line "tilt" can have on trapping efficiency, with tilted traps overcollecting by a maximum factor of 3 for tilt angles of up to 45° (Fig. 1.12A). The passage of internal waves also creates an "effective tilt" effect (t) with floating traps experiencing higher t angles, compared with moored traps,

especially when internal wave amplitude is greater than 20 m, period is less than 4 h and mean velocities are less than 20 cm s^{-1} (Gardner, 1985) (Fig. 1.12B).

For bottom-anchored traps, tilting and related hydrodynamic factors can be addressed by monitoring the behaviour of vertical moorings using current meters and tilt and pressure sensors, and by over-designing the buoyancy requirements of moorings in areas of known strong bottom currents (e.g., Asper, 1987b). For floating traps, it is essential that the traps are isolated from the effects of surface waves and that similar instrumentation is used to monitor the performance of the drifting mooring over the deployment period (U.S. JGOFS Report 10, 1989). Attempts to mitigate against the effects of wave action have included the use of bungy cords and surface buoys and drogues that are designed to reduce the drag of the floating array through the water (e.g., Staresinic et al., 1978; Knauer et al., 1979; U.S. GOFS Report 10, 1989; JGOFS Report 29, 1994). Staresinic et al. (1978) indicated that floating cylindrical traps (D=40.6 cm, AR=3) collected up to 300% more material than similar moored traps, whereas Baker et al. (1988) showed that relative trap efficiency in cylindrical traps decreased by 20-25% in the velocity range of 12-30 cm s^{-1} (R_t 24,000-60,000) for moored traps compared with floating traps. Gust et al. (1992, 1994) have shown that, even with precautions taken to minimise the effect of mooring line hydrodynamics on trapping efficiency, vertical excursions of up to 80 m for traps deployed deeper than 400 m can be experienced by floating trap arrays. These severe motions were associated with tether-line heaving at frequencies corresponding to surface wave energy (0.1 Hz). Miniaturised flow sensors used by Gust et al. (1994) also indicated that surface-tethered traps (cones and cylinders), deployed at depths ranging from 140 to 3200 m, experienced average water column approach velocities of up to 40 cm s^{-1}, irrespective of the array's drift velocity. Trapping efficiency seemed to be compromised by tether-line motions, with 2-6 times less material collected by a drifting conical sediment trap array, compared with a similar bottom-anchored array deployed just a few kilometres away. The bottom-moored trap did not experience the same mooring line motions as the surface-tethered array, where the peak frequency of motions (0.1 Hz) was directly related to wave action at the sea-surface (Gust et al., 1994). The recent work by Gust et al. (1992, 1994) accentuates several factors that

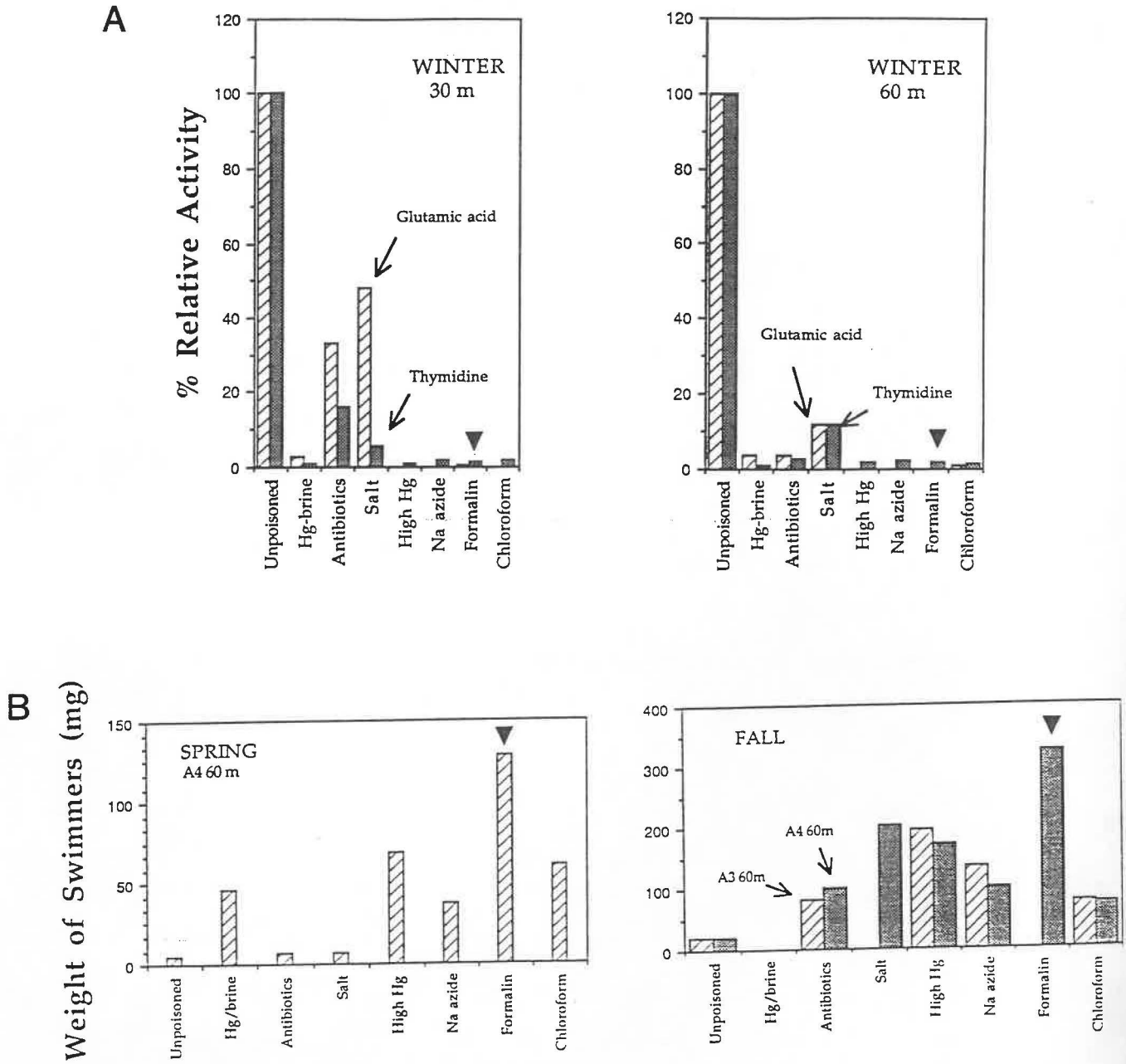

Fig. 1.13 (A) Effectiveness of different poisons and preservatives on microbial activity and (B) weight of >850 μm material (mostly zooplankton "swimmers"), highlighting the effect of different poisons and preservatives in sediment traps deployed in Dabob Bay, Washington, U. S. A. (from Lee et al., 1992). Note that bacterial activity is reduced severely in the presence of most poisons (A) and that, while formalin is a very good preservative, it also seems to result in the collection of higher amounts of "swimmers" preferentially (B). Northern hemisphere sample season and depth of sediment traps are shown in A and B. In B, **A3** and **A4** refer to sites in Dabob Bay

were previously considered inconsequential to trap collection efficiency, and serves as a warning to past and future sediment trap interpretations. Such hydrodynamic effects on trapping efficiency may only be overcome truly in the future with the technological development of neutrally buoyant sediment traps (e.g., Diercks & Asper, 1994).

1.6. Contamination effects - zooplankton swimmers, poisons and preservatives

The sediment trap method is subject to additional complexities in the form of sample contamination by marine zooplankton that swim actively into traps (known as "swimmers") and by the use of poisons and preservatives, as discussed below (Fig. 1.13). Zooplankton swimmers may either consume sinking material that has collected in sediment traps (e.g., Knauer et al., 1984; Lee et al., 1987) or contribute additional organic matter, such as faecal pellets and dissolved compounds (e.g., Lee et al., 1988, 1992). Furthermore, zooplankton may herniate upon contact with hypersaline brines (Harbison & Gilmer, 1986; Peterson & Dam, 1990) while some zooplankton, such as gelatinous salps and larvaceans, are difficult to discern or disentangle from sinking detrital material (Michaels et al., 1990; Silver & Gowing, 1991). Contamination by zooplankton swimmers on reported carbon and nitrogen fluxes in the upper ocean has been estimated at 50-100% (Karl & Knauer, 1989; Michaels et al., 1990) with the effect reducing below 200 m (Michaels et al., 1990), although swimmers can continue to be a contamination problem at water depths of up to 1500 m (Lee et al., 1988). Fluxes of other organic compounds, such as amino acids, lipids, carbohydrates and pigments, may be elevated by as much as 30% due to swimmer-related artefacts (Peterson & Dam, 1990; Lee et al., 1992; Wakeham et al., 1993) (Fig. 1.13B).

Efforts to mitigate against swimmer effects have included the use of poisons, such as chloroform, sodium azide, formalin and mercuric chloride, which kills the organisms before they are able to enter the trap and graze on sinking organic material (e.g., Knauer et al., 1979, 1984; Lee et al., 1992; Hedges et al., 1993; Wakeham et al., 1993) (Fig. 1.13A), the use of screens (e.g., Karl & Knauer, 1989; Karl et al., 1991b), careful removal (or "picking") of identifiable swimmers from flux samples (e.g., U.S. GOFS Report 10, 1989) and the development of specially designed traps that attempt to

exclude "swimmers" (e.g., traps with segregation chambers - "Labyrinth of Doom", Coale, 1990; Hansell & Newton, 1994; internally valved traps - "Indented Rotating Sphere (IRS)", Peterson et al., 1993). All of these techniques (with the possible exception of "swimmer" exclusion methods) require compromises to be made in terms of sample integrity. For example, certain poisons seem to increase preferentially the numbers of specific zooplankton collected in traps (Lee et al., 1992), and the use of screens may exclude larger sinking particles (Lee et al., 1988). The "picking" of zooplankton swimmers is extremely subjective and requires expert judgment as to what components should be regarded as part of the "true" flux. Silver & Gowing (1991) indicated that an average of 35% (range 11-80%) of organisms removed as swimmers during the VERTEX experiments (1980-1984) may have been participating in vertical migratory activities as part of their life histories. Similarly, simple pre-screening of trap samples to remove zooplankton swimmers (e.g., Karl et al., 1995) resulted in particle fluxes that were 63±12% higher than those fluxes calculated from samples where swimmers were removed manually (Michaels & Knap 1996).

Furthermore, in coastal environments, many live protozoans occupy micro-habitats within sinking marine snow (Shanks & Edmondson, 1990) and micro-organisms such as ciliates and dinoflagellates can form up to 17% of average particulate organic carbon fluxes (Heiskanen, 1995). Such organisms can be extremely difficult to remove successfully from trap samples due to their small size and involvement with larger particles that can legitimately be regarded as components of "particle flux" (i.e., Silver & Gowing, 1991). Larger "cryptic" zooplankton may also be a significant contaminant in trap samples, particularly those organisms that produce mucous feeding structures that entangle other particulates (Michaels et al., 1990). Despite the intuitive value of zooplankton exclusion devices at reducing the swimmer effect, recent designs have displayed variable results with Coale's (1990) "Labyrinth of Doom" removing 25-70% of swimmers based on amino acid content (Lee et al., 1988). Hansell & Newton's (1994) trap variant performed satisfactorily in coastal waters (>77% exclusion of copepod swimmers), but only achieved 37-72% exclusion rates in open ocean environments. The Indenting Rotating Sphere of Peterson et al. (1993) reduced the

swimmer-induced flux of >850 μm particles collected in cylindrical traps by 88% and <850 μm swimmer fluxes on average by 84% (range 59-97%).

Organic material in the ocean decomposes at rates varying from 0.1-1% d^{-1} in deep ocean samples (Gardner et al., 1983) to less than 10% d^{-1} in floating trap (Iseki et al., 1980; Lorenzen et al., 1981; Ducklow et al., 1985; Hansell & Newton, 1994) and sediment studies (Iturriaga, 1979). To prevent decomposition of sinking organic compounds collected in sediment traps, poisons and/or preservatives, such as formalin and mercuric chloride, are commonly used, depending on deployment period, and often in association with high density brines (e.g., Knauer et al., 1984; Lee et al., 1992; Hedges et al., 1993; Wakeham et al., 1993). As documented in many of these studies, the use of various poisons and preservatives can compromise sample integrity, including increasing swimmer-related effects (as described above), enhancing the dissolution of certain flux components, such as formalin on carbonates (up to 20% reduction in $CaCO_3$ flux, e.g., Honjo et al., 1992; Khripounoff & Crassous, 1994) and interfering with specific analyses, such as parameters that may indicate how significant intra-trap degradation might have been over a deployment period (i.e., formalin and DOC, mercuric chloride and mass flux, sodium azide and organics; Knauer et al., 1984; Hedges et al., 1993; Khripounoff & Crassous, 1994). Since decomposition effects are generally only a few percent per day, however, it has been recommended that for short-term deployments (<1 day) poisons and/or preservatives should not be employed (e.g., Iseki et al., 1980) with formalin suggested as the preferred biocide for longer term deployments of weeks to months (e.g., Knauer et al., 1984; U.S. GOFS Report 10, 1989; JGOFS Report 29, 1994). Formalin is the most effective poison at limiting microbial activity, compared with other poisons, and because formalin also acts as a preservative by solidifying the protein matrix of organisms, intracellular losses of material are reduced and the quantifiable removal of swimmers from trap samples can be achieved more successfully (e.g., Knauer et al., 1984; Lee et al., 1992). The use of formalin in traps does, however, limit the measurement of DOC in trap samples (Knauer et al., 1984), can decrease the apparent carbonate flux due to dissolution of $CaCO_3$ components (Honjo et al., 1992; Khripounoff & Crassous, 1994) and seems to

act as a preferential poison for euphausiids and calanoid copepods (Lee et al., 1992) (Fig. 1.13).

1.7. Sediment trap calibration

Despite the pervasive use of sediment traps in many oceanic environments and the plethora of associated hydrodynamic and sample integrity questions, traps in their various guises remain one of the more critical oceanographic tools that have not presently been calibrated by independent means. Early workers used comparisons between production and sediment accumulation rates of natural radionuclides, such as ^{210}Pb, ^{230}Th and ^{231}Pa, in oceanic environments and trap fluxes (e.g., Knauer et al., 1979; Lorenzen et al., 1981; Moore & Dymond, 1988) to suggest that traps seemed to perform adequately (i.e., within given measurement uncertainties of about 15%; Bacon, 1984; Bacon et al., 1985). Recent studies, based on mass balance modelling of ^{234}Th:^{238}U disequilibria in dissolved and particulate states in the upper 70-200 m of the water column (where particle scavenging results in ^{234}Th depletion), have led to suggestions that traps may underestimate actual sinking fluxes by as much as 80% (e.g., Clegg & Whitfield, 1990, 1993; Buesseler, 1991; Buesseler et al., 1992; Cochran et al., 1993; Michaels et al., 1994). Most recently, Murnane et al. (1996, p. 239) have proposed that a "33% trapping efficiency scenario produces results that are consistent with the water column ^{234}Th budget", rather than a 100% efficiency scenario that sediment trap enthusiasts would expect. Martin et al. (1993) refuted previous assertions by Buesseler et al. (1992) that trap fluxes in the upper 300 m were too low by factors of 4-7 on the basis of rapid regeneration and flux rates of organic material in the upper ocean. Martin et al.'s (1993) argument, however, was based on an assumption that suspended POC should be related to sinking POC, despite acknowledgments that sediment traps collect preferentially generally larger and faster sinking particles (e.g., McCave, 1975, 1984b; Walsh & Gardner, 1992). Mass balance approaches using ^{234}Th budget estimates have also resulted in ambiguous interpretations, with Buesseler et al. (1994) indicating that overtrapping occurs during periods of low productivity whereas during times of high biological productivity undertrapping trends were observed. It is, therefore, apparent that further studies are required to investigate the relationships

between carbon and thorium isotopes in size-fractionated sinking and suspended particulate matter samples before ^{234}Th-derived trap calibrations can be determined with accuracy. Furthermore, the errors involved in ^{234}Th modelling analyses can be large (up to ±1300% with error estimates for particulate fluxes of ±60-157%; Cochran et al., 1993; Buesseler et al., 1994).

Other calibration techniques that have been used with varying levels of success have included oxygen mass balance studies (e.g., Spitzer & Jenkins, 1989; Emerson et al., 1995) and comparisons of trap fluxes with sediment accumulation rates (e.g., Pennington, 1974; Soutar et al., 1977; Dymond et al., 1981; Moore & Dymond, 1988). Carbon fluxes calculated from oxygen mass balance modelling at the Bermuda Atlantic Time-series Study (BATS) site (Spitzer & Jenkins, 1989) were up to 300% higher than those measured using sediment traps (Michaels et al., 1994), whereas at the Hawaiian Ocean Time-series (HOT) station the mass balance calculations (Emerson et al., 1995) agreed to within the errors of data accuracy with the trap-derived fluxes (Karl et al., 1995, 1996). Neither of these studies, however, considered the effects of horizontal advection on particle dynamics (e.g., Michaels et al., 1994; Toggweiler, 1994), or other modes of carbon export such as vertically migrating zooplankton (Angel, 1989), which can represent between 8-70% of trap carbon flux at BATS (Longhurst et al., 1989; Dam et al., 1995), or downward transport of dissolved organic and inorganic carbon, which can be of the same magnitude as trap-derived particle fluxes (e.g., Toggweiler, 1989; Carlson et al., 1994; Michaels & Knap, 1996). The apparent carbon imbalance observed at BATS has been attributed to undertapping by sediment traps (Michaels et al., 1994) and/or pronounced horizontal advection into the region via the Gulf Stream (Toggweiler, 1994).

Sediment trap fluxes have displayed reasonable correlation with long-term sedimentation rates determined using radiogenic dating techniques (e.g., Soutar et al, 1977; Dymond et al., 1981), accumulation of sediment radionuclides (e.g., Moore et al., 1981; Bacon et al., 1985; Colley et al., 1995), lithostratigraphic correlation (e.g., Pennington, 1974; Soutar et al., 1977) or fluxes of inert particulate components (e.g., Walsh & Gardner, 1992). For short-term trap deployments in the open ocean, however,

such methods are not particularly useful as calibration tools since degradation rates of sinking particulate material are orders of magnitude different from the inherent accuracy of sediment accumulation measurements (i.e., rates of POC degradation - days to weeks, compared with absolute resolution of decades for ^{210}Pb and 100-1000 y for ^{14}C). High-resolution radiogenic chronostratigraphy in marine sediments using tracers such as ^{137}Cs are only valid in environments with sedimentation rates that are sufficiently high so as to mitigate against the disruption of the radiogenic profile by bioturbation. Thus, application of such technology to many open ocean sites would be inappropriate given the typically relatively low rates of sedimentation in the world's ocean basins (<5 cm 1000 y^{-1}). Furthermore, the use of inert constituent fluxes, such as aluminium, are often compromised in continental margin environments where relatively high sediment accumulation rates are expected, but resuspension and lateral advection can exaggerate and contaminate near-bottom sediment trap fluxes (e.g., Honjo et al., 1982a; Gardner & Richardson, 1992; Walsh & Gardner, 1992).

1.8. Summary of Chapter 1

(1) To the east of New Zealand, the ocean occasionally acts as a pronounced sink for atmospheric CO_2, but there is no information on how efficiently biologically fixed particles are removed from surface waters, and hence from further exchange with the atmosphere. Sinking of organic material is one of the important mechanisms by which this sequestration of carbon by the ocean can occur.

(2) The New Zealand JGOFS programme was instigated in 1992 to investigate the cycling of carbon within pelagic ecosystems in water masses across a globally important ocean front, the Subtropical Convergence. This frontal zone marks the northernmost boundary of the Southern Ocean, and separates cool, nutrient-rich subantarctic waters in the south from warm, saline, nutrient-depleted subtropical waters to the north. An integral component of the New Zealand JGOFS research initiative was the initiation of a sediment trap study, which involved designing and constructing

sediment traps to be deployed on free-drifting arrays for fieldwork scheduled in winter and spring 1993.

(3) A detailed literature search indicated that ideally traps needed to be axially symmetrical; cylinders with an aspect ratio of at least 3 have been recommended for use in oceanic environments where currents are expected to be less than 10 cm s^{-1} (U.S. GOFS Report 10, 1989). In regions where currents may exceed 10 cm s^{-1}, such as frontal zones, a higher aspect ratio should be used with 10 suggested for highly turbulent environments. In the case of multiple traps to be deployed at the same depth a separation distance of at least 3-trap diameters should be employed. A high-density basal brine (about 1-trap diameter deep) should ensure that samples are recovered relatively intact. For deployments lasting longer than 1 day, poisons and/or preservatives need to be used; formalin is recommended as an effective biocide, and has the added benefit of preserving sedimenting organic material and contaminants such as zooplankton "swimmers", that can be removed more easily than from solutions containing other poisons (e.g., mercuric chloride, chloroform, sodium azide). The effect of baffles on trapping efficiency of cylinders is poorly known, although baffles reduce turbulence across the entrances of funnelled traps. Hydromechanical effects of mooring line configuration on trapping efficiency have recently been identified as a potentially significant factor in trap performance, but are difficult to fully assess without state-of-the-art technology (e.g., minaturised pressure and velocity sensors). Independent calibration of sediment traps is notoriously difficult, with suggestions from new production measurements and modelling of thorium/uranium isotope tracers that traps may underestimate actual particulate fluxes by up to 70%. Nevertheless, previous studies have also indicated that there is often reasonable correlation between trap fluxes and fluxes estimated from sedimentation rates in deep-sea cores.

The results of the literature search and conclusions of this chapter are used in Chapter 2 to guide the design and construction of a sediment trap system that was subsequently used in particulate flux studies across the Subtropical Convergence region (Chapters 5 and 6).

Chapter 2

DESIGNING AND TESTING SEDIMENT TRAPS: Results of pilot studies conducted 1992–1995

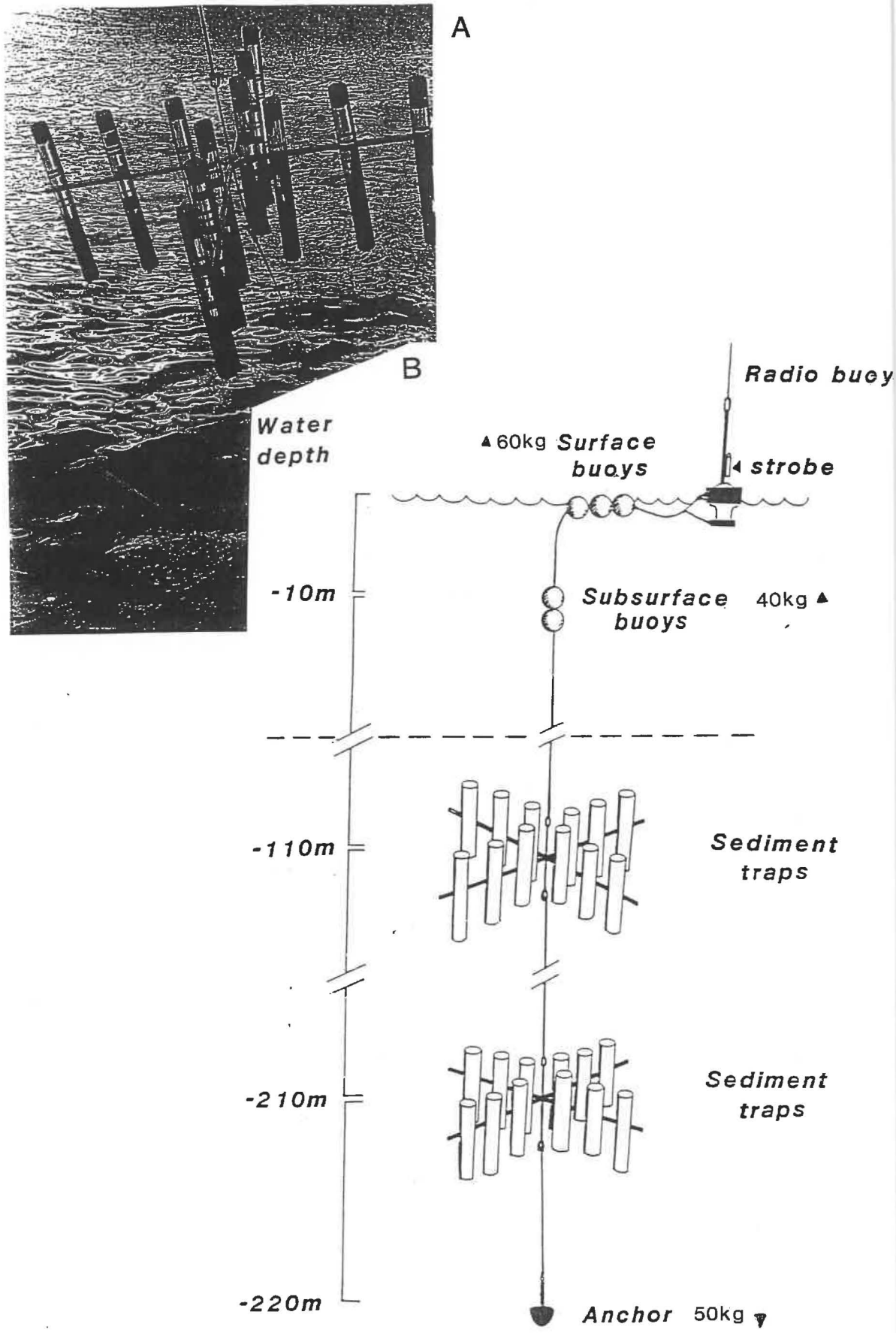

Fig. 2.1 NZOI-NIWA sediment trap cylinders arranged on a cross-frame during deployment (photograph), and a diagram outlining the mooring configuration used in free-floating deployments in winter and spring 1993.

Chapter 2

DESIGNING AND TESTING SEDIMENT TRAPS: results of pilot studies conducted 1992-95

2.1. NZOI-NIWA sediment trap design and rationale

A comprehensive literature search led to the author designing a NZOI-NIWA sediment trap system on the basis of the practical and theoretical considerations described in Sections 1.3-1.7 of Chapter 1. Since the sediment trap experiments were the first to be conducted in New Zealand waters, the NZOI-NIWA traps were designed with an overall conservative strategy in mind. Briefly, the traps were based upon previous studies demonstrating that axially symmetrical cylindrical traps perform, on average, as unbiased particle collectors (e.g., Lau, 1979; Hargrave & Burns, 1979; Bloesch & Burns, 1980; Gardner, 1980a, b; Blomquist & Håkanson, 1981; Butman, 1986; Butman et al., 1986). To maintain a degree of ruggedness the traps were constructed from 9 cm-diameter polycarbonate tubing cut into 95 cm lengths for each individual trap. These trap dimensions resulted in an aspect ratio (AR) of 10.6, in accordance with the recommendations of Bloesch & Burns (1980) for turbulent open ocean sediment trap studies. Although Gardner (1980a, b) suggested that ARs of 2-3 should be sufficient to ensure equivalent trapping efficiency, it was decided to pursue the more conservative AR of at least 10 (Bloesch & Burns, 1980). Baffles were constructed from polyvinyl chloride with dimensions similar to those baffles used in the VERTEX programme (e.g., Knauer et al., 1979; Martin et al., 1987), although the effect of baffles on trapping efficiency in cylindrical sediment traps has proven to be equivocal (e.g., Gardner, 1980b; U.S. GOFS Report 10, 1989).

Individual traps were held on a stainless cross-frame, capable of holding 8 or 12 cylinders, using 2-3 jubilee clips, similar to the cruciform design of the VERTEX MULTI-TRAPS (e.g., Knauer et al., 1979; Martin et al., 1987) (Fig. 2.1). A trap separation distance of at

least $3D_0$ (27 cm) was maintained on all cross-frames to minimise inter-trap hydrodynamic biases (e.g., Butman, 1984, *in* U.S. GOFS Report 10, 1989). Prior to each deployment, trap cylinders and baffles were washed in 1 M HCl, rinsed with distilled water and covered with plastic bags.

Trap cross-frames could be suspended at various depths in the water column using pre-cut mooring lines and shackles. In free-floating deployments, Taiyo-Musen radio-transmitter buoys, transmitting on Very High Frequencies (1982-1989 Hz), were used for tracking the mooring. A series of surface and near-surface Viny buoys reduced drag of the mooring through the water (e.g., Asper, 1987b). A bungy cord was not installed to reduce potential wave effects (e.g., Lohrenz et al., 1992; JGOFS Report 29, 1994; Karl et al., 1996) because, even by employing such a device, wave heaving can still be a significant problem (Gust et al., 1992, 1994). Uppermost traps were deployed below the depth of the mixed-layer to reduce turbulence effects (e.g., Gardner et al., 1995) on 11 mm-thick, braided Dacron mooring line. White xenon strobe lights attached to radio-transmitter buoy aerials facilitated night-time tracking and recovery of the drifting moorings. A 50 kg anchor at the bottom of each drifting array was used to ensure that the entire array remained as taut as possible during deployment and recovery.

Despite ongoing disagreement with regard the standardisation of poisons and/or preservatives in sediment trap studies (e.g., U.S. GOFS Report 10, 1989; Lee et al., 1992; Gardner, 1996), it was decided to use formalin in the NZOI-NIWA traps to ensure sample integrity during the collection period. Following the protocols developed for the Hawaii Ocean Time-series programme (HOT, Karl et al., 1990), 10 ml of concentrated formaldehyde (100% formalin) was added to 1.0 l of surface sea-water that had been pressure-filtered through 1.0 and 0.45 μm cellulose membrane filters using a Sartorius filtration system (<1 bar pressure). Fifty (50) g of ANALAR NaCl and a small amount (<5 ml) of dye were then added to this solution and dissolved prior to deployment. In general, 20.0 l of 1% formalin-brine solution was produced for each sample depth. The traps were assembled on the cross-frames and filtered sea-water added to a set height, and then the formalin-brine solution was back-filled gravitationally into the base of each trap, corresponding generally to brine heights of less than $1D_0$ (U.S. GOFS Report 10, 1989).

The dye was used to monitor the efficiency of the back-filling procedure and to establish the rate of diffusion of the formalin-brine solution into the overlying filtered sea-water during the deployment period. During deployment, trap openings were covered with plastic sheeting, held in place with dissolvable links (candy "Lifesaver" ring-rubber band; Knauer et al., 1979). The disslovable links took 12-15 min to dissolve in sea-water regardless of "Lifesaver" flavour.

Upon recovery, trap openings were covered immediately with clear plastic bags and sea-water was siphoned within 2-3 hours to at least 5 cm above the brine/sea-water interface, corresponding to the volume of recovered brine. Samples were processed for various parameters, including total mass, particulate carbon, phosphorus, nitrogen and individual pigmented compounds. Details of the methods used during specific flux determinations are provided in Chapters 5 and 6. Zooplankton swimmers were removed manually by screening (333 or 200 μm) and microscope picking techniques (e.g., Lee et al., 1988; U.S. GOFS Report 10, 1989; Michaels et al., 1990; Karl et al., 1996) after recovery. Each trap cylinder was then rinsed with a portion of <200 or <335 μm filtrate to recover all sinking particles. Material retained on the screen was rinsed into a 50 ml centrifuge tube, labelled and topped up with 2.5% formalin and refrigerated at 4°C. Solubilisation effects were not addressed as deployments were less than 72 h (e.g., Karl et al., 1996) and losses of organic material due to solubilisation were expected to be less than 10% (Lorenzen et al., 1981; Hansell & Newton, 1994). Furthermore, the use of high-density brines in the traps probably would have resulted in the herniation of zooplankton (e.g., Peterson & Dam, 1990) which would have compromised any attempts to measure directly particle solubilisation effects.

The next two sections in this chapter outline the methods employed and results obtained during two pilot studies that were undertaken in austral autumn 1992 (Nodder, in press) and 1993 to assess the practicality of sediment trap deployments using the sediment trap system developed in-house at NZOI-NIWA (Section 2.1). The impact of the chosen trap design on relative trapping efficiency was addressed subsequently in a series of small-scale field experiments in which potential hydrodynamic biases introduced by inter-trap interactions, baffles and brine volume were evaluated separately (Section 2.4). Errors

associated with particle degradation over time (days to weeks), sample handling and filtering were also assessed using simple laboratory tests.

2.2. North Chatham Rise sediment trap deployment

2.2.1. Methods

In austral autumn 1992 a research voyage (2-13 April) was undertaken to Chatham Rise onboard R. V. *Rapuhia* (NZOI cruise 2053) to conduct a series of floating and bottom-moored sediment trap experiments to measure fluxes of particulate material on either side of, and within, the STC frontal zone (Fig. 2.2). Unfortunately, only one sediment trap mooring could be deployed (NZOI station number U940) due to atrocious weather conditions. This experiment was a free-floating deployment in subtropical waters, north of the Chatham Rise, in water depths >1500 m. The 1992 pilot study is the subject of a note accepted for publication in *Limnology and Oceanography* (Nodder, in press).

In the 1992 pilot study, prior to deployment, traps were washed with 1 M HCl and rinsed with distilled water and capped with clear plastic bags. Traps were unbaffled and 0.6 l of high density brine (50‰ NaCl and 1% formalin, e.g., Karl et al., 1990) was back-filled into the bottom of each cylindrical trap. The volume of brine corresponded to a brine height equivalent to one trap diameter, as recommended by U.S. GOFS Report 10 (1989). Stainless steel cross-frames, each holding 12 traps, were deployed at 200, 300 and 500 m water depths, with Brancker temperature loggers positioned just below mid-water and lowermost trap sets. Prior to deployment, individual trap cylinders were covered with plastic sheeting, held in place with dissolvable links ("Lifesaver" ~ a ring-shaped candy, and rubber band; Knauer et al., 1979). The trap array was deployed for 72 h over the period 8-11 April 1992.

Upon recovery, water above the brine/sea-water interface was removed by opening drainage holes located at set heights along each cylinder. Trap solutions were pre-screened through a 335 μm plankton mesh to remove zooplankton "swimmers" (e.g. Karl & Knauer 1989). Approximately 0.5 l aliquots of trap solution were filtered using a low vacuum pump system (<20 cm Hg). From each depth, three cylinders were used for total mass (TM) flux

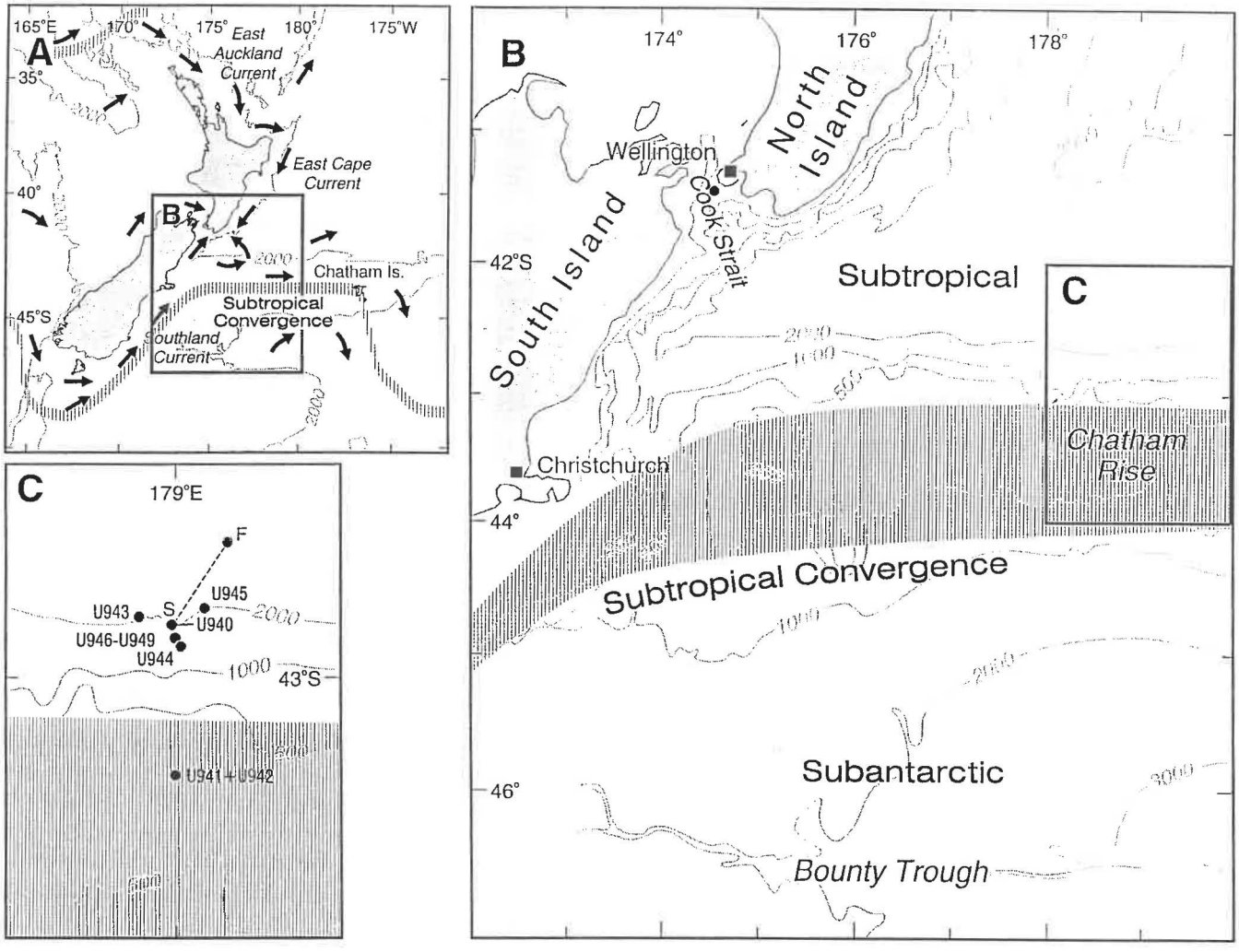

Fig. 2.2 Location of study area, showing relationship of Subtropical Convergence (shaded) to subantarctic and subtropical water masses in New Zealand region (A and B; after Heath 1985). Positions of CTD/nephelometer (U941-U949) and sediment trap (U940; **S** = start of drift deployment, **F** = finish) stations occupied during cruise 2053 in austral autumn 1992 are shown in C. The approximate location of the sediment trap station occupied in Cook Strait in March-April 1993 is also shown in B, marked with a closed circle.

determinations, six cylinders for particulate carbon/nitrogen (PC/PN) analyses, and the remaining three cylinders for particulate phosphorus/nitrogen (PP/PN). Onshore, PC/PN samples were analysed using a Perkin Elmer 2400 CHN analyser, while PP/PN samples were acid-digested and analysed using a Technicon Autoanalyzer II (Nodder et al., 1994a, b; Chapter 4). TM samples were desiccated under vacuum for 48 h to remove any water particles and re-weighed.

Conductivity-Temperature-Depth (CTD) casts were made near the deployment site of the free-floating sediment trap (Fig. 2.2) using a Guildline Model 8705 CTD. Independent nephelometer casts were conducted with a Chelsea Aquatracka III nephelometer, coupled with a 12 kHz ORE Model 265 HP pinger. Salinity (for CTD calibration purposes) and particulate matter samples were collected from depths of 5 m, 300 m and "near-bottom" (>1000 m depending on water depth). For total particulate matter analyses, approximately 3.0-5.0 l of sea-water were filtered through pre-weighed, 0.45 μm pore size, 47 mm diameter Nuclepore filters using an in-line Sartorius filtration system, connected directly to the taps of 5.0 l Niskin bottles. Niskin bottles were gently agitated periodically over the course of filtration to ensure that the majority of particles were recovered from each bottle (Gardner 1977). Particulate matter samples were washed with distilled water to remove sea-salts and then frozen until filters could be dried under heat lamps and re-weighed in the onland laboratory.

2.2.2. Results

The free-floating mooring was recovered in a water depth of 2390 m, approximately 50 km northeast of it's initial release position (Fig. 2.2), indicating an overall drift speed of about 0.2 m s^{-1}. The NE drift path was not correlated significantly with the 4-hourly dominant wind directions (NW-NE) over the deployment period (Fig. 2.3), suggesting that the drifting array was moved by relatively strong subsurface currents. Ekman depths (D_E) at the start and end of the deployment period were 130-160 m (Fig. 2.3), based on the relationship between wind speed (W) and latitude (F) (Pond & Pickard 1983):

$$D_E = 4.3W(\sin½F½)^{-½}$$

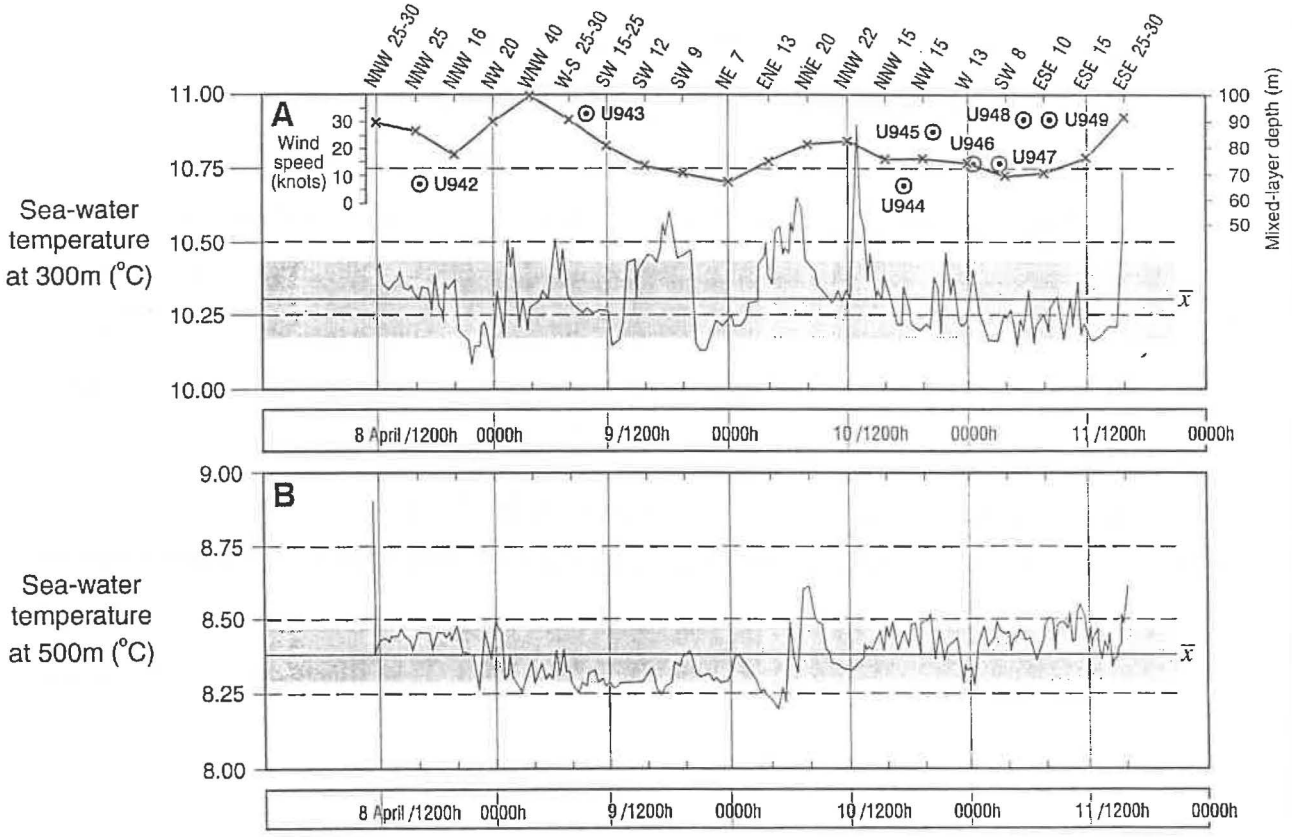

Fig. 2.3 Brancker temperature logger records at 300 m and 500 m water depths over sediment trap deployment period (1045 h, 8 April 1992 to 1518 h, 11 April 1992). Mean temperatures (± 1 standard deviation, as depicted by shaded area) are shown for the duration of each record. Four-hourly wind speeds and directions and maximum wind speeds (solid line) are also depicted. Mixed-layer depths (⊙) at selected CTD stations (U942-U949) are shown. Using the equation in Pond & Pickard (1983, refer to text), Ekman depths of 131-157 m are calculated for the starting and finishing latitudes of the sediment trap deployment, which were 42°40.45'S and 42°22.43'S, respectively.

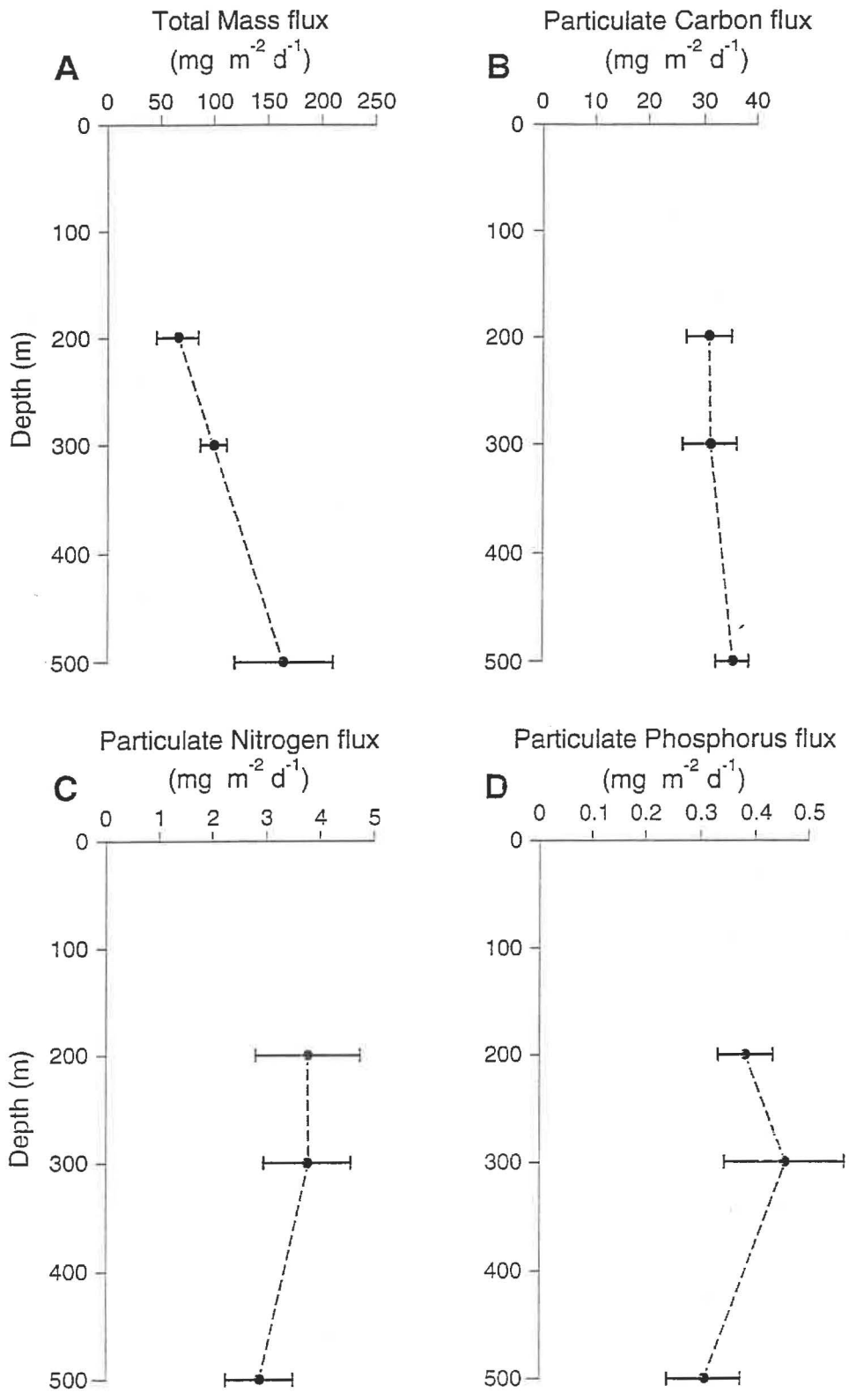

Fig. 2.4 Particulate fluxes in subtropical waters, east of New Zealand (station U940), in austral autumn, 1992: **A** Total mass (TM); **B** Total particulate carbon (inorganic + organic, PC); **C** Particulate nitrogen (PN); **D** Particulate phosphorus (PP). Error bars (±1 standard deviation) represent trap samples filtered for each parameter at each depth; for TM, n=3; PC, n=6; PN, n=9; PP, n=3.

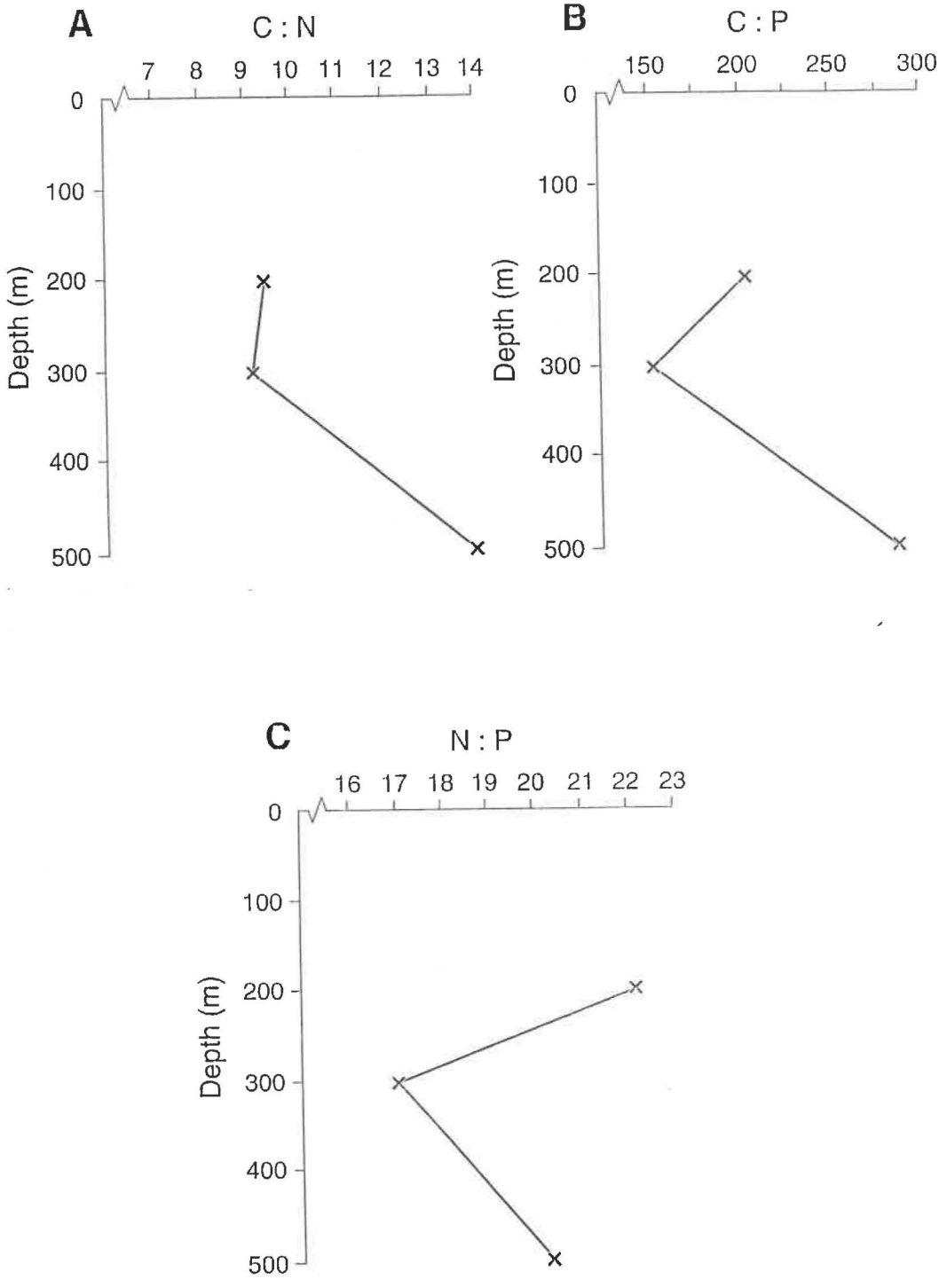

Fig. 2.5 Elemental molar ratios in sediment trap samples at subtropical station U940 in austral autumn 1992: **A** Total carbon:nitrogen; **B** Total carbon:phosphorus; **C** Nitrogen:phosphorus.

Persistent winds from the NW quadrant would have generated a net NE-directed Ekman transport due to the deflection of the Coriolis force to the left in the Southern Hemisphere (Pond & Pickard, 1983). Such currents would explain partially the predominant NE drift pattern of the mooring, possibly in association with observed semi-permanent oceanic currents in the region (Fig. 2.2).

TM fluxes increased with water depth, although standard deviations were in the order of 10-30% of the calculated mean flux for each depth (Fig. 2.4A). Average TM fluxes in the upper 200 m were approximately 1.5 and 2.5 times less than the fluxes measured at 300 and 500 m, respectively. Mean PC and PP fluxes showed no systematic variation with depth, while average PN fluxes decreased slightly with increasing depth (Fig. 2.4B-D). Correspondingly, C:N ratios increased with depth, whereas N:P ratios exhibited a range of values from which no obvious depth-related trends could be determined (Fig. 2.5A, C). C:P ratios were variable, but increased slightly from 200-300 m to 500 m (Fig. 2.5B). Average PC fluxes were typically between 20-50% of the total mass flux, and decreased in proportion with depth. Average PN and PP fluxes also decreased in relative proportion with depth, ranging from 2-6% and 0.2-0.6%, respectively, despite the observed increase in total mass flux over the same depth range. Note that the PC fluxes presented here are estimates of total PC flux, and do not distinguish between organic and inorganic (or carbonate) carbon.

Qualitative microscopic inspection (100x magnification) of filters from the three sediment trap sample depths reveals subtle differences in the types of organic material collected by the traps. At all depths, translucent and amorphous khaki- and yellow green organic masses are ubiquitous, with diatoms and silicoflagellates prominent at 200 m, diatoms and foraminifera at 300 m and numerous dark brown, ovoid faecal pellets (110-370 μm in length and 40-80 μm in width) common at 500 m.

Fluctuations in subsurface temperature of up to 0.5°C were recorded at 300 m and 500 m on the trap mooring (Fig. 2.3). Due to the relatively deep water depths of the loggers, there was no correlation of these fluctuations with surface wind conditions (Fig. 2.3). The Brancker temperature variations were similar, however, to the temperature gradients and ranges

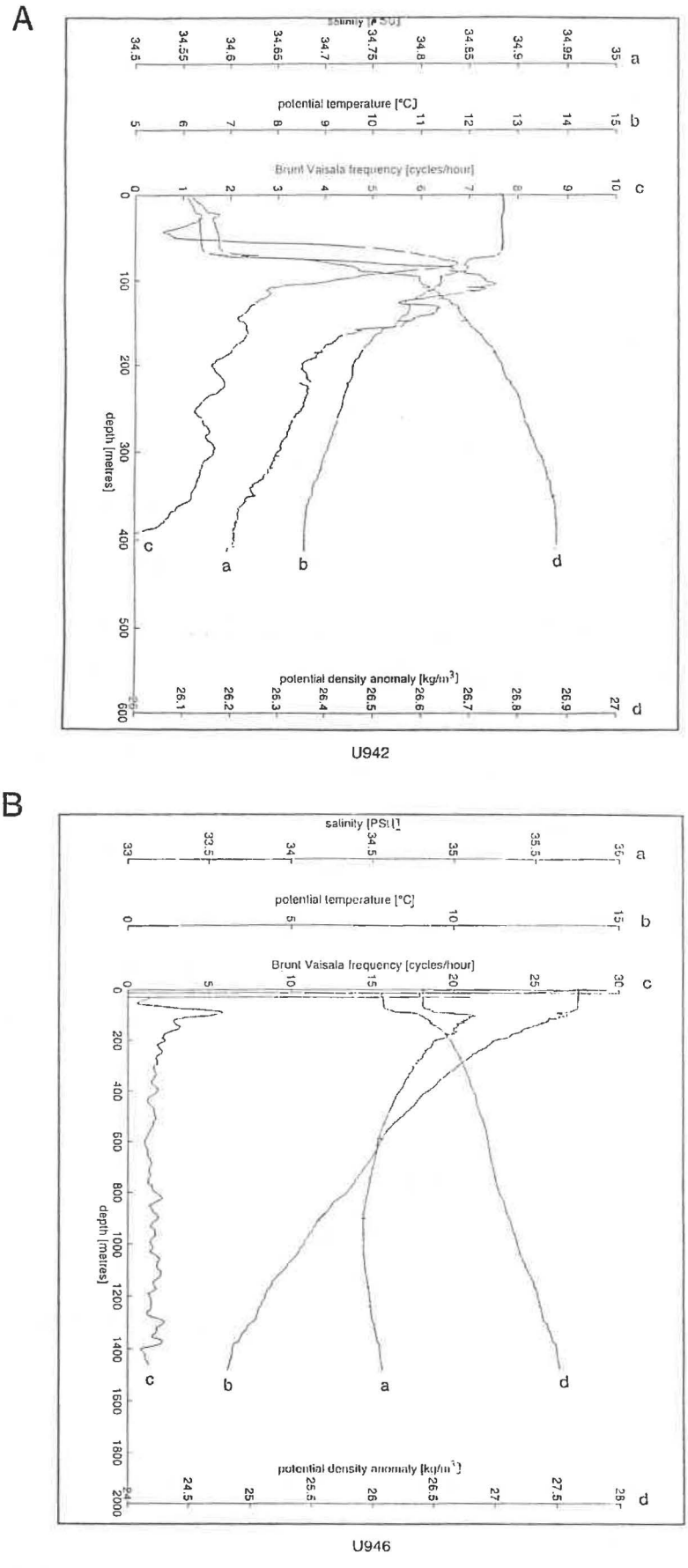

Fig. 2.6 Selected Conductivity-Temperature-Depth profiles for stations U942 (A) and U946 (B), north Chatham Rise, April 1992. Note scale changes in A and B.

measured using the CTD (Fig. 2.6). The overall temperature range recorded by the Brancker loggers indicated that the free-floating sediment trap array remained in subtropical water (e.g. Heath, 1985), as corroborated by the CTD data.

Mixed-layer temperatures and salinities at stations U943-U949 ranged from 13.8-14.2°C and 34.80-34.89 psu, respectively (Fig. 2.6). At U942, lower near-surface temperatures (12.7°C) and salinities (34.56-34.60 psu) were recorded, reflecting the location of the station within the STC. Mixed-layer depths, based on the initiation point of rapid temperature and salinity changes in the upper water column (e.g., Pond & Pickard, 1983; Gardner et al., 1995), varied from 65 m on the crest (U942) and northern flank (U944) of the Chatham Rise to between 70-90 m at the other stations in deeper water (Fig. 2.6). Below the mixed-layer, over depths < ca.800 m, temperature and salinity characteristics at all of the CTD stations were remarkably similar, confirming a subtropical origin (Heath, 1981, 1985). A salinity minimum of 34.46-34.48 psu at about 800-1100 m water depths on deeper casts (Fig. 2.6B) suggests the probable influence of Antarctic Intermediate Water (AAIW) (Heath, 1981, 1985), consistent with previous observations of this water mass on the northern flank of the Chatham Rise (e.g., Tomczak & Godfrey, 1994).

Water column total particulate concentrations varied from <0.05 to >0.5 mg l^{-1} and, with the exception of U942, concentration profiles decreased with increasing water depth (Fig. 2.7). At U942, a mid-water minimum was identified at 100 m, and the highest total particulate matter concentration (0.55 mg l^{-1}) occurred within 20 m of the sea-floor. Over a 12-h period, maxima in total particulate matter concentration at 5 m and 300 m at approximately 6-hourly intervals (Fig. 2.8) suggest a possible tidal influence (see Chapter 5). Alternatively, the temporal pattern in total particulate matter concentration may indicate horizontal advection of material into the area due to meso-scale physical phenomena, such as those associated with eddy formation (e.g., Barnes, 1985; Chiswell, 1994b). In contrast, there was no detectable change in total particulate matter concentrations at near-bottom depths over the same 12-hour sampling period (Fig. 2.8).

Since nephelometer casts were undertaken independent of the CTD, it was impossible to calibrate accurately the nephelometer with total particulate matter concentrations. The

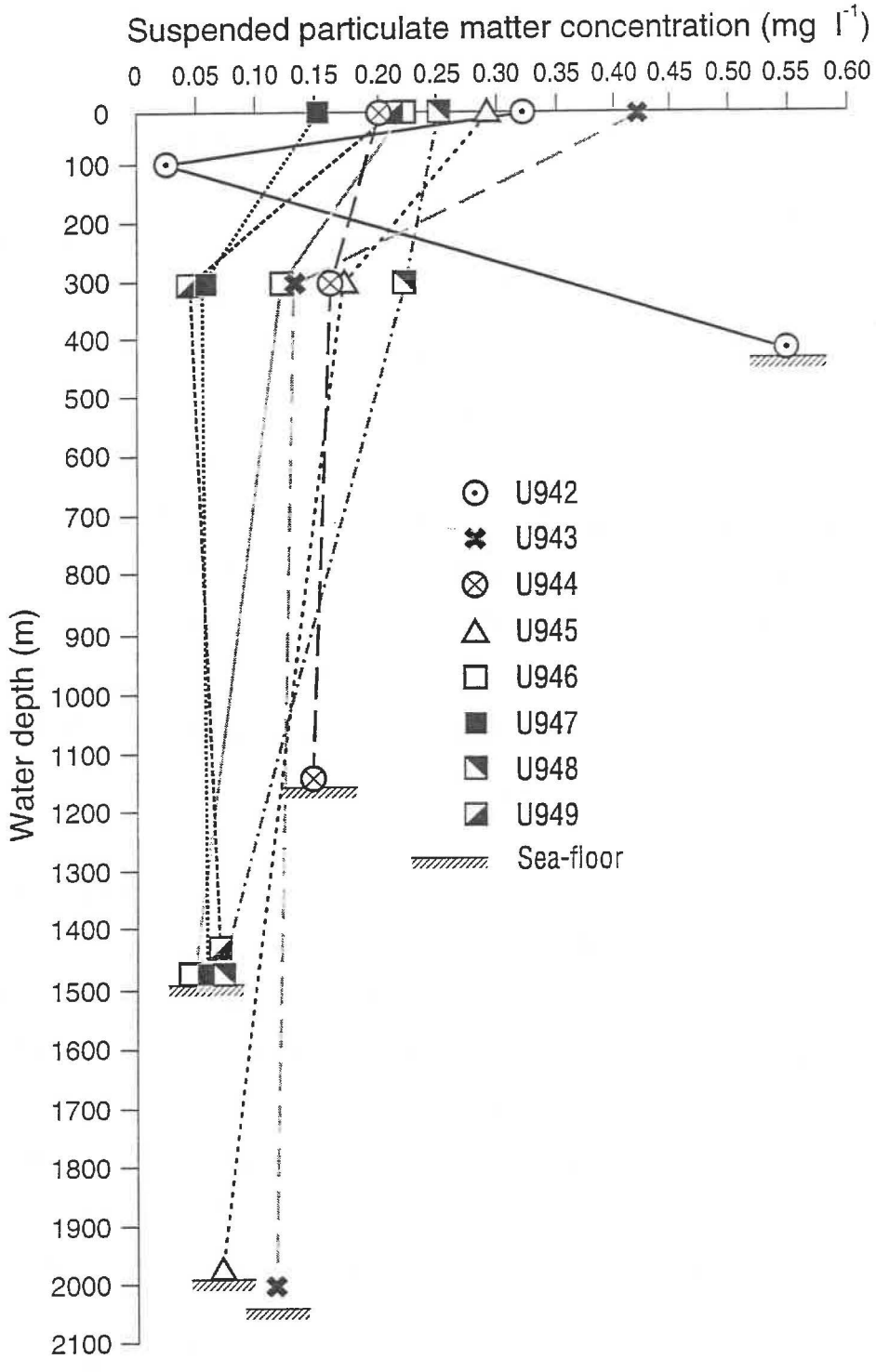

Fig. 2.7 Water column profiles of suspended particulate matter concentrations in April 1992. Station U942 is within the Subtropical Convergence while the other stations (U943-U949) are in subtropical waters on the north Chatham Rise slope. U946-U949 were conducted at the same position over 12 hours (refer Fig. 2.8).

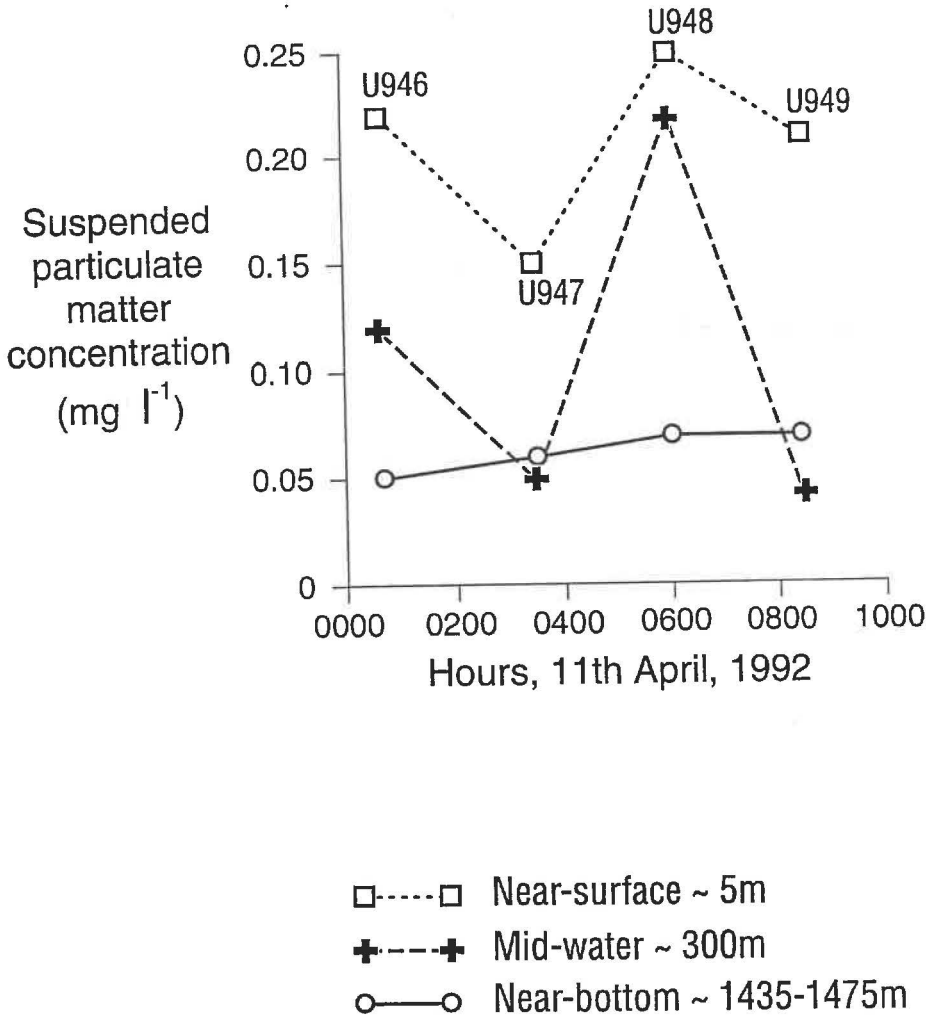

Fig. 2.8 Suspended particulate matter concentrations measured over 12 hours on 11 April 1992 in subtropical waters, north Chatham Rise (stations U946-U949, water depth 1490 m).

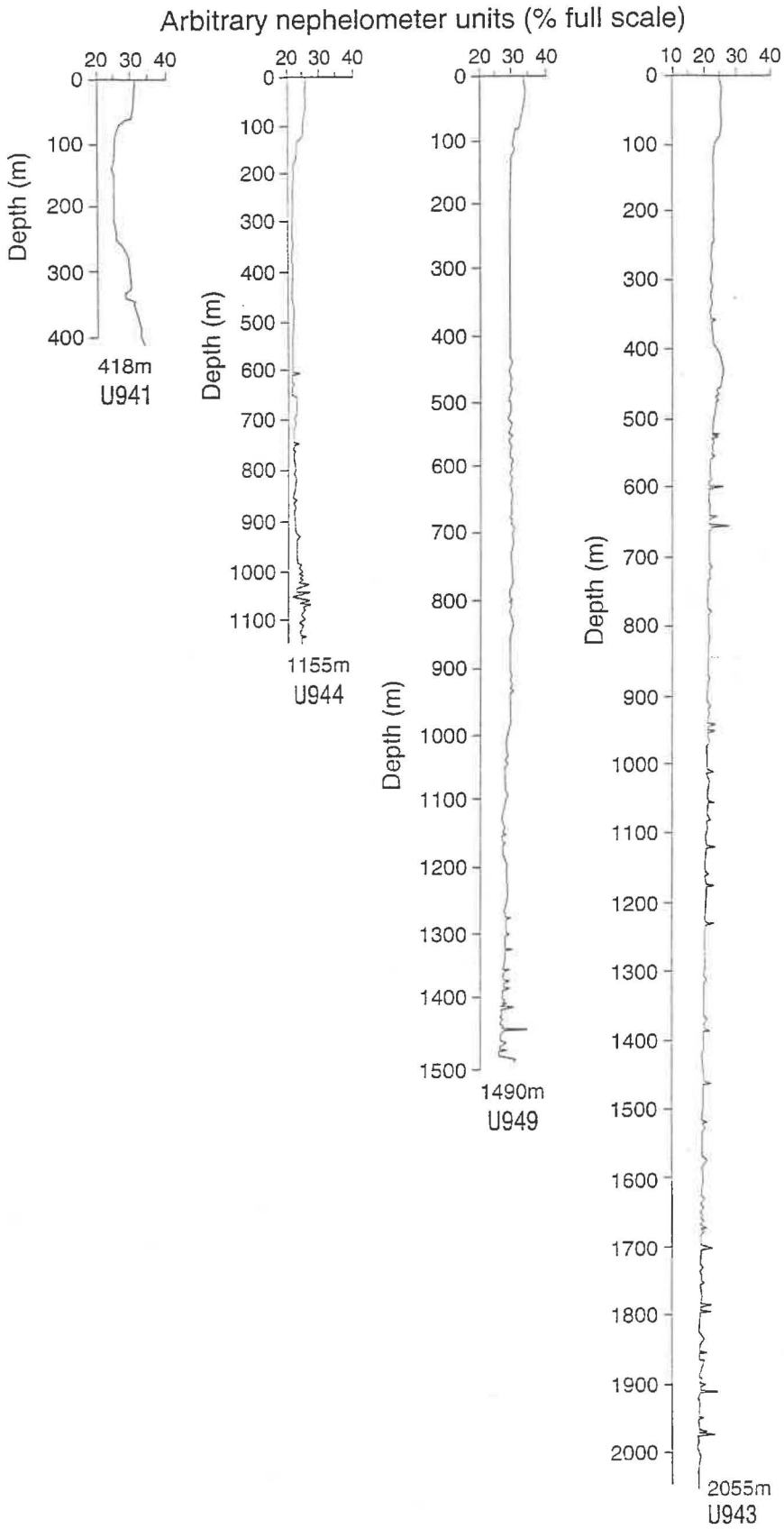

Fig. 2.9 Nephelometer water column profiles to the sea-floor on crest (U941) and northern flank of Chatham Rise (U943, U944 and U949). Spikes on the profiles below about 500 m are believed to be electronic artefacts.

nephelometer profiles, however, provide a qualitative indication of water column particulate material distribution (Fig. 2.9). At U944 and U949, similar profiles were observed with elevated concentrations of total particulate matter in the upper 80-130 m, a zone of lower concentrations throughout most of the remaining water column, and a basal 200-300 m thick region of slightly increased particulate matter concentration near to the sea-bed. In comparison, the deepest cast (U943) recorded the existence of a 90 m-thick upper layer of relatively high particulate matter concentrations and, except for a mid-water maximum at 400-450 m, a homogenous distribution of particles throughout the water column to the sea-floor. The station on the crest of the Chatham Rise (U941) exhibited relatively higher apparent concentrations in the top 60 m and bottom 165 m, compared with all of the other casts (Fig. 2.9).

2.2.3. Discussion

Many of the particles in the upper zone of relatively high particle concentration (Fig. 2.9) are likely to be dominantly biological in origin (e.g., Walsh & Gardner, 1992; Gardner et al., 1993). The highest apparent particulate matter concentrations were on Chatham Rise crest within the STC (stations U941/U942), a region of inferred high biological productivity (Bradford, 1983; Murphy et al., 1991; Comiso et al., 1993).

Increases in near-bottom particulate matter concentrations within 300 m of the sea-floor (Fig. 2.9) are inferred to represent sediment resuspended from the sea-floor on Chatham Rise. The resuspended material could then be advected horizontally, probably predominantly by tidal currents (e.g., Chiswell, 1994a). Strong across-rise flows (up to 20 $cm.s^{-1}$, Chiswell, 1994a) are inferred to be responsible for the observed mid-water increases in particle concentration on nephelometer profiles (Fig. 2.9), and to have contributed to increases in mass flux with depth (Fig. 2.4A). Meso-scale eddies could be an additional influence, particularly on the northern flank of the Chatham Rise where the East Cape Current impinges onto the Rise (e.g., Barnes, 1985; Chiswell, 1994a).

The observed increase in total mass fluxes with increasing water depth from 200 m to 500 m (Fig. 2.4A) is contrary to the expected reduction in particle abundance with depth due to

dissolution, decomposition and remineralisation processes below the euphotic zone (e.g., Bruland et al., 1989). Anomalous increases in particle flux with depth have been attributed to horizontal advective processes (Gardner et al., 1985; Gardner & Richardson, 1992), vertical migration and mid-water activities of mesopelagic zooplankton (Angel, 1989), patchiness of near-surface biological processes (Siegel et al., 1990) and *in situ* mid-water microbial production (Karl & Knauer, 1984a). Without complementary data on the water column distribution of phytoplankton, bacteria and zooplankton, it is impossible to suggest a single explanation for the depth increases in north Chatham Rise total mass flux data. Lateral advection, however, is likely to be an important process, given the observation of bottom nepheloid layers on the crest and on the northern flanks of the Chatham Rise (Fig. 2.9). Detachment of bottom resuspended layers from the crest of the Rise (e.g., U941) may have occurred to form the mid-water particulate matter concentration maxima at 400-450 m at more northerly sites (e.g., U943) (Fig. 2.9). Currents on the Rise crest of up to 20 $cm.s^{-1}$ (e.g., Chiswell, 1994a) are also sufficiently strong to erode and transport fine-grained sea-floor material (e.g., Lampitt, 1985).

Organic fluxes (PC, PP, PN), relative to TM flux, decreased proportionally with depth as more labile organic components are removed preferentially by dissolution and decomposition processes (Fig. 2.4B-D). The increased presence of faecal pellets in trap samples from 500 m confirms previous observations that such re-packaging processes are an important mechanism by which organic material is transported from surficial waters to the deep ocean (e.g., Bruland et al., 1989).

In comparison with the average C:N:P Redfield ratio of 106:16:1 proposed for marine organic materials (phytoplankton and zooplankton; Fleming, 1940; Redfield et al., 1963), trap samples in the present study have higher average ratios over most of the sampled depths (155-287:17-22:1; Fig. 2.5). These observations imply that the trapped samples comprised relatively refractory material, enriched in carbon, with nitrogen and phosphorus undergoing preferential recycling within the euphotic zone. A higher contribution of terrigenous or marine sediment material to the deeper trap, derived laterally from horizontal advective processes, or from contributions from sedimenting carbonate particles or vertically sinking

"marine snow" (Alldredge & Silver, 1988), may also explain the observed high C:N ratios (9 at 200 and 300 m; 14 at 500 m).

North Chatham Rise mass fluxes at 200 m are similar in magnitude to euphotic zone export flux measurements conducted at other oligotrophic locations (e.g., Sargasso Sea - averages range from 25-280 mg m^{-2} d^{-1} at 200 m, Lohrenz et al., 1992; central equatorial Pacific Ocean - averages range from 20-125 mg m^{-2} d^{-1} at 150 m, Karl et al., 1996) (refer to Table 5.5). Since *total* particulate carbon fluxes are reported by the present study, direct comparisons of these measurements can only be made with data-sets collected at the Hawaii time-series station ALOHA (Karl et al., 1996) and unpublished data obtained by the late J. M. Martin during the North Atlantic Bloom Experiment in 1989. In comparison, PC values at 200 m from north Chatham Rise fall within the range of mean fluxes measured from 1988-1993 at 150 m near Hawaii (13-57 mgC m^{-2} d^{-1}) and close to the overall mean (29.0±11.0, Karl et al., 1996). Significantly higher fluxes were observed during spring in north Atlantic Ocean (124-174 mgC m^{-2} d^{-1}, e.g., Martin et al., 1993) than have been measured at either Hawaii or north Chatham Rise due to sedimentation of phytoplankton "bloom' products in the Atlantic Ocean. PP and PN fluxes out of the surface mixed-layer, north of Chatham Rise, are comparable with values reported near Hawaii (Karl et al., 1996) and in northeast Pacific Ocean (Knauer et al., 1979; Martin et al., 1987). In contrast, PN fluxes in Sargasso Sea are substantially lower than those observed at all of these oligotropic locations, perhaps reflecting the importance of dissolved organic nitrogen cycling in the oceanic waters near Bermuda (e.g., Michaels & Knap, 1996).

There is only limited information on the magnitude of temporal and spatial variations of particulate fluxes in the Chatham Rise region. In other studies, significant temporal variations on both seasonal and annual time-scales have been observed at moored sediment trap locations (e.g., Deuser et al., 1981; Deuser, 1986; Newton et al., 1994; Honjo et al., 1995), as well as at time-series stations north of Hawaii (Karl et al., 1996) and near Bermuda (Lohrenz et al., 1992). Therefore, questions remain as to whether the flux results presented here are spatially or temporally representative of the Chatham Rise region. Subsequent sediment trap work in the same region in 1993 has gone some way towards filling these information gaps (Nodder & Alexander, 1997). The fluxes presented in Nodder (in press)

are the first direct measurements of export flux from the Southwest Pacific Ocean, and therefore provide a basis for future trap experiments in the region.

2.3. Sediment trap deployment in Cook Strait

2.3.1. Methods

In autumn 1993 a second pilot study was undertaken from 31 March-1 April in Cook Strait during commissioning voyages onboard R. V. *Akademik M. A. Lavrentyev* (NZOI-NIWA cruises 3004 & 3005) (Fig. 1.8 & 2.2). This study was designed to investigate the relative flushing rates of traps and the effect of baffles on trapping efficiency over a short-term deployment (1 day). A high-density brine was prepared prior to vessel departure using sea-water collected from Evans Bay, Wellington Harbour, and filtered through 47 mm-diameter Whatman GF/C glass-fibre filters (nominal pore size ~0.9 μm). Formalin (1%), NaCl (50‰) and a Fuschin Acid (red) dye were added to the sea-water. Twelve trap cylinders were deployed on one cross-frame set at 110 m in 250-300 m water depth in eastern Cook Strait. Baffles were placed randomly in six of the twelve cylinders, based on previous experience during April 1992 (Section 2.2), which indicated that a sample size of at least 4 was required to ensure standard errors of mass flux measurements would not exceed a "tolerable error" in order to assess the effect of baffles. An estimate of this "tolerable error" was calculated (Bhattacharyya & Johnson, 1978) based on the standard deviation of previous mass fluxes at 200 m water depth, north of Chatham Rise, in 1992 (section 2.2). Prior to deployment in eastern Cook Strait, cylinders were filled completely with dyed high-density brine solution and covered with plastic sheeting, held in place with dissolvable links, as described previously. The deployment commenced at 1007 hours on 31 March 1993, but was aborted due to severe weather and sea conditions at 1455 hours on 1 April 1993. No other ancillary data were collected during this pilot study.

Upon recovery, sea-water overlying dyed brine was siphoned off, traps capped with plastic bags and, once onshore, sample aliquots (250 and 500 ml) were extracted in triplicate from each cylinder using measuring cylinders. Subsamples were analysed for total mass, as described previously, except that filtered samples were oven-dried at 60 °C for successive

Table 2.1 Brine volume (%) recovered from traps deployed during storm conditions in Cook Strait pilot study, March-April 1993.

Trap Number†	Height of brine upon recovery (m)	Volume of brine upon recovery (m^3)	% brine solution retained	% brine solution lost
1	0.62	0.0040	66	34
2	0.60	0.0038	63	37
3	0.59	0.0038	63	37
4	Sample lost	-	-	-
5	0.56	0.0036	60	40
6	0.63*	0.0040	66	34
7	0.57	0.0037	61	39
8	0.56	0.0036	60	40
9	Sample lost	-	-	-
10	0.625*	0.0040	66	34
11	0.565	0.0036	60	40
12	0.60*	0.0038	63	37
		$\bar{x}$	62.8%	37.2%
		s	2.5	2.5

† Number corrsponds to position of trap cylinder on trap cross-frame.

* Volume actually equates to total brine recovered (i.e., the dyed portion), plus a small volume of ambient sea-water (< 0.0001 m^3, <2% total trap volume) not aspirated off.

24-h periods until they reached constant weight (within ±0.0050 mg of their original weight, Karl et al., 1990). Processing of some samples did not actually begin until between 40-70 days of trap recovery, in part due to the lengthy periods of time it took to filter some samples (i.e., up to 21 h). Blank samples were also filtered from a blank solution prepared 2 months after the voyage using identical methods to those used for preparation of the original brine solution; filtering times for the blank solution ranged from between 2 and 9 h for aliquots of 250 or 500 ml. Samples were rinsed with three 5 ml aliquots of ammonium formate, and stored frozen until filters could be weighed to constant weight using the drying-cooling cycle outlined by Karl et al. (1990).

2.3.2. Results

During the deployment, the array drifted approximately north under the influence of gale-force southerly winds to be recovered in a water depth of approximately 300 m. A total distance of about 3.6 km was covered at a drift rate of 0.2 km h^{-1} or 5 km d^{-1}. Upon recovery, the brine-filled traps were found to have lost on average 37% of their original brine volume, presumably due to flushing and wash-out of brine solution during deployment and/or retrieval (Table 2.1). Two samples were lost due to leakage out of previously drilled drainage holes in the sides of the traps (see methods used in Section 2.2). In general, an overall average total flux of about 30 g m^{-2} d^{-1} is indicated by the trap data (Table 2.2), excluding the obvious spurious data from cylinder 11, together with results from cylinders 1 and 12, which were all improperly subsampled and, consequently, did not recover all filtered material.

There appears to be little difference in the mass fluxes calculated using different filtration aliquots of trap solution (Table 2.2). Similarly, the reasonable correlations between replicate subsamples (standard deviation:mean ratio 0.01-0.12) suggests that the simple subsampling technique used in this study can be reproduced with moderate accuracy (generally better than 10%). Several data gaps are apparent in the subsampling results with two complete samples lost and various replicate subsamples discounted due to poor recovery of filtered material, including all the samples collected from cylinders 1, 11 and 12. Incomplete recovery of subsamples arose mainly from excessive filtration times which led to material drying onto

Table 2.2 Mass fluxes measured in Cook Strait pilot study, March-April 1993. Two different aliquots of trap sample solution (250 and 500 ml) were taken from each cylinder. Note that there were no substantial differences between fluxes calculated from filtering 250 ml rather than 500 ml of trap solution.

Trap number	Approximate volume filtered (l)	Average mass flux ± 1 *s* (g m^{-2} d^{-1})	Total average mass flux ± 1 *s* (g m^{-2} d^{-1})	Baffled (B) or not baffled
1	0.50	21.35 *(n=1)*	21.35 *(n=1)*	
2	0.25 0.50	30.05±1.10 *(n=2)* 27.15±1.63 *(n=3)*	28.31±2.03 *(n=5)*	
3	0.25 0.50	30.29±3.62 *(n=3)* 26.47 *(n=1)*	29.33±3.52 *(n=4)*	
4	0.25 0.50	Sample lost	-	B
5	0.25 0.50	35.98±1.89 *(n=3)* 29.06 *(n=1)*	35.63±5.21 *(n=4)*	B
6	0.25 0.50	27.12±0.20 *(n=3)* 29.30±1.54 *(n=3)*	28.21±1.55 *(n=6)*	
7	0.25 0.50	33.75±1.68 *(n=3)* 33.99±3.84 *(n=3)*	33.87±2.65 *(n=6)*	B
8	0.25	32.81±1.56 *(n=3)*	32.81±1.56 *(n=3)*	B
9	0.25 0.50	Sample lost	-	
10	0.25 0.50	25.84±1.70 *(n=3)* 30.19±2.09 *(n=3)*	28.01±2.92 *(n=6)*	
11	0.25 0.50	6.61±1.68 *(n=3)* 7.66±0.25 *(n=2)*	7.03±1.32 *(n=5)*	B
12	0.50	29.43±1.11 *(n=2)*	29.43±1.11 *(n=2)*	B

the base and sides of the filter funnels and/or loss of material during the weighing of the filtered samples to constant weight. These samples were, therefore, excluded from the final data analysis, although similar problems were encountered to some degree for most of the samples, suggesting that the fluxes presented in Table 2.2 are likely to be underestimates of the actual flux. The loss of these samples meant that the effect of baffles on trapping efficiency could not be tested statistically, although there is an indication that baffles might increase trapping efficiency since higher total average fluxes were measured in baffled traps, compared to those traps without baffles (Table 2.2). There seems to be minimal effect of inter-trap hydrodynamic interactions on trapping efficiency, although the aforementioned problems of sample integrity and retention suggested that further experimental work was required to evaluate fully these effects; *a posteriori* experiments conducted subsequently in Evans Bay in 1993-1995 were designed to address these effects (Section 2.4).

2.3.3. Discussion

The magnitude of the Cook Strait fluxes warrants further discussion since the measured fluxes are generally about two orders of magnitude higher than mass fluxes measured at mid-water column depths in continental shelf environments elsewhere (e.g., northwest Mediterranean Sea, 0.03-0.70, up to 1.3 g m^{-2} d^{-1}, Monaco et al., 1990; southern California, 0.2-0.8 g m^{-2} d^{-1}, Landry et al., 1992). The Cook Strait fluxes are similar in magnitude to those measured in both very shallow coastal environments (<30 m, e.g., Monaco et al., 1990; Lund-Hansen et al., 1994) and in continental slope settings where lateral transport of sediments may be enhanced by seasonal variations in meteorological and oceanographic physical features (e.g., Monaco et al., 1990). Monaco et al. (1990) observed mass fluxes at 600 m on the NW Mediterranean continental margin ranging from 8-21 g m^{-2} d^{-1}. The highest fluxes occurred in winter months, with the seasonality in fluxes attributed to the increased occurrence of storms, higher river discharges and the intensification of regional circulation patterns in winter (Monaco et al., 1990).

Cook Strait is recognised as a site of active sediment transport (e.g., Black, 1986; Carter et al., 1991) with recorded near-bottom tidal currents of >1 m s^{-1} down to 300 m water depth (e.g., Gilmour, 1960; Heath, 1986; Harris, 1990). The deployment of the traps during storm

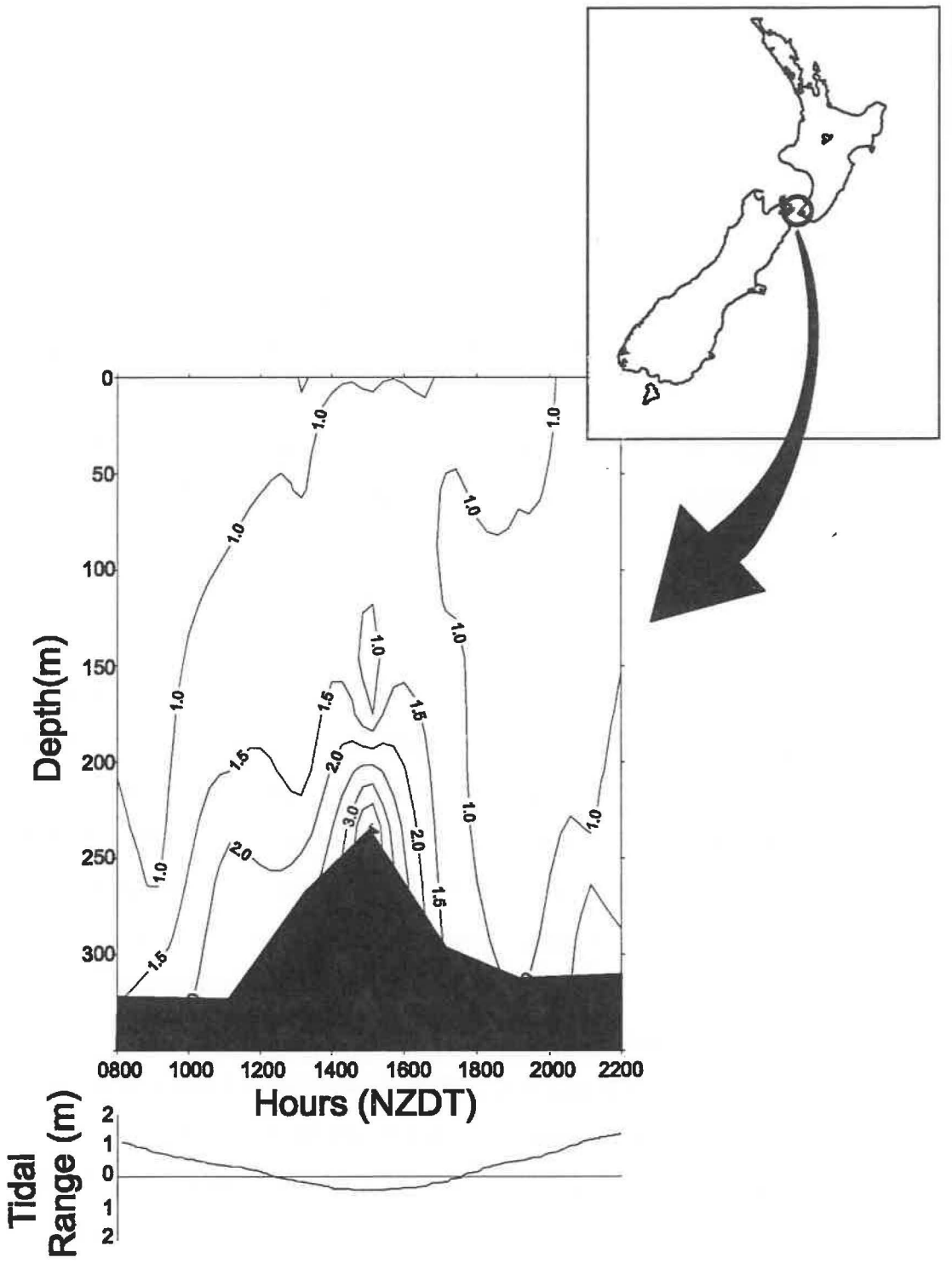

Fig. 2.10 Suspended particulate matter concentrations (mg l^{-1}) in Cook Strait in September 1986 (NIWA research voyage 2001, station Q898, 41°12.75'S 174°27.60'E) over one tidal cycle.

conditions, coupled with calculated high suspended sediment transport rates (Black, 1986) and the meterologically forced nature of circulation in the strait (Heath, 1986), suggests that the seemingly extreme fluxes of 20-35 g m^{-2} d^{-1}, measured in this short-term (<1 day), single trap deployment, should not be discounted entirely. Bottom sediments in Cook Strait are characterised by marked spatial heterogeneity (e.g., Carter, 1992), and suggest that a major source of particulate material, as collected by the sediment traps, may be the two major rivers in northeastern South Island, the Awatere and Wairau Rivers (e.g., Griffiths & Glasby, 1985). These rivers have been responsible for the formation of an extensive Holocene sandy and muddy sand wedge, east of Cloudy Bay (Carter, 1992). Suspended sediment loads from these two rivers dominate river discharges on the NE coast of South Island, north of Cape Campbell, with annual suspended loads of 1.5 and 4.7 x 10^6 tonnes, respectively (Griffiths & Glasby, 1985). Southerly swell in Cloudy bay has sufficient force to resuspend sediments to most shelf depths. Using a threshold for fine sand of 19-22 cm s^{-1} (Pickrill & Currie, 1983), and applying linear wave theory, it is estimated that 5-7 m high and 11-16 s long waves observed during the trap deployment would be capable of stirring fine sand down to depths of 160 m. Carter & Lewis (1995) reached similar conclusions for the swell reaching the south Wellington coast on the other side of Cook Strait to Cloudy Bay.

In addition, significant transport of suspended sediment through central Cook Strait has been well documented by Black (1986) and Carter (1992). Total particulate matter data (L. Carter, pers. comm., 1995) from the Narrows area in northern Cook Strait indicates strong apparent coupling between suspension of bottom sediments and tides with increases in near-bottom suspended solid concentrations at low tide, decreasing to concentrations of between 1-2 mg l^{-1} at high tide (Fig. 2.10). Higher tidal current speeds and, hence, enhanced sediment transport potential at low tide are expected from modelling results where surface flows in the order of 20-60 cm s^{-1} to the southeast are implied, compared with variable flows of less than 10 cm.s^{-1} only an hour before high tide (e.g., Bowman et al., 1980). Tidal streams are anticipated to reverse and flow strongly to the north in eastern Cook Strait a mere two hours after high tide (Bowman et al., 1980). Alternatively, vessel drift may have contributed to the apparent higher near-bottom fluxes since the highest SPM concentration of 4.3 mg l^{-1} is observed at the shallowest sampling site (Fig. 2.10) where resuspension may be anticipated to be a prominent process. Total particulate matter concentrations were generally consistent

throughout the water column (270-330 m) with values of 0.5-1.0 mg l^{-1} and maximum concentrations of 1-4 mg l^{-1} at near-bottom sampling depths (Fig. 2.10). Thus, suspended sediment swept by tides through central Cook Strait is likely to be another major source of material collected by the NZOI-NIWA sediment traps deployed in autumn 1993.

The traps were also deployed in a region characterised by predicted moderately low stratification (S~2-2.5, Bowman et al., 1980; 1983a, b), with shelf fronts also a feature of the area (Bowman et al., 1980). Southern Cook Strait is noted as the location of the confluence of waters associated with the northwards-flowing Southland Current, the eastward-directed D'Urville Current and the southwards-flowing East Cape Current (e.g., Heath, 1971; Bowman et al., 1983a, b; Barnes, 1985; Murdoch et al., 1990) (Fig. 1.7 & 2.2). This region may, therefore, be regarded as an area of significant tide-, wind- and/or upwelling-induced mixing, resulting in moderately low stratification indices, nutrient enrichment of surface waters (Bowman et al., 1983a, b), and possibly may contribute to the observed accumulation of spawning hoki (*Macruronus novaezelandiae*) in Cook Strait (Murdoch et al., 1990). In addition, propagating internal waves may suspend sediment through wave breaking at the sea-floor (L. Carter, pers. comm., 1997). Unfortunately, there are no other data that can be used usefully to verify the flux information; in particular, seasonal and interannual variations of particulate fluxes in Cook Strait remain unknown.

2.4. Factors affecting sediment trap efficiency: a posteriori sediment trap experiments in Evans Bay, Wellington Harbour

A series of five *a posteriori* experiments (I-V) were conducted in the shallow (<20 m) inner harbour waters of Evans Bay, Wellington Harbour (41°18.25'S 178°48.44'E) between 1993 and 1995 to evaluate trapping efficiency of the NZOI-NIWA traps (Fig. 1.8 and 2.1). The first experiment (I) was designed to gain an understanding of possible effects of brine volume and baffles on trapping efficiency, but could not be validated statistically, so that three specific studies were conducted subsequently to investigate: (a) inter-trap hydrodynamic interactions between trap cylinders placed in different positions on a cross-frame (Experiment II); (b) the effect of baffles (III); and (c) the effect of brine volume on

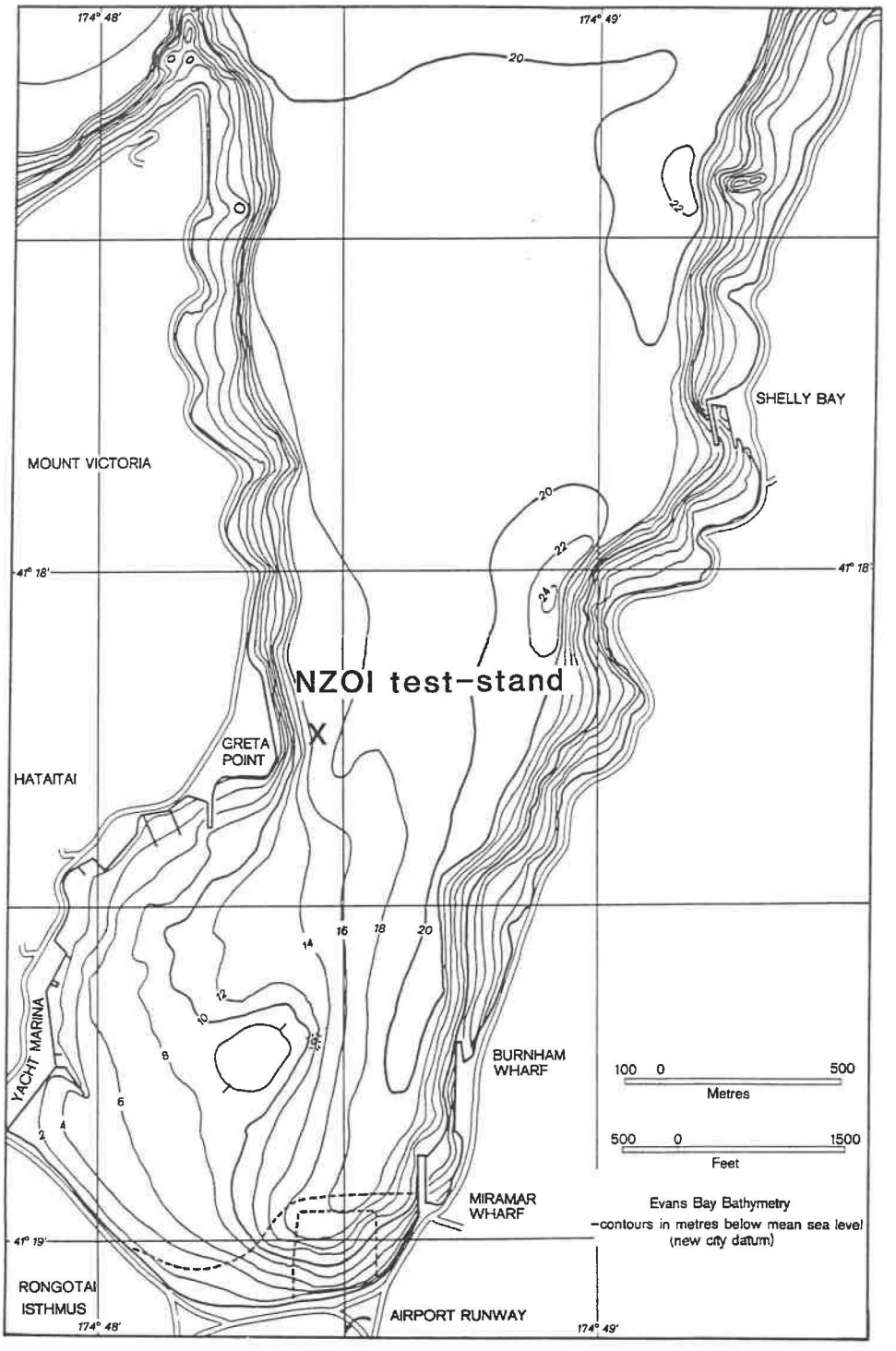

Fig. 2.11 Bathymetric map of Evans Bay, Wellington Harbour, showing location of permanent NZOI-NIWA test-stand (after Lewis & Carter, 1976).

trapping efficiency (IV). In addition, a 2-week dissolution experiment (V) was undertaken to evaluate the effectiveness of formalin as a preservative.

In each experiment, single sediment trap cross-frames, each holding twelve cylindrical traps, were bottom moored at depths of 4 m above the sea-floor using 30-50 kg anchors and 40 kg of buoyancy provided by two Viny buoys. Traps and baffles were washed using 1 M HCl, rinsed with distilled water and capped with plastic bags, prior to deployment. Brine solutions were prepared 1-2 days in advance from inner harbour sea-water that was pressure-filtered through 0.45 and 1.0 μm membrane filters, and mixed with 50 g ANALAR NaCl and 100 ml formalin for every litre of dyed filtered sea-water (e.g., Karl et al., 1990). Traps were typically deployed and recovered from a small boat (*Tara-iti* or *Matuku*), and traps were closed and opened by SCUBA divers using plastic bags and rubber bands. Spatial relationships between individual trap moorings were measured with ground-lines, and bearings taken by divers along the lines from a central permanent NZOI-NIWA test-stand to the traps, and *vice versa* (Fig. 2.11). Upon recovery, after deployments ranging from 1-6 days, sea-water overlying the basal brine was aspirated off and trap contents were pre-screened through a 200 mm mesh to remove zooplankton "swimmers" and poured into a 10 l Nalgene container from whence aliquots of trap solution were removed into measuring cylinders. Material retained on the mesh was transferred to a plastic flask, 30 cm^3 of sodium metahexaphosphate added and the sample shaken on a mechanical shaker for 15 min to breakdown completely any organic material. This solution was then combined with the originally sieved trap contents by being passed back through the 200 μm mesh; the >200 μm fraction was preserved in 2.5% pH-buffered formalin and stored in a refrigerator. Three aliquots of about 100 ml trap solution from each cylinder were then filtered through pre-weighed 25 mm diameter, 0.2 μm Nuclepore filters, and average mass fluxes for each cylinder calculated.

Ambient current flow characteristics over the course of each experiment were measured using a RDI Broad Band Acoustic Doppler Current Profiler (ADCP) with a frequency of 600 kHz (Abraham, 1997) (Experiment I) or an Aanderaa rotary current meter (Experiments II-IV). The current meter was moored 4 m above the sea-floor on the permanent NZOI-NIWA

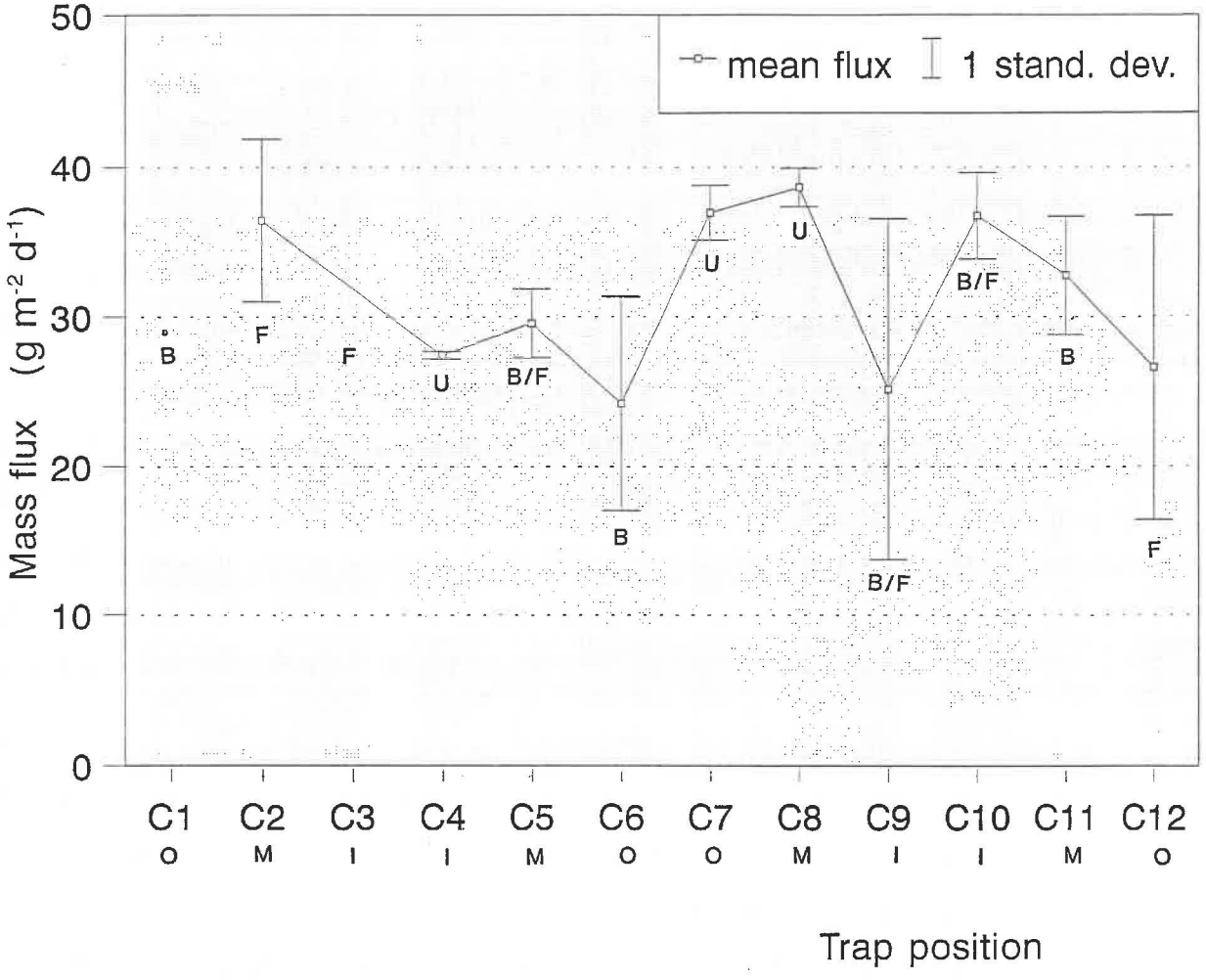

Fig. 2.12 (A) Average mass flux results (± 1 standard deviation) from Evans Bay, Wellington Harbour, in November, 1993 (Experiment I). Along x-axis, O = outer position on cross-frame, M = middle and I = inner position; B = baffled with basal brine, B/F = baffled and filled with brine, U = unbaffled with basal brine, F = unbaffled and filled with brine;

test-stand located in Evans Bay (Fig. 2.11), whereas the ADCP was bottom-moored in upward-viewing mode 10 m away from the test-stand.

2.4.1. Experiment I: Initial evaluation

In the initial experiment, in conjunction with the ADCP, the sediment trap array was moored approximately 10 m due east of the permanent mooring in a water depth of about 15 m for a period of 6 days from 18-24 November 1993. Six cylinders were filled completely with brine; the remaining six cylinders were back-filled with 1.5 l of brine beneath approximately 4.5 l of filtered sea-water. In each of these two preparations, three traps were baffled and three were unbaffled.

In addition, total particulate matter concentrations were determined from sea-water samples pumped from a depth of 15 m in the vicinity of the permanent NZOI-NIWA mooring site over a 24-h period from 0930 h 23 November to 1630 h 24 November 1993. Duplicate 2.0 l samples were collected every two hours and filtered onto pre-weighed 47 mm diameter, 0.45 μm Nuclepore filters under low vacuum (<8 mm Hg). Samples were rinsed completely with distilled water to remove sea-salts and stored frozen until re-weighing, following drying of the frozen filtered sample using a heat lamp. Total particulate matter samples were also collected from discrete water depths using a 1.5 l Nansen bottle on a hydro-line with a messenger at midday on 25 November from a small row-boat.

Absolute mass fluxes from Experiment I varied from 13 to 43 g m^{-2} d^{-1} (Fig. 2.12), with high amounts of variation between replicate subsamples due in part to excessive losses of collected sample material during the drying-to-constant-weight procedure. The loss of material from filters contributed to the complete disregard given to subsamples from cylinder 3, as well as several samples from other traps (Table 2.3). This initial experiment was unreplicated, in that, the sampling only represented one site at one location. In addition, the attempt to investigate the effect of several parameters on trapping efficiency (e.g., baffles, brine volume) without an understanding of how such parameters may themselves be influenced by other factors, such as trap hydrodynamic interactions, indicated that the experiment was flawed. Thus, although the results provided an initial appreciation of the

Table 2.3 Mass fluxes and %brine recovered from traps filled completely with high-density brine solution deployed 3 m above the sea-floor in 16.5 m water depth in Evans Bay, Wellington Harbour, November 1993 (Experiment I).

Trap number†	Total average mass flux ± 1 *s* ($g.m^{-2}.d^{-1}$)	Initial brine volume (l)	Recovered brine volume (l)	%brine recovered	%brine lost	Code*
1	29.41 *(n=1)*	1.50	2.18	-	-	B, o
2	36.42±5.45 *(n=3)*	6.04	2.27	37.6	62.4	F, m
3	Sample lost	6.04	2.34	38.7	61.3	F, i
4	27.44±0.23 *(n=2)*	1.50	1.28	-	-	U, i
5	29.54±2.29 *(n=2)*	6.04	2.30	38.1	61.9	B/F, m
6	24.18±7.12 *(n=2)*	1.50	2.34	-	-	B, o
7	36.95±1.83 *(n=2)*	1.50	2.75	-	-	U, o
8	38.62±1.29 *(n=2)*	1.50	2.69	-	-	U, m
9	25.12±11.40 *(n=3)*	6.04	2.72	37.6	62.4	B/F, i
10	36.72±2.89 *(n=3)*	6.04	2.05	33.9	66.1	B/F, i
11	32.74±3.95 *(n=2)*	1.50	2.11	-	-	B, m
12	26.60±10.15 *(n=3)*	6.04	2.18	36.0	64.0	F, o

† Number corresponds to position of trap cylinder on trap cross-frame.

* B=baffled with 1.5 l brine, F=brine-filled, unbaffled, U=1.5 l brine, unbaffled, B/F=baffled and brine-filled; o=outer position on trap cross-frame, m=middle, i=inner.

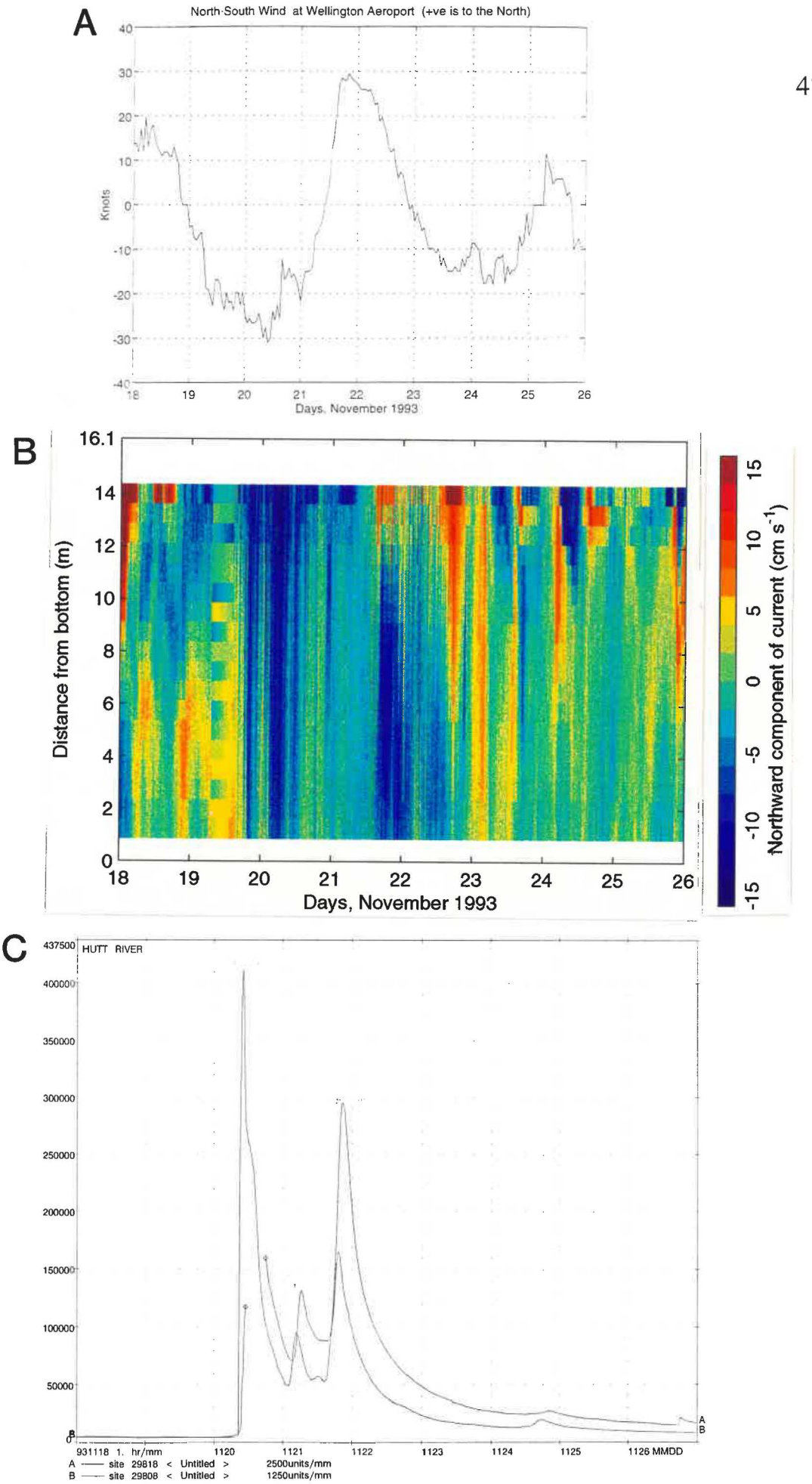

Fig. 2.13 (A) North-south winds at Wellington Airport over the duration of the experiment; (B) ADCP currents above the Evans Bay site; and (C) Hutt River flows measured at Birchville (a) and Kaitoke (b); note the change of y-axis scale for these sites; units are in l s^{-1}.

SUSPENDED PARTICULATE MATTER

24 H CYCLE, EVANS BAY

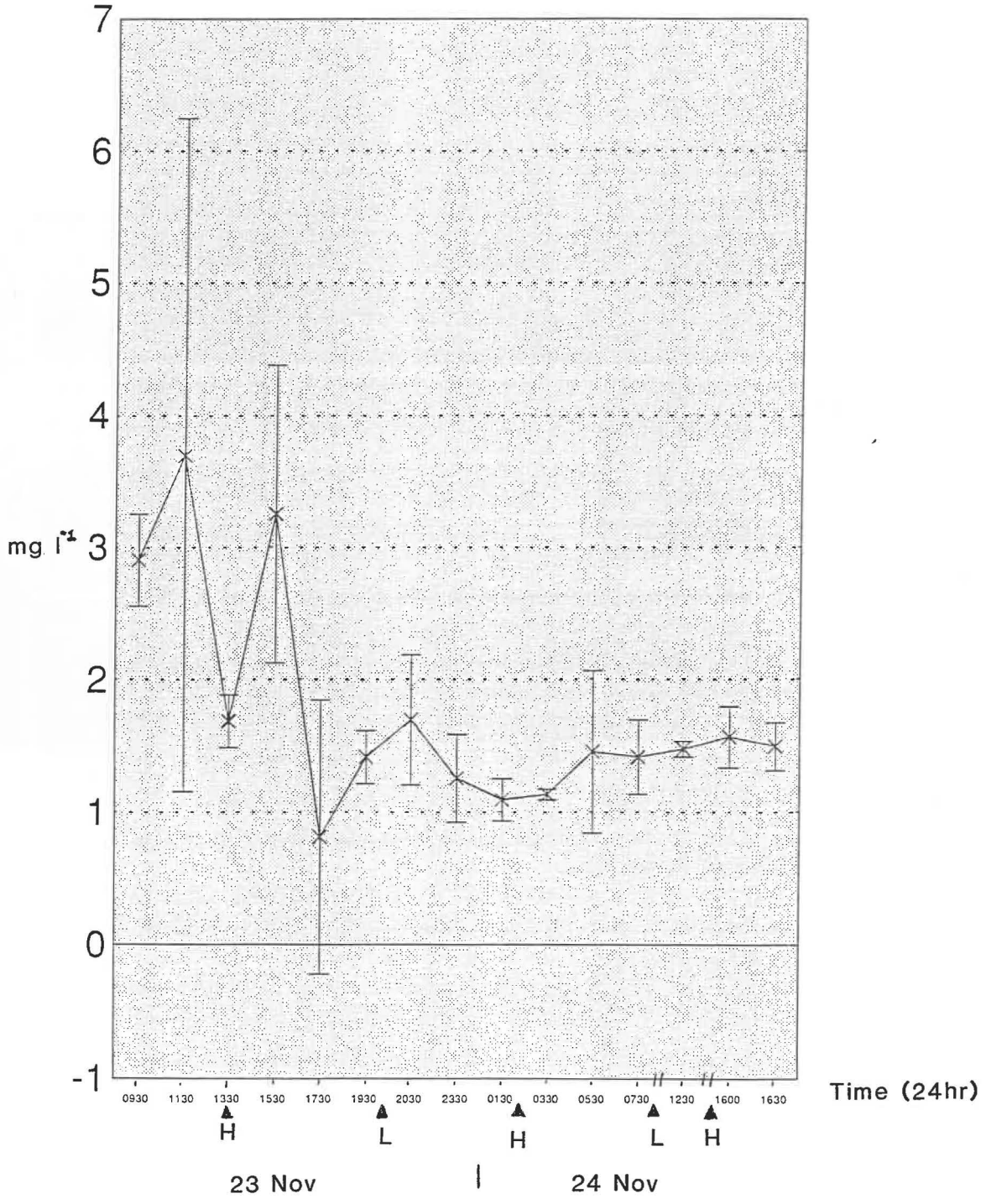

Fig. 2.14 Average suspended particulate matter concentrations (± 1 standard deviation) measured at Evans Bay over a 24 hour period in November 1993 (Experiment I). Along x-axis, H = high tide, L = low tide.

magnitude of fluxes in an inner harbour environment, the data could not provide a clear indication as to whether baffles and/or brine volume affected trapping efficiency (Fig. 2.11).

In the initial experiment, cylindrical traps completely filled with brine solution consistently lost 63% of this solution (Table 2.3). In comparison, only 37% was lost from traps deployed during storm conditions in Cook Strait (Table 2.1). The more energetic wave environment is likely to have led to highly turbulent conditions that resulted in greater washout from the NZOI-NIWA traps deployed in Evans Bay, particularly as the traps were fixed in position in the harbour. Current speeds of between 5-10 cm s^{-1} were measured by the ADCP over the depth range of the moored traps (Fig. 2.13B). In contrast, in Cook Strait, the traps were deployed on a free-floating array which is expected to reduce turbulence at trap mouths (e.g., Staresinic et al., 1978, although refer to recent work by Gust et al., 1992, 1994; see Section 1.5). Nonetheless, the mass fluxes measured in these two depositional environments are of the same order of magnitude with an overall average flux from the moored Evans Bay experiment of 31.32±7.3 g m^{-2} d^{-1} (±1 *s*, *n*=25) and from Cook Strait, 30.60±3.96 (±1 *s*, *n*=34, excluding cylinders 1, 11 & 12) (Section 2.2).

Total suspended particulate matter (SPM) samples collected over the first 8 h of Experiment I exhibited marked variability, possibly reflecting initial problems with the pumping system and contamination by nekton, such as fish (*Notolabrus celidotus*, New Zealand spotty) that were subsampled inadvertently by the pump. SPM concentrations of the early samples seemed to be higher (2-6 mg l^{-1}) and exhibited considerably more variablity, compared with the samples collected after 8 hours which occupied a relatively narrow band of concentrations, ranging from 1-2 mg l^{-1} (Fig. 2.14). The highly variable and relatively high SPM concentrations observed over the first 8 h may be attributed to additional material that had entered Wellington Harbour as a turbid estuarine layer arising from simultaneous flooding of the Hutt River (Fig. 2.13C). One may have, however, expected these trends to have persisted into the 24 November when the plume entered fully into Evans Bay. At this time the 2-3 m thick turbid layer endured in the bay until at least midday on 25 November near to the mooring site (Fig. 2.15). These observations are consistent with previous descriptions of the shallow vertical structure of such plumes in Wellington Harbour (i.e., <5 m thick; Booth, 1975; Heath, 1977). It is difficult to determine whether or not tides play a

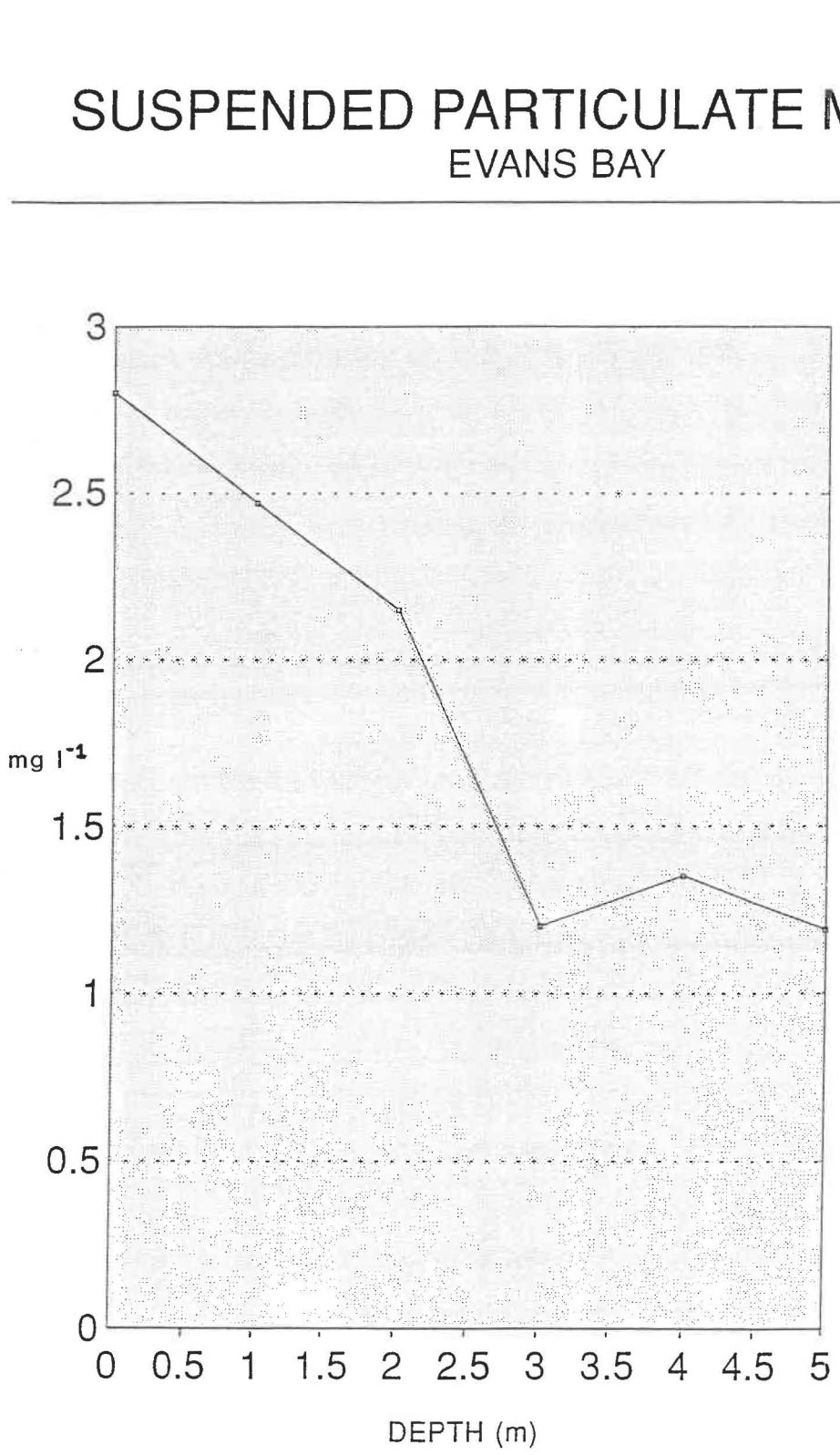

Fig. 2.15 Suspended particulate matter concentrations measured in upper 5 m of water column in Evans Bay on 25 November 1993 (Experiment I).

significant role in the advection of suspended material within Evans Bay, particularly since tidal currents in the inner harbour are often less than the currents generated by wind-forcing, such as seiching (e.g., Heath, 1977; Abraham, 1997). Intense seiches were observed on 20 and 22 November, closely associated with periods during which wind speeds were greater than 10 m s^{-1} (Abraham, 1997) (Fig. 2.13A). There is no obvious relationship between SPM concentration fluctuations and predicted high and low tides (Fig. 2.14) due mainly to the inherent variability associated with the duplicate SPM concentration results.

2.4.2. Experiment II: Inter-trap hydrodynamic interactions

Disturbance of the mean flow field by individual traps deployed on the same array may affect relative trapping efficiency depending on the horizontal spacing between each trap. Gardner (1980a) and Butman (1984, *in* U.S. GOFS Report 10, 1989) proposed that a minimum of three trap diameters cross-stream and ten diameters downstream should be employed to eliminate inter-trap hydrodynamic interactions. The cross-frame array designed for use at NZOI-NIWA had a trap spacing interval of at least 30 cm which is in accordance with these previous recommendations. The cross-frame was free to rotate in the horizontal plane to maintain the traps parallel to the mean flow. Accordingly, Experiment II in Evans Bay was designed to test the null hypothesis:

That there is no difference in the trapping efficiency of traps placed at any position on a moored NZOI-NIWA sediment trap cross-frame array.

This hypothesis assumed that there were no interactions between trap moorings on the scale of the distances between each moored array, and that the Evans Bay environment and particulate populations were essentially homogeneous. A summary of the experimental design for Experiment II was as follows:

Site:	Mooring sites	random	a=3
Position:	Inner, middle, outer	fixed	b=3
Replicates:	Cylinders	random	n=4

Linear equation: $x_{ijk} = \mu + S_i + P_j + SP_{j(I)} + e_{k(ji)}$

Table 2.4 Sources of variation for a sediment trap experiment designed to test the hypothesis that the position of traps on a cross-frame affects trapping efficiency, i.e., hydrodynamic biases are introduced to particulate flux determinations by inter-trap interactions (Evans Bay sediment trap experiment II).

SOURCE OF VARIATION	DEGREES OF FREEDOM (DF)	TABLE OF MULTIPLIERS			EXPECTED MEAN SQUARES (MS)	F-RATIO
		random (S) i	fixed (P) j	random (n) k		
Among (sites) A	2 *(a-1)*	1	3	4	$1\sigma_e^2 + n\sigma_{SP}^2 + pn\sigma_S^2$	MS(S)/RES
Among (positions) B	2 *(b-1)*	3	0	4	$1\sigma_e^2 + sn\sigma_P^2$	MS(P)/MS(SP)
A x B	4 *(a-1)(b-1)*	1	0	4	$1\sigma_e^2 + n\sigma_{SP}^2$	MS(SP)/RES
Residual	27 *ab(n-1)*	1	0	1	$1\sigma_e^2$	
TOTAL	35 *abn-1*					

The data were analysed statistically using a General Linear Model (GLM) Analysis of Variance (ANOVA) and a multiple comparison *a posteriori* procedure (Tukey test) since there are several possible alternative hypotheses (i.e., H_{A1}: $m_1>m_2=m_3$, H_{A2}: $m_1<m_2=m_3$, H_{A3}: $m_1=m_2>m_3$, etc) (Table 2.4). The computer programme employed for all statistical analyses was NCSS (Version 6.0). The same general form of the linear equation used in the experimental design for Experiment II was used in Experiments III and IV, except that in III only two fixed variables were being tested (i.e., baffled versus unbaffled traps).

In austral late winter (August) 1994, three arrays were placed randomly in water depths of between 16-18 m at locations in Evans Bay near the permanent NZOI-NIWA test-stand. All traps were baffled and back-filled with approximately 1.5 l of high-density brine containing 0.5% formalin as a poison/preservative. Ten 250 ml "time-zero" brine samples were filtered as blanks. The traps at sites A and C were capped after five days (10-15 August 1994), but site B was not located until 16 August (i.e., 6 day deployment). The site C mooring was recovered on 15 August and traps at sites A and B recovered the following day. Prior to being capped with plastic bags, traps at site A were well stratified with a strongly developed dyed basal brine layer. Upon recovery, however, dye in the site A traps was distributed homogeneously throughout the cylinders so that, upon recovery, trap contents were aspirated down to a level corresponding to 1.5 l, the original brine volume, once the sea-water/brine interface was recognised visually. Traps from other sites were aspirated to within 5 cm of the sea-water/dyed brine interface. Trap contents from all three sites were analysed in triplicate for mass flux. An Aanderaa current meter was deployed at the start and recovered at the end of the experiment, but malfunctioned so that there were no current data available to assess flow conditions during the sediment trap deployment in Experiment II.

At each of the three mooring sites, there are no significant differences in trapping efficiency due to cross-frame position (d.f. = 2, 4; F = 2.90; P = 0.167; power = 0.096), and hence there seems to be only minimal inter-trap hydrodynamic interactions (Table 2.5, Fig. 2.16). These observations support the previous contention that a three-diameter across-flow spacing of individual traps on an array would eliminate such biases (e.g., Gardner, 1980a; Butman, 1984, *in* U.S. GOFS Report 10, 1989). It does appear, however, that one of the primary assumptions made prior to the experiment, regarding inter-mooring interactions or

Table 2.5 Effect of trap position on mass flux determinations from Experiment II conducted in Evans Bay, Wellington Harbour, in August 1994. Traps were deployed 3 metres above the sea-floor in water depths of 18 (Sites A and B) and 17 m (Site C). Note that ANOVA analysis (α=0.05) indicates that, although there are significant differences between the three sites, trap cylinders in "outer" cross-frame positions collect similar amounts of material as those in "inner" or "middle" positions.

Trap position†	Mass fluxes ($g\ m^{-2}\ d^{-1}$) Site A	Mass fluxes ($g\ m^{-2}\ d^{-1}$) Site B	Mass fluxes ($g\ m^{-2}\ d^{-1}$) Site C
1 (O)	33.61±10.59	51.85±6.19	33.50±5.79 *(n=2)*
2 (M)	41.25±0.69	58.54±2.78	36.42±5.45
3 (I)	36.96±5.12	49.49±7.84	32.90±2.93 *(n=2)*
4 (I)	44.52±2.50	55.23±0.56	27.44±0.23 *(n=2)*
5 (M)	43.89±3.48	48.76±12.91	29.54±2.29 *(n=2)*
6 (O)	32.15±4.29	45.30±17.58 *(n=2)*	24.18±7.12 *(n=2)*
7 (O)	41.04±2.13	48.10±4.58	36.95±1.83 *(n=2)*
8 (M)	46.15±1.23	53.66±4.07	38.62±1.29 *(n=2)*
9 (I)	42.04±4.36	50.46±2.86	25.12±11.40
10 (I)	39.82±0.78	41.41±9.43	36.72±2.90
11 (M)	46.12±10.12	41.51± 6.79	32.74±3.95 *(n=2)*
12 (O)	42.22±3.96	57.26±1.96 *(n=2)*	26.60±10.15
Site mean, $\bar{x}$	40.81	50.13	31.73
Site standard deviation, s	4.54	5.59	5.02

† Position corresponds to position of trap cylinder on trap cross-frame arm; **I** = inner position on cross-frame, **M** = middle position, **O** = outer position.

§ Average mass fluxes ± 1 standard deviation are given; unless stated, n=3 in each case.

EVANS BAY II

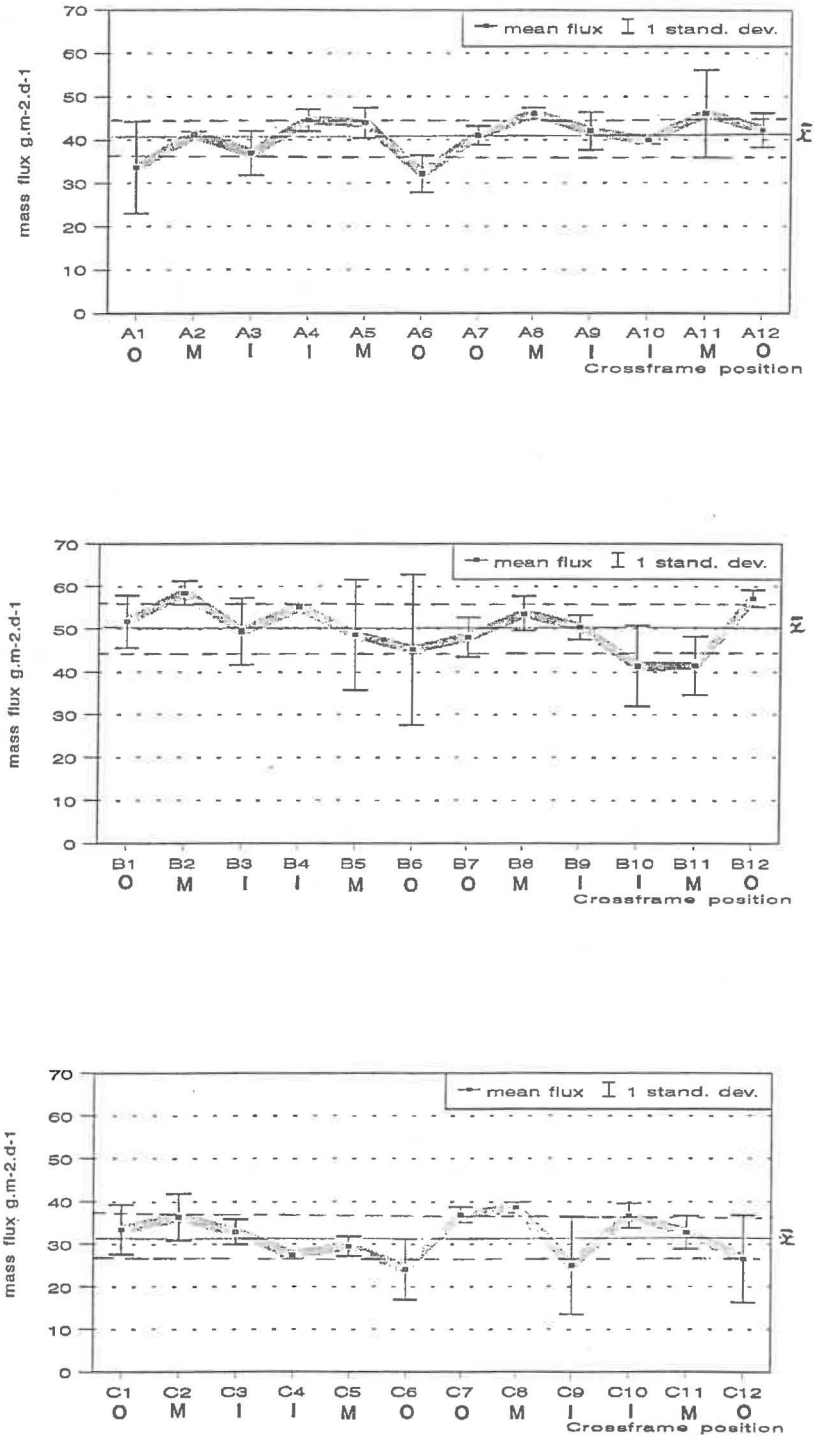

Fig. 2.16 Effect of trap cross-frame position on average mass fluxes (± 1 standard deviation) in Evans Bay, Wellington Harbour, in August 1994 (Experiment II). Along x-axis, **A, B** and **C** refer to the randomly chosen sites, **1-12** to cross-frame position and **O, M** and **I** to whether the traps were in "outer", "middle" or "inner" positions. Traps were deployed 3 m above the sea-floor in water depths of 18 m (Sites A and B) and 17 m (Site C).

homogeneity of the sampling environment, may have been violated since the three mooring sites have significantly different mean fluxes with 41 g m^{-2} d^{-1} at site A, 50 at site B and 32 at site C. Standard deviations ranged from 11-16% of the mean (Table 2.5, Fig 2.16). ANOVA tests indicate that while sites A and B are statistically similar, fluxes measured at both of these sites are significantly different to those at site C (d.f. = 2, 4; F = 16.50; P = 0.00).

These differences can be explained by: (a) analytical errors arising from problems with several defective filters detected during the filtration of subsamples from site C, and the loss of material from several samples during the weighing-drying process; and (b) the deployment of traps at site C in slightly shallower water (traps at a depth of 13.7 m in 16.8 m) than the other sites (traps at approximately 15 m in 18 m), where one may expect more wave-induced turbulence. This environmental effect could have led to increased penetration of eddies into trap cylinders, thereby reducing the amount of collected material due to increased flushing effects (e.g., Hawley, 1988).

The overnight capping of the traps at site A seems to have affected intra-trap mixing processes with the red dye in the traps distributed homogeneously throughout each recovered cylinder. It is proposed that the plastic bag used as a cap on each trap acted as a diaphram that transmitted vertical motions arising from surface wave activity into the traps, causing the trap contents to become extremely well mixed. The effect of this process on measured mass fluxes is unknown. Furthermore, the higher fluxes at site B can be partially explained by the longer deployment time due to the initial loss of the array.

2.4.3. Experiment III: Effect of baffles

Baffles are used widely in many sediment trap applications to minimise trap turbulence, although the actual effect of baffles has not been tested rigorously. Gardner (1980b) suggested that baffles may improve relative trapping efficiency, particularly in cones (e.g., Soutar et al., 1977), and that for cylinders, baffles should have aspect ratios of between 2-6. In field experiments, deep baffles also caused preferential collection of particles <63 mm in size (Gardner, 1980b). Butman (1986) indicated that relative particle collection efficiency

was increased in cylinders with identical aspect ratios (~3.0) by as much as 160% by using baffles with individual aspect ratios of ~8.0. In contrast, unpublished results from the VERTEX programme suggest that baffles may result in slight decreases in the collection of marine particulates, and that relatively consistent trapping efficiency may be achieved at baffle lengths greater than about 7 cm (Martin et al., *in* U.S. GOFS Report 10, 1989). In this unpublished study by Martin et al., deep baffles were also found to be associated with apparent increases in flushing rates while, in general, zooplankton "swimmer" effects were reduced by using baffles of any design.

In order to evaluate the effect of baffles on the sediment trapping efficiency of NZOI-NIWA traps, sediment trap Experiment III was conducted in Evans Bay in March 1995 (early austral autumn) to investigate the following null hypothesis:

That baffles make no difference to the trapping efficiency of traps placed at any position on a moored NZOI-NIWA sediment trap cross-frame array.

Once again, assumptions regarding site effects were made, although, based on the results from the previous experiment, sites were restricted to certain water depths so as to minimise the site differences apparent from the earlier Experiment II (Section 2.4.2). An Aanderaa current meter and vane was connected to the NZOI-NIWA permanent test-stand immediately prior to the first sediment trap deployment. Three trap arrays were bottom moored at random locations on 28 March 1995, each with cross-frames fitted with six randomly chosen baffled and six unbaffled cylinders. Based on the results from Experiment II, no mooring was located in water depths shallower than 16 m to minimise possible wave stirring activity as suggested by results at site C from the earlier experiment (Section 2.4.2). In Experiment III, each array was successfully recovered on the following day (29 March 1995), and trap contents overlying the dyed brine-sea-water interface immediately aspirated off in the laboratory. At site C, the plastic cap was left on the trap at position 6 on the cross-frame, thereby acting as a surrogate control. Aliquots of approximately 100 ml of trap solution were filtered in triplicate onto pre-weighed 0.2 μm Nuclepore filters for mass flux analyses for each cylinder.

Mass fluxes measured at each site during Experiment III ranged from 27-47 g m^{-2} d^{-1} and suggested that the trapping efficiency of NZOI-NIWA traps is not significantly affected by

Table 2.6 Effect of baffles on mass flux determinations from Experiment III conducted in Evans Bay, Wellington Harbour, in March 1995. Traps were deployed 3 metres above the sea-floor in water depths of 18 (Sites A and B) and 17 m (Site C). Note ANOVA analysis (α=0.05) indicates that there are no significant differences between baffled and unbaffled traps, nor between sites.

Trap number† Site A	Mass fluxes ($g\ m^{-2}\ d^{-1}$)§ Site A	Trap number† Site B	Mass fluxes ($g\ m^{-2}\ d^{-1}$)§ Site B	Trap number† Site C	Mass fluxes ($g\ m^{-2}\ d^{-1}$)§ Site C
1 (O)	41.27±0.77	1 (O) **B**	39.90±1.25	1 (O) **B**	34.09±2.39
2 (M)	46.85±0.40	2 (M)	42.30±1.43	2 (M)	34.12±0.80
3 (I) **B**	37.50±0.64	3 (I) **B**	42.94±0.37	3 (I)	40.14±1.74
4 (I) **B**	39.02±0.55	4 (I)	40.82±1.34	4 (I) **B**	38.59±0.66
5 (M)	34.07±0.93	5 (M) **B**	27.26±1.09	5 (M)	41.76±1.98
6 (O)	38.57±0.75	6 (O) **B**	41.82±1.54	6 (O) **B***	0.49±0.08
7 (O) **B**	38.46±2.32	7 (O)	31.67±1.16	7 (O)	47.28±1.51
8 (M)	37.97±1.74	8 (M)	34.47±1.53	8 (M) **B**	38.95±1.31
9 (I) **B**	30.34±0.71	9 (I) **B**	34.57±1.33	9 (I)	43.27±2.41
10 (I) **B**	34.66±1.04	10 (I) **B**	40.05±0.52	10 (I) **B**	29.97±1.87
11 (M) **B**	35.32±1.60	11 (M)	35.92±0.81	11 (M) **B**	33.26±1.82
12 (O)	40.64±0.16	12 (O)	42.92±1.59	12 (O)	38.15±2.64

Site mean, $\bar{x}$	37.89	37.89	38.14*
Site standard deviation, s	4.16	5.06	5.01
Baffled $\bar{x}_b$	35.88	37.76	34.97**
Baffled s_b	3.21	5.89	3.80
Unbaffled $\bar{x}_{ub}$	39.90	38.02	40.79
Unbaffled s_{ub}	4.25	4.64	4.50
Overall $\bar{x}$	37.97 (n=35)		
Overall s	4.61		

* n=11; cylinder 6 remained capped during experiment so data from this trap has been excluded.

** n=5 since data from cylinder 6 has been excluded.

† Number corresponds to position of trap cylinder on trap cross-frame; **I** = inner position on cross-frame, **M** = middle position, **O** = outer position, **B** = cylinders with baffles.

§ Average mass fluxes ± 1 standard deviation are given; n=3 in each case.

baffles (d.f. = 1, 4; F = 4.08; P = 0.181; power = 0.071; Table 2.6, Fig. 2.17). Note that tests between sites and interaction terms have one less degree of freedom than the general model described above for Experiment II because one trap at site C could not be used in the analysis, so that a mean value from all the traps at site C was used instead. There was no consistent pattern in flux at each site that could be tested statistically and attributed solely to a "baffle effect", although on average baffled traps seemed to collect slightly less than the overall mass flux mean of 37.97±4.61 g m^{-2} d^{-1} (n=35), whereas unbaffled traps collected slightly more than the overall mean, on average (Table 2.6). Currents at the height of the traps were generally between 2-7 cm s^{-1}, with a period of variable southward-directed flows on 28 March and stronger northward-flowing currents on 29 March. The water temperature was 17°C.

To investigate the effectiveness of baffles as zooplankton "swimmer" deterrents (e.g., Martin et al., *in* U.S. GOFS Report, 1989), identifiable zooplankton "swimmers" from Evans Bay were collected on a 200 μm mesh and enumerated (Table 2.7). Some inter-site variability is suggested by the "swimmer" data, and there are no substantial differences between the plankton collected by unbaffled and baffled traps, except at Site A. At sites A and B, the mean number of active "swimmers", represented by copepods and a ?polychaete species, in baffled traps was on average less than those recovered from unbaffled traps. Martin et al. (unpublished results, *in* U.S. GOFS Report 10, 1989) observed a similar trend as at sites A and B. The opposite trend was observed at site C (Table 2.7). For non-active plankton, such as passively settling diatoms, it seems that unbaffled traps collected slightly less on average, than baffled traps.

2.4.4. Experiment IV: Effect of brine volume

A dichotomy exists within the international sediment trap community regarding the manner in which high-density brines should be used in field studies using free-floating trap arrays. Traps are either filled up completely with brine, as in the VERTEX programme (Knauer et al., 1979) and at the two JGOFS time-series stations at Hawaii (Karl et al., 1990, 1996) and Bermuda (Lohrenz et al., 1992; Michaels & Knap, 1996), or are back-filled with a specific volume of brine that is markedly less than the total volume of the trap (e.g., Lee et al., 1992).

Evans Bay III

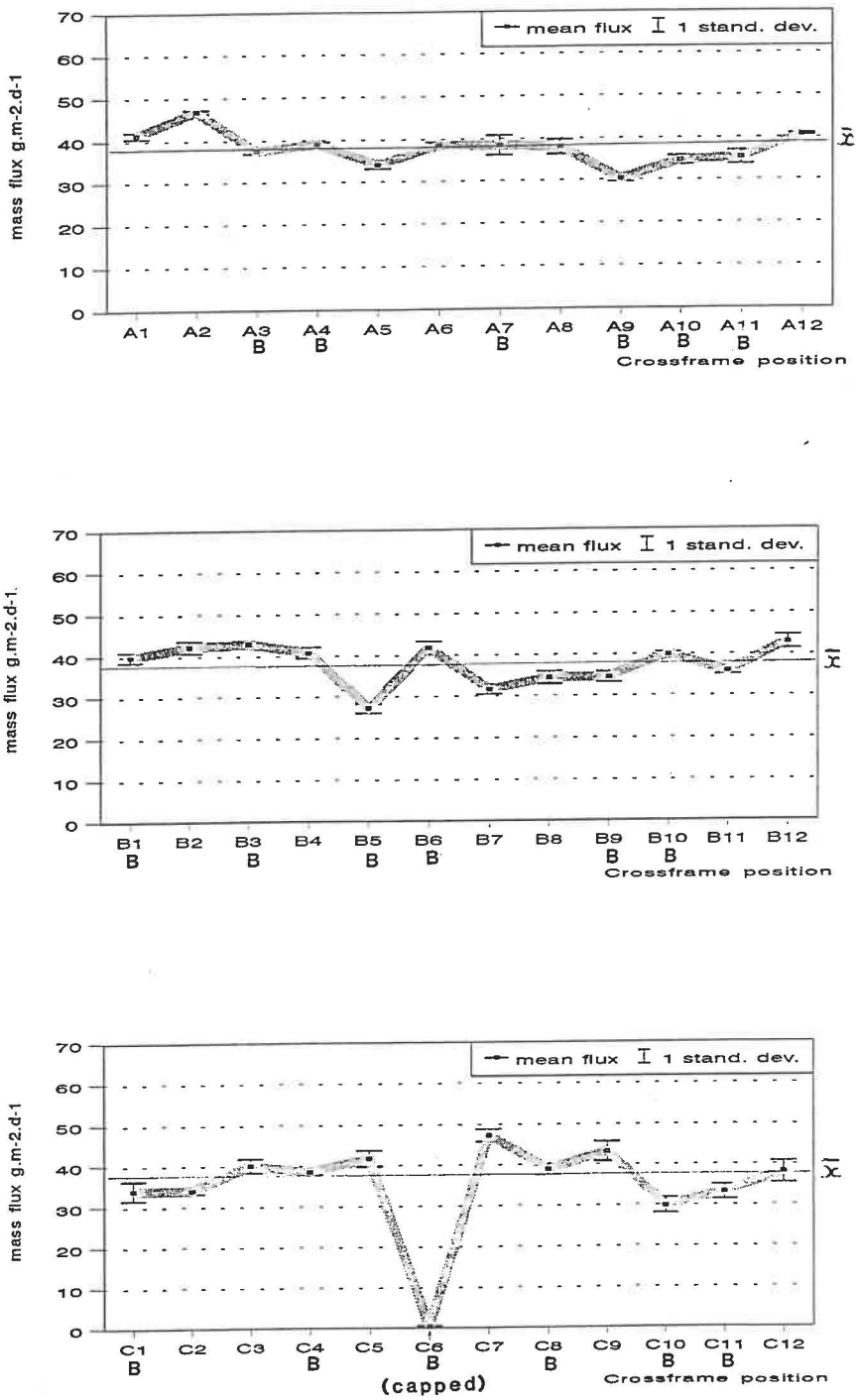

Fig. 2.17 Effect of baffles on average mass fluxes (± 1 standard deviation) in Evans Bay, Wellington Harbour, in March 1995 (Experiment III). Along x-axis, **A**, **B** and **C** refer to the randomly chosen sites, **1-12** to cross-frame position and **B** to whether traps were baffled or not (unlabeled). Traps were deployed 3 m above the sea-floor in water depths of 17 m (Sites A and C) and 17.5 m (Site B).

Table 2.7 Effect of baffles on average zooplankton "swimmers" abundance in Evans Bay sediment trap Experiment III in March 1995.

		Mean zooplankton "swimmer" (>200 μm) abundance*				
		Copepods	?Polychaetes	Medusae	Large worms	Diatoms
Site A	Baffled	65.50±24.98	28.83±5.74	6.00±5.51	2.50±1.64	12.50±6.92
	Unbaffled	92.83±34.98	38.17±15.80	7.17±3.87	3.67±1.51	9.50±3.08
Site B	Baffled	50.4±10.31	24.80±9.23	6.00±3.67	0.80±0.84	5.60±3.58
	Unbaffled	67.25±10.01	23.75±7.41	4.00±1.83	1.75±1.83	6.50±3.70
Site C	Baffled	63.20±18.30	24.20±10.83	2.00±0.71	2.00±0.71	8.80±3.42
	Unbaffled	40.00±5.34	21.00±6.00	0.60±0.55	1.40±1.14	8.20±4.09
All sites**	$\bar{x} \pm s_{baffled}$	60.06±19.28	26.13±8.35	4.75±4.19	1.81±1.33	9.19±5.59
	$\bar{x} \pm s_{unbaffled}$	68.40±31.79	28.60±13.34	4.13±3.82	2.40±1.55	8.27±3.56

* Average values ± 1 standard deviation are shown; typically, n = 4-6

** For baffled traps, n = 16; for unbaffled traps, n = 15

There are valid hydrodynamical reasons for arguing against the former practice since the addition of a high-density brine acts as a "false" bottom within the trap, thereby altering the trap's aspect ratio (Gardner, 1979; U.S. GOFS Report 10, 1989). Since aspect ratio is a critical factor affecting sediment trapping efficiency (e.g., Gardner, 1980a; Butman, 1986; Butman et al., 1986; and others), U.S. GOFS Report 10 (1989) recommended that a brine volume equivalent to a brine height of 1-trap diameter should be sufficient to ensure that trapping efficiency is not compromised.

The final field experiment (IV) in the series examining aspects of sediment trapping efficiency of the NZOI-NIWA trap system was conducted from 7-8 June 1995 (austral mid-winter) in Evans Bay, Wellington Harbour. This experiment was designed to test the following null hypothesis:

That brine volume does not influence the trapping efficiency of traps placed at any position on a moored NZOI-NIWA sediment trap cross-frame array.

Individual traps were either filled completely with a high-density, formalin-poisoned brine solution, as used in previous Evans Bay experiments, or back-filled with brine volumes equivalent to a brine height of either 2.5-trap diameters (as used during NZOI-NIWA research voyages 3009 and 3014 in 1993; Chapter 5) or 1-trap diameter, as recommended by U.S. GOFS Report 10 (1989). Three locations, spaced randomly around the permanent NZOI-NIWA test-stand in Evans Bay, were occupied by bottom-moored trap arrays for a period of 1 day. An Aanderaa current meter that was connected to the test-stand in March 1995 (Evans Bay Experiment III) remained there for the duration of the present investigation, and was not recovered until early July. Weather conditions during the sediment trap deployment period in June 1995 were extremely good with light northerly winds (5-7 knots, up to 10) and very calm to gently rippled seas. Accordingly, SCUBA divers used during the deployment and recovery phases reported clear water with visibility of between 2-5 m, compared to 1-2 m on previous dives when sea and weather conditions were moderately rough (10-20 knot southerly winds, 1 m wind-waves).

As in previous experiments, upon recovery, sea-water overlying the brine in each trap was aspirated off in the laboratory, and triplicate 100 ml aliquots of trap solution filtered onto pre-weighed 0.2 μm Nuclepore filters to determine mass flux differences between trap

Table 2.8 Effect of brine on mass flux determinations during Experiment IV conducted in Evans Bay, Wellington Harbour, in June 1995. Traps were deployed 3 metres above the sea-floor in water depths of 15 m (all sites). Note ANOVA analysis (α=0.05) indicates that there are no significant differences between brine-filled or unfilled traps, nor between sites.

Trap number†	Mass fluxes ($g\ m^{-2}\ d^{-1}$)§	Trap number†	Mass fluxes ($g\ m^{-2}\ d^{-1}$)§	Trap number†	Mass fluxes ($g\ m^{-2}\ d^{-1}$)§
Site A	Site A	Site B	Site B	Site C	Site C
1 (O) **2.5D**	9.52±0.59	1 (O) **F**	4.48±0.20	1 (O) **2.5D**	11.04±2.90
2 (M) **1D**	11.33±1.02	2 (M) **1D**	6.58±0.06	2 (M) **F**	5.93±0.25
3 (I) **F**	3.39±1.66	3 (I) **2.5D**	12.33±0.13	3 (I) **1D**	8.94±2.03
4 (I) **2.5D**	8.56±0.73	4 (I) **F**	3.72±0.52	4 (I) **F**	4.00±0.63
5 (M) **1D**	8.76±0.99	5 (M) **2.5D**	6.10±0.34	5 (M) **2.5D**	7.69±0.73
6 (O) **F**	5.73±0.36	6 (O) **2.5D**	7.07±0.44	6 (O) **1D**	8.61±1.28
7 (O) **1D**	9.54±0.81	7 (O) **1D**	5.79±0.14	7 (O) **1D**	8.17±0.18
8 (M) **2.5D**	8.67±2.52	8 (M) **F**	2.40±0.25	8 (M) **2.5D**	8.90±2.22
9 (I) **2.5D**	10.26±1.00	9 (I) **2.5D**	6.62±0.16	9 (I) **F**	4.70±0.05
10 (I) **F**	3.91±0.72	10 (I) **1D**	11.99±0.33	10 (I) **F**	5.64±0.62
11 (M) **F**	4.39±0.68	11 (M) **1D**	5.31±0.40	11 (M) **1D**	7.66±1.27
12 (O) **1D**	9.95±0.32	12 (O) **F**	5.60±0.51	12 (O) **2.5D**	9.60±0.66
$\bar{x}$	7.83		6.50		7.57
s	2.73		2.95		2.10
$\bar{x}_{1D}$	9.90		7.42		8.35
s_{1D}	1.08		3.09		0.56
$\bar{x}_{2.5D}$	9.25		8.03		9.31
$s_{2.5D}$	0.80		2.89		1.40
$\bar{x}_{FULL}$	4.36		4.05		5.07
s_{FULL}	1.00		1.34		0.88
Overall $\bar{x}$	7.30 (n=36)				
Overall s	2.61				

† Number corresponds to position of trap cylinder on trap cross-frame; **I** = inner position on cross-frame, **M** = middle position, **O** = outer position. **1D** = cylinders with basal brine corresponding to a height of the trap's external diameter (9.5 cm), **2.5D** = basal brine equivalent to 2.5 x height of the trap's external diameter, **F** = trap completely filled with brine.

§ Average mass fluxes ± 1 standard deviation are given; n=3 in each case, except for cylinder 8 at site A where n=2.

cylinders. It should be noted that, although it was intended to use volumes equivalent to exactly 1D- and 2.5D-brine heights (0.576 l and 1.472 l, respectively), it was not feasible to replicate these amounts for each trap due to bubbling during the back-filling process. Accordingly, actual brine volumes for the "1D" traps ranged from 0.960 to 2.016 l (average 1.536±0.353 l, ±1 standard deviation) and for the "2.5D" traps volumes were between 1.600 and 3.136 l with an average brine volume in these traps of 2.437±0.386 l. Traps filled with brine were recovered with variable amounts of high-density solution. There was only minimal leakage from traps during pre-deployment and post-recovery phases, so that the loss of solution may be related to upper trap flushing processes during the deployment period (e.g., Gardner, 1980a; Hawley, 1988). Trap volumes in the "FULL" traps ranged from as low as 2.432 l to a maximum of 5.856 l with an average brine volume in "FULL" traps of 4.460±1.183 l, out of a total trap volume of 6.044 l.

In general, the mean fluxes recorded on this very calm day in winter during Experiment IV were substantially less than the fluxes observed in other months in Evans Bay (Table 2.8 cf. Tables 2.3 and 2.4), ranging from 2 to 12 g m^{-2} d^{-1}. Current meter records collected at this time indicate that flows at the height of the moored traps were less than 5 cm s^{-1} and variable in direction (slightly to the north). The water temperature was 11°C. Furthermore, fluxes calculated for traps that were filled completely with brine were significantly different to fluxes derived from other traps (d.f. = 2, 4; F = 42.73; P = 0.002; power = 0.68). Fluxes in brine-filled traps were typically 2-3 times less than those fluxes from traps containing less brine (Table 2.8, Fig. 2.18). There was no clear pattern between those traps filled with 1D-brine volume, compared with those filled with 2.5D, although there was a tendency for the latter to trap slightly more material (Table 2.8, Fig. 2.18). These results confirm previous assertions that cylindrical traps filled completely with a high-density brine solution may under-estimate actual particulate fluxes. Therefore, important time-series sediment trap studies conducted at JGOFS sites in central equatorial Pacific and off Bermuda may be compromised, and may provide one possible explanation for the perceived failure of traps to accurately measure export flux (e.g., Buesseler, 1991; Buesseler et al., 1992, 1994; Michaels et al., 1994; Murnane et al., 1996).

EVANS BAY IV

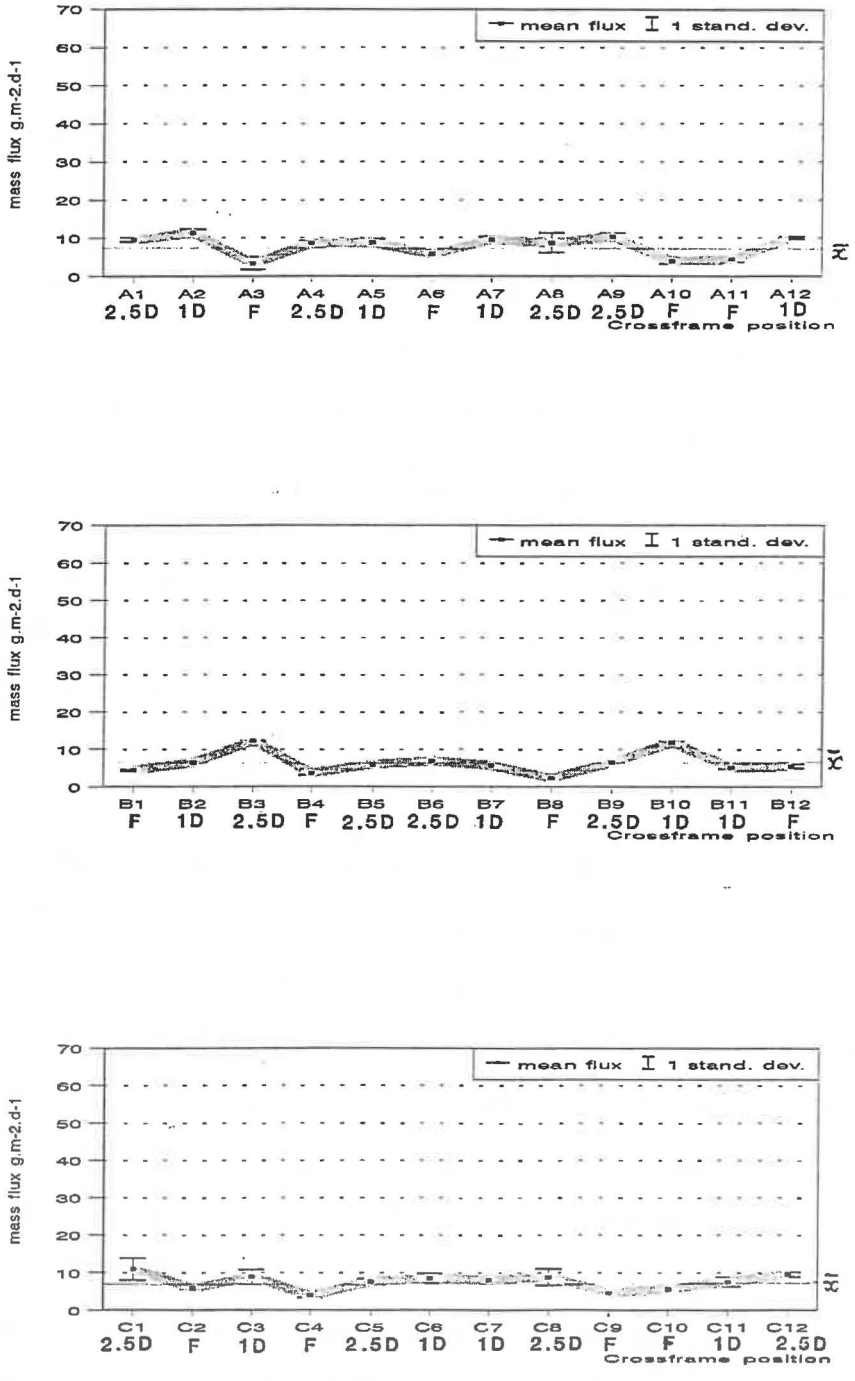

Fig. 2.18 Effect of brine volume on average mass fluxes (± 1 standard deviation) in Evans Bay, Wellington Harbour, in June 1995 (Experiment IV). Along x-axis, **A**, **B** and **C** refer to the randomly chosen sites, **1-12** to cross-frame position and **1D**, **2.5D** and **F** to volume of brine originally added to the traps; the two former volumes correspond to basal brines with heights above trap bottom of 1 and 2.5 trap diameters, respectively, and the latter (**F**) refers to traps that were filled completely with brine. Traps were deployed 3 m above the sea-floor in water depths of 15 m (all sites).

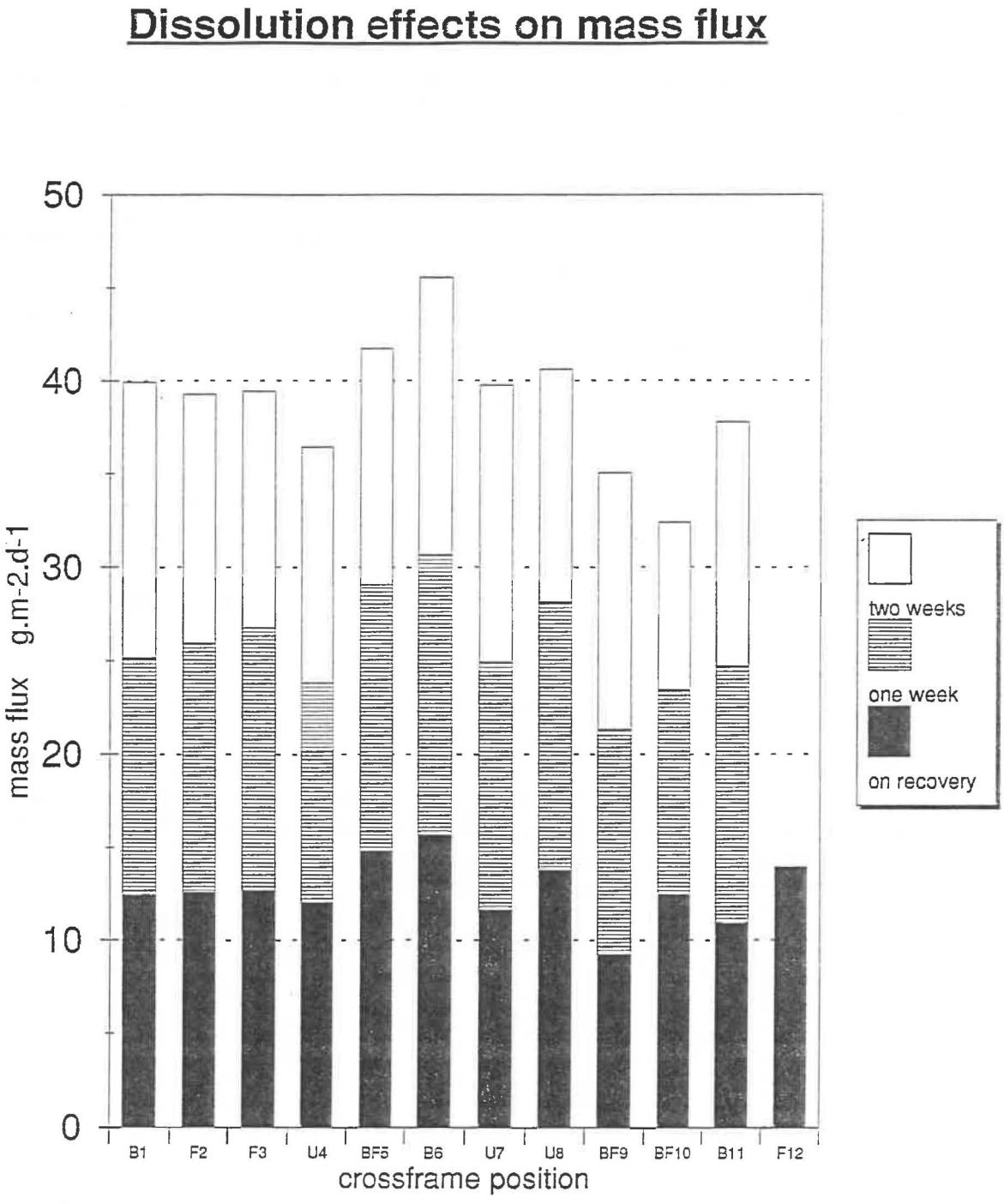

Fig. 2.19 Dissolution effects on mass flux over a two week period using sediment trap samples collected from Evans Bay, Wellington Harbour, in November 1993 (Experiment I). Trap solutions comprised a dyed 5% excess NaCl brine poisoned with 1% formalin. Along x axis, **1-12** refer to trap cross-frame position and **B**, **BF**, **U** and **F** relate to different trap treatments (refer to Table 2.3 for details).

Table 2.9 Changes in mass flux over a two week period from sediment trap samples collected in Evans Bay, Wellington Harbour, in November 1993 during Experiment I.

Trap number†	Mass flux upon recovery ($g\ m^{-2}\ d^{-1}$)	Mass flux after 1 week ($g\ m^{-2}\ d^{-1}$)	Mass flux after 2 weeks ($g\ m^{-2}\ d^{-1}$)	Average mass flux ± 1 *s* ($g\ m^{-2}\ d^{-1}$)	% difference* & % rate of change d^{-1}
1	27.63	28.87	29.07	28.52±0.78	105 (+0.4)
2	15.32	16.92	15.53	15.92±0.87	101 (+0.1)
3	15.47	17.41	15.40	16.09±1.14	100 (0.0)
4	33.46	33.70	35.00	34.05±0.83	105 (+0.4)
5	16.24	16.61	16.32	16.39±0.20	101 (+0.1)
6	32.22	31.81	30.85	31.63±0.70	96 (-0.3)
7	25.77	29.24	27.12	27.38±1.75	105 (+0.4)
8	29.74	31.50	29.52	30.25±1.89	99 (-0.1)
9	18.47	-	17.94	18.21±0.37	97 (-0.2)
10	15.37	15.54	16.09	15.66±0.38	105 (+0.4)
11	22.93	23.72	-	23.33±0.56	(104) (+0.3)
12	16.78	17.44	17.56	17.26±0.42	105 (+0.4)

† Number corresponds to position of trap cylinder on trap cross-frame.

* % difference = ($Flux_{at\ 2\ weeks}/Flux_{upon\ recovery}$ x 100), except for Trap 11.

2.4.5. Experiment V: Effectiveness of formalin as a preservative

An experiment to investigate dissolution rates in formalin-preserved trap samples was undertaken by retaining trap solutions from Experiment I in the dark and measuring the changes in total mass measurements over a period of 2 weeks. Subsamples were taken from each volume using measuring cylinders after agitating thoroughly the total sample between subsampling.

The sequential dissolution experiments indicate that there was only limited change in mass flux (typically <10%) over a two week period for sedimenting material collected in Evans Bay (Fig. 2.19). Many of the subsamples taken from the same cylinder actually revealed a slight increase in flux with time which was probably due to analytical errors associated with the technique or may reflect an enhancement in particle production, possibly by microbial activity (e.g., Ducklow et al., 1985). Previous incubation experiments using marine organic matter collected in shallow water sediment traps (<250 m) deployed for short periods (4-6 days) suggest decomposition rates that range from 3-8% d^{-1} (e.g., Iturriaga, 1979; Lorenzen et al., 1983b). These rates are an order of magnitude higher than the measurements suggested by this study (i.e., ±0.1-0.4% d^{-1}, Table 2.9). The decay of organic matter in deep ocean traps, on the other hand, occurs at similar rates (e.g., 0.1-1.0% d^{-1}, Gardner et al., 1983; Khripounoff & Crassous, 1994), suggesting that the material collected in Evans Bay may be predominantly refractory in nature. The observed increases in apparent mass flux with time are unlikely to be due to bacterial growth. Although the traps were recovered at the end of the Experiment I deployment with their inner walls covered with an organic slime which may host high densities and numbers of bacteria (e.g., Ducklow et al., 1985), it is recognised that formalin inhibits significantly bacterial production (e.g., Knauer et al., 1984; Lee et al., 1992; Hedges et al., 1993). The slight differences between mass fluxes measured over a 2-week period (range 1-23%, average 6%) are within expected errors of the subsampling technique (±10%, range 3-27%, Table 2.2), and therefore can be ignored.

2.5. Summary of Chapter 2

(1) A sediment trap system was designed and constructed at New Zealand Oceanographic Institute, NIWA, in 1992. An overall conservative design strategy was adopted since environmental conditions at proposed open ocean sampling sites near and within the Subtropical Convergence were poorly known. Since free-floating deloyments were to be undertaken in the New Zealand JGOFS field work planned for winter and spring 1993, the favoured design concept was to manufacture cylindrical polycarbonate traps with removeable baffles that could be mounted on stainless steel cross-frames holding 8 or 12 traps. Basal high-density brine solutions containing formalin as a poison/preservative would be used to maximise sample integrity over the planned deployment periods of 2-3 days. Laboratory analyses (for total mass, particulate carbon, nitrogen and phosphorus) would follow the protocols adopted by the Hawaiian Ocean Time-series programme (Karl et al., 1990).

(2) A sediment trap pilot study in subtropical waters on the northern flank of Chatham Rise in autumn 1992 was undertaken to assess the practicality of sediment trap deployments by NZOI-NIWA. The one deployment that was conducted was successful, and highlighted several logistic requirements that would have to be met for future trap deployments, including using less trap solution for mass flux determinations (problems with filter clogging), laboratory ventilation and brine dispensing. Results from this voyage indicated that resuspension of bottom sediments from the crest of the Rise is likely to be an important source of sinking particulate material. Trap samples were enriched in refractory carbon, relative to nitrogen and phosphorus, with Redfield ratios of 155-287:17-22:1 over sampled water depths of 200, 300 and 500 m. Mass fluxes at 200 m were similar to export flux measurements made at other oligotrophic oceanic sites (e.g., Lohrenz et al., 1992; Karl et al., 1996).

(3) A second pilot study in autumn 1993 in Cook Strait highlighted the potential significance of the strait as a zone of active sediment transport, with mass fluxes measured over just 1 day that were generally two orders of magnitude higher than similar fluxes measured at other continental shelf sites (e.g., Monaco et al., 1990; Landry et al., 1992).

Problems with high sediment loading in trap samples were encountered during filtration, despite filtering smaller volumes of trap solution than were used in the previous pilot study. Thus, statistical analysis to investigate the effects of inter-trap hydrodynamic biases and baffles on trapping efficiency could not be attempted.

(4) Four field and one laboratory experiment were conducted in Evans Bay, Wellington Harbour, to evaluate statistically the effects on trapping efficiency of inter-trap interactions, baffles and brine volume, and the effectiveness of formalin as a preservative. The first experiment (I) was compromised by lack of integrity of filtered mass flux samples due to excessive sediment loading arising from the traps being deployed for 6 days. A second experiment (II) was undertaken to determine whether cross-frame position affected the trapping efficiency of the NZOI-NIWA traps using three randomly chosen mooring sites in Evans Bay. Traps were deployed unavoidably for 5-6 days. Although strong inter-site differences were apparent, there were no significant differences in trapping efficiency due to cross-frame position, supporting previous assertions from flume studies (e.g., Gardner, 1980a; Butman, 1984, *in* U.S. GOFS Report 10, 1989).

(5) Experiment III, to evaluate the effect of baffles on trapping efficiency, had a statistical sampling design similar to that employed in Experiment II. After a 1 day deployment, three moorings were recovered and trap samples analysed for mass flux, which indicated that sediment trap efficiency was not significantly affected by baffles. Baffles may have reduced slightly the impact of zooplankton "swimmer" contamination (although not statistically validated). In Experiment IV the effect of different brine volumes on trapping efficiency was investigated, and indicated that traps filled completely with high-density brine solution, as used in many other JGOFS-affiliated studies (e.g., Martin et al., 1993; Lohrenz et al., 1992; Karl et al., 1996), collected 2-3 times less material than traps only partially filled with a basal brine. Finally, a two week dissolution experiment (V) indicated that formalin is an effective preservative of trapped material collected in Evans Bay, with measured decomposition rates of $<0.5\%\ d^{-1}$.

Chapter 3

THE BIO-PHYSICAL ENVIRONMENT OF CHATHAM RISE–SUBTROPICAL CONVERGENCE

Chapter 3

THE BIO-PHYSICAL ENVIRONMENT OF CHATHAM RISE AND SUBTROPICAL CONVERGENCE

3.1. Physical setting of Chatham Rise

3.1.1. Location and morphology

Chatham Rise is a broad, asymmetric submarine high, centred on ~43°30'S that extends 1700 km eastwards from Banks Peninsula on the east coast of South Island to approximately 500 km east of the Chatham Islands where it intersects the northern reaches of the Subantarctic Slope (CANZ, 1997; Fig. 3.1). Slopes on the northern flank of the Rise are typically steeper than those on the southern side, with maximum gradients of 1:5 compared to 1:25 (Krause, 1966). The northern margin descends to depths of 2500 m onto Hikurangi Plateau, a region of overthickened oceanic crust (10-15 km; Davy & Wood, 1994; Wood & Davy, 1994). The southern flank reaches depths of over 4000 m on the northern side of Bounty Trough, which is a starved rift basin of Cretaceous-Oligocene age that has also been an active conduit for sediment derived from Southern Alps erosion during late Cenozoic glaciations (e.g., Carter & Carter, 1993). Within the 500 m isobath, the crest of Chatham Rise ranges from 50 to 130 km in width, being narrowest in central regions at about 179°E (Fig. 3.1). Water depths along the gently undulating crest generally vary between 300-400 m, except at the Chatham Islands, which is the only presently emergent part of the Rise, and in the vicinity of four submerged banks, Mernoo, Veryan, Reserve and Matheson, all of which rise to within 200 m of the sea-surface (Fig. 3.1).

3.1.2. Tectonic setting and geological history

Chatham Rise is located to the south of the presently active, east-facing, obliquely convergent Hikurangi subduction-transform margin where the anomalously thick, oceanic

Pacific plate (Hikurangi Plateau, Davy & Wood, 1994) is being subducted beneath the continental Indo-Australian plate (e.g., Lewis & Pettinga, 1993). The Cretaceous-Cenozoic geological history of the Rise has been summarised by Wood et al. (1989) and Wood & Herzer (1993), and is outlined briefly here. Crustal thickness beneath Chatham Rise is estimated to be 23-26 km, thinning to the south towards Bounty Trough and east of Chatham Islands (Davy & Wood, 1994). Basement rocks on the Chatham Rise comprise Upper Paleozoic and Lower Mesozoic schists and greywackes of the Torlesse terrane (e.g., Norris, 1964; Wood et al., 1989). Extensional Late Cretaceous half-graben formation on normal faults occurred across entire Chatham Rise between 100-70 million years ago with half-grabens subsequently infilled by a >2 km-thick syn-tectonic sequence of terrestrial and shallow marine sediments (e.g., Wood et al., 1989; Carter & Carter, 1993; Barnes, 1994). Widespread calc-alkaline and basaltic volcanism accompanied Late Cretaceous extension and crustal subsidence (Wood et al., 1989; Wood & Herzer, 1993).

Early Cenozoic (Paleocene-Early Oligocene) sequences on the Rise thicken from less than 300 m on the crest to 1 km or more on the flanks, and are characterised by carbonate and authigenic sediments deposited in shelf-slope environments, punctuated by episodes of basaltic volcanism (Wood et al., 1989). Some Cretaceous faults underwent reactivation in the Eocene, creating localised depocentres over 500 m deep (e.g., Wood et al., 1989; Barnes, 1994). During the late Cenozoic, Chatham Rise remained tectonically stable and, as a consequence, sediments from this period are either absent or relatively thin over much of the Rise. Up to six periods (Wood & Herzer, 1993) of extensive erosion were interspersed with episodes of slow glauconitic and carbonate deposition. Extensive phosphatisation of lag gravels is inferred to have occurred during one phase of middle Late Miocene erosion in central and eastern parts of the Rise (e.g., Cullen, 1980; von Rad & Kudrass, 1984; Cullen, 1987). Since Pleistocene times, authigenic glauconitic greensand (40-80% of sediment samples; Norris, 1964) and foraminifera-rich carbonate sedimentation have persisted across the Rise, resulting in locally thick (<20 m) accummulations of sediment in topographic depressions along the crest (Norris, 1964; Pasho, 1976; McDougall, 1982; Falconer et al., 1984). Hemipelagic mud extends eastwards from South Island to 179°E, mantling northern and southern flanks of the Rise, while planktonic formanifera-rich oozes are common in Bounty Trough region. Little material has been introduced from external sources, except for

ice-rafted cobbles (Cullen, 1962), airborne volcanic deposits (Barnes & Shane, 1994; Carter et al., 1995) and aeolian dust deposited in glacial times (Stewart & Neall, 1984). Active normal faulting, including some reactivated Cretaceous and Eocene structures, is restricted primarily to the northwestern corner of the Rise in the North Mernoo Fault Zone (e.g., Lewis et al., 1985; Wood et al., 1989; Barnes, 1994). Within this zone, Barnes (1992) also described extensive scouring and deposition by late Quaternary mid-bathyal bottom currents. Localised areas on both the northern and southern slopes of Chatham Rise have undergone recent mass flows and slope failure (e.g., Barnes, 1992).

3.2. Physical oceanography

3.2.1. Water masses and fronts in Chatham Rise region

Water masses and fronts in the New Zealand region have been summarised by Deacon (1937), Wyrtki (1962), Heath (1985), Paterson & Whitworth (1990) and Tomczak & Godfrey (1994), among others. Of specific relevance to this study, however, is the distribution in space and time of the Subtropical Convergence (STC) and the oceanic water masses that are entrained into the frontal zone to the east of New Zealand (Fig. 3.2). To the south of the STC, **Subantarctic Surface** (SASW) and **Mode Waters** (SAMW) thicken northwards of the Antarctic Circumpolar Front (e.g., McCartney, 1977; Sievers & Nowlin, 1984). SAMW is characterised as a circum-polar, 300-700 m thick layer of nearly homogenous water, derived from deep vertical convective overturning in winter at the Subantarctic Front. Heath (1985) suggested that the weak thermal structure of surface waters on the Campbell Plateau (e.g., Heath & Bradford, 1980) may be attributed to SAMW formation. Throughout much of the South Pacific, a shallow oxygen minimum layer at 150-500 m lies above SAMW (e.g., Wyrtki, 1962; Paterson & Whitworth, 1990), with the overlying SASW identified by low temperatures and salinities and a weak oxygen maximum. This surface water mass is driven northwards from the Subantarctic Front by prevailing West Wind Drift, south of New Zealand. North of the STC, subtropical surface waters fill the upper 1 km of the Pacific Ocean, having formed as **Western South Pacific Central Water** (WSPCW) either within the STC between Tasmania and New Zealand (near 150°E; Szymanska & Tomczak, 1994) or in the Central Pacific Ocean (Heath, 1985).

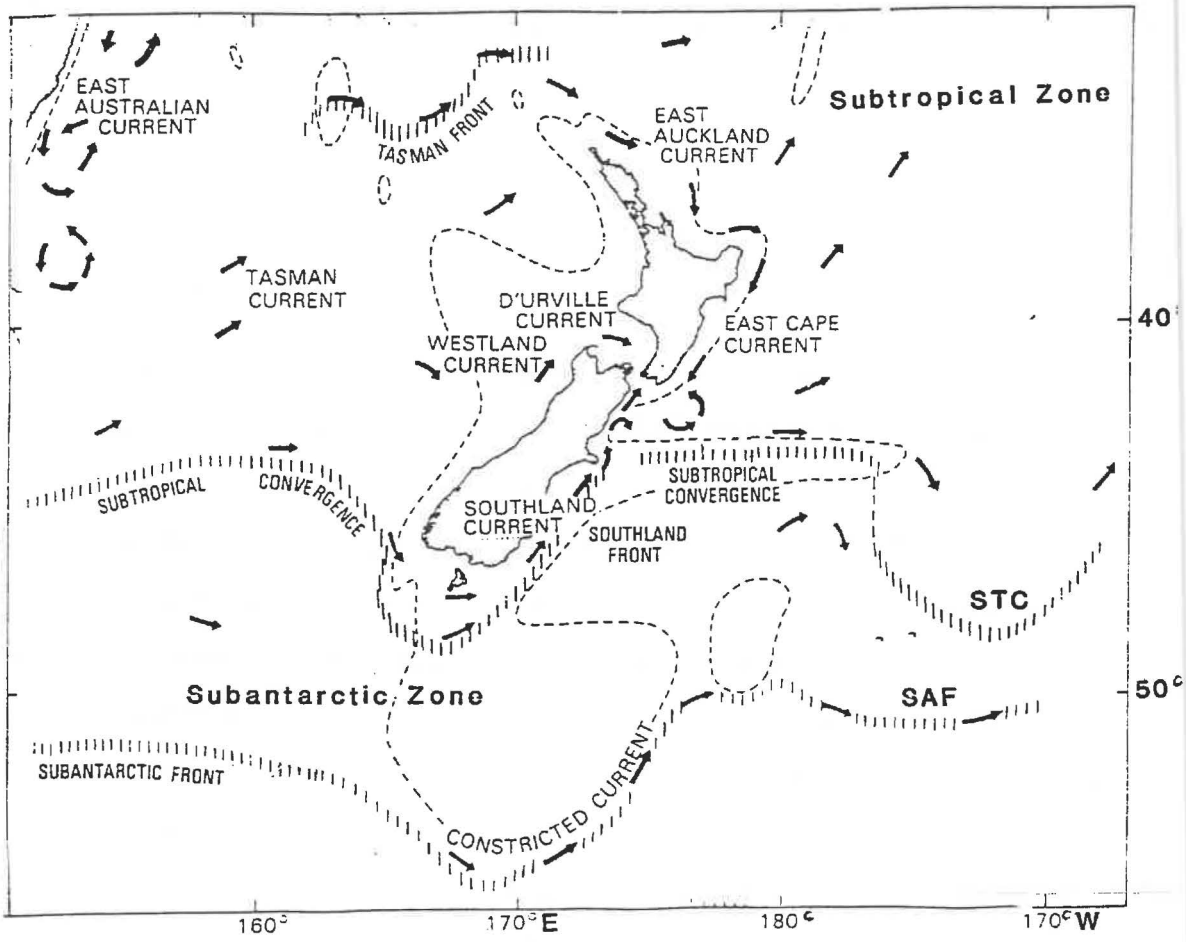

Fig. 3.2 Summary of ocean circulation patterns and position of fronts in Chatham Rise region (after Heath, 1985). STC = Subtropical Convergence, SAF = Subantarctic Front.

These northern and southern water masses meet at the STC which marks the zone in which warm (summer >15°C, winter >10°C), highly saline (35.7-35.8‰), nutrient-depleted subtropical waters to the north, interact and mix with cold (summer <14.5°C, winter <10°C), less saline (~34.5‰), nutrient-rich subantarctic waters to the south (Fig. 3.2). Early workers (e.g., Garner, 1959; Gilmour & Cole, 1979; Heath, 1975, 1981, 1985) identified the STC on the basis of surface temperature and salinity characteristics, such that the STC was regarded to follow the 10°C and 15°C surface isotherms in winter and summer, respectively, and the surface isohalines of 34.7-34.8‰, independent of season. Recent studies of Advanced Very High Resolution Radiometer (AVHRR) images over a 2 year period (1989-1990) by Chiswell (1994b) indicate that the STC zone is marked by pronounced gradients in temperature (i.e., over 2°C per 100 km) and has a winter sea-surface temperature range of 8-12°C in winter and 12-18°C in summer.

The New Zealand subcontinent intersects the west-east zonal passage of the STC across the south Tasman Sea and the South Pacific Ocean (e.g., Deacon, 1937). Compared with the east coast, the STC is more difficult to define accurately off the west coast of New Zealand. The STC frontal zone is located off the Fiordland coast (Chiswell, 1996), but is deflected south of here by the relatively shallow (<200 m) bathymetry of Puysegur Bank and Snares Platform (e.g., Stanton, 1973; Heath, 1975; Stanton & Ridgway, 1988; Butler et al., 1992 cf. Deacon, 1937; Wyrtki, 1962). The position of the frontal zone around southern New Zealand is therefore generally south of approximately 46°S latitude (Fig. 3.2). In central Tasman Sea between 40-44°S west of about 160°E, a strong southern front, centred on the 34.9‰ isohaline, and a weaker, less permanent northern front at 35.2‰ have been delineated within the STC, the latter influenced by both relic East Australia Current eddies and local wind field forcing (Jeffrey, 1986; Stanton & Ridgway, 1988). Recently, Szymanska and Tomczak (1994) have defined the Subtropical Front in the south Tasman Sea in summer as a region of enhanced sea-surface temperature and salinity gradients *within* the STC, as positioned by the 34.8‰ isohaline and the 13°C isotherm.

Along the east coast of South Island, New Zealand, warm, coastal surface waters are separated from cooler, offshore subantarctic waters by the Southland Front which is associated with the northwards-flowing Southland Current (e.g., Burling, 1961; Jillett, 1969; Heath, 1972; Chiswell, 1996). From satellite-derived sea-surface temperature data, the Southland Front exhibits limited spatial variability, but its strength is modulated annually, being strongest in winter (Chiswell, 1994b). Between Banks Peninsula and Kaikoura, a component of the Southland Current diverges eastwards and flows along the northern and southern flanks of the Chatham Rise (Barnes, 1985 cf. Heath, 1981). The northernmost flow bifurcation interacts and becomes mixed with southwards-flowing subtropical East Cape Current (Heath, 1972, 1981). Semi-permanent anticyclonic eddies have developed off southeast coast of North Island (e.g., Barnes, 1985; Vincent et al., 1991), presumably in response to the interaction between Southland and East Cape Currents. Evidence for flow within the southern bifurcation of the Southland Current on the Chatham Rise may be provided by Ridgway (1975) who suggested that a shallow trough in sea-surface elevation, relative to 200 dbar, indicated an easterly zonal flow at about 45°S. Ridgway (1975) also interpreted this zonal flow to represent the position of the STC. Thus, in this region, the STC is restricted geographically along Chatham Rise, paralleling the crest of the Rise out towards the Chatham Islands (Fig. 3.2), possibly due to the interplay of flows within the Southland and East Cape currents. East of the Chatham Rise, although data coverage is sparse, it appears that the STC swings abruptly towards the south (Ridgway, 1975) as the eastern flank of Chatham Rise becomes more submerged. Recently, Stramma et al. (1995) advocated the existence of a weak (i.e., geostrophic surface current <10 m s^{-1}, upper 1000 m transport <5 Sv) flow, referred to as the South Pacific Current (SPC) within the STC (or Subtropical Front, as preferred by these authors) to the east of the Chatham Islands. This current originated supposedly from the interaction between subtropical waters carried around southern New Zealand by the Southland Current and a larger volume (up to 6-9 Sv) of subtropical water derived from the north via the East Auckland and East Cape Currents. Furthermore, the SPC is inferred to act as a barrier to the northwards dispersal of Antarctic Intermediate Water and Subantarctic Mode Water and forms the southern closure of the South Pacific subtropical gyre (Stramma et al., 1995). A recent global ocean eddy-resolving circulation model suggests, however, that the strong jet streams associated with the ACC may mask the importance of the SPC (Semtner & Chervin, 1992).

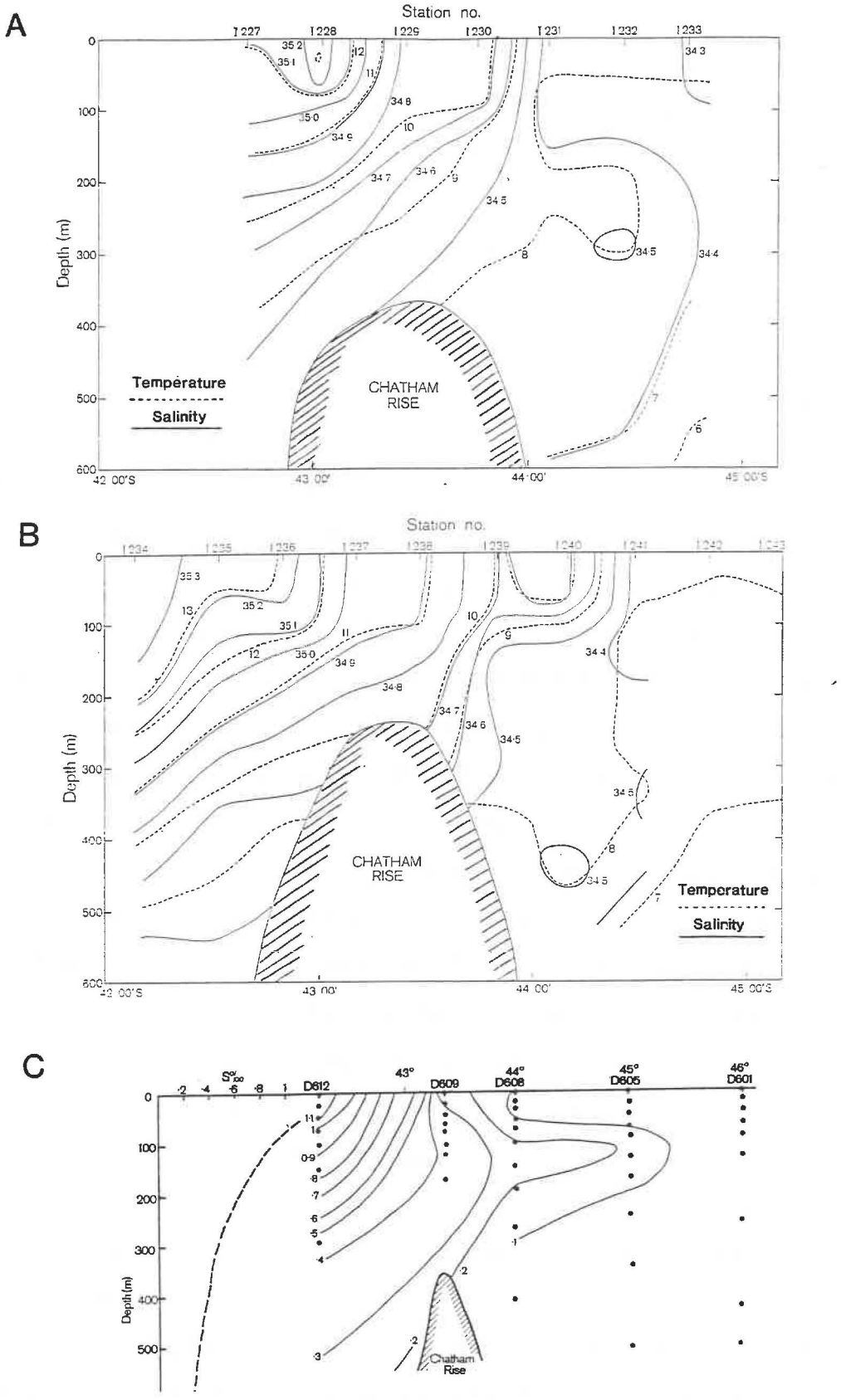

Fig. 3.3 North-south sections along longitudes 177°E (A), 179°E (B) and 177°40'E (C). Temperature (dashed line, °C) and salinity (solid line, ‰) data are shown for October 1976 in A and B (from Gilmour & Cole, 1979). In C, a salinity anomaly cross-section (‰) across the Subtropical Convergence is depicted from a survey in April 1967, showing the development of a sub-surface salinity tongue towards the south (from Heath, 1976).

3.2.2. Subtropical Convergence and Chatham Rise

On Chatham Rise, the STC is characterised by marked surface salinity and temperature gradients (e.g., 0.9‰ and 4°C within one degree of latitude, respectively; Heath, 1973), with the STC occupying a mean latitude of approximately 43°S east of New Zealand (e.g., Deacon, 1937; Garner, 1953, 1959; Heath, 1975; Ridgway, 1975; Gilmour & Cole, 1979; Vincent et al., 1991) (Fig. 3.2). Strong temperature gradients across the STC (i.e., >2°C over 100 km) have been recently observed from satellite imagery data (Chiswell, 1994b). The actual latitudinal position of the STC can vary considerably, however (e.g., Heath, 1975 cf. Vincent et al., 1991), and recent sea-surface temperature satellite imagery indicates that this zone is, in fact, represented by a complex, irregular front, characterised by large-scale meanders and eddy-like features, particularly near Mernoo Bank (e.g., Barnes, 1985; Vincent et al., 1991). In vertical profile, isohalines and isotherms slope upwards to the south (e.g., Heath, 1975; Gilmour & Cole, 1979) (Fig. 3.3). A subsurface tongue of high salinity water appears to extend southwards into the cooler, less saline subantarctic waters at depths of between 80-300 m to at least 47°S at certain times (e.g., Heath, 1968; Heath, 1975; Gilmour & Cole, 1979; Sparks et al., 1989; Vincent et al., 1991). Complex mixing patterns across the STC indicate that "old" (i.e., ^{14}C depleted) water is upwelled on to the southern flank of the Rise to a water depth of about 800 m (R. Sparks, pers. comm., 1991). High levels of bomb-^{14}C at 1000 m south of Bounty Trough suggests a typical vertical mixing time of 25-30 years (Sparks et al., 1989).

Seasonal migration of the STC has been postulated by Heath (1968, 1975) who suggested that the STC may be located further south in winter (September-October 1967) compared to summer (April 1967), contrary to observations of the STC in central Atlantic Ocean (Deacon, 1937). Heath (1975) attributed this apparently anomalous seasonal movement in the Chatham Rise area to thermal and density stratification of the water column in the summer. The resultant abrupt changes in vertical current gradient and associated increased vertical stresses were postulated to restrain the southward movement of subtropical water due to strong coupling between water above and below the depth of the Chatham Rise crest. Seasonal variations in wind patterns and strengths may also be a significant factor in

controlling the position of the STC (Heath, 1975). Chiswell (1994b) has also invoked an annual migration pattern associated with the position of the STC suggesting that the STC, as defined by the position of strongest sea-surface temperature gradient, migrates northwards from the southern flank of the Rise in spring to the northern flank in summer. Significant interannual variations of the position of the STC, however, can be observed when considering other data collected in different years in the same season (e.g., Ridgway, 1975; Robertson et al., 1978; Gilmour & Cole, 1979; Vincent et al., 1991). This observation may be addressed in the interpretations of Chiswell (1994b) who found that the inferred annual signal associated with the position of the STC only accounts for 30% of the total variance, and is probably influenced by mesoscale meanders and eddies not able to be resolved in his analysis (e.g., Vincent et al., 1991). Accordingly, both the strength and position of the STC during any individual month are likely to be different from their expected seasonal values.

3.2.3. Currents on Chatham Rise

Mean current flows in the vicinity of Chatham Rise have been inferred from calculations of the geostrophic current field by Heath (1968), Ridgway (1975) and Chiswell (1994a). Geostrophic currents are generally weak north and south of the STC with Heath (1968) reporting a maximum geostrophic current velocity of 11.2 cm s^{-1} in southern Hikurangi Trough region, associated with the occurrence of a semi-permanent anticyclonic eddy, known as the Waiarapa Eddy, in this area (e.g., Garner, 1967; Heath, 1975; Barnes, 1985, Vincent et al., 1991). Both Heath (1968) and Ridgway (1975) show a dominant mean northeastwards flow at about 46°S, south of the Rise, with very weak current speeds of between 1.7-8.8 cm s^{-1} (Heath, 1968). In addition, Stramma et al. (1995) calculated eastwards-flowing geostrophic surface velocities of <10 m s^{-1}, just to the north and east of the Chatham Islands, within the proposed South Pacific Current, as did Chiswell (1994b) over the Chatham Rise.

Quantitative measurements of current flow on the Chatham Rise using current meters have been reported only by Heath (1983, 1984), Greig & Gilmour (1992) and Chiswell (1994a). Heath (1983, 1984) presented results from a 34-day mooring on the Rise crest at approximately 179°30'E, while Greig & Gilmour (1992) outlined data collected during a

127-day mooring in Mernoo Saddle. Chiswell (1994a) collected 4- to 7-day current meter records at 150 m water depths from north, south and on top of the Rise, together with 150 kHz Acoustic Doppler Current Profiler (ADCP) data over the same region along 178.5°E. These data indicate that flows on the Rise are dominated by the lunar semi-diurnal tidal constituent M_2, but differ in the strength of the signal attributed to the diurnal tidal constituents (O_1 and K_1). Greig & Gilmour (1992) found that the currents associated with the latter two parameters were considerably less on their more westerly mooring than those recorded by Heath (1983, 1984) (i.e., 1.6 and 0.7 cm s^{-1} for O_1 and K_1, respectively cf. 4.9-7.6 and 3.4-5.4 cm s^{-1}), thereby disputing the presence of a trapped continental shelf wave along the crest of the Rise as proposed by the earlier work. Furthermore, Chiswell (1994a) argued that if the diurnal tide is a shelf tide then it only exists on the northern flank of the Rise. Along-rise (or zonal) currents appear to be strongest on top of the Rise and dominated by diurnal tides, whereas across-rise (meridional) currents are predominantly influenced by semi-diurnal tides (Chiswell, 1994a). Tidal flows in Mernoo Saddle were typically 12-15 cm s^{-1} with maximum currents of 30 cm s^{-1} (Greig & Gilmour, 1992), compared with generally <20 cm s^{-1} from the mid-rise moorings of Heath (1983) and Chiswell (1994a). A maximum along-rise flow of 37 cm s^{-1} was reported by Chiswell (1994a) at his central mooring (43°20'S 179°00'E).

The current meter data of Chiswell (1994a) is used to determine the Reynold's numbers that the traps described in Chapter 2 (Section 2.1) would be anticipated to experience during deployments on Chatham Rise. Using equation 7 (Section 1.4, Chapter 1) this analysis indicates that maximum Reynold's numbers, relative to the traps, of 13300-24700 might be expected based on current flows of between 20 and 40 cm s^{-1} (Chiswell, 1994a). Similarly, using the mean flow characteristics of the Subtropical Convergence frontal zone, described by Chiswell (1994a), average trap Reynold's numbers of 4000-8000 are anticipated. These calculations suggest that the high aspect ratio of the NZOI-NIWA traps should be sufficient to reduce intra-trap turbulence since Hawley (1988) showed that the basal tranquil zone in traps with relatively high aspect ratios remains intact even at Reynold's numbers of 4000 and 8000. At aspect ratios lower than 5, the tranquil zone in cylindrical traps was destroyed at progressively lower levels of turbulence (Hawley, 1988) (Fig. 1.11C, Section 1.4, Chapter 1).

Simple models of the diffusive-advective balance across the STC led Heath (1976, 1981) to suggest that mean flow was towards the north near the surface, decreased with depth (e.g., 4.6 to 1.84 cm s^{-1}; Heath, 1983) and directed southwards near the sea-floor. Chiswell (1994a) was unable to show conclusively any evidence of cross-frontal circulation patterns required to maintain the STC with convergence of flows only inferred for a narrow band at about 43°S. Considerable spatial heterogeneity is apparent in current flow speeds and directions within the STC. For example, Chiswell (1994a) observed mean westerly flows of 11 cm s^{-1} north of the Rise crest (42°56.5'S), 12 cm s^{-1} to the northeast on the crest itself (43°14.9'S), and 6 cm s^{-1} to the south at 44°S, over the same period of time. Similarly, in Mernoo Saddle, Greig & Gilmour (1992) observed that, although the net average flow was to the north at 3.1 cm s^{-1}, this flow was interrupted by strong southward currents that persisted for up to 10-12 days. Therefore, net southward flows in Mernoo Saddle lasted for up to 5 weeks, while the maximum recorded current speed was 67 cm s^{-1} to the south.

3.3. Biological processes

The strong hydrographic zonality associated with the STC, east of New Zealand, plays a significant role in influencing biological processes operating in the vicinity of Chatham Rise. For example, the position of the STC appears to control the distribution and abundance of many floral and faunal groups in this region, such as mesopelagic fishes (e.g., Robertson et al., 1978), planktonic foraminifera (e.g., Kustanowich, 1963), phytoplankton (F.H. Chang, pers. comm., 1991), copepods (e.g., Bradford & Jillett, 1980), dinoflagellate cysts (e.g., Sun & McMinn, 1994) and benthic organisms (e.g., Probert & McKnight, 1993).

The Southwest Pacific region is recognised as a zone of heightened atmospheric CO_2 uptake (ΔpCO_2>20 μatm, e.g., Takahashi & Azevedo, 1982; Murphy et al., 1991; Currie & Hunter, 1997) (Fig. 1.2), which is inferred to be related to high rates of biological productivity in the vicinity of the STC (Taniguchi & Nishizawa, 1971; Bradford, 1980b, 1983). From very limited historical data, surface production is higher in subtropical waters (>1.0 mgC m^{-3} h^{-1}; Bradford, 1980b) than in subantarctic waters (0.5-0.75 mgC m^{-3} h^{-1}), although water column-integrated production is reported to be higher in the latter (0.5-0.75 cf. 0.25-0.5 gC m^{-2} d^{-1};

Bradford, 1980c). Furthermore, enhanced biomass of benthic organisms on the southern flank of Chatham Rise, compared with expected depth-biomass trends in other deep ocean basins (e.g., Rowe, 1983), led Probert & McKnight (1993) to infer that high fluxes of organic matter to the sea-floor must be reaching, and being utilised by, benthic communities within the STC.

Previous studies have shown that, compared to subantarctic waters, subtropical water masses in the New Zealand region are generally depleted in nitrate (0-17 μM, compared with 15-25 μM; Zentara & Kamykowski, 1981) and dissolved reactive phosphorus (<0.3 μg l^{-1}, compared with >0.8 μg l^{-1}; Bradford & Roberts, 1978; Bradford & Taylor, 1980; Vincent et al., 1991). Furthermore, subtropical waters contain higher concentrations of dissolved reactive silica, relative to nitrate, than subantarctic waters, such that subantarctic surface waters are characterised by excess nitrate (>6 μM) at silicic acid depletion and subtropical-tropical waters of the South Pacific are in approximate nutrient balance (Zentara & Kamykowski, 1981; Kamykowski & Zentara, 1989). Vincent et al. (1991), however, showed that near-surface silica concentrations were highest in subantarctic waters (2.3 mmol m^{-3}), compared to subtropical waters, which had concentrations of 1.0-1.5 mmol m^{-3}. Ammonium concentrations in the top 90 m, measured in spring 1987, ranged from <0.2-0.8 μM, with a mid-water maximum of >0.6 μM at about 40-60 m, and highest values recorded atop and north of Chatham Rise (J. Grieve, pers. comm., 1991).

The standing stock and distribution of phytoplankton is estimated from the measurement of chlorophyll *a* in surface waters. Bradford (1980d) showed that non-winter chlorophyll *a* concentrations were generally uniform, typically ranging from 0.25-0.5 mg m^{-3}. Higher concentrations (up to 1.5 mg m^{-3}) were suggested for the western end of the Rise, north and south of Mernoo Saddle, and around the Chatham Islands (Bradford, 1980d). Taniguchi & Nishizawa (1971) also found that in winter 1968 surface chlorophyll *a* concentrations were generally higher in the STC than both south and north of the convergence zone (i.e., 140-220 mg m^{-2} cf. 90-140 mg m^{-2}). Vincent et al. (1991) showed that there was little relationship between physical and chemical variables across the Chatham Rise with highest chlorophyll *a* concentrations observed immediately south of Mernoo Saddle (1.5 mg m^{-3}) and lower values in subantarctic (<0.3 mg m^{-3}) than in subtropical and STC waters (0.3-0.9 mg m^{-3}).

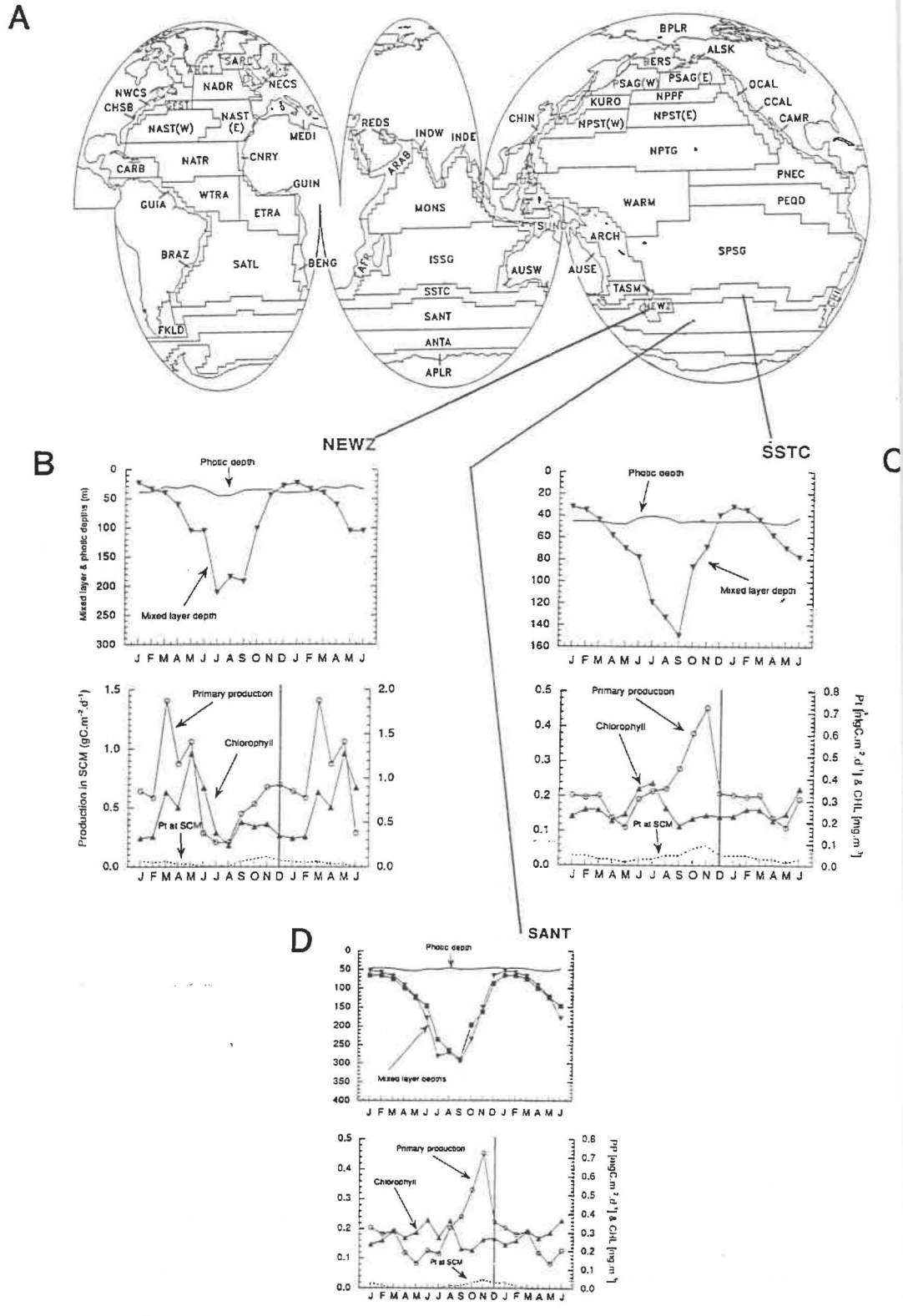

Fig. 3.4 Biogeochemical provinces of Longhurst (1995) on a 2° longitude x 2° latitude grid (A) and modelled annual production curves for New Zealand (NEWZ) (B), Subtropical Convergence-subtropical (SSTC) (C) and Subantarctic (SANT) (D). Note that CHL = chorophyll *a*, PP and Pt = primary production, SCM = sub-surface chlorophyll maximum (after Longhurst, 1995).

Discontinuities in the distribution of many zooplankton (e.g., aetideidae copepods, hyperiid amphipods, planktonic foraminifera recovered from sediment samples; see Bradford, 1983) and pelagic faunal groups (e.g., mesopelagic fishes, crustacea and cephalopods; Robertson et al., 1978) reveal a close spatial association with the STC (Bradford, 1983). Zooplankton biomass estimates by Bradford (1980a), on the other hand, integrated over 0-200 m water depths, indicate a more complex distribution pattern for zooplankton in the Chatham Rise region. Maximum non-winter biomass concentrations (>300 mg m^{-3} wet weight) occur over and just south of Mernoo Saddle while, in general, much of central Chatham Rise is characterised by relatively low values (<25 mg m^{-3}) with a patch of moderate biomass concentration (25-50 mg m^{-3}) located off southeast North Island, associated with semi-permanent eddies that form in this region (e.g., Barnes, 1985; Vincent et al., 1991). In addition, Chatham Rise is the location of several economically significant deep water fisheries, targeting orange roughy (*Hoplostethus atlanticus*), hoki (blue grenadier, *Macruronus novaezelandiae*) and oreo (Family Oreosomatidae), which contribute over $200 million export dollars annually to the New Zealand economy.

There is only limited information, however, regarding spatial and temporal variations in ecosystem structure and functioning in the oceans around New Zealand. Seasonal cycles of oceanic phytoplankton and zooplankton successions are not as well established as they are for other oligotrophic environments, such as northeast Pacific and Atlantic oceans (e.g., Parsons et al., 1984). Until recently, there has been no information collected on microzooplankton, bacterial and picophytoplankton biomass distributions in the Chatham Rise region. Coastal Zone Color Scanner (CZCS) satellite imagery suggests that phytoplankton pigment concentrations are enhanced along Chatham Rise, regardless of season (Comiso et al., 1993). Longhurst and various co-authors (e.g., Longhurst & Harrison, 1989; Longhurst, 1995; Longhurst et al., 1995) have extrapolated CZCS ocean colour data to predict primary production indices and more recently to model seasonal cycles of pelagic ecosystem functioning (Longhurst, 1995). This latter work subdivides the Southern Ocean into several biogeochemical provinces (Fig. 3.4), of which Longhurst's designations SPSG, NEWZ, SSTC and SANT are pertinent to this study. The SPSG province represents the South Pacific Ocean subtropical gyre, and is described by

Longhurst (1995, p. 150) as being "very poorly known". The NEWZ province is located over the Campbell Plateau, north of the Subantarctic Front and south of the STC (or SSTC of Longhurst), and is characterised by strong topographic control on chlorophyll biomass accumulation and productivity, which peak in summer, as documented originally by Heath & Bradford (1980). The SSTC represents the frontal zone of the Subtropical Convergence, and the SANT field extends across the Southern Ocean from about 35° to 55°S. The SANT province is characterised by deep winter mixing of 200-500 m and a latitudinal gradient in surface nitrate increasing southwards from 1-3 to 10-15 $\mu g\ l^{-1}$. The three SPSG, SSTC and SANT regions form part of Longhurst's (1995) *Westerlies domain* at mid-latitudes which is typified by winter-spring production with nutrient limitation occurring in early summer. Perhaps significantly in this domain, the depth of the photic zone is deeper than the mixed-layer only in summer months, and biological production is coupled with chlorophyll biomass accumulation, unlike the scenario suggested for higher latitudes (>55°S). In summary, the modelling work of Longhurst (1995) proposes that in STC and subtropical waters, primary production rates increase through austral autumn-winter and culminate in spring. Chlorophyll levels are limited by enhanced zooplankton grazing and sedimentation rates in spring. In contrast, subantarctic waters over Campbell Plateau sustain heightened primary production rates and chlorophyll concentrations through spring-summer due to interactions between shallow plateau topography and high wind stresses (Heath & Bradford, 1980; Longhurst, 1995).

3.4. Summary of Chapter 3

(1) The physiography of the Subtropical Convergence region east of New Zealand is dominated by the Chatham Rise, a submerged continental ridge that has undergone successive phases of submergence, emergence, deposition, erosion and volcanism over the last 100 million years. Planktonic ooze is the dominant modern sediment type to the south of the Rise beneath subantarctic waters, with hemipelagic muds present to the north below subtropical waters. Glauconitic sandy muds and exposed Miocene chalk with phosphatic nodules characterise the crest of the Chatham Rise at water depths of 300-400 m.

(2) Previous workers have regarded the STC to be bathymetrically constrained by Chatham Rise. Recent time-series AVHRR data suggest, however, that seasonally the STC may migrate over a 2° latitudinal range. Thus, it may be that the convergence zone is maintained by along-rise current systems, and that seasonal or interannual variations within these flows may in part control the position of the STC. This major ocean front is a dynamic mixing zone where warm, highly saline, nutrient-poor subtropical waters to the north interact with cold, nutrient-rich waters of subantarctic origin to the south. The STC is characterised by intense gradients in surface salinity and temperature, and by the presence of large-scale meanders and eddy features. Currents on the Rise crest are predominantly tidal with near-bottom speeds up to 20 cm s^{-1}.

(3) The STC forms a pronounced biogeographical barrier, marking the southern extent of many subtropical plankton species. Surface biological production is higher in subtropical waters, although integrated productivity is higher in subantarctic waters. The STC is characterised by higher levels of phytoplankton accumulation, regardless of season (e.g., Comiso et al., 1993), compared with the water masses on either side of the front. There is only limited information, however, on temporal and spatial variations in ecosystem functioning and structure across this region, except from pelagic production models developed by Longhurst (1995).

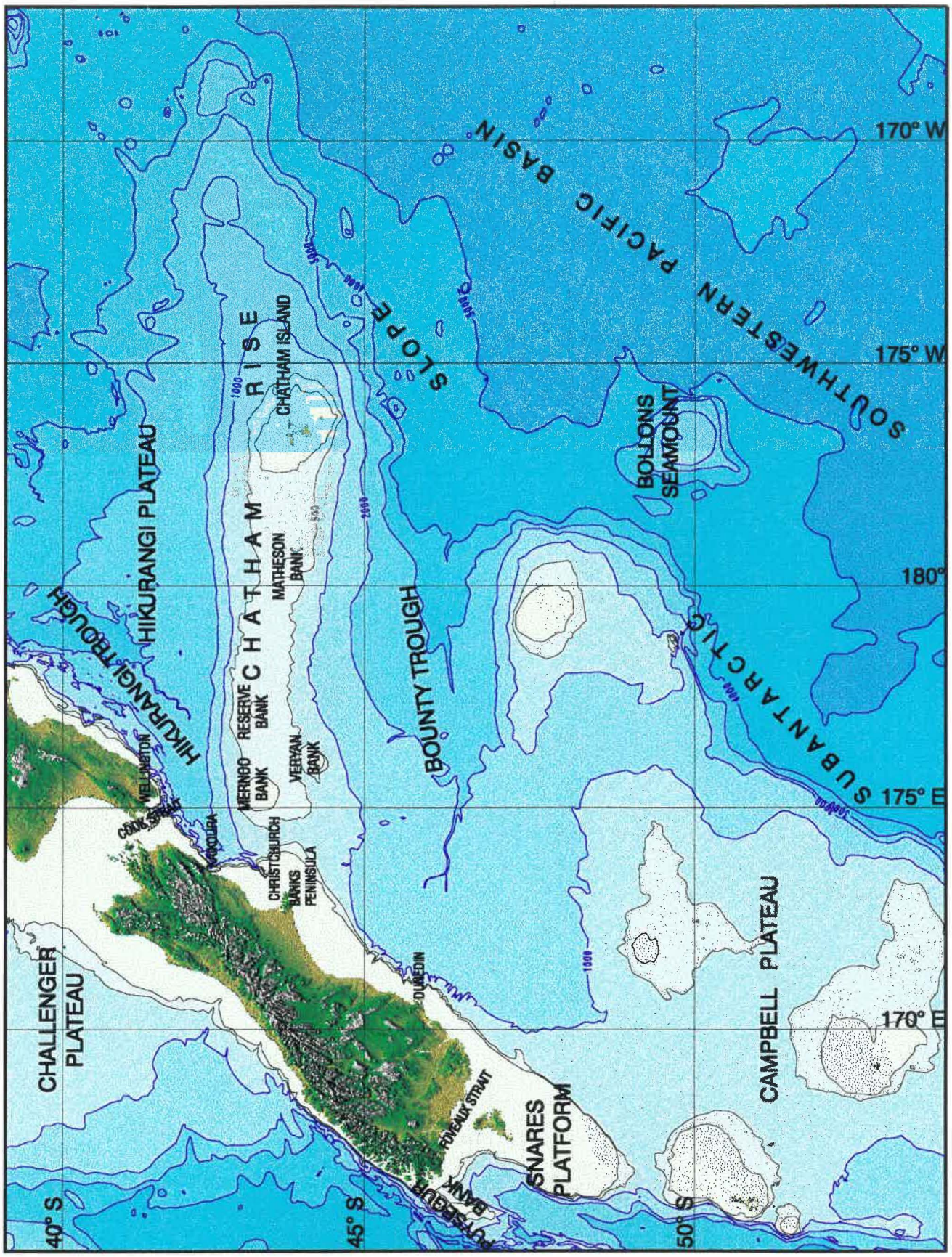

Figure 3.1 Bathymetric map of Chatham Rise region (from CANZ, 1997)
. Bathymetric contours are in meters.

Chapter 4

DYNAMICS OF CHATHAM RISE–SUBTROPICAL CONVERGENCE ECOSYSTEMS IN WINTER AND SPRING 1993

Chapter 4

DYNAMICS OF CHATHAM RISE-SUBTROPICAL CONVERGENCE ECOSYSTEMS IN WINTER AND SPRING 1993

4.1. Introduction

In order to understand the factors affecting particulate flux data collected from short-term, free-floating sediment trap arrays it is essential that the dominant biological and physical processes operating prior to and at the time of the trapping experiment are evaluated (e.g., Knauer et al., 1979; Martin et al., 1987, 1993; Landry et al., 1992; Lohrenz et ál., 1992; Karl et al., 1996). This chapter therefore focuses upon the physical and biological dynamics of Chatham Rise-Subtropical Convergence ecosystems studied in three water types that were sampled in 1993 as part of the New Zealand JGOFS research programme. The principal aim of the JGOFS-affiliated programme was to investigate seasonal changes in physical and biological variability across the STC region. This aim required contributions from a multidisciplinary team of scientists, with the author involved as the principal investigator for the sediment flux component of the programme. Thus, although part of a strongly collaborative project, the presentations and interpretations contained in this chapter are largely the author's own. This original analysis has been made to determine whether food web dynamics directly affect particulate fluxes east of New Zealand. As a consequence, the chapter represents the first interpretation of temporal and spatial differences in ecosystem functioning and structure across the Chatham Rise-STC region. In addition, the author co-ordinated the compilation of two NIWA internal reports that detail the methods used in the 1993 JGOFS voyages (Nodder et al., 1994a, b). The techniques employed in the food web studies are paraphrased by the author in the present chapter; these methods are not, however, evaluated critically. Work by JGOFS colleagues is acknowledged via reference to a series of recently submitted or in press scientific papers (Bradford-Grieve et al., 1997a, b; Chang & Gall, submitted; Currie & Hunter, 1997; James & Hall, 1997; Smith & Hall, in press; Safi & Hall, in press).

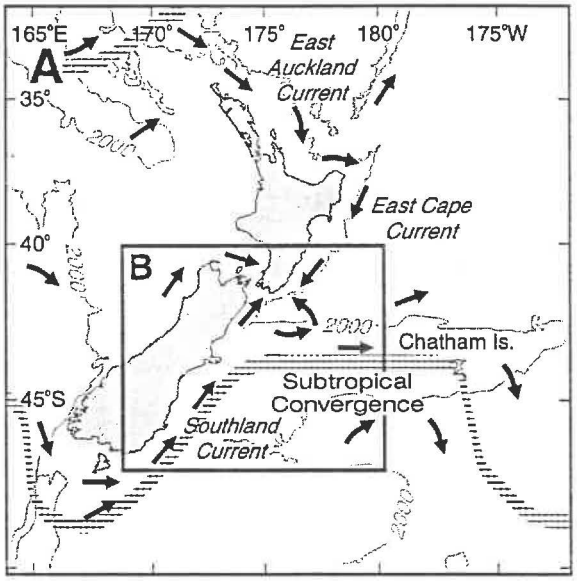

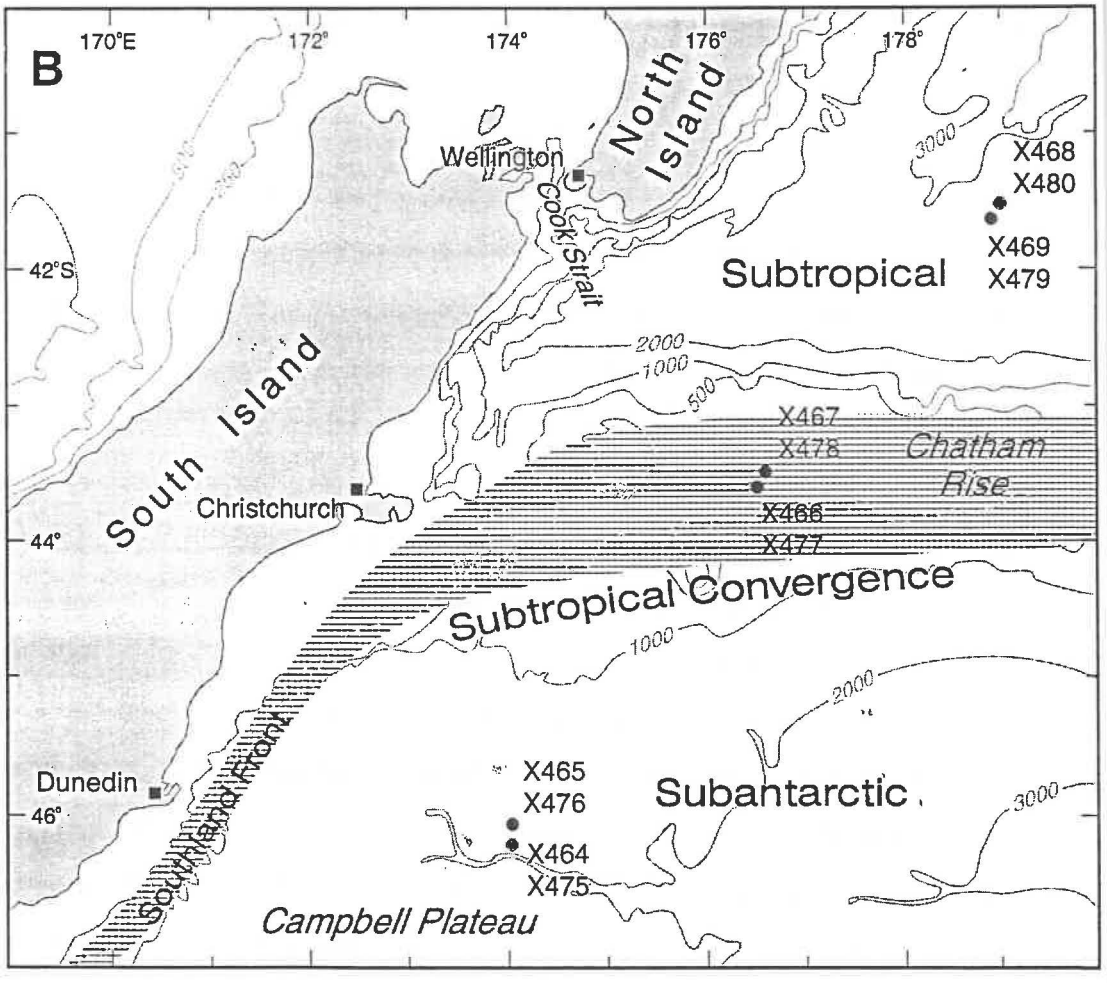

Fig. 4.1 Locality map showing nominal positions of stations occupied in Subtropical Convergence region during New Zealand JGOFS research voyages in June-July (austral early winter, X464-469) and October (spring, X475-X480) 1993. Bathymetric contours are in metres. Inset A is after Heath (1985) showing ocean circulation patterns and frontal positions around New Zealand.

4.2. Methods

Research voyages were conducted onboard R. V. *Akademik M. A. Lavrentyev* in early austral winter (12 June-4 July, NZOI-NIWA cruise 3009) and spring (1-21 October, NZOI-NIWA cruise 3014). For logistical reasons, water column sampling in each season was restricted to two stations (nominally 13 km apart) within each designated water type: subantarctic, Subtropical Convergence (STC) and subtropical (Fig. 4.1). *In situ* variations in certain physical and biological parameters were documented through time by undertaking sampling using a Conductivity-Temperature-Depth (CTD)-rosette system within 2 km of a Lagrangian drifting buoy deployed at each station. The free-floating buoys were tethered to subsurface sediment traps set below the mixed-layer (Nodder & Alexander, 1997) (Table 4.1). While several parameters were able to be monitored on time-scales of 3-4 h (e.g., temperature, salinity, nutrients, particulates), and other biological observations were made on the order of days (e.g., primary and bacterial production, and microbial, microzooplankton and mesozooplankton biomass and grazing rates), sediment trap results represented an integrated measure of export flux over each deployment period (generally 2-3 days).

As far as practical, sampling and analytical protocols were compatible with those recommended for other JGOFS studies (JGOFS Report 6, 1990). Water column temperature and salinity were measured using a Seabird 9/11*plus* CTD instrument package, connected to a 5 and 10 l Niskin bottle rosette for collecting sea-water samples (Singleton, 1993, 1994). CTD salinity measurements were calibrated using water samples run on a Guildline AutoSal salinometer, standardised with IAPSO Standard Seawater from Ocean Scientific International Ltd. Water column fluorometric information was obtained only during the spring voyage using a Chelsea Aquatracka fluorometer, interfaced with the Seabird CTD. Additional physical and biological information was collected while underway using a temperature sensor and fluorometer connected in-line to a surface sea-water pump, which extracted sea-water from the ship's moon pool from a depth of 4 m. Data was logged every 10 min to a LICOR LI-1000 data logger (Singleton, 1993, 1994). pCO_2 in surface waters and atmosphere were measured continuously during both voyages using a dual flow-through

Table 4.1 Sediment trap stations occupied during winter and spring 1993. Details of the deployments are summarised in Table 5.1 (Chapter 5).

1993 Season	NIWA research voyage*	Water type**	NIWA station	Water depth of traps (m)
Winter	3009	SA	X464B	120, 220, 300, 550
Winter	3009	SA	X465A	120, 220, 300, 550
Winter	3009	STC	X467A	110, 210
Winter	3009	ST	X468B	120, 220, 300, 550
Spring	3014	SA	X475A	150, 550
Spring	3014	SA	X476A	150, 300, 550
Spring	3014	STC	X477A	100, 220
Spring	3014	STC	X478A	100, 220
Spring	3014	ST	X479A	110, 300, 550
Spring	3014	ST	X480A	110, 550

* NIWA = National Institute of Water and Atmospheric Research (NZ) Ltd.

** SA = subantarctic, STC = Subtropical Convergence, ST = subtropical.

system that included a drying tube, an infra-red gas analyser and an equilibration chamber. The winter voyage was hampered by equipment malfunction and no measurements were taken (Currie & Hunter, 1997). Atmospheric pressure was logged manually every four hours.

Total alkalinity (TA) of discrete sea-water samples was determined by automated potentiometric titration (e.g., Dickson, 1981; Brewer et al., 1986). Samples were fixed with $HgCl_2$, stored in the dark and titrations performed in an open vessel against standardised HCl using a Metrohm 702 SM Titrino Autotitrator within 12 h of sampling. The precision of the method is estimated to be better than 0.2% (±3 $\mu eqkg^{-1}$).

Nitrate + nitrite (referred to as "nitrate" in following text), ammonium, urea and dissolved reactive phosphorus (DRP) and silica (DRSi) concentrations were measured from pre-screened (>200 μm) 500 ml aliquots, filtered through acid-rinsed, 25 mm Whatman GF/F filters, with filtrate collected in 250 ml, acid-washed polyethylene bottles. Samples were then run immediately on a Technicon AAII autoanalyser to determine DRP, ammonia and nitrate concentrations with the sample frozen for later analysis of urea and DRSi.

Particulate carbon (PC), phosphorus (PP) and nitrogen (PN) samples were prepared by filtering 500 ml of sea-water through a 25 mm diameter, precombusted (500°C for 4 hours) GF/F filter. For PP/PN samples, filters were also soaked in 10% HCl overnight and rinsed with distilled water. Filters were rinsed with filtered sea-water, and stored frozen until analyses could be conducted on PC/PN samples using a Perkin Elmer 2400 CHN Autoanalyser and a Technicon Autoanalyser II following modified acid-digestion methods (Downes, 1978) for PP/PN samples. Total suspended particulate matter (SPM) concentrations were determined by filtering between 2-8 l of sea-water through pre-weighed, 0.45 μm 47 mm diameter Nuclepore polycarbonate filters, rinsing with filtered sea-water and storing frozen. SPM samples were re-weighed in the laboratory following drying of each filtered sample under ultra-violet light for approximately 2-3 min.

Chlorophyll *a* samples were prepared for analysis by pre-screening sea-water samples through a 200 μm mesh to remove zooplankton and large debris, and filtering 500 ml

subsample of sea-water through a 25 mm diameter GF/F filter. Filters were then snap-frozen in liquid N_2 and stored frozen until further analysis. Samples were size-fractionated into <200 (total), <20 and <2 μm fractions using polycarbonate filters. Extraction of chlorophyll *a* was conducted in the onland laboratory using 90% acetone under low light and temperature (<20°C) conditions to avoid photodegradation using standard extraction techniques (e.g., Strickland & Parsons, 1972). Chlorophyll *a* concentrations were determined using a Perkin Elmer luminescence spectrofluorometer with excitation and emission wavelengths of 431 nm and 670 nm, respectively (Bradford-Grieve et al., 1997a).

Primary production incubations were conducted in deck incubators for 24 h using "clean" metal-free techniques (i.e., silicon o-rinds and closure cords in Niskin water bottles; Fitzwater et al., 1982). All containers were cleaned with 10% HCl and rinsed thoroughly between stations with sea-water. Duplicate light and dark samples were transferred into 180 ml polycarbonate bottles and innoculated with radio-active bicarbonate solution in Teflon vials under alkaline conditions. A final ^{14}C concentration of 0.25 μCi ml^{-1} was used with stock solutions made up fresh each day (Bradford-Grieve et al., 1997a). Incubations were carried out in shade cloth bags over 24 h in a deck incubator cooled with surface sea-water. Varying grades of shade cloth were used to simulate the range of light intensities that equated to those intensities experienced at the depths from which samples were taken. Samples were size-fractionated into <200, <20 and <2 μm size classes and filtered at low vacuum onto GF/F filters and then frozen. Uptake of radioactive ^{14}C was measured with a liquid scintillation counter after vapour acidification of samples and corrected for dissolved inorganic carbon concentration (Bradford-Grieve et al., 1997a). Photosynthetically available radiation (PAR) was estimated from light profiles conducted at mid-day using an underwater LICOR scalar light sensor after pre-dawn production samples had been collected and incubated.

Phytoplankton community composition was measured by microscopic counts of water samples preserved in acidic Lugol's solution. Cell carbon estimates were made using bio-volume corrections for diatoms, dinoflagellates and microflagellates, greater than 5 μm in diameter (Chang & Gall, submitted). Contributions by calcified phytoplankton (prymnesiophytes) could not be quantified due to dissolution in Lugol's solution.

Table 4.2 Summary of physical and chemical parameters measured in water types, east of New Zealand, during winter and spring 1993. Values in table are ranges from a series of stations occupied in each water type over periods of 2-3 days.

Parameters	SUBANTARCTIC		SUBTROPICAL CONVERGENCE		SUBTROPICAL	
	Winter 1993	Spring 1993	Winter 1993	Spring 1993	Winter 1993	Spring 1993
Temperature (°C)*	5.6-8.5	5.8-8.1	8.5-10.8	8.8-10.9	8.8-13.7	8.5-13.7
Salinity (psu)*	34.2-34.4	34.3-34.4	34.5-34.8	34.5-34.7	34.6-35.2	34.6-35.3
Sigma-t (σ_t)*	26.6-27.1	26.7-27.0	26.5-26.8	26.6-26.8	26.4-26.9	26.5-26.9
Mixed-layer depth (m)	80-120	50-60	110-120	14-70	110-140	10-15 (50-80)†
pCO_2^{sw} (µatm)	-	308	-	250	-	?250-260
TA (meq kg^{-1})	2.334-2.355	2.305-2.315	2.343-2.353	2.301-2.330	2.345-2.390	2.320-2.360
$NO_3^- + NO_2^-$ (µM)‡	15-19	16-18	8-14	4-9	2-7	3-8
NH_4^+ (µM)‡	<0.01-0.8	0-0.8	<0.01-0.3	0.1-0.8	<0.01-0.3	0.02-0.3
Urea (µM)‡	0.4-0.6	0.1-0.5	0.3-0.7	0.2-0.8	0.3-0.6	0.2-0.4
DRP (µM)‡	1.1-1.3	1.2-1.3	0.8-1.1	0.4-0.8	0.4-0.8	0.3-0.7
DRSi (µM)‡	2-5	3-4	1-6	1-3	1-4	2-7
PC <200 µm (µg l^{-1})‡	17-73	80-136	40-111	56-573	15-136	133-225
PP <200 µm (µg l^{-1})‡	0.5-1.3	0.5-2.8	0.9-1.9	1.3-8.5	0.7-1.7	3.2-4.9
PN <200 µm (µg l^{-1})‡	6-10	5-40	4-14	10-64	5-12	19-38
Suspended particulate matter (mg l^{-1})	0.3-0.8	0.2-0.4	0.5-0.9	0.6-1.9	0.4-0.9	0.3-0.9

* Based on deep-water pycnocline characteristics, i.e. below mixed-layer depth.

† Depth of remnant mixed-layer given in parentheses.

‡ Concentrations over the depth of the mixed-layer. Other parameters (unless stated) have concentration ranges over the sample depths at each station to a maximum depth of 550 m.

Picophytoplankton (<2 μm) biomass was determined by epifluoresence and distinctions were made between eukaryotic and prokaryotic forms (Bradford-Grieve et al., 1997a; James & Hall, 1997). Microscopic counts of autotrophic and heterotrophic picoplankton were made on samples preserved in 0.2% paraformaldehyde using epifluorescence (Safi & Hall, in press).

Samples were collected to determine water column (0-80 m) bacterial biomass and production using epifluoresence and ^{3}H-thymidine and leucine uptake techniques, respectively (Smith & Hall, in press). Dilution experiments were undertaken only on water samples collected from 10 m depth to investigate microzooplankton grazing impacts on bacteria (in spring only), picophytoplankton and total chlorophyll biomass (James & Hall, 1997). Microzooplankton (<200 μm) biomass and composition (ciliates, tintinids) analyses were undertaken on Lugol's solution-preserved samples (James & Hall, 1997). Mesozooplankton (>200 μm) community structure and biomass determinations were made on samples collected from four-hourly vertical bongo hauls, integrated over 0-100 m, and from depth-stratified, horizontal tows made using a Mulitple Opening and Closing Net and Environmental Sensing System (MOCNESS) (Bradford-Grieve et al., 1997b). MOCNESS tows were completed down to 1000 m in winter and 400 m in spring. Gut fluorescence techniques assessed community grazing rates on phytoplankton (Bradford-Grieve et al., 1997b).

4.3. Results

Obvious geographical and seasonal variations across the study area were apparent from many of the biological and physical parameters measured during the field programme in 1993 (Tables 4.2 & 4.3). For example, subantarctic waters were dissimilar physically and generally hosted less biomass than subtropical waters. High levels of seasonal variation were observed in certain parameters, such as chlorophyll *a* and other particulates, in the STC. Pronounced differences in bio-physical characteristics persisted across water types and seasons (Tables 4.2 & 4.3). These observations occurred despite times when there were marked changes in water column structure and biological characteristics at replicate stations, or at the same "station" sampled at different times.

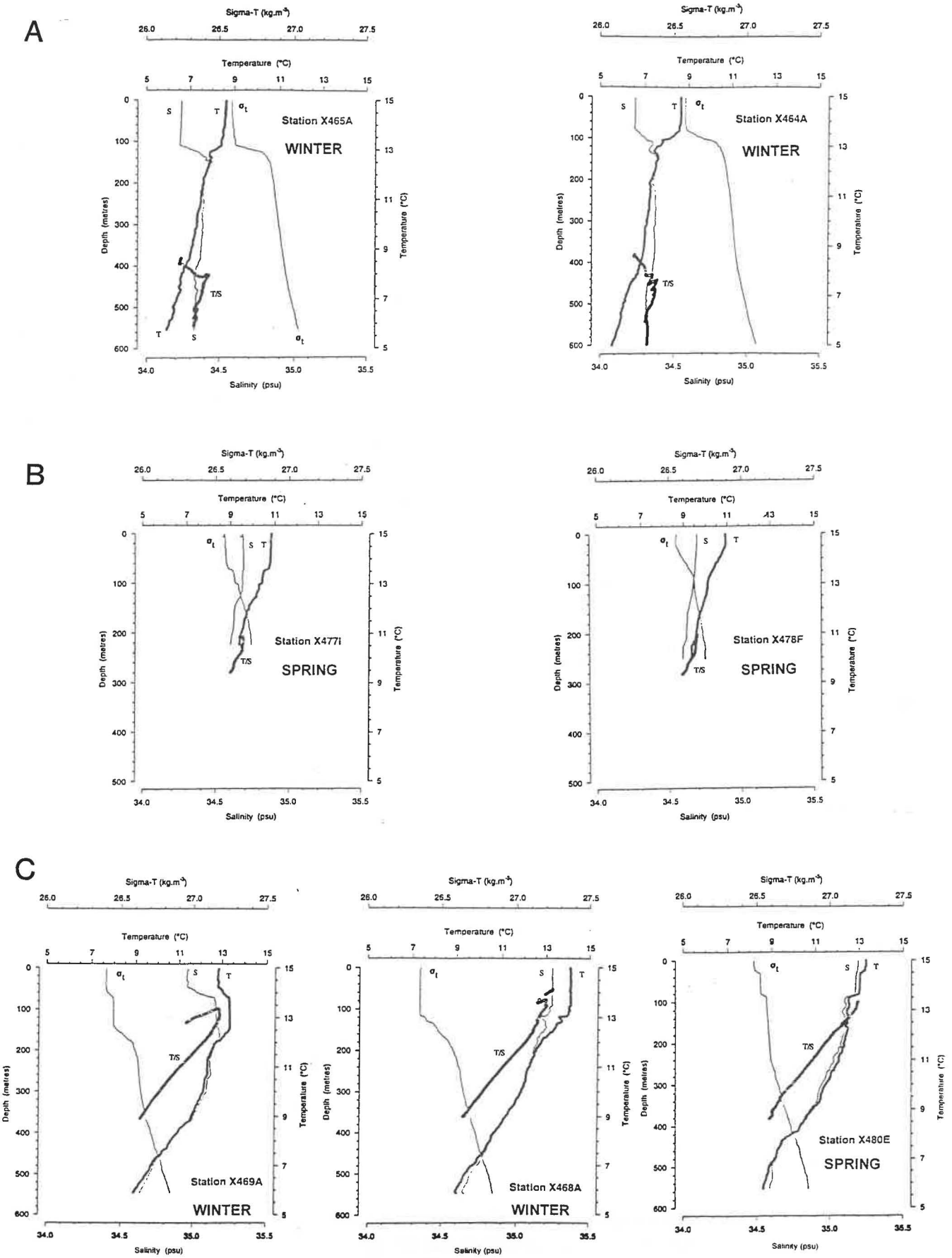

Fig. 4.2 Selected Conductivity-Temperature- Depth (CTD) profiles from subantarctic (A), Subtropical Convergence (B) and subtropical (C) water types, showing sea-water temperature (T), salinity (S) and density (σ_t). Stations are located nominally in Fig. 4.1. Temperature-salinity (T/S) plots are also shown for each CTD cast.

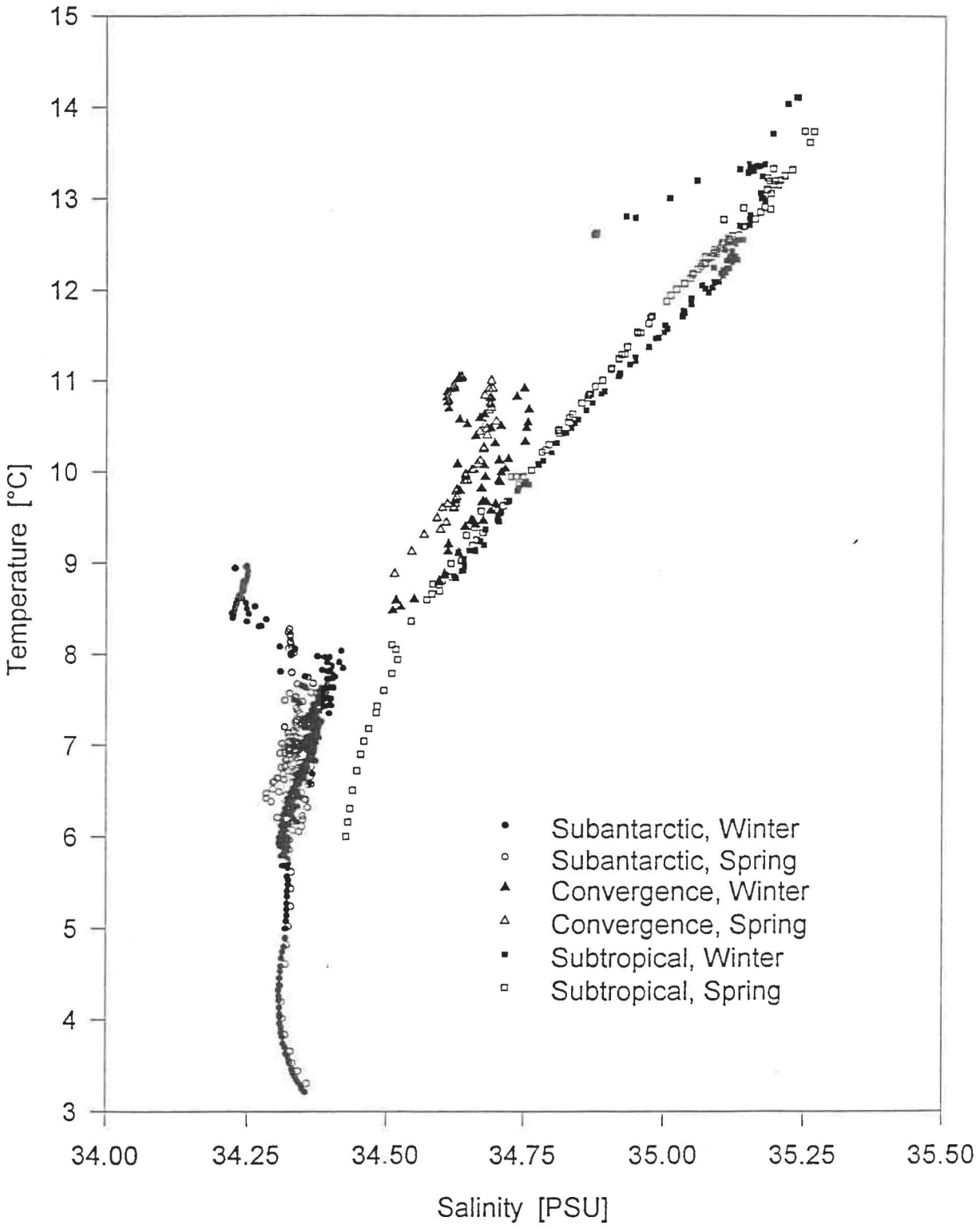

Fig. 4.3 Temperature-salinity plot for all stations occupied during New Zealand JGOFS research voyages in winter and spring 1993. Note the transition from colder, less saline subantarctic to warmer, more saline subtropical waters, with the STC intermediate in character between the other two water masses.

4.3.1. Physical water column structure

As expected from previous work (e.g., Heath, 1985), subantarctic waters were generally less saline, considerably colder, and had correspondingly higher density values than subtropical waters (Fig. 4.2 & 4.3), reflecting the origin of the subantarctic water mass as Australasian Subantarctic Mode Water (Heath, 1985). The STC exhibited physical attributes intermediate between subantarctic and subtropical water masses in both seasons (Fig. 4.3). In winter, temperature and salinity characteristics of the three water types fell on a semi-continuous mixing line, whereas in spring there was a distinct decoupling between STC and subtropical waters from subantarctic waters, which exhibited a much less variable salinity range (Fig. 4.3). Temperature and salinity characteristics of the three water types, however, did not vary markedly between the two seasons (Fig. 4.3) (Table 4.2). CTD profiles in subtropical waters indicate that complex sub-surface interleaving of water types occurred in this water mass, compared with structurely "simple" profiles observed in subantarctic waters in both seasons (Fig. 4.2). Subtropical waters exhibited physical attributes that mimicked its original source as Subtropical Surface Water (Wyrtki, 1962; Heath, 1985), otherwise known as Western South Pacific Central Water (Tomczak & Godfrey, 1994). A pronounced surface intrusion event was observed in subtropical waters (X469A, X468E) in winter when a 60 m thick layer of colder (>0.5°C), less saline (>1 psu) subantarctic water capped underlying subtropical waters (Fig. 4.2C). These observations highlight the influence of small-scale temporal (i.e., hours-days) and spatial events (<15 km, the initial separation of replicate stations) on water column structure and characteristics (see later discussion on biological variations related to this surface intrusion event).

Mixed-layer depths (MLD) were measured from the sea-surface to the initiation point of the most rapid rates of sea-water density change (Gardner et al., 1995). MLDs were always deeper in winter than in spring (Fig. 4.2; Table 4.2). In both seasons, subantarctic waters had more homogenous mixed-layers, compared with subtropical waters, where several shallow stratification events were apparent, particularly in spring (Fig. 4.2). Compared to winter observations, MLDs in the STC in spring were highly variable, ranging from strongly

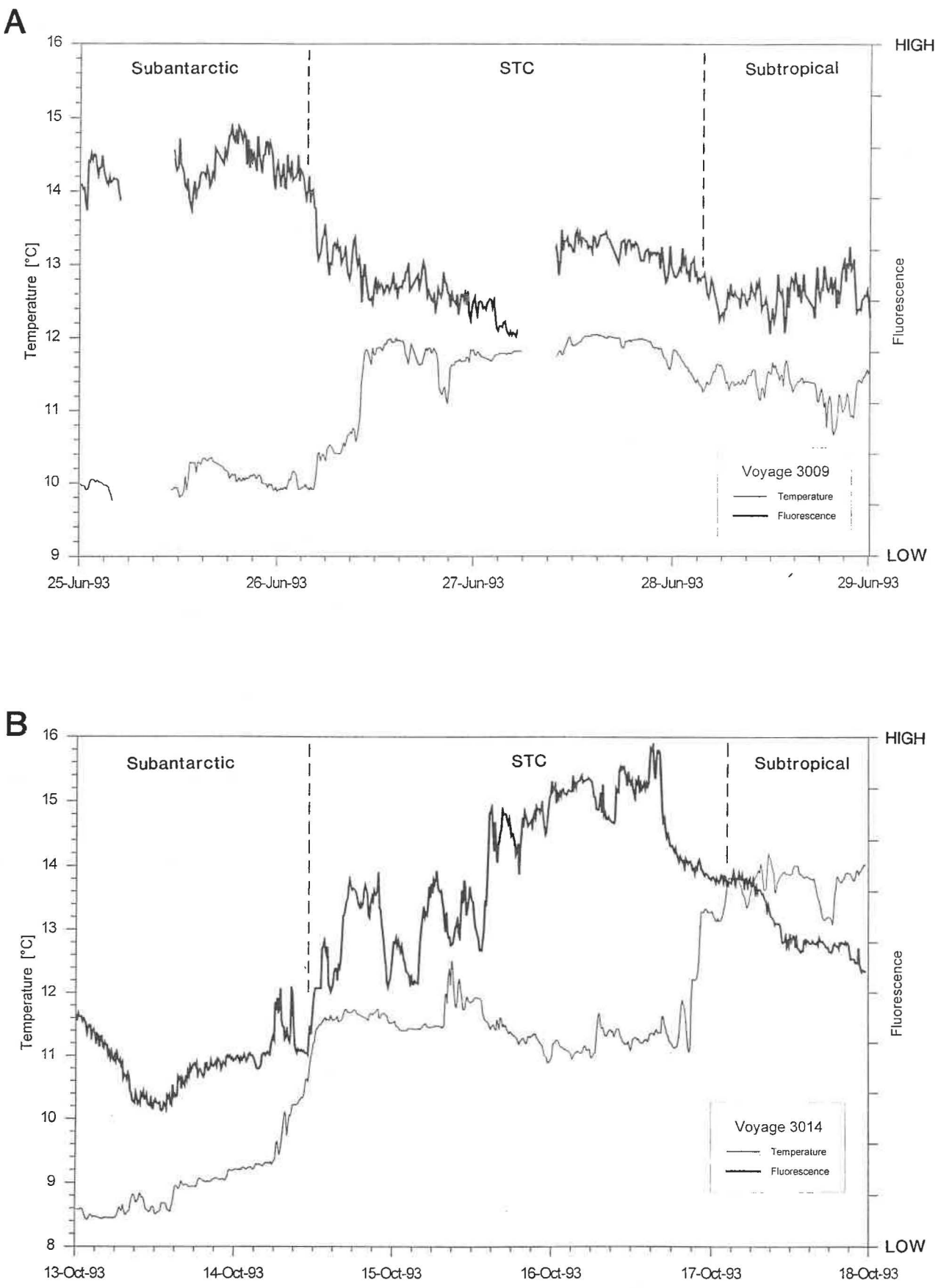

Fig. 4.4 Continuous sea-surface temperature (°C) and relative fluorescence (arbitrary units) across Subtropical Convergence region in winter (A) and spring (B) 1993. Note that data include times when the vessel was on station, hence the spiky nature of temperature, in particular, in the Subtropical Convergence (STC).

Alkalinity Profiles

Winter 1993

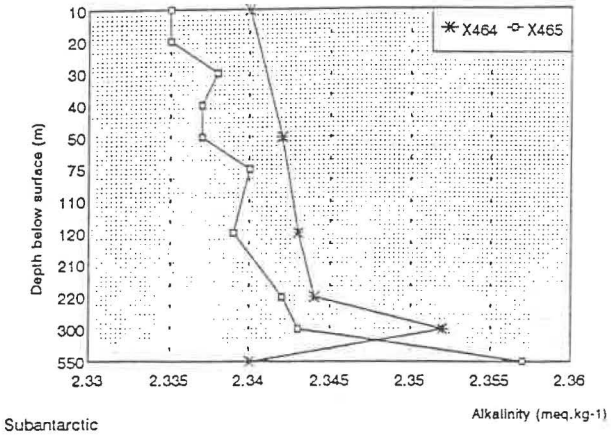

Subantarctic

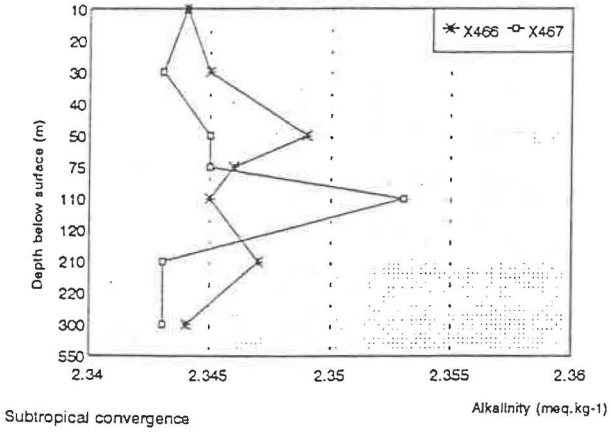

Subtropical convergence

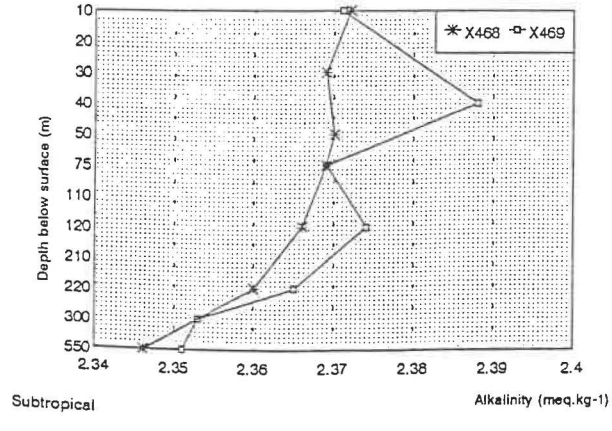

Subtropical

Spring 1993

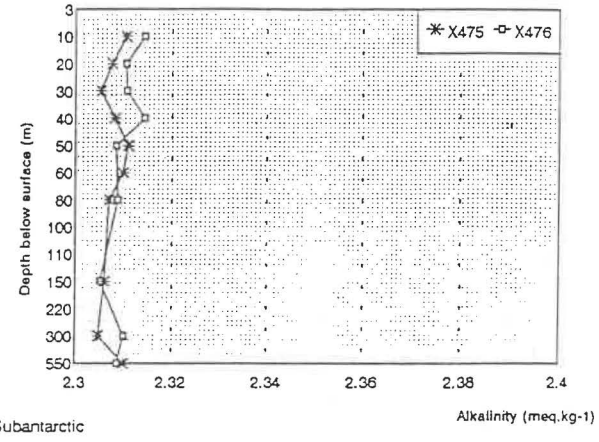

Subantarctic

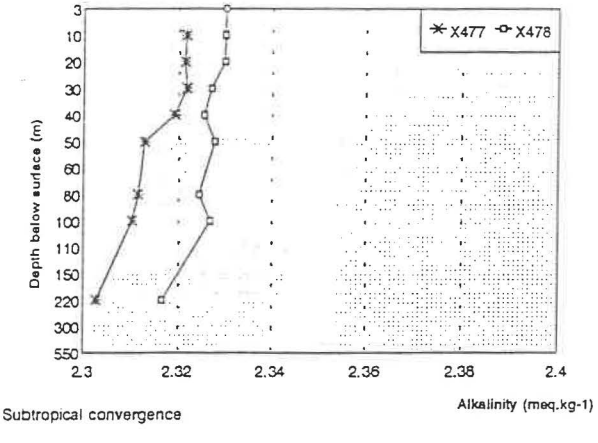

Subtropical convergence

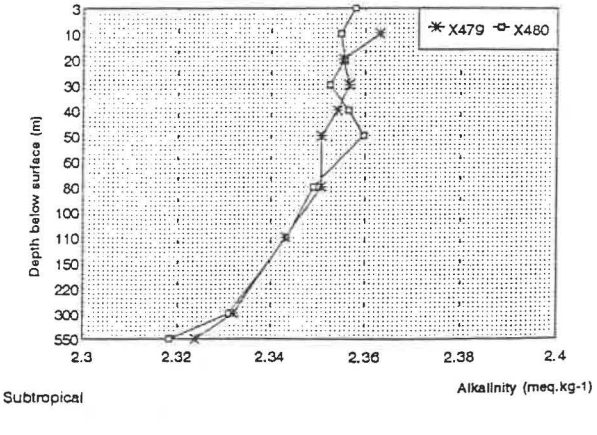

Subtropical

Fig. 4.6 Total alkalinity (meq kg^{-1}) profiles in subantarctic, STC and subtropical waters in winter and spring 1993.

Table 4.3 Summary of biological parameters measured in water types, east of New Zealand, during winter and spring 1993. Values in table are ranges from a series of stations occupied in each water type over periods of 2-3 days (data from Bradford-Grieve et al. (1997a, b), James & Hall (1997), Smith & Hall (in press) and NIWA unpublished data reports).

Parameters	SUBANTARCTIC		SUBTROPICAL CONVERGENCE		SUBTROPICAL	
	Winter 1993	Spring 1993	Winter 1993	Spring 1993	Winter 1993	Spring 1993
Integrated (0-75 m) primary production (mgC m^{-2} d^{-1})	28-62	230-271	249-275	977-995	100-197	625-1317
Integrated (0-100 m) <200µm chlorophyll *a* (mg m^{-2})	10-12	12-16	46-52	79-137	14-25	46-47
Production:biomass in mixed-layer (P_B)	2.3-6.0	14.2-23.0	4.8-6.0	7.1-12.6	4.0-14.4	13.7-28.8
<200µm chlorophyll *a* at 10 m (µg l^{-1})	0.10-0.13	0.15-0.20 (up to 0.90)	0.17-0.65	1.00-2.70	0.10-0.25	0.24-0.85
Chlorophyll *a* 200-20 µm in mixed-layer (µg l^{-1})	0	0-0.10	0.21-0.44	0.10-1.86	0-0.10	0.01-0.14
Chlorophyll *a* 20-2 µm in mixed-layer (µg l^{-1})	0.04-0.11	0.03-0.13	0.08-0.18	0.04-2.18	0.05-0.12	0.26-0.57
Chlorophyll *a* <2 µm in mixed-layer (µg l^{-1})	0.06-0.08	0.05-0.09	0.03-0.08	0.02-0.31	0.06-0.09	0.25-0.42
Mean bacterial numbers at 10 m ($\bar{x}$ 10^6 cells ml^{-1})*	0.47**	0.74	0.35**	1.06	0.34**	1.23
Mean bacterial production at 10 m (µgC l^{-1} h^{-1})*	0.084**	0.067	0.034**	0.532	0.018**	0.260
Autotrophic flagellates at 10 m (average no. cells ml^{-1})*	749	1342†	507	2792	316	3200‡
Heterotrophic flagellates at 10 m (average no. cells ml^{-1})*	185	530†	259	979	118	518‡
Ciliates at 10 m (average no. cells l^{-1})*	1362**	2670**	1383**	1604**	737**	2883**
% primary production removed by microzooplankton grazing at 10 m	71-121	41	119	100-126	117	74-82
Mean mesozooplankton biomass (0-100 m) (mgC m^{-3})*	1.9	2.7	1.4	5.6	1.0	37.6
Mean mesozooplankton community grazing (mgC m^{-2} d^{-1})*	1.6	2.6	4.8	18.2	3.8	33.7

* Mean of 2 stations in each water type, *n*=2 unless stated.
** Mean of 6 data-points from 2 stations, *n*=6.
† One data-point from 20 m water depth (X475).
‡ Data from one station only (X480), *n*=1.

developed, shallow (0-15 m) or deep (0-70 m) mixed-layers to occasions where no mixed-layer could be clearly defined. Thermocline and halocline development in all three water types generally coincided, especially in winter (Fig. 4.2). MLDs in subantarctic and subtropical waters in winter were generally deeper (by 40-55 and 80-95 m, respectively) than those expected solely from Ekman calculations using observed wind speeds (e.g., Pond & Pickard, 1983), whereas expected depth ranges of mixing across the two water masses due only to wind events were found in spring. Enhanced surface cooling and associated convective overturning processes in winter are the most likely explanation for these seasonal differences (Pond & Pickard, 1983).

4.3.2. Underway data: temperature, fluorescence and pCO_2

Underway sea-surface temperature varied by 2°C in winter and 5-6°C in spring as the vessel passed from subantarctic into subtropical waters (Fig. 4.4). Surface fluorescence decreased slightly from north to south through the STC in winter (Fig. 4.4). In contrast, fluorescence increased markedly within the STC in spring, reflecting relatively high phytoplankton biomass within the frontal zone, compared to the water masses on either side (Fig. 4.4). Surface fluorecence was also highest in subantarctic waters and decreased from south to north in winter despite low phytoplankton biomass (Section 4.3.5) in the colder subantarctic waters. Vincent et al. (1991) also noted that the relationship between fluorescence and chlorophyll *a* biomass in subantarctic waters was less precise than that observed in warmer waters to the north. Specifically, fluorescence per unit chlorophyll *a* was highest in subantarctic waters where extracted chlorophyll *a* concentrations were lowest, and *vice versa* in STC and subtropical waters. Vincent et al. (1991) surmised that cell size, taxonomic composition and physiological photo-adaption of the phytoplankton population could significantly affect relationships between *in vivo* fluorescence and extracted chlorophyll *a* measurements.

Mean atmospheric concentrations of CO_2 in winter and spring were 353.0±0.6 ppmv (dry air) and 353±1 ppmv, respectively (Currie & Hunter, 1997). In spring, a 1°C increase in surface water temperature from subantarctic to STC waters on the Chatham Rise was concomitant with a decrease in sea-water pCO_2 by about 60 μatm (Fig. 4.5). At the

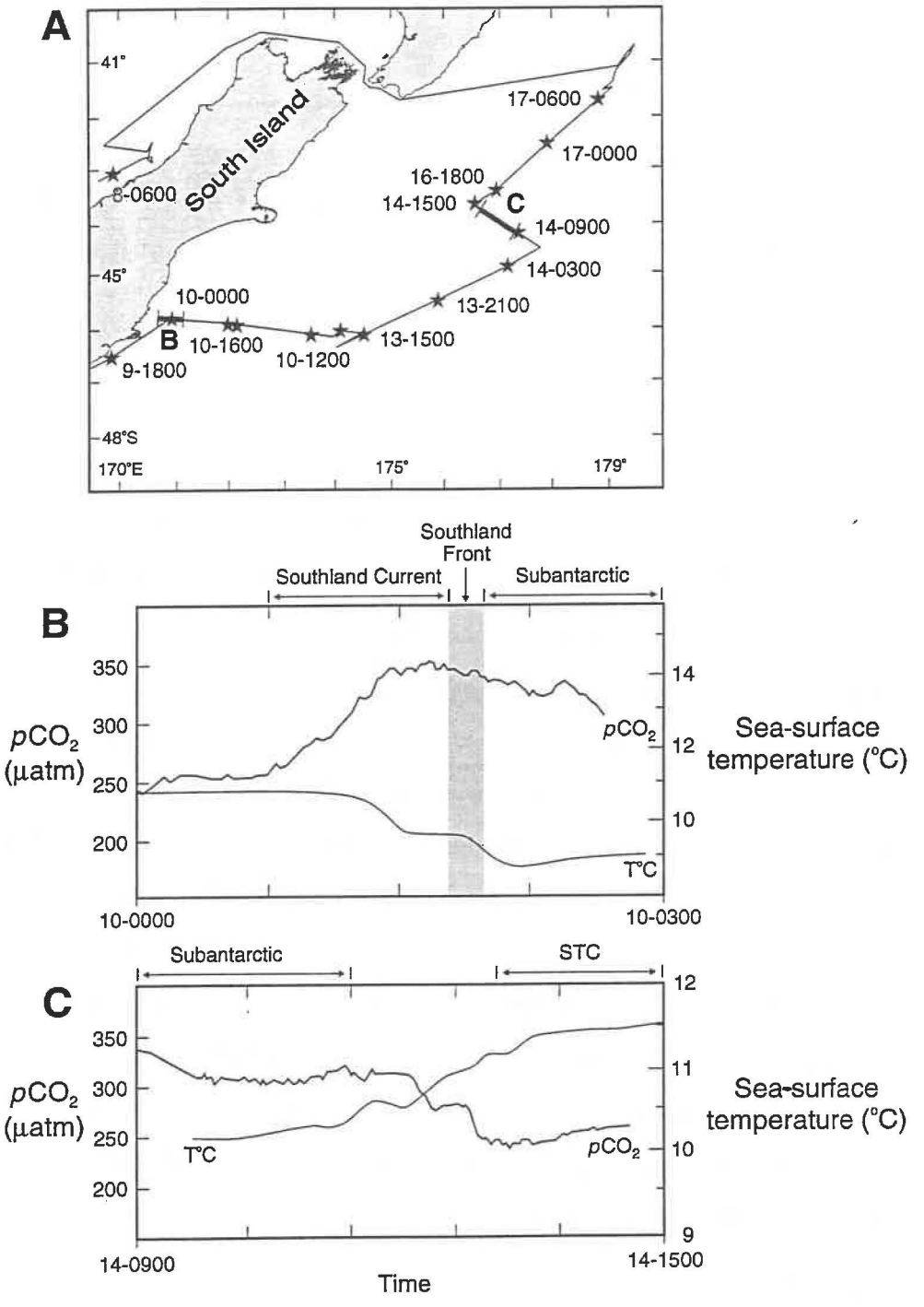

Fig. 4.5 (A) Location diagram of ship's track, showing dates and times, during spring 1993 ("13-1500" refers to the date - 13 October, 1993 - and the time - 1500 hours in New Zealand Standard Time). (B) and (C) Continuous pCO_2 (µatm) and sea surface temperature (°C) measurements across (B) the Southland Front and (C) Subtropical Convergence on the Chatham Rise. STC=Subtropical Convergence. Location of profiles shown in Fig. 4.5A.

transition from STC to warmer subtropical waters, there was an equivalent increase in sea-water pCO_2, although data from this crossing are not reliable (Currie & Hunter, 1997). Furthermore, sea-water pCO_2 increased by about 85-90 μatm as the vessel traversed across the Southland Front, off southeastern South Island, from modified coastal subtropical (Heath, 1972; Chiswell, 1996) into subantarctic surface waters (Fig. 4.5B). One might have expected pCO_2 in sea-water to decrease by about 20 μatm if this observation was due solely to a temperature change (Currie & Hunter, 1997); this anomalous situation is discussed further in Section 4.3.1.

4.3.3. Water chemistry: total alkalinity and dissolved inorganic nutrients

Winter total alkalinity (TA) values in subantarctic waters increased slightly with depth (0.01-0.02 meq kg^{-1}) (Table 4.2) (Fig. 4.6). In comparison, TA of STC waters in spring, and subtropical waters in both seasons, decreased by between 0.02-0.05 meq kg^{-1} with increasing depth. Winter TA values in all three water masses were generally higher than those in spring (Fig. 4.6). At the most northerly subtropical CTD stations (X468 & X469A) in winter, an increase in alkalinity was associated with a surface intrusion of cold, less saline water (Fig. 4.2). When the effects of salinity are taken into account, by normalising the TA data to 35‰, the increased TA at this station was not the result of simple dilution by the low salinity water (Currie & Hunter, 1997).

Dissolved inorganic nutrient concentrations (nitrate, DRP, DRSi) in the mixed-layer were generally higher in subantarctic waters, compared to the other two water types, regardless of season (Table 4.2) (Fig. 4.7-4.9). Subtropical waters typically recorded the lowest concentrations of nutrients, highlighting the nutrient-poor status of these waters. Notably, the low saline, cold water surface intrusion event observed at X469A (Fig. 4.2C) was accompanied by an increase in total alkalinity (as discussed above) and significant reduction in nitrate levels at depth (<7 μM at 550 m, compared with up to 22 μM at X468A, Fig. 4.7). Furthermore, DRP concentrations in surface waters (<100 m) at X469A were slightly elevated by 0.4 μM, compared with its paired station, (Fig. 4.8), while surface DRSi concentrations were slightly lower at X469A (by 0.5 μM), but were two times greater at 550 m (Fig. 4.9).

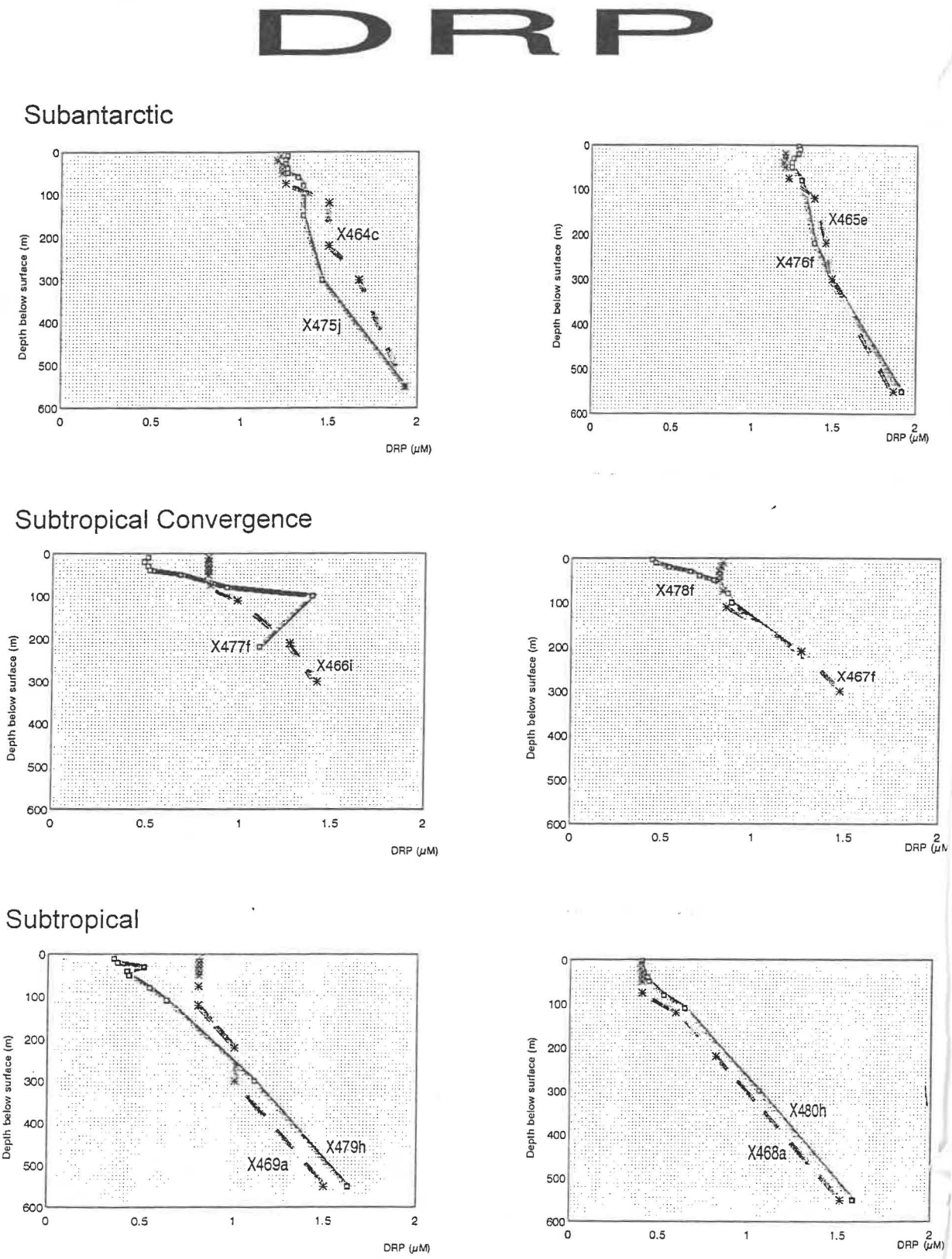

Fig. 4.8 Dissolved reactive phosphorus (DRP, μM) profiles at selected stations in subantarctic, STC and subtropical waters in winter (dashed line) and spring (solid line) 1993.

Nitrate

Subantarctic

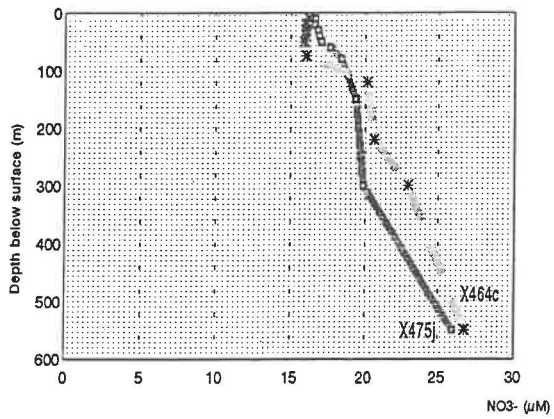

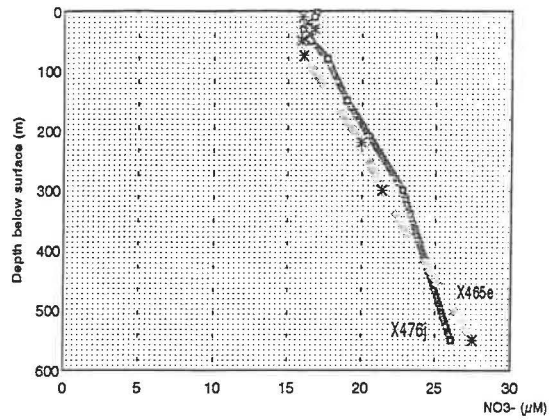

Subtropical Convergence

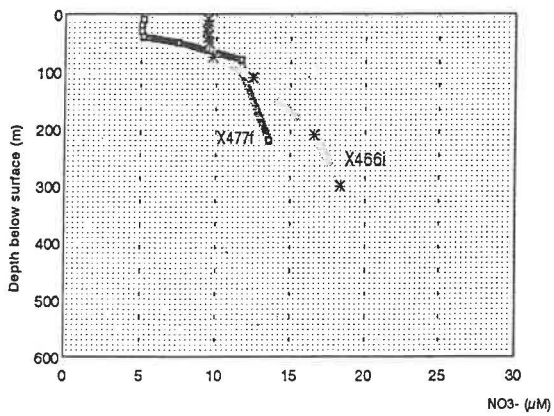

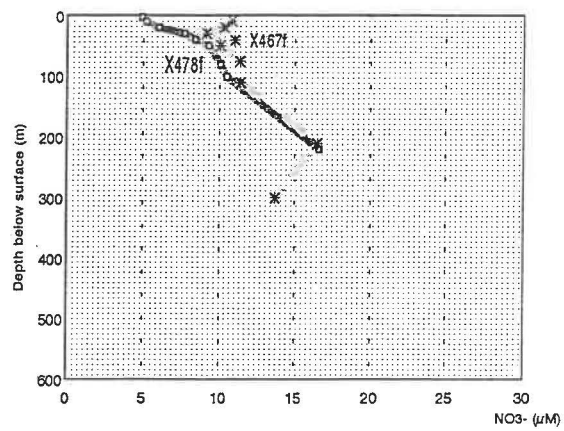

Subtropical

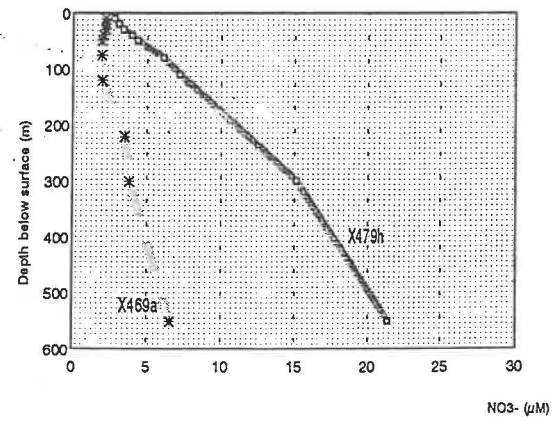

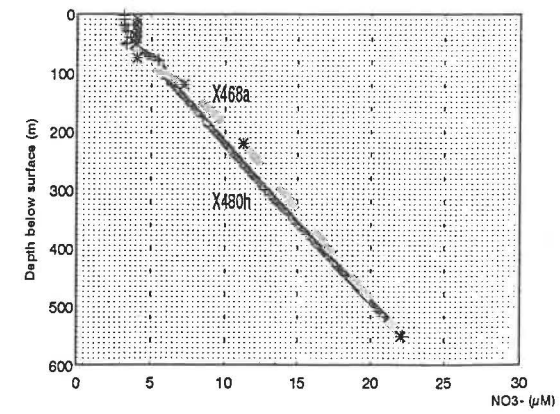

Fig. 4.7 Nitrate + nitrite (μM) profiles at selected stations in subantarctic, STC and subtropical waters in winter (dashed line) and spring (solid line) 1993.

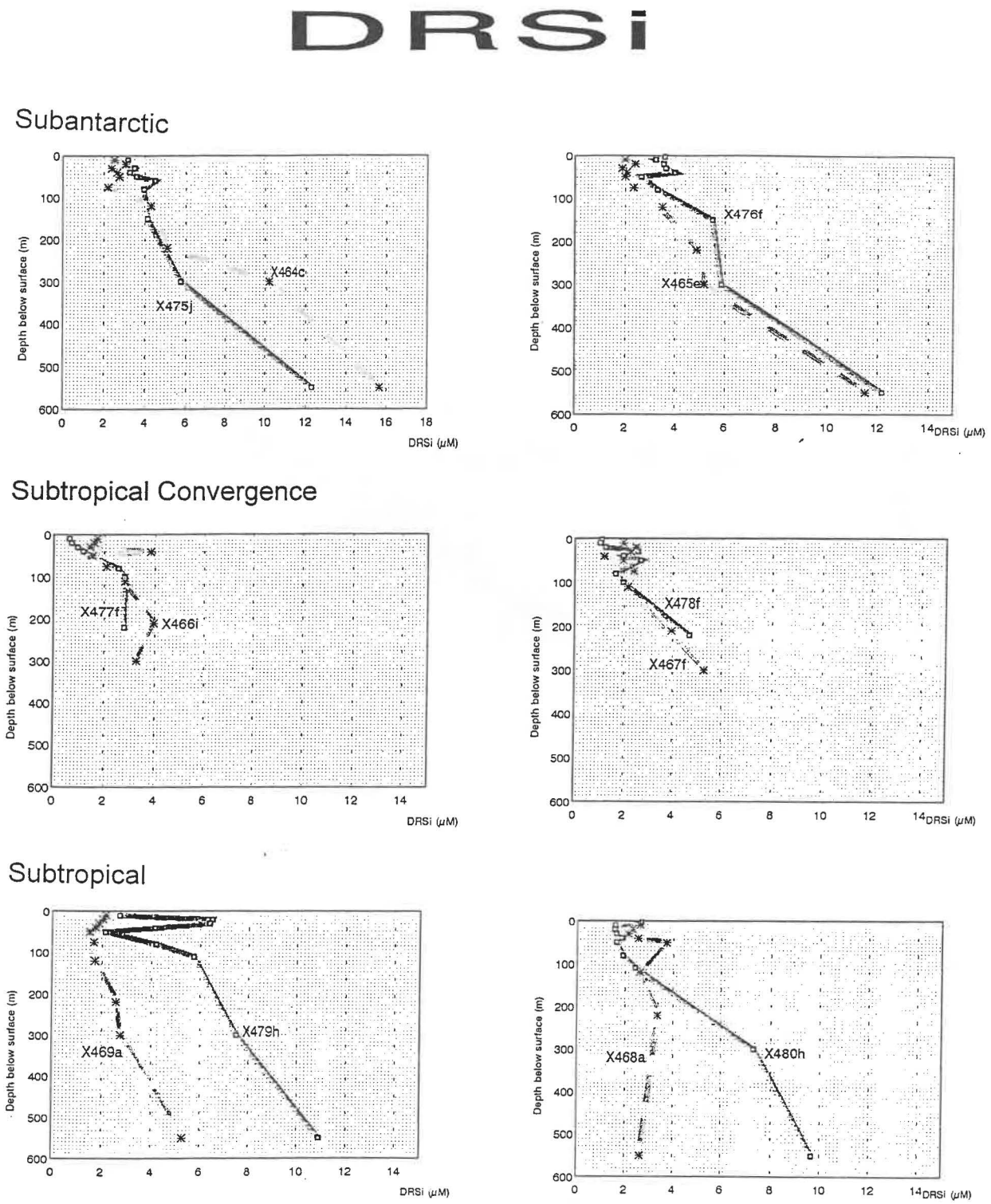

Fig. 4.9 Dissolved reactive silica (DRSi, μM) profiles at selected stations in subantarctic, STC and subtropical waters in winter (dashed line) and spring (solid line) 1993.

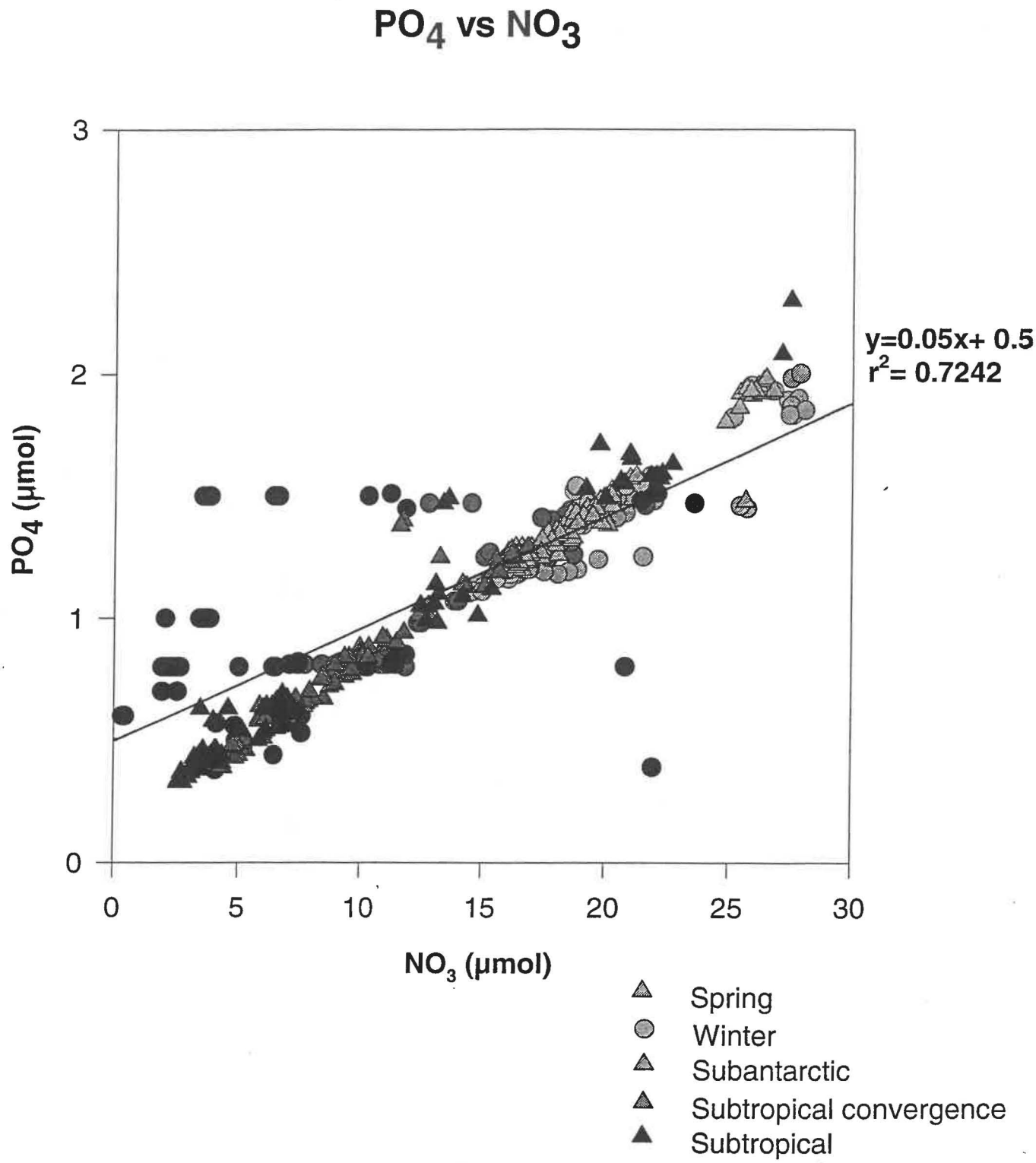

Fig. 4.10 Dissolved reactive phosphorus (PO_4) versus nitrate + nitrite (NO_3) concentrations (µmol = µM) across all stations and over all sampled depths in winter and spring 1993.

In STC waters, nitrate and DRP concentrations were slightly higher in winter, than in spring, with the apparent seasonal depletions in spring amounting to 2-5 μM nitrate and 0.3-0.4 μM DRP (Table 4.2) (Fig. 4.7 & 4.8). Spring values of DRSi concentration in subtropical and subantarctic waters were higher than corresponding measurements made in winter (Table 4.2) (Fig 4.9). Overall, nitrate and phosphate nutrients were well balanced in the three water types in both seasons, except for subtropical waters in winter when there seemed to be a slight excess of phosphate, relative to nitrate, in the system (Fig. 4.10). Weaker relationships were observed between these nutrients and silicate (Fig. 4.11 & 4.12), although overall silicate levels in subantarctic waters in spring, and to a lesser degree in subtropical waters in both seasons, were higher than expected from DRP concentrations (Fig. 4.12). The relationship between nitrate and DRSi suggests that, regardless of season, there is an excess of nitrate, relative to silicate, in subantarctic (~12 μM nitrate at 0 μM DRSi) and STC waters (~2 μM nitrate at 0 μM DRSi) (Fig. 4.13). In contrast, subtropical waters exhibit an apparently opposite, though highly variable, relationship wherein there is an excess of silicate of ~2 μM once all the nitrate has been consumed (Fig. 4.13).

Other nitrogenous compounds (urea and ammonium) displayed variable seasonal mixed-layer concentrations, with urea values slightly depressed in spring in subtropical waters by 0.1-0.4 μM (Table 4.2) (Fig. 4.14). Ammonium concentrations were relatively enhanced in STC in spring, compared to winter, and exhibited pronounced near-surface and mid-water concentration peaks down through the mixed-layer (Fig. 4.13).

4.3.4. Water column particulate populations

Water column particulate concentrations were variable between seasons and water types, although in general, higher values were observed in spring than in winter (Table 4.2) (Fig. 4.15-4.17). Concentrations of total particulate carbon, nitrogen and phosphorus were highest in upper parts of the water column as a function mainly of the vertical distribution of plankton. Particulate concentrations typically decreased down the water column, except for occasional mid-water and near-bottom increases in concentration during separate casts at the same station (Fig. 4.15-4.17). Some of these increases were matched by observable changes in particulate flux as measured using sediment traps (see later).

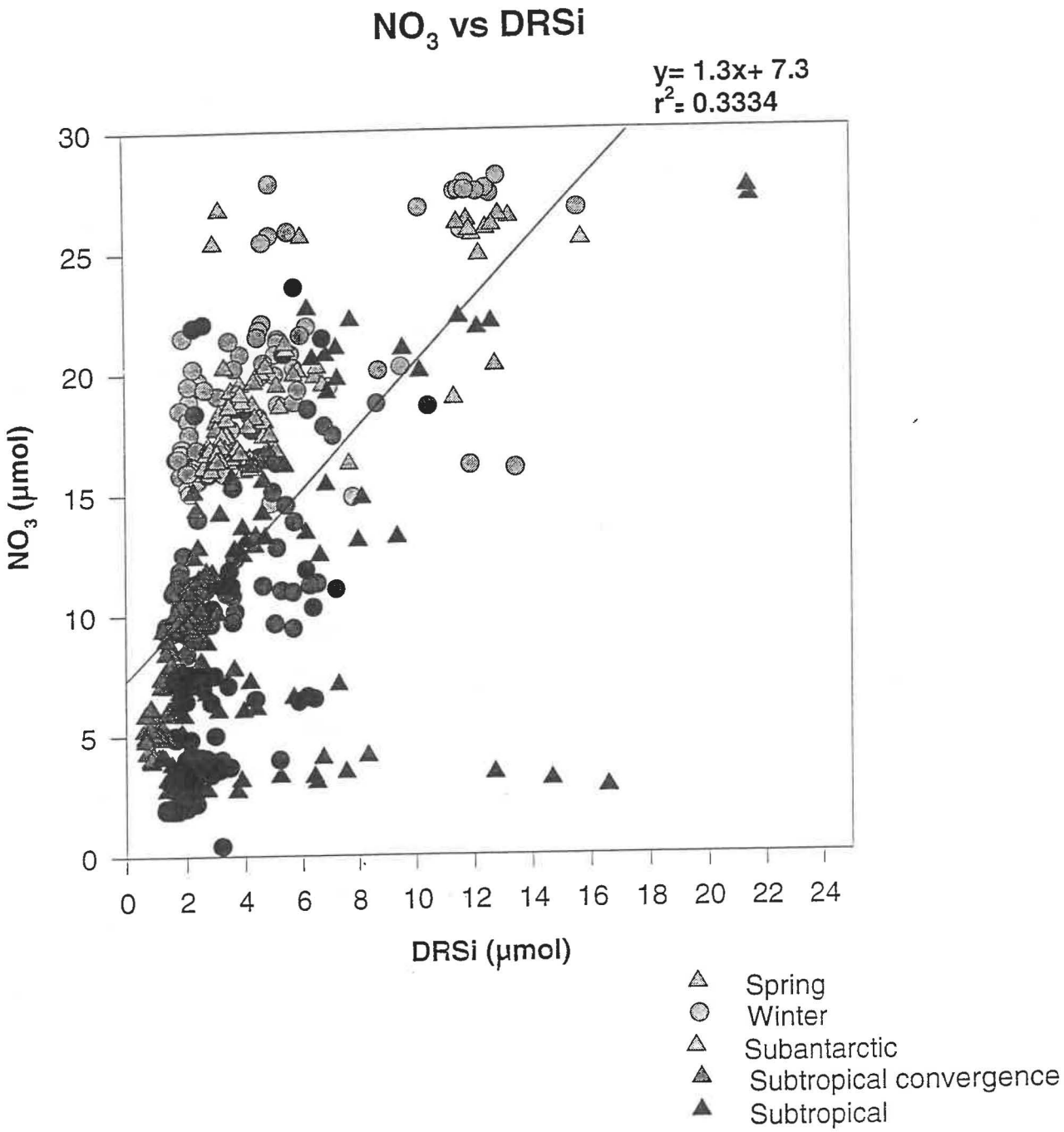

Fig. 4.11 Nitrate + nitrite (NO_3) versus dissolved reactive silicate (DRSi) concentrations (µmol = µM) across all stations and over all sampled depths in winter and spring 1993.

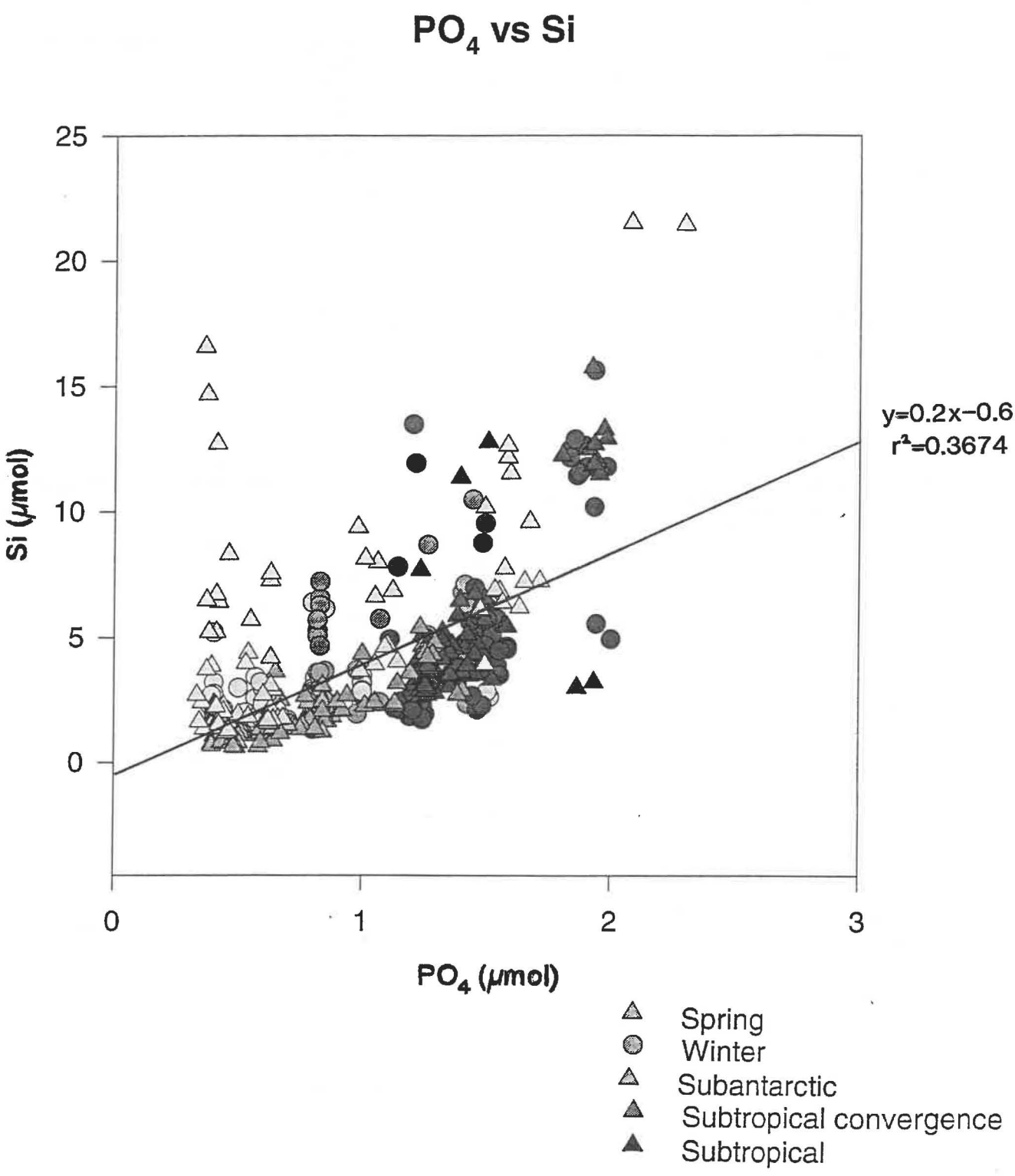

Fig. 4.12 Dissolved reactive phosphorus (PO_4) versus dissolved reactive silicate (Si) concentrations (µmol = µM) across all stations and over all sampled depths in winter and spring 1993.

NH_4

Subantarctic

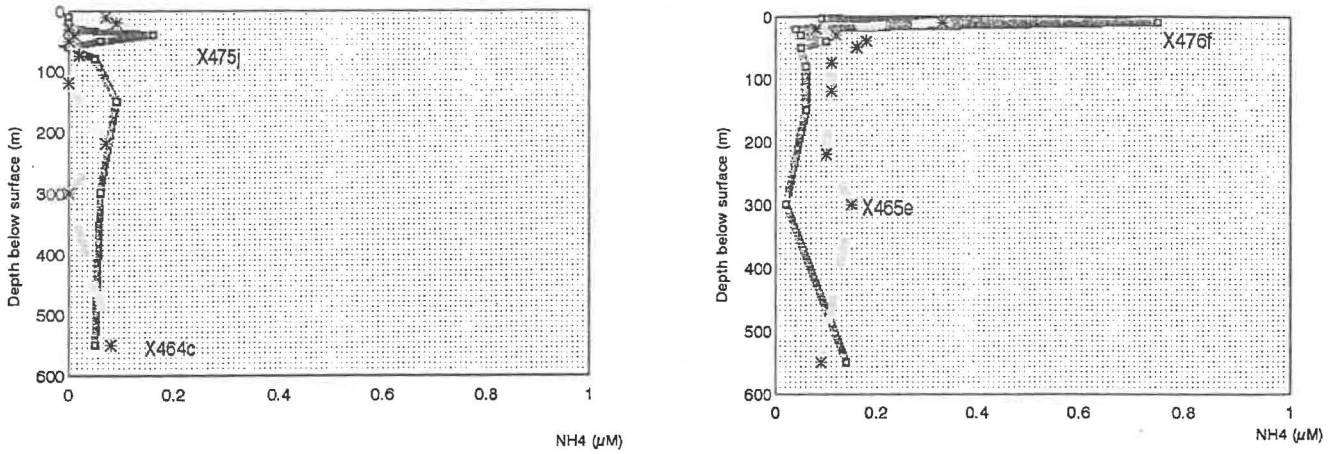

Subtropical Convergence

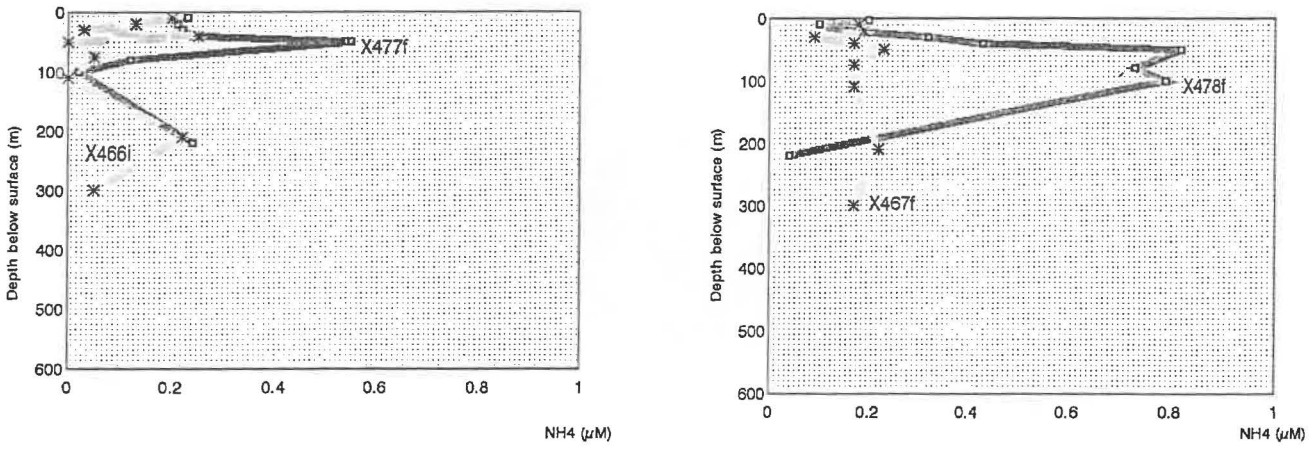

Subtropical

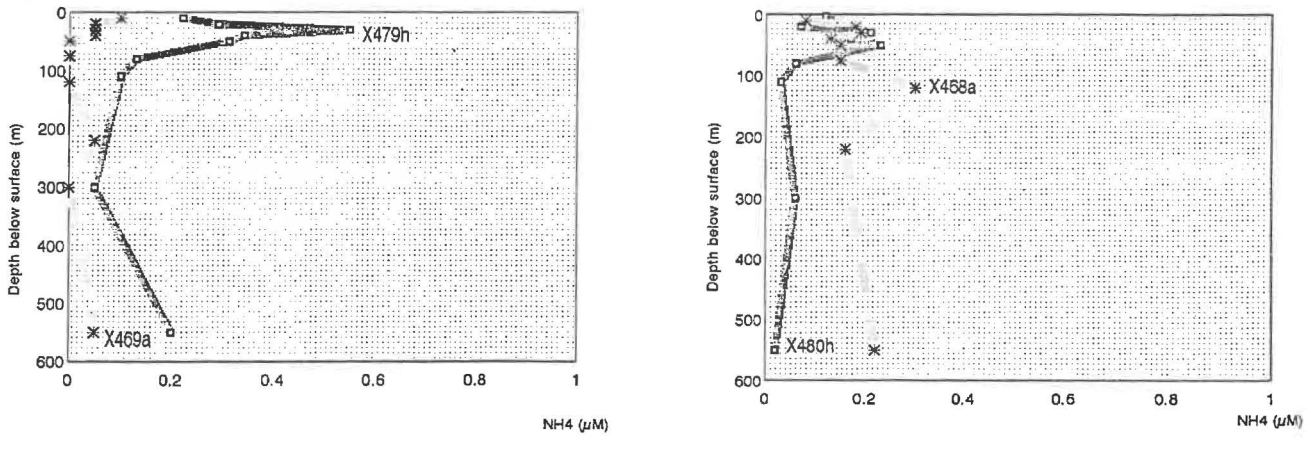

Fig. 4.13 Ammonium (NH_4, μM) profiles at selected stations in subantarctic, STC and subtropical waters in winter (dashed line) and spring (solid line) 1993.

Urea

Subantarctic

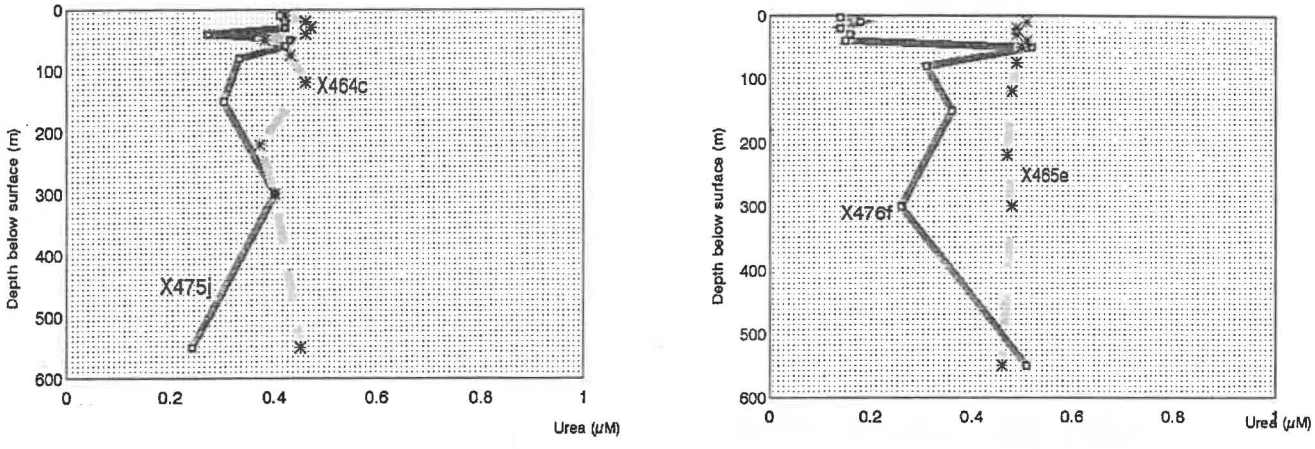

Subtropical Convergence

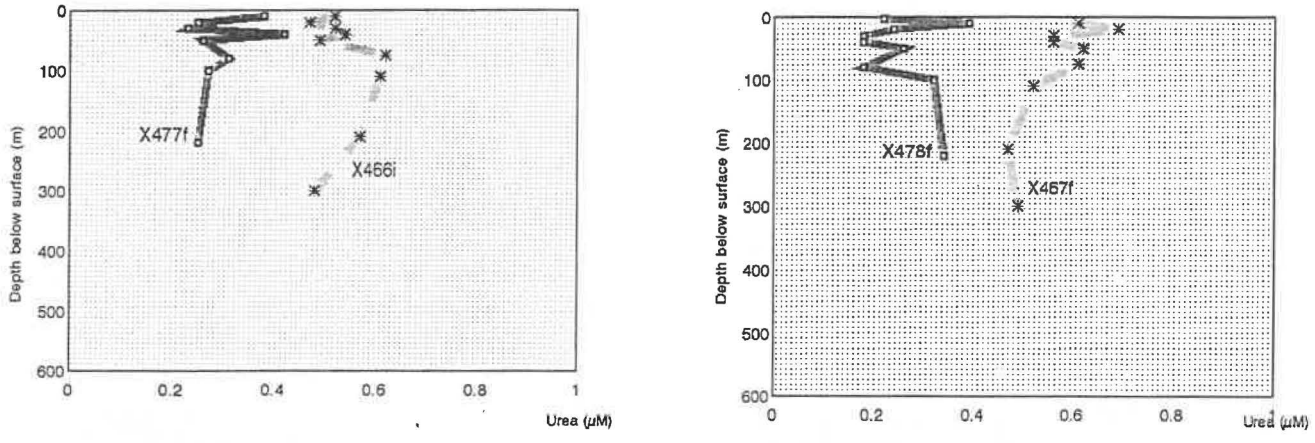

Subtropical

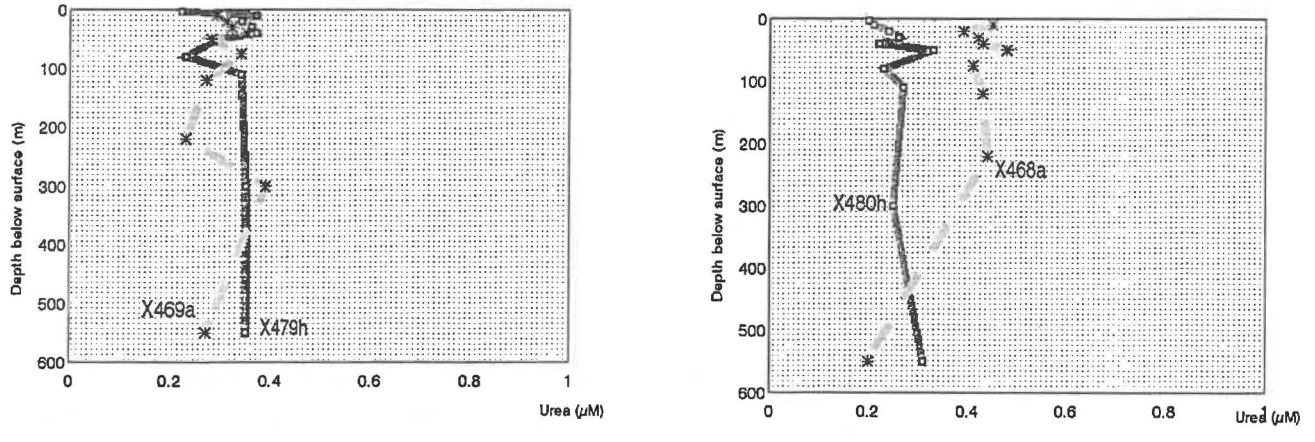

Fig. 4.14 Urea (μM) profiles at selected stations in subantarctic, STC and subtropical waters in winter (dashed line) and spring (solid line) 1993.

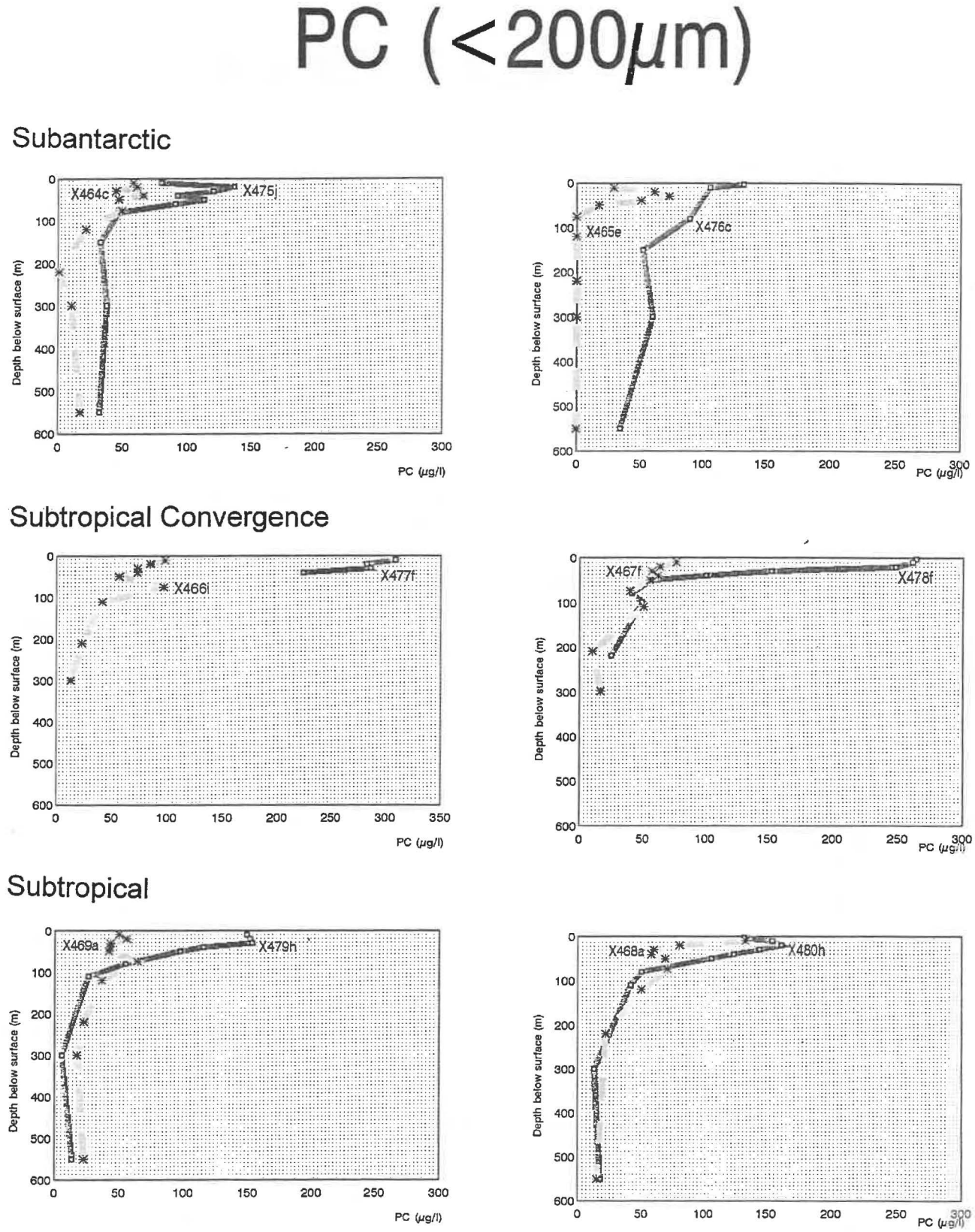

Fig. 4.15 Particulate carbon (<200 µm, µg l^{-1}) profiles at selected stations in subantarctic, STC and subtropical waters in winter (dashed line) and spring (solid line) 1993.

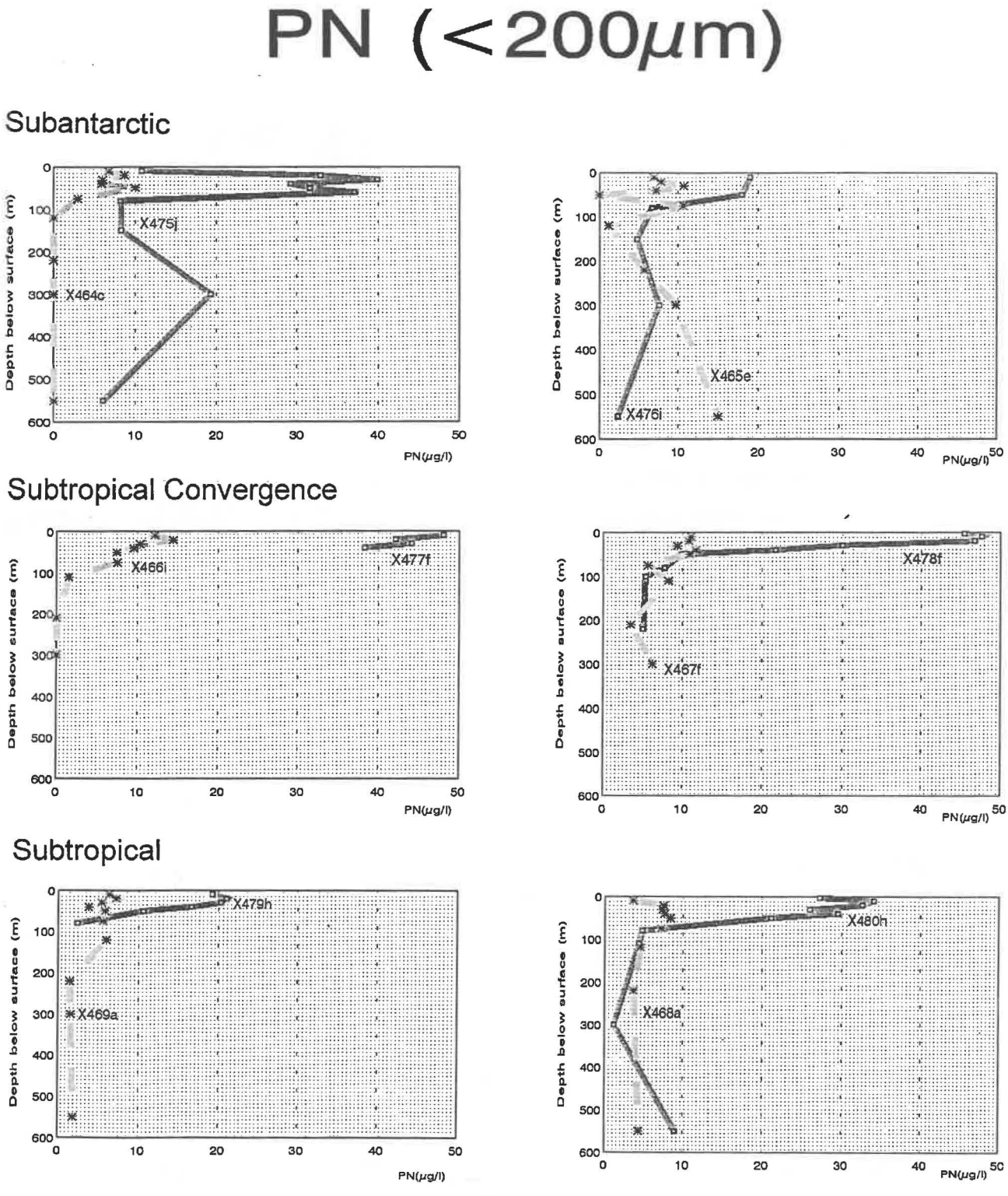

Fig. 4.16 Particulate nitrogen (<200 μm, μg l^{-1}) profiles at selected stations in subantarctic, STC and subtropical waters in winter (dashed line) and spring (solid line) 1993.

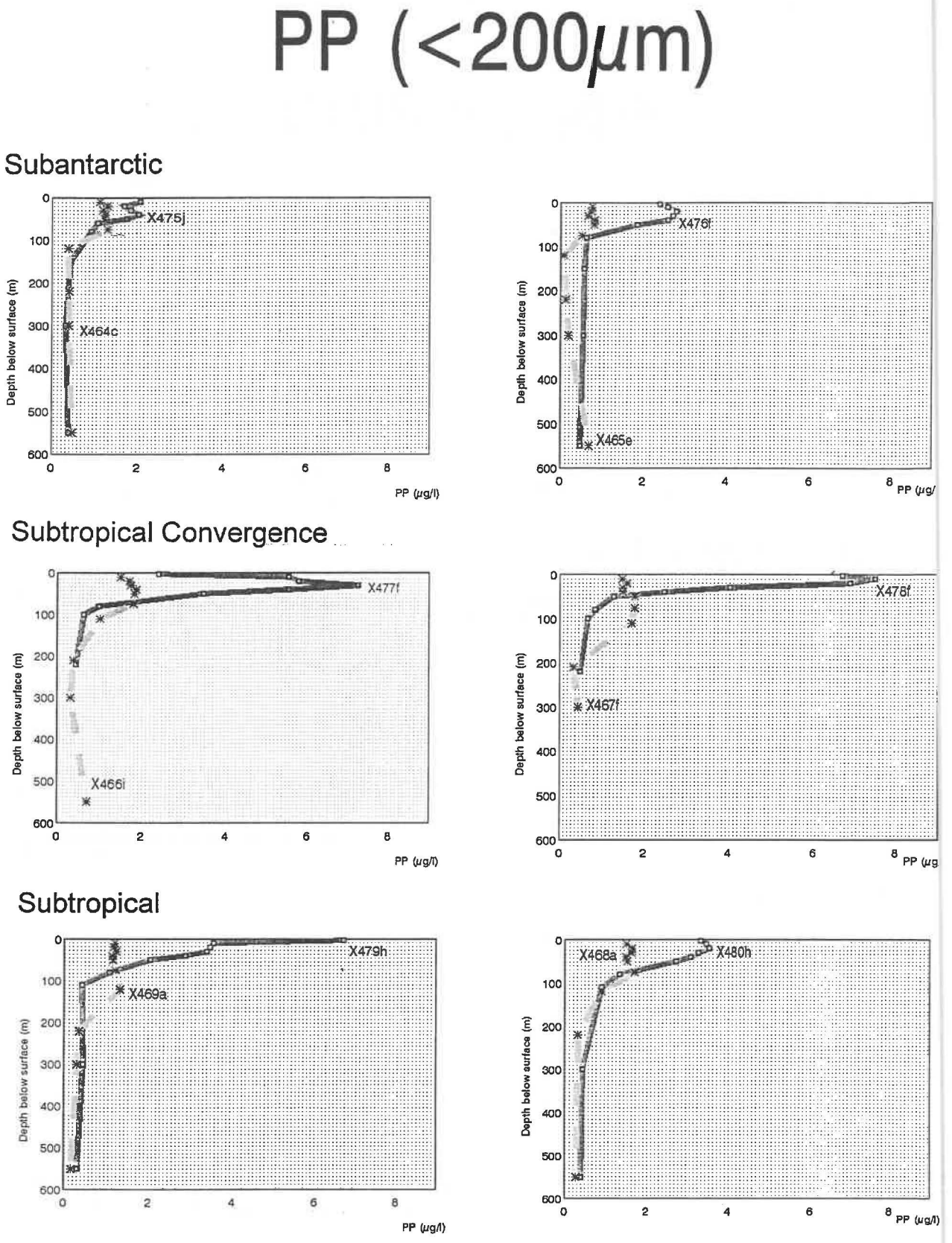

Fig. 4.17 Particulate phosphorus (<200 μm, μg l^{-1}) profiles at selected stations in subantarctic, STC and subtropical waters in winter (dashed line) and spring (solid line) 1993.

SPM concentrations were measured on duplicate samples in winter only and show a high degree of variation, ranging from 1-70%, but generally 5-40%. Thus, it is difficult to make statistically valid comparisons between the three water types (Fig. 4.18 & 4.19). Average SPM concentrations were higher generally in the STC in both seasons, with an increase observed in spring, compared to winter. In contrast, average SPM values observed in subantarctic waters were higher in winter (Table 4.2) (Fig. 4.18). SPM concentrations generally decreased or were similar with increasing depth in the three water types, except in winter at X465E (subantarctic), X466E and X467E (both STC).

4.3.5. Chlorophyll a, fluorescence, primary production and light regime

Chlorophyll *a* concentrations generally decreased down through the water column, with highest values observed within the mixed-layer (Fig. 4.20 & 4.21). Clearly defined sub-surface chlorophyll maxima were difficult to detect with the sampling intervals chosen. Overall, winter near-surface chlorophyll *a* (<200 μm) concentrations in the three water types were lower than those observed in spring (Table 4.3). Regardless of season, values of chlorophyll *a* were higher in the STC than in water masses to the north and south, with a 6-fold increase in near-surface chlorophyll *a* concentration observed in spring (Fig. 4.21). Subantarctic waters exhibited lower levels of chlorophyll *a* than subtropical waters. Similar observations were found across the three water types for fluorescence response, as measured during vertical CTD casts in spring, with maximum fluorescence of 25% in subantarctic waters, >50% in the STC and 30-35% in subtropical waters (Singleton, 1994). In spring, maximum depth zones of total fluorescence (>20% arbitrary units) were often deeper than the depth of the mixed-layer, although highest fluorescence responses were typically observed well above the MLD, in association with maximum chlorophyll *a* concentrations (Fig. 4.20 & 4.21). Maximum depths of fluorescence ranged from 80-123 m in subantarctic waters, 70-115 m in the STC and 70-100 m in subtropical waters.

Mean depth-integrated chlorophyll *a* concentrations did not vary substantially between seasons in subantarctic waters, but were enhanced in spring by 2-3 times in STC and subtropical waters (Table 4.3). Water column primary production, integrated to 1% light level, was substantially higher in STC and subtropical water types in spring by 4 and 6-7

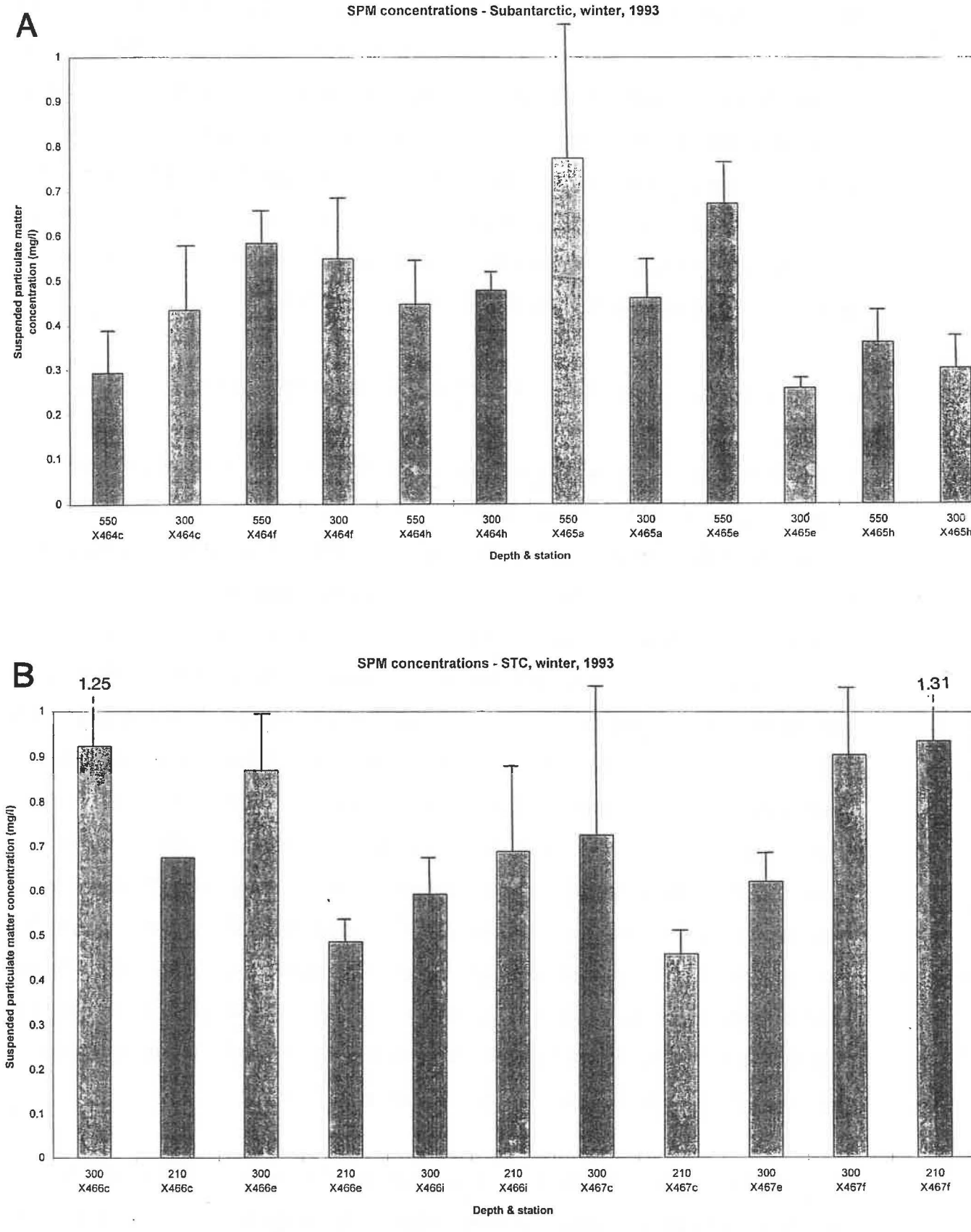

Fig. 4.18 Suspended particulate matter concentrations (SPM, mg l^{-1}) at selected depths and stations in subantarctic (A) and Subtropical Convergence (B) in winter 1993. Average values are shown ± 1 standard deviation.

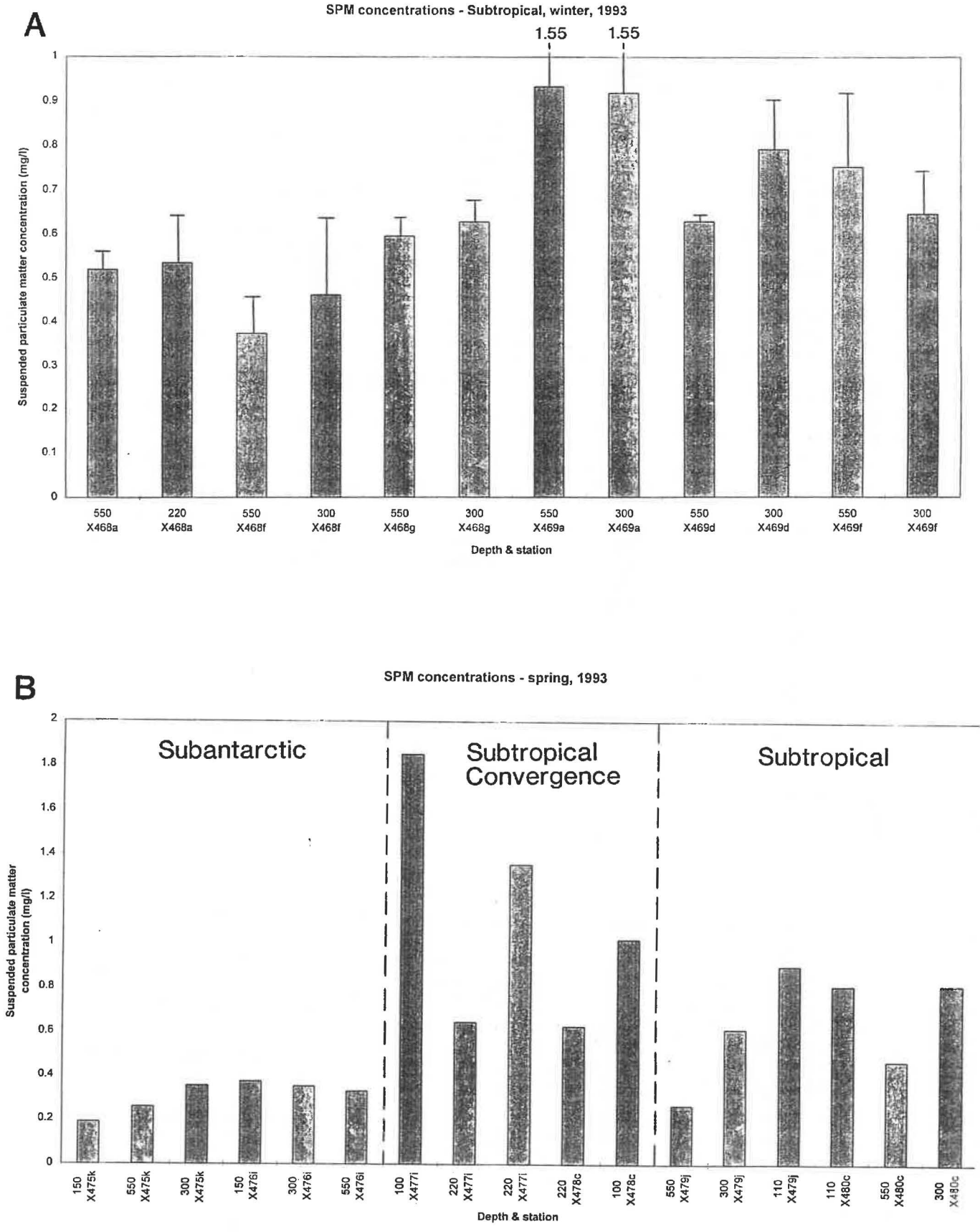

Fig. 4.19 Suspended particulate matter concentrations (SPM, mg l^{-1}) at selected depths and stations in (A) subtropical waters in winter and (B) across three water types in spring 1993. In A, average values are shown ± 1 standard deviation, while in B, samples were unreplicated.

Winter 1993

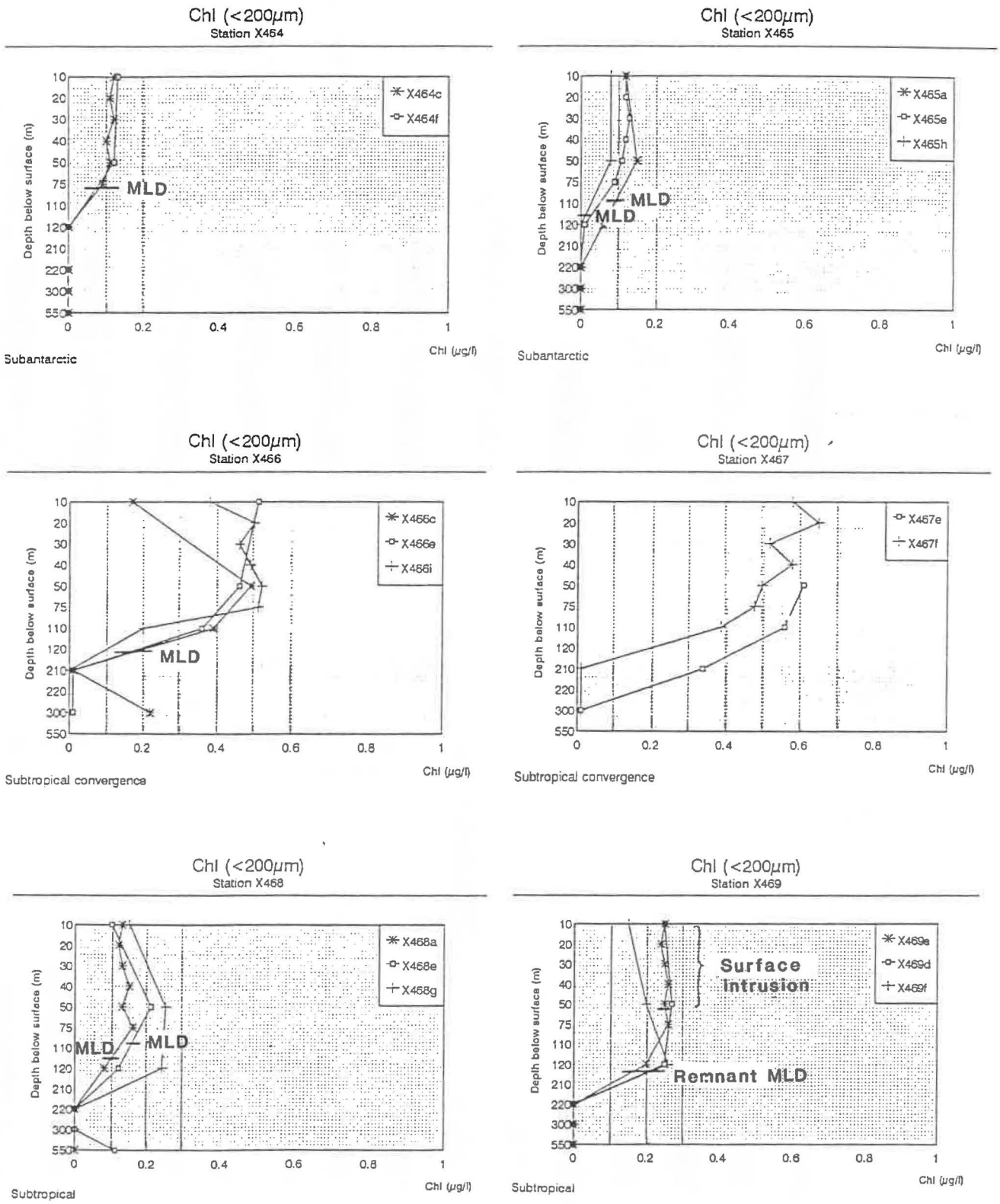

Fig. 4.20 Chlorophyll *a* concentrations (<200 μm, μg l^{-1}) profiles at selected stations in subantarctic, STC and subtropical waters in winter 1993.

Spring 1993

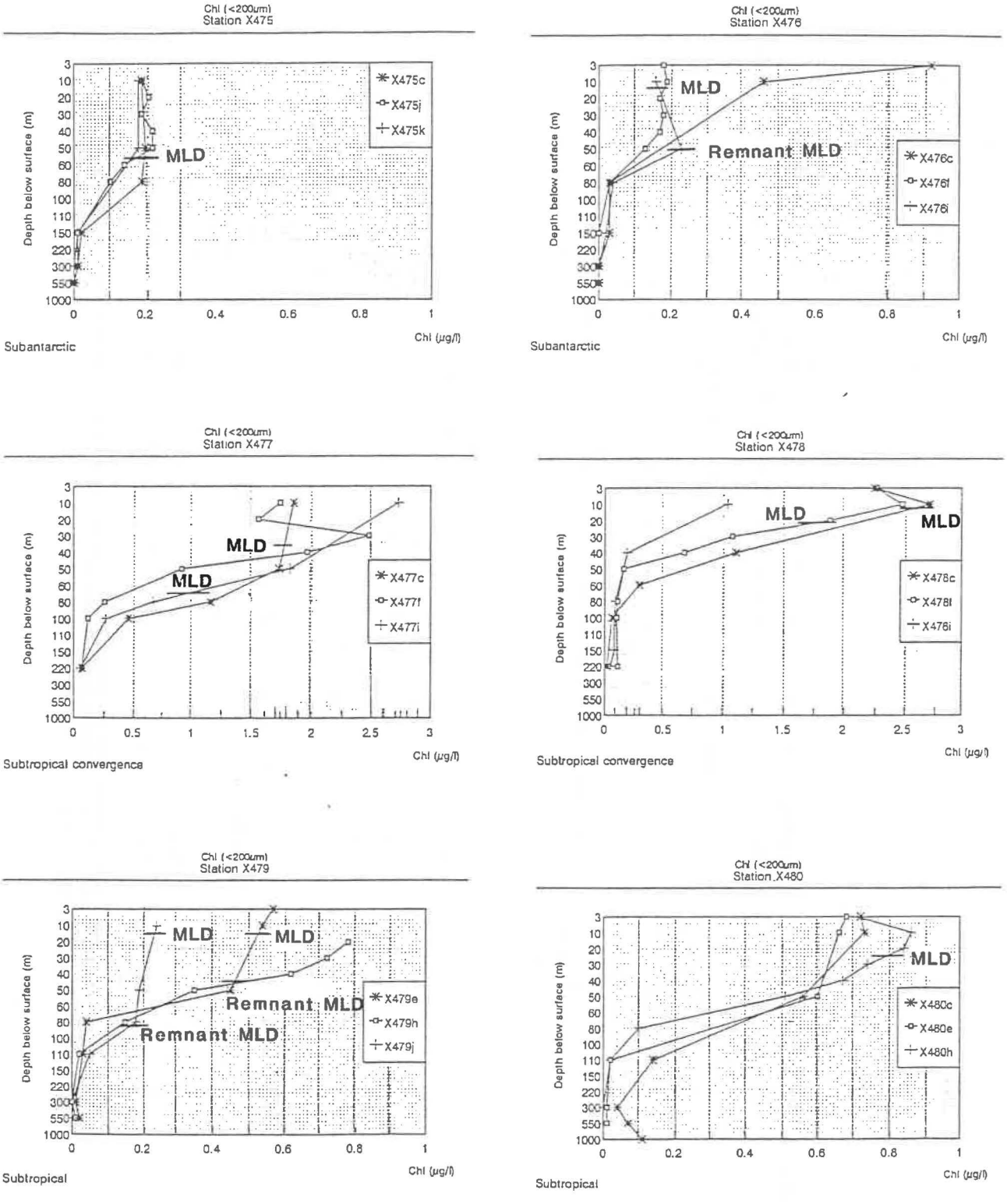

Fig. 4.21 Chlorophyll *a* concentrations (<200 µm, µg l^{-1}) profiles at selected stations in subantarctic, STC and subtropical waters in spring 1993.

Table 4.4 Size-fractionated primary production rates and chlorophyll *a* concentrations across three water types in winter and spring 1993 (Bradford-Grieve et al., 1997a). Depth to the 1% light level at each station is also shown.

Season & water type*	Station	1% light level (m)	% primary production				% chlorophyll *a*			
			20-200 µm	20-2 µm	<2 µm	<20 µm	20-200 µm	20-2 µm	<2 µm	<20 µm
Winter 1993										
SA	X464	29	12	22	66	88	35	21	44	65
	X465	30	49	7	43	50	10	45	45	90
STC	X466	-	60	24	15	39	62	24	15	39
	X467	47	70	9	20	29	67	21	12	33
ST	X468	55	54	19	27	46	0	51**	48	99
	X469	-	52	3	45	48	35	34	31	65
Spring 1993										
SA	X475	56 & 62	35	25	40	65	34	33	33	66
	X476	49	35	21	44	65	0	63**	38	101
STC	X477	29 & 18	82	6	12	18	79	13	8	21
	X478	-	71	7	22	29	64	23	13	36
ST	X479	42 & 38	46	21	32	53	16	49	35	84
	X480	55	33	18	49	67	0	55**	45	100

* SA=subantarctic, STC=Subtropical Convergence, ST=subtropical.

** Samples represent 2-200 µm fraction due to omission of pre-screening.

times, respectively, compared with winter. The highest proportional seasonal increase in integrated production was in subantarctic waters at the X464/X475 station pairing (8 times), while at the replicate station (X465/X476) this rate of increase was about half (Table 4.3). Production per unit biomass (P_B) was relatively low across all three water types in winter, ranging from 2-14 and increased in spring (Table 4.3). In the STC in spring, however, P_B ratios of 7-13 were about half those measured in subantarctic (14-23) and subtropical waters (14-28).

In subantarctic waters, production and chlorophyll biomass was variable between all phytoplankton size classes, with pico- and nanophytoplankton (<2 and 2-20 μm size-fractions) being important contributers to the algal biomass, particularly in spring (Bradford-Grieve et al., 1997a) (Table 4.4). Production and chlorophyll biomass in the STC in both seasons were dominated by microphytoplankton (20-200 μm), which were mainly diatoms (Bradford-Grieve et al., 1997a) (Table 4.5). Sixty to seventy percent of potential primary production in this size fraction occurred in winter, compared with 70-80% in spring. In subtropical waters in winter, 50% of production was occurring in the microphytoplankton population; this proportion reducing to 30-50% in spring. Production and biomass of picophytoplankton (<2 μm) in subtropical waters remained relatively constant between winter and spring at about 30-50%. Primary production varied between stations with production at X469 and X479 about 50% of the rate measured at X468 and X480, respectively (Bradford-Grieve et al., 1997a).

The photic zone (depth to 1% surface light level) in the three water types typically varied from 40-60 m in both seasons (Table 4.4). Relatively shallow photic zones were observed in subantarctic waters in winter (30 m) and in the STC in spring (20-30 m). The deepest 1% light level at 50-60 m was found in subantarctic waters in spring.

4.3.6. Planktonic community structure and functioning: algal groups, microbial populations and mesozooplankton communities

The phytoplankton community in subantarctic waters was generally characterised by microflagellates (50-60%) and dinoflagellates (30-45%) in both seasons (Chang & Gall,

Table 4.5 Phytoplankton cell carbon biomass in water types, east of New Zealand, during winter and spring 1993.

Season & water type*	Station	Total microflagellates** µgC l^{-1}	Total diatoms** µgC l^{-1}	Total dinoflagellates** µgC l^{-1}
Winter 1993				
SA	X464C	86.15	4.25	48.35
	X465E	63.30	17.85	26.55
	$\bar{x} \pm s$	**74.73±16.16**	**11.05±9.62**	**37.45±15.42**
STC	X466I	182.05	927.80	53.55
	X467F	178.40	1332.10	135.90
	$\bar{x} \pm s$	**180.23±2.58**	**1129.95±285.88**	**144.73±12.48**
ST	X468A	85.05	65.65	950.20
	X469A	90.00	83.60	182.75
	$\bar{x} \pm s$	**87.53±3.50**	**74.63±12.69**	**566.48±542.67**
Spring 1993				
SA	X475I	240.25	15.45	166.95
	X476F	245.22	10.14	251.27
	$\bar{x} \pm s$	**242.74±3.51**	**12.80±3.76**	**209.11±59.62**
STC	X477F	1186.30	3154.55	120.70
	X478D	1018.41	2165.95	187.30
	$\bar{x} \pm s$	**1102.36±118.72**	**2660.25±699.05**	**154.00±47.09**
ST	X479H	266.79	405.85	60.90
	X480H	368.54	24.46	21.73
	$\bar{x} \pm s$	**317.65±71.98**	**215.16±269.68**	**41.32±27.70**

* SA=subantarctic, STC=Subtropical Convergence, ST=subtropical.

** All values are integrated from 0 to 50 m water depths assuming that surface concentrations at 0 m are equal to concentrations in the uppermost sample (generally 10 m). Cell carbon contents were determined on the basis of microscopic identifications and counts of phytoplankton and assumptions regarding carbon content and cell geometry (data provided by F. H. Chang, pers. comm., 1997) (Chang & Gall, submitted).

submitted) (Table 4.5). Diatoms were present in small numbers and coccolithophorids were under-represented in all samples due to dissolution by acidic Lugol's solution. In subantarctic waters, smaller phytoplankton cells, predominantly <2 μm in size, were proportionally dominant in winter with picophytoplankton accounting for 40-70% of the estimated primary production and 40-45% of chlorophyll biomass, compared with 30-40% in spring. Bacterial biomass and production were higher in subantarctic waters in winter, compared with the other water types (Table 4.3), although bacterial production only accounted for 10-20% of daily production of phytoplankton standing stock in either season (Smith & Hall, in press). Spring bacterial productivity at two stations in subantarctic waters was variable; production at X475 was about half that measured at X476 (Smith & Hall, in press). Microzooplankton biomass and grazing on phytoplankton increased between seasons in subantarctic waters, and heterotrophic flagellates were present in higher numbers than autotrophic flagellates in spring (James & Hall, 1997) (Table 4.3). Grazing impact by microzooplankton was generally greater in subantarctic waters and on picophytoplankton rather than on total phytoplankton, compared with the other two water types. Mesozooplankton biomass and grazing in subantarctic environments did not increase substantially between winter and spring (Bradford-Grieve et al., 1997b) (Table 4.3).

In the STC, diatoms dominated the phytoplankton community (70-80%), with microflagellates (probably prymnesiophytes and cryptomonads, F. H. Chang, pers. comm., 1995) comprising 10-30% in both seasons (Table 4.5). Bacterial productivity increased substantially in spring with winter productivity only 5% of the spring rate, equivalent to a 26-fold increase between seasons (Smith & Hall, in press) (Table 4.3). Autotrophic flagellates dominated over heterotrophic flagellates in spring in the STC, while ciliate numbers were also substantially reduced in this season. Grazing rates of microzooplankton on phytoplankton, as a percentage of chlorophyll *a* standing stock and primary production removed per day, increased variably by an average of 3 times in the STC, but removed only about 30% of total biological production. Mesozooplankton biomass and grazing rates increased 3-4 times between seasons in the STC.

Seasonal variations in the phytoplankton population were apparent in subtropical waters with dinoflagellates dominating in winter (50-90%) and microflagellates predominating in spring

(40-90%) (Table 4.5). There were distinctive inter-station differences in phytoplankton composition, however, with dinoflagellates dominating phytoplankton cell carbon estimates at X468 (86%), but not the replicate station at X469, in winter (50%; Chang & Gall, submitted). Similarly, diatoms characterised station X479 in spring (55%), whereas at X480, diatoms were only a minor component (6%), compared with microflagellates (89%; Chang & Gall, submitted). Mesozooplankton and microzooplankton biomass estimates were highest in subtropical waters in spring with mesozooplankton grazing rates increasing from 4 to 28 mgC m^{-2} d^{-1}, a 7-fold increase between seasons. As was observed in the STC in spring, autotrophic flagellates dominated the microplankton community with relatively low numbers of heterotrophic flagellates and ciliates. Microzooplankton grazing on bacteria was only measured in spring, and removed almost all bacterial production and between 30-70% of bacterial biomass on a daily basis across the three water types (James & Hall, 1997).

Copepods were the dominant component of the mesozooplankton community, regardless of season and water type, although the dominant copepod species did vary, and in subantarctic waters, euphausiids and chaetognaths were also important (Bradford-Grieve et al., 1997b). There were no significant temporal differences in mesozooplankton community composition with omnivores comprising around 50-80% in both seasons (Bradford-Grieve et al., 1997b). Gelatinous metazoans, such as pteropods and salps, are known to produce fast sinking faecal pellets (e.g., Bruland & Silver, 1981), but were only minor components of mesozooplankton populations, except in subantarctic (one station only, X476) and subtropical waters (one station only, X480) in spring (20% of >1000 μm biomass, Bradford-Grieve et al., 1997b).

4.4. Discussion

4.4.1. Variations in pCO_2 and total alkalinity: effect of biological processes on water column chemistry

In spring, 1993, oceanic surface waters were undersaturated in CO_2 with respect to the atmosphere (average concentration of CO_2 in atmosphere was 353 μatm), suggesting that all oceanic water types east of New Zealand were acting as sinks for atmospheric CO_2 (Currie & Hunter, 1997). The temperature increase from subantarctic to STC waters should have

resulted in an increase in sea-water pCO_2, but observations indicate that pCO_2 in the STC was about 60 μatm less than that in subantarctic waters (Fig. 4.5C). The apparently anomalous depression in sea-water pCO_2 in the STC could be due to enhanced photosynthetic production in the STC in spring 1993, as suggested by the elevated primary productivity rates and chlorophyll *a* concentrations observed in the convergence zone (Table 4.3). The relatively low TA concentrations and high sea-water pCO_2 values in subantarctic waters may also reflect the influence of carbonate precipitation, while the observed, albeit subtle, decreases in TA with depth in STC and ST waters are likely to arise from the oxidation of sinking organic matter. One may have expected TA to increase with depth due to the enhanced dissolution of carbonate with increasing pressure (e.g., Baes et al., 1985); only the winter TA results reveal such a change with depth.

Observed lower primary production rates in winter suggest that photosynthetic processes are unlikely to have been responsible for the heightened TA concentrations measured in winter. The observed relative decrease in TA in spring may be partially explained by preferential uptake of ammonium during photosynthesis since the photosynthetic uptake of 1 mole of ammonium results in a concomitant 1 mole reduction in TA (Robertson & Watson, 1993). Support for this mechanism is suggested by relatively stable concentrations of nitrate and the slight reduction of ammonium in SA and ST waters in spring, compared to winter (Table 4.2). Unfortunately, no nitrogen uptake experiments were undertaken on either voyage to verify this inference. Alternatively, increased carbonate precipitation in spring may have also contributed to the observed lower TA concentrations, as perhaps evinced by the prevalence of calcium carbonate-precipitating zooplankton "swimmers", such as foraminifera and pteropods, collected in sediment traps in spring (Table 5.5, Section 5.3.6, Chapter 5).

Sea-water pCO_2 in surface waters, associated with other frontal regions in the Southern Ocean, is variable on many spatial and temporal scales (e.g., Goyet et al., 1991; Poisson et al., 1993). In subantarctic regions, in the Southwest Indian Ocean, sea-water pCO_2 is influenced predominantly by seasonal biological activity (i.e., lower pCO_2 in austral summer than in winter; Goyet et al., 1991), while in subtropical waters, variations in pCO_2^{sw} are due principally to changes in sea-surface temperature (i.e., higher in summer than in winter). Low pCO_2^{sw} values have been reported at seasonal scales in the STC in the Pacific (Murphy

et al., 1991) and Indian oceans (Inoue & Sugimura, 1988; Goyet et al., 1991), and are associated generally with elevated levels of biological activity (Metzl et al., 1991; Murphy et al., 1991), similar to the austral spring 1993 interpretations made in the Southwest Pacific Ocean. Note that no winter pCO_2 measurements were made in 1993 due to equipment malfunction, but given the elevated nature of phytoplankton chlorophyll *a* concentrations in monthly averaged Coastal Zone Color Scanner (CSCZ) across the Chatham Rise from 1978-86 (Comiso et al., 1993), and results of Murphy et al. (1991), it is anticipated that the Southwest Pacific Ocean may be a significant regional sink for atmospheric CO_2 over most seasons, including winter.

4.4.2. Seasonal changes in plankton community structure and functioning

Seasonal changes in plankton community structure can account for temporal and spatial patterns and modes of export fluxes out of the upper ocean (e.g., Legendre & le Fèvre, 1989; Passow & Peinert, 1993; Landry et al., 1994; Boyd & Newton, 1995; Deuser et al., 1995; Karl et al., 1996; Rivkin et al., 1996, and many others). Sediment trap data collected in 1993, however, shows that there were no statistically significant differences in total mass and particulate phosphorus export flux across three physically, chemically and biologically distinctive water types (Nodder & Alexander, 1997). This situation occurred despite marked seasonal variations in ecosystem community structure and function as discussed below.

Subantarctic. In winter, subantarctic waters supported high microbial productivity and biomass, and elevated microzooplankton biomass, compared to the same water mass in spring. These observations suggest that higher recycling rates of organic material within the upper water column may be expected, and hence reduced export flux (e.g., Landry et al., 1994). Average mass fluxes, however, were enhanced in winter, compared to spring (Nodder & Alexander, 1997), possibly due to the incorporation of dense terrigenous material into fast-sinking marine particles (e.g., Honjo & Manganini, 1993). Corrobative evidence is inferred from observations of higher concentrations of marine total suspended particulate material in winter compared to spring (0.3-0.8 cf. 0.2-0.4 mg l^{-1}, Table 4.2). The postulation that a proportion of this material is likely to be inorganic in origin is supported by other

observations, such as seasonal variations in "organic" particulate concentrations (e.g., chlorophyll *a*, particulate carbon and nitrogen) are opposite to the seasonal trend exhibited by total water column particulate populations (Table 4.2). In addition, inorganic substances may have been responsible for the high extinction coefficient, K_o, found at X464 in subantarctic waters in winter since chlorophyll *a* biomass was low (Bradford-Grieve et al., 1997a). In spring, however, it seems that phytoplankton accumulation in subantarctic waters had barely begun since spring nutrient concentrations were similar to winter levels and chlorophyll *a* biomass estimates remained low (Bradford-Grieve et al., 1997a) (Table 4.3).

Subtropical Convergence. Comparison of ecosystem dynamics in the two seasons in STC waters suggests that, although phytoplankton, mesozooplankton, microzooplankton and microbial processes appear to be reduced substantially in winter, compared with spring (Table 4.3 & 4.4), chlorophyll-derived pigment and phaeopigment fluxes were enhanced slightly in winter (Nodder & Gall, submitted). Microphytoplankton (mainly 200-20 μm diatoms) dominated biomass and productivity estimates in both seasons, such that the observed increase in total chlorophyllous fluxes in winter reflects the greater sedimentation potential of large cell phytoplankton aggregates in this season, compared with spring. In spring, despite substantial accumulation of large phytoplankton cells in the upper water column, production per unit biomass was lowest in the STC, compared with the other two water types. Furthermore, it was expected that maximal export rates of senescent and intact phytoplankton would be observed if a "bloom" situation had developed (e.g., Legendre, 1990; Head et al., 1994; Lochte et al., 1993). This anomalous observation may reflect the timing of the sediment trap experiment which may have preceded any spring "bloom" sedimentation event(s) (Bradford-Grieve et al., 1997a). Another explanation, however, may be that since phytoplankton accumulation was also associated with seasonal increases in meso- and microzooplankton grazing rates and significant bacterial productivity in spring, an intense recycling regime within the upper ocean food web could have been established at this time. As expected for a "bloom"-like scenario, the greatest winter-to-spring depletion of nutrients across the three water types was observed in the STC where near-surface new nitrogen (as nitrate) was reduced by up to 5 μM and dissolved reactive silica and phosphorus by 1.0 and 0.2-0.3 μM, respectively, in spring (Table 4.3). In contrast to observations of a coastal spring "bloom" presented by Rivkin et al. (1996), heterotrophic flagellates do not

appear to have been a prominent component of the microzooplankton spring STC community (Table 4.3). The low P_B value in STC in spring is also not supportive of full "bloom" development (e.g., Legendre, 1990). In addition, carbon specific doubling times of phytoplankton in the STC were no higher in spring, compared with winter (1.01 and 0.82 cf. 1.03 and 1.29 per day) suggesting that the spring "bloom" was probably winding down, perhaps in response to the limiting effect of low dissolved reactive silica concentrations (Bradford-Grieve et al., 1997a).

Since combined mesozooplankton grazing and sedimentation rates were generally less than 10% of chlorophyll *a* standing stock and intergrated primary production, and microzooplankton grazing on phytoplankton was also relatively low at about 40% of primary production (Table 4.3), it does not appear that zooplankton grazing and sinking were controlling the balance between algal biomass accumulation and consumption in the STC in spring. Perhaps, these observations in the STC frontal zone reflect the influence that physical aggregation by hydrodynamic forces, rather than biological production *per se*, can have on phytoplankton accumulation, particularly in frontal regions (e.g., Legendre & Le Fèvre, 1989; Legendre, 1990).

Subtropical. Subtropical waters experienced a marked seasonal increase in mesozooplankton biomass and grazing rates from winter-to-spring that was matched by elevated phaeopigment and estimated pellet fluxes in spring (Nodder & Gall, submitted). Microzooplankton biomass increased in spring, compared with winter, although grazing on phytoplankton and bacterial productivity were only occurring at moderate rates, compared with the STC (Table 4.3). Heterotrophic flagellates, relative to autotrophs, and photosynthetic dinoflagellates were conspicuous components of the plankton community in subtropical waters in winter, relative to spring, while phytoplankton production and biomass was concentrated in nano- and pico-size fractions in both seasons. Bacterial biomass and productivity were more pronounced in spring, compared with winter, highlighting the importance of the microbial loop during this season, although grazing pressure on bacteria by microzooplankton populations was exceedingly high (>200% of bacterial productivity; James & Hall, 1997). High nutrient levels and production per unit biomass in subtropical waters at this time suggest that phytoplankton accumulation was probably occurring,

associated with substantial increases in mesozooplankton biomass, dominated by *Neocalanus tonsus*, a herbivorous copepod that overwinters at water depths greater than 500 m and migrates into the upper ocean in spring to coincide with the timing of phytoplankton "bloom" periods (Jillett, 1968).

Certainly, while water column stratification was pronounced in subtropical waters at this time (i.e., most recent mixing events down to 15-25 m with remnant mixed-layers of 50-90 m), and may have resulted in concomittant reductions in vertical mixing strength and, hence, export flux (e.g., Barlow et al., 1995), nutrient concentrations (nitrate + nitrite and dissolved reactive silica and phosphorus) were not reduced significantly from winter values (Fig. 4.7-4.9). The location of sampling stations in the vicinity of a semi-permanent warm-core eddy (e.g., Barnes, 1985) may have limited winter primary production and conserved nutrient concentrations until spring due to deep winter mixing (e.g., Bradford et al., 1982). Given the dominance of herbivorous grazers and the inferred importance of the microbial loop at this time, it is proposed that subtropical waters in spring were the scene of pronounced food web recycling processes via a variety of mechanisms that probably included bacterial metabolism, microzooplankton grazing on phytoplankton and coprophagy and coprorhexy by mesozooplankton, as discussed in more detail in Chapter 6.

Despite these observations, the dominance of autotrophic processes in STC and subtropical waters in spring is obvious, as evinced by the presence of large (20-200 μm) diatoms in the frontal zone and one station in subtropical waters (X479) and the abundance of autotrophic flagellates, relative to heterotrophs, in both water types. The predominant grazing on bacteria by heterotrophic flagellates in subtropical waters in spring (James & Hall, 1997) is a little incongruous, as is the only moderate proportion of primary production being grazed by microzooplankton (60%), such that phytoplankton growth exceeded microzooplankton grazing (James & Hall, 1997). These authors suggested that growth-grazing decoupling resulted from unavailability of large (>20 μm) phytoplankton cells to microzooplankton consumers. Much of this plant material was not sedimenting out of the upper water column, however, since lower fluxes of carotenoids and chlorophylls were found in spring (Nodder & Gall, submitted), despite marked increases in phytoplankton biomass and productivity in subtropical waters (Table 4.3). In winter, subtropical waters were dinoflagellate-dominated

(80% of phytoplankton cell carbon on average, Table 4.5) and became microflagellate-dominated in spring (55% on average). The associated increase in the abundance of nano- and picophytoplankton (30-40 mg chlorophyll *a* m^{-2} cf. 7-14 in winter) indicates that small-sized cells were more prominent in spring (80-100% of total chlorophyll <200 μm) (Table 4.4). This situation would have encouraged relative accumulation of phytoplankton in the upper water column since the sedimentation rates of small particles are low (e.g., McCave, 1984b; Passow & Peinert, 1993; Boyd & Newton, 1995).

4.4.3. Influence of small-scale spatial and temporal variations on physical and biological processes

Substantial differences between many physical and biological parameters investigated in 1993 were obviously related to natural variations across the three geographically distinct water types and the two seasons that were studied (Tables 4.2 & 4.3). Relatively small-scale spatial and temporal processes, however, are also likely to play a significant role in determining the distribution of parameters of interest in the ocean (cf. Siegel et al., 1990). For example, marked changes in water column structure are apparent from CTD profiles conducted at supposed replicate stations (Fig. 4.2C), and at the same "station" at different times (Singleton, 1993, 1994). In Fig. 4.2C, a cold, low salinity surface intrusion event, representing a transient filament of subantarctic water (e.g., Barnes, 1985), was observed on CTD profiles at X469A, X468E and X468G. These stations were located to the north of other stations occupied in subtropical waters in winter 1993 (i.e., X469D and F, X468A). The two groupings of supposed replicate stations were separated spatially by 13-37 km and temporally by about 9 h (Singleton, 1993). Changes to several chemical and biological parameters were associated with this surface capping of subtropical water by what was subantarctic water (Table 4.6).

Similarly, two replicate stations in the STC in spring (X477 and X478) had significantly different total mass and particulate phosphorus fluxes (Nodder & Alexander, 1997), but did not have vastly different water column properties that could adequately explain this variability (Table 4.7). Thus, these differences in near-bottom flux are inferred to reflect differential contributions made to trap samples by re-suspension and lateral advection of

Table 4.6 Comparison of selected physical, chemical and biological parameters at two replicate stations in subtropical waters in winter 1993.

Parameter	X468A	X469A
Mixed-layer depth (m)	117	140 (56 - surface intrusion)
Mixed-layer temperature (°C)	13.9-14.1	13.3-13.4 (12.8-13.0)
Mixed-layer salinity (psu)	35.19-35.23	35.14-35.16 (34.95-35.01)
Alkalinity (meq kg^{-1})*	2.372 / 2.346	2.372 / 2.351
Nitrate (μM)*	4.1 / 22.0	2.2 / 6.6
Dissolved reactive phosphorus (μM)*	0.4 / 1.5	0.8 / 1.5
Dissolved reactive silica (μM)*	2.6 / 2.6	2.1 / 5.3
Ammonium (μM)*	0.05 / 0.22	0.10 / 0.08
Urea (μM)*	0.45 / 0.17	0.29 / 0.27
PC (<200 μM) μg l^{-1}*	134 / 70	50 / 42
PN (<200 μm) μg l^{-1}*	12 / 11	8 / 8
PP (<200 μm) μg l^{-1}*	1.5 / 1.5	1.2 / 1.2
Chlorophyll *a* <200 μm at 10 m (mg m^{-3})	0.13	0.25
Integrated (0-100 m) <200 μm chlorophyll *a* (mg m^{-2})	13.7	24.8
Integrated (0-1% light) primary production (mgC m^{-2} d^{-1})	197	100
% Primary production (<2 μm)	27	45
% Primary production (20-2 μm)	19	3
Dinoflagellates (μgC l^{-1})	950	182
Prokaryotic picophytoplankton (cells ml^{-1})**	2330 / 2180	1770 / 870
Tintinnids (individuals l^{-1})**	50-120	20-70
Autotrophic:heterotrophic flagellates**	4	2
Mesozooplankton community composition**	Low numbers of copepods, no euphausids, high numbers of foraminifera	High numbers of copepods, some euphausids, low numbers of foraminifera

* Values taken at 10 m (near-surface) and 550 m, separated by a slash mark.

** Values and observations taken from 0-50 m.

bottom sediments at this shallow setting on the crest of the Chatham Rise (e.g., Gardner & Richardson, 1992). The traps were positioned only 40-70 m above the sea-floor, within the depth range of previously observed mid-water nephelometer maxima (Section 2.2, Chapter 2). The unique presence of benthic crustaceans (cumaceans) in X478 sediment trap samples (Table 5.2, Chapter 5) supports this interpretation. There is also evidence to suggest that plumes of re-suspended sediment may be periodically entrained off the Chatham Rise (Fig. 2.9, Section 2.2, Chapter 2; also Carter & McCave, 1994); similar plumes may have been responsible for the observed increases in mass flux with depth in autumn 1992 (Section 2.2, Chapter 2; Nodder, in press) and in spring 1993 (Nodder & Alexander, 1997).

In addition, geological evidence of present-day bottom current erosion and/or non-deposition on the crest of Chatham Rise includes the existing erosional microtopography, the presence of glauconite in surficial sediments and the exposure of phosphatic nodules and underlying Miocene chalks at the surface (Cullen, 1987). Assuming the surficial sediments are non-cohesive, as suggested by the low effective cohesion values recorded by Meyer & Toan (1984), then the critical frictional velocity (u_*) can be derived from the equation:

$$\tau_o = \rho_w u_*^2$$

where τ_o = 0.2 Pa as determined from the shear stress/grain-size relationship of Dade et al. (1992) for a mean grain-size of 0.1 mm (Meyer & Toan, 1984), and ρ_w = density of sea-water = 1025 kg m^{-3}.

Accordingly,

$$u_* = 1.4 \text{ cm } s^{-1}.$$

Using the relationship:

$$u_{100}/ u_* = 5.6 \log_{10} [(u_* z_{100})/ \upsilon + 4.9$$

where u_{100} = critical erosion velocity 100 cm above the bed, z_{100} = height of 100 cm above the sea-bed and υ = kinematic viscosity of water = 0.0135 cm^2 s^{-1} (Young & Southard, 1978), then the erosion speed:

$$u_{100} = 38.3 \text{ cm } s^{-1}.$$

It is acknowledged, however, that the actual erosion resistance of such fine-grained deposits will also be highly dependent upon many other factors not evaluated by this study, including current flow dynamics, consolidation history of the sediment, effects of bioturbation and

Table 4.7 Comparison of selected physical, chemical and biological parameters at two replicate stations in the Subtropical Convergence in spring 1993.

Parameter	X477	X478
Mixed-layer depth (m)	36-70	14-?23
Mixed-layer temperature (°C)	10.7-10.9	10.9-11.0
Mixed-layer salinity (‰)	34.66-34.69	34.69
Integrated primary production (mgC m^{-2} d^{-1})	1011.5	861.9
Integrated (0-100 m) <200 μm chlorophyll *a* (mg m^{-2})	112	80
Chlorophyll *a* 20-2 μm (μg l^{-1})	0.04-0.37	0.49-2.18
Alkalinity (meq kg^{-1})	2.30-2.32	2.32-2.33
Dissolved reactive silica (μM)	0.6-2.6	1.3-2.7
Ammonium (subsurface maxima at 50-100 m)	<0.6	0.6-0.8
Picophytoplankton (cells ml^{-1})	810-1300	930-3300
Mesozooplankton biomass (mg m^{-2})	2300	1200
Mesozooplankton ingestion rate (μg pigment m^{-2} d^{-1})	550	360
Average mass flux at 220 m (mg m^{-2} d^{-1})	**313**	**1811**
Particulate phosphorus flux at 220 m (mg m^{-2} d^{-1})	**0.80**	**2.83**
Sediment trap "swimmer" population*	**F (A) + Co (A) + Po ± App ± Pt**	**F (C) + Co (A) + Po + Cu ± App ± Pt ± Ch**

* F=foraminifera, Co=copepods, Po=polychaetes, App=appendicularians, Pt=pteropods, Cu=cumaceans, Ch=chaetognaths; A=abundant, C=common, other genera are listed as "present"; + implies a dominant or subdominant component, ± a "presence and/or absence" dependent on specific stations (see Table 5.2, Chapter 5).

other biological processes, strength of interparticle interactions, chemical processes and sea-floor morphology (e.g., McCave, 1984a; Dade et al., 1992). If the grains are assumed to be totally non-cohesive and using quartz as a "typical" sediment type, then the Yalin parameter (Ξ) can be calculated from the expression:

$$\Xi^{0.5} = [(\rho_s - \rho_w)\, gD^3/\rho_w \upsilon]^{0.5} \text{ where:}$$

ρ_s = sediment density = 2.65 g cm^{-3} for quartz, g = acceleration due to gravity = 980.4 cm s^{-2} and D = grain diameter, approximated to 0.01 cm (Meyer & Toan, 1984). The Ξ value of 2.9 allows derivation of Shield's criterion (θ_t) from the modified Yalin curve in Miller et al. (1977), which is related to the frictional velocity of the sediment (u_*) by the equation:

$$\theta_t = \rho\, u_*^2/(\rho_s - \rho)gD$$

Since $\theta_t = 0.076$, u_* is equal to 1.08 cm s^{-1} for quartz. Assuming that flow in the bottom 1 m of the current has a logarithmic profile (Grant & Madsen, 1986), the threshold velocity (u_z) can be calculated from the Prandtl-von Kármán equation:

$$u_z = K^{-1} u_*^2 \ln (z/z_0).$$

In this expression, K = von Kármán's constant = 0.4, z = height of flow measurements above sea-floor = 100 cm and z_0 is a roughness length co-efficient, equivalent to 0.5 cm for sandy sea-floors (Heathershaw, 1981). From this equation,

$$u_{100} = 14.3 \text{ cm } s^{-1}.$$

From previous work, sufficiently strong bottom currents are likely to operate on the Chatham Rise, although in general currents are unidirectional with depth, and decrease in magnitude by as much as a factor of 2 over water depths of 0-250 m (Chiswell, 1994a). From a 34-day current meter record, Heath (1983) reported maximum current speeds of 24 cm s^{-1} within 17 m of the sea-floor on the crest of the Rise. Chiswell (1994a) noted maximum current speeds of about 40 cm s^{-1} at a water depth of 150 m. Such strong across-rise flows are inferred to be responsible for the observed mid-water increases in particle concentration (Section 2.2, Chapter 2) and may have contributed to increases in mass flux with depth in adjacent subtropical waters at this time (Section 2.2, Chapter 2).

4.5. Summary of Chapter 4

(1) The water masses of the Chatham Rise region were a prominent regional sink for atmospheric CO_2 in spring 1993. This observation was contemporaneous with marked spring increases in biological biomass and productivity. These data, satellite imagery and other studies of pCO_2 distribution suggest that the "biological pump" in the Southwest Pacific Ocean may have an important regional role in sequestering atmospheric carbon dioxide.

(2) There were substantial differences in physical, chemical and biological characteristics of subantarctic, Subtropical Convergence and subtropical water types studies in winter and spring 1993. Statistically significant differences in average particulate fluxes were not detected (Nodder & Alexander, 1997), however, which suggests that food web control of export particulate flux was not a dominating factor (cf. Legendre & le Fèvre, 1989; Rivkin et al., 1996).

- In **subantarctic** waters the incorporation of terrigenous material into sinking marine particles is inferred by higher average fluxes measured in winter, compared to spring. Relatively low rates of sedimentation in subantarctic waters in spring are also attributed to reduced levels of phytoplankton biomass accumulation, compared with STC and subtropical waters, and the predominance of small-sized algal cells, which are not involved significantly in passive sinking.
- In the **STC**, pronounced nutrient depletion, accumulation of large diatoms and elevated primary productivity in spring suggest that a seasonal phytoplankton "bloom" was occurring at the time of sampling. Consequently, maximum sedimentation rates were expected, but not measured because: (a) sedimentation of phytoplankton cells may have occurred soon after trap deployments were completed since productivity per unit biomass in the STC was surprisingly low and silicate levels were at limiting concentrations; (b) organic material was being recycled within the upper ocean food web as inferred from increases in mesozooplankton biomass and rates of grazing in spring. Bacterial productivity and microzooplankton and bacterial biomass were also elevated at this time; and

(c) phytoplankton cells may have been aggregated together by physical processes acting within the frontal zone.

- In **subtropical** waters mesozooplankton biomass and grazing increased substantially in spring, in association with increases in bacterial productivity and biomass. Although phytoplankton biomass increased substantially in spring from winter, pronounced recycling in the upper ocean ecosystem by meso- and microzooplankton, and the dominance of small-sized algal cells, meant that average particulate mass fluxes were lower in spring than in winter. Furthermore, the influence of a semi-permanent, warm-core eddy in subtropical waters in both seasons highlights the complexities involved in conducting food web studies in the vicinity of dynamic oceanic frontal zones.

(3) Processes operating at time- and space-scales smaller than seasons and water types may also be important in affecting the relative magnitude of export fluxes measured in subantarctic, STC and subtropical waters. In particular, elevated near-bottom mass fluxes at one station in the STC in spring (X480) are inferred to be related to the resuspension of sediments on the crest of Chatham Rise by across-rise tidal currents, as previously surmised by Nodder (in press) (Section 2.2, Chapter 2). Other factors affecting particulate fluxes are detailed in the following two chapters (Chapters 5 and 6).

Chapter 5

PARTICULATE FLUXES FROM CHATHAM RISE–SUBTROPICAL CONVERGENCE REGION

Chapter 5

PARTICULATE FLUXES IN CHATHAM RISE-SUBTROPICAL CONVERGENCE REGION

5.1. Introduction

Sediment traps have been used to investigate the fate of sinking particulate material in oceanic biogeochemical cycles (e.g., Knauer et al., 1979, 1990; Honjo et al., 1982a, b; Martin et al., 1987; 1993; Karl et al., 1991b, 1996; Lohrenz et al., 1992; and many others, see Section 1.3, Chapter 1). A recent Joint Global Ocean Flux Study (JGOFS) report has highlighted potential problems with the sediment trap technique (Gardner, 1996). Continued questions regarding the hydrodynamic performance of sediment traps have been raised, mainly on the basis of mass balance modelling of upper ocean ^{234}Th:^{238}U disequilibria (e.g., Buesseler et al., 1992, 1994; Michaels et al., 1994; Murnane et al., 1996) (Section 1.7, Chapter 1). The hydromechanics of mooring lines during free-floating deployments of sediment traps have been shown to affect absolute trapping efficiency (Gardner, 1985; Gust et al., 1992, 1994) (Section 1.5, Chapter 1). Furthermore, an enduring problem with sediment trap methods is sample contamination by marine zooplankton that swim actively into traps (known as "swimmers", e.g., Knauer et al., 1984; Lee et al., 1988, 1992; Karl & Knauer, 1989; Michaels et al., 1990; Peterson & Dam, 1990; Silver & Gowing, 1991) (Section 1.6, Chapter 1).

In Section 2.1, Chapter 2, a novel sediment trap system is described. This apparatus was constructed at NZOI-NIWA in 1992, primarily for deployment in two New Zealand JGOFS research voyages in 1993 (Fig. 4.1, Chapter 4). The free-floating sediment trap arrays were deployed in order to determine the sinking rates and composition of particulate matter exported from the upper ocean across an oceanic frontal zone, the Subtropical Convergence (STC). In this chapter the particulate flux data are used to investigate some of the sources of trapping variability associated with the hydrodynamic performance of

free-floating sediment traps. The question of zooplankton "swimmer" contamination is not addressed specifically, but is acknowledged as a significant problem in most upper ocean sediment trap studies (e.g., Lee et al., 1988, 1992; Michaels et al., 1990; Hedges et al., 1993) and is covered in a qualitative sense in Section 5.3.6.

5.2. Methods

As mentioned previously (Section 4.1, Chapter 4), two free-floating sediment trap arrays were deployed in each of subantarctic, STC and subtropical waters in winter and spring 1993. The configuration of the drifting arrays is described in Section 2.1 (Fig. 2.1, Chapter 2). Twelve or eight baffled cylinders were attached to four arms of stainless steel cross-frames deployed below the mixed-layer at depths ranging from 100 to 550 m in each of the water types (Table 4.1, Chapter 4). A basal 1% formalin-brine was back-filled carefully into the bottom of cylinders used for total mass, particulate carbon (PC), nitrogen (PN) and phosphorus (PP) determinations (e.g., Karl et al., 1990). In addition, pigment fluxes were investigated by using a single trap at each sample depth with a non-poisoned basal brine. The remainder of each trap was filled with filtered surface sea-water (<0.5 μm) that was prepared up to 2-3 days in advance of each deployment. A "time-zero" blank solution was retained and prepared as for each parameter, except pigments, at the time of each deployment. Upon recovery, samples were pre-screened into a 10.0 l Nalgene carboy through a 303 μm mesh in winter, and a 200 μm mesh in spring to remove large zooplankton "swimmers" (Karl et al., 1990).

Aliquots of 250 ml from each homogenised trap sample were removed for total mass analysis using measuring cylinders and were filtered onto pre-weighed, 0.2 μm pore size, 25 mm diameter Nuclepore polycarbonate filters. These hydrophobic filters were tared prior to research voyages by following the techniques in Karl et al. (1990) which involved a series of drying and weighing procedures (i.e., 60°C overnight, desiccated for 0.5 h and re-weighed on a Cahn electronic micro-balance with 10^{-7} resolution) until filters returned a constant weight that was within 0.0050 mg of their original weight. In spring, to estimate sample processing errors, 2-3 replicate subsamples were taken from individual cylinders and analysed for total mass flux.

For PC/PN and PP/PN analyses, 500 ml aliquots were filtered onto pre-combusted (500°C for 4 h), 25 mm diameter Whatman GF/F filters which were acid-washed for PP/PN determinations (Karl et al., 1990). In addition, similar volume subsamples were taken from PC/PN cylinders which would be later fumed in concentrated HCl overnight, oven-dried (60°C) and analysed for particulate organic carbon (POC) concentration. The contribution of particulate inorganic carbon (PIC) to export flux would be calculated by difference (i.e., PC-POC=PIC). All filters were rinsed with three 5 ml aliquots of 1 M ammonium formate to remove salt and excess formalin, and stored frozen. Pigment (PG) traps were covered with opaque plastic bags to prevent photodegradation. PG samples were prepared by filtering the entire volume of basal brine (typically 1.5 l) through a 47 mm Whatman GF/C filter under low light conditions. These pigment filters were snap-frozen in liquid nitrogen and stored frozen.

Onshore, all filters were inspected microscopically at 20-40x magnification, and zooplankton "swimmers" removed manually (e.g., U.S. GOFS Report 10, 1989; Michaels et al., 1990; Silver & Gowing, 1991). Total mass samples were re-weighed to constant weight (i.e., within 0.0050 mg) after thawing for 48 h in a desiccator, following the same drying-weighing routine used to tare the filters. PC/PN and POC/PON samples were analysed using a Perkin Elmer 2400 CHN Autoanalyser which was calibrated using acetanilide (approximately 0.5-1.0 mg) with machine blanks calculated by running helium and oxygen gases only. The analyser was operated by technical staff at NIWA, Hamilton, and samples were transported frozen up to Hamilton from Wellington. Filters were dried in an oven for at least 1 h at 65°C, wrapped in aluminium foil, pelletised and combusted, and C and N concentration measured in the gaseous phase. Values produced by the analyser were in µg of C and N per filter.

Concentration of POC was determined using a CHN analyser, as described above, following vapour acidification of the sample to remove particulate inorganic carbon (PIC), or carbonate. PIC was then determined from the difference between PC and POC. There is debate as to whether acid vapourisation extracts quantitatively *all* interstitial carbonate, and whether some organic carbon is also removed by the acidification process (e.g., Froelich, 1980; Welicky et al., 1983; Hedges & Stern, 1984; cf. Hurd & Spencer, 1991). In the present study, a modified version of the technique used by Hedges & Stern (1984) was employed, assuming that the

total carbonate content of the trapped samples was less than 50%. The vapourisation procedure was as follows: the frozen GF/F filters were oven-dried overnight at 50°C to remove H_2O. They were then transferred to a grid, marked on aluminium foil, covering a metal desiccator plate, and the plate placed inside a glass desiccator above a dish filled with concentrated HCl. The desiccator was sealed and left for 36 h to remove carbonate from the filters. Residual water and HCl were removed by further drying filters in an oven at 50°C for 2 h, prior to re-freezing and sending samples up to NIWA, Hamilton for analysis.

A Technicon Autoanalyser II measured PP/PN analyses using modified acid-digestion methods of Downes (1978) by technical staff at NIWA, Christchurch. Briefly, the acid digestion process begins by placing each filter in a 16 x 125 mm pyrex-glass test tube and drying at 60°C for one hour in a drying oven. 0.5 ml of acid digestion mixture (0.5 g SeO_2 and 34 g K_2SO_4 dissolved in 100 ml AR grade H_2SO_4) was added to the sample using a positive displacement transfer pipette, and the test tubes were placed in a Grant BT5 heating block (280°C) for 3 h. The volume in each cooled test tube was then made up to 10 ml using 9.5 ml Milli RQ water, sealed with acid-washed polyethene stoppers and shaken vigorously on a vortex shaker to dissolve the digest mixture. The test tubes were allowed to stand overnight and, immediately prior to analysis using the Technicon Autoanalyser, were re-shaken and centrifuged at 3000 r.p.m. The analysis determines the concentration of phosphorus and nitrogen as dissolved orthophosphate and ammonium, respectively (Downes, 1978). Details of calibration standard and reagent preparation and storage for PP/PN analyses are provided in Nodder et al. (1994a, b).

Flux calculations were made using equations in Karl et al. (1990) after correcting for "time-zero" blank effects, except for pigment analyses (see Section 6.3.1, Chapter 6). For total mass samples:

$$\text{mg (dry wt) m}^{-2}\,\text{d}^{-1} = \frac{[(W_a - W_b) - W_{blk}] \times V_r}{V_f \times 0.0064 \times t}$$

Table 5.1 Sources of variation for sediment trap experiments conducted in three distinctive water types (W) in winter and spring 1993. Two stations (S) were occupied in each water type. Particulate fluxes measured at two depths (D) at each station were used in the analysis. The experiments were designed to test the hypothesis that water types have significantly different particulate fluxes. The test statistic was based on the linear equation: $x_{ijkl} = \mu + W_i + S(W)_{j(i)} + D_k + WD_{ik} + DS(L)_{kj(i)} + e_{l(ijk)}$

SOURCE OF VARIATION	DEGREES OF FREEDOM (DF)		TABLE OF MULTIPLIERS				EXPECTED MEAN SQUARES (MS)	F-RATIO
			fixed (W) i	random (S) j	fixed (D) k	random (n) l		
Among (water types) A	2	*a-1*	0	2	2	2	$1\sigma_e^2 + nd\sigma_{S(L)}^2 + nsd\sigma_W^2$	MS[W]/MS[S(W)]
Among (depths) C	1	*c-1*	3	2	0	2	$1\sigma_e^2 + n\sigma_{DS(W)}^2 + wsn\sigma_D^2$	MS[D]/MS[DS(W)]
A x C	2	*(a-1)(c-1)*	0	2	0	2	$1\sigma_e^2 + n\sigma_{DS(W)}^2 + ns\sigma_{WD}^2$	MS(WD)/ MS[DS(W)]
Among (stations, nested in water type) B(A)	3	*a(b-1)*	1	1	2	2	$1\sigma_e^2 + nd\sigma_{S(L)}^2$	MS[S(W)]/MS[RES]
C x B(A)	3	*a(b-1)(c-1)*	1	1	0	2	$1\sigma_e^2 + n\sigma_{DS(W)}^2$	MS[DS(W)]/MS[RES]
Residual	12	*abc(n-1)*	1	1	1	1	$1\sigma_e^2$	
TOTAL	23	*abcn-1*						

where:

W_a	= filter weight after filtration (mg)
W_b	= filter weight before filtration (mg)
W_{blk}	= net filter weight of blank solution (mg)
V_r	= volume of recovered solution (l)
V_f	= volume filtered (l)
0.0064	= cross-sectional area of trap (m^2)
t	= period of deployment (d)

Other particulate fluxes (i.e., PC/POC/PN/PP/PG) were calculated as follows:

$$\text{mg C (or OC, N, P, PG) } m^{-2}\ d^{-1} = \frac{(C_s - C_{blk}) \times V_r}{V_f \times 0.0064 \times t}$$

where:

C_s	= carbon in filtered sample (mg)
C_{blk}	= carbon in blank sample (mg)
V_r	= volume of recovered solution (l)
V_f	= volume filtered (l)
0.0064	= cross-sectional area of trap (m^2)
t	= period of deployment (d)

A summary of the experimental design used in 1993 to test the hypothesis that water types can be characterised by the magnitude of particulate fluxes measured by free-floating sediment trap arrays was as follows:

Water type:	Subantarctic, STC, subtropical	fixed	a=3
Station:	Two free-floating trap arrays	random	b=2
Depth:	Shallow versus deep traps	fixed	c=2
Replicates:	Mass fluxes in cylinders	random	n=2

Linear equation: $x_{ijkl} = \mu + W_i + S(W)_{j(i)} + D_k + WD_{ik} + DS(L)_{kj(i)} + e_{l(ijk)}$

The data were analysed statistically using a General Linear Model (GLM) Analysis of Variance (ANOVA) and a multiple comparison *a posteriori* procedure (Tukey test) since there are several possible alternative hypotheses (i.e., H_{A1}: $m_1 > m_2 = m_3$, H_{A2}: $m_1 < m_2 = m_3$, H_{A3}: $m_1 = m_2 > m_3$, etc) (Table 5.1). The computer programme employed for all statistical analyses was NCSS (Version 6.0) as also used in Section 2.3, Chapter 2.

Qualitative microscopic analysis was undertaken on selected mass flux filters to identify the types of marine particles involved in export flux. Quantitative analysis could not be conducted for a variety of reasons. Specifically, since most mass flux samples were subjected to prolonged filtering times (3-6 h) due to pronounced filter clogging, lysis and physical destruction of cells are expected to have occurred, but to an unknown extent. Furthermore, in general, only one filter from each sample depth was available for microscopic analysis, and the winter data-set was incomplete since many filters had been halved for other analyses. Sample integrity was further compromised by the variable preservation states of several filters due to previous phases of freezing and thawing.

For qualitative microscope analysis, filters were mounted directly on glass microscope slides using emulsion oil and microscope cover slips. Filtered samples were viewed using a Nikon Model 104 camera with 100-200x magnification. Various components were identified to broad levels, including foraminifera, radiolaria, silicoflagellates, faecal pellets, marine aggregates, diatoms, dinoflagellates, inorganic mineral grains and zooplankton. An approximate and descriptive estimate was made as to relative abundance of the more common components in terms of "abundant", "common" and "rare" designations.

5.3. Results

Drift paths of free-floating sediment trap arrays deployed in winter and spring 1993 generally followed prevailing wind directions and speeds (Fig. 5.1; see Fig. 4.1 for geographic relationships between nominal starting positions of drifting traps). General westward drift patterns were observed for traps deployed in subantarctic and STC waters in spring. Traps deployed in subtropical waters drifted rapidly to NNE in both seasons due to entrainment of the trap arrays into a semi-permanent eddy identified recently by NIWA scientists (P. Sutton, pers. comm., 1996). In winter, traps in the STC were influenced by re-circulation processes, and variable drift patterns were observed for traps in subantarctic waters (Fig. 5.1). Typically, drift speeds were higher in spring, compared to winter, in all three water types (Table 5.2). Rough seas encountered during all deployments often resulted in moorings becoming entangled which would have affected trapping efficiency (e.g., Gust et al., 1994). It is assumed, however, that sampling positions of the traps would have been shallowed by only up to 10 m. In all cases, basal brines were recovered intact with minimal washout.

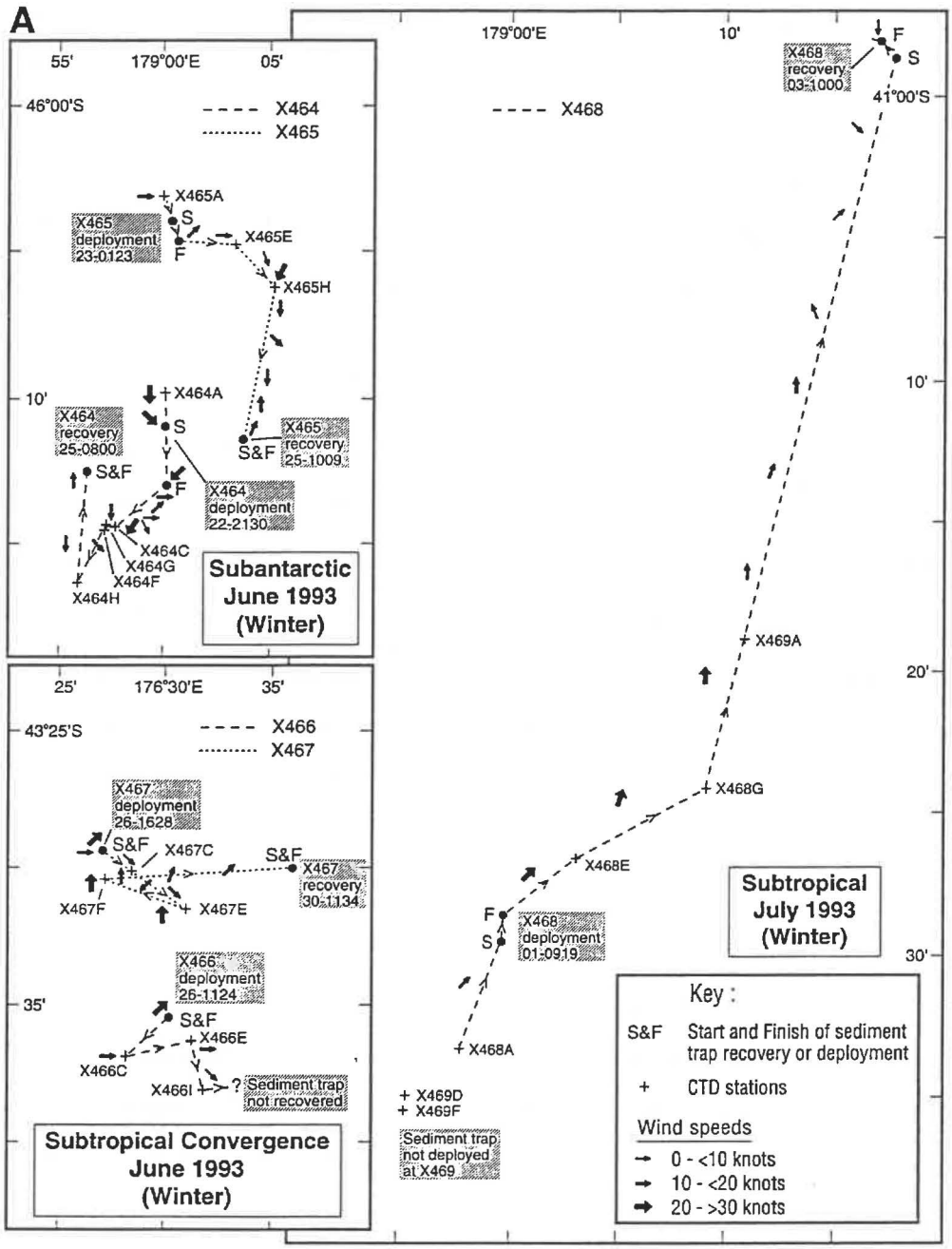

Fig. 5.1A Positions of CTD stations and sediment trap deployments and recoveries during winter (A) 1993. Dates and times of sediment trap operations are in the following format whereby "23-0123" refers to the date - 23 June 1993 (month given in figure title) - and the time - 0123 hours in New Zealand Standard Time (refer also to Table 5.1). Observed wind directions and speeds, as recorded by ship's officers every 4 h, are also depicted. Refer to Fig. 4.1, Section 4.2, Chapter 4 for geographical location of stations east of New Zealand.

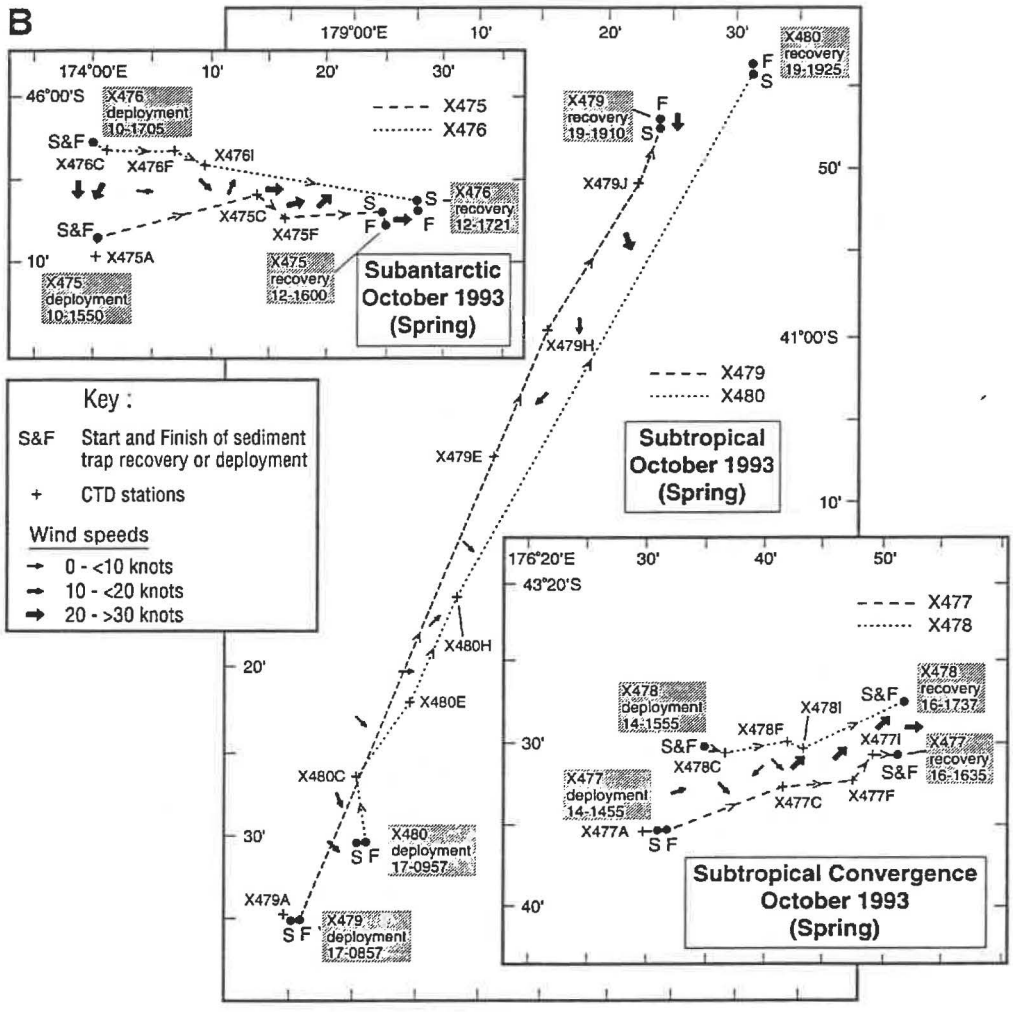

Fig. 5.1B Positions of CTD stations and sediment trap deployments and recoveries during spring (B) 1993. Dates and times of sediment trap operations are in the following format whereby "23-0123" refers to the date - 23 June 1993 (month given in figure title) - and the time - 0123 hours in New Zealand Standard Time (refer also to Table 5.1). Observed wind directions and speeds, as recorded by ship's officers every 4 h, are also depicted. Refer to Fig. 4.1, Section 4.2, Chapter 4 for geographical location of stations east of New Zealand.

One out of two arrays was recovered from STC in winter, allowing only one mooring to be deployed subsequently at subtropical stations. The lack of a full suite of flux measurements from two planned stations in STC and subtropical waters, and limited recovery of samples from one station (X464) in subantarctic waters, meant that statistical analyses for comparing inter-station differences could not be conducted in winter. Similarly, seasonal differences in particulate flux in the three water types were not able to be evaluated statistically.

5.3.1. Blank solutions

Problems with the preparation and analysis of blank brine samples became apparent due to the high levels of variation that were found between control "time-zero" blank samples (Fig. 5.2). These observations resulted in occasional anomalous "negative" fluxes (Appendices 3 & 4). Before average fluxes and error bars, as represented by ±1 standard deviation (s.d.), were calculated for each depth range, such unrealistic "negative" results were excluded from the final data set. Due to large amounts of variation associated with some of the original data, however, erroneous negative error bar limits persisted through subsequent analyses. Problems with such anomalous blank analyses have not been discussed widely in sediment trap literature. Karl et al. (1991a) reported blank values that ranged from 18-41% and 12-43% of the overall signal observed in trap samples for total mass and particulate phosphorus fluxes, respectively. Thus, it is anticipated that at times some errors may be introduced to particulate flux measurements due to high levels of blank variability.

The original "negative" fluxes from the 1993 trap samples have arisen mainly because of: (1) enhanced biological activity (i.e., bacteria) in the blank solutions which, despite the addition of formalin, may have led to remineralisation of ambient organic matter in the blank solutions; (2) *de novo* formation of particles by either agitation or bubble production during the filtration of surface sea-water, filling of traps or during trap deployment (e.g., Knauer, 1991); (3) airborne contamination, primarily during aspiration and filtering phases; and (4) the fact that sediment trap samples may not have been able to discriminate sufficiently between background "noise" and measurement of "true" vertical flux. Microbiological contamination of the large volumes of filtered sea-water (i.e., up to 600 l for two replicate stations) that were prepared up to 2-3 days in advance of some stations, is likely to be the main source of error; bacterial growth is likely to have occurred between the times that sea-

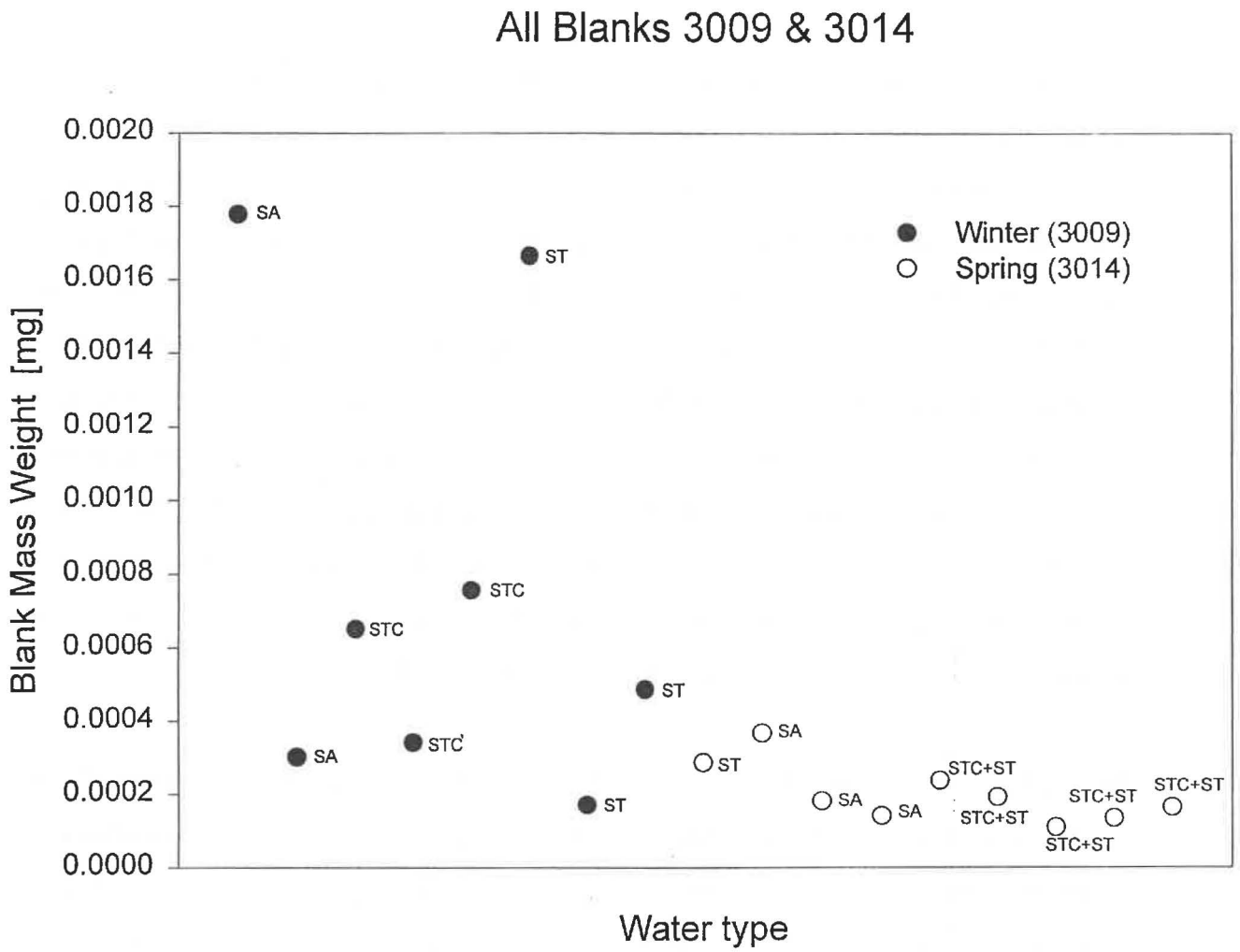

Fig. 5.2 Filtered mass weights (mg) of "time-zero" blank solutions from winter and spring 1993 sediment trap deployments. SA = subantarctic, STC = Subtropical Convergence, ST = subtropical.

water was filtered and the poison added. This contamination seemed to be a particular problem in winter in subantarctic and subtropical waters (Fig. 5.2). The effects of *de novo* particle formation and airborne contamination on the observed high blank solution variability cannot be evaluated with present data-sets. Finally, it may be that insufficient blank solution replicates were processed during the two voyages (i.e. 2-5 replicates/parameter/station pair in winter; 3-7 in spring), and that additional errors may have arisen because blank brine solutions were not exposed to the same physical conditions as trap samples (e.g., U.S. GOFS Report 10, 1989).

Thus, "control" values have not been used in subsequent statistical analyses (referred to as "uncorrected" fluxes) to correct trap fluxes to obtain absolute export rates, as documented in other sediment trap studies (e.g., Karl et al., 1990, 1996). In order to compare particulate fluxes from the STC data-set with work conducted in other oceanic environments, "absolute" fluxes have been estimated by excluding all blank values that lie outside ± 1 standard deviation of the average blank as determined from the total number of processed blanks. This approach had the effect of reducing the overall coefficient of variation between blank samples (from 84% to 50% in winter and 43% to 26% for spring). This approach, however, had minimal impact on specific mass flux samples (i.e., in winter, the same 9 out of 11 samples still had "negative" fluxes after corrections were made by excluding anomalous data points; similarly, in spring the same 3 samples remained "negative" after the above corrections were made). These "negative" values were subsequently neglected in further analyses.

Contamination of blank winter PP samples was also apparent from excessively high blank values (Fig. 5.3). This problem necessitated the use of spring PP blank corrections on the winter PP sediment trap data set in order to draw comparisons with other trap data-sets. As for the mass flux samples, statistical tests were conducted on "uncorrected" PP fluxes.

5.3.2. Total mass fluxes

Overall, mean coefficients of variation (C. V.) in uncorrected total mass flux for winter were 72% (1 s.d. 41%, n=12), compared with 34% (1 s.d. 23%, n=14) in spring (i.e., C. V. is standard deviation expressed as a percentage of mean flux). In winter, differences in flux measurements from cylinders at the same depth were substantial, which resulted in C. V.s for

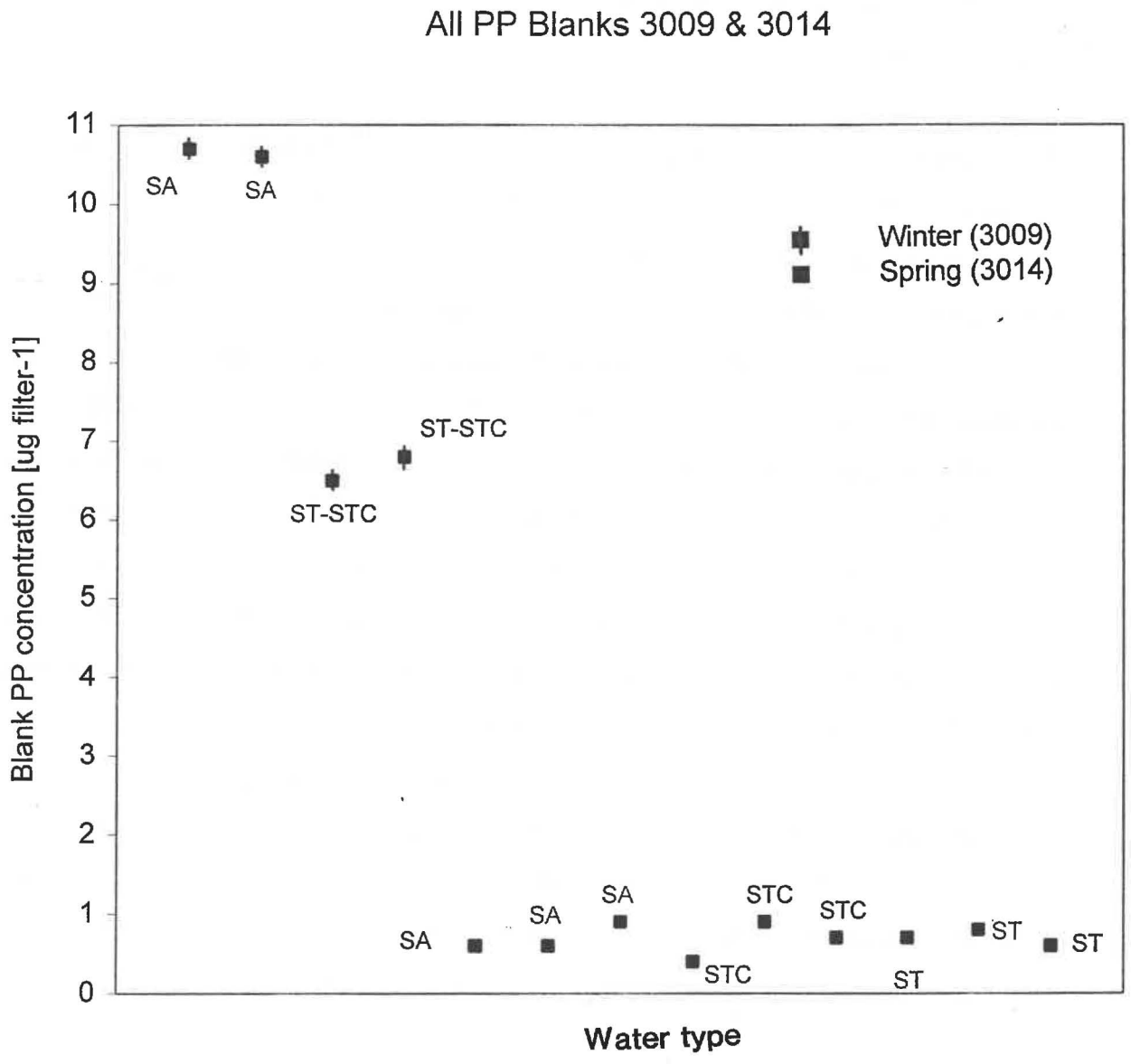

Fig. 5.3 Particulate phosphorus concentrations (μg filter^{-1}) in "time-zero" blank solutions from winter and spring 1993 sediment trap deployments. SA = subantarctic, STC = Subtropical Convergence, ST = subtropical.

Table 5.2 Sediment trap stations occupied, east of New Zealand, during winter and spring 1993, showing deployment and recovery positions, drift speeds and directions and sea-state conditions. SA = subantarctic, STC = Subtropical Convergence, ST = subtropical.

Season	Station & water mass	Final deployment position	Time of deployment	Final recovery position	Time of recovery	Cumulative distance (km)	Cumulative time (hours)	Minimum drift speed (km/h)*	Maximum drift speed (km/h)*	Mean drift speed† (km/h)	Overall drift direction T°	Wave conditions
Winter 1993	X464 SA	46°13.0'S 174°01.0'E	2038-2130 h 22/06/93	46°12.9'S 173°56.1'E	0625-0800 h 25/06/93	17.25	57.25	0.1	1.3	0.3	281	smooth-moderate seas, 2-5 m
	X465 SA	46°04.6'S 174°03.5'E	0005-0123 h 23/06/93	46°12.0'S 174°03.6'E	0855-1009 h 25/06/93	17.3	55.5	0.2	0.8	0.3	163	As for X464
	X466 STC	43°36.3'S 176°28.4'E	1050-1124 h 26/06/93	Sediment trap not recovered		-	-	-	-	-	-	-
	X467 STC	43°29.7'S 176°26.6'E	1600-1628 h 26/06/93	43°30.8'S 176°36.2'E	1134 h 30/06/93	22.9	69.25	0.2	0.6	0.3	097	slight-rough sea, 2-6 m
	X468 ST	41°28.8'S 179°00.4'E	0820-0919 h 01/07/93	40°58.0'S 179°16.9'E	0900-1000 h 03/07/93	65.6	48.75	1.1	1.5	1.4	022	smooth-moderate seas, 2-5 m
Spring 1993	X475 SA	46°08.6'S 174°00.2'E	1525-1550 h 10/10/93	46°08.3'S 174°25.1'E	1530-1600 h 12/10/93	34.0	47.5	0.6	1.0	0.7	089	slight-very rough seas, 3-6 m
	X476 SA	46°02.5'S 174°00.3'E	1637-1705 h 10/10/93	46°07.1'S 174°27.5'E	1700-1721 h 12/10/93	37.2	47.0	0.5	1.0	0.8	102	As for X475
	X477 STC	43°35.1'S 176°31.6'E	1430-1455 h 14/10/93	43°30.5'S 176°50.8'E	1635 h 16/10/93	29.4	49.5	0.5	1.0	0.6	072	smooth-very rough seas, 1-5 m
	X478 STC	43°29.9'S 176°35.3'E	1540-1555 h 14/10/93	43°27.2'S 176°51.5'E	1737 h 16/10/93	24.0	49.5	0.3	0.9	0.5	076	As for X477
	X479 ST	41°35.1'S 178°55.6'E	0832-0857 h 17/10/93	40°47.3'S 179°24.0'E	1736-1810 h 19/10/93	97.8	57.0	1.4	2.4	1.7	025	smooth-rough seas, 1-5 m
	X480 ST	41°29.8'S 179°00.5'E	0940-0957 h 17/10/93	40°44.1'S 179°31.4'E	1900-1925 h 19/10/93	97.2	57.5	1.4	1.9	1.7	027	As for X479

* Minimum and maximum drift speeds calculated from times and distances between individual stations (refer to Fig. 5.1).

† Mean drift speed averaged over the cumulative drift time and distance.

each depth that ranged from 10 to 123%. The high degree of variability may be due to inter-trap hydrodynamic interactions or could have arisen from sample processing errors. Furthermore, the small pore-size (0.2 μm) of the filters used in total mass analyses meant that filtering times of up to 6-7 h per sample were not unusual. It is likely that the preservation of intact filtered material will have been affected during the filtering process, although this factor was a consistent source of error over the two sampling seasons. Inter-trap hydrodynamic interactions were investigated in an *a posteriori* study (Section 2.4, Chapter 2), while the effect of sample processing errors was assessed more closely during subsequent spring trap deployments. The latter results indicate that sample processing errors varied from between <1% to 83% (average 34%) of the calculated mean flux for each cylinder in spring. In comparison, using all flux estimates derived from each cylinder (including subsamples used in evaluating sample processing errors), variations in mean flux at each depth ranged from 6-87% in spring.

Because of the wide range of variability between subsamples taken from the same cylinder and between cylinders at the same depth, analysis of variance (ANOVA) indicates that in subantarctic waters there were no significant differences in average mass flux between the two stations in spring nor over sampled water depths (>100 and 550 m) in both seasons (Table 5.3, Fig. 5.4A). In winter, there were no statistically discernible changes in mean flux with depth at stations in STC and subtropical water types (Table 5.3), despite a 2-fold increase in average flux between 120 m and 550 m in subtropical waters (Fig. 5.4). On average, relative fluxes in subtropical waters in winter (i.e., 420 mg m^{-2} d^{-1} at 120 m, increasing to 830-1020 mg m^{-2} d^{-1} over 220-550 m) were higher than equivalent fluxes in subantarctic and STC waters. One exception was at X465 where a near-surface flux of 600 mg m^{-2} d^{-1} was recorded at 120 m, which decreased from 750 mg m^{-2} d^{-1} at 220 m to 225-370 mg m^{-2} d^{-1} over 300-550 m (Fig. 5.4). Lowermost traps in the STC were set 130-190 m above the sea-floor in winter.

In spring, statistically significant differences in flux were observed between stations in the STC (Table 5.3). A significant interaction term, however, was found between stations and depths in the frontal zone. From investigation of the raw data (Fig. 5.4B), it is probable that this significant interaction was due to five-fold increases in average mass flux with depth at X478 (i.e., 185 mg m^{-2} d^{-1} at 100 m, increasing to 1810 mg m^{-2} d^{-1} at 220 m), compared with

Table 5.3 Summary of statistical analyses conducted on total mass fluxes determined from sediment trap experiments in winter and spring 1993 (see text for details). Experiments were designed to test the hypothesis that water types can be characterised by the magnitude of particulate fluxes.

Season	Water type*	Variable**	Station	Degrees of freedom	F ratio	Probability	Power at α of 0.05	Significance†
Winter 1993	SA	Depth	X465	1, 3	0.08	0.80	0.05	ns
		Depth	X464	1, 3	0.58	0.53	0.08	ns
Winter 1993	STC	Depth	X467	1, 5	0.004	0.95	0.05	ns
Winter 1993	ST	Depth	X468	1, 5	6.32	0.07	0.48	ns
Spring 1993	SA	Depth	X475	1, 4	1.65	0.30	0.15	ns
		Depth	X476	1, 4	6.92	0.08	0.44	ns
		Station		1, 9	0.28	0.61	0.11	ns
Spring 1993	STC	Depth	X477	1, 4	9.55	0.05	0.56	ns
		Depth	X478	1, 4	628.14	<<0.01	1.00	*
		Station		1, 9	320.56	<<0.01		*
		Depth & station		1, 9	329.55	<<0.01		*
Spring 1993	ST	Depth	X479	1, 4	26.16	0.02	0.91	*
		Depth	X480	1, 5	11.92	0.03	0.73	*
		Station		1, 10	0.31	0.60		ns
		Depth & station		1, 10	5.84	0.05		*
Spring 1993		**Water type**		**2, 3**	**1.60**	**0.39**	**0.07**	**ns**
		Water type (Depth & station)		**3, 12**	**107.72**	**<0.01**		*

* SA = subantarctic, STC = Subtropical Convergence, ST = subtropical.

** Variations between fluxes at shallowest and deepest sample depths of sediment traps (**Depth**), between stations (**Station**) and flux interactions between **Depth** and **Station** were tested in winter and spring. In addition, variations in fluxes across three water types (**Water type**) and interactions between **Depth** and **Station**, nested in **Water type** were tested in spring.

† ns = not significant, * = significant.

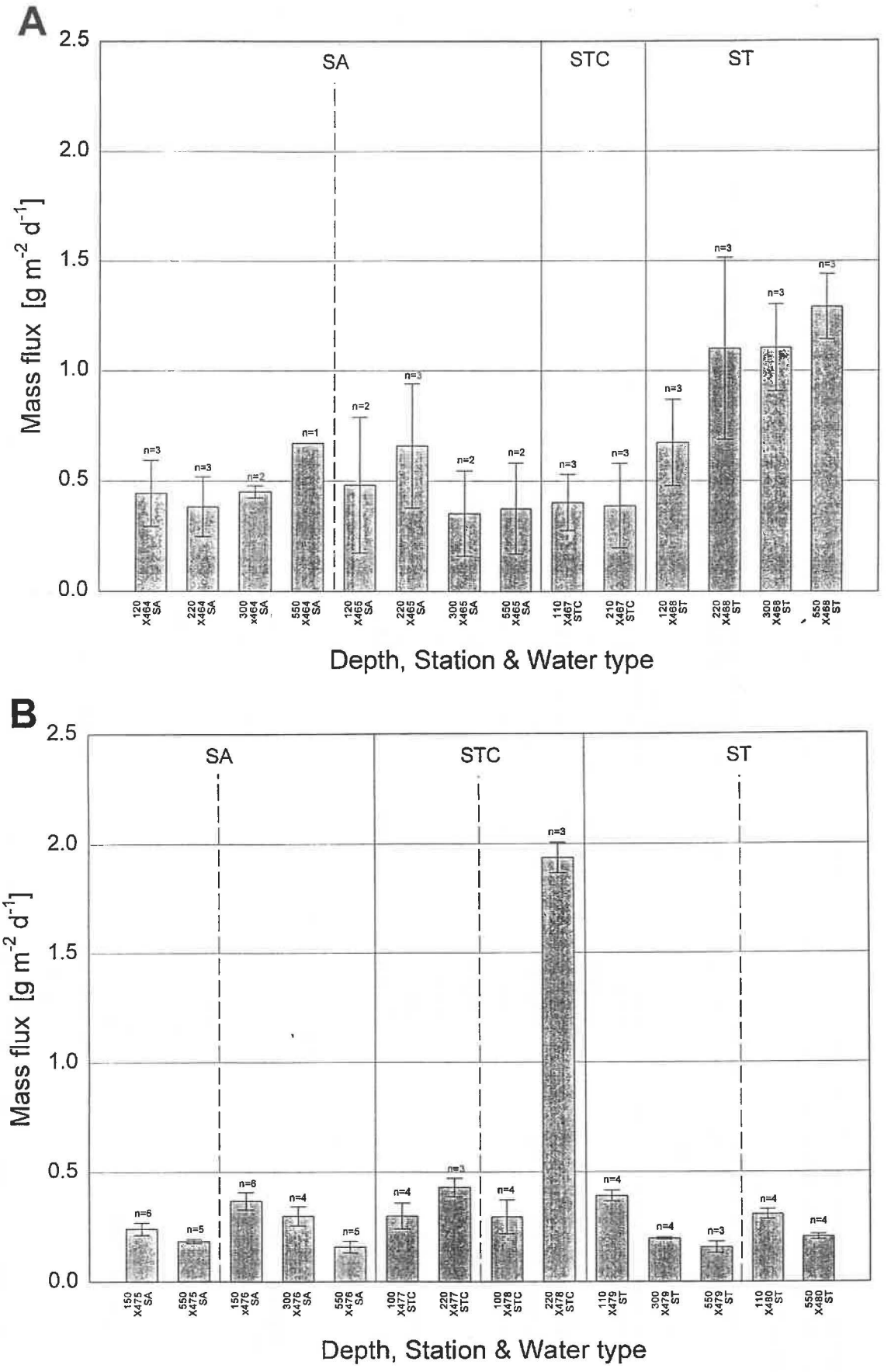

Fig. 5.4 Average uncorrected total mass fluxes (g m^{-2} d^{-1}) over specified depth ranges in water types across Chatham Rise in winter (A) and spring (B) 1993. Error bars are standard errors (S. E. = standard deviation/$\sqrt{n}$, where n = number of samples used in calculation of mean values).

those at X477 (190 mg m^{-2} d^{-1} in near-surface, increasing to 310 mg m^{-2} d^{-1} at near-bottom depths). Lowermost traps in STC waters in spring were 40-70 m above the sea-floor of Chatham Rise over the course of deployments, despite having been deployed originally in water depths of 300-400 m, as in winter. In subtropical waters, a significant interaction term between stations and depths is probably related to a relatively higher magnitude of flux reduction with depth found at X479, compared with a similar, though smaller, decrease in flux measured at X480 (Table 5.3, Fig. 5.4).

Because of significant flux variations on vertical and horizontal spatial scales of about 400 m (i.e., vertical separation of traps on drifting array) and 13 km (i.e., initial distance between stations), respectively, there were no statistically significant differences (i.e., d.f.=2, 3; F=1.60; P=0.39; power=0.07) between the fluxes measured in each of the water types in spring (Table 5.3). Significant interaction terms, however, were found between depths and stations, nested in water types (d.f.=3, 12; F=107.72; P<0.01), probably due mainly to the five-fold difference in flux measured over 100-220 m water depths at X478, compared with low levels of difference between fluxes at various depths observed at all other stations (Fig. 5.4).

Twice as many trap arrays were deployed in 1993 compared with other sediment trap studies that were also designed to characterise water masses by export flux (e.g., Knauer et al., 1979; Martin et al., 1987, 1993; Lohrenz et al., 1992; Karl et al., 1991a, b, 1996). The low levels of power for the above statistical tests (Table 5.3), however, suggest that more replication of trap arrays is required to reduce the chances of accepting a false null hypothesis. Thus, on the basis of results of the present study, more than two arrays need to be deployed if anticipated distinctions between seasons, water masses and water depths are to be unravelled statistically. The present study has shown that high levels of variability attributed mainly to subsampling variations can mask the very trends that researchers are trying to identify in efforts to understand upper ocean biogeochemical processes.

5.3.3. Particulate phosphorus fluxes

Particulate phosphorus (PP) fluxes were not evaluated for errors in sample processing procedures, except in the STC in spring where C. V.s for subsampling ranged from 5-15%

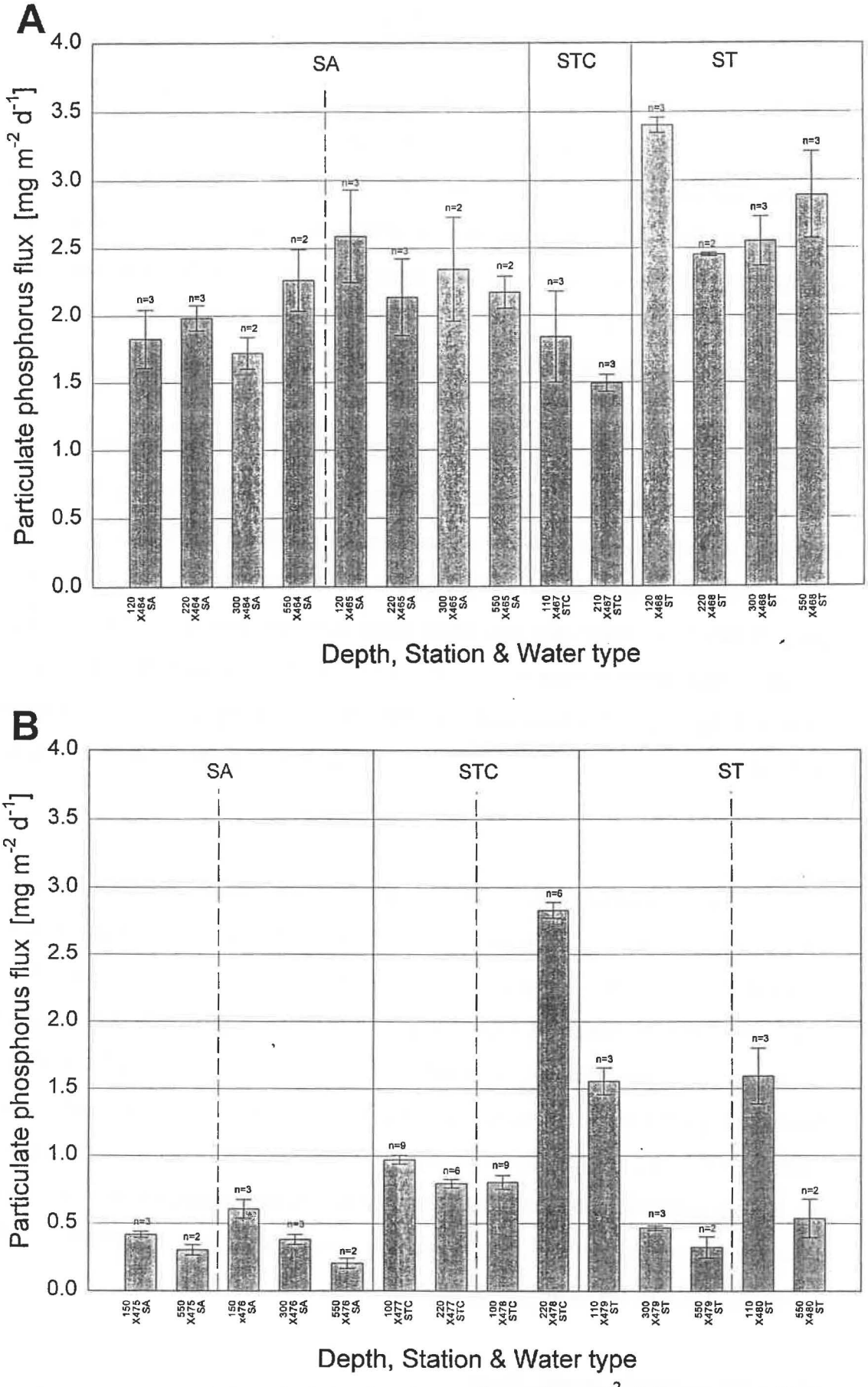

Fig. 5.5 Average uncorrected particulate phosphorus fluxes (mg m^{-2} d-1) over specified depth ranges in water types across Chatham Rise in winter (A) and spring (B) 1993. Error bars are standard errors (S. E. = standard deviation/$\sqrt{n}$, where n = number of samples used in calculation of mean values).

(mean C. V. 9%, n=4). It is anticipated, however, that similar degrees of variability as exhibited by mass flux subsamples would occur for phosphorus flux samples. Certainly, estimates of mean PP flux at specific depths were slightly higher in winter (C. V. range 1-32%, mean C. V. 15%, n=14) compared with spring, when C. V.s ranged from 4-25% (mean C. V. 12%, n=14). Average particulate phosphorus fluxes in winter ranged from 1.3-3.1 mg m^{-2} d^{-1}, compared with 0.2-2.8 mg m^{-2} d^{-1} in spring (Fig. 5.5).

Almost identical trends, as noted for total mass flux measurements using ANOVA (Table 5.3), were observed for particulate phosphorus fluxes across all water types (Table 5.4, Fig. 5.5). Obvious similarities between the two flux data-sets include statistically significant increases in flux with depth at X478 in spring, leading to perceived spatial incoherence between the two STC stations (Table 5.4, Fig. 5.5). Significant decreases in flux with water depth were also observed in spring in subtropical waters (Table 5.4). The main difference between the trends observed for particulate mass and phosphorus was a statistically significant decrease in phosphorus flux recorded in subantarctic waters at X476 but not at the paired station X475 (Table 5.4, Fig. 5.5), which resulted in a significant interaction term between station and water depth (Table 5.4).

Sample dissolution of particulate phosphorus has been observed in deep ocean moored traps (e.g., von Bodungen et al., 1991) and over lengthy deployments of free-floating traps (Knauer et al., 1990). It is anticipated, however, that dissolution of Chatham Rise trap samples over 2-3 days would be minimal given published loss rates for shallow water sediment trap material of only 3-8% d^{-1} (Iturriaga, 1979; Lorenzen et al., 1983; Gardner, 1996).

5.3.4. Particulate carbon and nitrogen fluxes

No carbon or nitrogen flux samples were obtained from the 1993 sediment trap deployments due to contamination of the samples with ammonium formate in the filter rinsing phase.

Significant geographical and temporal variations of particluate organic carbon (POC) flux have been recognised by many sediment trap studies (see references in Section 1.3, Chapter 1). A relatively conservative estimate of the contribution that POC makes to total mass flux can be made by assuming that POC comprises 10-30% of mass flux at the base of the

Table 5.4 Summary of statistical analyses conducted on particulate phosphorus fluxes determined from sediment trap experiments in winter and spring 1993 (see text for details). Experiments were designed to test the hypothesis that water types can be characterised by the magnitude of particulate fluxes.

Season	Water type*	Variable**	Station	Degrees of freedom	F ratio	Probability	Power at α of 0.05	Significance†
Winter 1993	SA	Depth	X464	1, 5	0.01	0.92	0.05	ns
		Depth	X465	1, 4	0.86	0.42	0.10	ns
Winter 1993	STC	Depth	X467	1, 5	1.01	0.37	0.12	ns
Winter 1993	ST	Depth	X468	1, 5	2.56	0.19	0.24	ns
Spring 1993	SA	Depth	X476	1, 4	19.77	0.02	0.83	*
		Depth	X475	1, 4	1.31	0.34	0.13	ns
		Depth & station		1, 9	13.03	0.011		*
Spring 1993	STC	Depth	X478	1, 4	212.83	<0.01	1.00	*
		Depth	X477	1, 4	4.08	0.14	0.29	ns
		Station		1, 9	140.46	<<0.01		*
		Depth & station		1, 9	189.48	<<0.01		*
Spring 1993	ST	Depth	X479	1, 4	81.34	<0.01	1.00	*
		Depth	X480	1, 4	11.49	<0.04	0.63	*
		Station		1, 9	0.87	0.39		ns

* SA = subantarctic, STC = Subtropical Convergence, ST = subtropical.

** Variations between fluxes at shallowest and deepest sample depths of sediment traps (**Depth**), between stations (**Station**) and flux interactions between **Depth** and **Station** were tested in winter and spring 1993.

† ns = not significant, * = significant

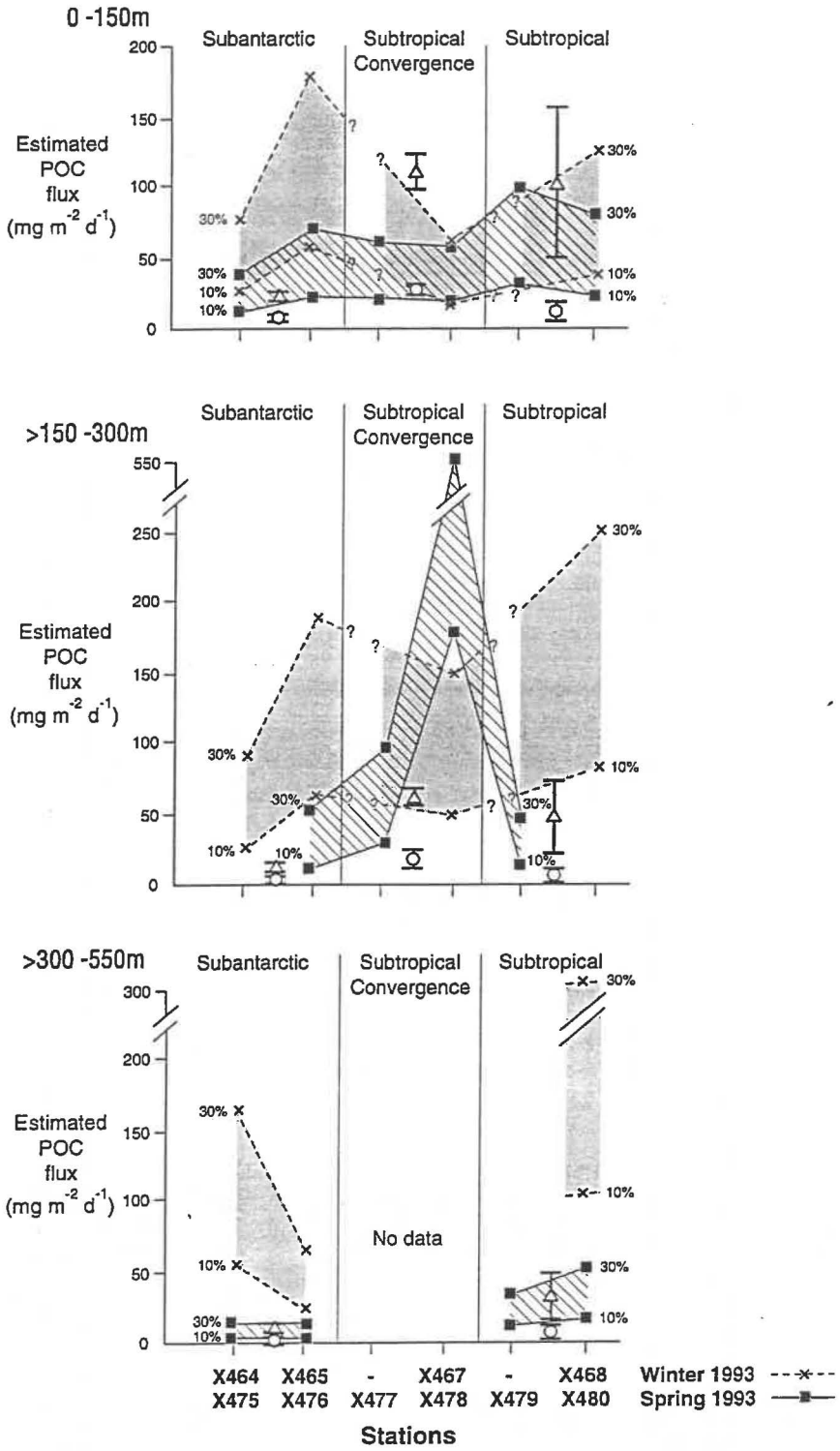

Fig. 5.6 Particulate organic carbon (POC) fluxes estimated from average mass flux measurements (Fig. 5.4), assuming that POC flux is between 10-30% of total mass flux (shaded for winter data-set and hatched for spring 1993). Calculations of POC flux, estimated from primary production information collected in winter (O) and spring (Δ) (Table 4.3, Chapter 4), using the equation of PACE et al. (1987), are depicted for comparison. The three graphs encompass the depth ranges sampled using sediment traps in the same seasons.

euphotic zone in oligotrophic environments (e.g., Eppley & Peterson, 1979; Betzer et al., 1984; Bishop, 1989). Previous sediment trap work from northern Chatham Rise (Nodder, in press) suggests that such an approximation is appropriate since *total* particulate carbon (i.e., organic + inorganic carbon) comprised between 20-40% of total mass flux (Fig. 2.4, Section 2.2, Chapter 2). This approximation allows ranges of average POC fluxes in winter and spring across the STC to be estimated (Fig. 5.6). These values are compared with POC fluxes determined from an empirical relationship between surface productivity, water depth and POC flux, developed by Pace et al. (1987) from the comprehensive VERTEX data set. This relationship was advocated by Bishop (1989) as providing a better model of relationships between primary productivity, export flux and depth in the water column than other similar equations (e.g., Eppley & Peterson, 1979; Suess, 1980; Betzer et al., 1984). The comparison of estimated POC flux with Pace et al.'s (1987) equation indicates that, on average, the POC fluxes approximated for winter from measured TM fluxes exceeded those expected from the empirical relationship. The estimated POC spring fluxes, however, follow more closely the empirical values, albeit at the lower hypothesised 10% limit (Fig. 5.6). Furthermore, it is likely that POC content of sinking particulate material may be closer to 2-5% of total mass flux (e.g., Wefer, 1989), thereby providing a much closer fit for the estimated winter and, especially, the estimated spring POC fluxes to Pace et al.'s equation.

It is noted, however, that subsequent work by Silver & Gowing (1991) on the same VERTEX data-set may have largely discredited the earlier work by showing that on average 36% of carbon exported from the euphotic zone was related to living organisms that were probably participating in vertical migration activities as part of their life histories. Karl et al. (1996) highlight the difficulties in using such empirical equations to predict carbon flux from primary productivity measurements, especially when production and export flux appear to be decoupled over lengthy time periods (i.e., up to 3 years). Thus, the discussion above regarding the derivation of particulate carbon fluxes from mass fluxes, while internally consistent, may not be especially valid in reality.

5.3.5. Microscopic analyses

Generally, flux components such as amorphous material, faecal pellets and individual planktonic particles (including silicoflagellates, foraminifera, radiolaria, diatoms,

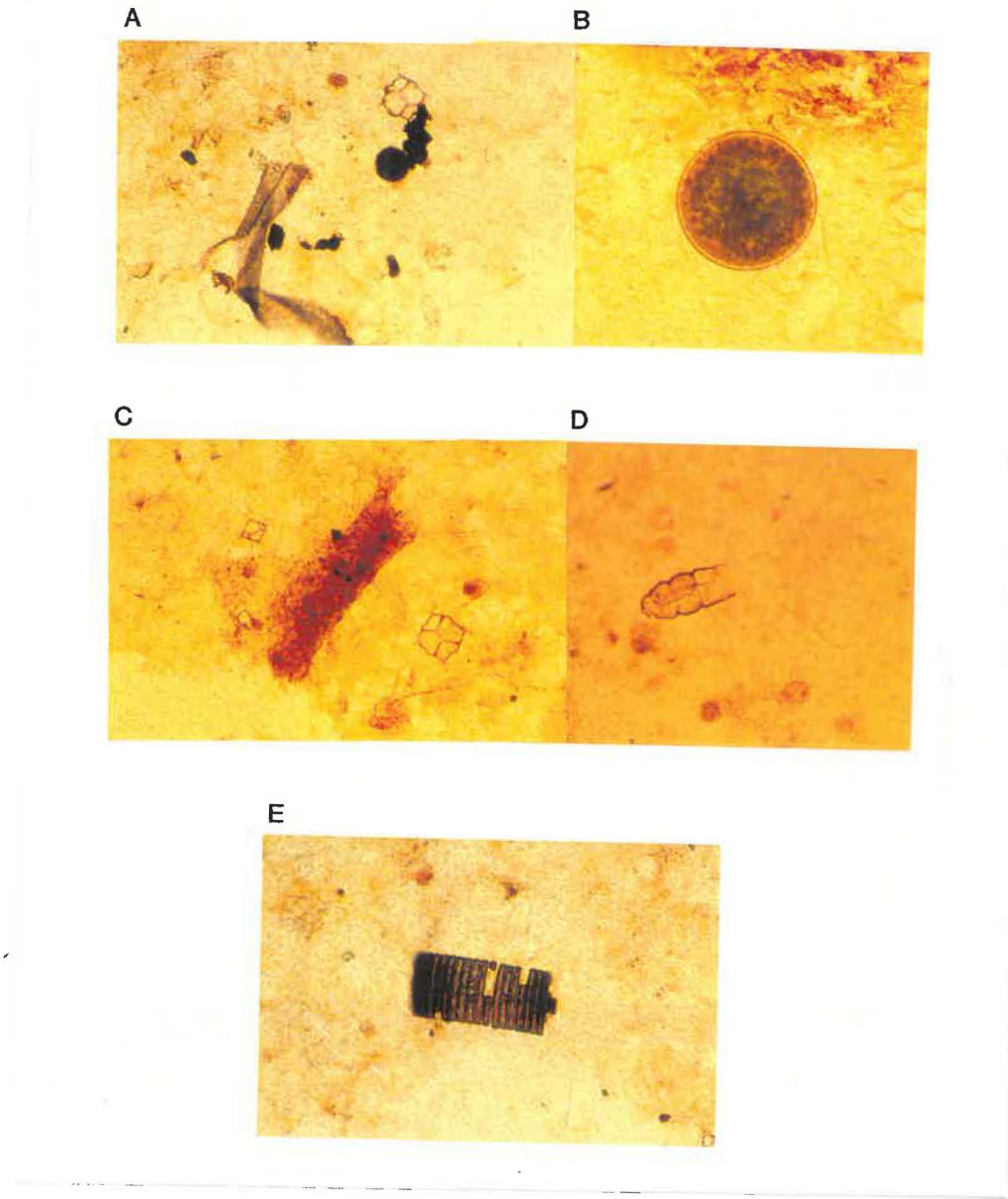

Fig. 5.7 Photo-micrographs of filtered sediment trap samples collected in winter 1993 (length of bar = 100 μm at 100 x magnification). (A) Web-like organic material and silicoflagellate (60 μm across) from 220 m in subantarctic waters (X465). (B) *Coscinodiscus* spp. (205 μm diameter) from 110 m in the STC (X467). (C) Faecal pellet (80 μm wide) and silicoflagellate from 120 m in subtropical waters (X468). (D) Tintinnid (140 long x 60 μm wide) from 200 m in subtropical waters (X468). (E) Box-like diatom (200 long x 95 μm wide) from 120 m in subtropical waters (X468).

dinoflagellates and microzooplankton) did not change substantially with water depth in the three water types (Fig. 5.7 & 5.8). Most 0.2 μm filters were covered by ubiquitous, yellow-brown to greenish-brown, amorphous, fine-grained material. There was often an observable decrease in the amount of material collected on filters from deeper trap depths. One obvious exception was at X478 in spring in the STC where the trap sample from 220 m comprised a substantial quantity of trapped material with a very different assemblage of collected particles, as described later. Most of the trap samples included unidentified microzooplankton, including tintiniids, foraminifera and radiolaria, as well as several forms of large (>50 μm) dinoflagellates.

In winter, trap samples from subantarctic waters contained many angular, transparent mineral grains, together with conspicuous small round diatoms (55-80 μm diameter) and web-like filaments and fragments (Fig. 5.7). Silicoflagellates were rare, as were large amorphous aggregates. Equant khaki faecal pellets and ovoid khaki-dark brown pellets were present in low numbers. Particulate fluxes in subtropical and STC in winter comprised abundant silicoflagellates (20-30 μm, up to 70 μm diameter), common large *Coscinodiscus* spp. diatoms (100-220 μm diameter) and occasional rectangular, khaki faecal pellets. Opaque red-brown mineral grains were also a feature of STC trap samples.

In spring, silicoflagellates, mainly 20-30 μm in diameter, were abundant in trap samples in subantarctic waters, as were small, round *Coscinodiscus* spp. (<60 μm diameter) (Fig. 5.8). Radiolarians and rare oval khaki-dark green and rectangular dark khaki faecal pellets were also present. Unusual light blue-yellow and red-brown translucent mineral grains occurred in small quantities. In subtropical waters, rectangular and elongate khaki-brown faecal pellets were common whereas silicoflagellate numbers seemed to be slightly lower than trap samples in subantarctic waters. Red-brown mineral grains were numerous, together with abundant *Coscinodiscus* spp. (190->200 and 40-90 μm diameters). Agglutinated foraminifera and copepod carcasses were present, though rare.

A broadly similar assemblage to that in subtropical waters was found at station X477 and in the 100 m trap sample at the paired station, X478, in the STC (Fig. 5.8). Silicoflagellates were probably more abundant in the STC, while faecal pellets were less

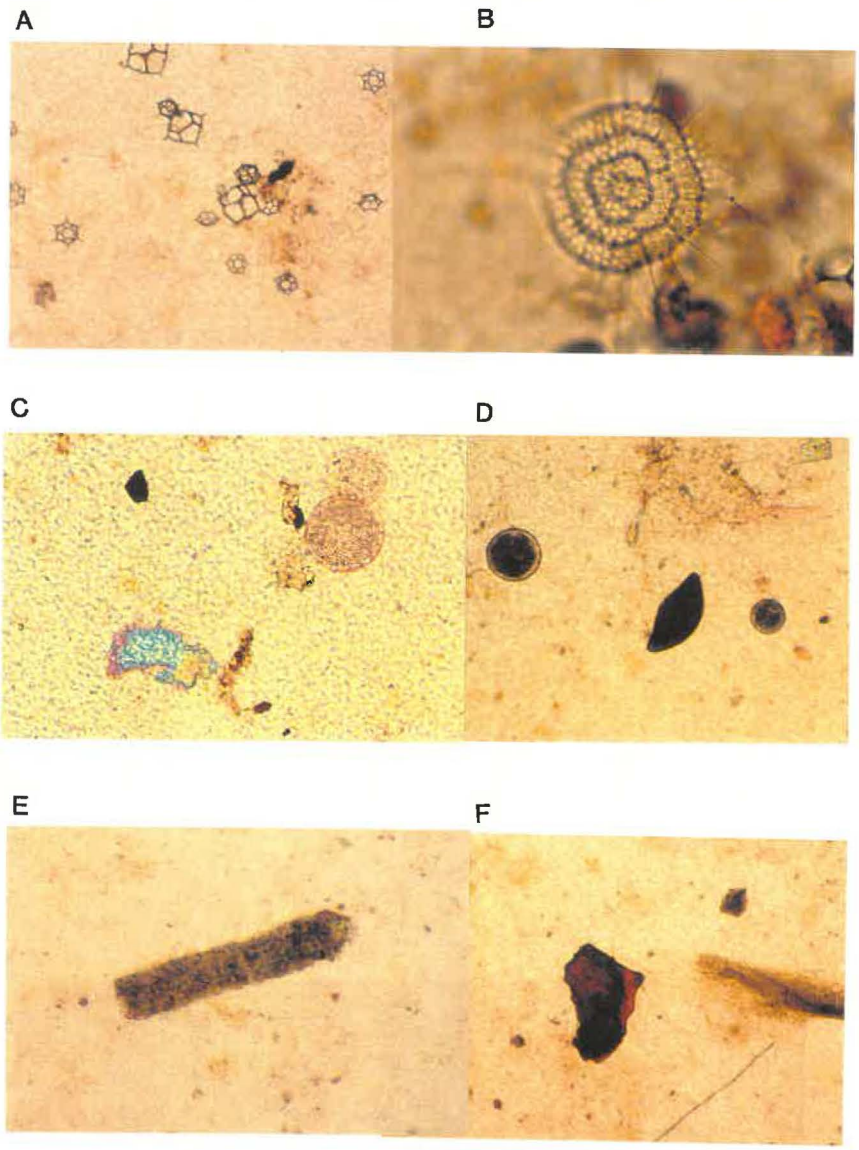

Fig. 5.8 Photo-micrographs of filtered sediment trap samples collected in spring 1993 (length of bar = 100 μm at 100 x magnification, 50 μm at 200 x magnification). (A) Silicoflagellates at 300 m in subantarctic waters (X476). Large silicoflagellate in centre of photograph is 60 μm across. (B) Radiolarian (110 μm diameter, 200 x) at 300 m in subantarctic waters (X476). (C) Pale blue-pink translucent mineral and *Coscinodiscus* spp. (60 μm diameter) at 550 m in subantarctic waters (X476). 200 x magnification. (D) Microzooplankton (60 μm long) and small *Coscinodiscus* spp. at 150 m in subantarctic waters (X476). (E) Rectangular faecal pellet (60 μm across) at 110 m in subtropical waters (X479). (F) Reddish-brown mineral grain (150 μm long x 100 μm wide) at 110 m in subtropical waters (X480).

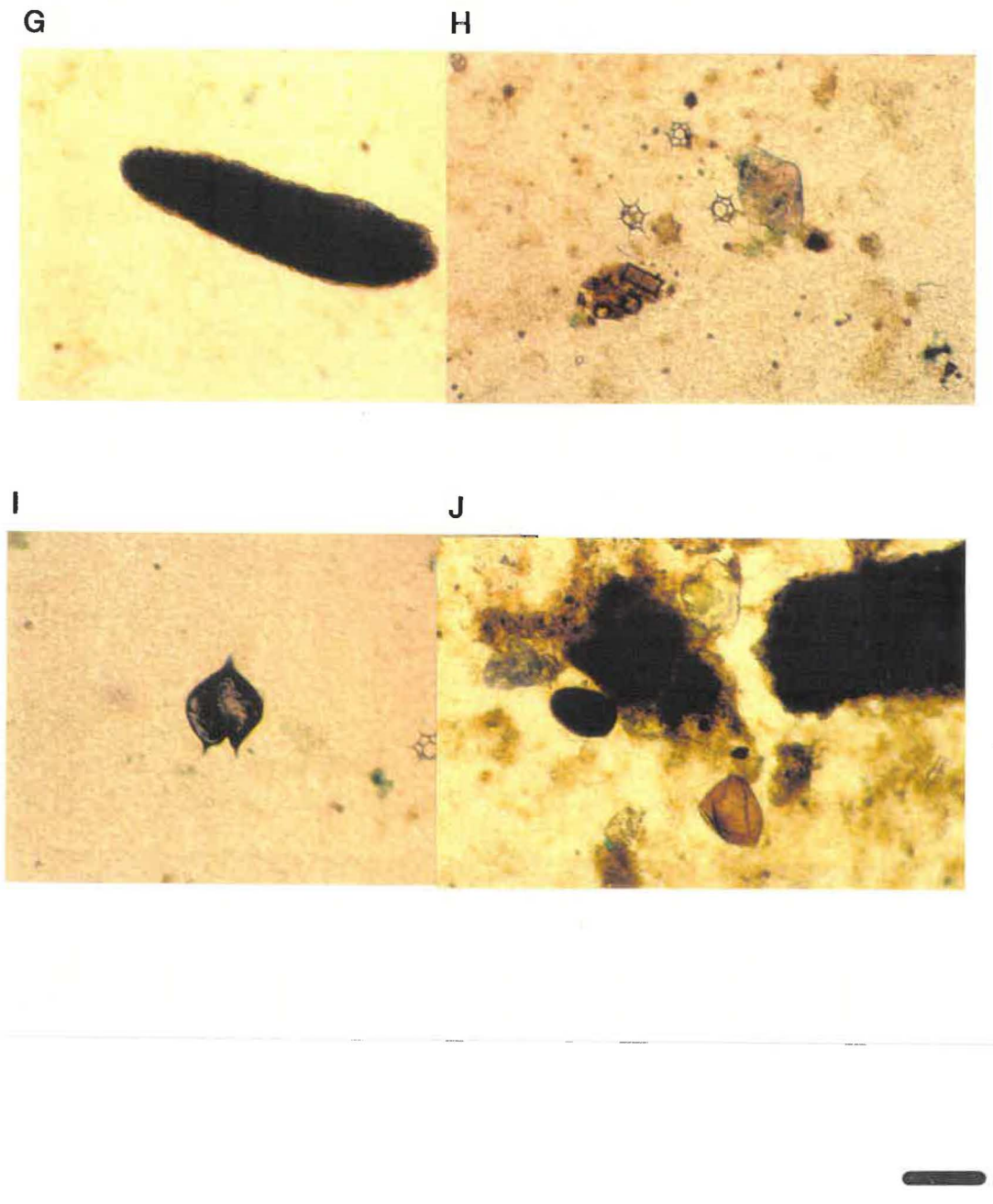

Fig. 5.8 (cont'd) (G) Large elongate faecal pellet (240 μm long, 200 x magnification) at 550 m in subtropical waters (X479). (H) Silicoflagellates and unidentifiable material at 220 m in the STC (X477). Silicoflagellate in centre of photograph is 30 μm across. (I) Unidentified dinoflagellate? (90 μm across) at 100 m in the STC (X480). (J) Faecal pellets (140 μm wide, 200 x), greenish (glauconite?) minerals and assorted debris at 220 m in the STC (X478).

Table 5.5 Qualitative appraisal of zooplankton "swimmers" collected in sediment traps in water types, east of New Zealand, in winter and spring 1993.

"Swimmer" type	Winter 1993*				Spring 1993*				
	X464 SA	X465 SA	X467 STC	X468 ST	X475 SA	X476 SA	X477 STC	X478 STC	X479 ST
Calanoid copepods	C	C	VA	A	C	C	A	A	VA
Foraminifera	✓	✓	✓	✓	A	A	A	C	C
Ostracods	✓	✓		✓					✓
Radiolarians	±	±	±	±					
Appendicularians			✓	✓			±	±	
Polychaetes			±				✓	✓	✓
Cumaceans								✓	
Pteropods							±	±	✓
Tintinnids									±
Chaetognaths								±	

* SA = subantarctic, STC = Subtropical Convergence, ST = subtropical, ± = may be present or absent in samples from the same station, ✓ = present in all samples, C = common in all samples, A = abundant, VA = very abundant.

common than in subtropical waters. In addition, radiolarians were conspicuous in the STC. By contrast, the deep trap sample at X478 contained considerably more material and comprised a vastly different assemblage to other trap samples from the STC, and indeed all other analysed samples. At X478, the assemblage at 220 m was characterised by very abundant irregular, subangular-rounded translucent mineral grains and common, large rectangular faecal pellets and "fluffy" amorphous aggregates. The most conspicuous component of fluxes at 220 m, however, was rounded, equant-elongate, green mineral grains that resembled glauconite pellets.

5.3.6. Zooplankton "swimmers"

Other workers have highlighted the problems associated with identification and removal of "swimmers" (e.g., U.S. GOFS Report 10, 1989; Michaels et al., 1990; Silver & Gowing, 1991; Gardner, 1996) (Section 1.6, Chapter 1) and, for the purposes of this study, all zooplankton that could have entered the sediment traps "alive" have been excluded. In certain cases, this approach could have included the removal of some organisms, such as radiolarians and foraminiferans, that may be more rigorously regarded as part of the "true" vertical particulate flux (e.g., Silver & Gowing, 1991). The zooplankton "swimmer" component has been assessed qualitatively using a scale of relative abundance and presence/absence criteria (Table 5.5).

Copepods were the dominant "swimmer" found at all stations in both seasons with foraminifera being a sub-dominant form in all three water masses in spring, especially in subantarctic waters. Radiolarians were observed in the "swimmer" population in winter, but were apparently replaced in spring by appendicularians, polychaetes and pteropods. A unique feature of one station in the STC (X478) in spring was the collection of large (3-5 mm long) cumaceans. In general, abundance of copepod "swimmers" seemed to be little changed between the two seasons (Table 5.5), suggesting that contamination of sediment trap samples by "swimmers" (e.g., Peterson & Dam, 1990) cannot fully explain the higher observed fluxes in winter, compared to spring. The high numbers of calanoid copepods found in the Chatham Rise traps may reflect observations that formalin appears to act as a preferential poison for such organisms (e.g., Lee et al., 1992). It is noted that other studies that have attempted to quantify the contaminant contribution made by swimmers use dry weights of zooplankton

classes (e.g., Lee et al., 1988, 1992; Peterson et al., 1993); this approach was not attempted by the present study.

5.4. Intra- and inter-trap variability

Sediment trap results exhibited more variability in winter than spring (Fig. 5.4), such that even a two-fold increase in mass flux with depth at the subtropical station (X468) was deemed non-significant by ANOVA analysis. It is difficult to determine the reasons for this variability, although it is probable that a significant proportion was introduced during sample processing since the simple method of preparing sample aliquots (i.e., thorough agitation of the homogenised sample solution in each cylinder and extraction of subsample aliquots using measuring cylinders) involved mean estimated errors of 34% (range<1-83%). These results were not anticipated since prior to undertaking the research voyages in 1993, laboratory work had suggested that coefficients of variation between 4 and 12% might have been expected (see Table 2.2, Section 2.3, Chapter 2). Results from *a posteriori* experiments, conducted in 1994-95, also exhibited lower degrees of variability between processed subsamples (i.e., range 1-45%, Tables 2.5, 2.6 & 2.8, Section 2.3, Chapter 2).

Although it is difficult to extract sample processing errors from many published floating sediment trap studies, Wassman (1991) suggested that (p.98) "variance between subsamples was generally greater than that between traps, depths and stations" deployed in a fjord in western Norway, while a literature search indicated that intra-trap sample replicates of particulate mass and organic carbon fluxes can vary from 1-35% (e.g., Staresinic et al., 1982; Nelson et al., 1987; Karl et al., 1991a; Landry et al., 1992). Sub-sampling from solutions combined from individual cylindrical traps deployed for 3 days at the same depth off Hawaii, however, resulted in C. V.s of between 8 and 83% for particulate carbon flux analyses (calculations performed on data from Hawaii Ocean Time-series (HOT) cruises 2-7; Chiswell et al., 1990). The time-series data collected off Hawaii show that the potential errors arising from subsampling protocols at this oligotrophic site are similar in range to those measured during spring sediment trap deployments across the STC region. In comparison, mean subsampling errors from rotary splitters used in other trap studies have been estimated at 4-6% (e.g. von Bodungen et al., 1991; Honjo & Manganini, 1993; Honjo et al., 1995).

Another potential source of flux variability in winter may have arisen from deployment of uppermost traps close to maximum depth of the mixed-layer in each water type (Table 4.2, Chapter 4), thereby affecting absolute trapping efficiency (e.g., Gardner, 1985). In addition, mooring line heaving effects, attributed to surface wave action, could have also affected trapping efficiency throughout the free-floating arrays in all water types and in both seasons (e.g., Gust et al., 1992, 1994).

It is unlikely that inter-trap interactions affected trapping variability in light of the results from an *a posteriori* experiment in 1994 that indicated there was no significant difference in mass flux between NZOI-NIWA traps deployed on the same cross-frame at the same depth (see Table 2.5, Section 2.3, Chapter 2). Substantial variability between samples taken from different cylinders at the same depth was considerable in winter, with C. V.s ranging from 10-123%. These observations could have been attributed to inter-trap variability (e.g., Honjo, 1978; Gardner, 1980a), but there was no systematic pattern to this variation which suggests that a substantial proportion was possibly due to subsampling errors, as discussed previously.

Similarly, it is unlikely that baffles contributed to the high levels of variability because a second *a posteriori* experiment in 1995 indicated that trapping efficiency should not be significantly affected by baffled or unbaffled NZOI-NIWA cylinders (see Table 2.6, Section 2.3, Chapter 2). C. V.s of mass flux determinations between individual traps at each depth were slightly less in spring than in winter, averaged 33% (1 s.d. 22%, range 6-87%, n=14). The coefficients of variation determined between individual cylinders deployed at the same depth in Chatham Rise region in 1993 are comparable with similar estimates made at JGOFS time-series stations off Hawaii and Bermuda which range from 1-79% (overall mean C. V. 21%, n=137) and 1-90% (20%, n=255), respectively (calculations made using U.S. JGOFS data-sets available on http://hahana.soest.hawaii.edu/hot/hot_jgofs.html and http://www.bbsr.edu/bats/bats.html). In addition, re-appraisal of particulate organic carbon flux data contained in the classic sediment trap paper by Knauer et al. (1979) indicates that variability between replicate traps ranged between 4 and 47% with the highest degrees of inter-trap variation occurring at their open ocean northeast Pacific site (i.e., 36% at 75 m, n=3; 6% at 575 m, n=2; 47% at

1050 m, n=3). Similarly, Hedges et al. (1993) compared cylindrical traps arranged within bottom-moored octagonal arrays and found C. V.s between cylinders in the same array of 7-15%. Furthermore, overall mean precision estimates for replicate traps in the first year of the HOT programme for total mass and particulate phosphorus flux were 18 and 32%, respectively (Karl et al., 1991a). Thus, despite substantially larger sample sizes in the HOT and BATS data-sets (n>100), the Chatham Rise results probably provide a reasonable estimation of total mass flux given the high degrees of variability that are seemingly inherent in such analyses from other sediment trap studies.

5.5. Inter-depth variations in flux: Effect of zooplankton and resuspension

Previous studies of upper ocean particle export have shown that fluxes generally decrease markedly within the top 500 m due to decomposition and remineralisation of sinking material (e.g., Knauer et al., 1979; Martin et al., 1987, 1993; Bruland et al., 1989). A pilot study in subtropical waters on northern flank of Chatham Rise in austral autumn reported near-bottom and mid-water increases in total particulate concentrations and mass flux which were attributed to resuspension and lateral advection of sediments from crest of Chatham Rise (Nodder, in press; Fig. 2.4, Section 2.2, Chapter 2). In winter and spring 1993 significant decreases in particulate flux with depth were only observed in mass and phosphorus flux in subtropical waters and in phosphorus flux at one station (X476) in subantarctic waters in spring. Non-significant flux variations with depth were generally observed in the three water types, particularly in winter. The non-significant results in winter are a reflection of higher sample variation between individual traps at each depth, as discussed earlier (Fig. 5.4).

Noteworthy occurrences of apparently increasing flux with water depth were observed in winter subtropical waters (X468) and in the STC in spring (X478). Such increases have been explained in other studies as being due to mid-water column microbial activity (e.g., Karl & Knauer, 1984a), the effect of horizontal advection on settling patterns of marine particles (e.g., Siegel et al., 1990), migrating zooplankton (e.g., Angel, 1989) or resuspension of sea-floor sediments (e.g., Gardner et al., 1985; Gardner & Richardson, 1992). There is no available data to verify the influence of microbial processes since bacterial analyses were not conducted below 80 m water depth on both voyages (Smith & Hall, in press). Similarly,

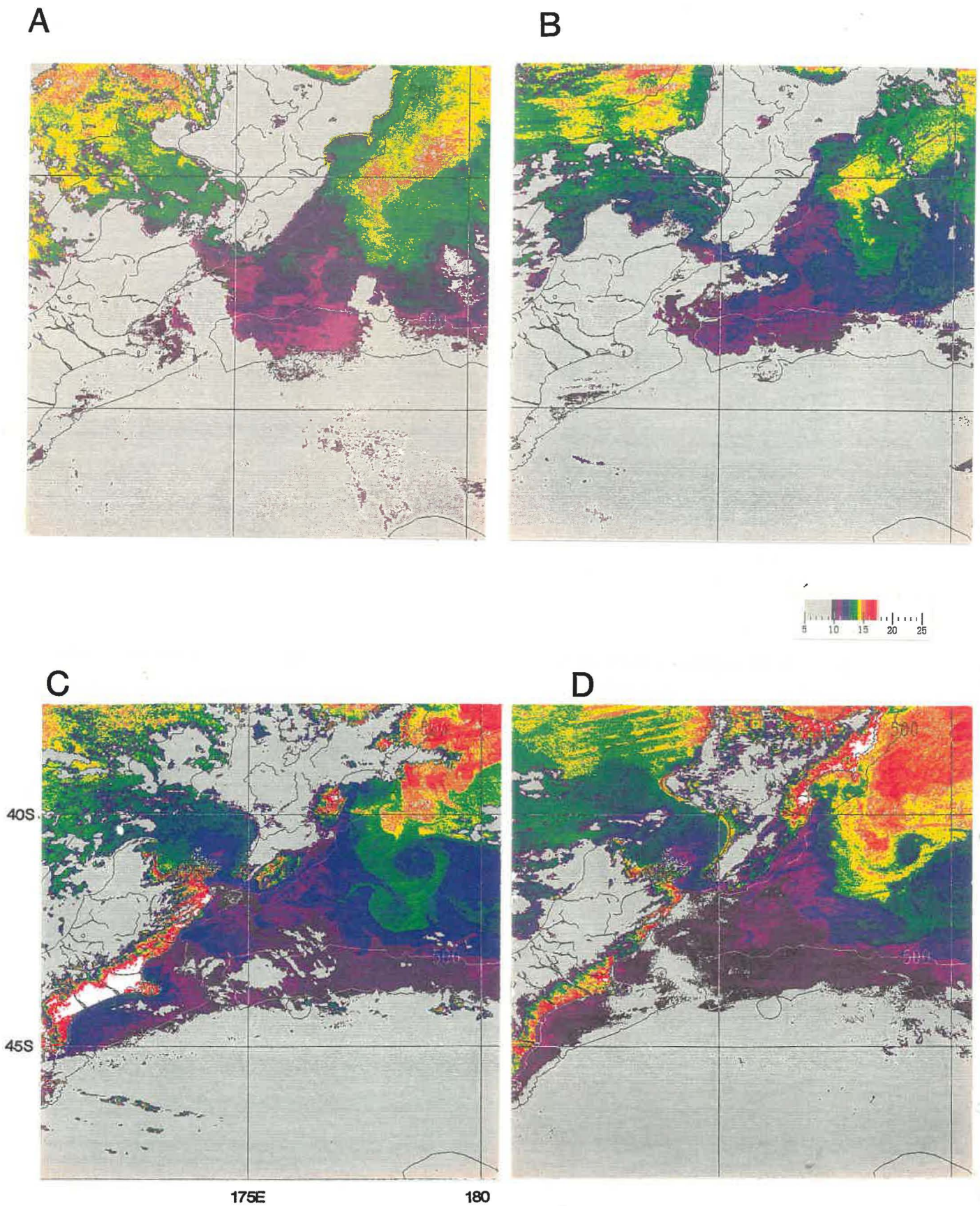

Fig. 5.9 Sea-surface temperature (°C) mosaics from AVHRR satellite imagery for 1603 h (UTC), 21 June (A); 0415 h, 23 June (B); 0444 h, 14 October (C) and 0512 h, 20 October (D) 1993. These were the "best" images selected from the periods of the winter and spring research voyages in 1993. Note the extensive cloud cover and lack of temperature resolution south of the Chatham Rise.

meso-scale oceanographic features cannot be evaluated due to inadequate sea-surface temperature data from satellite passes at the time of the trap deployments as a result of extensive cloud cover during the two sampling periods in 1993 (Fig. 5.9).

In winter subtropical waters, however, a statistically non-significant two-fold increase in flux with depth was associated with a reasonable proportion of mesozooplankton biomass (2 mgC m^{-3}, especially >1000 μm, mainly omnivores; Bradford-Grieve et al., 1997b) between 200-500 m water depths collected during stratified, night-time zooplankton tows. The presence of many large faecal pellets in trap samples in subtropical waters suggests that mesozooplankton may have directly contributed faecal material to trap samples during diel vertical migrations (e.g., Angel, 1989). The mid-water flux increase was also accompanied by increases in the water column particulate carbon concentration over 300-550 m (by 5-15 μg l^{-1}).

The only significant inter-station difference across water types and seasons was found between the STC station pair in spring (Fig. 5.4). The cause of this variation was substantial near-bottom increases in total particulate mass and phosphorus flux at X478, although at X477 mass fluxes were also observed to increase non-significantly with increasing water depth (Fig. 5.4). These anomalous mid-water increases are probably due to resuspension of bottom sediments on the crest of the Chatham Rise, as documented by Nodder (in press) (Section 2.2, Chapter 2). Microscopic examination of filtered trap samples indicates that at X478 there was a noticeable increase in large amorphous "fluffy" aggregates, inorganic mineral grains, and possibly glauconite in 220 m trap samples, compared to analogous samples from X477. Supporting data for a resuspension mechanism include 2-fold increases in chlorophyll *a* (<200 μm) concentration over water depths from 100 to 220 m during one cast at X478. The non-persistence of near-bottom increases in this and other parameters, such as water column particulate concentrations measured on other casts, may be explained by the periodic, semi-diurnal nature of tidal flows (Chiswell, 1994a) that are inferred to be responsible for resuspension events on and off the crest of the Chatham Rise (Nodder, in press). Lampitt (1985) showed that phytodetritus that had recently arrived on the sea-floor at 4000 m was readily disaggregated and resuspended by tidal currents at speeds in excess of 7 cm s^{-1}. Auffret et al. (1994) suggested that, while bottom resuspension at depths of 4700 m was not due specifically to

tidal oscillations, tidal currents affect near-bottom particle concentrations. Water depths on the Chatham Rise crest are less than 500 m (Fig. 3.1, Chapter 3) and there is evidence of localised erosion from seismic reflection profiles and bottom photographs (von Rad & Kudrass, 1984), adding further support to resuspension mechanisms.

5.6. Inter-station and inter-seasonal variability

Differences in plankton community structure affect material fluxes by influencing the mode of particle export and the efficiency of the biological pump at removing carbon from the upper ocean (e.g., Legendre & le Fèvre, 1989; Passow & Peinert, 1993; Boyd & Newton, 1995; Karl et al., 1996). Comparison between stations and across water types east of New Zealand, however, suggests that this factor may not always be significant with respect to total mass flux at least in winter and spring 1993. For example, no statistically significant differences were observed either across the three water types in spring nor between stations in subantarctic and subtropical waters in both seasons, despite distinct biological and physical differences in the overlying water column between seasons (e.g., Bradford-Grieve et al., 1997a, b; James & Hall, 1997; Smith & Hall, in press) (Tables 4.2 & 4.3, Chapter 4). For example in the spring STC, nitrate + nitrite and dissolved reactive phosphorus and silicate concentrations were relatively depleted at both stations, compared with winter values (lower by approximately 5 μM, 0.3-0.4 μM and 1 μM, respectively). Furthermore, in spring, ratios of production to biomass ratios in STC were low (7 and 13) and the phytoplankton community was dominated by large (20-200 μm) phytoplankton (mainly diatoms). These data suggest that phytoplankton biomass accumulation had probably ceased. At this time, since free-floating sediment trap measurements did not record a significant near-surface flux event in the STC, it is postulated that a phytoplankton-dominated sedimentation event may have occurred soon after the time of sampling (Bradford-Grieve et al., 1997a). If traps had been deployed for a longer period, then such an episodic event might have been captured (e.g., during the JGOFS North Atlantic Bloom experiment in 1989, free-floating traps were deployed for approximately 2 weeks and recorded substantial fluxes associated with the passage of a spring phytoplankton bloom; Martin et al. (1993)).

5.7. Independent validation of sediment trap fluxes

Particulate flux measurements may be calibrated independently using other techniques, including new production estimates (e.g., Eppley & Peterson, 1979; Suess, 1980; Knauer et al., 1990) and water column uranium-thorium disequilibria modelling (e.g., Buesseler et al., 1992, 1994; Murnane et al., 1996). No independent means of estimating the validity of sediment trap fluxes in the present study were undertaken at the time of sampling, however, so that approximate comparisons are made here with estimated rates of sediment accumulation across the STC region derived from other geological studies. This crude approximation indicates that when average mass fluxes, measured directly below the mixed-layer, are converted to geological rates of sediment accumulation (and *vice versa*), there is a reasonable comparison between the two independent measurements (Table 5.6). When estimates of water column decomposition are taken into account (based on an average six-fold reduction in flux between 150 and 2000 m reported by Martin et al. (1993) in North Atlantic), predicted transformed annual fluxes across the region are generally less than sedimentary accumulation rates (e.g., Fenner et al., 1992; Carter & Carter, 1993) (Table 5.6), especially for hemipelagic sediments beneath subtropical waters (Fenner et al., 1992). One explanation for this apparent discrepancy is that sea-floor deposition in vicinity of the subtropical sediment trap stations is probably dominated by channel overspill of turbidity currents flowing down the Hikurangi Channel (Lewis, 1994), rather than by hemipelagic processes (Fenner et al., 1992).

5.8. Implications of inherent sampling variability in sediment trap studies

If errors in Chatham Rise mass fluxes are systematic and estimated fluxes reflect the relative magnitude of actual measurements, then apparent relationships between particulate export and primary production rates can be examined. This analysis suggests that there is a weak association between average mass flux and integrated primary productivity (Fig. 5.10). A close coupling between the production of organic particles in the upper ocean and those sinking to the sea-floor has been inferred previously using moored and free-floating trap arrays (e.g., Eppley & Peterson, 1979; Suess, 1980; Pace et al., 1987; Asper et al., 1992; Newton et al., 1994). Recent time-series information from other oligotrophic environments suggests, however, that particle export, measured using drifting traps, is

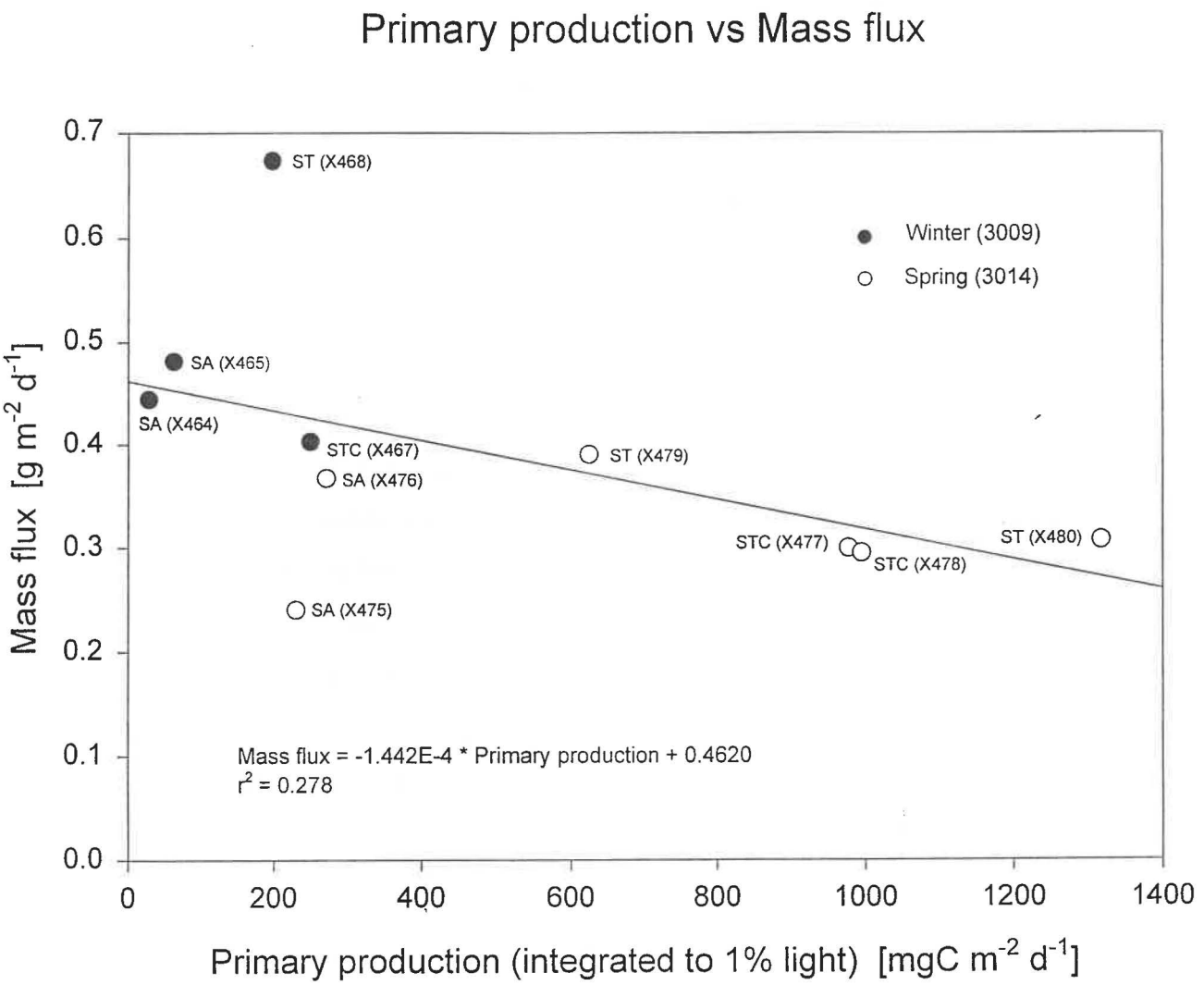

Fig. 5.10 Relationship between integrated primary production and average uncorrected total mass flux in winter and spring 1993. Mass fluxes are estimated from shallowest traps deployed below the mixed-layer in subantarctic (SA), Subtropical Convergence (STC) and subtropical (ST) waters. Primary production rates are integrated to the depth of the 1% surface light level (Bradford-Grieve et al., 1997b).

Table 5.6 Comparison of mass flux measurements with sediment accumulation rates across the Subtropical Convergence region.

Water mass	NIWA station	Latitude & longitude	Sedimentation rate (cm kyr^{-1})*	Accummulation rate (g cm^{-2} kyr^{-1})**	Near-surface mass flux (g m^{-2} d^{-1})	"Geological" near-surface flux (g cm^{-2} kyr^{-1})†	"Geological" near-bottom flux (g cm^{-2} kyr^{-1})‡	Reference
Subantarctic	Q217 (1940 m water depth)	46°28'S 175°04'E	3.0	3.0	-	-	-	Carter & Carter (1993)
	Average (South Chatham Rise - Bounty Trough)*		3.4	3.4	-	-	-	-
	X464	46°13'S 174°01'E	-	-	0.260	9.5	1.6	**This study**
	X465	46°05'S 174°04'E	-	-	0.600	21.9	3.7	**This study**
	X475	46°09'S 174°00'E	-	-	0.240	8.8	1.5	**This study**
	X476	46°03'S 174°00'E	-	-	0.120	4.4	0.7	**This study**
Subtropical	Q858 (3735 m water depth)	39°50'S 178°04'W	6.0	6.0	-	-	-	Fenner et al. (1992)
	Average (Hikurangi Plateau)*		7.7	7.7	-	-	-	-
	Average (North Chatham Rise)*		2.5	2.5	-	-	-	-
	X468	41°29'S 179°00'E	-	-	0.420	15.3	2.6	**This study**
	X479	41°35'S 178°56'E	-	-	0.260	9.5	1.6	**This study**
	X480	41°30'S 179°01'E	-	-	0.210	7.7	1.3	**This study**

* Sedimentation rate since end of oxygen isotope stage 2 dated at about 12,000 years (H. Neil and L. Carter, personal communication, 1997).

** Accummulation rate determined based on an average dry bulk density of 1 g cm^{-3}.

† Daily average near-surface mass flux rate converted to annual rate by multiplying by 365 days.

‡ Transformation of average near-surface mass flux to a near-bottom flux by assuming a six-fold reduction in flux with depth, based on results of Martin et al. (1993) in North Atlantic.

poorly correlated with primary production (Knauer et al., 1990; Lohrenz et al., 1992; Michaels et al., 1994; Karl et al., 1996; Michaels & Knap, 1996).

Karl et al. (1996) presented three hypotheses to account for the apparent decoupling between primary production and export flux: (1) temporal and spatial variations in the relative strength of components of the biological pump; (2) inadequacies and biases of the sediment trap method for accurately measuring the downward flux of biological particles and energy (e.g., Michaels et al., 1990; Buesseler et al., 1992, 1994; Murnane et al., 1996); and (3) influence of horizontal advection on oligotrophic carbon and energy cycling (e.g., Siegel et al., 1990; Michaels et al., 1994; Toggweiler, 1994).

The first hypothesis does not appear to be particularly robust for oceanic waters east of New Zealand (cf. Legendre & le Fèvre, 1989; Boyd & Newton, 1995) since, despite marked changes in plankton community structure and functioning across water types and seasons, particle export processes were not profoundly affected. With regard to the second hypothesis, it is acknowledged that the New Zealand traps may also exhibit similar shortcomings in terms of trapping efficiency as other traps used in JGOFS programmes (e.g., Buesseler et al., 1992, 1994; Murnane et al., 1996). Of relevance to the New Zealand results, Buesseler et al. (1994) suggested that MULTI-PIT traps used at Bermuda Atlantic Time Series station overcollect during periods of low productivity and undercollect when production rates are high. The effect of the third factor, namely horizontal advection, on trapping efficiency in the vicinity of the Chatham Rise is expected to be considerable (e.g., Heath, 1985; Chiswell, 1994a), but has not been quantified adequately to enable detailed discussion in this paper. Meso-scale eddy features have been detected in satellite imagery (Barnes, 1985; Vincent et al., 1991) and current meter records (Chiswell, 1994a) and bottom-eroding tidal currents are inferred to operate across the Chatham Rise (Nodder, in press; Section 2.2, Chapter 2). In addition, the northward drift paths of traps deployed in subtropical waters in both seasons (Fig. 5.1) suggest that traps were entrained in flows associated with a large semi-permanent eddy that lies centred above the Hikurangi Trough, north of Chatham Rise (P. Sutton, pers. comm., 1996).

Perhaps, a fourth hypothesis is also warranted, regarding variability introduced during subsampling procedures and/or arising from inter-trap interactions between individual

Table 5.7 Comparison of 1992 North Chatham Rise sediment trap results with some previous sediment trap experiments.

	Mass flux $mg\ m^{-2}\ d^{-1}$	POC flux* $mg\ m^{-2}\ d^{-1}$	PON flux* $mg\ m^{-2}\ d^{-1}$	POP flux* $mg\ m^{-2}\ d^{-1}$	References
NW Sargasso Sea (BATS 32°N) 100-400 m	10-270	1.2-5.4	0.1-1.1	-	Lohrenz et al. (1992)
W Atlantic slope (SEEP II 37-38°N)	67-456	9-33	-	-	Biscaye & Anderson (1994)**
120-400 m	235.0±178.5	19.3±11.0	-	-	
Central N Atlantic (NABE 46-47°N) <400 m	320-660	160-500	-	-	Martin et al. (1993)
NE Pacific (VERTEX 32-36°N)					
Coastal upwelling 250-700 m**	-	183.3±80.1	18.9±7.3	2.4±1.4	Knauer et al. (1979)
Coastal non-upwelling 250-700 m**	-	50.6±4.8	5.1±1.6	0.4±0.05	
Open ocean 75-575 m	-	47.3±34.2	2.7±2.6	0.2±0.2	
Central equatorial Pacific (HOT 22°N) 150 m	-	24.4±9.5†	3.8±1.5	0.4±0.2	Karl et al. (1995)
E Pacific (S California 34°N) 500 m	100-1210	18-54	-	-	Thunell et al. (1994)**
	513.7±269.0	32.7±10.6	-	-	
North Chatham Rise, SW Pacific 43°S	**44-205**	**25-38†**	**1.5-5.1**	**0.2-0.5**	**This study**
200-500 m	**114.2±47.8**	**31.9±4.5†**	**2.8±0.6**	**0.4±0.1**	

* POC = particulate organic carbon; PON = particulate organic nitrogen; POP = particulate organic phosphorus; ranges of values or calculated averages ± 1 standard deviation are given; only approximate values for the BATS data-set are listed; average fluxes for the El Niño period 1991-92 are taken from the HOT programme summary (Karl et al., 1995); BATS = Bermuda Atlantic Time-series Study 1989-1990, NABE = North Atlantic Bloom Study 1989, VERTEX = Vertical Transport & Exchange , HOT = Hawaii Ocean Time-series 1991-92.

** Moored cones (Thunell et al., 1994 - 7 months) or cylinders (Knauer et al., 1979 - 19-21 days; Biscaye & Anderson, 1994 - 10-20 days) used; in other studies, free-floating cylinders were deployed as drifting arrays for periods ranging from 3 days (Karl et al., 1995; Lohrenz et al., 1992; this study)to about 2-5 weeks (Martin et al., 1987; 1993). These comparisons assume that there is little difference in trapping efficiency between trap types, mooring configurations and analytical techniques used in each study (e.g. Honjo et al., 1992).

† Values represent total PC flux and include inorganic (PIC) and organic carbon. PIC flux is expected to be similar in magnitude to POC flux since even in regions where carbonate sedimentation dominates, such as the equatorial Pacific Ocean, PIC flux is only 1-6% higher than POC flux relative to total mass flux (Honjo et al., 1995).

cylinders deployed at the same depth, as discussed earlier in Section 5.4. Such analyses suggest that systematic errors in trap measurements may mask the seasonal and depth trends in particulate flux that researchers are attempting to document in studies of oceanic biogeochemical cycles across different water types. Given the low levels of power associated with many of the statistical tests conducted as part of the present study, it is suggested that more than two replicated stations are required to determine "across water mass/type" variations in upper ocean particulate flux, as measured using free-floating sediment trap arrays. Therefore, the use of single surface-tethered arrays at individual stations, as employed in many other sediment trap studies (e.g., Knauer et al., 1979, 1990; Karl & Knauer, 1984; Martin et al., 1987, 1993; Lohrenz et al., 1992; Karl et al., 1991b, 1996), is not advocated for studies that attempt to characterise fluxes for specific oceanic provinces (e.g., Martin et al., 1987). Perhaps, the use of deep ocean moored traps, which integrate fluxes over much wider temporal and spatial scales (e.g., Siegel et al., 1990), may be a more suitable method for establishing basin-wide sedimentation characteristics (e.g., Deuser et al., 1981; Honjo & Manganini, 1993; Newton et al., 1994; Honjo et al., 1995).

5.9. Comparison with other sediment trap data

The limited data-set collected in autumn 1992 during the North Chatham Rise NZOI sediment trap pilot study (Section 2.2, Chapter 2) can be compared directly with other sediment trap studies conducted in oceanographic provinces. These results suggest that there is little difference between the range of flux values observed east of New Zealand compared with other oligotrophic sites (Table 5.7).

In order to conduct a similar comparison with the 1993 sediment trap data, mass and particulate phosphorus fluxes were converted to absolute values by: (a) ignoring any blank values that lay outside an arbitrary chosen range of the mean blank ± 1 standard deviation; (b) subtracting specific mean mass blank values from raw data for each of the trap experiments, and excluding any fluxes that were "negative"; and (c) using the spring particulate phosphorus blank values to correct the winter data-set due to excessive contamination of the latter.

Table 5.8 Comparison of Southwest Pacific Ocean sediment trap studies in 1993 with some other trapping experiments.

	Sampling depth (m)	TM flux (mg m^{-2} d^{-1})	PC flux* (mg m^{-2} d^{-1})	POP flux* (mg m^{-2} d^{-1})	PON flux* (mg m^{-2} d^{-1})	References
NE Pacific (VERTEX)	250	250-300	52 + 252**	0.4 + 4**	6 + 25**	Knauer et al. (1979); Wakeham et al. (1984)
	575	-	14†	0.08†	1.2†	
Central Pacific (HOT) 1988-89	150	59-105	20-67	0.3-1.4	3-7	Chiswell et al. (1990)
	300	23-45	7-34	0.1-0.6	1-4	
	500	28-73	7-26	0.1-0.3	1-2	
E Pacific (S California)	100	220-242	26-35	-	5.3	‡Nelson et al. (1987); ‡Thunell et al. (1994)
	300	138-393	14-37	-	2.2	
	500	256-419	17-25	-	2.2	
Equatorial E Pacific (Peru)	15 and 50	500-6000	220-570	-	-	Staresinic et al. (1982)
Central N Atlantic (NABE)	150	545-774	84-150	-	18-28	Martin et al. (1993)
	300	417-490	36-72	-	7-11	
	500	247-393	24-48	-	4-7	
Equatorial W Atlantic (PARFLUX & BATS)	150	130-175	36-48	-	-	Lohrenz et al. (1992)
Antarctica (Bransfield Strait, RACER)	200	-	87-248	1.2-2.8	7-30	Karl et al. (1991b)
SW Pacific - SA: winter & spring, 1993§	**120(150)**	**22-603 (67-417)**	**13-348 (113)**	**1.3-3.0 (0.4-0.8)**	-	**This study**
	300	**266-370 (120-279)**	**33-166 (-)**	**1.4-2.5 (0.3-0.4)**	-	
	550	**29-556 (35-80)**	**8-269 (6-171)**	**1.9-2.3 (0.2-0.3)**	-	
SW Pacific - STC: winter & spring, 1993§	**110(100)**	**8-428 (109-441)**	**12-36 (-)**	**1.2-2.3 (0.7-1.2)**	-	**This study**
	210(220)	**504 (252-1965)**	**13-163 (78)**	**1.2-1.5 (0.7-3.0)**	-	
SW Pacific - ST: winter & spring, 1993§	**120(110)**	**36-714 (247-409)**	**77-348 (1-136)**	**3.0-3.2 (1.3-2.0)**	-	**This study**
	300	**482-1106 (151-174)**	**7-335 (21-635)**	**1.9-2.5 (0.4-0.5)**	-	
	550	**752-1235 (63-200)**	**3-416 (2-273)**	**2.1-3.2 (0.3-0.6)**	-	

* TM=total mass, PC = particulate carbon, POP = particulate organic phosphorus, PON = particulate organic nitrogen

** Coastal non-upwelling + upwelling.

† Open ocean.

‡ Moored or free-floating cones used; all other studies used free-floating cylinders, except Staresinic et al. (1982) where moored cones were also deployed

§ Ranges of values are given with spring values in parentheses; a dash indicates "no value". Note that for Antarctic and Central equatorial Pacific Ocean studies, total particulate carbon fluxes were estimated, whereas for the other studies, particulate *organic* carbon (POC) flux values were determined; in addition, the Southwest Pacific work (this study) was only able to estimate POC fluxes by assuming that they might typically range from 10-30% of mass flux.

Thus, average mass flux measurements for spring and winter in all three water types across the Chatham Rise may be between 1-2 orders of magnitude greater than fluxes observed in other open ocean environments, depending upon water depth (Table 5.8). The values are, however, similar in magnitude to fluxes that have been recorded from coastal and continental shelf settings (e.g., Knauer et al., 1979; Nelson et al., 1987; Thunell et al., 1994), suggesting that, assuming that there are only minimal differences in measured flux due to trap type (e.g., Dymond et al., 1981; Honjo et al., 1992), the oceanic waters to the east of New Zealand, perhaps not surprisingly, seem to have closer affinities with continental margin environments, rather than truly open ocean regimes. The fluxes are generally less than the highest fluxes measured at sites of active upwelling (e.g., Peru, Staresinic et al., 1982) and regions of very high biological production (e.g., Bransfield Strait, Antarctica, Karl et al., 1991b).

The relatively high fluxes of exported material from the euphotic zone in the vicinity of the Chatham Rise will influence the distribution and composition of mesopelagic (e.g., Robertson et al., 1978) and benthic communities in the region (e.g., Probert & McKnight, 1993). Chatham Rise presently supports economically important deep-water demersal trawl fisheries, such as orange roughy and oreo (Fenaughty & Uozumi, 1989) whose distribution may be linked with the quality and quantity of organic flux to the deep-sea. Probert & McKnight (1993) suggested that high benthic biomass estimates, observed on the southern flanks of the Chatham Rise, were inconsistent with expected biomass trends with increasing water depth (e.g., Rowe, 1983). They attributed this relatively high biomass to enhanced biological surface productivity and, supposedly, export flux, in the STC. Meridional and seasonal variations in primary productivity in 1993, however, were not coupled strongly with observed differences in particulate flux (Fig. 5.10), despite the observation in spring 1993 that the surface waters to the east of New Zealand were acting generally as a sink for atmospheric CO_2 (Fig. 4.5, Chapter 4). Relative to surrounding water types, substantial decreases in sea-water pCO_2 at the STC in spring highlight the importance of this region as a zone of elevated atmospheric CO_2 uptake via enhanced biological production. Since particulate fluxes do not seem to be coupled strongly with primary production it seems that it is the nutritional quality of sinking material, rather than the quantity, reaching the benthos that is important in benthic community structure and function on Chatham Rise. This facet is investigated in more detail in the following chapter by using photosynthetic pigments as tracers for the production and fate of sinking particulate organic matter.

5.10. Summary of Chapter 5

(1) Particulate flux measurements derived from short-term free-floating sediment trap deployments have been used to characterise oceanic provinces (e.g., Martin et al., 1987; Lohrenz et al., 1992; Karl et al., 1996). Results from New Zealand deployments in 1993, however, indicate that such inferences cannot be made without substantially improving the replication that is typically used. While most previous studies have only deployed one drifting array, it is recommended that more than two arrays are required to establish statistically any differences in water types.

(2) Significant variability can be introduced during simple subsampling procedures. These systematic errors may mask seasonal and depth trends in particulate flux that researchers are attempting to document in studies of oceanic biogeochemical cycles across different water types.

(3) Since particulate fluxes do not seem to be coupled strongly with primary production, it seems that benthic community structure and function on Chatham Rise is controlled mainly by the nutritional *quality*, rather than the *quantity*, of sinking material reaching the sea-floor. Furthermore, resupension of material from the crest of Chatham Rise has been confirmed as an important process in enhancing near-bottom particulate fluxes in waters of the Subtropical Convergence. Such processes must have implications for benthic communities that inhabit the Chatham Rise environment in terms of foraging activities and adaptive life histories.

Chapter 6

PHYTOPLANKTON FLUXES FROM CHATHAM RISE–SUBTROPICAL CONVERGENCE REGION:
Results from pigment tracer studies

Table 6.1 Summary of major pigments used as biomarkers in ocean process studies.

Pigment	Algal type or process
CHLOROPHYLLS	
chlorophyll *a*	all photosynthetic algae, except prochlorophytes
chlorophyll *b*	chlorophytes ("green" algae), prasinophytes
chlorophyll *c*'s	chromophytes
CAROTENOIDS	
fucoxanthin	diatoms, prymnesiophytes, chrysophytes
diatoxanthin, diadinoxanthin	diatoms, chrysophytes, dinoflagellates
19'hexanoyloxyfucoxanthin	prymnesiophytes
19'butanoyloxyfucoxanthin	pelagophytes, some prymnesiophytes
peridinin	photosynthetic dinoflagellates
zeaxanthin/lutein	cyanobacteria, chlorophytes
alloxanthin	cryptomonads
PHAEOPIGMENTS	
phaeophorbides, phaeophytins	grazed phytoplankton, faecal pellets, sediments
chlorophyllides	chlorophyllase, extraction & filtering artefact
chlorophyll allomer	oxygenated conditions

Chapter 6

PHYTOPLANKTON FLUXES FROM CHATHAM RISE-SUBTROPICAL CONVERGENCE REGION: results from pigment tracer studies

6.1. Applications of pigment tracers in marine process studies

Pigment and organic compound biomarkers provide a useful tool for investigating aspects of oceanic biogeochemical cycles. The production and subsequent transformation of chlorophyll and carotenoid pigments within marine phytoplankton communities can be traced by determining pigment concentrations in suspended particulate material from water bottle samples (e.g., Gieskes et al., 1978; Hallegraeff & Jeffrey, 1985; Barlow et al., 1993; Méjanelle et al., 1995) and in sinking particles collected by sediment traps (e.g., Cole et al., 1985; Welschmeyer & Lorenzen, 1985a, b; Head & Horne, 1993). Such data can provide information on temporal and spatial changes in phytoplankton community structure (e.g., Claustre, 1994), effects of zooplankton grazing on phytoplankton (e.g., Lopez et al., 1988; Strom, 1993; Landry et al., 1994, 1995), bacterial and enzymatic processes in the water column or within zooplankton guts (e.g., Nelson, 1989), and the influence of environmental conditions, such as light, oxygen and pH, on pigment degradation (e.g., Vernet & Lorenzen, 1987a, b). High-performance liquid chromatography (HPLC) has proven to be an extremely sensitive analytical technique for the unambiguous determination of photosynthetic chlorophyll derivatives, degradation products or phaeopigments, and carotenoids of eukaryotic and prokaryotic origin (e.g., Wright et al., 1991) (Table 6.1). Pigments have been used as diagnostic indicators of autotrophic assemblages (e.g., Barlow et al., 1993; Andersen et al., 1996), and their accumulative concentrations proposed as an estimator of overall phytoplankton biomass (Claustre, 1994). Chlorophyll *a* is taken as a universal indicator of phytoplankton biomass (but see Longhurst, 1991), while the presence of the carotenoids, 19'-hexanoyloxyfucoxanthin (19'HOF), lutein/zeaxanthin (together with chlorophyll *b*), peridinin and alloxanthin are used as evidence for prymnesiophytes, chlorophytes (or "green" algae), dinoflagellates and cryptophytes, respectively (Wright et al., 1991; Barlow et al., 1993). Peridinin, however, is not found in one species of photoautotrophic dinoflagellate,

Gryodinium (Bjørnland & Tangen, 1979) and, therefore, may not be singularly diagnostic of some dinoflagellates. 19'-butanoyloxyfucoxanthin (19'BOF) has been used as an indicator of chrysophytes (Williams & Claustre, 1991) and a new class of phytoplankton, the pelagophytes (Andersen et al., 1996). Barlow et al. (1993) indicate, however, that these correlations should be used with caution due the occurrence of 19'BOF in prymnesiophytes as well. Fucoxanthin, diadinoxanthin and diatoxanthin are common pigments found in diatoms, prymnesiophytes, chrysophytes, and some dinoflagellates, and Claustre (1994) has suggested that fucoxanthin may be used reliably to estimate diatom biomass. Chlorophyll *b* is a dominant pigment in the Chlorophyceae and Prasinophyceae (e.g., Vernet & Lorenzen, 1987a). The phaeopigments, phaeophorbide *a* and phaeophytin *a*, are signature pigments for faecal material and grazed phytoplankton (e.g., Shuman & Lorenzen, 1975; Lorenzen & Welschmeyer, 1983), and may degrade to colourless compounds in the euphotic zone under well lit and oxygenated conditions (Vernet & Lorenzen, 1987b). Chlorophyllides and allomers or oxidised chlorophyll variants are also regarded as degradation products of chlorophyll (e.g., Brown et al., 1977); the former compound is formed under the influence of the enzyme chlorophyllase, but may also be an extraction or filtering artefact (e.g., Wright et al., 1991). The production of chlorophyllides is generally regarded as a chemical step in the full degradation of chlorophyll to phaeophorbides (Brown et al., 1977). Chlorophyll *a* allomers provide an indication as to the oxygen status of the depositional environment prior to sediment deposition, with the transformation from natural chlorophyll occurring in well oxygenated conditions (Brown et al., 1977).

Seasonal successions of phytoplankton and zooplankton are linked intimately via processes of growth and grazing. In turn, temporal and spatial changes in planktonic community structure mediate the rates and modes at which organic material is exported from the upper ocean (e.g., Michaels & Silver, 1988; Legendre & le Fèvre, 1989; Passow and Peinert, 1993; Boyd & Newton, 1995; Karl et al., 1996; Rivkin et al., 1996). During periods of high phytoplankton growth and low zooplankton grazing pressure, such as occurs in spring in the north Atlantic Ocean (e.g., Lochte et al., 1993), seasonal upper ocean production events are typically followed by episodic pulses of rapidly sinking material to the deep ocean (e.g., Deuser et al., 1981; Billet et al., 1983; Deuser, 1986; Asper et al., 1992). Benthic communities respond opportunistically and quickly to the arrival of such labile material at the seabed (e.g., Graf, 1989; Smith et al., 1994). Specific localities, such as regions of coastal

upwelling (e.g., Peru; Staresinic et al., 1978) and within frontal zones (e.g., Olson et al., 1994), are characterised typically by elevated planktonic biomass and primary productivity, which are expected to lead to high particulate export from surface waters to the sea-floor (e.g., Peinert & Miquel, 1994).

This chapter focuses on the waters within and on either side of a circum-global ocean front, the Subtropical Convergence (STC) which is described fully in Chapter 3. Photosynthetic pigment fluxes were measured near the frontal zone to determine whether food quality, rather than food quantity, is important for fueling benthic metabolic requirements in the deep ocean interior. Pigments were employed as biomarkers for specific phytoplankton genera and as tracers for specific processes operating within the pelagic ecosystem.

6.2. Methods

Pigment samples were analysed using High-Performance Liquid Chromatography (HPLC), following the techniques described in Nodder & Gall (submitted) and Nodder et al. (1994a, b) (see Section 5.2, Chapter 5). Briefly, in the onland laboratory, each frozen filter was disrupted in cold 90% acetone using a probe sonicator (Ultrasonics W-225) and extracted at 4°C in the dark. The suspension was centrifuged at 2500 r.p.m. for 5 min, and the supernatant decanted and filtered through a Whatman GF/F filter. The filtrate was stored frozen at -20°C. Chloropigments and carotenoids were separated, identified and quantified using modified HPLC methods adapted from Mantoura and Llewellyn (1983) and Wright et al. (1991). The mobile phases consisted of Eluant A (0.35M ammonium sulphate (pH 6.7-6.8):methanol - 15:85) and Eluant B (90% acetone). Separation was conducted on an Alltech column (Hypersil C18, 5 μm, 250 x 4.6mm internal diameter) fitted with a guard column (Adsorbosphere C18, 5 μm). The column temperature was maintained at 40°C and the eluant flow rate at 1.5 ml min^{-1}. The Shimadzu HPLC system utilised three detectors: UV-VIS, photo-diode array and fluorescence (Hewlett Packard, HP-1046A). The system was washed with Eluant B for 15 min, then gradient-changed to Eluant A and stabilised for 30 min before sample injection. The filtrate was diluted to 66% acetone prior to injection to improve the resolution of polar pigments (Wright et al., 1991). A 150 μl aliquot of

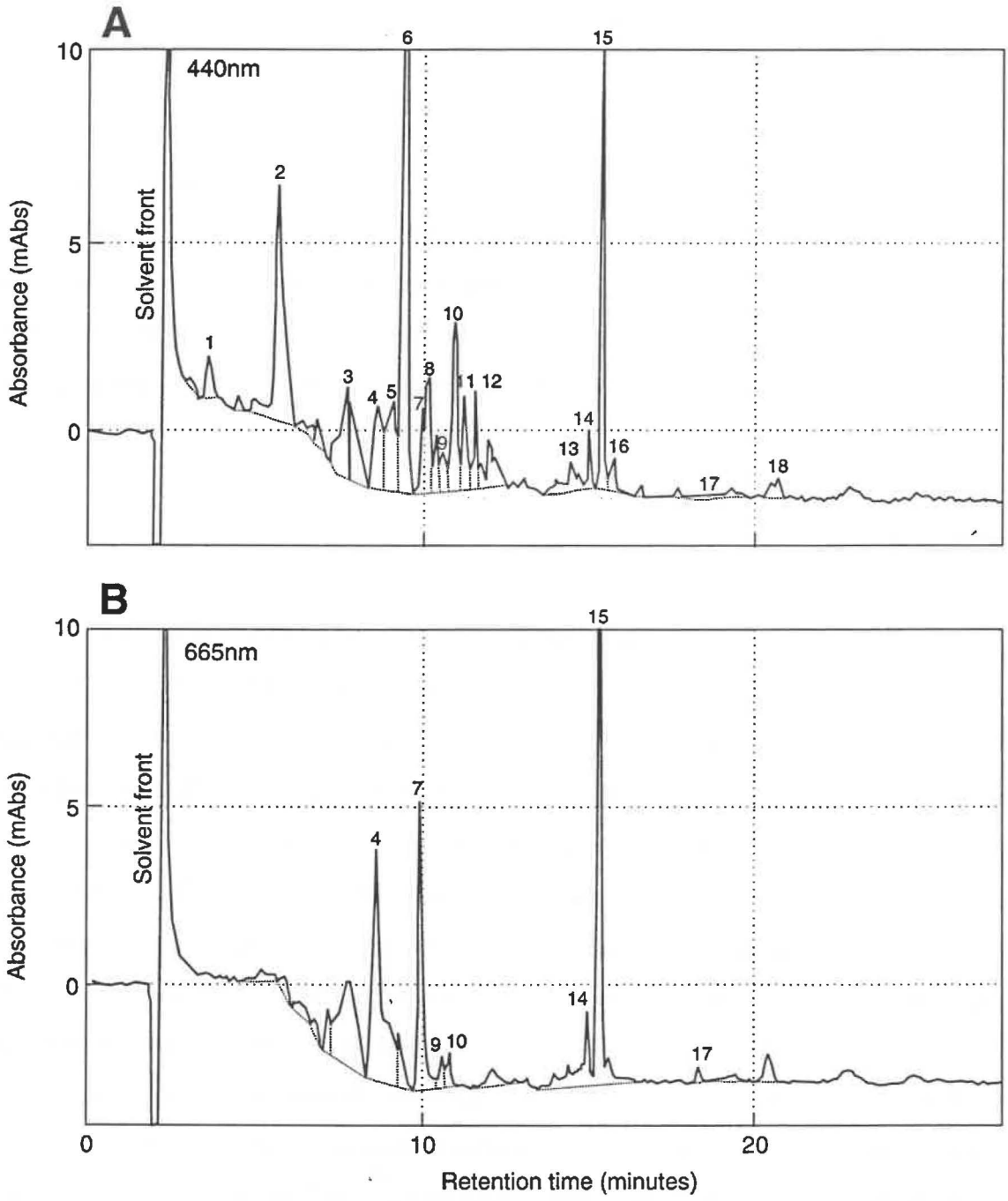

Fig. 6.1 Example of HPLC chromatogram of trap sample from 110 m at station X477 in Subtropical Convergence in spring at (A) 440 nm and (B) 665 nm. Peaks: *1* chlorophyll *c3*, *2* chlorophyll *c*'s, *3* peridinin, *4* phaeophorbide *a1*, *5* 19'BOF, *6* fucoxanthin, *7* phaeophorbide *a2*, *8* 19'HOF, *9* phaeophorbide *a3*, *10* diadinoxanthin/phaeophorbide *a4*, *11* alloxanthin, *12* zeaxanthin/lutein, *13* chlorophyll *b*, *14* chlorophyll *a* (allomer), *15* chlorophyll *a*, *16* echinone, *17* phaeophytin *a1*, *18* β,β-carotene. Refer to Fig. 4.1 and 5.1 for location of sediment trap station X477.

diluted sample was loaded and separated within 30 min using gradient elution [Time min (Eluant B %) = 0 (0), 10(100), 30(100), 32(0)]. Pigment detection was monitored on a UV-VIS detector at 440 nm as a general absorbance for all pigments. Fluorometric techniques (excitation 430 nm and emission 665 nm) were employed to detect chlorophyll *a* and its derivatives. Additionally, a photo-diode array detector (range 380-670nm) captured the spectra of eluted pigments.

Pigment identification was based on retention times and spectral characteristics in comparison with those obtained from separation of commercially available standards (chlorophyll *a*, chlorophyll *b*, lutein and β,β-carotene - Sigma Chemical Co.) and unialgal cultures of known pigment composition (Wright et al., 1991 - CSIRO, Division of Fisheries, Australia). Where possible, pigments were quantified against calibrated standards. In the absence of available standards, pigment quantification was based on published extinction coefficients measured at 440nm ($E^{1\%}$ at 440 nm) or by converting coefficients that had been measured at spectra maxima ($E^{1\%}$max) to $E^{1\%}$440nm (i.e., chlorophyll *a* and it's derivatives - Lorenzen & Newton Downs (1986); all other pigments - Rowan (1989)). Conversion was based on photo-diode array chromatograms from which ratios of peak heights measured at the spectra maxima and at 440 nm were determined, and the corresponding $E^{1\%}$max adjusted accordingly. Alternatively, extinction coefficients from Mantoura & Llewellyn (1983) were used. Fluorescence chromatograms were used to quantify chlorophyll *a* derivatives (phaeophytins and phaeophorbides) since these pigments have poor absorbances at 440 nm and appear in cluttered areas of the chromatogram. Spectrofluorometric extinction coefficients, under similar fluorescence conditions from Neveux & Panouse (1987), allowed calculation of conversion factors for phaeophytin and phaeophorbide extinction coefficients from the calibrated chlorophyll *a* standard solution.

6.3. Results

6.3.1. Photosynthetic pigment fluxes in STC region

Chromatographic analysis of trap samples provided clear resolution of many of the major photosynthetic pigments, such as chlorophyll *a*, fucoxanthin, 19'-hexanoyloxyfucoxanthin (19'HOF), 19'-butanoyloxyfucoxanthin (19'BOF), alloxanthin, β,β-carotene and phaeopigments (Fig. 6.1, 6.2, 6.3 and 6.4). Overall, pigment concentrations in trap samples

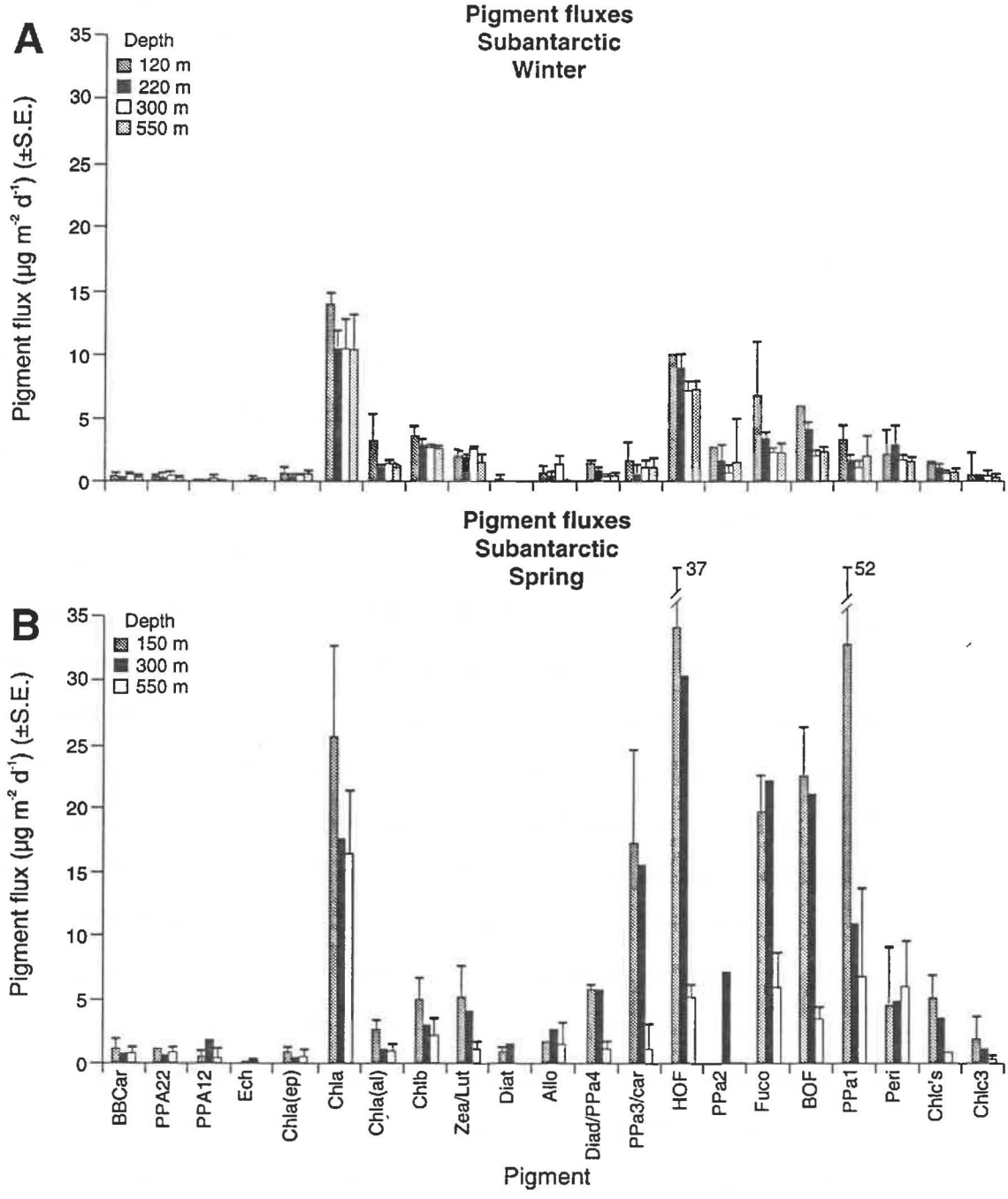

Fig. 6.2 Average pigment fluxes (µg m^{-2} d^{-1}) in winter (A) and spring (B) for all sample depths in subantarctic waters. Key: Allo=alloxanthin, BBCar=β,β-carotene, BOF=19'BOF, Chla=chlorophyll *a*, Chla(al)=chlorophyll *a* (allomer), Chla(ep)=chlorophyll *a* (epimer), Chlb=chlorophyll *b*, Chlc's=chlorophyll *c*'s, Chlc3=chlorophyll *c3*, Diad/PPhorba4=diadinoxanthin/phaeophorbide *a4*, Diat = diatoxanthin, Ech=echinone, Fuco=fucoxanthnin, HOF=19'HOF, Peri=peridinin, PPhorba1=phaeophorbide *a1*, PPhorba2=phaeophorbide *a2*, PPhorba3/car = phaeophorbide *a3*/carotenoid, PPhytina1 = phaeophytin *a1*, PPhytina2 = phaeophytin *a2*, Zea/Lut=zeaxanthin/lutein. Refer to Fig. 4.1 and 5.1 for location of sediment trap stations.

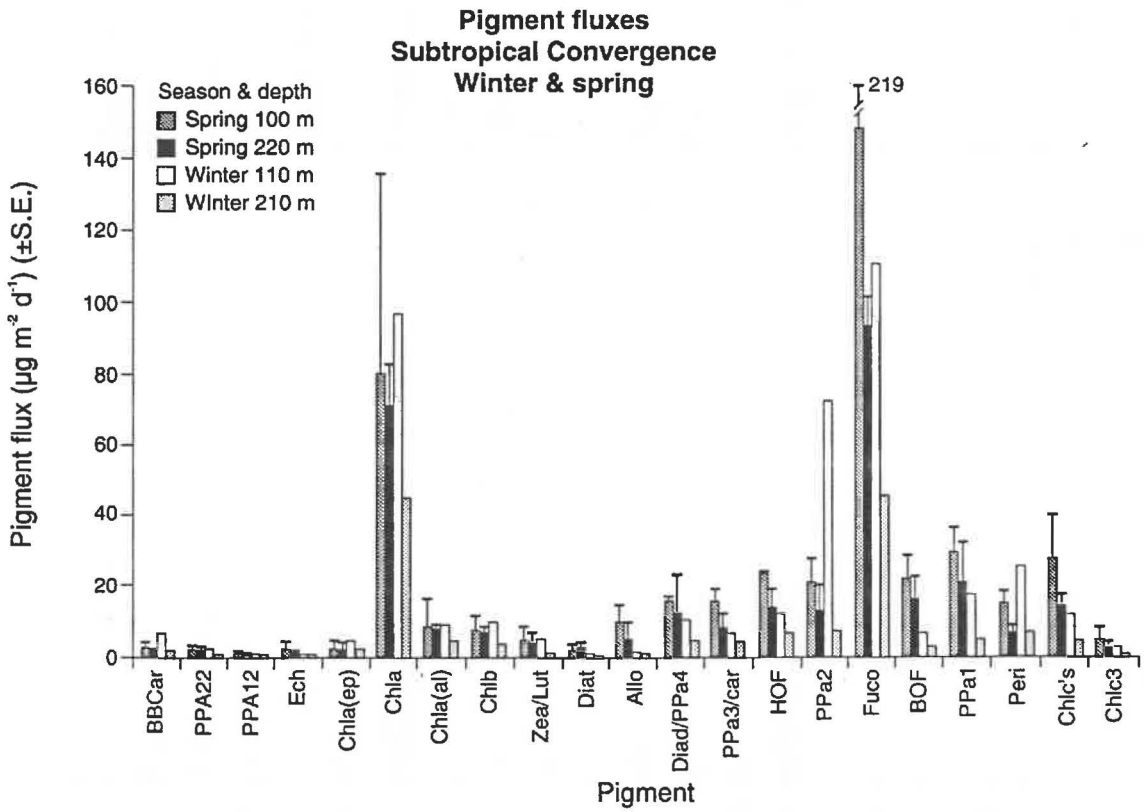

Fig. 6.3 Average pigment fluxes (µg m^{-2} d^{-1}) in winter and spring for all sample depths in Subtropical Convergence. Key = pigment identification as for Fig. 6.2. Refer to Fig. 4.1 and 5.1 for location of sediment trap stations.

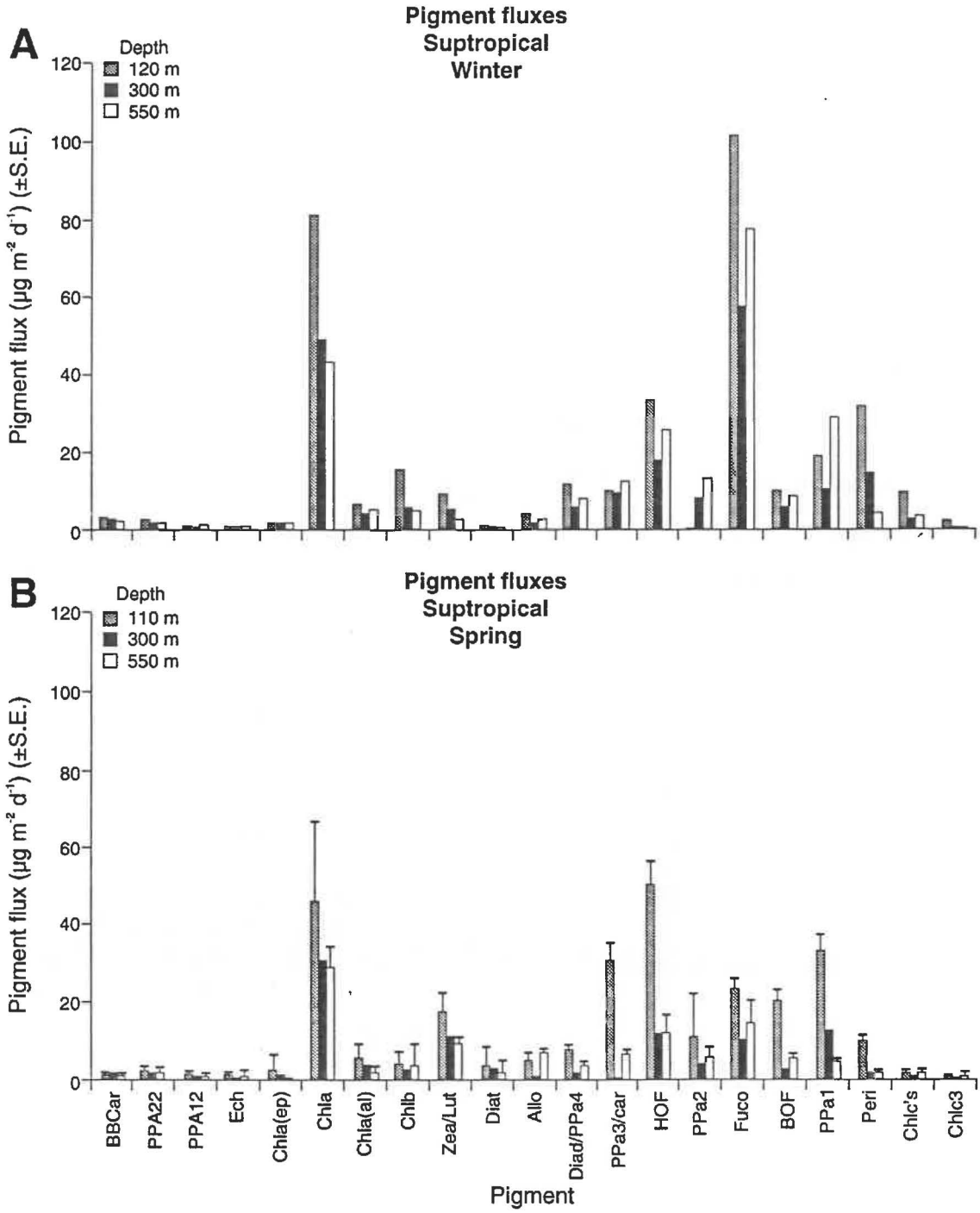

Fig. 6.4 Average pigment fluxes (µg m^{-2} d^{-1}) in winter (A) and spring (B) for all sample depths in subtropical waters. Key = pigment identification as for Fig. 6.2. Refer to Fig. 4.1 and 5.1 for location of sediment trap stations.

were low (<5 μg per trap) (Appendices 5C and D). Baseline resolution could not be achieved for all pigments and spectral analysis revealed that peaks sometimes comprised two or possibly more pigments (e.g., phaeophorbide *a3* and an unknown carotenoid with an average retention time of 9.44 minutes; peak 9, Fig. 6.1). Peridinin concentrations may have been overestimated due to co-elution of other pigments. The technique was not able to resolve the co-eluting pigments of diadinoxanthin/phaeophorbide *a4*, zeaxanthin/lutein, chlorophyll *a* and *b*/divinyl chlorophyll *a* and *b* and some of the chlorophyll *c* species (cf. Vidussi et al., 1996). For the purposes of the following discussion, regarding pigment budget estimates, the various co-eluting pigments are considered to be diadinoxanthin, zeaxanthin/lutein, chlorophyll *a*, *b* and chlorophyll *c*'s. Accordingly, estimates of total phaeopigment and total carotenoid fluxes are possibly slightly under- and overestimated, respectively.

Corrections were not made for "time-zero" effects since pigments were found only in trace amounts in blank solutions identically prepared on a research voyage to the Chatham Rise in September 1993 (RV3013). Pigment concentrations in these blank solutions were always <0.3 and typically <<0.1 μg per filtered sample. Identified pigments included chlorophyll *a* (with allomer and epimers), chlorophyll *b* and β, β-carotene.

The highest individual fluxes (>90 μg m^{-2} d^{-1}) were observed in the STC frontal zone for chlorophyll *a* and fucoxanthin, with the latter pigment exhibiting the highest measured flux of 219 μg m^{-2} d^{-1} (Fig. 6.3, Appendices 5E and F). Chlorophyll *a* and fucoxanthin fluxes were generally dominant and of comparable magnitude, and were lower than other pigment fluxes only on occasions, such as in subantarctic (where above 300 m, fluxes of 19'BOF, 19'HOF and phaeophorbide *a1* were higher; Fig. 6.2B) and subtropical waters (19'HOF at 110 m) in spring (Fig. 6.4B). Winter fluxes of chlorophyll *a* were higher than in the spring STC at 110 m and over all sample depths in subtropical waters (Fig. 6.4A & B). Fucoxanthin fluxes were enhanced, relative to other pigments, including chlorophyll *a*, in subantarctic and STC water types in spring and in winter subtropical waters. Fluxes of 19'HOF were higher proportionally in shallowest traps in subantarctic (30-40 μg m^{-2} d^{-1}) and subtropical waters (40-60 μg m^{-2} d^{-1}) in spring, as was 19'BOF (20-30 μg m^{-2} d^{-1}) . Fluxes of these carotenoids were typically less than 10 μg m^{-2} d^{-1} in other sediment trap samples. Fluxes of other identified pigments, such as peridinin, diadinoxanthin, chlorophyll *b*, *c3* and *c*'s, allomers and

epimers of chlorophyll *a*, alloxanthin and zeaxanthin/lutein, were generally less than 15 μg m^{-2} d^{-1} and often less than 5 μg m^{-2} d^{-1}. Exceptions included elevated near-surface fluxes of peridinin in winter at STC and subtropical sites (about 30 μg m^{-2} d^{-1}), and, in spring, fluxes of zeaxanthin/lutein in subtropical waters (about 20 μg m^{-2} d^{-1}) and chlorophyll *c* variants in the STC (10-40 μg m^{-2} d^{-1}). The carotenoids, diatoxanthin and β, β-carotene, and the bacterial pigment, echinone, were present only in trace amounts (typically <5 μg m^{-2} d^{-1}).

Phaeophorbides (*a1*, *a2* and possibly *a3*; note that these designations do not correspond necessarily to phaeophorbide *a* variants identified by previous workers, e.g., Vernet & Lorenzen, 1987a; Head & Horne, 1993, but see later discussion) were prominent components of vertical pigment flux in all three water types in both winter and spring, with near-surface fluxes of between 20 and 70 μg m^{-2} d^{-1} observed in the STC and subtropical waters (Fig. 6.3 and 6.4). Phaeophorbide fluxes were generally less than 30 μg m^{-2} d^{-1} in subantarctic waters in both seasons, except for a flux of 50 μg m^{-2} d^{-1} that was measured at 150 m in spring (Fig. 6.2). Only trace amounts of phaeophytins (typically <3 μg m^{-2} d^{-1}) were identified positively in any of the HPLC chromatograms. No carotenoid degradation products (e.g., Repeta & Gagosian, 1984) nor pyrophaeopigments or phaeoporphyrins (e.g., Head & Horne, 1993; Head et al., 1994) were identified definitively, although, it is possible that phaeophorbide *a3* may correspond to phaeoporphyrin *c* on the basis of retention times (Head & Horne, 1993).

6.3.2. Seasonal trends of pigment fluxes

For the purposes of this chapter, further discussion concentrates upon mean fluxes for pigments, determined by averaging fluxes calculated at each depth for the two stations sampled in each water type, except in STC and subtropical waters in winter when solitary free-floating arrays were deployed (e.g., Nodder & Alexander, 1997). Coefficients of variation (C. V. = standard deviation/mean %) for paired stations were dependent on specific pigment types with substantial differences observed for several of the minor pigments (i.e., C. V. averaging over 100 for echinone, diatoxanthin and alloxanthin and phaeophorbide *a3* across all stations in winter) (Appendix 5M). Variability was generally greater for these minor pigments and chlorophyll *a*-degradation products (phaeophorbides, phaeophytins, chlorophyll *a* allomer and epimer), regardless of season. One notable exception was

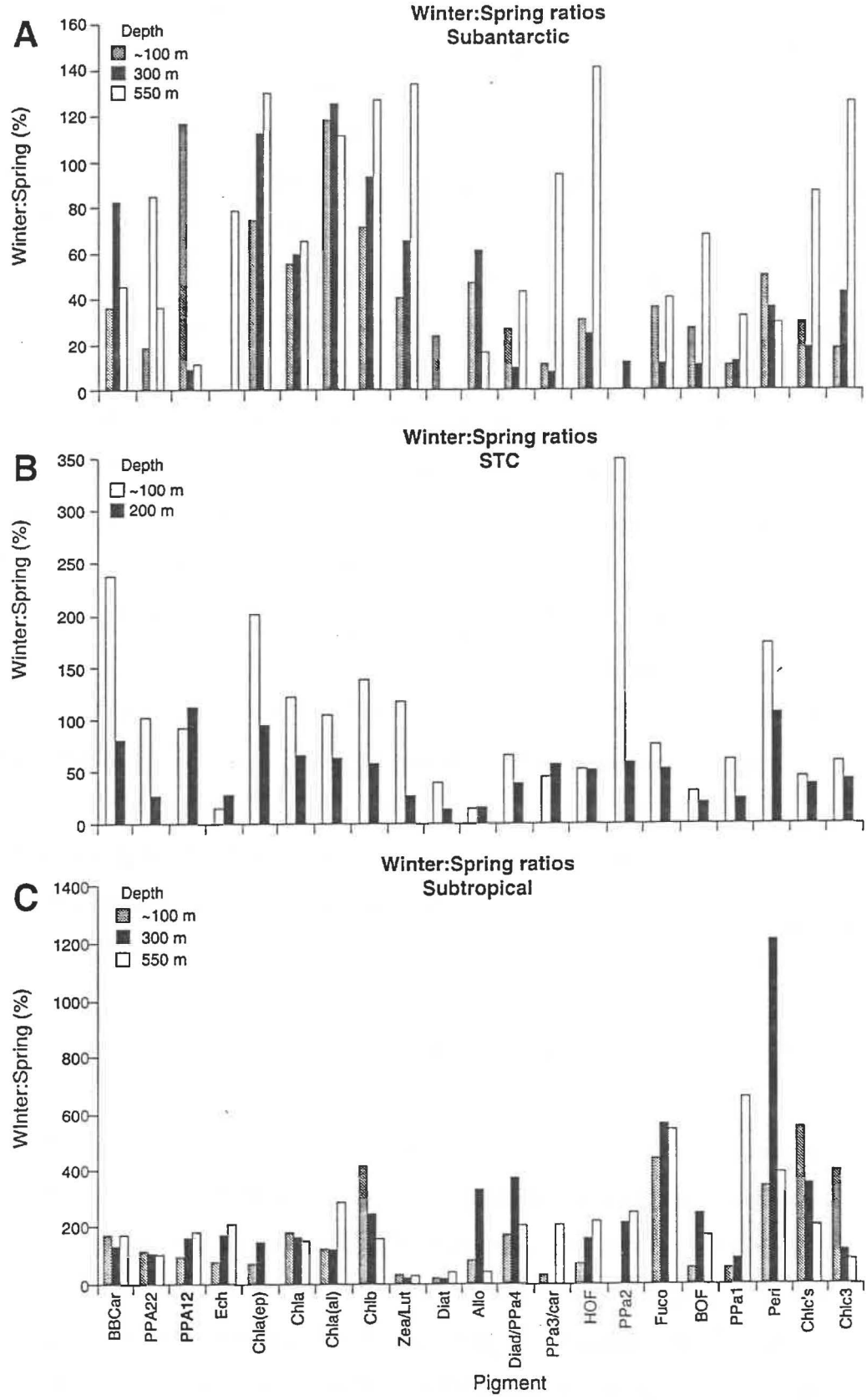

Fig. 6.5 Average seasonal differences of pigment fluxes at all sample depths in (A) subantarctic, (B) Subtropical Convergence and (C) subtropical waters. If pigment winter:spring ratio is less than 100%, then winter fluxes are less than equivalent spring fluxes, and *vice versa* if winter:spring ratio is greater than 100%.

chlorophyll *a* fluxes in the STC in spring at 100 m where a C. V. of 98% was observed due to substantially reduced flux at X477 (25 μg m^{-2} d^{-1} cf. 136 μg m^{-2} d^{-1} at X478). Peridinin fluxes were also highly variable between station pairs in both seasons, with average C. V.s of about 70%. A C. V. of 91% was found for peridinin flux in spring subtropical waters at 550 m, resulting from a low flux of <0.5 μg m^{-2} d^{-1} at X479, compared with 1.9 at X480. Across all water and pigments types, average C. V.s were 55% in spring and 59% in winter. A portion of this variability between stations could be attributed to inter-trap hydrodynamic interactions. This factor, however, is unlikely to be substantial given that "pigment" traps were placed consistently in the outer position of each cross-frame arm and that subsequent work has shown that trap position does not affect significantly trapping efficiency (Section 2.4.2, Chapter 2). Much of the variability between pigment fluxes measured at each station is therefore likely to either be "real" or, more probably, due to difficulties in quantifying pigment fluxes from homogenised sediment trap samples containing relatively low amounts of pigmented material (< 5 μg per trap) using HPLC.

On average, pigment fluxes, measured directly below the mixed-layer in the shallowest traps, were less in winter compared with spring in STC and subantarctic waters, whereas in subtropical waters fluxes of many of the identified pigments, including chlorophyll *a*, chlorophyll *b*, chlorophyll *c*'s, fucoxanthin and diadinoxanthin, were up to 5 times higher in winter (Fig. 6.5, Appendices 5G and H). The most extreme case for spring was a 12-times enhancement in peridinin flux observed at 300 m. In general, over most of the water column (100-550 m), average fluxes of various pigment species in winter were less than equivalent fluxes in spring in subantarctic and STC waters. Regardless of season or sample depth, pigment fluxes in subantarctic waters were markedly lower than equivalent fluxes measured in STC and subtropical water types (Fig. 6.2, Appendices 5E and F).

In all three water types, and in both seasons, total carotenoid fluxes typically exceeded total chlorophyll (including chlorophyll *a* degradation products) and phaeopigment fluxes over all water depths (Fig. 6.6). One exception was at X477 in the spring STC when the total chlorophyll flux of 255 μg m^{-2} d^{-1} at 100 m was higher than the total carotenoid flux of 194 μg m^{-2} d^{-1}. On a seasonal basis, total winter fluxes in subantarctic waters were variable and

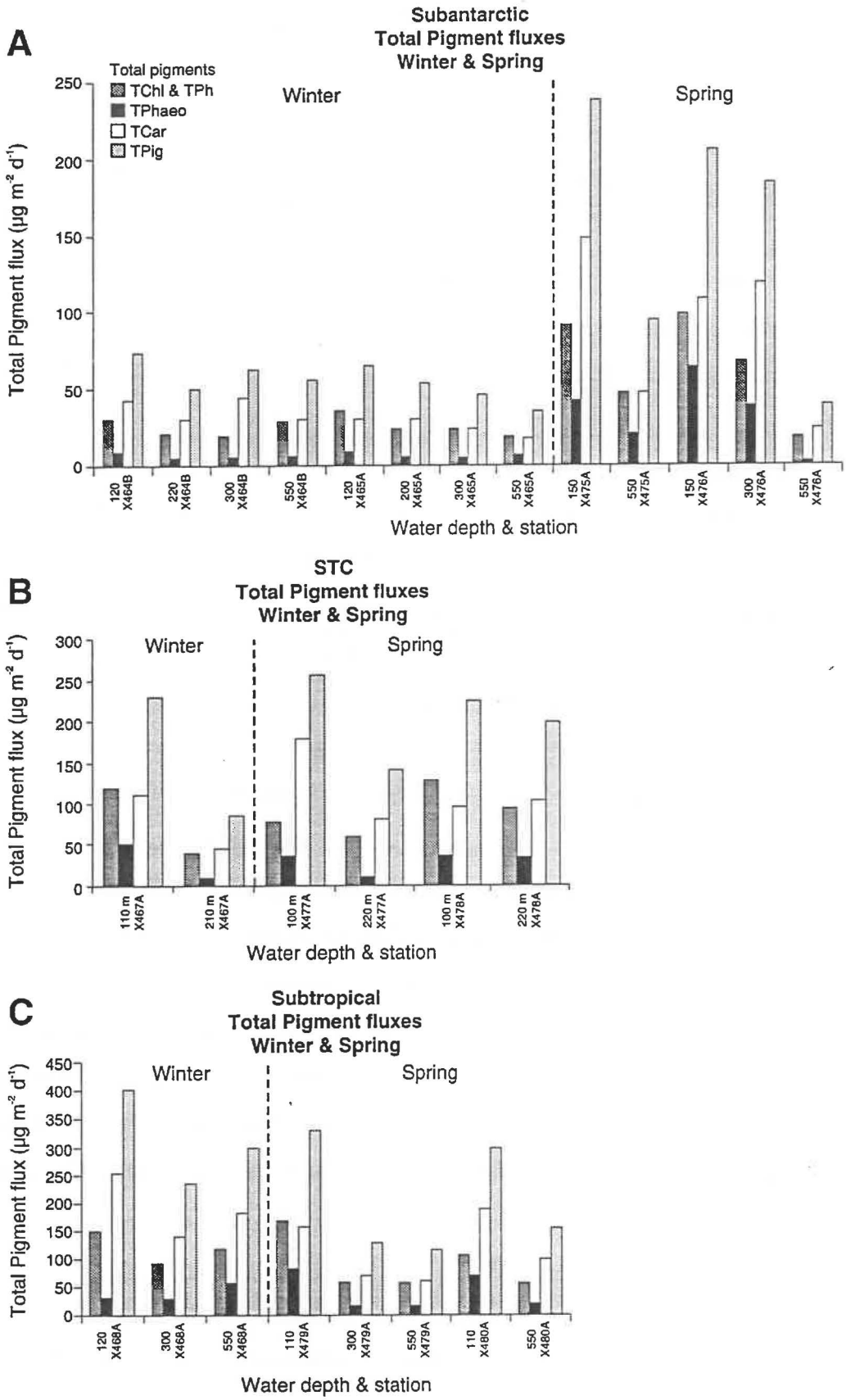

Fig. 6.6 Average total pigment fluxes (µg m^{-2} d^{-1}) in winter and spring at all sample depths in (A) subantarctic, (B) STC and (C) subtropical waters. Key: TChl=sum of all chlorophyll-derived pigments (including phaeopigments), TPhaeo=sum of all phaeopigments only, TCar=sum of all carotenoids, TPig=sum of all pigments (TChl+TCar).

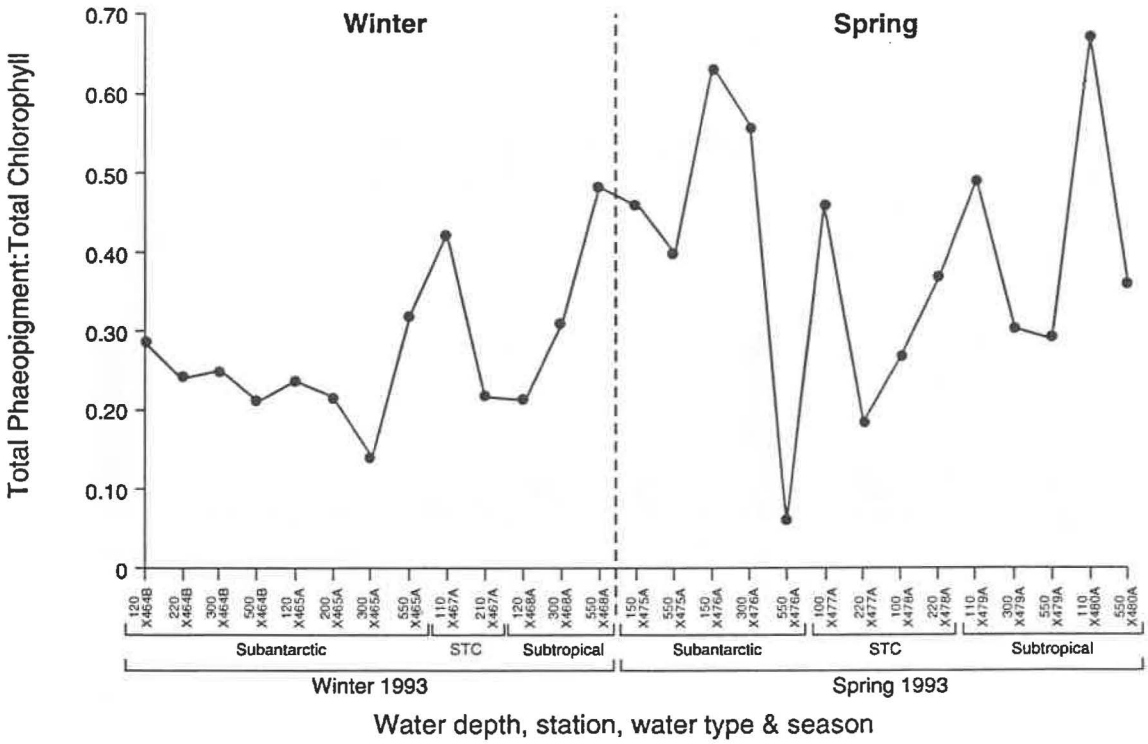

Fig. 6.7 Ratio of average total phaeopigment flux to total chlorophyll-derived flux in winter and spring for all depths and stations occupied in three water types. Key: STC=Subtropical Convergence.

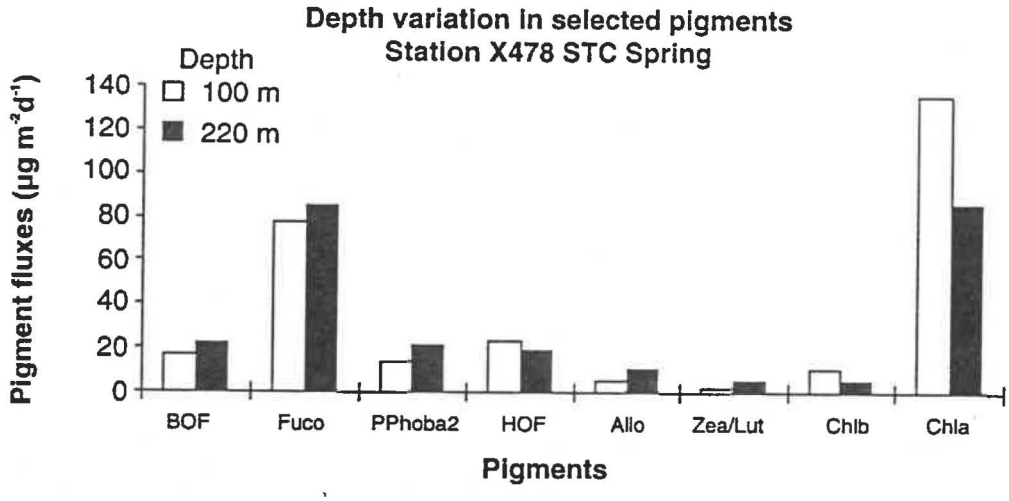

Fig. 6.8 Depth variation of selected pigments at station X478 in Subtropical Convergence in spring 1993. Several pigments (notably chlorophyll *a*, chlorophyll *b* and 19'HOF) exhibit slight decreases in flux with increasing depth, whereas fluxes of other compounds (phaeophorbide *a2*, fucoxanthin and 19'BOF) increase variably with depth by 10-50%.

between 10-70% of the corresponding spring values (Fig. 6.6). In contrast, in subtropical waters, total fluxes were up to 3 times higher in winter, particularly for total phaeopigment fluxes measured at 550 m traps. There was more variability in the seasonal comparison of fluxes in the STC zone with winter fluxes of chlorophyllous variants 1.2 to 1.4 times greater than in spring at the shallowest traps. Other pigment fluxes to the deeper traps in the STC, however, were 50-60% lower in winter, compared to spring (Fig. 6.6). Phaeopigments typically comprised 10-30% of the total chlorophyll-derived flux in subantarctic waters in winter, and varied from 6% at 550 m (X476) to 40-60% (all other depths and stations) in spring (Fig. 6.7). In the STC, this proportion ranged from 20-45% over both seasons. Total phaeopigment fluxes were generally elevated in subtropical waters, but exhibited more variability, ranging from 30-70% to 20-50% of total chlorophyll-derived material in spring and winter, respectively (Fig. 6.7). Interestingly, this percentage decreased with water depth in spring, but reversed in winter.

6.3.3. Depth variations of pigment fluxes

Regardless of season, photosynthetic pigment fluxes typically decreased in magnitude down the water column with most subsidary pigments following the general decreasing trend of chlorophyll *a* flux (Fig. 6.2, Appendix 5L). Exceptions occurred in STC waters in spring when chlorophyll *a* flux at X477 increased over 100 to 220 m depths; a trend that was followed by a very slight increase (<5 $\mu g\ m^{-2}\ d^{-1}$) in chlorophyll *b*. Increases in flux with depth for phaeophorbide *a2*, fucoxanthin, 19'BOF and other minor carotenoids (alloxanthin, zeaxanthin/lutein) by less than 10 $\mu g\ m^{-2}\ d^{-1}$ were also observed at X478, the replicate station of X477 (Fig. 6.8). Phaeopigment fluxes generally followed depth trends exhibited by the chlorin and carotenoid pigments, although phaeophorbide *a1* and *a2* fluxes increased from 300 to 550m in subtropical waters in winter (20 and 13 $\mu g\ m^{-2}\ d^{-1}$ for *a1*and *a2*, respectively), in opposition to the decreasing trends of the other chlorophyll-derived pigments (Fig. 6.2). In subantarctic waters, fluxes of several pigments were also observed to increase slightly with depth in winter, notably, chlorophyll *a* and 19'HOF (both only at X464).

6.4. Sources of sinking pigmented material

The relative contribution of various pigmented compounds to sediment trap samples can be used to infer sources of sinking material (e.g., Barlow et al., 1993, 1995; Letelier et al., 1993; Bustillos-Guzmán et al., 1995; Andersen et al., 1996; Llewellyn & Mantoura, 1996). In a qualitative sense, it is apparent that in both winter and spring 1993 in subantarctic waters, east of New Zealand, intact diatoms (fucoxanthin), prymnesiophytes (19'HOF) and pelagophytes (19'BOF) were characteristic components of export flux. Relatively minor contributions were made by photosynthetic dinoflagellates (peridinin), cryptophytes (alloxanthin), cyanobacteria or chlorophytes (zeaxanthin/lutein) and "green" algae (chlorophyll *b*) (e.g., Wright et al., 1991; Andersen et al., 1996). Spring fluxes of phaeopigments in subantarctic waters were relatively enhanced, compared with winter, suggesting that faecal pellet production by zooplankton grazing on phytoplankton (e.g., Welschmeyer & Lorenzen, 1985a), and/or sinking of senescent sinking algae (e.g., Head & Horne, 1993) were occurring during sampling (see later discussion). In the STC in winter and spring, phaeophorbides were a prominent feature of the sediment trap samples, particularly phaeophorbides *a1* and *a2* (Fig. 6.2). Fucoxanthin fluxes were higher than, or similar to, equivalent chlorophyll *a* fluxes at the same depth in both seasons, highlighting the significant role that sinking intact diatoms can play in export flux (e.g., Smetacek, 1985). Prymnesiophytes and pelagophytes also contributed minor amounts to pigment fluxes in both seasons in the STC (Fig. 6.2). Particle fluxes in subtropical waters in both seasons contained a similar pigment assemblage as that observed in the STC, with grazed or senescent phytoplankton and/or zooplankton faecal pellets (phaeophorbides), diatoms (fucoxanthin), dinoflagellates (peridinin), prymnesiophytes (19'HOF) and cyano-bacteria/chlorophytes (zeaxanthin/lutein) probably present in sediment trap samples. Fluxes of chlorophyll *a*, diatoms, chrysophytes and photosynthetic dinoflagellates were relatively enhanced in winter, compared with spring, in subtropical waters. Prochlorophytes (chlorophyll *b* and zeaxanthin) were probably present in sinking material in this water type in spring, together with variable amounts of cryptophytes (alloxanthin) in both seasons. Heightened winter fluxes of chlorophyll *c*'s and *c3* in subtropical waters may be related to sinking diatoms and/or prymnesiophytes (e.g., Andersen et al., 1996).

Table 6.2 Photosynthetic pigment concentrations (mg m^{-3}) at 10 m water depth in water types east of New Zealand in spring 1993. Refer to Fig. 5.1B, Section 5.3, Chapter 5 for location of stations.

Station	Water type*	Chl *a***	Chl *b*	Chl *c*'s	β,β-Car	Fuco	Per
X475K	SA	104.4	11.9	19.2	2.5	20.7	0.6
X476I	SA	131.6	17.0	18.1	2.1	18.2	0.6
X477I	STC	539.0	32.5	168.4	5.4	734.6	14.2
X477C	STC	608.5	161.1	90.4	7.0	273.2	7.7
X479J	ST	438.2	73.0	85.5	26.6	245.6	14.0
X480C	ST	301.0	58.8	66.0	10.7	153.0	17.3

		Diad	HOF	BOF	Allo	Zea/lut
X475K	SA	98.7	94.5	22.6	2.1	14.2
X476I	SA	80.4	77.0	18.8	1.7	12.8
X477I	STC	42.3	40.5	23.1	3.9	2.4
X477C	STC	128.6	123.2	47.4	9.6	3.9
X479J	ST	199.6	191.2	46.2	20.8	32.9
X480C	ST	142.1	136.1	37.5	24.2	7.3

* SA=subantarctic, STC=Subtropical Convergence, ST=subtropical.

** Chl = chlorophyll, Car = carotene, Fuco = fucoxanthin, Per = peridinin, Diad = diadinoxanthin, HOF = 19' hexanoyloxyfucoxanthin,
BOF = 19'-butanoyloxyfucoxanthin, Allo = alloxanthin, Zea/lut = zeaxanthin/lutein.

Water column HPLC pigment data were only collected from 10 m water depth in spring (F.H. Chang, pers. comm., 1996; Chang & Gall, submitted) (Table 6.2). Although direct comparison of this data-set with integrated flux measurements made at water depths ranging from 100-550m is difficult (due to pigment transformations with increasing depth), the HPLC data from 10 m provides the only indication as to what the dominant photosynthetic pigments were in the upper water column at the time of sediment trap sampling. At 10 m, chlorophyll *a* was the dominant near-surface pigment in all three water types (i.e., 100-130 mg m^{-3} in subantarctic waters; 540-610 in STC; 300-440 in subtropical), except in the STC at X477 where fucoxanthin was found in higher concentrations (735 mg m^{-3} of fucoxanthin, compared with 540 mg m^{-3} of chlorophyll *a*). Fucoxanthin was also a prominent pigment in subtropical waters (150-250 mg m^{-3}), together with diadinoxanthin and 19'HOF (140-200 mg m^{-3}). The latter two pigments were also found in subantarctic waters in concentrations only slightly less than chlorophyll *a* (80-100 mg m^{-3}). In general, pigment concentrations at 10 m in subantarctic waters were lower than for identical pigments in the other two water types. Observed pigment constituents of export flux in spring compare reasonably well with this 10 m data-set and with phytoplankton assemblages reported for both winter and spring (Table 6.3), although the use of acidic Lugol's solution as a preservative prevented a quantitative evaluation of the importance of calcium carbonate-secreting prymnesiophytes (F.H. Chang, pers. comm., 1996).

Nonetheless, these observations suggest that all of the major components of the phytoplankton standing stock, including free-swimming photosynthetic dinoflagellates (peridinin), contributed to the pool of sinking organic material across the three water types. Diatoms (fucoxanthin) and prymnesiophytes (19'HOF) were significant contributors to particulate flux, regardless of season, as observed by other studies elsewhere (e.g., Barlow et al., 1993, 1995; Llewellyn & Mantoura, 1996). The possible presence of cyanobacteria (zeaxanthin) in material collected by sediment traps requires a transport medium which may be provided by sinking faecal pellets (e.g., Pfannkuche & Lochte, 1993) or through incorporation into marine aggregates (e.g., Alldredge & Silver, 1988). Prochlorophytes have not been identified in phytoplankton assemblages east of New Zealand due to technological constraints (i.e., lack of flow cytometry equipment), and the difficulty of detecting near-surface prochlorophytes with standard epifluorescence microscopy (e.g., Chisholm et al., 1988). It is surmised that, based on the presence of chlorophyll *b* and zeaxanthin,

Table 6.3 Phytoplankton cell carbon biomass in water types, east of New Zealand, during winter and spring 1993. Refer to Fig. 5.1A & B, Section 5.3, Chapter 5 for location of stations.

Season & water type*	Station	Total microflagellates** $\mu gC\ l^{-1}$	Total diatoms** $\mu gC\ l^{-1}$	Total dinoflagellates** $\mu gC\ l^{-1}$
Winter 1993				
SA	X464C	86.15	4.25	48.35
	X465E	63.30	17.85	26.55
	$\bar{x} \pm s$	**74.73±16.16**	**11.05±9.62**	**37.45±15.42**
STC	X466I	182.05	927.80	53.55
	X467F	178.40	1332.10	135.90
	$\bar{x} \pm s$	**180.23±2.58**	**1129.95±285.88**	**144.73±12.48**
ST	X468A	85.05	65.65	950.20
	X469A	90.00	83.60	182.75
	$\bar{x} \pm s$	**87.53±3.50**	**74.63±12.69**	**566.48±542.67**
Spring 1993				
SA	X475I	240.25	15.45	166.95
	X476F	245.22	10.14	251.27
	$\bar{x} \pm s$	**242.74±3.51**	**12.80±3.76**	**209.11±59.62**
STC	X477F	1186.30	3154.55	120.70
	X478D	1018.41	2165.95	187.30
	$\bar{x} \pm s$	**1102.36±118.72**	**2660.25±699.05**	**154.00±47.09**
ST	X479H	266.79	405.85	60.90
	X480H	368.54	24.46	21.73
	$\bar{x} \pm s$	**317.65±71.98**	**215.16±269.68**	**41.32±27.70**

* SA=subantarctic, STC=Subtropical Convergence, ST=subtropical.

** All values are integrated from 0 to 50 m water depths assuming that surface concentrations at 0 m are equal to concentrations in the uppermost sample (generally 10 m). Cell carbon contents were determined on the basis of microscopic identifications and counts of phytoplankton and assumptions regarding carbon content and cell geometry (data provided by F. H. Chang, pers. comm., 1997) (Chang & Gall, submitted).

prochlorophytes and other small phytoplankton cells may have been incorporated into sinking particles in subtropical waters in spring. Definitive identification of prochlorophytes using HPLC, however, relies upon the presence of divinyl chorophyll *a* (Chisholm et al., 1988; Suzuki et al., 1995) which could not be distinguished by the HPLC method employed in the present study.

Dominant phytoplankton species in the waters east of New Zealand include the diatoms *Nitzschia* spp., *Thalassiosira* spp., *Chaetoceros* spp. and *Leptocylindricus danicus*, and the coccolithophorids *Emiliania huxleyi* and *Gephyrocapsa oceanica* (F. H. Chang, pers. comm., 1997). Most of these genera might be expected to exhibit enhanced sinking rates owing to their moderate size and the propensity of some of these organisms to bloom and form surface aggregations (e.g., Smetacek, 1985), particularly in spring in the STC when larger phytoplankton (20-200 μm) dominated the algal community (Bradford-Grieve et al,, 1997a). Similarly, at times when dinoflagellates, such as *Ceratium* spp., *Gyrodinium* spp. and *Gymnodinium* spp. (F. H. Chang, pers. comm., 1997), dominated the phytoplankton population, such as in subantarctic waters in spring and subtropical waters in winter, peridinin fluxes were also enhanced (Fig. 6.2B, 6.4A and 6.5), indicating that relatively smaller organisms can also contribute to export flux (e.g., Alledredge & Silver, 1988; Taylor, 1989) or in the production of non-pigmented faecal material, collected in sediment traps (e.g., Nöthig & von Bodungen, 1989; Buck & Newton, 1995).

The presence of undegraded pigments in sediment trap samples from 300-550 m depths in subtropical and subantarctic waters highlights the rapid rates at which organic material can sink through the water column below the mixed-layer (e.g., Smayda, 1970; Smetacek, 1985; Bruland et al., 1989). The quantity of pigmented material reaching the deep ocean east of New Zealand was, however, relatively small (<100 μg chl m^{-2} d^{-1} and <460 μg total pigments m^{-2} d^{-1}). Since HPLC only provides information on phototrophic pigments that are mainly associated with algal populations and attendant transformation processes, the contribution made by additional organic components, such as other lipids (fatty acids, waxes, sterols), carbohydrates and proteins (e.g., Lee & Wakeham, 1989; Wakeham & Lee, 1989, 1993), to export fluxes east of New Zealand remains unknown. Work is underway presently on contemporaneous sediment trap samples to discern the biochemical characteristics of other

lipids in sinking organic material using gas chromatographic techniques (J. K.Volkman, S. D. Nodder, E. L. Sikes & L. Robertson, unpublished data).

The relative contribution made by pigmented material to organic flux in oligotrophic waters is not expected to be significant since, even in highly productive coastal regions, chlorophyll-type pigments typically make up less than 0.1% of total organic carbon flux, compared with amino acids (15-34%), sugars (or polysaccharides, 20-30%) and other lipids (3-5%) (Wakeham et al., 1993). In Wakeham et al.'s study, up to two-thirds of total organic carbon in sediment traps could not be characterised using existing techniques. Biochemical transformations of pigments also occur during zooplankton metabolism, such as the well documeted conversion of chlorophyll *a* to phaeophorbide *a* during zooplankton grazing (Shuman & Lorenzen, 1975; Brown et al., 1977; Lee & Wakeham, 1989; Wakeham & Lee, 1989, 1993). Such processes affect specific compounds to differing degrees. For example, Cowie & Hedges (1996) showed that temperate copepod (*Calanus pacificus*) faecal pellets comprised mainly recalcitrant organic matter which they surmised may be unreactive aliphatic polymers and/or chitinous material (66% of total organic carbon), with only minor contributions from proteins (21%) and polysaccharides (7.5%). The lowest contribtion made to the biochemical composition of these herbivorous copepod faecal pellets was from chlorophyll-type pigments (5.3%). Contributions to export flux from terrestrial sources are also likely, but as yet unquantified, since oceanic sites east of New Zealand lie downstream from the uplifted landmass of New Zealand which intersects the west-to-east zonal passage of prevailing westerly winds and oceanic circulation patterns (Heath, 1985). Evidence of considerable offshore lateral advection is inferred from the presence of coastal zooplankton at STC sampling stations, approximately 200 km west of South Island (Bradford-Grieve et al., 1997b). A case has also been argued in Section 4.3.2 (Chapter 4) for the occurrence of terrigenous material in sinking material in subantarctic waters in winter.

6.5. Mid-water and near-bottom increases in pigment flux

The localised enhancement in near-bottom mass flux in the STC in spring at station X478 (Nodder & Alexander, 1997) (Chapter 5) is mirrored by increases in phaeophorbide *a2* (1.6x greater at depth than near-surface fluxes), fucoxanthin (1.1x) and other carotenoids (Fig. 6.8), suggesting that particulate material collected by these traps may have a dual origin,

originating as both "fresh" (i.e., undegraded carotenoids) and relatively degraded (phaeophorbide *a2*) organic matter. Depth-increases in pigment fluxes of chlorophyll *a* (2.3x) and chlorophyll *b* (2.5x) at the other spring STC station (X477) were matched by a statistically non-significant increase in mass flux with depth (Nodder & Alexander, 1997), and attest to the undegraded nature of generally labile pigmented marine particles that are apparently sinking out within the STC. Given the shallow nature of the Chatham Rise (300-400 m), these observations are not surprising on the basis of estimated marine organic aggregate sinking speeds of 50->100 m d^{-1} (e.g., Smayda, 1969, 1970; Small et al., 1979; Fowler & Knauer, 1986; Alldredge & Silver, 1988; Noji, 1991). In addition, phytodetritus can be resuspended and transported by deep ocean currents with speeds greater than only 7 cm s^{-1} (Lampitt, 1985). Near-bottom velocities of up to 20 cm s^{-1} have been measured on the Chatham Rise (Heath, 1983; Chiswell, 1994a). Thus, once at the sea-floor, sedimented organic matter within the STC may be resuspended readily by tidally driven currents and transported along and off the Rise (e.g., Nodder & Alexander, 1997; Nodder, in press) (Chapters 2 and 5).

The observed increase in total phaeopigments with depth in subtropical waters in winter (Fig. 6.6) is mirrored by a two-fold, though non-significant, depth increase in average mass flux (Nodder & Alexander, 1997) (Chapter 5). These observations are inferred to be related to mesozooplankton biomass which was also reasonably high (2 mgC m^{-3}) over 200-500 m water depths in night-time MOCNESS stratified tows (Bradford-Grieve et al., 1997b). Microscopic analysis of filtered trap samples from 220-550 m demonstrate that large faecal pellets (100-140 μm wide and >500 μm long) are prominent components of particulate flux at these depths (Nodder & Alexander, 1997), and indicates that this flux increase with depth was probably mediated by the effect of migrating mesozooplankton (e.g., Angel, 1989; Longhurst & Williams, 1992).

6.6. Pigment budget estimates and comparisons with other pigment flux studies

Total chlorophyll and phaeopigment flux at the base of the mixed-layer is used in this study as a measure of the relative amount of chlorophyll-derived material sinking out of the upper ocean as intact, grazed and/or senescent phytoplankton (e.g., Welschmeyer & Lorenzen,

Table 6.4 Relationships between primary production, chlorophyll *a* biomass and total chlorophyllous fluxes across three water types in winter and spring 1993.

Season & water type*	Integrated mean primary production** mgC m^{-2} d^{-1}	Integrated chlorophyll *a* (<200µm) mg m^{-2}	Production : biomass	Total Chloro- & phaeopigment fluxes				Mean mass flux mg m^{-2} d^{-1}¥
				mg pig m^{-2} d^{-1}†	mgC m^{-2} d^{-1}‡	%standing stock d^{-1}#	%production§	
Winter 1993								
SA	45.0	11.4	4.0	0.032	1.1	0.3	2.4	430
STC	262.0	49.1	5.4	0.239	8.0	0.5	3.1	192
ST	148.5	19.3	7.7	0.151	5.1	0.8	3.4	420
Spring 1993								
SA	250.5	14.0	17.9	0.094	3.4	0.7	1.4	178
STC	986.0	108.3	9.1	0.206	7.4	0.2	0.8	188
ST	971.0	46.6	20.8	0.138	5.0	0.3	0.5	236

* SA = subantarctic (sediment traps positioned at 120 m water depth in winter; 150 m in spring), STC = Subtropical Convergence (110 m; 100 m), ST = subtropical (120 m; 110 m).

** Primary production (^{14}C bicarbonate <200 µm uptake - 24 h incubations), integrated to 1% light level; chlorophyll *a* (<200 µm) are integrated to 100 m (Bradford-Grieve et al., 1997a).

† Pig = average total chlorophyll and phaeopigment concentrations determined using HPLC; no conversions to chl *a*-equivalent values (cf. Welschmeyer & Lorenzen, 1985a, b) were made on the basis of results of Conover et al. (1986).

‡ Total chloro- and phaeopigment fluxes converted to carbon, assuming average C:Chl ratios of 33.55 for winter data-set and 35.8 for spring (F. H. Chang, pers. comm. 1995).

\# Chlorophyll *a* flux rates as % standing stock are based on the depth-integrated mean chlorophyll *a* to 100 m.

§ Carbon-equivalent flux rates as % production are based on integrated mean primary production to 1% light level.

¥ Average mass flux values from 2 stations in each water type, except for STC and ST waters in winter when only 1 station was occupied (Nodder & Alexander, 1997). Particulate organic carbon (POC) flux estimated assuming that POC flux is approximately 10-30% of total mass flux (Wefer, 1989).

1985a, b; Landry et al., 1994, 1995). A complete pigment budget could not be undertaken because the contribution made by microzooplankton grazing to ecosystem functioning was only evaluated at 10 m water depth (James & Hall, 1997). Furthermore, the microzooplankton grazing impact on phytoplankton growth could not be determined as a function of depth-integrated chlorophyll *a* and phaeophorbide concentrations and light regime, as adopted originally by Welschmeyer & Lorenzen (1985b), because such measurements were not made in 1993. In any case, the pigment budget approach does not account adequately for the grazing effect of microzooplankton estimated in this manner (Landry et al., 1995). Furthermore, chlorophyllous pigment fluxes determined by the present study should be regarded as maximum values since 20-30% of the estimated flux could be due to herniated zooplankton "swimmers" (Peterson & Dam, 1990). In addition, Wakeham et al. (1993) showed that chlorophyll *a* and phaeopigment fluxes were sometimes enhanced up to three-fold in traps with a basal salt brine, compared to control traps filled with sea-water. To the author's knowledge, similar experiments have not been conducted to assess effects of various preservative/poison treatments on carotenoid fluxes.

Nonetheless, budget estimates suggest that less than 1% of the chlorophyll *a* standing stock and less than 4% of primary production were actually "lost" by sinking from the surface mixed-layers in winter and spring (Table 6.4). Studies in other oligotrophic environments concur with these results, with less than 1% d^{-1} of chlorophyll *a* standing stock exported from the euphotic zone in the central Pacific Ocean gyres (Welschmeyer & Lorenzen, 1985b) and northeast Atlantic Ocean (Lenz et al., 1993) (Table 6.5). Even in highly productive, coastal environments such as west coast of U.S.A. (e.g., Washington coast, Southern California Bight) chlorophyll flux constitutes, on average, less than 5% d^{-1} of chlorophyll *a* standing stock (Welschmeyer & Lorenzen, 1985a, b; Landry et al., 1994), or 3-5% of primary production, as reported by Barlow et al. (1995) from western Mediterranean Sea. Fluxes of chlorophyll *a* (range 0.01-0.14 mg m^{-2} d^{-1}) across the three water types east of New Zealand are similar to those measured in the northeast Atlantic (Lenz et al., 1993), central Pacific (Welschmeyer & Lorenzen, 1985b) and Mediterranean (Barlow et al., 1995). The highest value of 0.14 mg chl *a* m^{-2} d^{-1} encountered in the spring STC, compares reasonably with the maximum mean value of 0.15 mg m^{-2} d^{-1} observed during the North Atlantic Bloom Experiment in 1989 (Lenz et al., 1993) (Table 6.5), suggesting that the STC frontal zone may have been the scene of a spring phytoplankton "bloom". It is postulated that, despite near-

Table 6.5 Comparison of Southwest Pacific Ocean mesozooplankton grazing rates and pigment fluxes in winter and spring 1993, with other studies.

	Mesozooplankton grazing		Pigment sedimentation		Pigment fluxes mg m^{-2} d^{-1}					References
	% primary production	% chl *a* standing stock	% primary production	% chl *a* standing stock	Chl *a* flux	TPh flux	Fuco flux	19'HOF flux	Chl *b* flux	
NE Atlantic ("bloom")	<6*	2*	11 (at 150 m)**	1†	0.01-0.15†	-	-	-	-	Dam et al. (1993)* Martin et al. (1993)** Lenz et al. (1993)†
Mediterranean	-	-	3-5 (TChl) & 10-24 (TPh)	<0.3 (TChl)	0.01-0.09	0.03-0.62	0.01-0.14	0.01-0.19	0.003-0.05	Barlow et al. (1995)
Equatorial Pacific										
El Niño	6	3	-	-	-	-	-	-	-	Zhang et al. (1995)
Non-El Niño	5	2	-	-	-	-	-	-	-	Zhang et al. (1995)
S California										
Winter-Spring	29-44	6-18	-	-	-	1.7-2.1	-	-	-	Landry et al. (1994)
Autumn	16-24	8-15	-	-	-	0.4-1.0	-	-	-	Landry et al. (1994)
NE Pacific (Dabob Bay)	-	-	-	2.2 (TChl) & 15.1 (TPh)‡	0.2-5.5	0.7-38.0‡	-	-	-	Welschmeyer & Lorenzen (1985)
Central Pacific	-	-	-	0.07 (TChl) & 0.6 (TPh)‡	0.01-0.03	0.09-0.18‡	-	-	-	Welschmeyer & Lorenzen (1985)
SW Pacific										
Subantarctic										
Winter	**2.7**	**0.3**	**2.4**	**0.3**	**0.01-0.03 (0.007-0.02)¥**	**0.003-0.009**	**0.002-0.01**	**0.005-0.01**	**0.002-0.005**	**This study**
Spring	**1.4**	**0.4**	**1.4**	**0.7**	**0.02-0.05 (0.01-0.03)¥**	**0.001-0.06**	**0.004-0.02**	**0.005-0.04**	**0.001-0.007**	**This study**
STC										
Winter	**0.9**	**0.2**	**3.1**	**0.5**	**0.07-0.1 (0.05-0.1)¥**	**0.02-0.1**	**0.05-0.1**	**0.007-0.01**	**0.003-0.01**	**This study**
Spring	**1.5**	**0.3**	**0.8**	**0.2**	**0.09-0.19 (0.03-0.14)¥**	**0.02-0.07**	**0.08-0.22**	**0.009-0.02**	**0.003-0.01**	**This study**
Subtropical										
Winter	**1.5**	**0.3**	**3.4**	**0.8**	**0.06-0.12 (0.04-0.08)¥**	**0.03-0.06**	**0.06-0.1**	**0.02-0.03**	**0.005-0.02**	**This study**
Spring	**3.5**	**1.8**	**0.5**	**0.3**	**0.04-0.09 (0.02-0.07)¥**	**0.02-0.08**	**0.009-0.03**	**0.008-0.06**	**0.002-0.006**	**This study**

* Dam et al. (1993); ** Martin et al. (1993); † Lenz et al. (1993); ‡ Fluxes re-converted from chlorophyll *a*-equivalent values (e.g., Conover et al., 1986 cf. Welschmeyer & Lorenzen, 1985a, b).

¥ Chlorophyll *a* fluxes only. **Chl** chlorophyll, **TPh** Total phaeopigments, **Fuco** fucoxanthin, **19'HOF** 19'-hexanoyloxyfucoxanthin.

surface seasonal depletion of nutrients in the STC in spring (i.e., nitrate + nitrite reduced by 5 μM and dissolved reactive silica and phosphorus by 1.0 and 0.2-0.3 μM, respectively), the spring "bloom" was probably in declining phase, as reflected by low P_B values, carbon specific doubling times of phytoplankton that were not substantially different between winter and spring (1.01 and 0.82 cf. 1.03 and 1.29 per day), and the observation that dissolved reactive silica values were at limiting concentrations (Bradford-Grieve et al., 1997a). It is inferred that a phytoplankton-dominated sedimentation event probably occurred soon after sampling had been completed (Section 4.3.2., Chapter 4). Sedimentation events following spring "blooms" in the open ocean have been observed to occur a matter of days after the peak of the "bloom" (e.g., Asper et al., 1992; Lochte et al., 1993; Head et al., 1994; Newton et al., 1994; Buck & Newton, 1995).

There are relatively few published studies that investigate oceanic fluxes of photosynthetic pigments, other than chlorophyll *a* and its derivatives. Comparisons with one study by Barlow et al. (1995) in western Mediterranean Sea show that near-surface fluxes of fucoxanthin, 19'HOF and chlorophyll *b* in STC and subtropical waters in both seasons in 1993 are comparable (Table 6.5). The maximum flux ranges for 19'HOF and chlorophyll *b* in the Mediterranean Sea were a little higher than in the present study, reflecting the relative dominance of prymnesiophytes, prasinophytes and chlorophytes in the Mediterranean environment (Barlow et al., 1995). In general, fluxes of the same pigments in subantarctic waters were an order of magnitude less than those fluxes measured in Mediterranean Sea (Table 6.5), suggesting that prymnesiophytes and "green" algae are not as important contributors to pigment export in subantarctic waters as they are in the Mediterranean. Pollehne et al. (1993) presented ratios of selected carotenoid pigments, relative to chlorophyll *a*, in sediment trap samples from central Arabian Sea which for fucoxanthin and 19'HOF were generally similar to those observed in the present study (1-3 and 0.5-1.5, respectively). Exceptions include the STC in winter and spring, where chlorophyll *a*:19'HOF flux ratios were as high as 6-8 and chlorophyll *a*:fucoxanthin ratios were as low as 0.1 (X477), and subantarctic waters where chlorophyll *a* dominated over fuxoxanthin flux below 220 m. Low numbers of prymnesiophytes, relative to diatoms, are inferred from these ratios in STC samples, as corroborated by the dominance of phytoplankton >20 μm in size (Table 6.3). On the other hand, subantarctic waters in winter were dominated by small-sized, non-

diatomaceous phytoplankton cells (65-90%, Table 6.3) which explains the high observed chlorophyll *a*:fucoxanthin flux ratios of 4-5 below 220 m.

Fluxes of total phaeopigments (range 0.001-0.01 mg m^{-2} d^{-1} in subantarctic, and 0.02-0.10 mg m^{-2} d^{-1} in STC and subtropical) compare well with fluxes observed in other oligotrophic settings (Welschmeyer & Lorenzen, 1985b; Barlow et al., 1995), although subantarctic waters register substantially lower values by an order of magnitude, compared to the central Pacific gyres (Welschmeyer & Lorenzen, 1985a) and subarctic Pacific (Lorenzen et al., 1983). Mesozooplankton biomass in subantarctic waters is generally similar to that in other oligotrophic provinces at similar latitudes in the Northern Hemisphere (Bradford-Grieve et al., 1997b), such that it is hypothesised that other processes must be operating in subantarctic waters to ensure effective particle retention in the upper water column (see later discussion). Phaeopigment flux measurements conducted in continental margin and coastal environments are generally higher (>1 mg phaeopigment m^{-2} d^{-1}; e.g., Welschmeyer & Lorenzen, 1985a, b; Landry et al., 1994) than those observed during the present study, and have been equated with enhanced mesozooplankton grazing on phytoplankton (i.e., 16-44% of daily production and 6-18%.d^{-1} of chlorophyll *a* standing stock, Landry et al., 1994). In contrast, mesozooplankton grazing rates in oceanic waters east of New Zealand are less than 5% of primary production (Bradford-Grieve et al., 1997b) (Table 6.4). Similar rates are reported in oligotrophic environments elsewhere, for example <6% in equatorial Pacific (Zhang et al., 1995) and northeast Atlantic oceans (Dam et al., 1993).

Many other sediment trap studies show that phaeopigment fluxes generally dominate over chlorophyll *a* fluxes (i.e., phaeopigment:chlorophyll ratios of 8-50, Downs & Lorenzen, 1985; 6-18, Welschmeyer & Lorenzen, 1985b; 2-8, Barlow et al., 1995; 10, Landry et al., 1995). In contrast, Chatham Rise traps typically exhibit ratios of 0.4-3.4 which indicates that phaeopigments were not an important component of pigment flux, relative to chlorophyll *a*. Degradation of chlorophyll *a* to phaeopigments (phaeophytins and phaeophorbides) occurs in acidic conditions (such as found in zooplankton guts), oxygen and/or light (Daley & Brown, 1973; Brown et al., 1977; Vernet & Welschmeyer, 1987b). The relative abundance of undegraded chlorophyll *a* in trap samples east of New Zealand therefore implies, first, rapid removal rates of intact phytoplankton cells or aggregates before oxidation can proceed in the surface layers of the ocean and, second, relatively low

rates of zooplankton faecal pellet removal from the upper ocean since herbivory is regarded as one of the main pathways by which chlorophyll *a* is degraded to phaeopigments (Welschmeyer et al., 1984; Welschmeyer & Lorenzen, 1985a, b). Although original studies advocated a 100% molar conversion efficiency (Shuman & Lorenzen, 1975), it is apparent that mesozooplankton grazing results in variable conversion of chlorophyll *a* to phaeopigments, ranging from 0->90% (e.g., Conover et al., 1986; Lopez et al., 1988; Bautista & Harris, 1992; Head & Harris, 1994, 1996). In addition, faecal pellets generally only comprise <10% of particulate organic carbon flux and 1-3% of total mass flux at deep ocean sites (Urrère & Knauer, 1981; Pilskaln & Honjo, 1987), so that zooplankton contributions to pigment flux are difficult to quantify in the present study without *in situ* observations and rate measurements of pellet producers (e.g., Lopez et al., 1988; Head & Harris, 1992, 1994). Microzooplankton waste products may also contain phaeopigments (Daley, 1973; Strom, 1993, cf. Klein et al., 1986), but processes of reinjestion (Strom, 1993), photo-oxidation (SooHoo & Kiefer, 1982a, b) and low preservation potential of faecal aggregates (Stoecker, 1984), result in unbleached pellets that contain little or no pigmentation (Buck & Newton, 1995). Intact carotenoids and chlorins may survive ingestion by copepods (Pasternak & Drits, 1988; Kleppel et al., 1991; Nelson, 1989) and some microzooplankton (Kleppel & Pieper, 1984), although complete loss of grazed carotenoids has also been reported (Strom & Welschmeyer, 1991; Head & Harris, 1994). Thus, it is envisaged that undegraded chlorins and carotenoids are transported rapidly to the deep ocean near Chatham Rise as components of fast sinking intact diatom chains (e.g., Smetacek, 1985), marine aggregates (e.g., Alldredge & Silver, 1988) or mesozooplankton faecal pellets where gut conversion rates of chlorophyll *a* to phaeopigments are low (e.g., Conover et al., 1986).

6.7. Relationships of pigment fluxes to planktonic community structure and functioning: importance of upper ocean particle retention mechanisms

Since the flux of photosynthetic pigments and their derivatives out of the upper ocean, east of New Zealand, was only a small percentage of chlorophyll *a* standing stock (<1% d^{-1}) and daily production (<3%), consideration is now given to mechanisms by which organic particles may be retained preferentially in the upper water column. Increases in particle residence times in the upper water column will also result in enhanced photo-degradation

of photosynthetic pigments (e.g., Daley, 1973; SooHoo & Kiefer, 1982 a, b; Nelson, 1993), which will reduce the quantity of intact pigmented material available for sinking out of the upper mixed-layer. Processes which may act to increase particle residence times in the upper ocean include physical turbulence (e.g., Alldredge et al., 1987), microbial degradation (e.g., Honjo & Roman, 1978; Nelson, 1993), microzooplankton grazing (e.g., Lopez et al., 1988; Strom, 1993) and mesozooplankton coprophagy and coprorhexy (e.g., Bathmann et al., 1987; Lampitt et al., 1990; Noji et al., 1991; Green et al., 1992). Low coagulation rates of phytoplankton have also been suggested as a possible mechanism in reducing mass sedimentation during spring "blooms" (Kiørboe et al., 1996); parameters of "stickiness" were not measured in winter and spring 1993 so this factor can not be evaluated.

Because sedimentation of particles and mesozooplankton grazing are unlikely to be primary controls on phytoplankton accumulation rates in the upper ocean, east of New Zealand, it is proposed that grazing by microzooplankton is probably the dominant controlling factor. James and Hall (in press) show that microzooplankton grazing does have a significant impact on the phytoplankton community east of New Zealand. In winter 1993 20-90% of the chlorophyll *a* standing stock was potentially consumed by microzooplankton on a daily basis, with 4-60% d^{-1} grazed in spring. Grazing by microzooplankton as a function of daily production ranged from 70-120% in winter and 40-130% in spring across the three water types (James & Hall, 1997). In subantarctic waters, microzooplankton grazing was more pronounced in winter (20-60%chlorophyll *a* d^{-1}), but was not so important in spring (<5%d^{-1}). Waste products from microzooplankton are generally inferred to have negligible sinking rates (Hofman et al., 1981; Stoecker, 1984), so there is likely to be only minimal contribution of this material to sinking fluxes (<1-2% of total pellet flux, Urrère & Knauer, 1981; Gowing & Silver, 1985), although in coastal seas the contribution can be as much as 30-40% (Nöthig & von Bodungen, 1989; Buck & Newton, 1995).

Subantarctic phytoplankton biomass in spring, however, remained relatively low, despite the presence of high levels of macro-nutrients (Tables 4.2 & 4.3), which suggests that micro-nutrients may also limit phytoplankton growth in this region (e.g., Banse, 1996; Bradford-Grieve et al., 1997a). If there is a terrestrial source for micro-nutrients, then it is likely that this will be via aeolian processes in subantarctic waters since a persistent, northeastward-

flowing, shelf-break current operates at the Southland Front (Fig. 3.2, Chapter 3) along the eastern margin of South Island (e.g., Heath, 1972; Chiswell, 1996) which might preclude river-derived sediments from moving offshore into deep subantarctic waters. In subtropical and STC waters, direct terrestrial sediment sources in the form of rivers in eastern North Island and northern South Island, and from sediment carried by the Southland Current into the STC frontal zone, are likely. Terrestrial sediment may be entrained and carried offshore by semi-permanent oceanic currents in this region (e.g., Heath, 1985), forming the wide swath of hemipelagic sediment apron that is draped over the central portions of the Chatham Rise out to about 179°E (McDougall, 1975, 1982). The presence of coastal mesozooplankton at STC stations in 1993 (Bradford-Grieve et al., 1997b) indicates that significant lateral advection of particulate material from the coastal zone into the oceanic realm east of New Zealand is possible.

Biologically mediated mechanisms of particle degradation involving the other component of the microbial loop - bacteria - may also be an important process accentuating pigmented particle retention in the upper ocean. Bacterial processes became significant in spring in subtropical and STC waters, especially in the latter where bacterial productivity increased 26-fold between winter and spring (Smith & Hall, in press). Bacterial degradation of copepod faecal pellets is enhanced at higher temperatures (Honjo & Roman, 1978) which might partially explain the lack of phaeopigments in the lower latitude water types in spring, despite significant increases in mesozooplankton biomass (see later). It is postulated that intense recycling processes were operating in STC waters in spring since, although the plankton community in the frontal zone was dominated by large (20-200 μm) phytoplankton, including many chain-forming diatoms, such as *Lauderia annulata*, *Thalassiosira* spp. and *Chaetoceros* spp., these chlorophyll-containing organisms were not apparently sinking out in high numbers as a proportion of total phytoplankton biomass and production (Table 6.4). Relative to the other water types, however, fucoxanthin and total chorophyll-derived pigment fluxes were higher in the STC at this time (Fig. 6.3 & 6.5). These observations suggest that, while a significant proportion of the total biomass was being retained in the upper water column, chain-forming diatoms and probably other phytoplankton-derived marine aggregates were being actively exported in the STC in spring. As discussed previously, however, it is anticipated that a phytoplankton-dominated sedimentation event probably occurred soon after

sediment trap deployments were completed, and thus any maximal sedimentation episode was not sampled by the free-floating traps.

Phaeopigments, identified in trap samples in the present study, were dominated by phaeophorbides (especially *a1* and *a2*) (Fig. 6.2, 6.3 & 6.4). These pigments are typically associated with phytoplankton which have been either grazed by mesozooplankton and excreted as faecal pellets (e.g., Welschmeyer & Lorenzen, 1985a; Vernet & Lorenzen, 1987a), or have undergone physiological stress and are senescing (e.g., Head & Horne, 1993). Based on retention times, phaeophorbide *a1* in the present study may be phaeophorbide *a2*, a by-product of herbivorous mesozooplankton grazing as observed by Vernet & Lorenzen (1987a), whereas phaeophorbide *a2* in Chatham Rise trap samples may be a phaeophorbide *a*-like pigment found by Head et al. (1994) to form during the senescent stages of phytoplankton blooms. If this is the case, then products of mesozooplankton grazing tend to predominate over most depths since phaeophorbide *a1*:phaeophorbide *a2* ratios were generally >1, except at one station in subantarctic waters in winter (X465) and in the STC in both seasons (at X467 and X477). The proportionally high numbers of larger phytoplankton found in the STC, and the variable persistence of small size fractions (predominantly <20 μm) in the phytoplankton community in other water types (Table 6.3), may partially explain the high winter export of phaeophorbide *a*-like pigments in the STC. It is unclear why apparent sedimentation of senescing phytoplanton was important at X465 since 90% of the phytoplankton community were <20 μm in size (Table 6.3), and therefore potentially not involved in export processes (e.g., Bienfang & Harrison, 1984; Passow & Peinert, 1993). Perhaps the lower microzooplankton grazing coefficients observed at X465, compared with X464 (-0.49 and -1.28 for picophytoplankton and -0.25 and -0.78 for total chlorophyll, respectively, James & Hall, 1997) may explain partially this discrepancy since lowered microzooplankton grazing at X465 might allow preferentially more phytoplankton material to sink out of the upper ocean. In addition, it seems that mesozooplankton were obtaining only 1% of their carbon metabolic requirements from phytoplankton and were probably feeding mainly upon the microzooplankton community (Bradford-Grieve et al., 1997b), thereby resulting in increased fluxes of phytoplankton-related phaeopigments.

The proportionally high numbers of larger phytoplankton found in the STC, and the variable persistence of small size fractions (predominantly <20 μm) in the phytoplankton community

Table 6.6 Relationships between primary production, chlorophyll *a* biomass, mesozooplankton grazing and phaeopigment fluxes across three water types in winter and spring 1993.

Season & water type*	Integrated mean primary production**	Integrated chlorophyll *a* (<200µm)	Mesozooplankton community grazing rate**				Phaeopigment flux			
	mgC m^{-2} d^{-1}	mg m^{-2}	mgPh m^{-2} d^{-1}†	mgC m^{-2} d^{-1}‡	%standing stock d^{-1}#	%production§	mgPh m^{-2} d^{-1}†	mgC m^{-2} d^{-1}‡	%standing stock d^{-1}#	%production§
Winter 1993										
SA	45.0	11.4	0.031	1.2	0.3	2.7	0.008	0.3	0.1	0.7
STC	262.0	49.1	0.093	3.7	0.2	1.4	0.100	4.0	0.2	1.5
ST	148.5	19.3	0.056	2.2	0.3	1.5	0.032	1.3	0.2	0.9
Spring 1993										
SA	250.5	14.0	0.054	2.2	0.4	0.9	0.051	2.1	0.4	0.8
STC	986.0	108.3	0.370	14.8	0.3	1.5	0.070	2.8	0.1	0.3
ST	971.0	46.6	0.843	33.7	1.8	3.5	0.077	3.1	0.2	0.3

* SA = subantarctic (sediment traps positioned at 120 m water depth in winter; 150 m in spring), STC = Subtropical Convergence (110 m; 100 m), ST = subtropical (120 m; 110 m).

** Primary production (^{14}C bicarbonate <200 µm uptake - 24 h incubations; Bradford-Grieve et al., 1997a) integrated to 1% light level; chlorophyll *a* (<200 µm) and mesozooplankton (>200 µm) community grazing rates (gut fluorescence technique) are integrated to 100 m (Bradford-Grieve et al., 1997b).

† Ph grazing rates = average phaeopigment concentrations in mesozooplankton determined fluorometrically using a 90% acetone extract (Bradford-Grieve et al., 1997b); average Ph fluxes determined using HPLC (this study); no conversions to chl *a*-equivalent values (e.g., Welschmeyer & Lorenzen, 1985a, b) were made on the basis of results in Conover et al. (1986).

‡ Phaeopigment ingestion rates and fluxes converted to carbon, assuming a C:Ph ratio of 40 (Bradford-Grieve et al., 1997b).

\# Grazing and flux rates as % standing stock are based on the depth-integrated mean chlorophyll *a* to 100 m.

§ Carbon-equivalent grazing and flux rates as % production are based on integrated mean primary production to 1% light level.

in the other water types (Table 6.3), may partially explain the high winter export of phaeopigments in the STC, although it is difficult to determine the exact proportions that material derived from senescent phytoplankton or heterotrophic grazing contribute to total phaeopigment flux. In support of the latter process, however, three- and five-times of pigmented material grazed by mesozooplankton was being exported potentially as phaeopigments in STC and subtropical waters, respectively, in winter compared with spring (Table 6.6).

It is likely that direct sedimentation of phytoplankton cells or aggregates in subtropical waters was lower in spring than in winter due to the associated increase in the abundance of nano- and picophytoplankton (30-40 mg chlorophyll *a* m^{-2} cf. 7-14 in winter) in the phytoplankton community (80-100% of total chlorophyll <200 μm). This situation would have encouraged relative accumulation of phytoplankton in the upper water column since sedimentation rates of small cells are low (<1 m d^{-1}, Bienfang & Harrison, 1984; McCave, 1984b; Passow & Peinert, 1993; Boyd & Newton, 1995). In addition, faecal pellets produced by dominant copepods in warmer subtropical waters were probably more susceptible to rapid colonisation by bacteria and microheterotrophs (Honjo & Roman, 1978; Jacobsen & Azam, 1984; Lee & Fisher, 1992), compared with subantarctic waters, leading to increased rates of pellet decomposition in the upper water column.

Increased incidences of coprophagy and coprorhexy by copepod-dominated mesozooplankton communities (mainly *Neocalanus tonsus*, Bradford-Grieve et al., 1997b) are also anticipated in subtropical waters in spring. There is no direct evidence that rates of coprophagy and coprorhexy were particularly significant in this water type at this time, but circumstantial data support this assertion, notably that, associated with substantial increases in mesozooplankton biomass, community grazing rates were enhanced seasonally in subtropical waters in spring 15-fold, compared with only 2- and 4-fold seasonal grazing rate increases in subantarctic and STC waters (Table 6.6). Slightly higher metabolic requirements for the mesozooplankton community were also being met through herbivory in subtropical waters in winter (12-16%), compared with spring (3-4%), when carnivory and perhaps detritivory were important (Bradford-Grieve et al., 1997b). Furthermore, near-surface stratification (15-25 m mixed-layer depths) in subtropical waters in spring is likely to have accentuated these biologically mediated particle retention mechanisms in the upper water column (e.g., Alldredge et al., 1987).

Table 6.7 Ratios of primary production, mesozooplankton grazing and phaeopigment flux across three water types in winter and spring 1993.

Season & water type*	Grazing:Production (%)**	TPh flux:Grazing (%)**	Grazing x 0.3: TPh flux (%)†
Winter 1993			
SA	3.6	20.5	146.6
STC	1.9	80.1	37.4
ST	2.5	33.5	89.5
Spring 1993			
SA	1.1	73.3	40.9
STC	1.9	15.3	196.1
ST	2.9	11.0	273.1

* SA = subantarctic (sediment traps positioned at 120 m water depth in winter; 150 m in spring), STC = Subtropical Convergence (110 m; 100 m), ST = subtropical (120 m: 110 m).

** Carbon-equivalent values (mgC m^{-2} d^{-1}) as given in Table 6.6; TPh = Total phaeopigments only (Table 6.6).

† Assumes that 70% of phytoplankton ingested by mesozooplankton are assimilated with 30% repackaged into faecal pellets (Landry et al., 1994).

If one considers the amount of grazed material that was actually lost via direct sinking, there are distinct seasonal differences across all three water types (Table 6.6). Higher proportions were observed in winter, particularly in STC and subtropical waters (80 and 34% in winter cf. 15 and 11 in spring, respectively, Table 6.6). By comparison, in subantarctic waters, only 21% of grazed material was exported in winter, but this proportion increased to 73% in spring, in accordance with mesozooplankton grazing rates which increased from winter to spring (1.6 to 2.8 mgC m^{-2} d^{-1}, Table 6.6). As a proportion of phytoplankton standing stock and primary production, however, there was a seasonal reduction in the effect of mesozooplankton grazing on the phytoplankton community from winter to spring which was not matched by variations in phaeopigment fluxes (Table 6.6). Substantial reductions in the amount of grazed material being exported from the mixed-layer as phaeopigments from STC and subtropical waters in spring (Table 6.6) indicate that there are times when mesozooplankton faecal pellets do not sink out immediately and therefore may behave functionally as microzooplankton excretion products (e.g., Hofman et al., 1981; Alldredge et al., 1987; Landry et al., 1994), albeit probably with slower degradation rates (Nelson, 1993).

The processes responsible for this situation include vertical stratification, bacterial and protisan decomposition of pellet membranes and mesozooplankton coprophagy and coprorhexy, as discussed above. A conservative estimate of the importance of mesozooplankton faecal pellet production and export can be made by assuming that 70% of ingested phytoplankton are assimilated by mesozooplankton and the remaining 30% are repackaged into faecal pellets (Dam et al., 1993; Landry et al., 1994) (Table 6.7). This analysis suggests that, although the impact of mesozooplankton grazing on phytoplankton stocks and production was negligible (<3%), the export of faecal pellets was probably a prominent process in subantarctic waters in winter and in STC and subtropical waters in spring. Heightened pellet flux is also consistent with observed high grazing-to-production ratios in these water types at these times (Table 6.7). Qualitative microscopic analysis of filtered samples supports these observations since large rectangular faecal pellets (100-140 μm wide and 460-740 μm long) were a common feature of contemporaneous mass flux samples (see Fig. 5.8E, G & F, Section 5.3.5, Chapter 5).

6.8. Summary of Chapter 6

(1) The presence of undegraded photosynthetic pigments in sediment trap samples from water depths of 100-550 m suggests rapid removal of phytoplankton cells from surface waters east of New Zealand. Algal cells are exported presumably mainly as sinking intact phytoplankton chains, marine aggregrates or as unconverted pigments in zooplankton waste products. Unusually low levels of phaeophorbides in trap samples emphasise the importance of such transfer processes.

(2) Pigment budget estimates indicate that less than 1% d^{-1} of chlorophyll *a* standing stock and <4% of primary production were exported on average from the upper ocean during the study periods in winter and spring 1993. Effective particle retention mechanisms that could have prevented significant loses of pigmented material from surface waters include: (a) microzooplankton grazing; (b) microbial degradation; (c) mesozooplankton coprophagy and coprorhexy; and to a lesser extent (d) upper ocean turbulence and seasonal stratification. Of these mechanisms, microzooplankton grazing was potentially the most important process affecting pigment distribution across subantarctic, convergence and subtropical water types. Bacterial degradation, mesozooplankton grazing and stratification were probably especially important in subtropical waters in spring.

(3) It appears that the magnitude and composition of pigment fluxes are affected markedly by variations in planktonic community structure and function, unlike total mass and particulate phosphorus fluxes measured in contemporaneous sediment trap samples (Chapter 5). Since fluxes of photosynthetic pigments are often a relatively low proportion of the total flux of organic products (<1% of total organic carbon flux), it is inferred that the anomalously high benthic biomass estimates found on south Chatham Rise (Probert & McKnight, 1993) suggest that there are high energy food sources in sinking particulate material other than pigmented matter (e.g., Lee & Wakeham, 1989; Wakeham & Lee, 1989, 1993; Wakeham et al., 1993; Cowie & Hedges, 1996). The results of this preliminary study of pigment fluxes highlight the potential that a biomarker approach has for evaluating the dominant particle transformation processes occurring in the upper ocean as reflected in marine particulate fluxes.

Chapter 7

CONCLUSIONS

Chapter 7

CONCLUSIONS

Two themes were addressed by the present study: (1) sediment trap methods and technique development (Chapters 1 and 2); and (2) oceanic sediment fluxes east of New Zealand and relationships to the Chatham Rise-Subtropical Convergence ecosystem (Chapters 3, 4, 5 and 6). Accordingly, as an integral component of Theme 1, a sediment trap system was designed and constructed after an extensive literature search, which indicated that the use of axially symmetrical cylindrical traps should be the primary design criteria (Chapter 1). A conservative design strategy was adopted because critical temporal and spatial aspects of the bio-physical environment of Chatham Rise-Subtropical Convergence were poorly known (Chapter 3). A multiple trap array was constructed for baffled cylindrical traps with an aspect ratio of 10.6. The practicalities of free-floating sediment trap deployments were evaluated successfully in two pilot studies conducted in 1992 and 1993 (Sections 2.2 and 2.3, Chapter 2). The first deployment was in subtropical waters on the northern flank of Chatham Rise in austral autumn 1992 (Nodder, in press). A second deployment was in Cook Strait under storm conditions in autumn 1993. These two studies highlighted several logistic and technical requirements that were used to modify deployment and laboratory protocols for subsequent sediment trap deployments in 1993 (e.g., volume of trap solutions to be filtered for mass flux determinations reduced to 250 ml, aspiration methods modified, techniques employed for filling traps with high-density brine altered). Finally, under Theme 1, trapping efficiency of the NZOI-NIWA traps was assessed in four, short-term field experiments undertaken in Evans Bay, Wellington Harbour, in 1994 and 1995 (Section 2.4, Chapter 2). These deployments indicated that hydrodynamic interactions between cylinders on the same cross-frame were likely to be insignificant (Experiment II), that baffles did not affect trapping efficiency (Experiment III) and that traps filled completely with high-density brine solution collected 2-3 times less material than traps with basal brine heights equivalent to 1- and 2.5-trap diameters (Experiment IV).

As part of Theme 2, the author conducted fieldwork within the framework of the multi-disciplinary New Zealand Joint Global Ocean Flux Study (JGOFS) in winter and spring 1993, as principal investigator overseeing sediment trap deployments. This work was undertaken off eastern New Zealand in subantarctic and subtropical water masses either side of, and within, the Subtropical Convergence, a globally important oceanic frontal zone. The primary aim of the sediment trap work was to quantify and characterise the particulate flux of material from the upper ocean in a region regarded as a biologically mediated, natural sink for atmospheric CO_2 (Nodder and Alexander, 1997). The trap study was complemented by food web studies undertaken in the surface waters of each water type (Chapter 4). Despite marked changes in planktonic community structure and functioning between seasons and across water masses, no statistically significant variations in total mass and particulate phosphorus fluxes could be determined due to high levels of variability arising mainly from subsampling procedures (Chapter 5). The high degrees of variability associated with sediment trap samples collected in 1993 were not unusual, however, since similar levels of variation have been observed in more extensive temporal studies conducted at JGOFS time-series stations in equatorial central Pacific and western Atlantic oceans. In order to use particulate fluxes to characterise distinctive oceanic provinces, this study recommends that more than two free-floating sediment arrays would have to be deployed within each water mass to generate statistically valid conclusions (Chapter 5).

Average particulate fluxes from the north Chatham Rise pilot study (Section 2.2, Chapter 2) and 1993 JGOFS fieldwork (Chapter 5) are similar in magnitude to other fluxes measured at oligotrophic and continental margin sites. The extremely high daily fluxes observed in Cook Strait (Section 2.3, Chapter 2) highlight the significance of this corridor as a zone of active sediment transport. Resuspension of material from the crest of Chatham Rise by strong tidal currents is inferred to be a significant process affecting particulate fluxes in the region, resulting in anomalous increases in mass flux with depth in autumn 1992 and winter and spring 1993.

Since seasonal and spatial variations in Chatham Rise-Subtropical Convergence ecosystems were not mirrored by similar differences in particulate flux magnitude (Chapter 5), it is surmised that it is the nutritional quality, rather than quantity, of sinking material that is

critical to the well-being of benthic communities. The use of photosynthetic pigments as process tracers in sinking particles showed that undegraded pigments could be rapidly transferred from the upper ocean to depths of 550 m (Nodder & Gall, submitted) (Chapter 6). Furthermore, pigment budgets indicated that <5% of phytoplankton biomass (as represented by chlorophyll *a*) and integrated primary production were exported on a daily basis. These results suggest that other processes were operating in the upper water column to prevent pronounced sedimentation of organic material out of surface layers at the time of sampling. Of particular importance was microzooplankton grazing of phytoplankton, which leads to extensive recycling of organic particles in the upper ocean and hence pronounced photodegradation of pigments to undetectable colourless products. Other retention mechanisms of variable significance in the three water types include bacterial decomposition, physical turbulence and stratification, and mesozooplankton coprophagy and coprorhexy.

It appears that the magnitude and composition of pigment fluxes are affected markedly by variations in planktonic community structure and function, unlike total mass and particulate phosphorus fluxes (Chapter 5). Since fluxes of photosynthetic pigments are often a relatively low proportion of the total flux of organic products (<1% of total organic carbon flux), it is inferred that anomalously high benthic biomass estimates found on south Chatham Rise (Probert & McKnight, 1993) reflect high energy food sources in sinking particulate material rather than pigmented matter.

Finally, the Chatham Rise-Subtropical Convergence region acts as an oceanic sink for atmospheric CO_2 at least on seasonal time-scales (e.g., Murphy et al., 1991; Currie & Hunter, 1997). The strength of the "biological pump" in sequestering CO_2 is likely to be a dominant process in this region, but the efficiency at which carbon, bound in organically produced particles, is removed from the upper ocean by sinking has yet to be evaluated fully. Sediment trap results from winter and spring 1993 are equivocal from a statistical point of view. There is, however, indications from pigment flux data that rates of export flux are sufficiently rapid to transport undegraded pigmented material to at least 550 m depth. Furthermore, average particulate fluxes from across the region are similar in magnitude to fluxes measured in other continental margin settings, and carbon fluxes may be as much as 40% of the total mass flux in subtropical waters (Section 2.2, Chapter 2). These findings indicate that "biological pump"

efficiency, as inferred from export flux estimates, is potentially relatively high in the vicinity of the Subtropical Convergence near New Zealand, compared with other oligotrophic environments of the Southern Ocean.

More work is required, however, to determine the temporal and spatial variability of particulate fluxes in the Southwest Pacific Ocean in order to develop an understanding of how the "biological pump" functions in this region. Future studies will have to overcome the statistical design criteria suggested by the present study (i.e., three or more free-floating arrays to be deployed at any one time), and should investigate the collection of longer time-series measurements made possible by the use of deep ocean, bottom-moored, time-incremental sediment traps. In order to fully understand sediment trap interpretations, contemporaneous measurements of food web structure and processes must also be made.

The gradual accrual of biological oceanographic data in an oceanic region largely devoid of adequate data coverage in both time and space is a necessity if our understanding of the Southern Ocean "biological pump" is to improve. It is also critical that pelagic production cycles are established for the Southwest Pacific Ocean so that existing and future modelling work can be truly validated. An initial estimate of temporal and spatial variations in surface production may be provided from sediment trap studies since trap samples represent an integrated signal of upper ocean biogeochemical processes. The potential use of process tracers and biomarkers has been highlighted by the present study and should be expanded in the future to include other organic compounds and elements including isotopic studies for trap calibration purposes.

In conclusion, despite the shortcomings of the sediment trap method (i.e., hydrodynamic biases, zooplankton contamination, lack of independent calibration), traps remain the only technique available to the oceanographic community that provides a quantifiable measurement of export fluxes from the upper to deep ocean. Until modern technology develops a truly neutrally buoyant sediment trap system with zooplankton exclusion devices, relatively simple sediment trap arrays, as utilised by the present study, will continue to provide the best initial estimates of oceanic particulate fluxes from previously uncharacterised regions of the global ocean.

REFERENCES

REFERENCES

Abraham, E. (1997). Seiche modes of Wellington Harbour, New Zealand. *New Zealand Journal of Marine and Freshwater Research*, **31**, 191-200.

Alldredge, A.L. and M.W. Silver (1988). Characteristics, dynamics and significance of marine snow. *Progress in Oceanography,* **20**, 41-82.

Alldredge, A.L., C.C. Gotschalk and S. MacIntyre (1987). Evidence for sustained residence of macrocrustacean fecal pellets in surface waters off southern California. *Deep-Sea Research*, **34**, 1641-1652.

Andersen, R.A., R.R. Bidigare, M.D. Keller and M.L. Latasa (1996). A comparison of HPLC pigment signatures and electron microscopic observations for oligotrophic waters of North Atlantic and Pacific oceans. *Deep-Sea Research II*, **43**, 517-537.

Angel, M.V. (1989). Does mesopelagic biology affect vertical flux? In: *Productivity of the Ocean: Present and Past*, W.H. Berger, V.S. Smetacek and G. Wefer, editors, J. Wiley and Sons, New York, 155-173.

Archer, D.E. (1996). An atlas of the distribution of calcium carbonate in sediments of the deep ocean. *Global Biogeochemical Cycles*, **10**, 159-174.

Asper (1987a). Measuring the flux and sinking speed of marine snow aggregates. *Deep-Sea Research*, **34**, 1-17.

Asper, V. L. (1987b). A review of sediment trap technique. *Marine Technology Society Journal*, **21**, 18-25.

Asper, V.L., W.G. Deuser, G.A. Knauer and S.E. Lohrenz (1992). Rapid coupling of sinking particle fluxes between surface and deep ocean waters. *Nature*, **357**, 670-672.

Auffret, G., A. Khripounoff and A. Vangriesheim (1994). Rapid post-bloom resuspension in the northeastern Atlantic. *Deep-Sea Research I*, **41**, 925-939.

Bacon, M.P. (1984). Radionuclide fluxes and the in-situ calibration of deep-sea sediment traps. *EOS, Transactions of American Geophysical Union*, **65**, 225.

Bacon, M.P., C-A. Huh, A.P. Fleer and W.G. Deuser (1985). Seasonality in the flux of natural radionuclides and plutonium in the deep Sargasso Sea. *Deep-Sea Research*, **32**, 273-286.

Baes, Jr., C.F., A. Björkström and P.J. Mulholland (1985). Chapter 5 - Uptake of carbon dioxide by the oceans. In: *Atmospheric carbon dioxide and the global carbon*

cycle, J.R. Trabalka, editor, United States Department of Energy, Washington D.C., **DOE/ER-0239**, 81-111.

Baker E.T. and H.B. Milburn (1983). An instrument for the investigation of particle fluxes. *Continental Shelf Research*, **1**, 426-435.

Baker, E.T., H.B. Milburn and D.A. Tennant (1988). Field assessment of sediment trap efficiency under varying flow conditions. *Journal of Marine Research*, **46**, 573-592.

Banse, K. (1996). Low seasonality of low concentrations of surface chlorophyll in the Subantarctic water ring: mean underwater irradiance, iron or grazing? *Progress in Oceanography*, **37**, 241-291.

Barlow, R.J., R.F.C. Mantoura, M.A. Gough and T.W. Fileman (1993). Pigment signatures of the phytoplankton composition in the northeastern Atlantic during the 1990 spring bloom. *Deep-Sea Research II*, **40**, 459-477.

Barlow, R.J., R.F.C. Mantoura, R.D. Peinert, A.E.J. Miller and T.W. Fileman (1995). Distribution, sedimentation and fate of pigment biomarkers following thermal stratification in the western Alboran Sea. *Marine Ecology Progress Series*, **125**, 279-291.

Barnes, E. J. (1985). Eastern Cook Strait region circulation inferred from satellite-derived, sea-surface, temperature data. *New Zealand Journal of Marine and Freshwater Research*, **19**, 405-411.

Barnes, P.M. (1992). Mid-bathyal current scours and sediment drifts adjacent to the Hikurangi deep-sea turbidite channel, eastern New Zealand: evidence from echo character mapping. *Marine Geology*, **106**, 169-187.

Barnes, P.M. (1994). Inherited structural control from repeated Cretaceous to Recent extension in the North Mernoo Fault Zone, western Chatham Rise, New Zealand. *Tectonophysics*, **237**, 27-46.

Barnes, P.M. and P.A.R. Shane (1994). Late Neogene unconformity-bounded tuffaceous sequences: northwestern Chatham Rise, New Zealand. *New Zealand Journal of Geology and Geophysics*, **35**, 421-435.

Bathmann, U.V., T.T. Noji, M. Voss and R. Peinert (1987). Copepod fecal pellets: abundance, sedimentation and content at a permanent station in the Norwegian Sea in May/June 1986. *Marine Ecology Progress Series*, **38**, 45-51.

Bautista, B. and R.P. Harris (1992). Copepod gut contents, ingestion rates and grazing impact on phytoplankton in relation to size structure of zooplankton and phytoplankton during spring bloom. *Marine Ecology Progress Series*, **82**, 41-50.

Berger, W.H., V.S. Smetacek and G. Wefer (1989). Ocean productivity and paleoproductivity - an overview. In: *Productivity of the Ocean: Present and*

Past, W.H. Berger, V.S. Smetacek and G. Wefer, editors, J. Wiley and Sons, New York, 1-34.

Betzer, P.R., W.J. Showers, E.A. Laws, C.D. Winn, G.R. DiTullo and P.M. Kroopnick (1984). Primary productivity and particle fluxes on a transect of the equator at 154°W in the Pacific Ocean. *Deep-Sea Research*, **31**, 1-11.

Bhattacharyya, G.K. and R.A. Johnson (1978). Statistical concepts and methods, Wiley, New York, 639p.

Billet, D.S.M., R.S. Lampitt, A.L. Rice and R.F.C. Mantoura (1983). Seasonal sedimentation of phytoplankton to the deep sea benthos. *Nature*, **302**, 520-522.

Bienfang, P.K. and P.J. Harrison (1984). Sinking rate response of natural assemblages of temperate and subtropical phytoplankton to nutrient depletion. *Marine Biology*, **83**, 293-300.

Biscaye, P.E. and R.F. Anderson (1994). Fluxes of particulate matter on the slope of the southern Middle Atlantic Bight: SEEP-II. *Deep-Sea Research II*, **41**, 459-509.

Bishop, J.K.B. (1989). Regional extremes in particulate matter composition and flux: effects on the chemistry of the ocean interior. In: *Productivity of the Ocean: Present and Past*, W.H. Berger, V.S. Smetacek and G. Wefer, editors, J. Wiley and Sons, New York, 117-137.

Bishop, J.K.B., J.C. Stepien and P.H. Wiebe (1986). Particulate matter distributions, chemistry and flux in the Panama Basin: response to environmental forcing. *Progress in Oceanography*, **17**, 1-59.

Bjørnland, T. and K. Tangen (1979). Pigmentation and morphology of a marine Gyrodinium (Dinophyceae) with a major carotenoid different from peridinin and fucoxanthin. *Journal of Phycology*, **15**, 457-463.

Black, K.P. (1986). Sediment-transport rates in Cook Strait. *New Zealand Oceanographic Institute Field Report*, **24**, 14p.

Bloesch, J. and N.M. Burns (1980). A critical review of sedimentation trap technique. *Schweizerische Zeitschrift für Hydrologie*, **42**, 15-55.

Blomquist, S. and L. Håkanson (1981). A review on sediment traps in aquatic environments. *Archiv für Hydrobiologie*, **91**, 101-132.

Blomquist, S. and C. Kofoed (1981). Sediment trapping - A subaquatic in situ experiment. *Limnology and Oceanography*, **26**, 585-589.

von Bodungen, B., M. Wunsch and H. Fürderer (1991). Sampling and analysis of suspended particles in the North Atlantic. In: *Marine Particles: analysis and characterization*, D.C. Hurd and D.W. Spencer, editors, American Geophysical Union, *Geophysical Monograph*, **63**, 47-56.

Booth, J.D. (1975). Seasonal tidal variations in the hydrology of Wellington Harbour. *New Zealand Journal of Marine and Freshwater Research*, **9**, 333-354.

Bowman M.J., A.C. Kibblewhite and D.E. Ash (1980). M_2 Tidal effects in greater Cook Strait, New Zealand. *Journal of Geophysical Research*, **85**, 2728-2742.

Bowman M.J., A.C. Kibblewhite, S.M. Chiswell and R.A. Murtagh (1983a). Shelf fronts and tidal stirring in the greater Cook Strait, New Zealand. *Oceanologica Acta*, **6**, 119-129.

Bowman, M.J., A.C. Kibblewhite, R.A. Murtagh, S.M. Chiswell and B.G. Sanderson (1983b). Circulation and mixing in greater Cook Strait, New Zealand. *Oceanologica Acta*, **6**, 383-391.

Boyd, P. and P. Newton (1995). Evidence of the potential influence of planktonic community structure on the interannual variability of particulate organic carbon flux. *Deep-Sea Research I*, **42**, 619-639.

Bradford, J.M. (1980a). New Zealand Region, Zooplankton Biomass (0-200m). *New Zealand Oceanographic Institute Chart, Miscellaneous Series*, **41**.

Bradford, J.M. (1980b). New Zealand Region, Primary Productivity Surface. *New Zealand Oceanographic Institute Chart, Miscellaneous Series*, **42**.

Bradford, J.M. (1980c). New Zealand Region, Primary Productivity Integrated. *New Zealand Oceanographic Institute Chart, Miscellaneous Series*, **43**.

Bradford, J.M. (1980d). New Zealand Region, Surface Chlorophyll a. *New Zealand Oceanographic Institute Chart, Miscellaneous Series*, **44**.

Bradford, J. M. (1983). Plankton and primary productivity in the vicinity of the Chatham Rise. *New Zealand Oceanographic Institute Oceanographic Summary,* **21**, 14p.

Bradford, J.M. and F.H. Chang (1987). Standing stocks and productivity of phytoplankton off Westland, New Zealand, February 1982. *New Zealand Journal of Marine and Freshwater Research*, **21**, 71-90.

Bradford, J.M. and J.B. Jillett (1980). The marine fauna of New Zealand: Pelagic calanoid copepods: Family Aetideidae. *New Zealand Oceanographic Institute Memoir*, **86**, 102p.

Bradford, J.M. and P.E. Roberts (1978). Distribution of reactive phosphorus and plankton in relation to upwelling and surface circulation around New Zealand. *New Zealand Journal of Marine and Freshwater Research*, **12**, 1-15.

Bradford, J.M. and F.J. Taylor (1980). New Zealand region reactive phosphorus (October-April) - surface, 1:6 000 000. *New Zealand Oceanographic Institute Chart, Miscellaneous Series*, **46**.

Bradford, J.M., R.A. Heath, F.H. Chang and C.H. Hay (1982). The effect of warm-core eddies on oceanic productivity off northeastern New Zealand. *Deep-Sea Research*, **29**, 1501-1516.

Bradford-Grieve, J.M., F.H. Chang, M. Gall, S. Pickmere and F. Richards (1997a). Size-fractionated phytoplankton standing stocks and primary production during austral winter and spring 1993 in the Subtropical Convergence region near New Zealand. *New Zealand Journal of Marine and Freshwater Research*, **31**, 201-224.

Bradford-Grieve, J., R. Murdoch, M. James, M. Oliver and J. McLeod (1997b). Mesozooplankton biomass, composition and potential grazing pressure on phytoplankton during austral winter and spring 1993 in the Subtropical Convergence region near New Zealand. *Deep-Sea Research II.*

Brewer, P.G., A.L. Bradshaw and R.T. Williams (1986). Measurements of total carbon dioxide and alkalinity in the north Atlantic Ocean in 1981. In: *The Changing Carbon Cycle: a global analysis*, J. R. Trabalka and D. E. Reichle, editors, Springer-Verlag, New York, 348-370.

Broecker, W.S. and T-H. Peng (1982). *Tracers in the sea.* Lamont-Doherty Geological Observatory, Columbia University, New York, 690p.

Broecker, W.S. and T-H. Peng (1992). Interhemispheric transport of carbon dioxide by ocean circulation. *Nature*, **356**, 587-589.

Brown, S.R., R.J. Daley and R.N. McNeely (1977). Composition and stratigraphy of the fossil phorbin derivatives of Little Round Lake, Ontario. *Limnology and Oceanography*, **22**, 336-348.

Bruland, K.W. and M.W. Silver (1981). Sinking rates of fecal pellets from gelatinous zooplankton (salps, pteropods, doliolids). *Marine Biology*, **63**, 295-300.

Bruland, K.W. and 9 others (1989). Group Report: Flux to the Seafloor. In: *Productivity of the Ocean: Present and Past*, W.H. Berger, V.S. Smetacek and G. Wefer, editors, J. Wiley and Sons, New York, 193-215.

Buck, K.R. and J. Newton (1995). Fecal pellet flux in Dabob Bay during a diatom bloom: contribution of microzooplankton. *Limnology and Oceanography*, **40**, 306-315.

Buesseler, K.O. (1991). Do upper-ocean sediment traps provide an accurate record of particle flux? *Nature*, **353**, 420-423.

Buesseler, K.O., M.P. Bacon, J.K. Cochran and H.D. Livingston (1992). Carbon and nitrogen export during the JGOFS North Atlantic Bloom Experiment estimated from ^{234}Th:^{238}U disequilibria. *Deep-Sea Research*, **39**, 1115-1137.

Buesseler, K.O., A.F. Michaels, D.A. Siegel and A.H. Knap (1994). A three dimensional time-dependent approach to calibrating sediment trap fluxes. *Global Biogeochemical Cycles*, **8**, 179-193.

Burling, R.W. (1961). Hydrology of circumpolar waters south of New Zealand. *New Zealand Oceanographic Institute Memoir*, **10**, 66p.

Bustillos-Guzmán, J., H. Claustre and J.C. Marty (1995). Specific phytoplankton signatures and their relationship to hydrographic conditions in the coastal northwestern Mediterranean Sea. *Marine Ecology Progress Series*, **124**, 247-258.

Butler, E. C.V., J.A. Butt, E.J. Lindstrom, P.C. Tildesley, S. Pickmere and W.F. Vincent (1992). Oceanography of the Subtropical Convergence Zone around southern New Zealand. *New Zealand Journal of Marine and Freshwater Research*, **26**, 131-154.

Butman, C.A. (1986). Sediment trap biases in turbulent flows: results from a laboratory flume study. *Journal of Marine Research*, **44**, 645-693.

Butman, C.A., W.D. Grant and K.D. Stolzenbach (1986). Predictions of sediment trap biases in turbulent flows: a theoretical analysis based on observations from the literature. *Journal of Marine Research*, **44**, 601-644.

Carlson, C.A., H.W. Ducklow and A.F. Michaels (1994). Annual flux of dissolved inorganic carbon from the euphotic zone in the northwestern Sargasso Sea. *Nature*, **371**, 405-408.

CANZ (1997). New Zealand region bathymetry, 3rd edition, 1:4 000 000. *New Zealand Oceanographic Institute Chart, Miscellaneous Series*, **73**.

Carter, L. (1992). Acoustical characterisation of seafloor sediments and its relationship to active sedimentary processes in Cook Strait, New Zealand. *New Zealand Journal of Geology and Geophysics*, **35**, 289-300.

Carter, L. and R M. Carter (1993). Sedimentary evolution of the Bounty Trough: a Cretaceous rift basin, southwestern Pacific Ocean. In: *South Pacific Sedimentary Basins, Sedimentary Basins of the World*, **2**, P.B. Ballance, editor, Elsevier Science Publishers, 51-67.

Carter, L. and K. Lewis (1995). Variability of the modern sand cover on a tide and storm driven inner shelf, south Wellington, New Zealand. *New Zealand Journal of Geology and Geophysics*, **38**, 451-470.

Carter, L. and I.N. McCave (1994). Development of sediment drifts approaching an active plate margin under the SW Pacific Deep Western Boundary Current. *Paleoceanography*, **9**, 1061-1085.

Carter, L., I.C. Wright, N. Collins, J.S. Mitchell and G. Win (1991). Seafloor stability along the Cook Strait power cable corridor. In: *Coastal Engineering - Climate for*

change, R.G. Bell, T.M. Hume and T.R. Healy, editors, *Proceedings of the 10th Australian Conference on Coastal and Ocean Engineering*, Water Quality Centre, DSIR, Hamilton, 565-570.

Carter, L., C.S. Nelson, H. Neil and P.C. Froggatt (1995). Correlation, dispersal, and preservation of the Kawakawa Tephra and other late Quaternary tephra layers in the Southwest Pacific Ocean. *New Zealand Journal of Geology and Geophysics*, **38**, 29-36.

Chang, F.H., J.M. Bradford-Grieve, W.F. Vincent and P.H. Woods (1995). Nitrogen uptake by the summer size-fractionated phytoplankton assemblages in the Westland, New Zealand, upwelling system. *New Zealand Journal of Marine and Freshwater Research*, **29**, 147-161.

Chang, F.H. and M. Gall (submitted). Winter and spring phytoplankton assemblages and photosynthetic pigments in the Subtropical Convergence region near New Zealand. *New Zealand Journal of Marine and Freshwater Research.*

Chisholm, S.W., R.J. Olsen, E.R. Zettler, R. Goericke, J.B. Waterbury and N.A. Welschmeyer (1988). A novel free-living prochlorophyte abundant in the oceanic euphotic zone. *Nature*, **334**, 340-343.

Chiswell, S.M. (1994a). Acoustic Doppler Current Profiler measurements over the Chatham Rise. *New Zealand Journal of Marine and Freshwater Research*, **28**, 167-178.

Chiswell, S.M. (1994b). Variability in sea surface temperature around New Zealand from AVHRR images. *New Zealand Journal of Marine and Freshwater Research*, **28**, 179-192.

Chiswell, S.M. (1996). Variability in the Southland Current, New Zealand. *New Zealand Journal of Marine and Freshwater Research*, **30**, 1-17.

Chiswell, S., E. Firing, D. Karl, R. Lukas and C. Winn (1990). Hawaii Ocean Time-series Data Report 1 1988-1989. *School of Ocean and Earth Science and Technology (University of Hawaii) Technical Report 1*, 269p.

Ciasis, P., P.P. Tans, M. Trolier, J.M.C. White, and R.J. Francey (1995). A large northern hemisphere terrestrial CO_2 sink indicated by the $^{13}C/^{12}C$ Ratio of Atmospheric CO_2. *Science,* **269**, 1098-1102.

Claustre, H. (1994). The trophic status of various oceanic provinces as revealed by phytoplankton pigment signatures. *Limnology and Oceanography*, **39**, 1206-1210.

Clegg, S.L. and M. Whitfield (1990). A generalized model for the scavenging of trace metals in the open ocean. I. Particle cycling. *Deep-Sea Research*, **37**, 809-832.

Clegg, S.L. and M. Whitfield (1993). Application of a generalized scavenging model to time-series ^{234}Th and particle data obtained during the JGOFS North Atlantic Bloom Experiment. *Deep-Sea Research I*, **40**, 1529-1545.

Coale, K.H. (1990). Labyrinth of doom: A device to minimize the "swimmer" component in sediment trap collections. *Limnology and Oceanography*, **35**, 1376-1381.

Cochran, J.K., K.O. Buesseler, M.P. Bacon and H.D. Livingston (1993). Thorium isotopes as indicators of particle dynamics in the upper ocean: results from the JGOFS North Atlantic Bloom Experiment. *Deep-Sea Research I*, **40**, 1569-1595.

Cole J.J., S. Honjo and N. Caraco (1985). Seasonal variation in the flux of algal pigments to a deep water site in the Panama Basin. *Hydrobiologia,* **122**, 193-197.

Colley, S., J. Thomson and P.P. Newton (1995). Detailed ^{230}Th, ^{232}Th and ^{210}Pb fluxes recorded by the 1989/90 BOFS sediment trap time-series at 48°N, 20°W. *Deep-Sea Research*, **42**, 833-848.

Comiso, J.C., C.R. McClain, C.W. Sullivan, J.P. Ryan and C.L. Leonard (1993). Coastal Zone Colour Scanner pigment concentrations in the Southern Ocean and relationships to geophysical surface features. *Journal of Geophysical Research*, **98 (C2)**, 2419-2451.

Conover, R.J., R. Durvasula, S. Roy and R. Wang (1986). Probable loss of chlorophyll-derived pigments during passage through the gut of zooplankton, and some of the consequences. *Limnology and Oceanography*, **31**, 878-887.

Cowie, G.L. and J.I. Hedges (1996). Digestion and alteration of the biochemical constituents of a diatom (*Thalassiosira weissflogil)* ingested by an herbivorous zooplankton (*Calanus pacificus)*. *Limnology and Oceanography*, **41**, 581-594.

Cullen, D.J. (1962). The significance of a glacial erratic from the Chatham Rise, east of New Zealand. *New Zealand Journal of Geology and Geophysics*, **5**, 309-313.

Cullen, D.J. (1980). Distribution, composition and age of submarine phosphorites on Chatham Rise, east of New Zealand. *SEPM Special Publication*, **29**, 139-148.

Cullen, D.J. (1987). The submarine phosphate resource on central Chatham Rise. *New Zealand DMFS (DSIR) report*, **2**, 22p.

Currie, K.I. and K.A. Hunter (1997). Surface water carbon dioxide in the waters associated with the Subtropical Convergence, east of New Zealand. *Deep-Sea Research II.*

Dade, W.B., A.R.M. Nowell and P.A. Jumars (1992). Predicting erosion resistance of muds. *Marine Geology*, **105**, 285-297.

Daley, R.J. (1973). Experimental characterization of lacustrine chlorophyll diagenesis. II. Bacterial, viral and herbivore grazing effects. *Archiv für Hydrobiologie*, **74**, 409-439.

Daley, R.J. and S.R. Brown (1973). Experimental characterization of lacustrine chlorophyll diagenesis. *Archiv für Hydrobiologie*, **72**, 277-304..

Dam, H.G., C.A. Miller and S.H. Jónasdóttir (1993). The trophic role of mesozooplankton at 47N, 20W during the North Atlantic Bloom Experiment. *Deep-Sea Research II*, **40**, 197-212.

Dam, H.G., X. Zhang, M. Butler and M.R. Roman (1995). Mesozooplankton grazing and metabolism at the equator in the central Pacific: implications for carbon and nitrogen fluxes. *Deep-Sea Research II*, **42**, 735-756.

Davy, B. and R. Wood (1994). Gravity and magnetic modelling of the Hikurangi Plateau. *Marine Geology*, **118**, 139-151.

Deacon, G.E.R. (1937). Hydrology of the Southern Ocean. *"Discovery" Reports*, **15**, 1-124.

Denning, S.A., I.Y. Fung and D. Randall (1995). Latitudinal gradient of atmospheric CO_2 due to seasonal exchange with land biota. *Nature*, **376**, 240-243.

Deuser, W.G. (1986). Seasonal and interannual variations in deep-water particle fluxes in the Sargasso Sea and their relation to surface hydrology. *Deep-Sea Research*, **33**, 225-246.

Deuser, W.G., E.H. Ross and R.F. Anderson (1981). Seasonality in the supply of sediment to the deep Sargasso Sea and implications for the rapid transfer of matter to the deep ocean. *Deep-Sea Research*, **28**, 495-505.

Deuser, W.G., T.D. Jickells, P. King and J.A. Commeau (1995). Decadal and annual changes in biogenic opal and carbonate fluxes to the deep Sargasso Sea. *Deep-Sea Research I*, **42**, 1923-1932.

Dickson, A.G. (1981). An exact definition of total alkalinity and a procedure for the estimation of alkalinity and total inorganic carbon from titration data. *Deep-Sea Research*, **28**, 609-623.

Diercks, A. and V. Asper (1994). Neutrally buoyant sediment traps: the first designs. *EOS, Transactions of American Geophysical Union*, **75**, 22.

Diercks. A.R. and V.L. Asper (1997). In situ settling speeds of marine snow aggregates below the mixed layer: Black sea and Gulf of Mexico. *Deep-Sea Research*, **44**, 385.

Downes, M.T. (1978). An improved hydrazine reduction method for the automated determination of low nitrate levels in freshwater. *Water Research*, **12**, 673-675.

Downs, J.N. and C.J. Lorenzen (1985). Carbon:pheopigment ratios of zooplankton fecal pellets as an index of herbivorous feeding. *Limnology and Oceanography*, **30**, 1024-1036.

Ducklow, H.W., S.M. Hill and W.D. Gardner (1985). Bacterial growth and the decomposition of particulate organic carbon collected in sediment traps. *Continental Shelf Research*, **4**, 445-464.

Dugdale, R.C. and J.J. Goering (1967). Uptake of new and regenerated forms of nitrogen in primary productivity. *Limnology and Oceanography*, **12**, 196-206.

Dunbar R.B. and W.H. Berger (1981). Fecal pellet flux to modern bottom sediment of Santa Barbara Basin (California) based on sediment trapping. *Geological Society of America Bulletin*, **92**, 212-218.

Dymond, J. and R. Collier (1988). Biogenic particle fluxes in the equatorial Pacific: evidence for both high and low productivity during the 1982-83 El Nino. *Global Biogeochemical Cycles*, **2**, 129-137.

Dymond, J., K. Fischer, M. Clauson, R. Cobler, W. Gardner, M.-J. Richardson, W. Berger, A. Soutar and R. Dunbar (1981). A sediment trap intercomparison study in the Santa Barbara Basin. *Earth and Planetary Science Letters*, **53**, 409-418.

Emerson, S. P.D. Quay, C. Stump, D. Wilbur and R. Schudlich (1995). Chemical tracers of productivity and respiration in the subtropical Pacific Ocean. *Journal of Geophysical Research*, **100**, 15873-15887.

Enting, I.G. and J.V. Mansbridge (1989). Seasonal sources and sinks of atmospheric CO_2: direct inversion of filtered data. *Tellus*, **41B**, 111-126.

Eppley, R.W. and B.J. Peterson (1979). Particulate organic matter flux and planktonic new production in the deep ocean. *Nature*, **282**, 677-680.

Eppley, R.W., E.H. Renger and P.R. Betzer (1983). The residence of particulate organic carbon in the surface layer of the ocean. *Deep-Sea Research*, **30**, 311-323.

Falconer, R.K.H., U. von Rad and R. Wood (1984). Regional structure and high-resolution seismic stratigraphy of the Central Chatham Rise. *Geologisches Jahrbuch*, **D65**, 29-56.

Fenaughty, J.M. and Y. Uozumi (1989). A survey of demersal fish stocks on the Chatham Rise, New Zealand, March, 1983. *New Zealand Ministry of Agriculture and Fisheries, Fisheries Technical Report*, **12**, 42p.

Fenner, J., L. Carter and R. Stewart (1992). Late Quaternary paleoclimatic and paleoceanographic change over northern Chatham Rise, New Zealand. *Marine Geology*, **108**, 383-404.

Fitzwater, S.E., G.A. Knauer and J.H. Martin (1982). Metal contamination and its effect on primary production measurements. *Limnology and Oceanography*, **27**, 544-551.

Fleming, R.H. (1940). The composition of plankton and units for reporting population and production. *Proceedings of Sixth Pacific Science Congress of California 1939*: 535-540.

Fowler, S.W. and G.A. Knauer (1986). The role of large particles in the transport of elements and organic compounds through oceanic water column. *Progress in Oceanography*, **16**, 147-194.

Fowler, S.W. and L.F. Small (1972). Sinking rates of euphausiid fecal pellets. *Limnology and Oceanography*, **17**, 293-296.

Francey, R.J., P.P. Tans, C.E. Allison, I.G. Enting, J.W.C. White and M. Trolier (1995). Changes in oceanic and terrestrial carbon uptake since 1982. *Nature.* **373**, 326-330.

Froelich, P.N. (1980). Analysis of organic carbon in marine sediments. *Limnology and Oceanography*, **25**, 564-572.

Gardner, W.D. (1977). Incomplete extraction of rapidly settling particles from water samples. *Limnology and Oceanography*, **22**, 764-768.

Gardner, W.D. (1979). Correctional reply to a paper by G. A. Knauer, J. H. Martin and K. W. Bruland, Fluxes of particulate carbon, nitrogen, and phosphorus in the upper water column of the northeast Pacific. *Deep-Sea Research*, **26A**, 965.

Gardner, W.D. (1980a). Sediment trap dynamics and calibration: a laboratory evaluation. *Journal of Marine Research*, **38**, 17-39.

Gardner, W.D. (1980b). Field assessment of sediment traps. *Journal of Marine Research*, **38**, 41-52.

Gardner, W.D. (1985). The effect of tilt on sediment trap efficiency. *Deep-Sea Research*, **32**, 349-361.

Gardner, W.D., editor, (1996). Sediment trap technology and sampling in surface waters. *Report on JGOFS Sediment Trap Symposium, Villefranche sur Mer, May, 1995*, 24p.

Gardner, W.D. and M.-J. Richardson (1992). Particle export and resuspension fluxes in the western North Atlantic. In: *Deep-sea food chains and the global carbon cycle*, G.T. Rowe and V. Pariente, editors, NATO ASI Series C, **360**, Klumer Academic Publishers, The Netherlands, 339-364.

Gardner, W.D., K.R. Hinga and J. Marra (1983). Observations on the degradation of biogenic material in the deep ocean with implications on accuracy of sediment trap fluxes. *Journal of Marine Research*, **41**, 195-214.

Gardner, W.D., J.B. Southard, and C.D. Hollister (1985). Sedimentation and resuspension in the Northwest Atlantic. *Marine Geology*, **65**, 199-242.

Gardner, W.D., I.D. Walsh and M.-J. Richardson (1993). Biophysical forcing of particle production and distribution during a spring bloom in the North Atlantic. *Deep-Sea Research II*, **40**, 171-195.

Gardner, W.D., S.P. Chung, M.-J. Richardson and I.D. Walsh (1995). The oceanic mixed-layer-pump. *Deep-Sea Research II*, **42**, 757-775.

Garner, D.M. (1953). Physical characteristics of inshore surface waters between Cook Strait and Banks Peninsula. *New Zealand Journal of Science and Technology, Section B,* **35**, 239-246.

Garner, D.M. (1959). The Subtropical Convergence in New Zealand surface waters. *New Zealand Journal of Geology and Geophysics*, **2**, 315-337.

Garner, D.M. (1967). Hydrology of the southern Hikurangi trench. *New Zealand Oceanographic Institute Memoir*, **39**, 36p.

Gattuso, P.P., M. Pichon and M. Frankignoulle (1995). Biological control of air-sea CO_2 fluxes: effect of photosynthetic and calcifying marine organisms and ecosystems. *Marine Ecology Press Series,* **129**, 307-312.

Gieskes, W.W.C., G.W. Kraay and S.B. Tijssen (1978). Chlorophylls and their degradation products in the deep pigment maximum layer of the tropical north Atlantic. *Netherlands Journal of Sea Research*, **12**, 195-204.

Gilmour A.E. (1960). Currents in Cook Strait. *New Zealand Journal of Geology and Geophysics*, **3**, 410-431.

Gilmour, A.E. and A.G. Cole (1979). The Subtropical Convergence east of New Zealand. *New Zealand Journal of Marine and Freshwater Research*, **13**, 553-557.

Gooday, A.J. (1988). A response of benthic foraminifera to the deposition of phytodetritus in the deep sea. *Nature*, **332**, 70-73.

Gowing, M.M. and M.W. Silver (1985). Minipellets: a new and abundant size class of marine fecal pellets. *Journal of Marine Research*, **43**, 395-418.

Goyet, C., C. Beauverger, C. Brunet and A. Poisson (1991). Distribution of carbon dioxide partial pressure in surface waters of the Southwest Indian Ocean. *Tellus*, **43**, 1-11.

Graf, G. (1989). Benthic-pelagic coupling in a deep-sea benthic community. *Nature*, **341**, 437-439.

Grant, W.D. and O.S. Madsen (1986). The continental-shelf bottom boundary layer. *Annual Review of Fluid Mechanics*, **18**, 265-305.

Green, E.P., R.P Harris and A. Duncan (1992). The production and ingestion of faecal pellets by nauplii of marine calanoid copepods. *Journal of Plankton Research*, **14**, 1631-1643.

Greig, M.J. and A.E. Gilmour (1992). Flow through the Mernoo Saddle, New Zealand. *New Zealand Journal of Marine and Freshwater Research*, **26**, 155-165.

Griffiths, G.A. and G.P. Glasby (1985). Input of river-derived sediments to the New Zealand continental shelf, I. Mass. *Estuarine, Coastal and Shelf Science*, **21**, 773-787.

Gust, G., R.H. Byrne, R.E. Bernstein, P.R. Betzer and W. Bowles (1992). Particle fluxes and moving fluids: experience from synchronous trap collections in the Sargasso Sea. *Deep-Sea Research*, **39**, 1071-1083.

Gust, G., A.F. Michaels, R. Johnson, W.G. Deuser and W. Bowles (1994). Mooring line motions and sediment trap hydromechanics: *in situ* intercomparison of three common deployment designs. *Deep-Sea Research*, **41**, 831-857.

Hall, J. A., D. P. Barrett and M. R. James (1993). The importance of phytoflagellate, heterotrophic flagellate and ciliate grazing on bacteria and picophytoplankton sized prey in a coastal marine environment. *Journal of Plankton Research*, **15**, 1075-1086.

Hallegraeff, G.M. and S.W. Jeffrey (1985). Description of new chlorophyll *a* alteration products in marine phytoplankton. *Deep-Sea Research*, **32**, 697-705.

Hansen, D.A. and J.A. Newton (1994). Design and evaluation of a "swimmer"-segregating particle interceptor trap. *Limnology and Oceanography*, **39**, 1487-1495.

Harbison, G.R. and R.W. Gilmer (1986). The feeding rates of the pelagic tunicate *Pegea confederata* and two other salps. *Limnology and Oceanography*, **21**, 517-528.

Hargrave, B.T. (1985). Particle sedimentation in the ocean. *Ecological Modelling*, **30**, 229-246.

Hargrave, B.T. and N.M. Burns (1979). Assessment of sediment trap collection efficiency. *Limnology and Oceanography*, **24**, 1124-1137.

Hargrave B., G. Siddall, G. Steeves and G. Awalt (1994). A current-activated sediment trap. *Limnology and Oceanography*, **39**, 383-390.

Harris, T.F.W. (1990). Greater Cook Strait: Form and flow. DSIR Marine and Freshwater, Wellington, 212p.

Hawley, N. (1988). Flow in cylindrical sediment traps. *Journal of Great Lakes Research*, **14**, 76-88.

Head, E.J.H. and L.R. Harris (1994). Feeding selectivity by copepods grazing on natural mixtures of phytoplankton determined by HPLC analysis of pigments. *Marine Ecology Progress Series*, **110**, 75-83.

Head, E.J.H. and L.R. Harris (1996). Chlorophyll destruction by *Calanus* spp. grazing on phytoplankton: kinetics, effects of ingestion rate and feeding history, and a mechanistic interpretation. *Marine Ecology Progress Series*, **135**, 223-235.

Head, E.J.H and E.P.W. Horne (1993). Pigment transformations and vertical flux in an area of convergence in the North Atlantic. *Deep-Sea Research I*, **40**, 329-346.

Head, E.J.H., B.T. Hargrave and D.V. Subba Rao (1994). Accumulation of a pheophorbide *a*-like pigment in sediment traps during late stages of a spring bloom: a product of dying algae? *Limnology and Oceanography*, **39**, 176-181.

Heath R.A. (1968). Geostrophic currents derived from oceanic density measurements north and south of the Subtropical Convergence east of New Zealand. *New Zealand Journal of Marine and Freshwater Research*, **2**, 659-677.

Heath, R.A. (1971). Hydrology and circulation in central and southern Cook Strait, New Zealand. *New Zealand Journal of Marine and Freshwater Research*, **5**, 178-199.

Heath R.A. (1972). The Southland current. *New Zealand Journal of Marine and Freshwater Research*, **6**, 497-533.

Heath R.A. (1973). Low cloud boundaries coincident with oceanic convergences. *New Zealand Journal of Marine and Freshwater Research*, **7**, 209-216.

Heath R.A. (1975). Oceanic circulation and hydrology off the southern half of the South Island, New Zealand. *New Zealand Oceanography Institute Memoir*, **72**, 36p.

Heath R.A. (1976). Models of the diffusive-advective balance at the Subtropical Convergence. *Deep-Sea Research*, **23**, 1153-1164.

Heath, R.A. (1977). Circulation and hydrography of Wellington Harbour. *New Zealand Oceanographic Institute Oceanographic Summary*, **12**, 8p.

Heath R.A. (1981). Physical oceanography of the waters over the Chatham Rise. *New Zealand Oceanographic Institute Oceanographic Summary,* **18**, 15p.

Heath, R.A. (1983). Observations of Chatham Rise currents. *New Zealand Journal of Marine and Freshwater Research*, **17**, 321-330.

Heath R.A. (1984). Summary of current observations from the Chatham Rise (SO-17 Cruise). *Geologisches Jahrbuch*, **D65**, 25-26.

Heath, R.A. (1985). A review of the physical oceanography of the seas around New Zealand - 1982. *New Zealand Journal of Marine and Freshwater Research*, **19**, 79-124.

Heath. R.A. (1986). In what direction is the mean flow through Cook Strait - evidence of 1 to 4 week variability? *New Zealand Journal of Marine and Freshwater Research*, **20**, 119-137.

Heath, R.A. and J.M. Bradford (1980). Factors affecting phytoplankton production over the Campbell Plateau, New Zealand. *Journal of Plankton Research*, **2**, 169-181.

Heathershaw, A.D. (1981). Comparisons of measured and predicted sediment transport rates in tidal currents. *Marine Geology*, **42**, 75-104.

Hedges, J.I. and J.H. Stern (1984). Carbon and nitrogen determinations of carbonate-containing solids. *Limnology and Oceanography*, **29**, 657-663.

Hedges, J.I., C. Lee, S.G. Wakeham, P.J. Hernes and M.L. Peterson (1993). Effects of poisons and preservatives on the fluxes and elemental compositions of sediment trap materials. *Journal of Marine Research*, **51**, 651-668.

Heiskanen, A.-S. (1995). Contamination of sediment trap fluxes by vertically migrating phototrophic micro-organisms in the coastal Baltic Sea. *Marine Ecology Press Series.* **122**, 45-58.

Hesshaimer, V., M. Heimann and I. Levin (1994). Radiocarbon evidence for a smaller oceanic carbon dioxide sink than previously believed. *Nature*, **370**, 201-203.

Heussner S., C. Ratti and J. Carbonne (1990). The PPS 3 time-series sediment trap and the sample processing techniques used during the ECOMARGE experiment. *Continental Shelf Research*, **10**, 943-958.

Hinga K.R., J. McN. Sieburth and G.R. Heath (1979). The supply and use of organic material at the deep-sea floor. *Journal of Marine Research*, **37**, 557-579.

Hofmann, E.E., J.M. Klinck and G.-A. Paffenhöfer (1981). Concentrations and vertical fluxes of zooplankton fecal pellets on a continental shelf. *Marine Biology*, **61**, 327-335.

Honjo, S. (1978). Sedimentation of materials in the Sargasso Sea at a 5,367 m deep station. *Journal of Marine Research*, **36**, 469-492.

Honjo, S. (1980). Material fluxes and modes of sedimentation in the mesopelagic and bathypelagic zones. *Journal of Marine Research*, **38**, 53-97.

Honjo, S. and K.W. Doherty (1988). Large aperture time-series sediment traps; design objectives, construction and application. *Deep-Sea Research*, **35**, 133-149.

Honjo, S. and S.J. Manganini (1993). Annual biogenic particle fluxes to the interior of the North Atlantic Ocean, studied at 34°N 21°W and 48°N 21°W. *Deep-Sea Research*, **40**, 587-607.

Honjo, S. and M.R. Roman (1978). Marine copepod fecal pellets: production, preservation and sedimentation. *Journal of Marine Research*, **36**, 45-57.

Honjo, S., J.F. Connell and P.L. Sachs (1980). Deep-ocean sediment trap; design and function of PARFLUX Mark II. *Deep-Sea Research*, **27**, 745-753.

Honjo, S., S.J. Manganini and J.J. Cole (1982a). Sedimentation of biogenic matter in the deep ocean. *Deep-Sea Research*, **29**, 609-625.

Honjo, S., S.J. Manganini and L.J. Poppe (1982b). Sedimentation of lithogenic particles in the deep ocean. *Marine Geology*, **50**, 199-220.

Honjo S., K.W. Doherty, Y.C. Agrawal and V.L. Asper (1984). Direct optical assessment of large amorphous aggregates (marine snow) in the deep ocean. *Deep-Sea Research*, **31**, 67-76.

Honjo, S., D.W. Spencer and W.D. Gardner (1992). A sediment trap intercomparison experiment in the Panama Basin, 1979. *Deep-Sea Research*, **39**, 333-358.

Honjo, S., J. Dymond, R. Collier and S.J. Manganini (1995). Export production of particles to the interior of the equatorial Pacific Ocean during the 1992 EqPac experiment. *Deep-Sea Research II*, **42**, 831-870.

Hurd, D.C. and D.W. Spencer, editors, (1991). *Marine particles: analysis and characterization, Geophysical Monograph*, **63**, American Geophysical Union, Washington, D.C., 472p.

Inoue, H. and Y. Sugimura (1988). Distribution and variations of oceanic carbon dioxide in the western North Pacific, eastern Indian and Southern Ocean, south of Australia. *Tellus*, **40**, 308-320.

Iseki, K., F. Whitney and C.S. Wong (1980). Biochemical changes of sediment matter in sediment trap in shallow coastal waters. *Bulletin of the Plankton Society of Japan*, **27**, 27-36.

Iturriaga, R. (1979). Bacterial activity related to sedimenting particulate matter. *Marine Biology*, **55**, 157-169.

Iverson, R.L. and W.E. Esaias (1995). Global ocean primary and export particulate organic carbon production determined using CZCS data. *EOS, Transactions of American Geophysical Union, April*, S185.

Jacobsen T.R. and F. Azam (1984). Role of bacteria in copepod fecal pellet decomposition: colonization, growth rates and mineralization. *Bulletin of Marine Science*, **35**, 495-502.

Jannasch H.W., O.C. Zafiriou and J.W. Farrington (1980). A sequencing sediment trap for time-series studies of fragile particles. *Limnology and Oceanography*, **25**, 939-943.

Jahnke, R.A. (1996). The global ocean flux of particulate organic carbon: areal distribution and magnitude. *Global Biogeochemical Cycles*, **10**, 71-88.

James, M.R. and J.A. Hall (1997). Microzooplankton grazing in different water masses associated with the Subtropical Convergence off the South Island, New Zealand. *Deep-Sea Research II.*

Jeffrey, M.Z. (1986). Climatological features of the Subtropical Convergence in Australian and New Zealand waters. *Ocean Sciences Institute Report*, **17**, The University of Sydney, New South Wales, 56p.

JGOFS Report 6 (1990). *Joint Global Ocean Flux Study Core Measurement Protocols - Reports of the Core Measurement Working Groups*, Scientific Committee on Oceanic Research, 40p.

JGOFS Report 29 (1994). *Protocols for the Joint Global Ocean Flux Study (JGOFS) Core Measurements*, Scientific Committee on Oceanic Research, 170p.

Jickells, T.D., W.G. Deuser and A.H. Knap (1984). The sedimentation rates of trace elements in the Sargasso Sea measured by sediment trap. *Deep-Sea Research*, **31**, 1169-1178.

Jickells, T.D., P.P. Newton, P. King, R.S. Lampitt and C. Boutle (1991). A comparison of sediment trap records of particle fluxes from 19 to 48°N in the northeast Atlantic and their relation to surface water productivity. *Deep-Sea Research I*, **43**, 971-986.

Jillett, J.B. (1968). *Calanus tonsus* (Copepoda Calanoida) in southern New Zealand waters with notes on the male. *Australian Journal of Marine and Freshwater Research*, **19**, 19-30.

Jillett, J.B. (1969). Seasonal hydrography of waters off the Otago Peninsula, southeastern New Zealand. *New Zealand Journal of Marine and Freshwater Research*, **3**, 349-375.

Jumars, P.A. and R.A. Wheatcroft (1989). Responses of benthos to changing food quality and quantity, with a focus on deposit feeding and bioturbation. In: *Productivity of the Ocean: Present and Past*, W.H. Berger, V.S. Smetacek and G. Wefer, editors, J. Wiley and Sons, New York, 235-253.

Kamykowski, D. and S.-J. Zentara (1989). Circumpolar plant nutrient covariation in the Southern Ocean: patterns and processes. *Marine Ecology Progress Series*, **58**, 101-111.

Karl, D.M. and G.A. Knauer (1984a). Vertical distribution, transport, and exchange of carbon in the northeast Pacific Ocean: evidence for multiple zones of biological activity. *Deep-Sea Research*, **31**, 221-243.

Karl, D.M. and G.A. Knauer (1984b). Detritus-microbe interactions in the marine pelagic environment: selected results from the VERTEX experiment. *Bulletin of Marine Science*, **35**, 550-565.

Karl, D.M. and G.A. Knauer (1989). Swimmers: a recapitulation of the problem and a potential solution. *Oceanography*, **2**, 32-35.

Karl, D.M., C.D. Winn, D.V.W. Hebel and R. Letelier, compilers, (1990). Chapter 18 - Sediment trap protocols. In: *Hawaii Ocean Time-series Program field and laboratory protocols, September, 1990*, 66-69.

Karl, D.M., J.E. Dore, D.V. Hebel and C. Winn (1991a). Particulate C, N, P and total mass analysis in US-JGOFS HOT. In: *Marine particles: analysis and characterization*, D.C. Hurd and D.W. Spencer, editors, *Geophysical Monograph*, **63**, American Geophysical Union, Washington, D.C., 71-77.

Karl, D.M., B.D. Tilbrook and G. Tien (1991b). Seasonal coupling of organic matter production and particle flux in the western Bransfield Strait, Antarctica. *Deep-Sea Research*, **38**, 1097-1126.

Karl, D.M., R. Letelier, D. Hebel, L. Tupas, J. Dore, J. Christian and C. Winn (1995). Ecosystem changes in the North Pacific subtropical gyre attributed to the 1991-92 El Niño. *Nature*, **373**, 230-234.

Karl, D.M., J.R. Christian, J.E. Dore, D.V. Hebel, R.M. Letelier, L.M. Tupas and C.D. Winn (1996). Seasonal and interannual variability in primary production and particle flux at Station ALOHA. *Deep-Sea Research II*, **43**, 539-568.

Keeling, C.D. and M. Heimann (1986). Meridional eddy diffusion model of the transport of atmospheric carbon dioxide: 2. Mean annual carbon cycle. *Journal of Geophysical Research*, **91**, 7782-7796.

Keeling, C.D., S.C. Piper and M. Heimann (1989). A three-dimensional model of atmospheric CO_2 transport based on observed winds: 4. Mean annual gradients and interannual variations. In: *Aspects of climate variability in the pacific and the western Americas*, D.H. Peterson, editor, *American Geophysical Monograph*, **55**, 305-363.

Keeling, F.R. and S.R. Shertz (1992). Seasonal and interannual variations in atmospheric oxygen and implications for the global carbon cycle. *Nature*, **358**, 723-727.

Kiørboe, T., J.L.S. Hansen, A.L. Alldredge, G.A. Jackson, U. Passow, H.G. Dam, D.T. Drapeau, A. Waite and C.M. Garcia (1996). Sedimentation of plankton during a diatom bloom: Rates and mechanisms. *Journal of Marine Research*, **54**, 1123-1148.

Klein, B., W.W.C. Gieskes and G.G. Kraay (1986). Digestion of chlorophylls and carotenoids by the marine protozoan *Oxyrrhis marina* studied by h.p.l.c. analysis of algal pigments. *Journal of Plankton Research*, **8**, 827-836.

Kleppel G.S. and R.E. Pieper (1984). Phytoplankton pigments in the gut contents of planktonic copepods from coastal waters off southern California. *Marine Biology*, **78**, 193-198.

Kleppel, G.S., D.V. Holliday and R.E. Pieper (1991). Trophic interactions between copepods and microzooplankton: a question about the role of diatoms. *Limnology and Oceanography*, **36**, 172-178.

Knauer, G.A. (1991). Determination of mass flux, inorganic and organic C and N flux in rapidly sinking particles. In: *Marine particles: analysis and characterization*, D.C. Hurd and D.W. Spencer, editors, *Geophysical Monograph*, **63**, American Geophysical Union, Washington, D.C., 79-82.

Knauer, G.A., J.H. Martin and K.W. Bruland (1979). Fluxes of particulate carbon, nitrogen, and phosphorus in the upper water column of the northeast Pacific. *Deep-Sea Research*, **26A**, 97-108.

Knauer, G.A., D.M. Karl, J.H. Martin and C.N. Hunter (1984). *In situ* effects of selected preservatives on total carbon, nitrogen and metals collected in sediment traps. *Journal of Marine Research*, **42**, 445-462.

Knauer, G.A., D.G. Redalje, W.G. Harrison and D.M. Karl (1990). New production at the VERTEX time-series site. *Deep-Sea Research*, **37**, 1121-1134.

Knox, G.A. (1994). The biology of the Southern Ocean. *Studies in Polar Research*, Cambridge University Press, Cambridge, 444p.

Krause, D.C. (1966). Geology and geomagnetism of the Bounty region east of the South Island, New Zealand. *New Zealand Oceanographic Institute Memoir*, **30**, 32p.

Krause, N.C. (1987). Application of portable traps for obtaining point measurements of sediment transport rates in the surf zone. *Journal of Coastal Research*, **3**, 139-152.

Kremling, K. and P. Streu (1993). Saharan dust influenced trace element fluxes in deep North Atlantic subtropical waters. *Deep-Sea Research I*, **40**, 1155-1168.

Khripounoff, A. and P. Crassous (1994). Particulate material degradation in sediment traps at 2000 m depth on the Meriadzeck terrace (Bay of Biscay). *Deep-Sea Research*, **41**, 821-829.

Kustanowich, S. (1963). Distribution of planktonic foraminifera in surface sediments of the South-west Pacific Ocean. *New Zealand Journal of Geology and Geophysics*, **6**, 534-565.

Lampitt, R.S. (1985). Evidence for the seasonal deposition of detritus to the deep-sea floor and its subsequent resuspension. *Deep-Sea Research*, **32**, 885-897.

Lampitt, R.S., T. Noji and B. von Bodungen (1990). What happens to zooplankton faecal pellets? Implications for material flux. *Marine Biology*, **104**, 15-23.

Landry, M.R., W.K. Peterson and C. C. Andrews (1992). Particulate flux in the water column overlying Santa Monica Basin. *Progress in Oceanography*, **30**, 167-195.

Landry, M.R., C.J. Lorenzen and W.K. Peterson (1994). Mesozooplankton grazing in the Southern California Bight. II. Grazing impact and particulate flux. *Marine Ecology Progress Series*, **115**, 73-85.

Landry, M.R., W.K. Peterson and C.J. Lorenzen (1995). Zooplankton grazing, phytoplankton growth, and export flux: inferences from chlorophyll tracer methods. *ICES Journal of Marine Science*, **52**, 337-345.

Lau, Y.L. (1979). Laboratory study of cylindrical sedimentation traps. *Journal of Fisheries Research Board of Canada*, **36**, 1288-1291.

Lee, B.-G. and N.S. Fisher (1992). Degradation and elemental release rates from phytoplankton debris and their geochemical implications. *Limnology and Oceanography*, **37**, 1345-1360.

Lee, C. and S.G. Wakeham (1989). Organic matter in seawater: Biogeochemical processes. In: *Chemical Oceanography*, **9**, J.P. Riley, editor, Academic Press Ltd, 1-51.

Lee, C., J.A. McKenzie and M. Sturm (1987). Carbon isotope fractionation and changes in the flux and composition of particulate matter resulting from biological activity during a sediment trap experiment in Lake Greifen, Switzerland. *Limnology and Oceanography*, **32**, 83-96.

Lee, C., S.G. Wakeham and J.I. Hedges (1988). The measurement of oceanic particle flux - are "swimmers" a problem? *Oceanography*, **1**, 34-36.

Lee, C., J.I. Hedges, S.G. Wakeham and N. Zhu (1992). Effectiveness of various treatments in retarding microbial activity in sediment trap material and their effects on the collection of swimmers. *Limnology and Oceanography*, **37**, 117-130.

Legendre, L. (1990). The significance of microalgal blooms for fisheries and for the export of particulate organic carbon in the oceans. *Journal of Plankton Research*, **12**, 681-699.

Legendre, L. and J. le Fèvre (1989). Hydrodynamical singularities as controls of recycled versus export production in oceans. In: *Productivity of the Ocean: Present and Past*, W.H. Berger, V.S. Smetacek and G. Wefer, editors, J. Wiley and Sons, New York, 49-63.

Lenz, J., A. Morales and J. Gunkel (1993). Mesozooplankton standing stock during the North Atlantic spring bloom study in 1989 and its potential grazing pressure on phytoplankton: a comparison between low, medium and high latitudes. *Deep-Sea Research II*, **40**, 559-572.

Letelier, R.M., R.R. Bidigare, D.V. Hebel, M.E. Ondrusek, C.D. Winn and D.M. Karl (1993). Temporal variability of phytoplankton community structure at the U.S.-JGOFS time-series Station ALOHA (22°45'N, 158°00'W) based on HPLC pigment analysis. *Limnology and Oceanography*, **38**, 1420-1437.

Lewis, K.B. (1994). The 1500-km long Hikurangi Channel: trench-axis channel that escapes its trench, crosses a plateau, and feeds a fan drift. *Geo-Marine Letters*, **14**, 19-28.

Lewis, K.B. and L. Carter (1976). Depths, sediments and faulting on each side of the Rongotao Isthmus, Wellington. *New Zealand Oceanographic Institute Oceanographic Summary*, **11**, 31p.

Lewis, K.B. and J.R. Pettinga (1993). The emerging, imbricate frontal wedge of the Hikurangi margin. In: *South Pacific Sedimentary Basins, Sedimentary Basins of the World*, **2**, P.B. Ballance, editor, Elsevier Science Publishers, 225-250.

Lewis, K.B., D.J. Bennett, R.H. Herzer and C.C. von der Borch (1985). Seismic stratigraphy and structure adjacent to an evolving plate boundary, western Chatham Rise, New Zealand. In: *Initial reports of the Deep Sea Drilling Project, Leg 90*, J.P. Kennett, C.C. von der Borch, and others, U.S. Government Printing Office, Washington D.C., 1325-1337.

Llewellyn C.A. and R.F.C. Mantoura (1996). Pigment biomarkers and particle carbon in the upper water column compared to the ocean interior of the northeast Atlantic. *Deep-Sea Research*. **43**, 1165-1184.

Lochte, K., H.W. Ducklow, M.J.R. Fasham and C. Stienen (1993). Plankton succession and carbon cycling at 47°N 20°W during the JGOFS North Atlantic Bloom Experiment. *Deep-Sea Research II*, **40**, 91-114.

Lohrenz, S.E., G.A. Knauer, V.L. Asper, M. Tuel, A.F. Michaels and A.H. Knap (1992). Seasonal variability in primary production and particle flux in the northwestern Sargasso Sea: U.S. JGOFS Bermuda Atlantic Time-series Study. *Deep-Sea Research*, **39**, 1373-1391.

Longhurst, A. and R. Williams (1992). Carbon flux by seasonal vertical migrant copepods is a small number. *Journal of Plankton Research*, **14**, 1495-1509.

Longhurst A., S. Sathyendranath, T. Platt and C. Caverhill (1995). An estimate of global primary production in the ocean from satellite radiometer data. *Journal of Plankton Research*, **17**, 1245-1271.

Longhurst, A.R. (1991). Role of the marine biosphere in the global carbon cycle. *Limnology and Oceanography,* **36**, 1507-1526

Longhurst, A.R. (1995). Seasonal cycles of pelagic production and consumption. *Progress in Oceanography*, **36**, 77-167.

Longhurst, A.R. and W.G. Harrison (1989). The biological pump: Profiles of plankton production and consumption in the upper ocean. *Progress in Oceanography,* **22**, 47-123.

Longhurst, A.R., A. Bedo, W.G. Harrison, E.J.H. Head, E.P. Horne, B. Irwin and C. Morales (1989). NFLUX: a test of vertical nitrogen flux by diel migrant biota. *Deep-Sea Research*, **36**, 1705-1719.

Lopez, M.D.G., M.E. Huntley and P.F. Sykes (1988). Pigment destruction by *Calanus pacificus*: impact on the estimation of water column fluxes. *Journal of Plankton Research*, **10**, 715-734.

Lorenzen, C.J. and J. Newton Downs (1986). The specific absorption coefficients of chlorophyllide *a* and pheophorbide *a* in 90% acetone, and comments on the fluorometric determination of chlorophyll and pheopigments. *Limnology and Oceanography*, **31**, 44-452.

Lorenzen, C.J. and N.A. Welschmeyer (1983). The *in situ* sinking rates of herbivore fecal pellets. *Journal of Plankton Research*, **5**, 929-933.

Lorenzen, C.J., F.R. Shuman and J.T. Bennett (1981). In situ calibration of a sediment trap. *Limnology and Oceanography*, **26**, 580-585.

Lorenzen, C.J., N.A. Welschmeyer and A.E. Copping (1983a). Particulate organic carbon flux in the subarctic Pacific. *Deep-Sea Research*, **30**, 639-643.

Lorenzen, C.J., N.A. Welschmeyer, A.E. Copping and M. Vernet (1983b). Sinking rates of organic particles. *Limnology and Oceanography*, **28**, 766-769.

Ludwig, W., J-L. Probst and S. Kempe (1996). Predicting the oceanic input of organic carbon by continental erosion. *Global Biogeochemical Cycles*, **10**, 23-41.

Lund-Hansen, L.C., M Pejrup, J. Valeur and A. Jensen (1994). Eddy diffusion coefficients of suspended particulate matter: Effects of wind energy transfer and stratification. *Estuarine, Coastal and Shelf Science*, **38**, 559-568.

Mantoura, R.F.C. and C.A. Llewellyn (1983). The rapid determination of algal chlorophyll and carotenoid pigments and their breakdown products in natural waters by reverse-phase high-performance liquid chromatography. *Analytica Chimica Acta*, **151**, 297-314.

McCartney, M.S. (1977). Subantarctic mode water. *Deep-Sea Research*, **24**, 103-119.

McCave, I.N. (1975). Vertical flux of particles in the ocean. *Deep-Sea Research*, **22**, 491-502.

McCave, I.N. (1984a). Erosion, transport and deposition of fine-grained marine sediments. In: *Fine-grained sediments: deep-water processes and facies*, Stow, D.A.V. and D.J.W. Piper, editors, Blackwell Scientific Publications, 35-69.

McCave, I.N. (1984b). Size spectra and aggregation of suspended particles in the deep ocean. *Deep-Sea Research*, **31**, 329-353.

McDougall, J.C. (1975). Cook sediments. *New Zealand Oceanographic Institute Chart, Oceanic Series, 1:1 000 000.*

McDougall, J.C. (1982). Bounty sediments. *New Zealand Oceanographic Institute Chart, Oceanic Series, 1:1 000 000.*

Martin, J.H., G.A. Knauer, D. M. Karl and W. W. Broenkow (1987). VERTEX: carbon cycling in the northeast Pacific. *Deep-Sea Research*, **34**, 267-285.

Martin, J.H., S.E. Fitzwater, R. M. Gordon, C. N. Hunter and S. J. Tanner (1993). Iron, primary production and carbon-nitrogen flux studies during the JGOFS North Atlantic Bloom Experiment. *Deep-Sea Research*, **40**, 115-134.

Méjanelle, L., J. Laureillard, J. Fillaux, A. Saliot and C. Lambert (1995). Winter distribution of algal pigments in small- and large-size particles in the northeastern Atlantic. *Deep-Sea Research I*, **42**, 117-133.

Metzl, N., C. Beauverger, C. Brunet, C. Goyet and A. Poisson (1991). Surface water carbon dioxide in the southwest Indian sector of the Southern Ocean: a highly variable CO_2 source/sink region in summer. *Marine Chemistry*, **35**, 85-95.

Meyer, K.W. and D.V. Toan (1984). Chatham Rise phosphorite investigation (SONNE-17 cruise): soil mechanic properties and implications for mining. *Geologisches Jahrbuch*, **D65**, 195-208.

Michaels, A.F. and M.W. Silver (1988). Primary production, sinking fluxes and the microbial food web. *Deep-Sea Research*, **35**, 473-490.

Michaels, A.F. and A.H. Knap (1996). Overview of the U.S. JGOFS Bermuda Atlantic Time-series Study and the Hydrostation S program. *Deep-Sea Research II*, **43**, 157-198.

Michaels, A.F., M.W. Silver, M.M. Gowing and G.A. Knauer (1990). Cryptic zooplankton "swimmers" in upper ocean sediment traps. *Deep-Sea Research*, **37**, 1285-1296.

Michaels, A.F., N.R. Bates, K.O. Buesseler, C.A. Carlson and A.H. Knap (1994). Carbon-cycle imbalances in the Sargasso Sea. *Nature*, **372**, 537-540.

Miller, M.C., I.N. McCave and P.D. Komar (1977). Threshold of sediment motion under unidirectional currents. *Sedimentology*, **24**, 507-527.

Millero, F.J. (1995). Thermodynamics of the carbon dioxide system in the oceans. *Geochimica et Cosmochimica Acta*, **59**, 661-677.

Monaco, A., T Courp, S Heussner, J Carbonne and S.W. Fowler (1990). Seasonality and composition of particulate fluxes during ECOMARGE-I, western Gulf of Lions. *Continental Shelf Research*, **10**, 959-987.

Moore, W.S. and J. Dymond (1988). Correlation of ^{210}Pb removal with organic carbon fluxes in the Pacific Ocean. *Nature*, **331**, 339-341.

Moore, W.S., K.W. Bruland and J. Michel (1981). Fluxes of uranium and thorium series isotopes in the Santa Barbara Basin. *Earth and Planetary Science Letters*, **53**, 391.

Murdoch R.C., R. Guo and A. McCrone (1990). Distribution of hoki (*Macruronus novaezelandiae)* eggs and larvae in relation to hydrography in eastern Cook Strait, September 1987. *New Zealand Journal of Marine and Freshwater Research*, **24**, 529-539.

Murnane, R.J., J.K. Cochran, K.O. Buesseler and M.P. Bacon (1996). Least-squares estimates of thorium, particle and nutrient cycling rate constants from JGOFS North Atlantic Bloom experiment. *Deep-Sea Research I*, **43**, 239-258.

Murphy, P.P., R.A. Feely, R.H. Gammon, D.E. Harrison, K.C. Kelly and L. Waterman (1991). Assessment of the air-sea exchange of CO_2 in the South Pacific during austral autumn. *Journal of Geophysical Research*, **96**, 20 455-20 465.

Murray, J.W., E. Johnson and C. Garside (1995). A. U.S. JGOFS Process study in the equatorial Pacific (EqPac). *Deep-Sea Research*, **42**, 275-293.

Nair, R.R., V. Ittekkot, S.J. Manganini, V. Ramaswamy, B. Haake, E.T. Degens, B.M. Desai and S. Honjo (1989). Increased particle flux to the deep ocean related to monsoons. *Nature*, **338**, 749-751.

Nelson, J.R. (1989). Phytoplankton pigments in macrozooplankton feces: variability in carotenoid alterations. *Marine Ecology Progress Series*, **52**, 129-144.

Nelson, J.R. (1993). Rates and possible mechanism of light-dependent degradation of pigments in detritus derived from phytoplankton. *Journal of Marine Research*, **51**, 155-179.

Nelson, J.R., J.R Beers, R.W. Eppley, G.A. Jackson, J.J. McCarthy and A. Soutar (1987). A particle flux study in the Santa Monica-San Pedro Basin off Los Angeles: particle flux, primary production, and transmissometer survey. *Continental Shelf Research*, **7**, 307-328.

Neveux, J. and M. Panouse (1987). Spectrofluorometric determination of chlorophylls and pheophytins. *Archiv für Hydrobiologie*, **109**, 567-581.

Newton, P.P., R.S. Lampitt, T.D. Jickells, P. King and C. Boutle (1994). Temporal and spatial variability of biogenic particle fluxes during the JGOFS northeast Atlantic process studies at 47°N, 20°W. *Deep-Sea Research I*, **41**, 1617-1642.

Noji, T.T. (1991). The influence of macrozooplankton on vertical particulate flux. *Sarsia*, **76**, 1-9.

Noji, T.T., K. W. Estep, F. MacIntyre and F. Norrbin (1991). Image analysis of faecal material grazed upon by three species of copepods: evidence for coprorhexy, coprophagy and coprochaly. *Journal of the Marine Biological Association of the U.K.*, **71**, 465-480.

Nodder, S.D., compiler, and others (1994a). *Field and laboratory protocols - NIWA Carbon Flux Research Voyage 3009, 12 June-4 July, 1993.*

Nodder, S.D., compiler, and others (1994b). *Field and laboratory protocols - NIWA Carbon Flux Research Voyage 3014, 1-22 October, 1993.*

Nodder, S.D. (in press). Short-term sediment trap fluxes from Chatham Rise, Southwest Pacific Ocean. *Limnology and Oceanography.*

Nodder, S.D. and B.L. Alexander (1997). Sources of variability in geographical and seasonal differences in particulate fluxes from short-term sediment trap deployments, east of New Zealand. *Deep-Sea Research II.*

Nodder, S.D. and M. Gall (submitted). Pigment fluxes within the Subtropical Convergence region, east of New Zealand: Relationships to planktonic community structure. *New Zealand Journal of Marine and Freshwater Research.*

Norris, R.M. (1964). Sediments of the Chatham Rise. *New Zealand Oceanographic Institute Memoir*, **26**, 39p.

Nöthig, E-M. and B. von Bodungen (1989). Occurrence and vertical flux of faecal pellets of probably protozoan origin in the southeastern Weddell Sea (Antarctica). *Marine Ecology Progress Series*, **56**, 281-289.

Olson, D.B., G.L. Hitchcock, A.J. Mariano, C.J. Ashjian, G. Peng, R.W. Nero and G.P. Podestá (1994). Life on the edge: marine life and fronts. *Oceanography*, **7**, 52-60.

Pace, M.L., G.A. Knauer, D.M. Karl and J.H. Martin (1987). Primary production, new production and vertical flux in the eastern Pacific Ocean. *Nature*, **325**, 803-804.

Parsons, T.R., M. Takahashi and B. Hargrave (1984). *Biological Oceanographic Processes* (3rd edition), Pergamon Press, 330p.

Pasho, D.W. (1976). Distribution and morphology of Chatham Rise phosphorites. *New Zealand Oceanographic Institute Memoir*, **77**, 28p.

Passow, U. and R. Peinert (1993). The role of plankton in particle flux: two case studies from the northeast Atlantic. *Deep-Sea Research*, **40**, 573-585.

Pasternak, A.F. and A.V. Drits (1988). Possible degradation of chlorophyll-derived pigments during gut passage of herbivorous copepods. *Marine Ecology Progress Series*, **49**, 187-190.

Paterson S.L. and T. Whitworth (1990). Physical Oceanography. In: *Antarctic sector of the Pacific*, G.P. Glasby, editor, Elsevier Oceanography Series, Amsterdam, 55-93.

Peinert, R. and J.-C. Miquel (1994). The significance of frontal processes for vertical particle fluxes: A case study in the Alboran Sea (SW Mediterranean Sea). *Journal of Marine Systems*, **5**, 377-389.

Pennington, W. (1974). Seston and sediment formation in five Lake District lakes. *Journal of Ecology*, **62**, 215-251.

Peterson, B.J. (1981). Perspectives on the importance of oceanic particulate flux in the global carbon cycle. *Ocean Scientific Engineering*, **6**, 71-108.

Peterson, W. and H.G. Dam (1990). The influence of copepod "swimmers" on pigment fluxes in brine-filled vs. ambient seawater-filled sediment traps. *Limnology and Oceanography*, **35**, 448-455.

Peterson, M.L., P.J. Hernes, D.S. Thoreson, J.I. Hedges, C. Lee and S.G. Wakeham (1993). Field evaluation of a valved sediment trap. *Limnology and Oceanography*, **38**, 1741-1761.

Pfannkuche, O. and K. Lochte (1993). Open ocean pelago-benthic coupling: cyanobacteria as tracers of sediment trap faeces. *Deep-Sea Research I*, **40**, 727-737.

Pickrill, R.A. and R.G. Currie (1983). Computer programs to estimate wave generated orbital velocities and threshold erosion velocities. *Current Research, Part A, Geological Survey of Canada Paper 83-1A*, 253-261.

Pilskaln, C.H. and S. Honjo (1987). The fecal pellet fraction of biogeochemical particle fluxes to the deep sea. *Global Biogeochemical Cycles*, **1**, 31-48.

Platt, T. and W.G. Harrison (1985). Biogenic fluxes of carbon and oxygen in the ocean. *Nature*, **318**, 55-58.

Poisson, A., N. Metzl, C. Brunet, B. Schauer, B. Bres, D. Ruiz-Pino and F. Louanchi (1993). Variability of sources and sinks of CO_2 in the western Indian and Southern Oceans during the year 1991. *Journal of Geophysical Research*, **98**, 22759-22778.

Pollehne, F., B. Klein and B. Zeitzschel (1993). Low light adaption and export production in the deep chlorophyll maximum layer in the northern Indian Ocean. *Deep-Sea Research II*, **40**, 737-752.

Pond, S. and G.L. Pickard (1983). *Introductory dynamical oceanography* (2nd edition). Pergamon Press, 329p.

Probert, P.K. and D.G. McKnight (1993). Biomass of bathyal macrobenthos in the region of the Subtropical Convergence, Chatham Rise, New Zealand. *Deep-Sea Research I*, **40**, 1003-1007.

von Rad, U. and H-R. Kudrass, compilers, (1984). Geology of the Chatham Rise phosphorite deposits, east of New Zealand: results of a prospection cruise with R/V Sonne (1981). *Geologisches Jahrbuch*, **D65**, 252p.

Ratmeyer, V. and G. Wefer (1996). A high resolution camera system (ParCa) for imaging particles in the ocean: system design and a three-month deployment. *Journal of Marine Research*, **54**, 589-603.

Redfield, A.C., B.H. Ketchum and F.A. Richards (1963). The influence of organisms on the composition of sea-water. In: *The Sea, Volume 2*, M. N. Hill, editor, Interscience Publishers, John Wiley & Sons, 26-77.

Reimers, C.E. (1989). Control of benthic fluxes by particulate supply. In: *Productivity of the Ocean: Present and Past*, W.H. Berger, V.S. Smetacek and G. Wefer, editors, J. Wiley and Sons, New York, 217-233.

Repeta, D.J. and R.B. Gagosian (1984). Transformation reactions and recycling of carotenoids and chlorins in the Peru upwelling region (15°S, 75°W). *Geochimica et Cosmochimica Acta*, **48**, 1265-1277.

Reynolds, C.S., S. W. Wiseman and W.D. Gardner (1981). An annotated bibliography of aquatic sediment traps and trapping methods. *Occasional Publication*, **11**, Freshwater Biological Association, 54p.

Ridgway N.M. (1975). Hydrology of the Bounty Islands region. *New Zealand Oceanographic Institute, Memoir*, **75**, 27p.

Rivkin, R.B., L. Legendre, D. Deibel and 16 others (1996). Vertical flux of biogenic carbon in the ocean: is there food web control? *Science*, **272**, 1163-1166.

Robertson, J.E. and A.J. Watson (1993). Estimation of primary production by observation of changes in the mesoscale carbon dioxide field. *ICES Marine Science Symposium*, **197**, 207-214.

Robertson, D.A., P.E. Roberts and J.B. Wilson (1978). Mesopelagic faunal transition across the Subtropical Convergence east of New Zealand. *New Zealand Journal of Marine and Freshwater Research*, **12**, 295-312.

Rowan, K.S. (1989). Photosynthetic pigments of algae. Cambridge University Press, Cambridge.

Rowe, G.T. (1983). Biomass and production of the deep-sea macrobenthos. In: *Deep-sea biology*, G.T. Rowe, editor, Wiley, New York, 97-121.

Rowe, G.T. and W.D. Gardner (1979). Sedimentation rates in the slope water of the northwestern Atlantic Ocean measured directly with sediment traps. *Journal of Marine Research*, **37**, 581-600.

Safi, K.A. and J.A. Hall (in press). Factors influencing autotrophic and heterotrophic nanoflagellate abundance in five water masses surrounding New Zealand. *New Zealand Journal of Marine and Freshwater Research.*

Sarmiento, J.L. (1995). Modeling the oceanic uptake of anthropogenic carbon. *U.S. JGOFS Newsletter*, January, 1995.

Sarmiento, J.L. and E.T. Sundquist (1992). Revised budget for the oceanic uptake of anthropogenic carbon dioxide. *Nature*, **356**, 589-593.

Semtner, A.J., Jr. and R.M. Chervin (1992). Ocean general circulation from a global eddy-resolving model. *Journal of Geophysical Research*, **97(C4)**, 5493-5550.

Shanks, A.L. and E.W. Edmondson (1990). The vertical flux of metazoans (holoplankton, meiofauna, and larval invertebrates). due to their association with marine snow. *Limnology and Oceanography*, **35**, 455-463.

Shuman, F.R. and C.J. Lorenzen (1975). Quantitative degradation of chlorophyll by a marine herbivore. *Limnology and Oceanography*, **20**, 580-586.

Siegel, D.A., T.C. Granata, A.F. Michaels and T.D. Dickey (1990). Mesoscale eddy diffusion, particle sinking, and the interpretation of sediment trap data. *Journal of Geophysical Research*, **95**, 5305-5311.

Siegenthaler, U. and J.L. Sarmiento (1993). Atmospheric carbon dioxide and the ocean. *Nature*, **365**, 119-125.

Sievers H.A. and W.D. Nowlin, Jr. (1984). The stratification and water masses at Drake Passage. *Journal of Geophysical Research*, **89**, 10489-10514.

Silver, M.W. and M.M. Gowing (1991). The "Particle" Flux: origins and biological components. *Progress in Oceanography*, **26**, 75-113.

Singleton, R.J. (1993). CTD data from voyage 3009 West Coast South Island/Subtropical Convergence Carbon Flux, June 1993. *NIWA Marine, NZOI Biology Section Report*, **1993/3**, 81p.

Singleton, R.J. (1994). CTD data from voyage 3014 West Coast South Island/Subtropical Convergence Carbon Flux, October 1993. *NIWA Marine, NZOI Biology Section Report*, **1994/1**, 103p.

Small, L.F., S.W. Fowler and M.Y. Ünlü (1979). Sinking rates of natural copepod fecal pellets. *Marine Biology*, **51**, 233-241.

Smayda, T.J. (1969). Some measurements of the sinking rate of fecal pellets. *Limnology and Oceanography*, **14**, 621-625.

Smayda, T.J. (1970). The suspension and sinking of phytoplankton in the sea. *Oceanography and Marine Biology Annual Review*, **8**, 353-414.

Smetacek, V. (1985). Role of sinking in diatom life-history cycles: ecological, evolutionary and geological significance. *Marine Biology*, **84**, 239-251.

Smith, Jr., K.L., R.S. Kaufmann and R.J. Baldwin (1994). Coupling of near-bottom pelagic and benthic processes at abyssal depths in the eastern North Pacific Ocean. *Limnology and Oceanography*, **39**, 1101-1118.

Smith, R. and J.A. Hall (in press). Bacterial abundance and production in different water masses around South Island, New Zealand. *New Zealand Journal of Marine and Freshwater Research.*

SooHoo, J.B. and D.A. Kiefer (1982a). Vertical distribution of phaeopigments - I. A simple grazing and photooxidative scheme for small particles. *Deep-Sea Research*, **29**, 1539-1551.

SooHoo, J.B. and D.A. Kiefer (1982b). Vertical distribution of phaeopigments - II. Rates of production and kinetics of photooxidation. *Deep-Sea Research*, **29**, 1553-1563.

Soutar, A., S.A. Kling, P.A. Crill, E. Duffrin and K.W. Bruland (1977). Monitoring the marine environment through sedimentation. *Nature*, **266**, 136-139.

Sparks, R.J., D.C, Lowe, C.B. Taylor and G. Wallace (1989). Radiocarbon and tritium distributions in the waters of the Chatham Rise. *Institute of Nuclear Sciences (DSIR) INS-Report*, **412**.

Spencer, D.W., P.G. Brewer, A. Fleer, S. Honjo, S Krishnaswami and Y. Nozaki (1978). Chemical fluxes from a sediment trap experiment in the deep Sargasso Sea. *Journal of Marine Research*, **36**, 493-523.

Spitzer, W.S. and W.J. Jenkins (1989). Rates of vertical mixing, gas exchange and new production: estimates from seasonal gas cycles in the upper ocean near Bermuda. *Journal of Marine Research*, **47**, 169-196.

Stanton, B.R. (1973). Circulation along the eastern boundary of the Tasman Sea. In: *Oceanography of the South Pacific 1972*, R. Fraser, compiler, New Zealand National Commission for UNESCO, Wellington, 141-147.

Stanton, B.R. and N.M. Ridgway (1988). An oceanographic survey of the Subtropical Convergence zone in the Tasman Sea. *New Zealand Journal of Marine and Freshwater Research*, **22**, 583-593.

Staresinic, N., G.T. Rowe, D. Shaughnessey and A.J. Williams III (1978). Measurement of the vertical flux of particulate organic matter with a free-drifting sediment trap. *Limnology and Oceanography*, **23**, 559-563.

Staresinic, N., K. von Bröckel, N. Smodlaka and C.H. Clifford (1982). A comparison of moored and free-drifting sediment traps of two different designs. *Journal of Marine Science*, **40**, 273-292.

Stewart, R.B. and V.E. Neall (1984). Chronology of paleoclimatic change at the end of the last glaciation. *Nature*, **311**, 47-48.

Stocker, T.F., W.S. Broecker and D.G. Wright (1994). Carbon uptake experiments with a zonally-averaged global circulation model. *Tellus*, **46B**, 103-122.

Stoecker, D.K. (1984). Particle production by plankton ciliates. *Limnology and Oceanography*, **29**, 930-940.

Stramma, L., R.G. Peterson and M Tomczak (1995). The South Pacific Current. *Journal of Physical Oceanography*, **25**, 77-91.

Strickland, J.D.H. and T.R. Parsons (1972). A practical handbook of seawater analyses (2nd edition). *Fisheries Research Board of Canada Bulletin*, **167**, 310p.

Strom, S.L. (1993). Production of pheopigments by marine protozoa: results of laboratory experiments analysed by HPLC. *Deep-Sea Research I*, **40**, 57-80.

Strom, S.L. and N.A. Welschmeyer (1991). Pigment-specific rates of phytoplankton growth and microzooplankton grazing in the open subarctic Pacific Ocean. *Limnology and Oceanography*, **36**, 50-63.

Suess, E. (1980). Particulate organic carbon flux in the oceans - surface productivity and oxygen utilization. *Nature*, **288**, 260-263.

Sullivan, C. W., K. R. Arrigo, C. R. McClain, J. C. Comiso and J. Firestone (1993). Distributions of phytoplankton blooms in the Southern Ocean. *Science*, **262**, 1832-1837.

Sun, X. and A. McMinn (1994). Recent dinoflagellate cyst distribution associated with the Subtropical Convergence on the Chatham Rise, east of New Zealand. *Marine Micropaleontology*, **23**, 345-356.

Suzuki, K., N. Handa, H. Kiyosawa and J. Ishizaka (1995). Distribution of the prochlorophyte *Prochlorococcus* in the central Pacific Ocean as measured by HPLC. *Limnology and Oceanography*, **40**, 983-989.

Szymanska, K. and M. Tomczak (1994). Subduction of central water near the Subtropical Front in the southern Tasman Sea. *Deep-Sea Research*, **41**, 1373-1386.

Takahashi, T. and A.E.G. Azevedo (1982). The oceans as a CO_2 reservoir. In: *Interpretation of climate and photochemical models, ozone and temperature measurements*, R.A. Reck and J.R. Hummel, editors, *AIP Conference Proceedings*, **82**, 83-109.

Taniguchi, A. and S. Nishizawa (1971). Primary production in the sea area east of New Zealand in winter 1968. *Kaiyo Report*, **3**, 17-25.

Tans, P.P., I.Y. Fung and T. Takahashi (1990). Observational constraints on the global atmospheric CO_2 budget. *Science*, **247**, 1431-1438.

Taylor, G.T. (1989). Variability in the vertical flux of microorganisms and biogenic material in the epipelagic zone of a North Pacific central gyre station. *Deep-Sea Research*, **36**, 1287-1308.

Thunell, R.C., C.H. Pilskaln, E. Tappa and L. Reynolds-Sautter (1994). Temporal variability in sediment fluxes in the San Pedro Basin, Southern California Bight. *Continental Shelf Research*, **14**, 333-352.

Toggweiler, J.R. (1989). Is the downward dissolved organic matter (DOM) flux important in carbon transport? In: *Productivity of the Ocean: Present and Past*, W.H. Berger, V.S. Smetacek and G. Wefer, editors, J. Wiley and Sons, New York, 65-83.

Toggweiler, J.R. (1994). Vanishing in Bermuda. *Nature*, **372**, 505-506.

Tomczak, M. and J.S. Godfrey (1994). *Regional oceanography: an introduction.* Elsevier Science Ltd, 422p.

Tsunogai, S. and S. Noriki (1991). Particulate fluxes of carbonate and organic carbon in the ocean. Is the marine biological activity working as a sink of the atmospheric carbon. *Tellus*, **43B**, 256-266.

Turley, C.M. and P.J. Mackie (1994). Biogeochemical significance of attached and free-living bacteria and the flux of particles in the NE Atlantic Ocean. *Marine Ecology Progress Series*, **115**, 191-203.

Urrère, M.A. and G.A. Knauer (1981). Zooplankton fecal pellet fluxes and vertical transport of particulate organic material in the pelagic environment. *Journal of Plankton Research*, **3**, 369-387.

U.S. GOFS Report 10 (1989). Sediment trap technology and sampling. *Report of the U.S. GOFS Working Group on Sediment Trap Technology and Sampling, November, 1988*, G.A. Knauer and V.L. Asper, co-chairs, 94p.

Vernet, M. and C.J. Lorenzen (1987a). The relative abundance of pheophorbide *a* and pheophytin *a* in temperate marine waters. *Limnology and Oceanography*, **32**, 352-358.

Vernet, M. and C.J. Lorenzen (1987b). The presence of chlorophyll *b* and the estimation of phaeopigments in marine phytoplankton. *Journal of Plankton Research*, **9**, 255-265.

Vidussi, F., H. Claustre, J. Bustillos-Guzmàn, C. Cailliou and J.-C. Marty (1996). Determination of chlorophylls and carotenoids of marine phytoplankton: separation of chlorophyll *a* from divinyl-chlorophyll *a* and zeaxanthin from lutein. *Journal of Plankton Research*, **18**, 2377-2382.

Villareal, T.A., M.A. Altabet and K. Culver-Rymsza (1993). Nitrogen transport by migrating diatom mats in the North Pacific Ocean. *Nature*, **363**, 709-712.

Vincent, W.F., C. Howard-Williams, P. Tildesley and E. Butler (1991). Distribution and biological properties of oceanic water masses around the South Island, New Zealand. *New Zealand Journal of Marine and Freshwater Research*, **25**, 21-42.

Volk, T. and M.I. Hoffert (1985). Ocean carbon pumps: Analysis of relative strengths and efficiencies in ocean-driven atmospheric CO_2 changes. In: *The carbon cycle and atmospheric CO_2: Natural variations Archean to present*, E.T. Sundquist and W.S. Broecker, editors, American Geophysical Union, Washington, D.C., 99-110.

Wakeham, S. and C. Lee (1993). Production, transport, and alteration of particulate organic matter in the marine water column. In: *Organic Geochemistry*, M. Engel and S. Macko, editors, Plenum Press, New York, 145-169.

Wakeham, S.G. and C. Lee (1989). Organic geochemistry of particulate matter in the ocean: The role of particles in oceanic sedimentary cycles. *Organic Geochemistry*, **14**, 83-96.

Wakeham, S.G., C. Lee, J.W. Farrington and R.B. Gagosian (1984). Biogeochemistry of particulate organic matter in the oceans: results from sediment trap experiments. *Deep-Sea Research*, **31**, 509-528.

Wakeham, S.G., J.I. Hedges, C. Lee and T.K. Pease (1993). Effects of poisons and preservatives on the composition of organic matter in a sediment trap experiment. *Journal of Marine Research*, **51**, 669-696.

Wallace, D.W.R. (1995). Monitoring global ocean carbon inventories. *Ocean Observing System Development Panel Background Report*, **5**, 54p.

Walsh, I.D. and W.D. Gardner (1992). A comparison of aggregate profiles with sediment trap fluxes. *Deep-Sea Research*, **39**, 1817-1834.

Walsh, J.J. (1989). How much shelf production reaches the deep sea. In: *Productivity of the Ocean: Present and Past*, W.H. Berger, V.S. Smetacek and G. Wefer, editors, J. Wiley and Sons, New York, 175-191.

Wassman, P. (1991). Sampling and analysis of marine particles with PERNOCO. In: *Marine particles: analysis and characterization*, D.C. Hurd and D.W. Spencer, editors, *Geophysical Monograph*, **63**, American Geophysical Union, Washington, D.C., 97-99.

Wefer, G. (1989). Particle flux in the ocean: effects of episodic production. In: *Productivity of the Ocean: Present and Past*, W.H. Berger, V.S. Smetacek and G. Wefer, editors, J. Wiley and Sons, New York, 139-153.

Wefer, G., E. Suess, W. Balzer, G. Lieberzeit, P.J. Muller, C.A. Ungerer and W. Zenk (1982). Fluxes of biogenic components from sediment trap deployment in circumpolar waters of the Drake Passage. *Nature*, **299**, 145-147.

Wefer, G., G. Fischer, D. Fueetterer and R. Gersonde (1988). Seasonal particle flux in the Bransfield Strait, Antarctica. *Deep-Sea Research*, **35**, 891-898.

Weliky, K., E. Suess, C. A. Ungerer, P.J. Müller and K. Fischer (1983). Problems with accurate carbon measurements in marine sediments and particulate matter in seawater: A new approach. *Limnology and Oceanography*, **28**, 1252-1259.

Welschmeyer, N.A. and C.J. Lorenzen (1985a). Role of herbivory in controlling phytoplankton abundance: annual pigment budget for a temperate marine fjord. *Marine Biology*, **90**, 75-86.

Welschmeyer, N.A. and C.J. Lorenzen (1985b). Chlorophyll budgets: zooplankton grazing and phytoplankton growth in a temperate fjord and the Central Pacific Gyres. *Limnology and Oceanography*, **30**, 1-21.

Welschmeyer, N.A., A.E. Copping, M Vernet and C.J. Lorenzen (1984). Diel fluctuation in zooplankton grazing rate as determined from the downward vertical flux of pheopigments. *Marine Biology*, **83**, 263-270.

Wiebe, P.H., S.H. Boyd and C. Winget (1976). Particulate matter sinking to the deep-sea floor at 2000 m in the Tongue of the Ocean, Bahamas, with a description of a new sedimentation trap. *Journal of Marine Research*, **34**, 341-354.

Williams, R. and H. Claustre (1991). Photosynthetic pigments as biomarkers of phytoplankton populations and processes involved in the transformation of particulate organic matter at the Biotrans site (47°N, 20°W). *Deep-Sea Research*, **38**, 347-355.

Wood, R. and B. Davy (1994). The Hikurangi Plateau. *Marine Geology*, **118**, 153-173.

Wood, R.A. and R.H. Herzer (1993). The Chatham Rise, New Zealand. In: *South Pacific Sedimentary Basins, Sedimentary Basins of the World*, **2**, P.B. Ballance, editor, Elsevier Science Publishers, 329-349.

Wood, R.A., P.B. Andrews, R.H. Herzer and others (1989). Cretaceous-Cenozoic geology of the Chatham Rise region, South Island. *New Zealand Geological Survey Basin Studies*, **3**.

Woolf, D.K. (1993). Bubbles and the air-sea transfer velocity of gases. *Atmosphere-Ocean*, **31**, 517-540.

Wright, S.W., S.W. Jeffrey, R.F.C. Mantoura, C.A. Llewellyn, T. Bjørnland, D. Repeta and N. Welschmeyer (1991). Improved HPLC method for the analysis of chlorophylls and carotenoids from marine phytoplankton. *Marine Ecology Progress Series*, **77**, 183-196.

Wyrtki K. (1962). The subsurface water masses in the Western South Pacific Ocean. *Australian Journal of Marine and Freshwater Research*, **13**, 18-47

Young, R.A. and J.B. Southard (1978). Erosion of fine-grained marine sediments: sea floor and laboratory experiments. *Bulletin of the Geological Society of America*, **89**, 663-672.

Zeitzschel, B., P. Diekmann and L. Uhlmann (1978). A new multisample sediment trap. *Marine Biology*, **46**, 285-288.

Zentara, S.J. and D. Kamykowski (1981). Geographic variations in the relationship between silicic acid and nitrate in the South Pacific Ocean. *Deep-Sea Research A*, **28**, 455-465.

Zhang, X., H.G. Dam, J.R. White and M.R. Roman (1995). Latitudinal variations in mesozooplankton grazing and metabolism in the central tropical Pacific during the JGOFS EqPac study. *Deep-Sea Research II*, **42**, 695-714.

APPENDICES

APPENDIX 1: Sediment trap results - North Chatham Rise (NZOI-NIWA research voyage 2053, April 1992, station U940).

A=200 m, B=300 m, C=500 m.

1A. Mass fluxes

Trap code	Filter number	Tared filter weight W_t (g)	Volume filtered V_f (l)	Brine volume V_r (l)	Filtered weight W_f (g)	Mass difference W_f-W_t (g)	Blank weight W_{blk} (g)	Total weight W_T (g)	Trap area A (m^2)	Duration t (d)	Total mass flux $TM=W_TV_r(V_fAt)^{-1}$ ($g\ m^{-2}\ d^{-1}$)
A1	14.39	0.009149	0.710	0.5731	0.010862	0.001713	0.00023	0.001483	0.0064	3	0.062363
A2	40.104	0.009211	0.670	0.5731	0.012149	0.002938	0.00023	0.002709	0.0064	3	0.120666
A7	10.19	0.009151	0.675	0.5731	0.012099	0.002948	0.00023	0.002719	0.0064	3	0.120214
B7	17.25	0.009184	0.520	0.5731	0.014766	0.005582	0.00023	0.005353	0.0064	3	0.307261
B9	110	0.004527	0.550	0.5731	0.005239	0.000712	0.00023	0.000482	0.0064	3	0.026175
B10	101.16	0.009246	0.530	0.5731	0.009087	-0.000159	0.00023	-0.000388	0.0064	3	-0.021880
C4	34.37	0.009269	0.500	0.5731	0.012890	0.003621	0.00023	0.003392	0.0064	3	0.202477
C5	33.11	0.009347	0.520	0.5731	0.012390	0.003043	0.00023	0.002813	0.0064	3	0.161494
C9	12	0.004553	0.510	0.5731	0.007152	0.002599	0.00023	0.002370	0.0064	3	0.138698
Blank	5	0.004578	0.500	~	~	~	0.00023	-0.000230	0.0064	~	-0
Blank	13	0.004707	0.500	~	~	~	0.00023	-0.000230	0.0064	~	-0
Blank	15	0.004586	0.500	~	0.005820	0.001234	0.00023	0.001005	0.0064	~	-0
Blank	18	0.004686	0.500	~	0.004852	0.000166	0.00023	-6.39E-05	0.0064	~	-0
Blank	20	~	0.500	~	~	~	0.00023	-0.000230	0.0064	~	-0
Blank	35	0.004667	0.500	~	0.005631	~	0.00023	-0.000230	0.0064	~	-0
Blank	38	0.004740	0.500	~	0.004911	0.000171	0.00023	-5.83E-05	0.0064	~	-0
Blank	103	0.004569	0.500	~	0.005623	0.001054	0.00023	0.000824	0.0064	~	-0

1B. Particulate carbon and nitrogen fluxes - North Chatham Rise (April 1992)

Trap code	Volume filtered V_f (l)	Carbon C_s (μg $filter^{-1}$)	Nitrogen N_s (μg $filter^{-1}$)	C blank C_{blk} (μg)	N blank N_{blk} (μg)	Total C_T C_s-C_{blk} (mg)	Total N_T N_s-N_{blk} (mg)	C:N	PC flux $PC=C_TV_r(V_rAt)^{-1}$ (mg m^{-2} d^{-1})	PN flux $PN=N_TV_r(V_rAt)^{-1}$ (mg m^{-2} d^{-1})
A11	0.49	584.8	77.8	76.8	5.9	0.5177	0.0714	7.3	31.53	4.35
A12	0.50	603.1	86.3	65.2	6.6	0.536	0.0799	6.7	31.99	4.77
A5	0.51	591.8	63.5	80.1	4.1	0.5247	0.0571	9.2	30.70	3.34
A6	0.71	601.3	77.8	102.1	9	0.5342	0.0714	7.5	22.45	3.00
A8	0.49	578.3	83.3	61.7	7	0.5112	0.0769	6.7	31.14	4.68
A9	0.48	660.7	90	70	6.8	0.5936	0.0836	7.1	36.91	5.20
B1	0.55	494.4	66.7	67.4	7.4	0.4273	0.0603	7.1	23.19	3.27
B11	0.46	524.1	69.4	72.3	11.2	0.457	0.063	7.3	29.65	4.09
B12	0.50	679.8	90.4	57	5.4	0.6127	0.084	7.3	36.57	5.01
B2	0.50	557.5	75.9	56.4	6.1	0.4904	0.0695	7.1	29.27	4.15
B5	0.54	581.8	73.8	59.3	5.1	0.5147	0.0674	7.6	28.45	3.72
B6	0.43	562.1	74.7	71.1	6.6	0.495	0.0683	7.3	34.36	4.74
C10	0.50	693.3	67.9	77.8	6.2	0.6262	0.0615	10.2	37.38	3.67
C11	0.47	650.1	62.1	82.4	7.2	0.583	0.0557	10.5	37.02	3.54
C12	0.51	718.3	61.8	50	5.1	0.6512	0.0554	11.8	38.11	3.24
C2	0.51	638.1	55.9	53.4	5.1	0.571	0.0495	11.5	33.41	2.90
C3	0.46	536.6	47.2	52.7	5.5	0.4695	0.0408	11.5	30.46	2.65
C7	0.54	641.8	55.7	51.3	5.2	0.5747	0.0493	11.7	31.76	2.73

1C. Particulate phosphorus and nitrogen fluxes - North Chatham Rise (April 1992)

Trap code	Volume filtered V_f (l)	Phosphorus P_s (μg $filter^{-1}$)	Nitrogen N_s (μg $filter^{-1}$)	P blank P_{blk} (μg)	N blank N_{blk} (μg)	Total P_T P_s- P_{blk} (mg)	Total N_T N_s- N_{blk} (mg)	P:N	N:P	PP flux $PP=P_TV_r$ $(V_rAt)^{-1}$ (mg m^{-2} d^{-1})	PN flux $PN=N_TV_r$ $(V_rAt)^{-1}$ (mg m^{-2} d^{-1})
A3	0.51	7.24	51.1	0.75	3.51	0.00646	0.04727	0.14	7.32	0.38	2.77
A4	0.55	7.06	49	0.98	5.92	0.00628	0.04517	0.14	7.19	0.34	2.45
A10	0.50	7.76	61.74	0.79	3.99	0.00698	0.05791	0.12	8.3	0.42	3.46
B3	0.54	9.65	67.87	0.78	3.55	0.00887	0.06404	0.14	7.22	0.49	3.54
B4	0.57	10.98	61.84	0.88		0.0102	0.05801	0.18	5.69	0.53	0.304
B8	0.54	6.74	51.71	0.84	4.29	0.00596	0.04788	0.13	8.03	0.33	2.65
C1	0.50	6.21	46.91	0.67	2.87	0.00543	0.04308	0.13	7.93	0.32	2.57
C6	0.53	6.69	54.12	0.64	3.3	0.00591	0.05029	0.12	8.51	0.33	2.83
C8	0.51	4.5	28.56	0.71	2.8	0.00372	0.02473	0.15	6.65	0.22	1.45

1D. Suspended particulate matter (SPM) concentrations North Chatham Rise (April 1992)

Station	Date	Time	Depth (m)	Filtered weight (mg)	Concentration SPM (mg l^{-1})
U942	APR 9 1992	1610	407	1.35	0.55
U942	APR 9 1992	1610	100	0.08	0.02
U942	APR 9 1992	1610	4.5	0.65	0.32
U943	APR 10 1992	0940	2033	0.55	0.12
U943	APR 10 1992	0940	300	0.57	0.13
U943	APR 10 1992	0940	5	0.84	0.42
U944	APR 10 1992	1720	1143	0.65	0.15
U944	APR 10 1992	1720	299	0.68	0.16
U944	APR 10 1992	1720	5	0.65	0.20
U945	APR 10 1992	2040	1977	0.38	0.08
U945	APR 10 1992	2040	290	0.70	0.17
U945	APR 10 1992	2040	5	0.67	0.29
U946	APR 11 1992	0040	1476	0.25	0.05
U946	APR 11 1992	0040	299	0.51	0.12
U946	APR 11 1992	0040	5	0.50	0.22
U947	APR 11 1992	0330	1475	0.35	0.06
U947	APR 11 1992	0330	302	0.27	0.05
U947	APR 11 1992	0330	5	0.85	0.15
U948	APR 11 1992	0600	1475	0.16	0.07
U948	APR 11 1992	0600	300	1.04	0.22
U948	APR 11 1992	0600	5	0.91	0.25
U948	APR 11 1992	0600	1475	0.19	0.07
U949	APR 11 1992	0830	1435	0.35	0.07
U949	APR 11 1992	0830	300	0.20	0.04
U949	APR 11 1992	0830	5	0.66	0.21

APPENDIX 2: Sediment trap results - Cook Strait (NZOI-NIWA research voyages 3004 and 3005, March-April 1993).

Trap code	Filter number	Tared filter weight W_t (g)	Volume filtered V_f (l)	Brine height H_b (m)	Brine volume $V_r=AH_b$ (l)	Filtered weight W_f (g)	Mass difference W_f-W_t (g)	Blank weight W_{blk} (g)	Total weight W_T (g)	Trap area A (m^2)	Duration t (d)	Total mass flux $TM=W_TV_r(V_fAt)^{-1}$ ($g\ m^{-2}\ d^{-1}$)
12	1	0.004633	0.500	0.600	3.840	0.08330	0.078667	0.000272	0.078395	0.0064	1.4	67.19571
12	2	0.004534	0.500	0.600	3.840	~	~	0.000272	~	0.0064	1.4	~
12	6	0.004584	0.500	0.600	3.840	0.040110	0.035526	0.000272	0.035254	0.0064	1.4	30.21737
1	7	0.004581	0.480	0.655	4.192	0.026760	0.022179	0.000272	0.021907	0.0064	1.4	21.35290
1	8	0.004530	0.460	0.655	4.192	0.032160	0.027630	0.000272	0.027358	0.0064	1.4	27.82519
1	21	0.004578	0.420	0.655	4.192	0.028510	0.023932	0.000272	0.023660	0.0064	1.4	26.35595
11	24	0.004586	0.250	0.620	3.968	0.007593	0.003007	0.000272	0.002735	0.0064	1.4	4.845211
11	28	0.004731	0.500	0.620	3.968	0.009974	0.005243	0.000272	0.004971	0.0064	1.4	4.402709
11	29	0.004534	0.250	0.620	3.968	0.009428	0.004894	0.000272	0.004622	0.0064	1.4	8.187011
11	30	0.004566	0.240	0.620	3.968	0.008525	0.003959	0.000272	0.003687	0.0064	1.4	6.803762
11	31	0.004718	0.490	0.620	3.968	0.013657	0.008940	0.000272	0.008668	0.0064	1.4	7.833601
11	32	0.004634	0.490	0.620	3.968	0.013186	0.008552	0.000272	0.008280	0.0064	1.4	7.483382
8	36	0.004629	0.240	0.610	3.904	0.022208	0.017580	0.000272	0.017308	0.0064	1.4	31.42135
8	42	0.004496	0.240	0.610	3.904	0.023770	0.019274	0.000272	0.019002	0.0064	1.4	34.49822
8	43	0.004663	0.250	0.610	3.904	0.023589	0.018926	0.000272	0.018654	0.0064	1.4	32.51126
7	44	0.004694	0.260	0.610	3.904	0.026150	0.021456	0.000272	0.021184	0.0064	1.4	35.50099
7	46	0.004678	0.250	0.610	3.904	0.024230	0.019552	0.000272	0.019280	0.0064	1.4	33.60211
7	47	0.004616	0.230	0.610	3.904	0.021863	0.017247	0.000272	0.016975	0.0064	1.4	32.15685
7	50	0.004696	0.5005	0.610	3.904	0.043230	0.038534	0.000272	0.038262	0.0064	1.4	33.30946
7	23	0.004704	0.500	0.610	3.904	0.040008	0.035304	0.000272	0.035032	0.0064	1.4	30.52789
7	111	0.004579	0.430	0.610	3.904	0.042470	0.037891	0.000272	0.037619	0.0064	1.4	38.11902
10	54	0.004630	0.490	0.625	4.000	0.036070	0.031440	0.000272	0.031168	0.0064	1.4	28.39614
10	179	0.004545	0.260	0.625	4.000	0.020591	0.016046	0.000272	0.015774	0.0064	1.4	27.08482
10	90	0.004577	0.260	0.625	4.000	0.020299	0.015722	0.000272	0.015450	0.0064	1.4	26.52867
10	76	0.004557	0.490	0.625	4.000	0.037410	0.032854	0.000272	0.032582	0.0064	1.4	29.68431
10	69	0.004634	0.460	0.625	4.000	0.038370	0.033736	0.000272	0.033464	0.0064	1.4	32.47632
10	131	0.004650	0.240	0.625	4.000	0.017777	0.013128	0.000272	0.012856	0.0064	1.4	23.91276

Trap code	Filter number	Tared filter weight W_t (g)	Volume filtered V_f (l)	Brine height H_b (m)	Brine volume $V_r=AH_b$ (l)	Filtered weight W_f (g)	Mass difference W_f-W_t (g)	Blank weight W_{blk} (g)	Total weight W_T (g)	Trap area A (m^2)	Duration t (d)	Total mass flux $TM=W_TV_r(V_fAt)^{-1}$ ($g\ m^{-2}\ d^{-1}$)
2	91	0.004591	0.270	0.620	3.968	0.022708	0.018117	0.000272	0.017845	0.0064	1.4	29.26990
2	161	0.004680	0.500	0.620	3.968	0.035940	0.031260	0.000272	0.030988	0.0064	1.4	27.44616
2	112	0.004339	0.230	0.620	3.968	0.020620	0.016281	0.000272	0.016009	0.0064	1.4	30.82459
2	188	0.004693	0.510	0.620	3.968	0.034220	0.029527	0.000272	0.029255	0.0064	1.4	25.40359
2	98	0.004612	0.500	0.620	3.968	0.037180	0.032569	0.000272	0.032297	0.0064	1.4	28.60547
2	132	0.004664	0.250	0.620	3.968	0.019783	0.015119	0.000272	0.014847	0.0064	1.4	26.30058
3	114	0.004633	0.500	0.610	3.904	0.051050	0.046417	0.000272	0.046145	0.0064	1.4	40.21225
3	162	0.004703	0.490	0.610	3.904	0.033700	0.028997	0.000272	0.028725	0.0064	1.4	25.54299
3	55	0.004640	0.470	0.610	3.904	0.033460	0.028820	0.000272	0.028548	0.0064	1.4	26.46538
3	77	0.004588	0.250	0.610	3.904	0.021736	0.017148	0.000272	0.016876	0.0064	1.4	29.41211
3	62	0.004575	0.260	0.610	3.904	0.021069	0.016494	0.000272	0.016222	0.0064	1.4	27.18472
3	80	0.004559	0.240	0.610	3.904	0.023700	0.019141	0.000272	0.018869	0.0064	1.4	34.25676
6	173	0.004695	0.250	0.630	4.032	0.020063	0.015368	0.000272	0.015096	0.0064	1.4	27.17316
6	115	0.004561	0.250	0.630	4.032	0.019776	0.015215	0.000272	0.014943	0.0064	1.4	26.89812
6	143	0.004573	0.450	0.630	4.032	0.035630	0.031058	0.000272	0.030786	0.0064	1.4	30.78550
6	63	0.004563	0.500	0.630	4.032	0.035620	0.031057	0.000272	0.030785	0.0064	1.4	27.70632
6	94	0.004629	0.505	0.630	4.032	0.037900	0.033271	0.000272	0.032999	0.0064	1.4	29.40496
6	149	0.004725	0.260	0.630	4.032	0.020764	0.016039	0.000272	0.015767	0.0064	1.4	27.28973
5	57	0.004581	0.495	0.575	3.680	0.039880	0.035299	0.000272	0.035027	0.0064	1.4	29.06297
5	78	0.004626	0.495	0.575	3.680	0.042640	0.038014	0.000272	0.037742	0.0064	1.4	31.31584
5	138	0.004659	0.240	0.575	3.680	0.025170	0.020511	0.000272	0.020239	0.0064	1.4	34.63519
5	174	0.004728	0.505	0.575	3.680	0.041720	0.036992	0.000272	0.036720	0.0064	1.4	29.86438
5	180	0.004558	0.235	0.575	3.680	0.026180	0.021622	0.000272	0.021350	0.0064	1.4	37.31400
5	126	0.004578	0.245	0.575	3.680	0.029610	0.025032	0.000272	0.024760	0.0064	1.4	41.50717

Trap code	Filter number	Tared filter weight W_t (g)	Volume filtered V_f (l)	Brine height H_b (m)	Brine volume $V_r=AH_b$ (l)	Filtered weight W_f (g)	Mass difference W_f-W_t (g)	Blank weight W_{blk} (g)	Total weight W_T (g)	Trap area A (m^2)	Duration t (d)	Total mass flux $TM=W_TV_r(V_fAt)^{-1}$ ($g\ m^{-2}\ d^{-1}$)
Blank	70	0.004640	0.475	~	0	0.004882	0.000242	0.000272	-0.00003	0.0064	~	-0
Blank	72	0.004675	0.510	~	0	0.005001	0.000326	0.000272	5.42E-05	0.0064	~	-0
Blank	139	0.004663	0.490	~	0	0.005013	0.000350	0.000272	7.76E-05	0.0064	~	-0
Blank	106	0.004553	0.490	~	0	0.004848	0.000295	0.000272	2.33E-05	0.0064	~	-0
Blank	125	0.004697	0.495	~	0	0.005132	0.000435	0.000272	0.000163	0.0064	~	-0
Blank	167	0.004751	0.270	~	0	0.005053	0.000302	0.000272	2.98E-05	0.0064	~	-0
Blank	155	0.004681	0.260	~	0	0.004900	0.000219	0.000272	-5.33E-05	0.0064	~	-0
Blank	127	0.004572	0.250	~	0	0.004764	0.000193	0.000272	-7.95E-05	0.0064	~	-0
Blank	58	0.004626	0.265	~	0	0.004825	0.000199	0.000272	-7.29E-05	0.0064	~	-0
Blank	83	0.004627	0.240	~	0	0.004786	0.000160	0.000272	-0.000113	0.0064	~	-0

APPENDIX 3: Sediment trap results - New Zealand JGOFS, Chatham Rise (NZOI-NIWA research voyage 3009, June-July 1993).

3A. Mass fluxes.

Trap code	Station	Trap depth (m)	Cylinder position	Filter number	Tared filter weight W_t (g)	Volume filtered V_f (l)	Brine height H_b (m)	Brine volume $V_r=AH_b$ (l)	Filtered weight W_f (g)	Mass difference W_f-W_t (g)	Blank weight W_{blk} (g)	Total weight W_T (g)	Trap area A (m^2)	Duration t (d)	Total mass flux $TM=W_TV_r(V_fAt)^{-1}$ ($g\ m^{-2}\ d^{-1}$)
6550.4	X464	550	4	53	0.004680	0.25	0.33	2.112	~	-0.00468	0.000302	-0.004982	0.0064	2.3	-2.859177
6550.6	X464	550	6	217	0.004508	0.24	0.21	1.344	0.006272	0.001764	0.000302	0.001462	0.0064	2.3	0.556272
6300.3	X464	300	3	133	0.004523	0.25	0.30	1.920	0.005335	0.000812	0.000302	0.000510	0.0064	2.3	0.266087
6300.6	X464	300	6	145	0.004633	0.25	0.33	2.112	0.005466	0.000834	0.000302	0.000532	0.0064	2.3	0.305150
6220.4	X464	220	4	134	0.004656	0.25	0.255	1.632	0.006074	0.001418	0.000302	0.001116	0.0064	2.3	0.494922
6220.5	X464	220	5	119	0.004538	0.25	0.24	1.536	0.004926	0.000388	0.000302	8.66E-05	0.0064	2.3	0.036146
6220.11	X464	220	11	87	0.004635	0.25	0.25	1.600	0.005463	0.000828	0.000302	0.000526	0.0064	2.3	0.228652
6120.3	X464	120	3	128	0.004652	0.25	0.29	1.856	0.006117	0.001466	0.000302	0.001164	0.0064	2.3	0.586910
6120.5	X464	120	5	156	0.004594	0.25	0.33	2.112	0.005180	0.000586	0.000302	0.000284	0.0064	2.3	0.163106
6120.6	X464	120	6	152	0.004667	0.25	0.45	2.880	0.004997	0.000330	0.000302	2.78E-05	0.0064	2.3	0.021757
7550.1	X465	550	1	210	0.004463	0.25	0.28	1.792	0.004826	0.000363	0.000302	6.12E-05	0.0064	2.4	0.028560
7550.2	X465	550	2	205	0.004803	0.25	0.32	2.048	0.005894	0.001091	0.000302	0.000789	0.0064	2.4	0.420907
7300.2	X465	300	2	164	0.004596	0.25	0.35	2.240	0.005532	0.000937	0.000302	0.000635	0.0064	2.4	0.370242
7300.8	X465	300	8	286	0.004529	0.25	0.39	2.496	0.004775	0.000246	0.000302	-5.58E-05	0.0064	2.4	-0.036270
7220.1	X465	220	1	68	0.004609	0.25	0.38	2.432	0.006239	0.001630	0.000302	0.001328	0.0064	2.4	0.841003
7220.3	X465	220	3	96	0.004524	0.25	0.35	2.240	0.005963	0.001439	0.000302	0.001137	0.0064	2.4	0.663133
7220.10	X465	220	10	232	0.004770	0.25	0.38	2.432	0.004938	0.000168	0.000302	-0.000134	0.0064	2.4	-0.084740
7120.4	X465	120	4	60	0.004639	0.25	0.48	3.072	0.004856	0.000217	0.000302	-8.46E-05	0.0064	2.4	-0.067680
7120.6	X465	120	6	121	0.004556	0.25	0.37	2.368	0.005836	0.001280	0.000302	0.000978	0.0064	2.4	0.603162
7120.11	X465	120	11	168	0.004599	0.25	0.39	2.496	~	-0.004599	0.000302	-0.004901	0.0064	2.4	-3.185325
Blk3	~	~	~	73	0.004509	0.25	~	0	0.006287	0.001778	0.000302	0.001477	0.0064	~	-0
Blk3	~	~	~	176	0.004605	0.25	~	0	0.004907	0.000302	0.000302	-3.79E-19	0.0064	~	-0
9210.5	X467	210	5	95	0.004652	0.25	0.45	2.880	0.005154	0.000502	0.000583	-8.14E-05	0.0064	3.8	-0.038558
9210.7	X467	210	7	117	0.004496	0.25	0.41	2.624	0.004864	0.000368	0.000583	-0.000216	0.0064	3.8	-0.093048
9210.12	X467	210	12	109	0.004633	0.25	0.43	2.752	0.00633	0.001697	0.000583	0.001114	0.0064	3.8	0.504277

3A. (cont'd) Mass fluxes - NZ JGOFS, Chatham Rise (June-July 1993).

Trap code	Station	Trap depth (m)	Cylinder position	Filter number	Tared filter weight W_t (g)	Volume filtered V_f (l)	Brine height H_b (m)	Brine volume $V_r=AH_b$ (l)	Filtered weight W_f (g)	Mass difference W_f-W_t (g)	Blank weight W_{blk} (g)	Total weight W_T (g)	Trap area A (m^2)	Duration t (d)	Total mass f $TM=W_TV_r(V_fAt)^{-1}$ (g m^{-2} d^{-1}
9110.5	X467	110	5	129	0.004619	0.24	0.34	2.176	0.005225	0.000606	0.000583	2.27E-05	0.0064	3.8	0.008463
9110.6	X467	110	6	159	0.004502	0.25	0.32	2.048	0.005496	0.000994	0.000583	0.000410	0.0064	3.8	0.138240
9110.7	X467	110	7	189	0.004553	0.25	0.36	2.304	0.006265	0.001712	0.000583	0.001129	0.0064	3.8	0.427832
Blk4	~	~	~	144	0.004499	0.175	~	0	0.005150	0.000651	0.000583	6.79E-05	0.0064	~	-0
Blk4	~	~	~	137	0.004632	0.085	~	0	~	~	0.000583	-0.000583	0.0064	~	-0
Blk4a	~	~	~	85	0.004677	0.25	~	0	0.005019	0.000342	0.000583	-0.000241	0.0064	~	-0
Blk4a	~	~	~	120	0.004636	0.25	~	0	0.005393	0.000757	0.000583	0.000173	0.0064	~	-0
Blk4a	~	~	~	163	0.004709	0.25	~	0	0.006374	0.001665	0.000583	0.001082	0.0064	~	-0
10550.3	X468	550	3	220	0.004414	0.25	0.41	2.624	0.005646	0.001232	0.000315	0.000917	0.0064	2.0	0.752104
10550.6	X468	550	6	249	0.004507	0.25	0.44	2.816	0.006038	0.001531	0.000315	0.001216	0.0064	2.0	1.070256
10550.1	X468	550	1	141	0.004674	0.24	0.43	2.752	0.006367	0.001694	0.000315	0.001379	0.0064	2.0	1.235085
10300.3	X468	300	3	213	0.004341	0.23	0.425	2.720	0.005853	0.001512	0.000315	0.001197	0.0064	2.0	1.106109
10300.5	X468	300	5	282	0.004832	0.25	0.39	2.496	0.005765	0.000933	0.000315	0.000618	0.0064	2.0	0.482196
10300.7	X468	300	7	124	0.004563	0.25	0.39	2.496	0.00609	0.001527	0.000315	0.001212	0.0064	2.0	0.945204
10220.2	X468	220	2	86	0.004527	0.25	0.45	2.880	0.005265	0.000738	0.000315	0.000423	0.0064	2.0	0.380700
10220.6	X468	220	6	65	0.004624	0.25	0.405	2.592	0.005502	0.000878	0.000315	0.000563	0.0064	2.0	0.456273
10220.8	X468	220	8	130	0.004645	0.25	0.425	2.720	0.006914	0.002269	0.000315	0.001954	0.0064	2.0	1.661155
10120.5	X468	120	5	221	0.004451	0.24	0.37	2.368	0.005427	0.000976	0.000315	0.000661	0.0064	2.0	0.509675
10120.7	X468	120	7	74	0.004650	0.25	0.40	2.560	0.005857	0.001207	0.000315	0.000892	0.0064	2.0	0.713920
10120.1	X468	120	1	274	0.004471	0.23	0.39	2.496	0.004828	0.000357	0.000315	4.22E-05	0.0064	2.0	0.035778
Blk5	~	~	~	135	0.004555	0.25	~	0	0.004726	0.000171	0.000315	-0.000144	0.0064	~	-0
Blk5	~	~	~	84	0.004473	0.25	~	0	0.004959	0.000486	0.000315	0.000171	0.0064	~	-0
Blk5	~	~	~	59	0.004492	0.25	~	0	0.004780	0.000288	0.000315	-2.69E-05	0.0064	~	-0

3B. Particulate phosphorus fluxes - NZ JGOFS, Chatham Rise (June-July 1993).

Trap code	Station	Trap depth (m)	Cylinder position	Volume filtered V_f (l)	Brine height H_b (m)	Brine volume $V_r=Ah_b$ (l)	Trap area A (m^2)	Duration t (d)	Phosphorus P_s ($\mu g\ filter^{-1}$)	P blank P_{blk} ($\mu g\ filter^{-1}$)	Total P_T P_s-P_{blk} (μg)	P flux $PP=P_TV_r$ $(V_rAt)^{-1}$ ($mg\ m^{-2}\ d^{-1}$)
6550.1	X464	550	1	0.49	0.29	1.856	0.0064	2.3	7.9	0.7	7.2	1.852706
6550.7	X464	550	7	0.50	0.305	1.952	0.0064	2.3	9.4	0.7	8.7	2.307391
6300.2	X464	300	2	0.48	0.26	1.664	0.0064	2.3	6.8	0.7	6.1	1.436594
6300.7	X464	300	7	0.48	0.29	1.856	0.0064	2.3	7.0	0.7	6.3	1.654891
6220.2	X464	220	2	0.45	0.275	1.76	0.0064	2.3	7.5	0.7	6.8	1.806763
6220.6	X464	220	6	0.49	0.34	2.176	0.0064	2.3	7.1	0.7	6.4	1.930790
6220.8	X464	220	8	0.49	0.28	1.792	0.0064	2.3	7.3	0.7	6.6	1.639752
6120.2	X464	120	2	0.46	0.24	1.536	0.0064	2.3	6.3	0.7	5.6	1.270321
6120.7	X464	120	7	0.48	0.48	3.072	0.0064	2.3	4.3	0.7	3.6	1.565217
6120.12	X464	120	12	0.50	0.33	2.112	0.0064	2.3	7.6	0.7	6.9	1.980000
7550.3	X465	550	3	0.48	0.3	1.92	0.0064	2.4	8.8	0.7	8.1	2.109375
7550.5	X465	550	5	0.50	0.28	1.792	0.0064	2.4	8.8	0.7	8.1	1.890000
7300.4	X465	300	4	0.45	0.29	1.856	0.0064	2.4	7.3	0.7	6.6	1.772222
7300.7	X465	300	7	0.50	0.42	2.688	0.0064	2.4	7.8	0.7	7.1	2.485000
7220.5	X465	220	5	0.47	0.39	2.496	0.0064	2.4	7.8	0.7	7.1	2.454787
7220.8	X465	220	8	0.44	0.28	1.792	0.0064	2.4	6.6	0.7	5.9	1.564394
7220.12	X465	220	12	0.50	0.315	2.016	0.0064	2.4	7.5	0.7	6.8	1.785000
7120.5	X465	120	5	0.49	0.48	3.072	0.0064	2.4	5.2	0.7	4.5	1.836735
7120.7	X465	120	7	0.45	0.38	2.432	0.0064	2.4	6.8	0.7	6.1	2.146296
7120.10	X465	120	10	0.49	0.43	2.752	0.0064	2.4	8.9	0.7	8.2	2.998299
Blk3	~	~	~	0.50	~	0	0.0064	~	10.7	0.7	10.0	-0
Blk3	~	~	~	0.50	~	0	0.0064	~	10.6	0.7	9.9	-0
9210.1	X467	210	1	0.50	0.41	2.624	0.0064	3.8	7.4	0.67	6.73	1.452263
9210.3	X467	210	3	0.48	0.42	2.688	0.0064	3.8	6.5	0.67	5.83	1.342434
9210.9	X467	210	9	0.50	0.41	2.624	0.0064	3.8	6.4	0.67	5.73	1.236474

3B. (cont'd) Particulate phosphorus fluxes - NZ JGOFS, Chatham Rise (June-July 1993).

Trap code	Station	Trap depth (m)	Cylinder position	Volume filtered V_f (l)	Brine height H_b (m)	Brine volume $V_r=Ah_b$ (l)	Trap area A (m^2)	Duration t (d)	Phosphorus P_s ($\mu g\ filter^{-1}$)	P blank P_{blk} ($\mu g\ filter^{-1}$)	Total P_T P_s-P_{blk} (μg)	P flux $PP=P_TV_r$ $(V_rAt)^{-1}$ ($mg\ m^{-2}\ d^{-1}$)
9110.3	X467	110	3	0.50	0.41	2.624	0.0064	3.8	6.3	0.67	5.63	1.214895
9110.8	X467	110	8	0.50	0.385	2.464	0.0064	3.8	8.2	0.67	7.53	1.525816
9110.10	X467	110	10	0.50	0.42	2.688	0.0064	3.8	11.3	0.67	10.63	2.349789
Blk4	~	~	~	0.44	~	0	0.0064	~	~	0.67	-0.67	-0
Blk4	~	~	~	0.43	~	0	0.0064	~	~	0.67	-0.67	-0
Blk4a	~	~	~	0.50	~	0	0.0064	~	~	0.67	-0.67	-0
Blk4a	~	~	~	0.50	~	0	0.0064	~	~	0.67	-0.67	-0
10550.2	X468	550	2	0.50	0.39	2.496	0.0064	2.0	7.2	0.7	6.5	2.535000
10550.5	X468	550	5	0.49	0.415	2.656	0.0064	2.0	8.2	0.7	7.5	3.176020
10550.8	X468	550	8	0.50	0.36	2.304	0.0064	2.0	6.6	0.7	5.9	2.124000
10300.2	X468	300	2	0.47	0.4	2.56	0.0064	2.0	6.3	0.7	5.6	2.382979
10300.1	X468	300	1	0.50	0.44	2.816	0.0064	2.0	6.3	0.7	5.6	2.464000
10300.12	X468	300	12	0.50	0.37	2.368	0.0064	2.0	5.9	0.7	5.2	1.924000
10220.3	X468	220	3	0.50	0.425	2.72	0.0064	2.0	5.8	0.7	5.1	2.167500
10220.11	X468	220	11	0.50	0.4	2.56	0.0064	2.0	6.1	0.7	5.4	2.160000
10120.3	X468	120	3	0.49	0.38	2.432	0.0064	2.0	8.7	0.7	8.0	3.102041
10120.8	X468	120	8	0.50	0.39	2.496	0.0064	2.0	9.0	0.7	8.3	3.237000
10120.11	X468	120	11	0.48	0.42	2.688	0.0064	2.0	7.6	0.7	6.9	3.018750
Blk5	~	~	~	0.50	~	0	0.0064	~	6.5	0.7	5.8	-0
Blk5	~	~	~	0.50	~	0	0.0064	~	6.8	0.7	6.1	-0

3C. Suspended particulate matter concentrations - NZ JGOFS, Chatham Rise (June-July 1993).

Station	Date	Time	Depth (m)	Filtered weight (mg)	Concentration SPM (mg l^{-1})
X462j	JUN 19 1993	1330	75	13.34	1.9333
X463b	JUN 20 1993	0600	90	7.17	3.5850
X463b	JUN 20 1993	0600	90	10.09	3.3633
X463b	JUN 20 1993	0600	80	13.09	2.0778
X463b	JUN 20 1993	0600	80	13.53	2.1075
X464c	JUN 24 1993	0600	550	0.85	0.3697
X464c	JUN 24 1993	0600	300	1.92	0.3316
X464c	JUN 24 1993	0600	300	1.35	0.5400
X464c	JUN 24 1993	0600	550	1.31	0.2183
X464f	JUN 24 1993	1330	300	1.78	0.4450
X464f	JUN 24 1993	1330	300	2.13	0.6554
X464f	JUN 24 1993	1330	550	2.12	0.5300
X464f	JUN 24 1993	1330	550	2.24	0.6400
X464h	JUN 24 1993	2130	300	1.49	0.4627
X464h	JUN 24 1993	2130	550	2.11	0.5275
X464h	JUN 24 1993	2130	550	1.43	0.3686
X464h	JUN 24 1993	2130	300	1.98	0.4950
X465a	JUN 22 1993	2230	300	3.64	0.5275
X465a	JUN 22 1993	2230	300	1.58	0.3950
X465a	JUN 22 1993	2230	550	2.68	1.0113
X465a	JUN 22 1993	2230	550	2.16	0.5400
X465e	JUN 23 1993	0600	550	1.25	0.6281
X465e	JUN 23 1993	0600	550	1.25	0.7184
X465e	JUN 23 1993	0600	300	1.68	0.2650
X465e	JUN 23 1993	0600	300	1.65	0.2511
X465h	JUN 23 1993	1500	550	1.90	0.2758
X465h	JUN 23 1993	1500	300	1.09	0.2725
X465h	JUN 23 1993	1500	550	1.14	0.4471
X465h	JUN 23 1993	1500	300	1.00	0.3333
X466c	JUN 26 1993	1400	300	4.62	1.1550
X466c	JUN 26 1993	1400	300	2.43	0.6943
X466c	JUN 26 1993	1400	210	2.50	0.6757
X466e	JUN 26 1993	2130	210	2.10	0.5250
X466e	JUN 26 1993	2130	210	1.55	0.4493
X466e	JUN 26 1993	2130	300	3.11	0.7775
X466e	JUN 26 1993	2130	300	2.60	0.9630
X466i	JUN 27 1993	0600	300	2.20	0.5500
X466i	JUN 27 1993	0600	300	1.91	0.6367
X466i	JUN 27 1993	0600	210	2.49	0.8300
X466i	JUN 27 1993	0600	210	2.20	0.5500
X467c	JUN 27 1993	1400	210	1.81	0.5070
X467c	JUN 27 1993	1400	210	1.65	0.4125
X467c	JUN 27 1993	1400	300	2.91	0.9932
X467c	JUN 27 1993	1400	300	1.85	0.4625
X467e	JUN 27 1993	2130	300	2.74	0.6850
X467e	JUN 27 1993	2130	300	2.01	0.5583
X467f	JUN 28 1993	0600	210	2.68	0.6700
X467f	JUN 28 1993	0600	300	3.04	0.7600
X467f	JUN 28 1993	0600	210	2.89	1.2042

3C. (cont'd) Suspended particulate matter concentrations.

Station	Date	Time	Depth (m)	Filtered weight (mg)	Concentration SPM (mg l^{-1})
X467f	JUN 28 1993	0600	300	2.53	1.0542
X468a	JUL 1 1993	0530	220	1.53	0.3825
X468a	JUL 1 1993	0530	220	1.14	0.4750
X468a	JUL 1 1993	0530	220	2.64	0.6600
X468a	JUL 1 1993	0530	550	1.64	0.5467
X468a	JUL 1 1993	0530	550	1.98	0.4950
X468a	JUL 1 1993	0530	220	1.82	0.6256
X468f	JUL 1 1993	1400	550	1.12	0.2917
X468f	JUL 1 1993	1400	550	1.83	0.4575
X468f	JUL 1 1993	1400	300	2.27	0.6168
X468f	JUL 1 1993	1400	300	1.23	0.3075
X468g	JUL 1 1993	2130	550	2.28	0.6423
X468g	JUL 1 1993	2130	300	2.07	0.5914
X468g	JUL 1 1993	2130	300	2.66	0.6650
X468g	JUL 1 1993	2130	550	2.20	0.5500
X469a	JUL 2 1993	600	550	1.98	0.4950
X469a	JUL 2 1993	0600	550	3.91	1.3719
X469a	JUL 2 1993	0600	300	3.90	1.3684
X469a	JUL 2 1993	0600	300	1.88	0.4700
X469d	JUL 2 1993	1400	300	3.51	0.8775
X469d	JUL 2 1993	1400	300	2.40	0.7059
X469d	JUL 2 1993	1400	550	2.53	0.6325
X469d	JUL 2 1993	1400	550	2.38	0.6263
X469f	JUL 2 1993	2130	550	2.45	0.6125
X469f	JUL 2 1993	2130	550	3.09	0.8905
X469f	JUL 2 1993	2130	300	1.98	0.6851
X469f	JUL 2 1993	2130	300	2.43	0.6075

APPENDIX 4: Sediment trap results - New Zealand JGOFS, Chatham Rise (research voyage 3014, October, 1993)

4A. Mass fluxes.

Trap code	Station	Trap depth (m)	Cylinder position	Filter number	Tared filter weight W_t (g)	Volume filtered V_f (l)	Brine height H_b (m)	Brine volume $V_r=AH_b$ (l)	Filtered weight W_f (g)	Mass difference W_f-W_t (g)	Blank weight W_{blk} (g)	Total weight W_T (g)	Trap area A (m^2)	Duration t (d)	Total mass flux $TM=W_TV_r(V_fAt)^{-1}$ ($g\ m^{-2}\ d^{-1}$)
6150.4	X476	150	4	391	0.004505	0.250	0.42	2.688	0.004970	0.000465	0.000162	0.000303	0.0064	2.0	0.254940
6150.4	X476	150	4	313	0.004708	0.250	0.42	2.688	0.005081	0.000373	0.000162	0.000211	0.0064	2.0	0.177660
6150.5	X476	150	5	384	0.004379	0.255	0.35	2.240	0.004902	0.000523	0.000162	0.000362	0.0064	2.0	0.248088
6150.5	X476	150	5	331	0.004373	0.240	0.35	2.240	0.005107	0.000734	0.000162	0.000573	0.0064	2.0	0.417448
6150.5	X476	150	5	364	0.004341	0.240	0.35	2.240	0.004834	0.000493	0.000162	0.000332	0.0064	2.0	0.241719
6150.10	X476	150	10	343	0.004455	0.250	0.51	3.264	0.004700	0.000245	0.000162	8.35E-05	0.0064	2.0	0.085170
6300.2	X476	300	2	383	0.004306	0.250	0.47	3.008	0.004764	0.000458	0.000162	0.000297	0.0064	2.0	0.278710
6300.2	X476	300	2	356	0.004427	0.280	0.47	3.008	0.004731	0.000304	0.000162	0.000143	0.0064	2.0	0.119598
6300.10	X476	300	10	367	0.004245	0.280	0.32	2.048	0.004684	0.000439	0.000162	0.000278	0.0064	2.0	0.158571
6300.12	X476	300	12	363	0.004493	0.270	0.45	2.880	0.004806	0.000313	0.000162	0.000152	0.0064	2.0	0.126250
6550.3	X476	550	3	386	0.004504	0.250	0.39	2.496	0.004768	0.000264	0.000162	0.000102	0.0064	2.0	0.079950
6550.3	X476	550	3	376	0.004482	0.260	0.39	2.496	0.004725	0.000243	0.000162	8.15E-05	0.0064	2.0	0.061125
6550.7	X476	550	7	347	0.004361	0.235	0.445	2.848	0.004421	6.00E-05	0.000162	-0.000102	0.0064	2.0	-0.096101
6550.7	X476	550	7	339	0.004452	0.210	0.445	2.848	0.004592	0.000140	0.000162	-2.15E-05	0.0064	2.0	-0.022780
6550.7	X476	550	7	348	0.004475	0.250	0.445	2.848	0.004693	0.000218	0.000162	5.65E-05	0.0064	2.0	0.050285
5150.3	X475	150	3	337	0.004475	0.240	0.39	2.496	0.004774	0.000299	0.000162	0.000138	0.0064	2.0	0.111719
5150.3	X475	150	3	299	0.004551	0.250	0.39	2.496	0.004854	0.000303	0.000162	0.000141	0.0064	2.0	0.110370
5150.8	X475	150	8	314	0.004735	0.250	0.37	2.368	0.005003	0.000268	0.000162	0.000107	0.0064	2.0	0.078810
5150.8	X475	150	8	297	0.004563	0.255	0.37	2.368	0.004858	0.000295	0.000162	0.000134	0.0064	2.0	0.096853
5150.8	X475	150	8	303	0.004499	0.260	0.37	2.368	0.004755	0.000256	0.000162	9.45E-05	0.0064	2.0	0.067240
5150.11	X475	150	11	298	0.004621	0.250	0.39	2.496	0.005101	0.000480	0.000162	0.000319	0.0064	2.0	0.248430
5550.2	X475	550	2	326	0.004298	0.255	0.46	2.944	0.004519	0.000221	0.000162	5.95E-05	0.0064	2.0	0.053667
5550.2	X475	550	2	324	0.004623	0.255	0.46	2.944	0.004854	0.000231	0.000162	6.95E-05	0.0064	2.0	0.062686
5550.2	X475	550	2	321	0.004601	0.255	0.46	2.944	0.004801	0.000200	0.000162	3.85E-05	0.0064	2.0	0.034725

4A. (cont'd) Mass fluxes - NZ JGOFS, Chatham Rise (October 1993).

Trap code	Station	Trap depth (m)	Cylinder position	Filter number	Tared filter weight W_t (g)	Volume filtered V_f (l)	Brine height H_b (m)	Brine volume $V_r=AH_b$ (l)	Filtered weight W_f (g)	Mass difference W_f-W_t (g)	Blank weight W_{blk} (g)	Total weight W_T (g)	Trap area A (m^2)	Duration t (d)	Total mass flux $TM=W_TV_r(V_fAt)^{-1}$ ($g\ m^{-2}\ d^{-1}$)
5550.4	X475	550	4	308	0.004593	0.250	0.40	2.560	0.004802	0.000209	0.000162	4.75E-05	0.0064	2.0	0.038000
5550.4	X475	550	4	308	0.004593	0.250	0.40	2.560	0.004802	0.000209	0.000162	4.75E-05	0.0064	2.0	0.038000
Blk3	~	~	~	353	0.004403	0.270	~	0	0.004771	0.000368	0.000162	0.000207	0.0064	~	-0
Blk3	~	~	~	301	0.004454	0.260	~	0	0.004636	0.000182	0.000162	2.05E-05	0.0064	~	-0
Blk3	~	~	~	361	0.004415	0.270	~	0	0.004556	0.000141	0.000162	-2.05E-05	0.0064	~	-0
7100.4	X477	100	4	336	0.004361	0.280	0.360	2.304	0.004726	0.000365	0.000168	0.000197	0.0064	2.1	0.120367
7100.5	X477	100	5	373	0.004302	0.265	0.345	2.208	0.004748	0.000446	0.000168	0.000278	0.0064	2.1	0.172097
7100.10	X477	100	10	394	0.004523	0.250	0.385	2.464	0.005166	0.000643	0.000168	0.000475	0.0064	2.1	0.348040
7100.10	X477	100	10	374	0.004256	0.280	0.385	2.464	0.004605	0.000349	0.000168	0.000181	0.0064	2.1	0.118250
7220.2	X477	220	2	354	0.004467	0.235	0.350	2.240	0.005111	0.000644	0.000168	0.000476	0.0064	2.1	0.337305
7220.7	X477	220	7	388	0.004525	0.250	0.365	2.336	0.005026	0.000501	0.000168	0.000333	0.0064	2.1	0.231236
7220.7	X477	220	7	333	0.004412	0.260	0.365	2.336	0.005138	0.000726	0.000168	0.000558	0.0064	2.1	0.372755
8220.2	X478	220	2	350	0.004346	0.250	0.420	2.688	0.006940	0.002594	0.000168	0.002426	0.0064	2.1	1.940480
8220.2	X478	220	2	385	0.004438	0.270	0.420	2.688	0.006942	0.002504	0.000168	0.002336	0.0064	2.1	1.730074
8220.3	X478	220	3	329	0.004561	0.275	0.415	2.656	0.007181	0.002620	0.000168	0.002452	0.0064	2.1	1.761756
8100.2	X478	100	2	375	0.004524	0.290	0.550	3.520	0.004783	0.000259	0.000168	9.06E-05	0.0064	2.1	0.081823
8100.7	X478	100	7	345	0.004468	0.260	0.315	2.016	0.004853	0.000385	0.000168	0.000217	0.0064	2.1	0.124962
8100.9	X478	100	9	387	0.004559	0.250	0.320	2.048	0.005421	0.000862	0.000168	0.000694	0.0064	2.1	0.422766
8100.9	X478	100	9	393	0.004560	0.280	0.320	2.048	0.004929	0.000369	0.000168	0.000201	0.0064	2.1	0.109170
Blk4	~	~	~	320	0.004377	0.250	~	0	0.004616	0.000239	0.000168	7.06E-05	0.0064	~	-0
Blk4	~	~	~	341	0.004357	0.250	~	0	0.004400	4.30E-05	0.000168	-0.000125	0.0064	~	-0
Blk4	~	~	~	323	0.004348	0.250	~	0	0.004389	4.10E-05	0.000168	-0.000127	0.0064	~	-0
Blk4	~	~	~	295	0.004592	0.200	~	0	0.004785	0.000193	0.000168	2.46E-05	0.0064	~	-0
Blk4	~	~	~	330	0.004461	0.210	~	0	0.004571	0.000110	0.000168	-5.84E-05	0.0064	~	-0
Blk4	~	~	~	358	0.004446	0.250	~	0	0.004581	0.000135	0.000168	-3.34E-05	0.0064	~	-0
Blk4	~	~	~	311	0.004653	0.250	~	0	0.004818	0.000165	0.000168	-3.4E-06	0.0064	~	-0

4A. (cont'd) Mass fluxes - NZ JGOFS, Chatham Rise (October 1993).

Trap code	Station	Trap depth (m)	Cylinder position	Filter number	Tared filter weight W_t (g)	Volume filtered V_f (l)	Brine height H_b (m)	Brine volume $V_r=AH_b$ (l)	Filtered weight W_f (g)	Mass difference W_f-W_t (g)	Blank weight W_{blk} (g)	Total weight W_T (g)	Trap area A (m^2)	Duration t (d)	Total mass flux $TM=W_TV_r(V_fAt)^{-1}$ (g m^{-2} d^{-1})
9110.1	X479	110	1	398	0.004282	0.250	0.465	2.976	0.004754	0.000472	0.000168	0.000304	0.0064	2.4	0.235290
9110.1	X479	110	1	406	0.004265	0.250	0.465	2.976	0.004732	0.000467	0.000168	0.000299	0.0064	2.4	0.231415
9110.3	X479	110	3	414	0.004563	0.250	0.515	3.296	0.005103	0.000540	0.000168	0.000372	0.0064	2.4	0.318957
9110.10	X479	110	10	404	0.004424	0.250	0.405	2.592	0.004975	0.000551	0.000168	0.000383	0.0064	2.4	0.258255
9300.4	X479	300	4	413	0.004455	0.250	0.330	2.112	0.004793	0.000338	0.000168	0.000170	0.0064	2.4	0.093280
9300.4	X479	300	4	407	0.004437	0.250	0.330	2.112	0.004817	0.000380	0.000168	0.000212	0.0064	2.4	0.116380
9300.8	X479	300	8	412	0.004478	0.250	0.360	2.304	0.004803	0.000325	0.000168	0.000157	0.0064	2.4	0.093960
9300.9	X479	300	9	408	0.004424	0.250	0.345	2.208	0.004768	0.000344	0.000168	0.000176	0.0064	2.4	0.100970
9550.5	X479	550	5	369	0.004262	0.275	0.420	2.688	0.004529	0.000267	0.000168	9.86E-05	0.0064	2.4	0.062745
9550.5	X479	550	5	352	0.004278	0.265	0.420	2.688	0.004572	0.000294	0.000168	0.000126	0.0064	2.4	0.082943
9550.7	X479	550	7	325	0.004453	0.260	0.420	2.688	0.004611	0.000158	0.000168	-1.04E-05	0.0064	2.4	-0.007000
10110.2	X480	110	2	395	0.004366	0.250	0.360	2.304	0.004845	0.000479	0.000168	0.000311	0.0064	2.4	0.186360
10110.2	X480	110	2	410	0.004430	0.250	0.360	2.304	0.004917	0.000487	0.000168	0.000319	0.0064	2.4	0.191160
10110.5	X480	110	5	396	0.004296	0.250	0.290	1.856	0.004871	0.000575	0.000168	0.000407	0.0064	2.4	0.196523
10110.1	X480	110	1	402	0.004516	0.250	0.385	2.464	0.005097	0.000581	0.000168	0.000413	0.0064	2.4	0.264752
10550.1	X480	550	1	411	0.004409	0.250	0.370	2.368	0.004684	0.000275	0.000168	0.000107	0.0064	2.4	0.065737
10550.4	X480	550	4	401	0.004498	0.250	0.295	1.888	0.004926	0.000428	0.000168	0.000260	0.0064	2.4	0.127637
10550.4	X480	550	4	397	0.004404	0.250	0.295	1.888	0.004874	0.000470	0.000168	0.000302	0.0064	2.4	0.148287
10550.7	X480	550	7	403	0.004381	0.250	0.275	1.760	0.004826	0.000445	0.000168	0.000277	0.0064	2.4	0.126775

4B. Particulate phosphorus fluxes - NZ JGOFS, Chatham Rise (October 1993).

Trap code	Station	Trap depth (m)	Cylinder position	Volume filtered V_f (l)	Brine height H_b (m)	Brine volume $V_r=Ah_b$ (l)	Trap area A (m^2)	Duration t (d)	Phosphorus P_s ($\mu g\ filter^{-1}$)	P blank P_{blk} ($\mu g\ filter^{-1}$)	Total P_T P_s-P_{blk} (μg)	P flux $PP=P_TV_r$ $(V_rAt)^{-1}$ ($mg\ m^{-2}\ d^{-1}$)
6150.3	X476	150	3	0.50	0.430	2.752	0.0064	2.0	2.0	0.7	1.3	0.559000
6150.6	X476	150	6	0.49	0.390	2.496	0.0064	2.0	2.6	0.7	1.9	0.756122
6150.11	X476	150	11	0.47	0.400	2.560	0.0064	2.0	1.9	0.7	1.2	0.510638
6300.3	X476	300	3	0.49	0.415	2.656	0.0064	2.0	1.7	0.7	1.0	0.423469
6300.5	X476	300	5	0.50	0.460	2.944	0.0064	2.0	1.6	0.7	0.9	0.414000
6300.7	X476	300	7	0.50	0.440	2.816	0.0064	2.0	1.4	0.7	0.7	0.308000
6550.1	X476	550	1	0.50	0.410	2.624	0.0064	2.0	1.1	0.7	0.4	0.164000
6550.8	X476	550	8	0.50	0.405	2.592	0.0064	2.0	1.3	0.7	0.6	0.243000
5150.4	X475	150	4	0.50	0.360	2.304	0.0064	2.0	1.8	0.7	1.1	0.396000
5150.6	X475	150	6	0.50	0.340	2.176	0.0064	2.0	2.1	0.7	1.4	0.476000
5150.9	X475	150	9	0.50	0.380	2.432	0.0064	2.0	1.7	0.7	1.0	0.380000
5550.7	X475	550	7	0.49	0.540	3.456	0.0064	2.0	1.2	0.7	0.5	0.275510
5550.8	X475	550	8	0.50	0.365	2.336	0.0064	2.0	1.6	0.7	0.9	0.328500
Blk3	~	~	~	0.50	~	0	0.0064	2.0	0.6	0.7	-0.1	-0
Blk3	~	~	~	0.50	~	0	0.0064	2.0	0.6	0.7	-0.1	-0
Blk3	~	~	~	0.50	~	0	0.0064	2.0	0.9	0.7	0.2	-0
7100.2	X477	100	2	0.48	0.300	1.920	0.0064	2.1	4.2	0.67	3.53	1.050595
7100.2	X477	100	2	0.50	0.300	1.920	0.0064	2.1	4.7	0.67	4.03	1.151429
7100.2	X477	100	2	0.48	0.300	1.920	0.0064	2.1	4.4	0.67	3.73	1.110119
7100.7	X477	100	7	0.50	0.340	2.176	0.0064	2.1	3.7	0.67	3.03	0.981143
7100.7	X477	100	7	0.49	0.340	2.176	0.0064	2.1	3.4	0.67	2.73	0.902041
7100.7	X477	100	7	0.49	0.340	2.176	0.0064	2.1	3.5	0.67	2.83	0.935083
7100.9	X477	100	9	0.50	0.355	2.272	0.0064	2.1	3.3	0.67	2.63	0.889190
7100.9	X477	100	9	0.50	0.355	2.272	0.0064	2.1	3.3	0.67	2.63	0.889190
7100.9	X477	100	9	0.47	0.355	2.272	0.0064	2.1	3.0	0.67	2.33	0.838045

4B. (cont'd) Particulate phosphorus fluxes - NZ JGOFS, Chatham Rise (October 1993).

Trap code	Station	Trap depth (m)	Cylinder position	Volume filtered V_f (l)	Brine height H_b (m)	Brine volume $V_r=Ah_b$ (l)	Trap area A (m^2)	Duration t (d)	Phosphorus P_s ($\mu g\ filter^{-1}$)	P blank P_{blk} ($\mu g\ filter^{-1}$)	Total P_T P_s-P_{blk} (μg)	P flux $PP=P_TV_r(V_rAt)^{-1}$ ($mg\ m^{-2}\ d^{-1}$)
7220.4	X477	220	4	0.50	0.380	2.432	0.0064	2.1	3.0	0.67	2.33	0.843238
7220.4	X477	220	4	0.50	0.380	2.432	0.0064	2.1	2.5	0.67	1.83	0.662286
7220.4	X477	220	4	0.48	0.380	2.432	0.0064	2.1	3.0	0.67	2.33	0.878373
7220.6	X477	220	6	0.48	0.355	2.272	0.0064	2.1	3.0	0.67	2.33	0.820585
7220.6	X477	220	6	0.50	0.355	2.272	0.0064	2.1	3.0	0.67	2.33	0.787762
7220.6	X477	220	6	0.50	0.355	2.272	0.0064	2.1	3.0	0.67	2.33	0.787762
8220.5	X478	220	5	0.50	0.345	2.208	0.0064	2.1	9.7	0.67	9.03	2.967000
8220.5	X478	220	5	0.50	0.345	2.208	0.0064	2.1	9.9	0.67	9.23	3.032714
8220.5	X478	220	5	0.48	0.345	2.208	0.0064	2.1	9.1	0.67	8.43	2.885268
8220.7	X478	220	7	0.50	0.355	2.272	0.0064	2.1	8.7	0.67	8.03	2.714905
8220.7	X478	220	7	0.50	0.355	2.272	0.0064	2.1	8.6	0.67	7.93	2.681095
8220.7	X478	220	7	0.47	0.355	2.272	0.0064	2.1	8.2	0.67	7.53	2.708359
8100.5	X478	100	5	0.46	0.320	2.048	0.0064	2.1	3.0	0.67	2.33	0.771843
8100.5	X478	100	5	0.48	0.320	2.048	0.0064	2.1	2.9	0.67	2.23	0.707937
8100.5	X478	100	5	0.49	0.320	2.048	0.0064	2.1	2.8	0.67	2.13	0.662391
8100.6	X478	100	6	0.50	0.395	2.528	0.0064	2.1	2.6	0.67	1.93	0.726048
8100.6	X478	100	6	0.48	0.395	2.528	0.0064	2.1	2.5	0.67	1.83	0.717113
8100.6	X478	100	6	0.50	0.395	2.528	0.0064	2.1	2.7	0.67	2.03	0.763667
8100.11	X478	100	11	0.49	0.340	2.176	0.0064	2.1	3.0	0.67	2.33	0.769874
8100.11	X478	100	11	0.48	0.340	2.176	0.0064	2.1	4.0	0.67	3.33	1.123214
8100.11	X478	100	11	0.50	0.340	2.176	0.0064	2.1	3.8	0.67	3.13	1.013524
Blk4	~	~	~	0.50	~	0	0.0064	2.1	0.4	0.67	-0.27	-0
Blk4	~	~	~	0.50	~	0	0.0064	2.1	0.9	0.67	0.23	-0
Blk4	~	~	~	0.50	~	0	0.0064	2.1	0.7	0.67	0.03	-0
9110.5	X479	110	5	0.53	0.420	2.688	0.0064	2.4	5.1	0.7	4.4	1.452830
9110.8	X479	110	8	0.50	0.350	2.240	0.0064	2.4	6.8	0.7	6.1	1.779167

4B. (cont'd) Particulate phosphorus fluxes - NZ JGOFS, Chatham Rise (October 1993).

Trap code	Station	Trap depth (m)	Cylinder position	Volume filtered V_f (l)	Brine height H_b (m)	Brine volume $V_r=Ah_b$ (l)	Trap area A (m^2)	Duration t (d)	Phosphorus P_s ($\mu g\ filter^{-1}$)	P blank P_{blk} ($\mu g\ filter^{-1}$)	Total P_T P_s-P_{blk} (μg)	P flux $PP=P_TV_r(V_fAt)^{-1}$ ($mg\ m^{-2}\ d^{-1}$)
9110.12	X479	110	12	0.50	0.420	2.688	0.0064	2.4	4.8	0.7	4.1	1.435000
9300.3	X479	300	3	0.53	0.465	2.976	0.0064	2.4	2.0	0.7	1.3	0.475236
9300.6	X479	300	6	0.47	0.385	2.464	0.0064	2.4	2.0	0.7	1.3	0.443706
9300.12	X479	300	12	0.54	0.365	2.336	0.0064	2.4	2.4	0.7	1.7	0.478781
9550.2	X479	550	2	0.58	0.280	1.792	0.0064	2.4	2.1	0.7	1.4	0.281609
9550.8	X479	550	8	0.52	0.380	2.432	0.0064	2.4	1.9	0.7	1.2	0.365385
10110.6	X480	110	6	0.50	0.305	1.952	0.0064	2.4	5.9	0.7	5.2	1.321667
10110.7	X480	110	7	0.50	0.345	2.208	0.0064	2.4	7.6	0.7	6.9	1.983750
10110.11	X480	110	11	0.50	0.310	1.984	0.0064	2.4	6.4	0.7	5.7	1.472500
10550.3	X480	550	3	0.30	0.340	2.176	0.0064	2.4	2.0	0.7	1.3	0.613889
10550.8	X480	550	8	0.50	0.345	2.208	0.0064	2.4	2.3	0.7	1.6	0.460000
Blk5	~	~	~	0.50	~	0	0.0064	2.4	0.7	0.7	0	-0
Blk5	~	~	~	0.50	~	0	0.0064	2.4	0.8	0.7	0.1	-0
Blk5	~	~	~	0.50	~	0	0.0064	2.4	0.6	0.7	-0.1	-0

4C. Suspended particulate matter (SPM) concentrations - NZ JGOFS, Chatham Rise (October 1993).

Station	Date	Time	Depth (m)	Filtered weight (mg)	Concentration SPM (mg l^{-1})
X475k	OCT 13 1993	1330	150	1.73	0.1885
X475k	OCT 13 1993	1330	550	2.49	0.2567
X475k	OCT 13 1993	1330	300	3.48	0.3544
X476i	OCT 11 1993	1330	150	2.90	0.3742
X476i	OCT 11 1993	1330	300	3.03	0.3523
X476i	OCT 11 1993	1330	550	3.06	0.3290
X477i	OCT 16 1993	1330	100	6.67	1.8528
X477i	OCT 16 1993	1330	220	5.26	0.6454
X477i	OCT 16 1993	1330	220	6.54	1.3568
X478c	OCT 15 1993	1330	220	4.76	0.6271
X478c	OCT 15 1993	1330	100	5.16	1.0178
X479j	OCT 19 1993	1330	550	2.61	0.2650
X479j	OCT 19 1993	1330	300	5.82	0.6140
X479j	OCT 19 1993	1330	110	6.16	0.8993
X480c	OCT 17 1993	1330	110	4.05	0.8100
X480c	OCT 17 1993	1330	550	2.74	0.4684
X480c	OCT 17 1993	1330	300	4.07	0.8134

APPENDIX 5: HPLC pigment analyses and fluxes - New Zealand JGOFS, Chatham Rise (NZOI-NIWA research voyages 3009 and 3014, June-July and October 1993).

5A. Chromatogram characteristics

PIGMENT CODE	Pigment	Average retention time RT (min)	Notes on resolution	RF	Cali-brated	Ratio
chl	unknown chlorophyll	2.98	Unknown (Looks like a chlorophyll *c* derivative. No red peak at 665nm)	1.88E-04		
Chlc3	chlorophyll *c3*	3.44	Sometimes similar to RT 2.98, but in general good resolution. Very similar in spectra to Chl *c*'s	1.15E-04		
chl	unknown chlorophyll	4.07	Unknown (similar to RT 2.98)	1.88E-04		
Chlc's	chlorophyll *c*'s	5.11	Mixture of chlorophyll *c1*, chlorophyll *c2* and Mg2,4D. In some cases resolution affected, such as on the elution gradient shoulder	1.15E-04		
car	unknown carotenoid	6.02	Unknown (peridinin-like)	1.88E-04		
chl	unknown chlorophyll	6.31	Unknown (chlorophyll *a*-like derivative in very small amounts)	1.88E-04		
Peri	peridinin	6.87	In clustered region of chromatogram. Maybe overestimated in some cases	3.69E-04		
car	unknown carotenoid	7.05	Unknown (sometimes co-elutes with peridinin. A combination of peaks. Similar to peridinin and a chlorophyll peak absorbing strongly in the red)	1.88E-04		
PPa1	phaeophorbide *a1*	7.57	Close to 19'BOF. Not baseline-resolved when peaks are in appreciable amounts	5.26E-04		
BOF	19'butanoloxyfucoxanthin	7.90	Affected by phaeophorbide *a1* to some degree	2.74E-04		
Fuco	fucoxanthin	8.26	Small amounts of phaeophorbide *a* co-elute with this peak	3.82E-04		
PPa2	phaeophorbide *a2*	8.71	Shoulder peak to 19'HOF	5.26E-04		
HOF	19'hexanoloxyfucoxanthin	8.91	Highest peak in triplet. Affected by two shoulder peaks	2.74E-04		
car	unknown carotenoid	9.11	Unknown (varies between chromatograms)	1.88E-04		
PPa3/car	phaeophorbide *a3*	9.44	Also interfered with by various unknown carotenoids	5.26E-04		
Diad/PPa4	diadinoxanthin	9.73	Diadinoxanthin and phaeophorbide *a4* run together producing a combined spectra. The contribution of each peak cannot be determined quantitatively	1.87E-04		
car	unknown carotenoid	9.89	Unknown (fucoxanthin-like. Could be Anthaxanthin)	1.88E-04		
car	unknown carotenoid	10.19	Unknown	1.88E-04		
Allo	alloxanthin	10.37	Identified as being halfway between zeaxanthin/lutein and diadinoxanthin. Sometimes spectra is fucoxanthin-like	1.88E-04		
car	unknown carotenoid	10.46	Unknown (combination of carotenoids)	1.88E-04		
Diat	diatoxanthin	10.73	If present, only in trace amounts, next to zeaxanthin/lutein	2.29E-04		
Zea/Lut	zeaxanthin/lutein	10.93	Zeaxanthin and lutein co-elute. Unable to quantify exact contributions. May be diatoxanthin, but the last major peak before the dip has been consistently ascribed to zeaxanthin/lutein on all chromatograms	1.99E-04		
car	unknown carotenoid	11.20	Unknown (maybe zea/lutein. Fucoxanthin-like spectra in some cases)	1.88E-04		
Chlb	chlorophyll *b*	14.07	Good resolution	4.82E-04	3.38E-04	0.70124
car/chl	unknown carotenoid or chlorophyll	14.43	Unknown (carotenoid and chlorophyll)	1.88E-04		
Chla(al)	chlorophyll *a* allomer	14.67	Good resolution	4.96E-04		
Chla	chlorophyll *a*	15.05	Good resolution	4.96E-04	3.82E-04	0.77016
Chla(ep)	chlorophyll *a* epimer	15.22	Sometimes merges with echinone	4.96E-04		
Ech	echinone	15.61	On shoulder of chlorophyll *a* (epimer)	1.99E-04		
car	unknown carotenoid	16.35	Unknown	1.88E-04		
car	unknown carotenoid	17.53	Unknown	1.88E-04		
PPA1	phaeophytin *a1*	18.37	Present in very low amounts	5.26E-04		
PPA2	phaeophytin *a2*	20.09	Shoulder of β, β-carotene. Sometimes merges. Shoulders have been cut off manually in most cases	5.26E-04		
BBCar	β, β-carotene	20.36	Sometimes merges with phaeophytin *a2*	1.74E-04	1.26E-04	0.72413

5B. Chromatogram calculations

Response Factor (ng $\mu V.sec^{-1}$)

$$RF = \frac{MF \times CF}{E(440nm)1\% \times 100}$$

MF	Machine Factor (3.125E-8 abs units.ml UV/VIS BASELINE)
CF	Correction factors for chlorophylls and carotenoids (1.2)
E(440nm)1%	Extinction coefficient of a 1% solution through a 1 cm path length
100	Converts to a 100% solution

Solution concentration (ng μl^{-1})

$$SC = \frac{PA \times RF}{IV}$$

PA	Peak Area ($\mu V.sec$)
RF	Response Factor (ng $\mu V.sec^{-1}$)
IV	Injection Volume (μl). Typically 73.31μl.

Original concentration ($\mu g\ l^{-1}$)

$$OC = \frac{SC \times EV \times DF}{SA}$$

EV	Extract Volume (μl). Typically 2500μl.
DF	Dilution Factor.
SA	Sample Amount

5C. Original baseline concentration of pigments in sediment traps (μg trap^{-1}) - NZ JGOFS, Chatham Rise, winter 1993).

SAMPLE NAME	FILE NAME	IV	DIL	TIME	chl	Chlc3	chl	Chlc's	car	chl	Peri	car	PPa1	BOF	Fuco
X467A 9-110-2P1	300935	73.31	1.93	0	0.00E+00	4.44E-02	9.22E-03	1.68E-01	2.27E-02	5.12E-03	3.44E-01	7.20E-02	2.11E-01	6.54E-02	1.46E+00
X467A 9-110-2P2	300936	73.31	2.02	39	3.87E-03	3.15E-02	6.71E-03	1.34E-01	4.40E-03	3.45E-02	2.83E-01	8.93E-02	2.09E-01	9.09E-02	1.22E+00
X467A 9-210-6	300937	73.31	2.08	77	2.39E-02	2.34E-02	4.28E-03	1.26E-01	0.00E+00	1.78E-02	1.74E-01	6.46E-02	1.17E-01	6.65E-02	1.13E+00
X465A 7-300-5	300947	73.31	1.96	460	1.19E-03	3.66E-04	2.13E-03	5.67E-03	0.00E+00	0.00E+00	2.42E-02	1.01E-02	1.17E-02	2.78E-02	4.00E-02
X464B 6-550-8	300948	73.31	2	497	1.19E-03	2.18E-03	1.31E-03	1.96E-02	1.96E-03	7.17E-03	1.33E-02	4.41E-02	9.36E-03	4.04E-02	4.08E-02
X464B 6-120-1	300949	73.31	2	535	0.00E+00	4.88E-03	0.00E+00	3.05E-02	8.80E-03	1.60E-02	6.02E-02	1.71E-02	7.42E-02	8.92E-02	1.55E-01
X464B 6-300-4	300950	73.31	2.01	572	0.00E+00	1.02E-02	2.32E-03	1.22E-02	2.08E-03	7.62E-03	2.90E-02	0.00E+00	2.60E-02	3.82E-02	3.25E-02
X465A 7-200-6	300951	73.31	2.04	610	0.00E+00	1.50E-03	1.65E-03	1.57E-02	4.62E-03	0.00E+00	2.22E-02	1.84E-03	1.81E-02	6.24E-02	5.19E-02
X464B 6-220-10	300952	73.31	1.99	647	2.61E-03	4.66E-03	2.91E-03	1.34E-02	4.52E-03	9.04E-03	6.74E-02	0.00E+00	3.79E-02	6.72E-02	5.56E-02
X465A 7-550-4	300953	73.31	1.94	685	1.53E-03	3.75E-03	2.71E-03	9.84E-04	1.06E-03	8.12E-03	4.00E-02	1.07E-02	5.76E-02	3.57E-02	3.15E-02
X465A 7-120-12	300954	73.31	2.05	722	0.00E+00	4.10E-03	0.00E+00	1.22E-02	1.02E-03	9.88E-03	8.29E-03	0.00E+00	2.77E-02	9.42E-02	5.34E-02
X468A 10-120-6	V300955	73.31	2.01	1369	4.90E-03	2.86E-02	2.84E-03	1.21E-01	1.43E-02	2.28E-02	4.09E-01	1.23E-01	2.42E-01	1.32E-01	1.30E+00
X468A 10-300-1	V300956	73.31	2.03	1406	9.11E-03	3.66E-03	0.00E+00	3.26E-02	1.04E-02	1.67E-02	1.89E-01	7.81E-02	1.32E-01	7.48E-02	7.36E-01
X468A 10-550-1	V300957	73.31	2.03	1444	7.36E-03	4.24E-03	1.62E-03	4.78E-02	0.00E+00	1.88E-02	5.54E-02	1.84E-01	3.71E-01	1.09E-01	9.90E-01

5C. (cont'd) Original baseline concentration of pigments in sediment traps (μg trap^{-1}) - NZ JGOFS, Chatham Rise, winter 1993).

SAMPLE NAME	PPa2	HOF	car	PPa3/car	Diad/PPa4	car	car	Allo	car	Diat	Zea/Lut	car	Chlb	car/chl
X467A 9-110-2P1	8.36E-02	1.47E-01	5.22E-02	6.91E-02	1.33E-01	6.61E-02	1.41E-01	1.60E-02	4.50E-02	8.22E-03	1.02E-01	5.57E-02	2.47E-01	3.68E-02
X467A 9-110-2P2	1.68E+00	1.42E-01	7.17E-02	9.45E-02	1.14E-01	7.24E-02	1.23E-01	1.43E-02	3.78E-02	6.13E-03	2.36E-02	4.47E-02	8.76E-02	2.45E-02
X467A 9-210-6	1.84E-01	1.74E-01	6.86E-02	1.01E-01	1.07E-01	7.16E-02	1.04E-01	1.72E-02	2.54E-02	7.77E-03	2.24E-02	4.47E-02	1.28E-01	3.61E-02
X465A 7-300-5	1.51E-02	1.07E-01	0.00E+00	8.28E-03	8.78E-03	1.24E-02	4.31E-03	1.25E-02	1.89E-02	0.00E+00	3.56E-02	2.28E-03	7.06E-02	1.56E-02
X464B 6-550-8	3.36E-02	1.52E-01	0.00E+00	3.34E-02	1.47E-02	1.80E-02	5.92E-03	7.02E-03	4.64E-03	0.00E+00	3.14E-02	1.67E-03	6.66E-02	1.64E-02
X464B 6-120-1	3.91E-02	1.51E-01	0.00E+00	6.10E-03	2.14E-02	1.35E-02	1.08E-02	3.83E-03	1.27E-02	6.46E-03	2.60E-02	9.07E-03	5.79E-02	1.91E-02
X464B 6-300-4	9.48E-03	1.12E-01	0.00E+00	2.62E-02	6.10E-03	2.95E-01	0.00E+00	3.66E-02	0.00E+00	0.00E+00	4.33E-02	1.52E-02	4.93E-02	1.75E-02
X465A 7-200-6	2.83E-02	1.52E-01	0.00E+00	2.22E-02	2.14E-02	4.10E-02	0.00E+00	0.00E+00	2.26E-02	0.00E+00	2.86E-02	1.60E-03	6.91E-02	2.17E-02
X464B 6-220-10	2.86E-02	1.24E-01	2.86E-03	7.69E-04	1.07E-02	2.01E-02	1.63E-03	1.18E-02	4.28E-03	0.00E+00	3.14E-02	1.64E-03	5.45E-02	1.81E-02
X465A 7-550-4	1.94E-02	6.84E-02	0.00E+00	6.43E-03	2.18E-03	4.41E-03	4.88E-04	0.00E+00	7.96E-03	0.00E+00	1.58E-02	1.10E-03	5.09E-02	1.89E-02
X465A 7-120-12	4.64E-02	1.58E-01	0.00E+00	4.86E-02	2.62E-02	8.31E-03	1.02E-02	2.14E-02	0.00E+00	0.00E+00	3.72E-02	1.38E-03	9.85E-02	3.08E-03
X468A 10-120-6	0.00E+00	4.22E-01	1.16E-01	1.25E-01	1.54E-01	7.60E-02	1.15E-01	5.00E-02	4.93E-02	7.54E-03	6.38E-02	9.32E-02	2.87E-01	4.70E-02
X468A 10-300-1	1.02E-01	2.29E-01	9.37E-02	1.15E-01	7.18E-02	5.44E-02	4.20E-02	2.64E-02	3.97E-02	4.81E-03	3.01E-02	5.51E-02	9.72E-02	1.93E-02
X468A 10-550-1	1.70E-01	3.28E-01	1.14E-01	1.57E-01	9.85E-02	9.75E-02	5.73E-02	3.11E-02	5.84E-02	8.05E-03	3.28E-02	7.91E-02	9.23E-02	3.20E-02

5C. (cont'd) Original baseline concentration of pigments in sediment traps (μg trap^{-1}) - NZ JGOFS, Chatham Rise, winter 1993).

SAMPLE NAME	Chla(al)	Chla	Chla(ep)	Ech	car	car	PPA1	PPA2	BBCar
X467A 9-110-2P1	1.57E-01	1.66E+00	8.39E-02	1.97E-03	1.10E-02	9.29E-03	7.79E-03	5.33E-02	1.41E-01
X467A 9-110-2P2	1.29E-01	1.41E+00	6.38E-02	5.02E-03	1.10E-02	7.96E-03	1.26E-02	1.14E-02	9.50E-02
X467A 9-210-6	1.47E-01	1.43E+00	7.15E-02	5.49E-03	8.24E-03	7.95E-03	1.46E-02	1.16E-02	6.40E-02
X465A 7-300-5	3.57E-02	2.60E-01	1.24E-02	1.08E-03	1.08E-02	9.03E-03	1.44E-03	1.18E-02	1.50E-02
X464B 6-550-8	2.85E-02	2.65E-01	1.44E-02	1.09E-03	7.16E-03	6.04E-03	5.38E-04	7.07E-03	1.34E-02
X464B 6-120-1	2.06E-02	2.46E-01	2.56E-02	0.00E+00	4.44E-03	7.86E-03	1.44E-03	6.13E-03	1.57E-02
X464B 6-300-4	2.31E-02	1.51E-01	9.06E-03	8.25E-04	3.23E-03	1.95E-03	3.39E-03	3.82E-03	9.26E-03
X465A 7-200-6	2.61E-02	2.38E-01	0.00E+00	7.85E-03	5.03E-03	3.16E-04	2.16E-03	3.07E-03	7.77E-03
X464B 6-220-10	2.03E-02	1.75E-01	1.27E-02	0.00E+00	4.34E-03	2.80E-03	1.18E-03	4.28E-03	7.12E-03
X465A 7-550-4	1.60E-02	1.44E-01	1.15E-02	0.00E+00	4.06E-03	3.24E-03	6.61E-04	2.12E-03	5.87E-04
X465A 7-120-12	1.05E-01	3.04E-01	0.00E+00	6.18E-03	4.68E-04	8.86E-04	2.46E-03	0.00E+00	0.00E+00
X468A 10-120-6	1.10E-01	1.35E+00	2.84E-02	7.89E-03	4.97E-03	7.79E-03	8.73E-03	2.69E-02	4.98E-02
X468A 10-300-1	6.49E-02	8.19E-01	2.90E-02	6.98E-03	3.12E-03	1.27E-03	3.02E-03	1.78E-02	4.26E-02
X468A 10-550-1	7.72E-02	7.27E-01	2.56E-02	1.28E-02	4.33E-03	5.95E-03	9.25E-03	1.87E-02	3.47E-02

5D. Original baseline concentration of pigments in sediment traps (μg trap^{-1}) - NZ JGOFS, Chatham Rise, spring 1993).

SAMPLE NAME	FILE NAME	IV	DIL	TIME	chl	Chlc3	chl	Chlc's	car	chl	Peri	car	PPa1	BOF	Fuco
X476A 6A1	V301423	73.31	2	113	2.03E-02	3.82E-02	2.37E-03	8.03E-02	2.91E-03	6.57E-03	0.00E+00	4.33E-02	6.42E-01	2.49E-01	2.21E-01
X476A 6B6	V301424	73.31	2	150	2.33E-02	1.09E-02	0.00E+00	4.37E-02	5.53E-03	7.84E-03	6.40E-02	3.74E-02	1.40E-01	2.71E-01	2.85E-01
X475A 5A1	V301425	73.31	2	188	1.03E-02	7.69E-03	1.26E-03	4.90E-02	1.01E-01	0.00E+00	1.19E-01	1.46E-01	1.96E-01	3.32E-01	2.85E-01
X476A 6C4	V301426	73.31	1.85	225	7.22E-04	1.12E-03	0.00E+00	1.05E-02	0.00E+00	9.25E-03	3.87E-02	2.24E-02	0.00E+00	4.44E-02	4.44E-02
X475A 5B6	V301427	73.31	2.09	263	3.06E-03	2.89E-03	0.00E+00	1.02E-02	8.13E-03	5.47E-04	1.20E-01	3.62E-02	1.78E-01	5.15E-02	1.10E-01
X478A 8A12	V301428	73.31	1.94	301	1.45E-02	4.03E-02	1.38E-02	2.04E-01	1.10E-01	2.89E-02	1.56E-01	6.89E-02	5.03E-01	2.27E-01	1.04E+00
X477A 7B8	V301429	73.31	1.7	-582	9.73E-03	4.58E-02	1.87E-02	2.41E-01	0.00E+00	2.11E-02	6.58E-02	2.41E-02	1.30E-01	1.23E-01	1.37E+00
X477A 7A1	V301430	73.31	2	-541	2.02E-03	1.05E-01	4.57E-02	5.62E-01	8.18E-02	2.18E-02	2.51E-01	4.21E-02	2.96E-01	3.62E-01	2.94E+00
X478A 8B4	V301431	73.31	2	-503	1.71E-02	2.10E-02	2.71E-02	1.52E-01	1.50E-01	4.55E-03	1.19E-01	5.58E-02	4.39E-01	3.04E-01	1.14E+00
X480A 10B2	V301432	73.31	1.87	-466	6.05E-03	1.38E-02	0.00E+00	3.83E-02	1.28E-02	1.51E-02	2.87E-02	2.39E-02	6.70E-02	1.05E-01	3.01E-01
X479A 9B11	V301433	73.31	2	-428	2.32E-03	4.24E-03	0.00E+00	1.14E-02	2.09E-01	3.60E-02	1.88E-02	2.04E-02	1.90E-01	3.70E-02	1.59E-01
X479A 9A6	V301434	73.31	2	-390	1.68E-02	1.06E-02	0.00E+00	3.41E-02	0.00E+00	1.03E-02	1.58E-01	6.58E-02	4.61E-01	2.68E-01	3.36E-01
X480A 10A1	V301435	73.31	2	-353	1.41E-02	6.97E-03	0.00E+00	1.93E-02	8.55E-03	1.75E-02	1.31E-01	5.94E-02	5.54E-01	3.37E-01	3.80E-01
X479A 9C3	V301436	73.31	1.97	874	0.00E+00	0.00E+00	0.00E+00	1.98E-02	6.46E-03	1.10E-02	6.16E-03	6.91E-03	6.91E-02	5.63E-02	1.42E-01

5D. (cont'd) Original baselin concentration of pigments in sediment traps (μg trap^{-1}) - NZ JGOFS, Chatham Rise, spring 1993).

SAMPLE NAME	PPa2	HOI	car	PPa3/car	Diad/PPa4	car	car	Allo	car	Diat	Zea/Lut	car	Chlb	car/chl
X476A 6A1	0.00E+00	4.96E 01	0.00E+00	1.33E-01	7.72E-02	3.95E-02	3.53E-02	2.23E-02	4.66E-02	1.12E-02	9.93E-02	~	1.25E-01	3.16E-02
X476A 6B6	9.20E-02	3.90E 01	1.10E-01	1.99E-01	7.49E-02	4.16E-02	4.32E-02	3.50E-02	3.91E-02	1.91E-02	5.26E-02	~	5.88E-02	1.14E-02
X475A 5A1	0.00E+00	3.78E 01	1.19E-01	3.11E-01	7.40E-02	9.00E-02	4.02E-02	2.25E-02	2.76E-02	1.29E-02	3.32E-02	~	6.07E-02	9.71E-03
X476A 6C4	0.00E+00	5.99E 02	0.00E+00	0.00E+00	1.36E-02	1.80E-02	4.18E-03	2.46E-03	2.80E-03	0.00E+00	1.85E-02	~	5.51E-02	1.39E-02
X475A 5B6	0.00E+00	7.53E 02	0.00E+00	3.66E-02	2.06E-02	2.70E-02	2.60E-02	3.70E-02	2.43E-02	2.21E-03	1.21E-02	~	2.01E-02	4.36E-03
X478A 8A12	1.83E-01	3.15E 01	6.88E-02	1.59E-01	2.07E-01	8.93E-02	3.02E-02	7.03E-02	0.00E+00	1.84E-02	3.22E-02	~	6.14E-02	1.39E-02
X477A 7B8	7.03E-02	1.24E 01	5.16E-02	5.16E-02	8.85E-02	5.61E-02	5.69E-02	0.00E+00	7.01E-02	4.07E-02	3.22E-02	~	1.51E-01	2.64E-02
X477A 7A1	3.80E-01	3.19E 01	1.59E-01	2.55E-01	2.11E-01	0.00E+00	3.29E-02	1.88E-01	2.56E-02	2.47E-02	8.65E-02	~	2.08E-01	5.93E-02
X478A 8B4	2.91E-01	2.51E 01	1.24E-01	1.57E-01	2.29E-01	0.00E+00	8.27E-02	1.35E-01	0.00E+00	2.65E-02	7.36E-02	~	1.03E-01	2.09E-02
X480A 10B2	1.29E-01	2.38E 01	6.35E-02	8.88E-02	6.33E-02	3.64E-01	3.65E-02	1.04E-01	0.00E+00	4.53E-02	1.17E-01	~	1.12E-01	5.05E-02
X479A 9B11	5.76E-02	1.78E 01	3.47E-02	0.00E+00	2.33E-02	0.00E+00	1.26E-01	9.60E-03	0.00E+00	4.10E-02	1.67E-01	~	4.76E-02	0.00E+00
X479A 9A6	3.38E-01	6.73E 01	1.61E-01	4.33E-01	1.04E-01	2.12E-01	0.00E+00	6.26E-02	0.00E+00	9.56E-02	1.93E-01	~	1.80E-02	2.02E-02
X480A 10A1	0.00E+00	8.74E 01	1.74E-01	4.95E-01	1.21E-01	2.20E-01	0.00E+00	8.31E-02	1.19E-01	0.00E+00	3.38E-01	~	5.20E-02	8.59E-03
X479A 9C3	3.87E-02	1.24E 01	4.07E-02	9.52E-02	5.02E-02	1.62E-01	0.00E+00	9.95E-02	0.00E+00	0.00E+00	1.61E-01	~	1.20E-01	8.63E-03

5D. (cont'd) Original baseline concentration of pigments in sediment traps (μg trap^{-1}) - NZ JGOFS, Chatham Rise, spring 1993).

SAMPLE NAME	Chla(al)	Chla	Chla(ep)	Ech	car	car	PPA1	PPA2	BBCar
X476A 6A1	5.13E-02	5.52E-01	1.28E-02	0.00E+00	1.06E-02	3.74E-02	2.83E-03	1.50E-02	2.48E-02
X476A 6B6	2.22E-02	3.61E-01	5.79E-03	0.00E+00	6.99E-03	8.56E-03	8.36E-03	1.22E-02	1.57E-02
X475A 5A1	3.86E-02	3.01E-01	1.71E-02	0.00E+00	0.00E+00	8.64E-03	0.00E+00	1.44E-02	1.34E-02
X476A 6C4	1.99E-02	2.92E-01	8.14E-03	0.00E+00	7.93E-03	1.24E-03	2.39E-02	7.73E-03	1.25E-02
X475A 5B6	1.23E-02	1.84E-01	1.13E-02	1.20E-03	6.29E-03	9.50E-03	1.39E-03	1.03E-02	1.12E-02
X478A 8A12	4.20E-02	4.31E-01	1.00E-02	1.45E-02	8.96E-03	9.78E-03	7.86E-03	2.69E-02	3.80E-02
X477A 7B8	1.27E-01	9.77E-01	2.44E-02	7.35E-03	5.86E-03	2.24E-03	6.43E-03	3.29E-02	4.42E-02
X477A 7A1	2.62E-01	2.36E+00	7.17E-02	5.08E-02	8.35E-03	5.96E-03	1.69E-02	4.40E-02	7.22E-02
X478A 8B4	1.41E-01	1.49E+00	6.10E-02	1.65E-02	7.59E-03	5.72E-03	8.18E-03	1.86E-02	4.52E-02
X480A 10B2	1.59E-01	1.33E+00	6.69E-02	1.89E-02	5.83E-03	5.71E-03	1.88E-02	1.95E-02	3.30E-02
X479A 9B11	6.28E-02	6.07E-01	2.40E-02	5.01E-03	4.08E-03	7.61E-03	2.22E-03	1.99E-02	3.89E-02
X479A 9A6	4.98E-02	6.85E-01	0.00E+00	1.44E-02	8.72E-03	5.26E-03	1.19E-02	3.14E-02	3.05E-02
X480A 10A1	5.46E-02	5.12E-01	2.47E-02	5.93E-03	7.14E-03	2.23E-02	3.09E-03	3.72E-02	3.74E-02
X479A 9C3	1.43E-02	4.81E-01	0.00E+00	0.00E+00	4.41E-03	5.53E-03	0.00E+00	1.16E-02	1.81E-02

5E. Pigment fluxes (μg m^{-2} d^{-1}) - NZ JGOFS, Chatham Rise, winter 1993

	STC		SA								ST		
	X467A		X464B				X465A				X468A		
Pigment	110	210	120	220	300	550	120	200	300	550	120	300	550
TChl	238.665	81.539	30.145	20.642	18.800	27.089	34.844	22.444	22.405	17.657	150.863	94.001	117.938
TPhaeo	100.161	17.641	8.623	4.943	4.681	5.705	8.152	4.812	3.146	5.609	31.515	28.919	56.711
TCar	219.904	89.724	42.639	29.462	43.477	28.316	27.998	29.319	22.890	16.013	252.498	140.418	181.545
TPig	458.569	171.263	72.784	50.104	62.277	55.405	62.842	51.763	45.296	33.670	403.362	234.419	299.482
BBCar	7.032	1.904	0.773	0.350	0.456	0.661	0.000	0.366	0.707	0.028	2.817	2.412	1.965
PPA22	2.664	0.477	0.417	0.291	0.260	0.480	0.000	0.200	0.769	0.138	2.104	1.388	1.462
PPA12	0.840	0.601	0.097	0.080	0.230	0.037	0.160	0.141	0.094	0.043	0.682	0.236	0.723
Ech	0.287	0.226	0.000	0.000	0.056	0.074	0.402	0.511	0.070	0.000	0.616	0.546	0.998
Chla(ep)	4.676	2.264	1.338	0.665	0.474	0.751	0.000	0.000	0.620	0.575	1.708	1.742	1.539
Chla	97.133	45.277	12.861	9.161	7.898	13.840	15.230	11.948	13.023	7.237	81.274	49.284	43.758
Chla(al)	9.058	4.640	1.076	1.063	1.209	1.491	5.269	1.311	1.787	0.804	6.617	3.901	4.646
Chlb	9.624	3.679	2.754	2.592	2.344	3.165	4.487	3.149	3.220	2.320	15.669	5.313	5.049
Zea/Lut	5.181	0.922	1.765	2.136	2.942	2.133	2.420	1.865	2.319	1.028	4.984	2.349	2.562
Diat	0.590	0.319	0.439	0.000	0.000	0.000	0.000	0.000	0.000	0.000	0.589	0.376	0.629
Allo	1.249	0.708	0.260	0.800	2.485	0.477	1.393	0.000	0.813	0.000	3.908	2.065	2.427
Diad/PPa4	10.142	4.417	1.452	0.724	0.414	0.996	1.705	1.396	0.572	0.142	12.021	5.607	7.695
PPa3/car	6.726	4.146	0.415	0.052	1.779	2.271	3.163	1.446	0.539	0.418	9.793	8.983	12.261
HOF	11.897	7.155	10.243	8.433	7.628	10.353	10.273	9.866	6.989	4.455	32.940	17.925	25.617
PPa2	72.675	7.586	2.657	1.945	0.644	2.281	3.024	1.844	0.984	1.262	0.000	7.982	13.262
Fuco	110.256	46.446	10.541	3.778	2.210	2.775	3.479	3.381	2.605	2.051	101.888	57.506	77.360
BOF	6.426	2.735	6.058	4.563	2.594	2.746	6.133	4.066	1.812	2.326	10.279	5.843	8.494
PPa1	17.255	4.829	5.038	2.575	1.768	0.636	1.805	1.182	0.760	3.747	18.937	10.329	29.003
Peri	25.799	7.174	4.090	4.582	1.971	0.906	0.540	1.442	1.576	2.604	31.974	14.762	4.328
Chlc's	12.451	5.188	2.072	0.913	0.827	1.332	0.796	1.020	0.369	0.064	9.466	2.543	3.732
Chlc3	3.118	0.960	0.331	0.316	0.691	0.148	0.267	0.098	0.024	0.244	2.233	0.286	0.331

5F. Pigment fluxes ($\mu g\ m^{-2}\ d^{-1}$) - NZ JGOFS, Chatham Rise, spring, 1993

	STC				SA					ST				
	X477A		X478A		X475A		X476A			X479A			X480A	
Pigment	100	220	100	220	150	550	150	300	550	110	300	550	110	550
TChl	157.438	119.178	255.286	187.073	90.224	46.232	97.953	65.117	16.164	170.277	57.971	55.710	106.712	54.331
TPhaeo	71.761	21.637	67.440	67.961	41.000	18.338	61.645	36.171	0.917	82.683	17.533	16.028	70.909	19.289
TCar	357.237	162.375	194.048	206.723	146.665	45.983	107.175	117.104	23.344	158.504	69.602	60.297	189.856	99.913
TPig	514.675	281.553	449.333	393.796	236.889	92.215	205.128	182.221	39.509	328.781	127.573	116.006	296.568	154.244
BBCar	2.045	2.380	3.891	2.434	1.401	0.887	0.760	0.707	0.632	1.555	1.831	1.436	1.764	0.854
PPA22	2.001	2.448	3.275	1.385	1.174	0.956	1.121	0.604	0.808	1.267	1.299	2.041	2.422	0.755
PPA12	0.585	0.479	1.257	0.609	0.221	0.653	0.000	1.869	0.108	1.223	0.145	0.773	0.201	0.000
Ech	1.080	0.547	3.783	1.229	0.000	0.000	0.000	0.000	0.094	1.228	0.326	0.938	0.386	0.000
Chla(ep)	0.575	1.400	4.109	3.494	0.772	0.348	1.029	0.490	0.681	3.352	1.204	0.000	1.239	0.000
Chla	24.693	55.958	135.454	85.648	33.186	21.690	18.090	17.548	11.040	66.481	30.406	34.357	25.691	24.100
Chla(al)	2.405	7.285	15.030	8.098	3.085	1.334	2.323	1.196	0.738	7.994	3.147	2.497	2.739	0.715
Chlb	3.200	7.867	10.851	5.382	6.848	3.217	3.321	3.012	1.100	5.097	2.167	0.819	2.369	5.456
Zea/Lut	6.440	2.395	2.399	5.476	2.598	0.942	7.758	4.108	1.449	12.573	10.871	10.502	22.011	7.601
Diat	1.835	3.031	1.368	1.973	1.008	0.173	0.872	1.495	0.000	6.224	2.668	0.000	0.000	2.948
Allo	14.025	0.000	5.227	10.076	1.758	2.893	1.739	2.731	0.192	4.077	0.625	6.477	5.408	6.773
Diad/PPa4	15.709	6.581	15.436	17.034	5.778	1.611	6.035	5.849	1.060	6.789	1.515	3.269	7.872	4.119
PPa3/car	18.946	3.838	11.853	11.696	24.290	2.858	10.374	15.539	0.000	28.173	0.000	6.195	32.210	5.783
HOF	23.754	9.245	23.469	18.691	29.530	5.886	38.753	30.430	4.678	43.835	11.615	8.081	56.915	15.480
PPa2	28.241	5.232	13.640	21.634	0.000	0.000	0.000	7.189	0.000	22.011	3.751	2.519	0.000	8.390
Fuco	218.896	102.306	77.212	85.070	22.276	8.580	17.269	22.233	3.471	21.879	10.349	9.218	24.720	19.612
BOF	26.918	9.171	16.893	22.599	25.970	4.021	19.464	21.161	3.468	17.478	2.408	3.669	21.951	6.860
PPa1	21.987	9.640	37.414	32.637		13.871	50.149	10.970	0.000	30.010	12.339	4.500	36.076	4.361
Peri	18.711	4.897	11.581	8.889	9.279	9.367	0.000	5.002	3.026	10.297	1.224	0.401	8.507	1.866
Chlc's	41.826	17.938	15.148	11.301	3.830	0.798	6.277	3.412	0.821	2.218	0.742	1.291	1.255	2.494
Chlc3	7.799	3.404	2.995	1.561	0.601	0.226	2.982	0.853	0.088	0.688	0.276	0.000	0.454	0.900

5G. Average pigment fluxes (μg m^{-2} d^{-1}) - NZ JGOFS, Chatham Rise, winter, 1993

	STC		SA				ST		
Pigment	110	210	120	220	300	550	120	300	550
TChl	238.665	81.539	32.494	21.543	20.602	22.373	150.863	94.001	117.938
TPhaeo	100.161	17.641	8.388	4.878	3.914	5.657	31.515	28.919	56.711
TCar	219.904	89.724	35.319	29.390	33.184	22.165	252.498	140.418	181.545
TPig	458.569	171.263	67.813	50.934	53.786	44.538	403.362	234.419	299.482
BBCar	7.032	1.904	0.386	0.358	0.582	0.344	2.817	2.412	1.965
PPA22	2.664	0.477	0.208	0.246	0.514	0.309	2.104	1.388	1.462
PPA12	0.840	0.601	0.129	0.110	0.162	0.040	0.682	0.236	0.723
Ech	0.287	0.226	0.201	0.256	0.063	0.037	0.616	0.546	0.998
Chla(ep)	4.676	2.264	0.669	0.333	0.547	0.663	1.708	1.742	1.539
Chla	97.133	45.277	14.045	10.554	10.461	10.539	81.274	49.284	43.758
Chla(al)	9.058	4.640	3.173	1.187	1.498	1.148	6.617	3.901	4.646
Chlb	9.624	3.679	3.621	2.870	2.782	2.742	15.669	5.313	5.049
Zea/Lut	5.181	0.922	2.092	2.001	2.631	1.580	4.984	2.349	2.562
Diat	0.590	0.319	0.219	0.000	0.000	0.000	0.589	0.376	0.629
Allo	1.249	0.708	0.826	0.400	1.649	0.239	3.908	2.065	2.427
Diad/PPa4	10.142	4.417	1.579	1.060	0.493	0.569	12.021	5.607	7.695
PPa3/car	6.726	4.146	1.789	0.749	1.159	1.345	9.793	8.983	12.261
HOF	11.897	7.155	10.258	9.149	7.309	7.404	32.940	17.925	25.617
PPa2	72.675	7.586	2.840	1.894	0.814	1.772	0.000	7.982	13.262
Fuco	110.256	46.446	7.010	3.579	2.407	2.413	101.888	57.506	77.360
BOF	6.426	2.735	6.095	4.314	2.203	2.536	10.279	5.843	8.494
PPa1	17.255	4.829	3.421	1.878	1.264	2.192	18.937	10.329	29.003
Peri	25.799	7.174	2.315	3.012	1.773	1.755	31.974	14.762	4.328
Chlc's	12.451	5.188	1.434	0.967	0.598	0.698	9.466	2.543	3.732
Chlc3	3.118	0.960	0.299	0.207	0.357	0.196	2.233	0.286	0.331

5H. Average pigment fluxes (μg m^{-2} d^{-1}) - NZ JGOFS, Chatham Rise, spring 1993

	STC		SA			ST		
Pigment	100	220	150	300	550	110	300	550
TChl	206.362	153.125	94.089	65.117	31.198	138.494	57.971	55.021
TPhaeo	69.600	44.799	51.322	36.171	9.627	76.796	17.533	17.659
TCar	275.642	184.549	126.920	117.104	34.664	174.180	69.602	80.105
TPig	482.004	337.674	221.008	182.221	65.862	312.674	127.573	135.125
BBCar	2.968	2.407	1.081	0.707	0.759	1.660	1.831	1.145
PPA22	2.638	1.917	1.148	0.604	0.882	1.844	1.299	1.398
PPA12	0.921	0.544	0.111	1.869	0.381	0.712	0.145	0.387
Ech	2.432	0.888	0.000	0.000	0.047	0.807	0.326	0.469
Chla(ep)	2.342	2.447	0.900	0.490	0.514	2.295	1.204	0.000
Chla	80.073	70.803	25.638	17.548	16.365	46.086	30.406	29.228
Chla(al)	8.717	7.691	2.704	1.196	1.036	5.367	3.147	1.606
Chlb	7.026	6.624	5.085	3.012	2.159	3.733	2.167	3.138
Zea/Lut	4.419	3.935	5.178	4.108	1.196	17.292	10.871	9.052
Diat	1.602	2.502	0.940	1.495	0.086	3.112	2.668	1.474
Allo	9.626	5.038	1.748	2.731	1.542	4.743	0.625	6.625
Diad/PPa4	15.572	11.808	5.906	5.849	1.335	7.330	1.515	3.694
PPa3/car	15.400	7.767	17.332	15.539	1.429	30.191	0.000	5.989
HOF	23.612	13.968	34.141	30.430	5.282	50.375	11.615	11.780
PPa2	20.940	13.433	0.000	7.189	0.000	11.005	3.751	5.455
Fuco	148.054	93.688	19.772	22.233	6.026	23.299	10.349	14.415
BOF	21.906	15.885	22.717	21.161	3.744	19.714	2.408	5.265
PPa1	29.700	21.139	32.732	10.970	6.936	33.043	12.339	4.430
Peri	15.146	6.893	4.639	5.002	6.197	9.402	1.224	1.133
Chlc's	28.487	14.619	5.053	3.412	0.810	1.737	0.742	1.892
Chlc3	5.397	2.483	1.791	0.853	0.157	0.571	0.276	0.450

5I. Standard deviations in pigment flux ($\mu g\ m^{-2}\ d^{-1}$) - NZ JGOFS, Chatham Rise, winter 1993

	STC		SA				ST		
Pigment	110	210	120	220	300	550	120	300	550
TChl	***	***	3.323	1.274	2.550	6.669	***	***	***
TPhaeo	***	***	0.333	0.093	1.085	0.068	***	***	***
TCar	***	***	10.352	0.101	14.558	8.700	***	***	***
Tpig	***	***	7.029	1.173	12.008	15.369	***	***	***
BBCar	***	***	0.546	0.011	0.178	0.448	***	***	***
PPA22	***	***	0.295	0.064	0.360	0.242	***	***	***
PPA12	***	***	0.044	0.043	0.096	0.005	***	***	***
Ech	***	***	0.284	0.362	0.010	0.052	***	***	***
Chla(ep)	***	***	0.946	0.470	0.104	0.125	***	***	***
Chla	***	***	1.675	1.971	3.624	4.669	***	***	***
Chla(al)	***	***	2.965	0.175	0.409	0.486	***	***	***
Chlb	***	***	1.225	0.394	0.619	0.598	***	***	***
Zea/Lut	***	***	0.463	0.192	0.440	0.781	***	***	***
Diat	***	***	0.310	0.000	0.000	0.000	***	***	***
Allo	***	***	0.801	0.566	1.182	0.337	***	***	***
Diad/PPa4	***	***	0.178	0.475	0.111	0.604	***	***	***
PPa3/car	***	***	1.943	0.985	0.877	1.310	***	***	***
HOF	***	***	0.021	1.013	0.452	4.171	***	***	***
PPa2	***	***	0.260	0.071	0.240	0.721	***	***	***
Fuco	***	***	4.994	0.281	0.279	0.512	***	***	***
BOF	***	***	0.052	0.351	0.553	0.297	***	***	***
PPa1	***	***	2.286	0.985	0.713	2.200	***	***	***
Peri	***	***	2.510	2.220	0.279	1.200	***	***	***
Chlc's	***	***	0.903	0.075	0.324	0.897	***	***	***
Chlc3	***	***	0.046	0.155	0.472	0.068	***	***	***

5J. Standard deviations in pigment flux ($\mu g\ m^{-2}\ d^{-1}$) - NZ JGOFS, Chatham Rise, spring 1993

	STC			SA			ST	
Pigment	100	220	150	300	550	110	300	550
TChl	69.189	48.009	5.466	***	21.261	44.947	***	0.974
TPhaeo	3.055	32.756	14.598	***	12.319	8.326	***	2.306
TCar	115.392	31.358	27.924	***	16.008	22.169	***	28.013
TPig	46.203	79.368	22.458	***	37.269	22.778	***	27.038
BBCar	1.306	0.038	0.454	***	0.180	0.148	***	0.412
PPA22	0.901	0.751	0.038	***	0.104	0.817	***	0.910
PPA12	0.475	0.092	0.157	***	0.385	0.723	***	0.547
Ech	1.911	0.483	0.000	***	0.066	0.595	***	0.663
Chla(ep)	2.499	1.481	0.182	***	0.235	1.494	***	0.000
Chla	78.320	20.994	10.674	***	7.530	28.843	***	7.252
Chla(al)	8.927	0.575	0.539	***	0.421	3.715	***	1.260
Chlb	5.410	1.757	2.494	***	1.497	1.929	***	3.279
Zea/Lut	2.857	2.179	3.649	***	0.358	6.674	***	2.051
Diat	0.331	0.748	0.096	***	0.122	4.401	***	2.085
Allo	6.221	7.125	0.013	***	1.909	0.941	***	0.209
Diad/PPa4	0.194	7.391	0.181	***	0.390	0.765	***	0.601
PPa3/car	5.015	5.556	9.840	***	2.021	2.855	***	0.291
HOF	0.202	6.679	6.522	***	0.854	9.249	***	5.232
PPa2	10.324	11.598	0.000	***	0.000	15.564	***	4.151
Fuco	100.186	12.188	3.541	***	3.613	2.009	***	7.349
BOF	7.089	9.495	4.601	***	0.391	3.163	***	2.257
PPa1	10.909	16.261	24.632	***	9.808	4.289	***	0.098
Peri	5.042	2.822	6.561	***	4.483	1.265	***	1.036
Chlc's	18.864	4.693	1.730	***	0.017	0.681	***	0.851
Chlc3	3.397	1.304	1.683	***	0.098	0.165	***	0.636

5K. Average winter:spring ratios (%) for pigment fluxes, NZ JGOFS, Chatham Rise, 1993.

	STC		SA			ST		
Pigment	"100"	"200"	"100"	300	550	"100"	300	550
Allo	13.0	14.0	47.3	60.4	15.5	82.4	330.5	36.6
BBCar	236.9	79.1	35.7	82.3	45.3	169.7	131.7	171.6
BOF	29.3	17.2	26.8	10.4	67.7	52.1	242.6	161.3
Chla	121.3	63.9	54.8	59.6	64.4	176.4	162.1	149.7
Chla(al)	103.9	60.3	117.3	125.3	110.7	123.3	124.0	289.2
Chla(ep)	199.6	92.5	74.3	111.7	128.8	74.4	144.7	0.0
Chlb	137.0	55.5	71.2	92.4	127.0	419.8	245.2	160.9
Chlc's	43.7	35.5	28.4	17.5	86.2	545.0	342.8	197.2
Chlc3	57.8	38.7	16.7	41.9	125.1	391.1	103.5	73.6
Diad/PPhorba4	65.1	37.4	26.7	8.4	42.6	164.0	370.2	208.3
Diat	36.9	12.8	23.4	0.0	0.0	18.9	14.1	42.6
Ech	11.8	25.4	0.0	0.0	79.0	76.4	167.3	213.0
Fuco	74.5	49.6	35.5	10.8	40.0	437.3	555.7	536.7
HOF	50.4	51.2	30.0	24.0	140.2	65.4	154.3	217.5
Peri	170.3	104.1	49.9	35.4	28.3	340.1	1205.9	381.8
PPhorba1	58.1	22.8	10.5	11.5	31.6	57.3	83.7	654.6
PPhorba2	347.1	56.5	0.0	11.3	0.0	0.0	212.8	243.1
PPhorba3/car	43.7	53.4	10.3	7.5	94.1	32.4	0.0	204.7
PphytinA1	91.2	110.6	116.5	8.7	10.5	95.8	163.1	186.9
PPhytinA2	101.0	24.9	18.2	85.1	35.1	114.1	106.9	104.6
Zea/Lut	117.2	23.4	40.4	64.0	132.2	28.8	21.6	28.3
TChl	115.7	53.2	34.5	31.6	71.7	108.9	162.2	214.4
TPhaeo	143.9	39.4	16.3	10.8	58.8	41.0	164.9	321.2
TCar	79.8	48.6	27.8	28.3	63.9	145.0	201.7	226.6
TPig	95.1	50.7	30.7	29.5	67.6	129.0	183.8	221.6

5L. Pigment degradation rates from near-surface traps to deepest traps, NZ JGOFS, Chatham Rise, 1993.

	Spring 1993						Winter 1993			
	STC	STC	SA	SA	ST	ST	STC	SA	SA	ST
Pigment	X477A	X478A	X475A	X476A	X479A	X480A	X467A	X464B	X465A	X468A
	100	100	150	150	110	110	110	120	120	120
TChl	-0.319	-0.568	-0.110	-0.204	-0.260	-0.119	-1.571	-0.007	-0.040	-0.077
TPhaeo	-0.418	0.004	-0.057	-0.152	-0.151	-0.117	-0.825	-0.007	-0.006	0.059
TCar	-1.624	0.106	-0.252	-0.210	-0.223	-0.204	-1.302	-0.033	-0.028	-0.165
TPig	-1.943	-0.463	-0.362	-0.414	-0.484	-0.323	-2.873	-0.040	-0.068	-0.242
Allo	0.003	-0.012	-0.001	0.000	0.000	-0.002	-0.051	0.000	0.000	-0.002
BBCar	0.004	-0.016	-0.001	-0.001	0.002	-0.004	-0.022	0.000	0.000	-0.001
BOF	-0.001	-0.005	0.001	0.000	-0.001	0.000	-0.002	0.000	0.000	0.000
Chla	-0.004	-0.021	0.000	0.000	-0.001	-0.001	-0.001	0.000	-0.001	0.001
Chla(al)	0.007	-0.005	-0.001	-0.001	-0.008	-0.003	-0.024	-0.001	0.001	0.000
Chla(ep)	0.261	-0.415	-0.029	-0.018	-0.073	-0.004	-0.519	0.002	-0.019	-0.087
Chlb	0.041	-0.058	-0.004	-0.004	-0.012	-0.005	-0.044	0.001	-0.010	-0.005
Chlc's	0.039	-0.046	-0.009	-0.006	-0.010	0.007	-0.059	0.001	-0.005	-0.025
Chlc3	-0.034	0.026	-0.004	-0.016	-0.005	-0.033	-0.043	0.001	-0.003	-0.006
Diad/PPhorba4	0.010	0.005	-0.002	-0.002	-0.014	0.007	-0.003	-0.001	0.000	0.000
Diat	-0.117	0.040	0.003	-0.004	0.005	0.003	-0.005	0.001	-0.003	-0.003
Ech	-0.076	0.013	-0.010	-0.012	-0.008	-0.009	-0.057	-0.001	-0.004	-0.010
Fuco	-0.126	-0.001	-0.054	-0.026	-0.050	-0.060	-0.026	0.004	-0.006	0.006
HOF	-0.121	-0.040	-0.059	-0.085	-0.081	-0.094	-0.047	0.000	-0.014	-0.017
Peri	-0.192	0.067	0.000	0.000	-0.044	0.019	-0.651	-0.001	-0.004	0.031
PPhorba1	-0.972	0.065	-0.034	-0.034	-0.029	-0.012	-0.638	-0.018	-0.003	-0.057
PPhorba2	-0.148	0.048	-0.055	-0.040	-0.031	-0.034	-0.037	-0.008	-0.009	-0.004
PPhorba3/car	-0.103	-0.040	-0.004	-0.125	-0.058	-0.072	-0.124	-0.010	0.005	0.023
PPhytinA1	-0.115	-0.022	0.000	0.008	-0.022	-0.015	-0.186	-0.007	0.005	-0.064
PPhytinA2	-0.199	-0.032	-0.008	-0.014	-0.002	0.003	-0.073	-0.002	-0.002	-0.013
Zea/Lut	-0.037	-0.012	-0.001	-0.007	-0.002	0.001	-0.022	0.000	0.000	-0.004

5M. Co-efficients of variation (CV) for pigment flux samples

	Spring						Winter				Average	Average	Average
	CZ		SA		ST		SA				CV	CV	CV
PIGMENTS*	100	220	150	550	110	550	120	220	300	550	Winter	Spring	Total
TChl	33.528	31.353	5.809	68.148	32.454	1.771	10.226	5.914	12.376	29.809	14.581	28.844	23.139
TPhaeo	4.390	73.117	28.444	127.955	10.842	13.057	3.970	1.907	27.735	1.200	8.703	42.967	29.262
TCar	41.863	16.992	22.001	46.181	12.728	34.970	29.311	0.345	43.869	39.250	28.194	29.123	28.751
TPig	9.586	23.504	10.162	56.587	7.285	20.010	10.366	2.302	22.325	34.507	17.375	21.189	19.663
BBCar	43.997	1.589	41.969	23.752	8.912	35.964	141.421	3.113	30.633	130.046	76.304	26.031	46.140
PPhytinA2	34.138	39.207	3.281	11.814	44.299	65.085	141.421	26.170	70.036	78.204	78.958	32.971	51.366
PPhytinA1	51.588	16.890	141.421	101.165	101.519	141.421	34.500	38.810	59.519	11.526	36.089	92.334	69.836
Ech	78.603	54.329	**	141.421	73.772	141.421	141.421	141.421	15.755	141.421	110.005	97.909	103.285
Chla(ep)	106.680	60.517	20.204	45.725	65.105	**	141.421	141.421	18.943	18.807	80.148	59.646	68.758
Chla	97.810	29.651	41.633	46.016	62.585	24.813	11.924	18.672	34.644	44.300	27.385	50.418	41.205
Chla(al)	102.410	7.477	19.934	40.661	69.229	78.436	93.447	14.768	27.270	42.343	44.457	53.025	49.598
Chlb	77.003	26.518	49.042	69.334	51.682	104.490	33.835	13.736	22.253	21.791	22.904	63.011	46.968
Zea/Lut	64.656	55.358	70.475	29.962	38.597	22.663	22.135	9.590	16.741	49.446	24.478	46.952	37.962
Diat	20.646	29.909	10.228	141.421	141.421	141.421	141.421	**	**	**	141.421	80.841	89.495
Allo	64.627	141.421	0.764	123.786	19.846	3.152	96.947	141.421	71.694	141.421	112.871	58.933	80.508
Diad/PPhorba4	1.243	62.598	3.071	29.206	10.441	16.281	11.303	44.794	22.543	106.135	46.194	20.473	30.762
PPhorba3/car	32.568	71.539	56.774	141.421	9.456	4.858	108.635	131.555	75.639	97.414	103.311	52.769	72.986
HOF	0.856	47.816	19.102	16.174	18.360	44.415	0.208	11.073	6.182	56.334	18.449	24.454	22.052
PPhorba2	49.304	86.340	**	**	141.421	76.108	9.140	3.767	29.532	40.684	20.781	88.293	54.537
Fuco	67.668	13.009	17.906	59.951	8.623	50.984	71.231	7.846	11.605	21.219	27.975	36.357	33.004
BOF	32.362	59.776	20.253	10.436	16.046	42.872	0.860	8.142	25.095	11.717	11.454	30.291	22.756
PPhorba1	36.729	76.925	75.255	141.421	12.980	2.217	66.808	52.462	56.411	100.376	69.014	57.588	62.158
Peri	33.291	40.943	141.421	72.351	13.457	91.373	108.438	73.701	15.751	68.381	66.568	65.473	65.911
Chlc's	66.219	32.103	34.241	2.068	39.214	44.970	62.951	7.798	54.159	128.451	63.340	36.469	47.217
Chlc3	62.933	52.505	93.969	62.331	28.975	141.421	15.241	74.651	131.998	34.647	64.134	73.689	69.867
										Overall average CV:	**55.542**	**59.345**	**54.663**

* Key to pigments: TChl=sum of all chlorophyll-derived pigments (including phaeopigments), TPhaeo=sum of all phaeopigments only, TCar=sum of all carotenoids, TPig=sum of all pigments (TChl+TCar); Allo=alloxanthin, BBCar=β, β-carotene, BOF=19'BOF, Chla=chlorophyll *a*, Chla(al)=chlorophyll *a* (allomer), Chla(ep)=chlorophyll *a* (epimer), Chlb=chlorophyll *b*, Chlc's=chlorophyll *c*'s, Chlc3=chlorophyll *c3*, Diad/PPhorba4=diadinoxanthin/phaeophorbide *a4*, Diat = diatoxanthin, Ech=echinone, Fuco=fucoxanthnin, HOF=19'HOF, Peri=peridinin, PPhorba1=phaeophorbide *a1*, PPhorba2=phaeophorbide *a2*, Pphorba3/car = phaeophorbide *a3*/carotenoid, PPhytina1=phaeophytin *a1*, PPhytina2=phaeophytin *a2*, Zea/Lut=zeaxanthin/lutein.

** Only one value, hence no CV calculated. Note only one station occupied in Subtropical Convergence (STC) and subtropical waters in winter, so only samples from subantarctic waters can be used to calculate a CV.

APPENDIX 6: Evans Bay experiments

6A. Experiment I (initial) & V (effect of formalin as a preservative).

B=baffled, U=unbaffled, F=brine full, BLK=blank.

	Trap code	Filter number	Tared filter weight W_t (mg)	Volume filtered V_f (l)	Brine height H_b (m)	Brine volume $V_r=Ah_b$ (l)	Filtered weight W_f (mg)	Mass difference W_f-W_t	Blank weight W_{blk} (mg)	Total weight W_T (mg)	Trap area A (m^2)	Duration t (d)	Total mass flux $TM=W_TV_r(V_fAt)^{-1}$ ($g\ m^{-2}\ d^{-1}$)
Upon recovery	B1	420	4.411	0.1	0.325	2.080	27.630	23.219	0.292	22.927	0.0064	6	12.41879
	F2	436	4.271	0.1	0.70	4.480	15.317	11.046	0.292	10.754	0.0064	6	12.54633
	F3	439	4.367	0.1	0.70	4.480	15.472	11.105	0.292	10.813	0.0064	6	12.61517
	U4	424	4.418	0.1	0.25	1.600	33.460	29.042	0.292	28.750	0.0064	6	11.97917
	BF5	429	4.269	0.1	0.76	4.864	16.238	11.969	0.292	11.677	0.0064	6	14.79087
	B6	434	4.374	0.1	0.34	2.176	32.220	27.846	0.292	27.554	0.0064	6	15.61393
	U7	432	4.642	0.1	0.335	2.144	25.774	21.132	0.292	20.840	0.0064	6	11.63567
	U8	415	4.427	0.1	0.33	2.112	29.740	25.313	0.292	25.021	0.0064	6	13.76155
	BF9	419	4.318	0.1	0.40	2.560	18.467	14.149	0.292	13.857	0.0064	6	9.23800
	BF10	426	4.415	0.1	0.70	4.480	15.366	10.951	0.292	10.659	0.0064	6	12.43550
	B11	438	4.464	0.1	0.36	2.304	22.934	18.470	0.292	18.178	0.0064	6	10.90680
	F12	417	4.367	0.1	0.69	4.416	16.779	12.412	0.292	12.120	0.0064	6	13.93800
	BLK	457	4.494	0.1	0	0	4.763	0.269	0.292	~	0	0	-0
	BLK	442	4.466	0.1	0	0	4.827	0.361	0.292	~	0	0	-0
	BLK	458	4.580	0.1	0	0	4.827	0.247	0.292	~	0	0	-0
After one week	B1	440	4.617	0.1	0.325	2.080	28.870	24.253	0.761	23.492	0.0064	6	12.72483
	F2	449	4.671	0.1	0.70	4.480	16.917	12.246	0.761	11.485	0.0064	6	13.39917
	F3	446	4.536	0.1	0.70	4.480	17.413	12.877	0.761	12.116	0.0064	6	14.13533
	U4	441	4.537	0.1	0.25	1.600	33.700	29.163	0.761	28.402	0.0064	6	11.83417
	BF5	456	4.574	0.1	0.76	4.864	16.613	12.039	0.761	11.278	0.0064	6	14.28547
	B6	464	4.436	0.1	0.34	2.176	31.810	27.374	0.761	26.613	0.0064	6	15.08070
	U7	450	4.644	0.1	0.335	2.144	29.240	24.596	0.761	23.835	0.0064	6	13.30788
	U8	454	4.688	0.1	0.33	2.112	31.500	26.812	0.761	26.051	0.0064	6	14.32805
	BF9	447	4.612	0.1	0.40	2.560	~	-4.612	0.761	-5.373	0.0064	6	-3.582
	BF10	444	4.468	0.1	0.70	4.480	15.539	11.071	0.761	10.310	0.0064	6	12.02833
	B11	455	4.652	0.1	0.36	2.304	23.721	19.069	0.761	18.308	0.0064	6	10.98480
	F12	451	4.692	0.1	0.69	4.416	17.438	12.746	0.761	11.985	0.0064	6	13.78275

	Trap code	Filter number	Tared filter weight W_t (mg)	Volume filtered V_f (l)	Brine height H_b (m)	Brine volume $V_r=Ah_b$ (l)	Filtered weight W_f (mg)	Mass difference W_f-W_t	Blank weight W_{blk} (mg)	Total weight W_T (mg)	Trap area A (m^2)	Duration t (d)	Total mass flux $TM=W_TV_r(V_fAt)^{-1}$ ($g\ m^{-2}\ d^{-1}$)
	BLK	460	4.596	0.1	~	0	5.654	1.058	0.761	~	0	0	0
	BLK	462	4.386	0.1	~	0	4.907	0.521	0.761	~	0	0	0
	BLK	453	4.617	0.1	~	0	5.322	0.705	0.761	~	0	0	0
After two weeks	B1	421	4.311	0.1	0.325	2.080	29.070	24.759	0.165	24.594	0.0064	6	13.32175
	F2	423	4.507	0.1	0.70	4.480	15.528	11.021	0.165	10.856	0.0064	6	12.66533
	F3	437	4.415	0.1	0.70	4.480	15.397	10.982	0.165	10.817	0.0064	6	12.61983
	U4	428	4.445	0.1	0.25	1.600	35.000	30.555	0.165	30.390	0.0064	6	12.66250
	BF5	425	4.412	0.1	0.76	4.864	16.319	11.907	0.165	11.742	0.0064	6	14.87320
	B6	430	4.521	0.1	0.34	2.176	30.850	26.329	0.165	26.164	0.0064	6	14.82627
	U7	459	4.523	0.1	0.335	2.144	27.120	22.597	0.165	22.432	0.0064	6	12.52453
	U8	422	4.314	0.1	0.33	2.112	29.520	25.206	0.165	25.041	0.0064	6	13.77255
	BF9	427	4.294	0.1	0.40	2.560	17.943	13.649	0.165	13.484	0.0064	6	8.98933
	BF10	448	4.688	0.1	0.70	4.480	16.085	11.397	0.165	11.232	0.0064	6	13.10400
	B11	452	4.563	0.1	0.36	2.304	~	-4.563	0.165	-4.728	0.0064	6	-2.8368
	F12	445	4.544	0.1	0.69	4.416	17.558	13.014	0.165	12.849	0.0064	6	14.77635
	BLK	443	4.464	0.1	~	0	4.651	0.187	0.165	0.022	0	0	0
	BLK	465	4.496	0.1	~	0	4.698	0.202	0.165	0.037	0	0	0
	BLK	470	4.545	0.1	~	0	4.759	0.214	0.165	0.049	0	0	0
	BLK	469	4.486	0.1	~	0	4.543	0.057	0.165	-0.108	0	0	0

6B. Experiment II (effect of trap position on trapping efficiency), Evans Bay.

Trap code	Filter number	Tared filter weight W_t (mg)	Volume filtered V_f (l)	Brine height H_b (m)	Brine volume $V_r=Ah_b$ (l)	Filtered weight W_f (mg)	Mass difference W_f-W_t	Blank weight W_{blk} (mg)	Total weight W_T (mg)	Trap area A (m^2)	Duration t (d)	Total mass flux $TM=W_TV_r(V_fAt)^{-1}$ ($g\ m^{-2}\ d^{-1}$)
A1a	277	0.00463	0.098	0.36	2.304	0.02639	0.02176	0.000031	0.021729	0.0064	5	15.96416
A1b	231	0.00462	0.098	0.36	2.304	0.05447	0.04985	0.000031	0.049819	0.0064	5	36.60171
A1c	207	0.00455	0.10	0.36	2.304	0.04369	0.03914	0.000031	0.039109	0.0064	5	28.15848
A2a	184	0.00458	0.099	0.25	1.600	0.06895	0.06437	0.000031	0.064339	0.0064	5	32.49444
A2b	102	0.00454	0.092	0.25	1.600	0.06520	0.06066	0.000031	0.060629	0.0064	5	32.95054
A2c	187	0.00454	0.10	0.25	1.600	0.07177	0.06723	0.000031	0.067199	0.0064	5	33.59950
A3a	229	0.00448	0.098	0.15	0.960	0.08663	0.08215	0.000031	0.082119	0.0064	5	25.13847
A3b	92	0.00460	0.092	0.15	0.960	0.09778	0.09318	0.000031	0.093149	0.0064	5	30.37467
A3c	251	0.00464	0.10	0.15	0.960	0.11539	0.11075	0.000031	0.110719	0.0064	5	33.21570
A4a	64	0.00459	0.10	0.35	2.240	0.05868	0.05409	0.000031	0.054059	0.0064	5	37.84130
A4b	66	0.00465	0.093	0.35	2.240	0.05132	0.04667	0.000031	0.046639	0.0064	5	35.10462
A4c	27	0.00462	0.098	0.35	2.240	0.05218	0.04756	0.000031	0.047529	0.0064	5	33.94929
A5a	280	0.00454	0.10	0.34	2.176	0.05495	0.05041	0.000031	0.050379	0.0064	5	34.25772
A5b	281	0.00481	0.099	0.34	2.176	0.06052	0.05571	0.000031	0.055679	0.0064	5	38.24416
A5c	3	0.00475	0.102	0.34	2.176	0.05410	0.04935	0.000031	0.049319	0.0064	5	32.87933
A6a	288	0.00468	0.10	0.345	2.208	0.04687	0.04219	0.000031	0.042159	0.0064	5	29.08971
A6b	201	0.00452	0.098	0.345	2.208	0.03612	0.03160	0.000031	0.031569	0.0064	5	22.22715
A6c	203	0.00467	0.096	0.345	2.208	0.04073	0.03606	0.000031	0.036029	0.0064	5	25.89584
A7a	379	0.00441	0.102	0.35	2.240	0.05514	0.05073	0.000031	0.050699	0.0064	5	34.79343
A7b	381	0.00451	0.098	0.35	2.240	0.04955	0.04504	0.000031	0.045009	0.0064	5	32.14929
A7c	334	0.00430	0.10	0.35	2.240	0.04949	0.04519	0.000031	0.045159	0.0064	5	31.61130
A8a	409	0.00437	0.098	0.32	2.048	0.06188	0.05751	0.000031	0.057479	0.0064	5	37.53731
A8b	399	0.00440	0.098	0.32	2.048	0.06180	0.05740	0.000031	0.057369	0.0064	5	37.46547
A8c	340	0.00450	0.098	0.32	2.048	0.05935	0.05485	0.000031	0.054819	0.0064	5	35.80016
A9a	142	0.00455	0.096	0.345	2.208	0.05584	0.05129	0.000031	0.051259	0.0064	5	36.84241
A9b	99	0.00455	0.099	0.345	2.208	0.05364	0.04909	0.000031	0.049059	0.0064	5	34.19264
A9c	113	0.00462	0.096	0.345	2.208	0.04629	0.04167	0.000031	0.041639	0.0064	5	29.92803
A10a	154	0.00454	0.098	0.355	2.272	0.04930	0.04476	0.000031	0.044729	0.0064	5	32.40570
A10b	52	0.00471	0.098	0.355	2.272	0.04894	0.04423	0.000031	0.044199	0.0064	5	32.02172
A10c	153	0.00467	0.099	0.355	2.272	0.04819	0.04352	0.000031	0.043489	0.0064	5	31.18908

Trap code	Filter number	Tared filter weight W_t (mg)	Volume filtered V_f (l)	Brine height H_b (m)	Brine volume $V_r=Ah_b$ (l)	Filtered weight W_f (mg)	Mass difference W_f-W_t	Blank weight W_{blk} (mg)	Total weight W_T (mg)	Trap area A (m^2)	Duration t (d)	Total mass flux $TM=W_TV_r(V_fAt)^{-1}$ ($g\ m^{-2}\ d^{-1}$)
A11a	253	0.00484	0.10	0.345	2.208	0.04499	0.04015	0.000031	0.040119	0.0064	5	27.68211
A11b	293	0.00478	0.095	0.345	2.208	0.06021	0.05543	0.000031	0.055399	0.0064	5	40.23717
A11c	435	0.00433	0.096	0.345	2.208	0.06394	0.05961	0.000031	0.059579	0.0064	5	42.82241
A12a	234	0.00486	0.10	0.335	2.144	0.05034	0.04548	0.000031	0.045449	0.0064	5	30.45083
A12b	123	0.00466	0.098	0.335	2.144	0.05470	0.05004	0.000031	0.050009	0.0064	5	34.18983
A12c	338	0.00456	0.092	0.335	2.144	0.05506	0.05050	0.000031	0.050469	0.0064	5	36.75460
B1a	284	0.00461	0.10	0.335	2.144	0.06894	0.06433	0.000031	0.064299	0.0064	6	35.90028
B1b	148	0.00449	0.10	0.335	2.144	0.07237	0.06788	0.000031	0.067849	0.0064	6	37.88236
B1c	199	0.00474	0.10	0.335	2.144	0.05842	0.05368	0.000031	0.053649	0.0064	6	29.95403
B2a	360	0.00448	0.09	0.382	2.445	0.05885	0.05437	0.000031	0.054339	0.0064	6	38.43981
B2b	392	0.00440	0.087	0.382	2.445	0.06063	0.05623	0.000031	0.056199	0.0064	6	41.12647
B2c	212	0.00454	0.098	0.382	2.445	0.06239	0.05785	0.000031	0.057819	0.0064	6	37.56268
B3a	248	0.00452	0.10	0.38	2.432	0.05109	0.04657	0.000031	0.046539	0.0064	6	29.47470
B3b	400	0.00435	0.09	0.38	2.432	0.05982	0.05547	0.000031	0.055439	0.0064	6	39.01263
B3c	276	0.00448	0.10	0.38	2.432	0.05273	0.04825	0.000031	0.048219	0.0064	6	30.53870
B4a	368	0.00446	0.10	0.415	2.656	0.05728	0.05282	0.000031	0.052789	0.0064	6	36.51239
B4b	196	0.00445	0.10	0.415	2.656	0.05833	0.05388	0.000031	0.053849	0.0064	6	37.24556
B4c	215	0.00440	0.10	0.415	2.656	0.05756	0.05316	0.000031	0.053129	0.0064	6	36.74756
B5a	263	0.00475	0.099	0.355	2.272	0.06626	0.06151	0.000031	0.061479	0.0064	6	36.74250
B5b	245	0.00456	0.10	0.355	2.272	0.04282	0.03826	0.000031	0.038229	0.0064	6	22.61883
B5c	380	0.00445	0.10	0.355	2.272	0.06905	0.06460	0.000031	0.064569	0.0064	6	38.20333
B6a	278	0.00495	0.098	0.39	2.496	0.03804	0.03309	0.000031	0.033059	0.0064	6	21.92689
B6b	292	0.00455	0.096	0.39	2.496	0.06145	0.05690	0.000031	0.056869	0.0064	6	38.50505
B6c	260	0.00441	0.10	0.39	2.496	X				0.0064	6	
B7a	254	0.00450	0.10	0.38	2.432	0.05850	0.05400	0.000031	0.053969	0.0064	6	34.18037
B7b	226	0.00457	0.10	0.38	2.432	0.04972	0.04515	0.000031	0.045119	0.0064	6	28.57537
B7c	256	0.00464	0.098	0.38	2.432	0.05649	0.05185	0.000031	0.051819	0.0064	6	33.48847
B8a	4	0.00477	0.089	0.44	2.816	0.05142	0.04665	0.000031	0.046619	0.0064	6	38.41266
B8b	382	0.00433	0.10	0.44	2.816	0.05343	0.04910	0.000031	0.049069	0.0064	6	35.98393
B8c	218	0.00457	0.098	0.44	2.816	0.04869	0.04412	0.000031	0.044089	0.0064	6	32.99177
B9a	242	0.00468	0.10	0.215	1.376	0.09711	0.09243	0.000031	0.092399	0.0064	6	33.10964
B9b	351	0.00424	0.10	0.215	1.376	0.10408	0.09984	0.000031	0.099809	0.0064	6	35.76489
B9c	283	0.00458	0.10	0.215	1.376	0.09409	0.08951	0.000031	0.089479	0.0064	6	32.06331

Trap code	Filter number	Tared filter weight W_t (mg)	Volume filtered V_f (l)	Brine height H_b (m)	Brine volume $V_r=Ah_b$ (l)	Filtered weight W_f (mg)	Mass difference W_f-W_t	Blank weight W_{blk} (mg)	Total weight W_T (mg)	Trap area A (m^2)	Duration t (d)	Total mass flux $TM=W_TV_r(V_fAt)^{-1}$ ($g\ m^{-2}\ d^{-1}$)
B10a	194	0.00470	0.10	0.42	2.688	0.03482	0.03012	0.000031	0.030089	0.0064	6	21.06230
B10b	214	0.00448	0.098	0.42	2.688	0.05154	0.04706	0.000031	0.047029	0.0064	6	33.59214
B10c	262	0.00471	0.08	0.42	2.688	0.03700	0.03229	0.000031	0.032259	0.0064	6	28.22663
B11a	200	0.00443	0.10	0.36	2.304	0.05926	0.05483	0.000031	0.054799	0.0064	6	32.87940
B11b	285	0.00483	0.10	0.36	2.304	0.04581	0.04098	0.000031	0.040949	0.0064	6	24.56940
B11c	243	0.00456	0.10	0.36	2.304	0.04730	0.04274	0.000031	0.042709	0.0064	6	25.62540
B12a	247	0.00522	0.097	0.34	2.176	X				0.0064	6	
B12b	287	0.00443	0.092	0.34	2.176	0.06796	0.06353	0.000031	0.063499	0.0064	6	39.1117
C1a	273	0.00482	0.104	0.34	2.176	0.05088	0.04606	0.000031	0.046029	0.0064	5	30.09588
C1b	275	0.00454	0.11	0.34	2.176	X				0.0064	5	
C1c	365	0.00442	0.094	0.34	2.176	0.03700	0.03258	0.000031	0.032549	0.0064	5	23.54609
C2a	195	0.00452	0.101	0.355	2.272	0.05317	0.04865	0.000031	0.048619	0.0064	5	34.17771
C2b	252	0.00442	0.08	0.355	2.272	0.03422	0.02980	0.000031	0.029769	0.0064	5	26.41999
C2c	294	0.00475	0.11	0.355	2.272	0.04641	0.04166	0.000031	0.041629	0.0064	5	26.86963
C3a	216	0.00470	0.10	0.365	2.336	0.03855	0.03385	0.000031	0.033819	0.0064	5	24.68787
C3b	238	0.00459	0.102	0.365	2.336	X				0.0064	5	
C3c	222	0.00458	0.09	0.365	2.336	0.03913	0.03455	0.000031	0.034519	0.0064	5	27.99874
C4a	197	0.00462	0.10	0.2	1.280	0.05989	0.05527	0.000031	0.055239	0.0064	5	22.09560
C4b	271	0.00475	0.095	0.2	1.280	0.05663	0.05188	0.000031	0.051849	0.0064	5	21.83116
C4c	147	0.00460	0.10	0.2	1.280	X				0.0064	5	
C5a	239	0.00435	0.10	0.36	2.304	0.03903	0.03468	0.000031	0.034649	0.0064	5	24.94728
C5b	264	0.00458	0.088	0.36	2.304	X				0.0064	5	
C5c	230	0.00458	0.10	0.36	2.304	0.03566	0.03108	0.000031	0.031049	0.0064	5	22.35528
C6a	97	0.00464	0.10	0.37	2.368	0.02539	0.02075	0.000031	0.020719	0.0064	5	15.33206
C6b	349	0.00445	0.10	0.37	2.368	X				0.0064	5	
C6c	233	0.00457	0.10	0.37	2.368	0.03621	0.03164	0.000031	0.031609	0.0064	5	23.39066
C7a	269	0.00492	0.09	0.43	2.752	X				0.0064	5	
C7b	224	0.00435	0.10	0.43	2.752	0.03998	0.03563	0.000031	0.035599	0.0064	5	30.61514
C7c	146	0.00456	0.10	0.43	2.752	0.03778	0.03322	0.000031	0.033189	0.0064	5	28.54254
C8a	246	0.00484	0.10	0.42	2.688	X				0.0064	5	
C8b	211	0.00458	0.10	0.42	2.688	0.04229	0.03771	0.000031	0.037679	0.0064	5	31.65036
C8c	136	0.00457	0.098	0.42	2.688	0.03982	0.03525	0.000031	0.035219	0.0064	5	30.18771

Trap code	Filter number	Tared filter weight W_t (mg)	Volume filtered V_f (l)	Brine height H_b (m)	Brine volume $V_r=Ah_b$ (l)	Filtered weight W_f (mg)	Mass difference W_f-W_t	Blank weight W_{blk} (mg)	Total weight W_T (mg)	Trap area A (m^2)	Duration t (d)	Total mass flux $TM=W_TV_r(V_fAt)^{-1}$ (g m^{-2} d^{-1})
C9a	225	0.00435	0.10	0.355	2.272	0.04396	0.03961	0.000031	0.039579	0.0064	5	28.10109
C9b	346	0.00438	0.10	0.355	2.272	0.03549	0.03111	0.000031	0.031079	0.0064	5	22.06609
C9c	209	0.00476	0.095	0.355	2.272	0.01841	0.01365	0.000031	0.013619	0.0064	5	10.17841
C10a	279	0.00471	0.098	0.32	2.048	0.05351	0.04880	0.000031	0.048769	0.0064	5	31.84914
C10b	228	0.00452	0.10	0.32	2.048	0.04997	0.04545	0.000031	0.045419	0.0064	5	29.06816
C10c	250	0.00451	0.10	0.32	2.048	0.04712	0.04261	0.000031	0.042579	0.0064	5	27.25056
C11a	267	0.00461	0.106	0.33	2.112	0.04314	0.03853	0.000031	0.038499	0.0064	5	23.97108
C11b	206	0.00454	0.10	0.33	2.112	X				0.0064	5	
C11c	236	0.00475	0.104	0.33	2.112	0.0496	0.04485	0.000031	0.044819	0.0064	5	28.44283
C12a	366	0.00434	0.10	0.34	2.176	0.04091	0.03657	0.000031	0.036539	0.0064	5	24.84652
C12b	265	0.00454	0.10	0.34	2.176	0.02223	0.01769	0.000031	0.017659	0.0064	5	12.00812
C12c	237	0.00443	0.104	0.34	2.176	0.04580	0.04137	0.000031	0.041339	0.0064	5	27.02935

	Filter number	Tared filter weight (mg)	Volume filtered (l)	Filtered weight (mg)	Blank mass difference (mg)	Conc. Blank (mg l^{-1})	Corrected conc. (mg l^{-1})
Blank1	235	0.00476	0.25	0.00481	5E-05	0.0002	2E-05
Blank2	208	0.00449	0.23	0.00455	6E-05	0.000261	2.4E-05
Blank3	359	0.0044	0.25	0.00446	6E-05	0.00024	2.4E-05
Blank4	240	0.00454	0.25	0.00457	3E-05	0.00012	1.2E-05
Blank5	258	0.00452	0.25	0.00452	0	0	0
Blank6	244	0.00473	0.25	0.00476	3E-05	0.00012	1.2E-05
Blank7	219	0.00458	0.24	0.00459	1E-05	4.17E-05	4E-06
Blank8	257	0.00485	0.245	0.00512	0.00027	0.001102	0.000108
Blank9	355	0.00421	0.235	0.00439	0.00018	0.000766	7.2E-05
Blank10	259	0.00446	0.25	0.00454	8E-05	0.00032	3.2E-05
				AV BLK	7.7E-05	0.000317	3.08E-05
				SD BLK	8.43E-05	0.000349	3.37E-05

6C. Experiment III (effect of baffles on trapping efficiency), Evans Bay.

Trap code	Filter number	Tared filter weight W_t (mg)	Volume filtered V_f (l)	Brine height H_b (m)	Brine volume $V_r=Ah_b$ (l)	Filtered weight W_f (mg)	Mass difference W_f-W_t	Blank weight W_{blk} (mg)	Total weight W_T (mg)	Trap area A (m^2)	Duration t (d)	Total mass flux $TM=W_TV_r(V_fAt)^{-1}$ ($g\ m^{-2}\ d^{-1}$)
A1a	524	0.00478	0.10	0.315	2.016	0.01802	0.01324	0.000078	0.013162	0.0064	1	41.46030
A1b	506	0.00481	0.099	0.315	2.016	0.01824	0.01343	0.000078	0.013352	0.0064	1	42.48364
A1c	516	0.00470	0.098	0.315	2.016	0.01753	0.01283	0.000078	0.012752	0.0064	1	40.98857
A2a	588	0.00472	0.096	0.33	2.112	0.01868	0.01396	0.000078	0.013882	0.0064	1	47.71938
A2b	587	0.00467	0.10	0.33	2.112	0.01900	0.01433	0.000078	0.014252	0.0064	1	47.03160
A2c	537	0.00484	0.096	0.33	2.112	0.01859	0.01375	0.000078	0.013672	0.0064	1	46.99750
A3a	548	0.00468	0.096	0.32	2.048	0.01620	0.01152	0.000078	0.011442	0.0064	1	38.14000
A3b	555	0.00471	0.094	0.32	2.048	0.01606	0.01135	0.000078	0.011272	0.0064	1	38.37277
A3c	554	0.00464	0.101	0.32	2.048	0.01644	0.01180	0.000078	0.011722	0.0064	1	37.13901
A4a	536	0.00465	0.095	0.335	2.144	0.01579	0.01114	0.000078	0.011062	0.0064	1	39.00811
A4b	581	0.00448	0.098	0.335	2.144	0.01627	0.01179	0.000078	0.011712	0.0064	1	40.03592
A4c	539	0.00472	0.098	0.335	2.144	0.01627	0.01155	0.000078	0.011472	0.0064	1	39.21551
A5a	580	0.00475	0.10	0.40	2.560	0.01323	0.00848	0.000078	0.008402	0.0064	1	33.60800
A5b	570	0.00474	0.098	0.40	2.560	0.01328	0.00854	0.000078	0.008462	0.0064	1	34.53878
A5c	538	0.00471	0.098	0.40	2.560	0.01348	0.00877	0.000078	0.008692	0.0064	1	35.47755
A6a	590	0.00470	0.096	0.36	2.304	0.01539	0.01069	0.000078	0.010612	0.0064	1	39.79500
A6b	583	0.00482	0.102	0.36	2.304	0.01592	0.01110	0.000078	0.011022	0.0064	1	38.90118
A6c	571	0.00476	0.098	0.36	2.304	0.01526	0.01050	0.000078	0.010422	0.0064	1	38.28490
A7a	585	0.00468	0.098	0.435	2.784	0.01308	0.00840	0.000078	0.008322	0.0064	1	36.93949
A7b	596	0.00470	0.097	0.435	2.784	0.01336	0.00866	0.000078	0.008582	0.0064	1	38.48629
A7c	599	0.00481	0.096	0.435	2.784	0.01405	0.00924	0.000078	0.009162	0.0064	1	41.51531
A8a	531	0.00473	0.102	0.41	2.624	0.01481	0.01008	0.000078	0.010002	0.0064	1	40.20412
A8b	532	0.00474	0.096	0.41	2.624	0.01381	0.00907	0.000078	0.008992	0.0064	1	38.40333
A8c	535	0.00475	0.093	0.41	2.624	0.01317	0.00842	0.000078	0.008342	0.0064	1	36.77656
A9a	575	0.00486	0.098	0.13	0.832	0.02747	0.02261	0.000078	0.022532	0.0064	1	29.88939
A9b	573	0.00474	0.098	0.13	0.832	0.02839	0.02365	0.000078	0.023572	0.0064	1	31.26898
A9c	560	0.00463	0.094	0.13	0.832	0.02664	0.02201	0.000078	0.021932	0.0064	1	30.33149
A10a	594	0.00473	0.098	0.37	2.368	0.01437	0.00964	0.000078	0.009562	0.0064	1	36.10143
A10b	557	0.00473	0.098	0.37	2.368	0.01382	0.00909	0.000078	0.009012	0.0064	1	34.02490
A10c	549	0.00468	0.094	0.37	2.368	0.01370	0.00902	0.000078	0.008942	0.0064	1	35.19723
A11a	589	0.00463	0.098	0.18	1.152	0.02411	0.01948	0.000078	0.019402	0.0064	1	35.63633
A11b	597	0.00478	0.101	0.18	1.152	0.02387	0.01909	0.000078	0.019012	0.0064	1	33.88277
A11c	598	0.00452	0.098	0.18	1.152	0.02479	0.02027	0.000078	0.020192	0.0064	1	37.08735

Trap code	Filter number	Tared filter weight W_t (mg)	Volume filtered V_f (l)	Brine height H_b (m)	Brine volume $V_r=Ah_b$ (l)	Filtered weight W_f (mg)	Mass difference W_f-W_t	Blank weight W_{blk} (mg)	Total weight W_T (mg)	Trap area A (m^2)	Duration t (d)	Total mass flux $TM=W_TV_r(V_fAt)^{-1}$ ($g\ m^{-2}\ d^{-1}$)
A12a	561	0.00469	0.098	0.355	2.272	0.01612	0.01143	0.000078	0.011352	0.0064	1	41.12204
A12b	562	0.00483	0.095	0.355	2.272	0.01593	0.01110	0.000078	0.011022	0.0064	1	41.18747
A12c	568	0.00476	0.102	0.355	2.272	0.01658	0.01182	0.000078	0.011742	0.0064	1	40.86676
B1a	515	0.00469	0.093	0.36	2.304	0.01518	0.01049	0.000078	0.010412	0.0064	1	40.30452
B1b	518	0.00473	0.096	0.36	2.304	0.01524	0.01051	0.000078	0.010432	0.0064	1	39.12000
B1c	514	0.00473	0.097	0.36	2.304	0.01602	0.01129	0.000078	0.011212	0.0064	1	41.61155
B2a	595	0.00453	0.097	0.38	2.432	0.01593	0.01140	0.000078	0.011322	0.0064	1	44.35423
B2b	553	0.00474	0.094	0.38	2.432	0.01529	0.01055	0.000078	0.010472	0.0064	1	42.33362
B2c	541	0.00468	0.094	0.38	2.432	0.01505	0.01037	0.000078	0.010292	0.0064	1	41.60596
B3a	558	0.00474	0.10	0.33	2.112	0.01802	0.01328	0.000078	0.013202	0.0064	1	43.56660
B3b	586	0.00476	0.098	0.33	2.112	0.01758	0.01282	0.000078	0.012742	0.0064	1	42.90673
B3c	565	0.00468	0.098	0.33	2.112	0.01768	0.01300	0.000078	0.012922	0.0064	1	43.51286
B4a	547	0.00472	0.097	0.38	2.432	0.01501	0.01029	0.000078	0.010212	0.0064	1	40.00577
B4b	546	0.00469	0.101	0.38	2.432	0.01570	0.01101	0.000078	0.010932	0.0064	1	41.13030
B4c	569	0.00464	0.097	0.38	2.432	0.01561	0.01097	0.000078	0.010892	0.0064	1	42.66969
B5a	542	0.00468	0.10	0.37	2.368	0.01215	0.00747	0.000078	0.007392	0.0064	1	27.35040
B5b	579	0.00486	0.088	0.37	2.368	0.01133	0.00647	0.000078	0.006392	0.0064	1	26.87545
B5c	574	0.00471	0.098	0.37	2.368	0.01245	0.00774	0.000078	0.007662	0.0064	1	28.92796
B6a	578	0.00468	0.102	0.33	2.112	0.01805	0.01337	0.000078	0.013292	0.0064	1	43.00353
B6b	572	0.00461	0.093	0.33	2.112	0.01609	0.01148	0.000078	0.011402	0.0064	1	40.45871
B6c	559	0.00471	0.098	0.33	2.112	0.01761	0.01290	0.000078	0.012822	0.0064	1	43.17612
B7a	550	0.00482	0.102	0.19	1.216	0.02167	0.01685	0.000078	0.016772	0.0064	1	31.24196
B7b	540	0.00475	0.092	0.19	1.216	0.01995	0.01520	0.000078	0.015122	0.0064	1	31.23022
B7c	545	0.00473	0.098	0.19	1.216	0.02195	0.01722	0.000078	0.017142	0.0064	1	33.23449
B8a	543	0.00466	0.10	0.22	1.408	0.02093	0.01627	0.000078	0.016192	0.0064	1	35.62240
B8b	567	0.00476	0.10	0.22	1.408	0.01982	0.01506	0.000078	0.014982	0.0064	1	32.96040
B8c	577	0.00475	0.098	0.22	1.408	0.02069	0.01594	0.000078	0.015862	0.0064	1	35.60857
B9a	576	0.00470	0.10	0.37	2.368	0.01420	0.00950	0.000078	0.009422	0.0064	1	34.86140
B9b	563	0.00472	0.098	0.37	2.368	0.01374	0.00902	0.000078	0.008942	0.0064	1	33.76061
B9c	564	0.00452	0.098	0.37	2.368	0.01424	0.00972	0.000078	0.009642	0.0064	1	36.40347
B10a	566	0.00463	0.102	0.28	1.792	0.01956	0.01493	0.000078	0.014852	0.0064	1	40.77020
B10b	600	0.00452	0.10	0.28	1.792	0.01909	0.01457	0.000078	0.014492	0.0064	1	40.57760
B10c	592	0.00471	0.092	0.28	1.792	0.01787	0.01316	0.000078	0.013082	0.0064	1	39.81478

Trap code	Filter number	Tared filter weight W_t (mg)	Volume filtered V_f (l)	Brine height H_b (m)	Brine volume $V_r=Ah_b$ (l)	Filtered weight W_f (mg)	Mass difference W_f-W_t	Blank weight W_{blk} (mg)	Total weight W_T (mg)	Trap area A (m^2)	Duration t (d)	Total mass flux $TM=W_TV_r(V_fAt)^{-1}$ ($g\ m^{-2}\ d^{-1}$)
B11a	593	0.00463	0.096	0.21	1.344	0.02125	0.01662	0.000078	0.016542	0.0064	1	36.18563
B11b	584	0.00464	0.098	0.21	1.344	0.02122	0.01658	0.000078	0.016502	0.0064	1	35.36143
B11c	591	0.00457	0.099	0.21	1.344	0.02208	0.01751	0.000078	0.017432	0.0064	1	36.97697
B12a	556	0.00461	0.101	0.325	2.080	0.01871	0.01410	0.000078	0.014022	0.0064	1	45.12030
B12b	582	0.00468	0.099	0.325	2.080	0.01771	0.01303	0.000078	0.012952	0.0064	1	42.51919
B12c	544	0.00462	0.10	0.325	2.080	0.01770	0.01308	0.000078	0.013002	0.0064	1	42.25650
C1a	473	0.00464	0.096	0.39	2.496	0.01351	0.00887	0.000078	0.008792	0.0064	1	35.71750
C1b	9	0.00467	0.097	0.39	2.496	0.01266	0.00799	0.000078	0.007912	0.0064	1	31.81113
C1c	122	0.00461	0.098	0.39	2.496	0.01377	0.00916	0.000078	0.009082	0.0064	1	36.14265
C2a	529	0.00468	0.10	0.33	2.112	0.01497	0.01029	0.000078	0.010212	0.0064	1	33.69960
C2b	530	0.00478	0.092	0.33	2.112	0.01449	0.00971	0.000078	0.009632	0.0064	1	34.54957
C2c	525	0.00472	0.096	0.33	2.112	0.01507	0.01035	0.000078	0.010272	0.0064	1	35.31000
C3a	504	0.00460	0.096	0.33	2.112	0.01592	0.01132	0.000078	0.011242	0.0064	1	38.64438
C3b	512	0.00465	0.092	0.33	2.112	0.01614	0.01149	0.000078	0.011412	0.0064	1	40.93435
C3c	533	0.00464	0.102	0.33	2.112	0.01771	0.01307	0.000078	0.012992	0.0064	1	42.03294
C4a	467	0.00430	0.099	0.40	2.560	0.01387	0.00957	0.000078	0.009492	0.0064	1	38.35152
C4b	61	0.00461	0.094	0.40	2.560	0.01390	0.00929	0.000078	0.009212	0.0064	1	39.20000
C4c	93	0.00456	0.096	0.40	2.560	0.01416	0.00960	0.000078	0.009522	0.0064	1	39.67500
C5a	466	0.00436	0.101	0.355	2.272	0.01677	0.01241	0.000078	0.012332	0.0064	1	43.34515
C5b	48	0.00472	0.095	0.355	2.272	0.01548	0.01076	0.000078	0.010682	0.0064	1	39.91695
C5c	71	0.00466	0.096	0.355	2.272	0.01645	0.01179	0.000078	0.011712	0.0064	1	43.31000
C6a	81	0.00468	0.10	0.29	1.856	0.00503	0.00035	0.000078	x	Trap sealed during deployment		
C6b	41	0.00455	0.098	0.29	1.856	0.00494	0.00039	0.000078	x			
C6c	472	0.00438	0.096	0.29	1.856	0.00472	0.00034	0.000078	x			
C7a	468	0.00436	0.101	0.40	2.560	0.01653	0.01217	0.000078	0.012092	0.0064	1	47.88911
C7b	175	0.00452	0.10	0.40	2.560	0.01614	0.01162	0.000078	0.011542	0.0064	1	46.16800
C7c	89	0.00469	0.10	0.40	2.560	0.01706	0.01237	0.000078	0.012292	0.0064	1	49.16800
C8a	88	0.00471	0.10	0.33	2.112	0.01715	0.01244	0.000078	0.012362	0.0064	1	40.79460
C8b	183	0.00457	0.098	0.33	2.112	0.01601	0.01144	0.000078	0.011362	0.0064	1	38.25980
C8c	49	0.00466	0.094	0.33	2.112	0.01584	0.01118	0.000078	0.011102	0.0064	1	38.97511
C9a	471	0.00441	0.094	0.37	2.368	0.01599	0.01158	0.000078	0.011502	0.0064	1	45.27383
C9b	100	0.00471	0.10	0.37	2.368	0.01585	0.01114	0.000078	0.011062	0.0064	1	40.92940
C9c	45	0.00474	0.10	0.37	2.368	0.01696	0.01222	0.000078	0.012142	0.0064	1	44.92540

Trap code	Filter number	Tared filter weight W_t (mg)	Volume filtered V_f (l)	Brine height H_b (m)	Brine volume $V_r=Ah_b$ (l)	Filtered weight W_f (mg)	Mass difference W_f-W_t	Blank weight W_{blk} (mg)	Total weight W_T (mg)	Trap area A (m^2)	Duration t (d)	Total mass flux $TM=W_TV_r(V_fAt)^{-1}$ ($g\ m^{-2}\ d^{-1}$)
C10a	474	0.00456	0.10	0.32	2.048	0.01476	0.01020	0.000078	0.010122	0.0064	1	32.39040
C10b	22	0.00465	0.10	0.32	2.048	0.01371	0.00906	0.000078	0.008982	0.0064	1	28.74240
C10c	56	0.00470	0.10	0.32	2.048	0.01412	0.00942	0.000078	0.009342	0.0064	1	29.89440
C11a	534	0.00485	0.098	0.31	1.984	0.01603	0.01118	0.000078	0.011102	0.0064	1	35.11857
C11b	527	0.00477	0.101	0.31	1.984	0.01514	0.01037	0.000078	0.010292	0.0064	1	31.58931
C11c	528	0.00463	0.101	0.31	1.984	0.01584	0.01121	0.000078	0.011132	0.0064	1	34.16752
C12a	510	0.00466	0.10	0.40	2.560	0.01364	0.00898	0.000078	0.008902	0.0064	1	35.60800
C12b	521	0.00461	0.102	0.40	2.560	0.01480	0.01019	0.000078	0.010112	0.0064	1	39.65490
C12c	523	0.00475	0.10	0.40	2.560	0.01497	0.01022	0.000078	0.010142	0.0064	1	40.56800

	Filter number	Tared filter weight (mg)	Volume filtered (l)	Filtered weight (mg)	Blank mass difference (mg)	Conc. Blank ($mg\ l^{-1}$)	Corrected conc. ($mg\ l^{-1}$)
Blank1	511	0.00459	0.25	0.00482	0.00023	0.00092	9.2E-05
Blank2	501	0.0046	0.25	0.00479	0.00019	0.00076	0.000076
Blank3	502	0.00465	0.251	0.00486	0.00021	0.000837	0.000084
Blank4	519	0.00464	0.25	0.00482	0.00018	0.00072	7.2E-05
Blank5	522	0.00467	0.25	0.00483	0.00016	0.00064	6.4E-05
Blank6	520	0.00465	0.251	0.00485	0.0002	0.000797	8E-05
			AV BLK	0.004828	0.000195	0.000779	0.000078
			SD BLK	2.48E-05	2.43E-05	9.66E-05	9.72E-06

6D. Experiment IV (effect of brine volume on trapping efficiency), Evans Bay.

Trap code	Filter number	Tared filter weight W_t (mg)	Volume filtered V_f (l)	Brine height H_b (m)	Brine volume $V_r=Ah_b$ (l)	Filtered weight W_f (mg)	Mass difference W_f-W_t	Blank weight W_{blk} (mg)	Total weight W_T (mg)	Trap area A (m^2)	Duration t (d)	Total mass flux $TM=W_TV_r(V_fAt)^{-1}$ (g m^{-2} d^{-1})
A1a	651	0.00449	0.104	0.25	1.600	0.00837	0.00388	7.47E-05	0.003805	0.0064	1	9.147436
A1b	646	0.00455	0.096	0.25	1.600	0.00844	0.00389	7.47E-05	0.003815	0.0064	1	9.935764
A1c	632	0.00455	0.094	0.25	1.600	0.00851	0.00396	7.47E-05	0.003885	0.0064	1	10.333330
A2a	659	0.00457	0.104	0.305	1.952	0.00845	0.00388	7.47E-05	0.003805	0.0064	1	11.159870
A2b	614	0.00449	0.098	0.305	1.952	0.00810	0.00361	7.47E-05	0.003535	0.0064	1	11.002820
A2c	601	0.00462	0.102	0.305	1.952	0.00899	0.00437	7.47E-05	0.004295	0.0064	1	12.843890
A3a	517	0.00475	0.106	0.87	5.568	0.00512	0.00037	7.47E-05	0.000295	0.0064	1	2.423962
A3b	503	0.00470	0.10	0.87	5.568	0.00535	0.00065	7.47E-05	0.000575	0.0064	1	5.005400
A3c	509	0.00466	0.104	0.87	5.568	0.00540	0.00074	7.47E-05	0.000665	0.0064	1	5.565769
A4a	505	0.00473	0.10	0.395	2.528	0.00689	0.00216	7.47E-05	0.002085	0.0064	1	8.237067
A4b	526	0.00475	0.098	0.395	2.528	0.00723	0.00248	7.47E-05	0.002405	0.0064	1	9.694966
A4c	552	0.00473	0.098	0.395	2.528	0.00706	0.00233	7.47E-05	0.002255	0.0064	1	9.090374
A5a	513	0.00466	0.10	0.25	1.600	0.00790	0.00324	7.47E-05	0.003165	0.0064	1	7.913333
A5b	500	0.00478	0.098	0.25	1.600	0.00856	0.00378	7.47E-05	0.003705	0.0064	1	9.452381
A5c	508	0.00465	0.10	0.25	1.600	0.00863	0.00398	7.47E-05	0.003905	0.0064	1	9.763333
A6a	627	0.00464	0.102	0.88	5.632	0.00554	0.00090	7.47E-05	0.000825	0.0064	1	7.120523
A6b	639	0.00469	0.102	0.88	5.632	0.00552	0.00083	7.47E-05	0.000755	0.0064	1	6.516601
A6c	617	0.00453	0.098	0.88	5.632	0.00533	0.00080	7.47E-05	0.000725	0.0064	1	6.513197
A7a	648	0.00459	0.101	0.255	1.632	0.00884	0.00425	7.47E-05	0.004175	0.0064	1	10.541680
A7b	654	0.00473	0.094	0.255	1.632	0.00811	0.00338	7.47E-05	0.003305	0.0064	1	8.966596
A7c	643	0.00473	0.10	0.255	1.632	0.00872	0.00399	7.47E-05	0.003915	0.0064	1	9.984100
A8a	649	0.00456	0.096	0.41	2.624	0.00596	0.00140	7.47E-05	0.001325	0.0064	1	5.660278
A8b	640	0.00466	0.096	0.41	2.624	0.00696	0.00230	7.47E-05	0.002225	0.0064	1	9.504028
A8c	607	0.00456	0.094	0.41	2.624	0.00688	0.00232	7.47E-05	0.002245	0.0064	1	9.793475
A8d	650	0.00459	0.094	0.41	2.624	0.00734	0.00275	7.47E-05	0.002675	0.0064	1	11.669010
A9a	641	0.00458	0.102	0.34	2.176	0.00754	0.00296	7.47E-05	0.002885	0.0064	1	9.617778
A9b	635	0.00456	0.10	0.34	2.176	0.00777	0.00321	7.47E-05	0.003135	0.0064	1	10.660130
A9c	620	0.00470	0.098	0.34	2.176	0.00813	0.00343	7.47E-05	0.003355	0.0064	1	11.640950
A10a	624	0.00473	0.10	0.80	5.120	0.00534	0.00061	7.47E-05	0.000535	0.0064	1	4.282667
A10b	672	0.00467	0.096	0.80	5.120	0.00529	0.00062	7.47E-05	0.000545	0.0064	1	4.544444
A10c	636	0.00473	0.102	0.80	5.120	0.00552	0.00079	7.47E-05	0.000715	0.0064	1	5.610458

Trap code	Filter number	Tared filter weight W_t (mg)	Volume filtered V_f (l)	Brine height H_b (m)	Brine volume $V_r=Ah_b$ (l)	Filtered weight W_f (mg)	Mass difference W_f-W_t	Blank weight W_{blk} (mg)	Total weight W_T (mg)	Trap area A (m^2)	Duration t (d)	Total mass flux $TM=W_TV_r(V_fAt)^{-1}$ ($g\ m^{-2}\ d^{-1}$)
A11a	637	0.00469	0.102	0.625	4.000	0.00564	0.00095	7.47E-05	0.000875	0.0064	1	5.363562
A11b	667	0.00447	0.094	0.625	4.000	0.00520	0.00073	7.47E-05	0.000655	0.0064	1	4.357270
A11c	631	0.00478	0.104	0.625	4.000	0.00578	0.00100	7.47E-05	0.000925	0.0064	1	5.560897
A12a	663	0.00465	0.10	0.31	1.984	0.00814	0.00349	7.47E-05	0.003415	0.0064	1	10.587530
A12b	644	0.00461	0.104	0.31	1.984	0.00802	0.00341	7.47E-05	0.003335	0.0064	1	9.941859
A12c	625	0.00451	0.098	0.31	1.984	0.00786	0.00335	7.47E-05	0.003275	0.0064	1	10.360750
B1a	692	0.00455	0.094	0.55	3.520	0.00542	0.00087	3.53E-05	0.000835	0.0064	1	4.883688
B1b	675	0.00463	0.092	0.55	3.520	0.00549	0.00086	3.53E-05	0.000825	0.0064	1	4.930072
B1c	700	0.00464	0.101	0.55	3.520	0.00551	0.00087	3.53E-05	0.000835	0.0064	1	4.545215
B2a	679	0.00448	0.096	0.15	0.960	0.00877	0.00429	3.53E-05	0.004255	0.0064	1	6.647917
B2b	697	0.00457	0.096	0.15	0.960	0.00883	0.00426	3.53E-05	0.004225	0.0064	1	6.601042
B2c	698	0.00461	0.101	0.15	0.960	0.00917	0.00456	3.53E-05	0.004525	0.0064	1	6.719802
B3a	676	0.00470	0.098	0.43	2.752	0.00763	0.00293	3.53E-05	0.002895	0.0064	1	12.701090
B3b	694	0.00458	0.098	0.43	2.752	0.00747	0.00289	3.53E-05	0.002855	0.0064	1	12.525580
B3c	684	0.00444	0.101	0.43	2.752	0.00740	0.00296	3.53E-05	0.002925	0.0064	1	12.451550
B4a	655	0.00464	0.10	0.88	5.632	0.00510	0.00046	3.53E-05	0.000425	0.0064	1	3.737067
B4b	609	0.00458	0.101	0.88	5.632	0.00516	0.00058	3.53E-05	0.000545	0.0064	1	4.745611
B4c	670	0.00458	0.096	0.88	5.632	0.00506	0.00048	3.53E-05	0.000445	0.0064	1	4.076111
B5a	702	0.00456	0.096	0.34	2.176	0.00627	0.00171	3.53E-05	0.001675	0.0064	1	5.931111
B5b	708	0.00461	0.10	0.34	2.176	0.00659	0.00198	3.53E-05	0.001945	0.0064	1	6.611867
B5c	701	0.00455	0.102	0.34	2.176	0.00647	0.00192	3.53E-05	0.001885	0.0064	1	6.282222
B6a	690	0.00452	0.098	0.365	2.336	0.00646	0.00194	3.53E-05	0.001905	0.0064	1	7.093912
B6b	682	0.00455	0.102	0.365	2.336	0.00652	0.00197	3.53E-05	0.001935	0.0064	1	6.923072
B6c	696	0.00460	0.098	0.365	2.336	0.00672	0.00212	3.53E-05	0.002085	0.0064	1	7.764320
B7a	695	0.00460	0.094	0.19	1.216	0.00748	0.00288	3.53E-05	0.002845	0.0064	1	5.749858
B7b	689	0.00451	0.096	0.19	1.216	0.00753	0.00302	3.53E-05	0.002985	0.0064	1	5.907153
B7c	688	0.00448	0.10	0.19	1.216	0.00768	0.00320	3.53E-05	0.003165	0.0064	1	6.012867
B8a	707	0.00467	0.10	0.38	2.432	0.00533	0.00066	3.53E-05	0.000625	0.0064	1	2.373733
B8b	680	0.00467	0.10	0.38	2.432	0.00546	0.00079	3.53E-05	0.000755	0.0064	1	2.867733
B8c	677	0.00464	0.10	0.38	2.432	0.00535	0.00071	3.53E-05	0.000675	0.0064	1	2.563733
B9a	706	0.00454	0.099	0.36	2.304	0.00643	0.00189	3.53E-05	0.001855	0.0064	1	6.744242
B9b	704	0.00453	0.098	0.36	2.304	0.00647	0.00194	3.53E-05	0.001905	0.0064	1	6.996735
B9c	709	0.00462	0.098	0.36	2.304	0.00648	0.00186	3.53E-05	0.001825	0.0064	1	6.702857

Trap code	Filter number	Tared filter weight W_t (mg)	Volume filtered V_f (l)	Brine height H_b (m)	Brine volume $V_r=Ah_b$ (l)	Filtered weight W_f (mg)	Mass difference W_f-W_t	Blank weight W_{blk} (mg)	Total weight W_T (mg)	Trap area A (m^2)	Duration t (d)	Total mass flux $TM=W_TV_r(V_fAt)^{-1}$ ($g\ m^{-2}\ d^{-1}$)
B10a	687	0.00466	0.099	0.27	1.728	0.00902	0.00436	3.53E-05	0.004325	0.0064	1	11.794550
B10b	693	0.00470	0.096	0.27	1.728	0.00906	0.00436	3.53E-05	0.004325	0.0064	1	12.163130
B10c	699	0.00457	0.099	0.27	1.728	0.00917	0.00460	3.53E-05	0.004565	0.0064	1	12.449090
B11a	710	0.00456	0.095	0.19	1.216	0.00737	0.00281	3.53E-05	0.002775	0.0064	1	5.549333
B11b	703	0.00448	0.101	0.19	1.216	0.00715	0.00267	3.53E-05	0.002635	0.0064	1	4.956304
B11c	705	0.00455	0.10	0.19	1.216	0.00760	0.00305	3.53E-05	0.003015	0.0064	1	5.727867
B12a	686	0.00468	0.10	0.45	2.880	0.00592	0.00124	3.53E-05	0.001205	0.0064	1	5.421000
B12b	685	0.00457	0.10	0.45	2.880	0.00587	0.00130	3.53E-05	0.001265	0.0064	1	5.691000
B12c	660	0.00462	0.098	0.45	2.880	0.00605	0.00143	3.53E-05	0.001395	0.0064	1	6.404082
C1a	613	0.00458	0.098	0.49	3.136	0.00734	0.00276	4.67E-05	0.002713	0.0064	1	13.566670
C1b	602	0.00459	0.102	0.49	3.136	0.00632	0.00173	4.67E-05	0.001683	0.0064	1	8.086601
C1c	618	0.00449	0.101	0.49	3.136	0.00711	0.00262	4.67E-05	0.002573	0.0064	1	12.484490
C2a	622	0.00452	0.101	0.84	5.376	0.00536	0.00084	4.67E-05	0.000793	0.0064	1	6.598020
C2b	507	0.00467	0.106	0.84	5.376	0.00556	0.00089	4.67E-05	0.000843	0.0064	1	6.683019
C2c	551	0.00485	0.097	0.84	5.376	0.00562	0.00077	4.67E-05	0.000723	0.0064	1	6.263918
C3a	616	0.00456	0.102	0.20	1.280	0.01043	0.00587	4.67E-05	0.005823	0.0064	1	11.418300
C3b	661	0.00451	0.104	0.20	1.280	0.00868	0.00417	4.67E-05	0.004123	0.0064	1	7.929487
C3c	645	0.00461	0.10	0.20	1.280	0.00860	0.00399	4.67E-05	0.003943	0.0064	1	7.886667
C4a	666	0.00460	0.101	0.67	4.288	0.00532	0.00072	4.67E-05	0.000673	0.0064	1	4.466667
C4b	669	0.00467	0.09	0.67	4.288	0.00524	0.00057	4.67E-05	0.000523	0.0064	1	3.895926
C4c	615	0.00458	0.096	0.67	4.288	0.00536	0.00078	4.67E-05	0.000733	0.0064	1	5.118056
C5a	662	0.00468	0.096	0.375	2.400	0.00698	0.00230	4.67E-05	0.002253	0.0064	1	8.802083
C5b	630	0.00466	0.10	0.375	2.400	0.00672	0.00206	4.67E-05	0.002013	0.0064	1	7.550000
C5c	638	0.00457	0.097	0.375	2.400	0.00656	0.00199	4.67E-05	0.001943	0.0064	1	7.512887
C6a	671	0.00455	0.10	0.19	1.216	0.00998	0.00543	4.67E-05	0.005383	0.0064	1	10.228330
C6b	665	0.00465	0.101	0.19	1.216	0.00894	0.00429	4.67E-05	0.004243	0.0064	1	7.982508
C6c	653	0.00482	0.10	0.19	1.216	0.00909	0.00427	4.67E-05	0.004223	0.0064	1	8.024333
C7a	621	0.00460	0.101	0.315	2.016	0.00736	0.00276	4.67E-05	0.002713	0.0064	1	8.462376
C7b	626	0.00455	0.101	0.315	2.016	0.00722	0.00267	4.67E-05	0.002623	0.0064	1	8.181683
C7c	606	0.00467	0.104	0.315	2.016	0.00753	0.00286	4.67E-05	0.002813	0.0064	1	8.521154
C8a	612	0.00471	0.10	0.44	2.816	0.00743	0.00272	4.67E-05	0.002673	0.0064	1	11.762670
C8b	623	0.00467	0.106	0.44	2.816	0.00660	0.00193	4.67E-05	0.001883	0.0064	1	7.817610
C8c	634	0.00470	0.10	0.44	2.816	0.00657	0.00187	4.67E-05	0.001823	0.0064	1	8.022667

Trap code	Filter number	Tared filter weight W_t (mg)	Volume filtered V_f (l)	Brine height H_b (m)	Brine volume $V_r=Ah_b$ (l)	Filtered weight W_f (mg)	Mass difference W_f-W_t	Blank weight W_{blk} (mg)	Total weight W_T (mg)	Trap area A (m^2)	Duration t (d)	Total mass flux $TM=W_TV_r(V_fAt)^{-1}$ ($g\ m^{-2}\ d^{-1}$)
C9a	608	0.00467	0.086	0.915	5.856	0.00523	0.00056	4.67E-05	0.000513	0.0064	1	5.461628
C9b	668	0.00463	0.099	0.915	5.856	0.00525	0.00062	4.67E-05	0.000573	0.0064	1	5.298990
C9c	611	0.00456	0.101	0.915	5.856	0.00520	0.00064	4.67E-05	0.000593	0.0064	1	5.375248
C10a	658	0.00458	0.106	0.84	5.376	0.00543	0.00085	4.67E-05	0.000803	0.0064	1	6.366038
C10b	642	0.00471	0.104	0.84	5.376	0.00544	0.00073	4.67E-05	0.000683	0.0064	1	5.519231
C10c	652	0.00448	0.096	0.84	5.376	0.00530	0.00082	4.67E-05	0.000773	0.0064	1	6.766667
C11a	629	0.00466	0.102	0.255	1.632	0.00831	0.00365	4.67E-05	0.003603	0.0064	1	9.008333
C11b	605	0.00454	0.098	0.255	1.632	0.00767	0.00313	4.67E-05	0.003083	0.0064	1	8.022959
C11c	610	0.00464	0.102	0.255	1.632	0.00728	0.00264	4.67E-05	0.002593	0.0064	1	6.483333
C12a	656	0.00454	0.098	0.375	2.400	0.00735	0.00281	4.67E-05	0.002763	0.0064	1	10.573980
C12b	604	0.00476	0.10	0.375	2.400	0.00741	0.00265	4.67E-05	0.002603	0.0064	1	9.762500
C12c	619	0.00456	0.104	0.375	2.400	0.00717	0.00261	4.67E-05	0.002563	0.0064	1	9.242788

	Filter number	Tared filter weight (mg)	Volume filtered (l)	Filtered weight (mg)	Blank mass difference (mg)	Average weight (mg)	Conc. Blank ($mg\ l^{-1}$)	Corrected conc. ($mg\ l^{-1}$)	Average Blank conc.	Std dev. Blank conc.
Blank A	603	0.00468	0.285	0.00487	0.00019	0.000187	0.000667	0.000076	7.47E-05	2.38E-05
Blank A	647	0.00461	0.255	0.00481	0.00020	0.000187	0.000784	8.00E-05		
Blank A	628	0.00462	0.25	0.00478	0.00016	0.000187	0.000640	6.40E-05		
Blank A	633	0.00459	0.24	0.00470	0.00011	0.000187	0.000458	4.40E-05		
Blank A	664	0.00451	0.25	0.00480	0.00029	0.000187	0.001160	0.000116		
Blank A	657	0.00465	0.25	0.00482	0.00017	0.000187	0.000680	0.000068		
Blank B	683	0.00472	0.25	0.00480	8.0E-05	8.83E-05	0.000320	3.20E-05	3.53E-05	1.88E-05
Blank B	674	0.00452	0.25	0.00465	0.00013	0.000088	0.000520	0.000052		
Blank B	673	0.00451	0.25	0.00458	7.0E-05	0.000088	0.000280	2.80E-05		
Blank B	691	0.00460	0.245	0.00464	4.0E-05	0.000088	0.000163	0.000016		
Blank B	678	0.00448	0.24	0.00464	0.00016	0.000088	0.000667	6.40E-05		
Blank B	681	0.00449	0.24	0.00454	5.0E-05	0.000088	0.000208	2.00E-05		
Blank C	711	0.00442	0.25	0.00453	0.00011	0.000117	0.000440	4.40E-05	4.67E-05	1.00E-05
Blank C	718	0.00451	0.25	0.00462	0.00011	0.000117	0.000440	4.40E-05		
Blank C	717	0.00477	0.25	0.00490	0.00013	0.000117	0.000520	0.000052		
Blank C	716	0.00453	0.25	0.00463	1.0E-04	0.000117	0.000400	4.00E-05		
Blank C	719	0.00437	0.251	0.00453	0.00016	0.000117	0.000637	6.40E-05		
Blank C	715	0.00469	0.249	0.00478	9.0E-05	0.000117	0.000361	3.60E-05		

APPENDIX 7B: Microscopic descriptions - Spring 1993

Station: X479 (Subtropical) **Filter number:** 404
Depth (m): 110
Comments: Significant more and larger sized material than at 300 m

Particle Type	Description	Size (μm)	Abundance
Coscinodiscus spp.	Round with green/brown textured centre; many partial outlines, smaller spheres have reddish-brown centre - finely structured	Diameter- 180, 240, 250, 220, 250, 240, 90, 240, 70, 35, 90, 60	Abundant
Silicoflagellates	Skeletal geodesic forms; spiny	50, 65, 35, 30, 35	Present
Translucent flakes	Flat with brown gunge & ragged edges	400 x 700 long	Abundant
Box-like diatoms	Series of adjoining rectangles <10 μm wide, greenish centres, partial outlines common	100 x 50, 100 x 80, 130 x 90	
Ovoid faecal pellets	Amorphous, olive-green, no obvious membrane, dark internal blotches	250 x 60, 170 x 130	Common
Foraminifera	Agglutinated	160 x 60, 300 x 50, 250 x 50, 70 x 250, 200 x 50	Common
Foraminifera	Planktonic (*Globigerina*)	90 across	
Zooplankton	Copepod legs and moult (300 across x 450 long)		
Large dinoflagellate?	Brownish colour	200 long	Rare
Round diatom?	With 3 triangular segments	Diameter - 50, 80, 60	
Spiny "umbrella" diatom?		60 long	
Elongate diatom	Internal specks	140 long	
Armoured dinoflagellate?	Trapezoid shape, external patterning and plates	100 high, 110 along base, 40 across top	
Mineral grains	Translucent, red-brown		Abundant

Station: X479 (Subtropical) **Filter number:** 413
Depth (m): 300

Particle Type	Description	Size (μm)	Abundance
Coscinodiscus spp.	Round with green/brown textured centre; many partial outlines	Diameter- 75, 150, 210, 40, 40, 95, 100	Common-abundant
Silicoflagellates	Skeletal geodesic forms; spiny	20, 25, 35	Common
Opaque flakes	Black, irregular - ?soot	100, 110 across	Rare
Box-like diatom	Series of adjoining rectangles <10 μm wide, greenish centres, partial outlines common	70 x 50	Present
Ovoid faecal pellets	Amorphous, olive-green, no obvious membrane, dark internal blotches	120 x 50, 200 x 60	Rare-common
Rectangular faecal pellets	Amorphous, khaki-brown	770 x 50, 120 x 50	Rare-common
Microzooplankton?	Pale, translucent with green centre, internal structure, rounded form	70 x 50	
Microzooplankton?	?"Jellybean" shape, black, opaque	140 long	
?unknown	Numerous very small indistinguishable brown, green and bright blue particles, many shapes - rods, rounded, irregular	generally <2, up to 40	Abundant
Diatom?	Translucent "lip-like" form with green centre, elongated	230 x 30	

Station: X479 (Subtropical) **Filter number:** 369
Depth (m): 550
Comments: Staining of particles by blue food colouring used for dying brine in traps

Particle Type	Description	Size (μm)	Abundance
Coscinodiscus spp.	Round with green to brown textured centre; many partial outlines, smaller forms have pale red/brown centre	Diameter- 40, 100, 90, 210, 140, 60	Common
Silicoflagellates		20, 30, 30, 35	Present
Opaque flakes	?soot		
Box-like diatom		90 x 80	
Ovoid faecal pellets	Olive-green, comprising speckled organic matter and occasional brown crystals, no evidence of membrane	140 x 60, 310 x 100, 50 x 190, 70 x 190, 50 x 120, 70 x 200, 50 x 130, 60 x 240	Common
Foraminifera	Large flakey white (?calcite) rounded form with spines	150 diameter	
Foraminifera	Partial chambers, planktonic with spines	50 diameter	
Zooplankton moult			
Chain diatom?	Comprisng many small rectangular internal forms linked with fine tendrils	30 wide x 680 long	
Mineral grains	Translucent, brown, well-moderate rounded, irregular and equant	250, 110, 60, 30 across	Abundant-common
Pelagic gastropod	Conical like *Struthialaria*	160 high x 90 across	

Station: X480 (Subtropical) **Filter number:** 402
Depth (m): 110
Comments: Lots of detrital organic material <5 μm so difficult to discern, filter stained green

Particle Type	Description	Size (μm)	Abundance
Coscinodiscus spp.	Round with green/brown textured centre; many partial outlines, smaller translucent forms	Diameter- 190, 210, 200, 100	Abundant
Silicoflagellates		30, 50	Present
Opaque flakes	?soot		
Box-like diatom	Reddish-brown pigment	60 x 100	
Ovoid faecal pellets			Present
Foraminifera	Agglutinated; panktonic form covered in O/M	60-70 wide x 260-280 long	Common
?Microzooplankton	Rounded form with dark khaki-green centre		
Zooplankton moult	Copepod	850 long x 400	Common
Amorphous organic matter	Large, elongate, ragged pieces of khaki-green, semi-translucent O/M, irregular, diffuse outline		
Armoured dinoflagellates?	Discrete outer plates	100 long x 130 high, 160 x 110	
?Tintinnids	"Mushroom" form (110 μm high); "Eiffel Tower" form (210 μm high)		
Elongate diatom?		250 long	

Station: X480 (Subtropical) **Filter number:** 411
Depth (m): 550
Comments: Less material than at Station X479

Particle Type	Description	Size (μm)	Abundance
Coscinodiscus spp.	Round with green/red-brown textured centre; many partial outlines, smaller forms translucent with less noticeable internal structure	Diameter- 90, 40-50, 90, 210, 170	Common
Silicoflagellates		20, 30, 30, 25, 30-35	Present
Opaque flakes	?soot		
Ovoid faecal pellets	Khaki-brown containing many well rounded pelletal (or cellular - picoplankton?) material <6-10 μm in size; no apparent membrane	120 x 500, 290 x 70, 210 x 50, 310 x 70, 170 x 60, 150 x 50	Common
Mineral grains	Red-brown, translucent		Common
Copepod eggs?	Light yellow-khaki brown globules aggregated together with dark spheres in centres of globules	245 long x 110 across	

Station: X478 (STC) **Filter number:** 393
Depth (m): 100
Comments: Filter stained blue-green; ubiquitous "green" material

Particle Type	Description	Size (μm)	Abundance
Coscinodiscus spp.	Round with green/brown textured centre; many partial outlines	Diameter- 150, 100, 60, 140, 260, 200, 185, 90, 90	Common
Silicoflagellates		Generally 20-30, up to 80	Very abundant
Rectangular faecal pellets	Opaque, dark khaki-green, not as plentiful as in ST slides	340 long x 150 wide	Rare
Radiolaria	Many spines, round	160, up to 160	
Needle diatom?	Mesh of needles	60-100 long	
Tintinnid?	"Mushroom" form	160 long x 100 wide	
Radiolarian	Double ring with numerous short spines segmenting the ring	155 diameter	Present
Armoured dinoflagellate?	Rounded triangular form with discrete external plates, khaki-brown	80 high	
?unknown	Solid, round with radiating segments	50 diameter	
Mineral grains	Brown-yellow, translucent		
Dinoflagellate	"Turban with pointy tips"	90 across	
Cylindrical diatom? Or moult?	Patterned cylinder with sharp pointed end (?)- triangular pattern		

Station: X478 (STC) **Filter number:** 385
Depth (m): 220
Comments: Numerous "fluffy" amorphous aggregates prominent

Particle Type	Description	Size (μm)	Abundance
Coscinodiscus spp.	Round with green/brown textured centre; many partial outlines		Common
Silicoflagellates	Less than in shallower trap	20-30	Abundant
Box-like diatom		30 high	
Rectangular faecal pellets	Opaque-khaki brown	300 long x 90-140 wide	Common
Foraminifera	Brown, planktonic - covered with O/M?	180 high	
Radiolaria	Large form	Diameter - 210, 310	
Mineral grains	Irregular, subangular-rounded, translucent		Very abundant
?Glauconite	Rounded, green-dark green, equant-elongate	160 x 290	
?Dinoflagellate	Large, khaki-brown, solid with external markings	80 across	
Tintinnids	"Mushroom" form	160 long	

Station: X477 (STC) **Filter number:** 336
Depth (m): 100
Comments: Significant less material than at Station X478, although similar in composition

Particle Type	Description	Size (μm)	Abundance
Copepod carcass		260 long x 90 wide body	Rare

Station: X477 (STC) **Filter number:** 388
Depth (m): 220

Particle Type	Description	Size (μm)	Abundance
Coscinodiscus spp.	Round with green/brown textured centre	Diameter- 230	Common
Silicoflagellates		30	Common
Ovoid faecal pellets	Dark khaki-green with numerous small black particles	210 long x 70 wide, 170 x 40	Rare
?Needle diatom	Haphazard radiating spicules ?	120 long	
Mineral grains	Translucent, subrounded-subangular	<50 long	Abundant
?Glauconite	Green, rounded-ovoid particles	80 long	

Station: X476 (Subantarctic) **Filter number:** 384
Depth (m): 150
Comments: Conspicuous absence of well-formed faecal pellets

Particle Type	Description	Size (μm)	Abundance
Coscinodiscus spp.	Round with green/brown textured centre; many smaller forms	Diameter - <60	Common
Silicoflagellates		20-30, up to 60	Abundant
Translucent flakes	Light brown, amorphous		Rare
Opaque flakes		up to 200	
Mineral grains	Subrounded, brown-yellow & dark reddish-brown; transparent grains that reflect light (becoming light blue and yellow in colour - ?micas)	< 30	
?Dinoflagellate	Armoured, reddish brown	90 across	
Radiolaria	Large, numerous spines		
Microzooplankton?	Triangular with rounded base, pale brown	130 wide x 60 high	
?unknown	Central round form with 6 rectangular "spines" radiating out on two separate levels	Diameter - 70, "spines" - 20 long	

Station: X465 (Subantarctic) **Filter number:** 367
Depth (m): 300
Comments: Contrasts ST slides with khaki-brown detrital material that seems to be more fragmented

Particle Type	Description	Size (μm)	Abundance
Coscinodiscus spp.	Round with green/brown textured centre; many partial outlines, smaller versions dominate	Diameter- 70, 40, 70, 70	Common
Silicoflagellates		25, 50, 35, 30	Very abundant
Opaque flakes	?soot	90-100 long x 40-50 wide	
Box-like diatom		60 high	
Chain diatom?	Consisting of numerous opaque "jellybean" forms within a straight, transparent strip	30 wide x 1000 long	
Foraminifera			
Radiolaria	May be clear and finely detailed or brown in colour, needle spines, intricate internal skeleton	Diameter - 110, 150	
Mineral grains	Translucent, brown		
Microzooplankton?	Triangular with rounded base, pale brown	75 wide x 50 high	Common
Radiolarian?	Round with radiating internal rib-like structure, multi-layered	70 diameter	

Station: X476 (Subantarctic) **Filter number:** 376
Depth (m): 550

Particle Type	Description	Size (μm)	Abundance
Coscinodiscus spp.	Round with green/brown textured centre; many partial outlines	Diameter- 50-60	
Silicoflagellates		20-30	Abundant
Ovoid faecal pellets	Dark green-khaki with black specks	220 long x 80, 370 x 80, 290 x 75	Rare
Radiolaria	Large forms	Diameter - 180, 160	
Mineral grains	Translucent, brown-opaque, subrounded; transparent grains (?micas - light blue & yellow under reflected light)		Common
?unknown	Central round form with 6 rectangular "spines" radiating out on two separate levels	Diameter - 60, "spines" - 10 long	
?unknown	Yellow-green, well rounded, translucent equant particle	200 across	
?pellet	Flattened ovoid, brown-yellow	310 long x 190 wide	

Station: X475 (Subantarctic) **Filter number:** 303
Depth (m): 150
Comments: Similar composition to 150 m sample at station X476

Particle Type	Description	Size (μm)	Abundance
Silicoflagellates		20-30	Abundant
Rectangular faecal pellets	Very diffuse outline with dark specks	860 long x 110 wide	
?Tintinnid or foraminifera	Scuptured external shell	180 high x 110 wide	
?Mineral grain	Brown with apparent blemishes, irregular, angular	235 high x 210 wide	

Station: X475 (Subantarctic) **Filter number:** 324
Depth (m): 550
Comments: Similar composition as 150 m sample at same station, although less material

APPENDIX 7A: Microscopic descriptions - Winter 1993

Station: X468 (Subtropical) **Filter number:** 221
Depth (m): 120
Comments: Ubiquitous yellow-brown amorphous masses (smothers entire filter)

Particle Type	Description	Size (μm)	Abundance
Coscinodiscus spp.	Round with green/reddish brown textured centre; many partial outlines	Diameter - 160, 95, 90, 130, 60, 50	Common
Silicoflagellates	Skeletal geodesic forms; spiny	20-30 up to 70	Abundant
Opaque flakes	?soot		
Box-like diatom	Series of adjoining rectangles <10 μm wide, greenish centres, partial outlines common	95 x 200 long, 60 x 110	
Rectangular faecal pellets	Khaki-brown, with black specks	390 long x 60-80	Present
Chain diatom	Rounded forms linked together	10 across	
?unknown	Crystalline "body" with needle tip, hard	215 long x 25 wide "body" & 115 long needle	
Rod-like diatom	Narrow ellipsoid with paired vertical divisions	175 long x 10 wide	
Zooplankton remains	Copepod carcass & unattached legs, etc		Rare
Aggregates	Rounded	100 diameter	
?Microzooplankton	"Jellybean" with internal structure	120 x 90 high	
?Needle diatom	Very narrow needles joined at common point, larger ones have some internal structure	140 long	
?Egg	Transparent with internal "yolk"	60 diameter	

Station: X468 (Subtropical) **Filter number:** 130
Depth (m): 220
Comments: Badly tainted by corroded aluminium foil; 1/2 filter

Station: X468 (Subtropical) **Filter number:** 213
Depth (m): 300
Comments: Similar composition as at 120 m, but less material, numerous desiccation cracks and flaking + nylon

Particle Type	Description	Size (μm)	Abundance
Coscinodiscus spp.	Round with green/brown textured centre; many partial outlines	Diameter - 40-60	Common
Silicoflagellates	Skeletal geodesic forms; spiny		Common
Tintinnids?	"Mushroom" (140 μm long x 60 μm), "Rocket" (205 μm long x 55 μm)		

Station: X468 (Subtropical) **Filter number:** 249
Depth (m): 550
Comments: Similar composition as at 300 and 120 m, but significantly less material than at near-surface depth; 1/2 filter

Station: X467 (STC) **Filter number:** 159
Depth (m): 110
Comments: Ubiquitous yellow/red-brown amorphous masses, covering filter, with sporadic lime green semi-regular forms; 1/2 filter

Particle Type	Description	Size (μm)	Abundance
Coscinodiscus spp.	Round with green/brown textured centre; many smaller varieties (30-65 μm diameter)	Diameter - 205, 100, 95, 100, 100, 85, 85, 80	Common
Silicoflagellates		20-30	Abundant
Box-like diatom		80 high	
Rectangular faecal pellets	Khaki green-brown	460 x 100, 740 x 130, 550 x 100, 500 x 140	
?Foraminifera	Open aperture, short spikes, rounded cone	140 long x 60 wide	
Radiolaria	Partial form with scalloped "wings"	80 across	
Mineral grains	Opaque/dark red-brown irregular, subrounded-subangular		
?Needle diatom	Very narrow needles joined at common point, larger ones have some internal structure	140 long needles	
Tabular diatom?	Faint, wavy outline with vertical internal segments		
?unknown	Crystalline "body" with needle tip, hard	100 long	
Zooplankton remains			Rare

Station: X467 (STC) **Filter number:** 117
Depth (m): 210
Comments: Filter covered by very fine, light brown amorphous material, similar composition to 110 m but less material; 1/2 filter

Particle Type	Description	Size (μm)	Abundance
Radiolaria	Fine needle spines, fine internal structure	Diameter - 200	
?Radiolaria	Brown internal core and numerous protruding fine needle spines	Diameter - 150	
?unknown	Tusk-like with solid external sheath	>550 long x 85 wide	
?Dinoflagellate	Rounded, armoured upper with 2 protruding spikes	170 high x 105 wide	
?Diatom	Elongate	260 long x 40 high	

Station: X464 (Subantarctic) **Filter number:** 156
Depth (m): 120
Comments: Filter covered by very fine, light brown amorphous material, rare large particles; 1/2 filter

Particle Type	Description	Size (μm)	Abundance
Coscinodiscus spp.	Round with red-brown textured centre; mostly smaller variety	Diameter - 60, 55, 60, 80	Common
Silicoflagellates			Rare, less than in other samples
Opaque flakes	Angular-subangular		Common
Rounded faecal pellets	Khaki-brown, equant, sometimes embedded with red-brown grains	60-70 across	Rare
Ovoid faecal pellets	Dark-brown-khaki brown	40 wide	Rare
?Foraminifera	High profile, rounded, textured surface	70 diameter	
Radiolaria	Fragmented		
Mineral grains	Transparent, angular		Common
?egg	Transparent with "yolk"	80 diameter	
Web-like fragments	?from appendicularians		
Elongate diatoms	Many vertical internal divisions	70 long x 10 wide	Common
?Tintinnid	3 stacked rounded chambers, external scupturing	130 long x 65 wide	
?Rod-like & branched forms		20-25 wide generally, up to 40, down to 10	

Station: X464 (Subantarctic) **Filter number:** 119
Depth (m): 220
Comments: Ubiquitous very fine light brown amorphous material - streaked across filter + nylon and possibly 2 "live" copepods; similar composition and amount of material as at 120 m, less faecal pellets; 1/2 filter

Particle Type	Description	Size (μm)	Abundance
Coscinodiscus spp.	Round with red-brown textured centre; many smaller versions	Diameter - 40-60, 1 large form - 265	
Ovoid faecal pellets			Less than at 120 m
Zooplankton carcass			Present
?Needle diatoms			
?Tintinnid	"Dalek" form with needle point on top	110 long x 35 wide	
?Dinoflagellate	Rounded, armoured with external plates	90 x 70	
?Radiolaria	Rod-like with many fine needle spines and rounded, protruding ends	360 x 55	

Station: X464 (Subantarctic) **Filter number:** 145
Depth (m): 300
Comments: Similar composition as 120 m, although less material and no widespread light brown amorphous material, rare aggregates + nylon

Particle Type	Description	Size (μm)	Abundance
?Microzooplankton	Rounded triangular form	115 long x 60 wide, smaller version - 50 x 35	
Radiolarian	Distinct centre and numerous radiationg fine needle spines	45 diameter	
?unknown	Elongate with cross-hatched pattern	30 wide	

Station: X464 (Subantarctic) **Filter number:** 217
Depth (m): 550
Comments: Problems with flattening filter out + nylon contaminants; 1/2 filter, filter covered with very fine amorphous indistinguishable material, rare large particles, similar composition to 120 m, but less material

Particle Type	Description	Size (μm)	Abundance
Coscinodiscus spp.	Round with green/brown textured centre	Diameter - 110	
Silicoflagellates		20-30	Less than at other depths
Box-like diatom		80 high	
Ovoid faecal pellets		50 wide	
Mineral grains	Pale translucent, surounded-subangular		
?Glauconite	Lime-green, one grain		
Rounded aggreagates	Dark brown-khaki	180 across	

Station: X465 (Subantarctic) **Filter number:** 232
Depth (m): 220

Particle Type	Description	Size (μm)	Abundance
Coscinodiscus spp.	Round with green/brown textured centre; many smaller varieties	Diameter - 190 (large one)	large versions rare, others abundant
Silicoflagellates			Common
Opaque flakes	Reddish tinge, angular grains	Up to 160 across	
Rectangular faecal pellets	One khaki pellet	90-100 wide	
Mineral grains	Translucent, angular		Common
?Tintinnid	"Dalek"		
Zooplankton carcass			Present
?Web-like forms	?remains from appendicularian	Up to 70 wide	Very common

Station: X465 (Subantarctic) **Filter number:** 286
Depth (m): 300
Comments: Similar composition and amount on filter as at 220 m

Particle Type	Description	Size (μm)	Abundan
Coscinodiscus spp.	Round with green/brown textured centre; many partial outlines	Diameter - 40-50	Common
Silicoflagellates		20-30 up tp 80	Rare
Opaque flakes	?soot		
Box-like diatom		60-100 wide	
Rectangular faecal pellets	Khaki	75-80 wide	
Mineral grains	Translucent, angular		Common
?Web-like forms	?remains of appendicularians		
Elongate diatoms	Vertical internal segments	70 long x 40 wide	Common
Zooplankton carcass	?copepod		
Large elongate diatom	Internal vertical segments, reddish tinge?	140 long x 10 wide	
?Egg	Transparent with internal "yolk"	70 diameter	
?Tintinnid	"Dalek"		
Large patterned fragment		680 wide	